PROTEINS BINDING NKG2D, CD16 AND CLEC12A

[0001] This application claims priority to U.S. Provisional Application No. 63/020,798, filed on May 6, 2020, the entirety of which is incorporated herein by reference.

SEQUENCE LISTING

[0002] This application incorporates by reference in its entirety the Computer Readable Form (CRF) of a Sequence Listing in ASCII text format. The Sequence Listing text file is entitled "14247-540-228_SEQ_LISTING," was created on May 3, 2021, and is 291,375 bytes in size.

FIELD OF THE INVENTION

[0003] The present application relates to multispecific binding proteins that bind NKG2D, CD16 and CLEC12A on a cell, pharmaceutical compositions comprising such proteins, and therapeutic methods using such proteins and pharmaceutical compositions, including for the treatment of cancer.

BACKGROUND

[0004] Despite substantial research efforts, cancer continues to be a significant clinical and financial burden in countries across the globe. According to the World Health Organization (WHO), it is the second leading cause of death. Surgery, radiation therapy, chemotherapy, biological therapy, immunotherapy, hormone therapy, stem-cell transplantation, and precision medicine are among the existing treatment modalities. Despite extensive research in these areas, a highly effective, curative solution, particularly for the most aggressive cancers, has yet to be identified. Furthermore, many of the existing anti-cancer treatment modalities have substantial adverse side effects.

[0005] Cancer immunotherapies are desirable because they are highly specific and can facilitate destruction of cancer cells using the patient's own immune system. Fusion proteins such as bi-specific T-cell engagers are cancer immunotherapies described in the literature that bind to tumor cells and T-cells to facilitate destruction of tumor cells. Antibodies that bind to certain tumor-associated antigens have been described in the literature. *See, e.g.*, WO 2016/134371 and WO 2015/095412.

[0006] Natural killer (NK) cells are a component of the innate immune system and make up approximately 15% of circulating lymphocytes. NK cells infiltrate virtually all tissues and were originally characterized by their ability to kill tumor cells effectively without the need for prior sensitization. Activated NK cells kill target cells by means similar to cytotoxic T cells – *i.e.*, via cytolytic granules that contain perforin and granzymes as well as via death receptor pathways. Activated NK cells also secrete inflammatory cytokines such as IFN-γ and chemokines that promote the recruitment of other leukocytes to the target tissue.

[0007] NK cells respond to signals through a variety of activating and inhibitory receptors on their surface. For example, when NK cells encounter healthy self-cells, their activity is inhibited through activation of the killer-cell immunoglobulin-like receptors (KIRs). Alternatively, when NK cells encounter foreign cells or cancer cells, they are activated via their activating receptors (*e.g.*, NKG2D, NCRs, DNAM1). NK cells are also activated by the constant region of some immunoglobulins through CD16 receptors on their surface. The overall sensitivity of NK cells to activation depends on the sum of stimulatory and inhibitory signals. NKG2D is a type-II transmembrane protein that is expressed by essentially all natural killer cells where NKG2D serves as an activating receptor. NKG2D is also be found on T cells where it acts as a costimulatory receptor. The ability to modulate NK cell function via NKG2D is useful in various therapeutic contexts including malignancy.

[0008] C-type lectin domain family 12 member A (CLEC12A), also known as C-type lectin-like molecule-1 (CLL-1) or myeloid inhibitory C-type lectin-like receptor (MICL), is a member of the C-type lectin/C-type lectin-like domain (CTL/CTLD) superfamily. Members of this family share a common protein fold and have diverse functions, such as cell adhesion, cell-cell signaling, glycoprotein turnover, and roles in inflammation and immune response. CLEC12A, a type II transmembrane glycoprotein, is overexpressed in over 90% of acute myeloid leukemia patient on leukemic stem cells, but not on normal haematopoietic cells.

[0009] Despite many efforts undertaken by several biotech and pharma companies, development of specific CLEC12A targeted biologics is hindered by the absence of antibodies with good developability characteristics. The challenges in discovering CLEC12A antibodies may be attributed to the complexity of the antigen. CLEC12A is a monomeric heavily glycosylated protein with six potential N-glycosylation sites within an extracellular domain having 201 amino acids. Four out of six N-glycosylation sites are clustered in the membrane

proximal domain of the molecule and are likely to be involved in presentation of the target on the cell surface. Variations in the glycosylation status of CLEC12A on the surface of different cell types has been reported (Marshall *et al.*, (2006) *Eur J Immunol.* 36(8):2159-69).

[0010] Therefore, there remains a need in the field for new and useful proteins that bind CLEC12A for use in treatment of cancer.

SUMMARY

[0011] The present application provides multispecific binding proteins that bind to the NKG2D receptor and CD16 receptor on natural killer cells, and CLEC12A. Such proteins can engage more than one kind of NK-activating receptor, and may block the binding of natural ligands to NKG2D. In certain embodiments, the proteins can agonize NK cells in humans. In some embodiments, the proteins can agonize NK cells in humans and in other species such as rodents and cynomolgus monkeys. Formulations containing any one of the proteins disclosed herein; cells containing one or more nucleic acids expressing the proteins, and methods of enhancing tumor cell death using the proteins are also provided.

[0012] Accordingly, in one aspect, the present application provides a protein comprising:

(a) a first antigen-binding site that binds NKG2D;

(b) a second antigen-binding site that binds CLEC12A; and

(c) an antibody Fc domain or a portion thereof sufficient to bind CD16, or a third antigen-binding site that binds CD16;

wherein the second antigen-binding site that binds CLEC12A comprises:

(i) a heavy chain variable domain (VH) comprising complementarity-determining region 1 (CDR1), complementarity-determining region 2 (CDR2), and complementarity-determining region 3 (CDR3) comprising the amino acid sequences of SEQ ID NOs: 137, 272, and 273, respectively; and a light chain variable domain (VL) comprising CDR1, CDR2, and CDR3 comprising the amino acid sequences of SEQ ID NOs: 140, 141, and 142, respectively;

(ii) a VH comprising CDR1, CDR2, and CDR3 comprising the amino acid sequences of SEQ ID NOs: 137, 138, and 139, respectively; and a VL comprising CDR1, CDR2, and CDR3 comprising the amino acid sequences of SEQ ID NOs: 140, 141, and 142, respectively;

(iii) a VH comprising CDR1, CDR2, and CDR3 comprising the amino acid sequences of

SEQ ID NOs: 251, 196, and 246, respectively; and a VL comprising CDR1, CDR2, and CDR3 comprising the amino acid sequences of SEQ ID NOs: 198, 199, and 201, respectively;

(v) a VH comprising CDR1, CDR2, and CDR3 comprising the amino acid sequences of SEQ ID NOs: 221, 166, and 223, respectively; and a VL comprising CDR1, CDR2, and CDR3 comprising the amino acid sequences of SEQ ID NOs: 240, 226, and 179, respectively;

(v) a VH comprising CDR1, CDR2, and CDR3 comprising the amino acid sequences of SEQ ID NOs: 206, 166, and 241, respectively; and a VL comprising CDR1, CDR2, and CDR3 comprising the amino acid sequences of SEQ ID NOs: 245, 239, and 179, respectively;

(vi) a VH comprising CDR1, CDR2, and CDR3 comprising the amino acid sequences of SEQ ID NOs: 221, 236, and 223, respectively; and a VL comprising CDR1, CDR2, and CDR3 comprising the amino acid sequences of SEQ ID NOs: 152, 226, and 179, respectively;

(vii) a VH comprising CDR1, CDR2, and CDR3 comprising the amino acid sequences of SEQ ID NOs: 159, 170, and 183, respectively; and a VL comprising CDR1, CDR2, and CDR3 comprising the amino acid sequences of SEQ ID NOs: 186, 188, and 189, respectively;

(viii) a VH comprising CDR1, CDR2, and CDR3 comprising the amino acid sequences of SEQ ID NOs: 197, 202, and 207, respectively; and a VL comprising CDR1, CDR2, and CDR3 comprising the amino acid sequences of SEQ ID NOs: 211, 212, and 214, respectively;

(ix) a VH comprising CDR1, CDR2, and CDR3 comprising the amino acid sequences of SEQ ID NOs: 220, 222, and 257, respectively; and a VL comprising CDR1, CDR2, and CDR3 comprising the amino acid sequences of SEQ ID NOs: 224, 225, and 227, respectively; or

(x) a VH comprising CDR1, CDR2, and CDR3 comprising the amino acid sequences of SEQ ID NOs: 230, 231, and 232, respectively; and a VL comprising CDR1, CDR2, and CDR3 comprising the amino acid sequences of SEQ ID NOs: 233, 234, and 235, respectively.

[0013] In some embodiments, the second antigen-binding site that binds CLEC12A comprises a VH comprising CDR1, CDR2, and CDR3 comprising the amino acid sequences of SEQ ID NOs: 137, 272, and 273, respectively; and a VL comprising CDR1, CDR2, and CDR3 comprising the amino acid sequences of SEQ ID NOs: 140, 141, and 142, respectively. In some embodiments, the second antigen-binding site that binds CLEC12A comprises a VH comprising CDR1, CDR2, and CDR3 comprising the amino acid sequences of SEQ ID NOs: 137, 138, and 139, respectively; and a VL comprising CDR1, CDR2, and CDR3 comprising the amino acid sequences of SEQ ID NOs: 140, 141, and 142, respectively.

[0014] In certain embodiments, the VH comprises an amino acid sequence at least 90% identical to SEQ ID NO:335, and the VL comprises an amino acid sequence at least 90% identical to SEQ ID NO:336. In certain embodiments, the VH comprises an amino acid sequence at least 90% identical to SEQ ID NO:270, and the VL comprises an amino acid sequence at least 90% identical to SEQ ID NO:271. In certain embodiments, the VH comprises an amino acid sequence at least 90% identical to SEQ ID NO:178, and the VL comprises an amino acid sequence at least 90% identical to SEQ ID NO:289. In certain embodiments, the VH comprises the amino acid sequence of SEQ ID NO:335, and the VL comprises the amino acid sequence of SEQ ID NO:336. In certain embodiments, the VH comprises the amino acid sequence of SEQ ID NO:270, and the VL comprises the amino acid sequence of SEQ ID NO:271. In certain embodiments, the VH comprises the amino acid sequence of SEQ ID NO:178, and the VL comprises the amino acid sequence of SEQ ID NO:289. In certain embodiments, the VH and the VL comprise the amino acid sequences of SEQ ID NOs: 143 and 144; 147 and 144; 244 and 144; 178 and 144; 256 and 144; 143 and 163; 143 and 167; 143 and 171; or 174 and 175, respectively.

[0015] In some embodiments, the second antigen-binding site is present as a single-chain fragment variable (scFv), and wherein the scFv comprises an amino acid sequence selected from SEQ ID NOs: 274, 145, 146, 149, 150, 153, 154, 156, 157, 160, 161, 164, 165, 168, 169, 172, 173, 176, 177, 180, and 181. In certain embodiments, the scFv comprises the amino acid sequence of SEQ ID NO:274. In certain embodiments, the scFv comprises the amino acid sequence of SEQ ID NO:180.

[0016] In some embodiments, the second antigen-binding site that binds CLEC12A comprises a VH comprising CDR1, CDR2, and CDR3 comprising the amino acid sequences of SEQ ID NOs: 251, 196, and 246, respectively; and a VL comprising CDR1, CDR2, and CDR3 comprising the amino acid sequences of SEQ ID NOs: 198, 199, and 201, respectively.

[0017] In certain embodiments, the second antigen-binding site that binds CLEC12A comprises:

(i) a VH comprising CDR1, CDR2, and CDR3 comprising the amino acid sequences of SEQ ID NOs: 195, 196, 187, respectively; and a VL comprising CDR1, CDR2, and CDR3 comprising the amino acid sequences of SEQ ID NOs: 198, 199, 201, respectively;

(ii) a VH comprising CDR1, CDR2, and CDR3 comprising the amino acid sequences of SEQ ID NOs: 192, 196, and 187, respectively; and a VL comprising CDR1, CDR2, and

CDR3 comprising the amino acid sequences of SEQ ID NOs: 198, 199, and 201, respectively; or

(iii) a VH comprising CDR1, CDR2, and CDR3 comprising the amino acid sequences of SEQ ID NOs: 192, 196, and 213, respectively; and a VL comprising CDR1, CDR2, and CDR3 comprising the amino acid sequences of SEQ ID NOs: 198, 199, and 201, respectively.

[0018] In certain embodiments, the VH comprises an amino acid sequence at least 90% identical to SEQ ID NO:148, and the VL comprises an amino acid sequence at least 90% identical to SEQ ID NO:203.

[0019] In certain embodiments, the VH comprises the amino acid sequence of SEQ ID NO:148, and the VL comprises the amino acid sequence of SEQ ID NO:203. In certain embodiments, the VH and the VL comprise the amino acid sequences of SEQ ID NOs: 162 and 203; 210 and 203; 162 and 218; 148 and 218; or 210 and 218, respectively. In some embodiments, second the antigen-binding site is present as an scFv, and wherein the scFv comprises an amino acid sequence selected from SEQ ID NOs: 184, 185, 204, 205, 208, 209, 215, 216, 252, 253, 254, and 255. In certain embodiments, the scFv comprises the amino acid sequence of SEQ ID NO:204.

[0020] In certain embodiments, the second antigen-binding site of a preceding embodiment binds CLEC12A in a glycosylation independent manner.

[0021] In another aspect, the present application provides a protein comprising:

(a) a first antigen-binding site that binds NKG2D;

(b) a second antigen-binding site that binds CLEC12A; and

(c) an antibody Fc domain or a portion thereof sufficient to bind CD16, or a third antigen-binding site that binds CD16;

wherein the second antigen-binding site binds CLEC12A in a glycosylation independent manner.

[0022] In some embodiments of a protein disclosed herein, the second antigen-binding site binds human CLEC12A with a dissociation constant (K_D) smaller than or equal to 20 nM as measured by surface plasmon resonance (SPR). In certain embodiments, the second antigen-binding site binds human CLEC12A with a K_D smaller than or equal to 1 nM as measured by SPR. In certain embodiments, the second antigen-binding site binds human CLEC12A comprising a K244Q substitution.

[0023] In some embodiments of a protein disclosed herein, the protein comprises an antibody Fc domain or a portion thereof sufficient to bind CD16.

[0024] In some embodiments of a protein disclosed herein, the first antigen-binding site that binds NKG2D is a Fab fragment, and the second antigen-binding site that binds CLEC12A is an scFv.

[0025] In some embodiments of a protein disclosed herein, the first antigen-binding site that binds NKG2D is an scFv, and the second antigen-binding site that binds CLEC12A is a Fab fragment.

[0026] In some embodiments of a protein disclosed herein, the protein further comprises an additional antigen-binding site that binds CLEC12A. In certain embodiments, the first antigen-binding site that binds NKG2D is an scFv, and the second and the additional antigen-binding sites that bind CLEC12A are each a Fab fragment. In certain embodiments, the first antigen-binding site that binds NKG2D is an scFv, and the second and the additional antigen-binding sites that bind CLEC12A are each an scFv. In certain embodiments, the amino acid sequences of the second and the additional antigen-binding sites are identical. In certain embodiments, the amino acid sequences of the second and the additional antigen-binding sites are different.

[0027] In another aspect, the present application provides a protein comprising:

(a) a first antigen-binding site that binds NKG2D;

(b) a second antigen-binding site that binds CLEC12A; and

(c) an antibody Fc domain or a portion thereof sufficient to bind CD16, or a third antigen-binding site that binds CD16;

wherein the first antigen-binding site that binds NKG2D is a Fab fragment, and the second antigen-binding site that binds CLEC12A is an scFv.

[0028] In some embodiments of a protein disclosed herein, the scFv that binds NKG2D is linked to an antibody constant domain or a portion thereof sufficient to bind CD16, via a hinge comprising Ala-Ser or Gly-Ser. In certain embodiments, the hinge further comprises an amino acid sequence Thr-Lys-Gly.

[0029] In some embodiments of a protein disclosed herein, each scFv that binds CLEC12A is linked to an antibody constant domain or a portion thereof sufficient to bind CD16, via a hinge comprising Ala-Ser or Gly-Ser. In certain embodiments, the hinge further comprises an amino acid sequence Thr-Lys-Gly.

[0030] In some embodiments of a protein disclosed herein, within the scFv that binds NKG2D, the heavy chain variable domain of the scFv forms a disulfide bridge with the light chain variable domain of the scFv. In certain embodiments, the disulfide bridge is formed between C44 of the heavy chain variable domain and C100 of the light chain variable domain, numbered under the Kabat numbering scheme

[0031] In some embodiments of a protein disclosed herein, within each scFv that binds CLEC12A, the heavy chain variable domain of the scFv forms a disulfide bridge with the light chain variable domain of the scFv. In certain embodiments, the disulfide bridge is formed between C44 of the heavy chain variable domain and C100 of the light chain variable domain, numbered under the Kabat numbering scheme.

[0032] In some embodiments of a protein disclosed herein, within the scFv that binds NKG2D, the heavy chain variable domain is linked to the light chain variable domain via a flexible linker. In certain embodiments, the flexible linker comprises $(G_4S)_4$.

[0033] In some embodiments of a protein disclosed herein, within each scFv that binds CLEC12A, the heavy chain variable domain is linked to the light chain variable domain via a flexible linker. In certain embodiments, the flexible linker comprises $(G_4S)_4$.

[0034] In some embodiments of a protein disclosed herein, within the scFv that binds NKG2D, the heavy chain variable domain is positioned at the C-terminus of the light chain variable domain.

[0035] In some embodiments of a protein disclosed herein, within each scFv that binds CLEC12A, the heavy chain variable domain is positioned at the C-terminus of the light chain variable domain.

[0036] In some embodiments of a protein disclosed herein, within the scFv that binds NKG2D, the heavy chain variable domain is positioned at the N-terminus of the light chain variable domain.

[0037] In some embodiments of a protein disclosed herein, within each scFv that binds CLEC12A, the heavy chain variable domain is positioned at the N-terminus of the light chain variable domain.

[0038] In some embodiments of a protein disclosed herein, the Fab fragment that binds NKG2D is not positioned between an antigen-binding site and the Fc or the portion thereof.

[0039] In some embodiments of a protein disclosed herein, no Fab fragment that binds CLEC12A is positioned between an antigen-binding site and the Fc or the portion thereof.

[0040] In some embodiments of a protein disclosed herein, the first antigen-binding site that binds NKG2D comprises a VH comprising CDR1, CDR2, and CDR3 comprising the amino acid sequences of SEQ ID NOs: 81, 82, and 112, respectively; and a VL comprising CDR1, CDR2, and CDR3 comprising the amino acid sequences of SEQ ID NOs: 86, 77, and 87, respectively. In certain embodiments, the first antigen-binding site that binds NKG2D comprises:

(i) a VH comprising CDR1, CDR2, and CDR3 comprising the amino acid sequences of SEQ ID NOs: 81, 82, and 97, respectively; and a VL comprising CDR1, CDR2, and CDR3 comprising the amino acid sequences of SEQ ID NOs: 86, 77, and 87, respectively; or

(ii) a VH comprising CDR1, CDR2, and CDR3 comprising the amino acid sequences of SEQ ID NOs: 81, 82, and 84, respectively; and a VL comprising CDR1, CDR2, and CDR3 comprising the amino acid sequences of SEQ ID NOs: 86, 77, and 87, respectively.

[0041] In some embodiments of a protein disclosed herein, the VH of the first antigen-binding site comprises an amino acid sequence at least 90% identical to SEQ ID NO:95, and the VL of the first antigen-binding site comprises an amino acid sequence at least 90% identical to SEQ ID NO:85. In certain embodiments, the VH of the first antigen-binding site comprises the amino acid sequence of SEQ ID NO:95, and the VL of the first antigen-binding site comprises the amino acid sequence of SEQ ID NO:85.

[0042] In some embodiments of a protein disclosed herein, the antibody Fc domain is a human IgG1 antibody Fc domain. In some embodiments, the antibody Fc domain or the portion thereof comprises an amino acid sequence at least 90% identical to SEQ ID NO:118. In certain embodiments, at least one polypeptide chain of the antibody Fc domain comprises one or more mutations, relative to SEQ ID NO:118, at one or more positions selected from Q347, Y349, L351, S354, E356, E357, K360, Q362, S364, T366, L368, K370, N390, K392, T394, D399, S400, D401, F405, Y407, K409, T411, and K439, numbered according to the EU numbering system. In certain embodiments, at least one polypeptide chain of the antibody Fc domain comprises one or more mutations, relative to SEQ ID NO:118, selected from Q347E, Q347R, Y349S, Y349K, Y349T, Y349D, Y349E, Y349C, L351K, L351D, L351Y, S354C, E356K, E357Q, E357L, E357W, K360E, K360W, Q362E, S364K, S364E, S364H, S364D, T366V, T366I, T366L, T366M, T366K, T366W, T366S, L368E, L368A, L368D, K370S, N390D,

N390E, K392L, K392M, K392V, K392F, K392D, K392E, T394F, D399R, D399K, D399V, S400K, S400R, D401K, F405A, F405T, Y407A, Y407I, Y407V, K409F, K409W, K409D, T411D, T411E, K439D, and K439E, numbered according to the EU numbering system. In certain embodiments, one polypeptide chain of the antibody heavy chain constant region comprises one or more mutations, relative to SEQ ID NO:118, at one or more positions selected from Q347, Y349, L351, S354, E356, E357, K360, Q362, S364, T366, L368, K370, K392, T394, D399, S400, D401, F405, Y407, K409, T411 and K439; and the other polypeptide chain of the antibody heavy chain constant region comprises one or more mutations, relative to SEQ ID NO:136, at one or more positions selected from Q347, Y349, L351, S354, E356, E357, S364, T366, L368, K370, N390, K392, T394, D399, D401, F405, Y407, K409, T411, and K439, numbered according to the EU numbering system. In certain embodiments, one polypeptide chain of the antibody heavy chain constant region comprises K360E and K409W substitutions relative to SEQ ID NO:118; and the other polypeptide chain of the antibody heavy chain constant region comprises Q347R, D399V and F405T substitutions relative to SEQ ID NO:136, numbered according to the EU numbering system. In certain embodiments, one polypeptide chain of the antibody heavy chain constant region comprises a Y349C substitution relative to SEQ ID NO:118; and the other polypeptide chain of the antibody heavy chain constant region comprises an S354C substitution relative to SEQ ID NO:136, numbered according to the EU numbering system.

[0043] In another aspect, the present application provides a protein comprising:

(a) a first polypeptide comprising the amino acid sequence of SEQ ID NO:259;

(b) a second polypeptide comprising the amino acid sequence of SEQ ID NO:260; and

(c) a third polypeptide comprising the amino acid sequence of SEQ ID NO:261.

[0044] In another aspect, the present application provides a protein comprising:

(a) a first polypeptide comprising the amino acid sequence of SEQ ID NO:276;

(b) a second polypeptide comprising the amino acid sequence of SEQ ID NO:260; and

(c) a third polypeptide comprising the amino acid sequence of SEQ ID NO:261.

[0045] In another aspect, the present application provides a pharmaceutical composition comprising a protein disclosed herein and a pharmaceutically acceptable carrier.

[0046] In another aspect, the present application provides a pharmaceutical formulation comprising a protein disclosed herein and a buffer at pH 7.0 or higher. In some embodiments, the pH of the formulation is between 7.0 and 8.0. In some embodiments, the buffer comprises citrate. In certain embodiments, the concentration of citrate is 10 to 20 mM. In some embodiments, the buffer further comprises phosphate. In some embodiments, the buffer further comprises a sugar or sugar alcohol. In certain embodiments, the sugar or sugar alcohol is a disaccharide. In certain embodiments, the disaccharide is sucrose. In some embodiments, the concentration of the sugar or sugar alcohol in the pharmaceutical formulation is 200 to 300 mM. In certain embodiments, the concentration of the sugar or sugar alcohol in the pharmaceutical formulation is about 250 mM. In some embodiments, the buffer further comprises a nonionic surfactant. In certain embodiments, the nonionic surfactant comprises a polysorbate. In certain embodiments, the polysorbate is polysorbate 80. In some embodiments, the concentration of polysorbate 80 in the pharmaceutical formulation is 0.005% to 0.05%. In certain embodiments, the concentration of polysorbate 80 in the pharmaceutical formulation is about 0.01%. In some embodiments, the concentration of NaCl, if any, is about 1 mM or lower in the pharmaceutical formulation. In some embodiments, the concentration of the protein is 10 to 200 mg/mL. In certain embodiments, the concentration of the protein is about 20 mg/mL.

[0047] In some embodiments, the pharmaceutical formulation comprises about 20 mM citrate, about 250 mM sucrose, and about 0.01% polysorbate 80, at pH 7.0. In certain embodiments, the pharmaceutical formulation comprises about 20 mg/mL of the protein, about 20 mM potassium phosphate, about 10 mM sodium citrate, and about 125 mM sodium chloride, at pH 7.8.

[0048] In another aspect, the present application provides a cell comprising one or more nucleic acids encoding a protein disclosed herein.

[0049] In another aspect, the present application provides a method of enhancing tumor cell death, the method comprising exposing the tumor cell and a natural killer cell to an effective amount of a protein, a pharmaceutical composition, or a pharmaceutical formulation disclosed herein.

[0050] In another aspect, the present application provides a method of treating cancer, the method comprising administering to a subject in need thereof an effective amount of a protein, a pharmaceutical composition, or a pharmaceutical formulation disclosed herein. In some

embodiments, the cancer is a hematologic malignancy. In certain embodiments, the hematologic malignancy is selected from the group consisting of acute myeloid leukemia (AML), myelodysplastic syndrome (MDS), acute lymphoblastic leukemia (ALL), myeloproliferative neoplasms (MPNs), lymphoma, non-Hodgkin lymphomas, and classical Hodgkin lymphoma.

[0051] In some embodiments, the AML is selected from undifferentiated acute myeloblastic leukemia, acute myeloblastic leukemia with minimal maturation, acute myeloblastic leukemia with maturation, acute promyelocytic leukemia (APL), acute myelomonocytic leukemia, acute myelomonocytic leukemia with eosinophilia, acute monocytic leukemia, acute erythroid leukemia, acute megakaryoblastic leukemia (AMKL), acute basophilic leukemia, acute panmyelosis with fibrosis, and blastic plasmacytoid dendritic cell neoplasm (BPDCN). In certain embodiments, the AML is characterized by expression of CLL-1 on the AML leukemia stem cells (LSCs). In certain embodiments, the LSCs further express a membrane marker selected from CD34, CD38, CD123, TIM3, CD25, CD32, and CD96.

[0052] In some embodiments, the AML is a minimal residual disease (MRD). In certain embodiments, the MRD is characterized by the presence or absence of a mutation selected from *FLT3-ITD* ((Fms-like tyrosine kinase 3)-internal tandem duplications (ITD)), *NPM1* (Nucleophosmin 1), *DNMT3A* (DNA methyltransferase gene *DNMT3A)*, and *IDH* (Isocitrate dehydrogenase 1 and 2 (IDH1 and IDH2)).

[0053] In certain embodiments, the MDS is selected from MDS with multilineage dysplasia (MDS-MLD), MDS with single lineage dysplasia (MDS-SLD), MDS with ring sideroblasts (MDS-RS), MDS with excess blasts (MDS-EB), MDS with isolated del(5q), and MDS, unclassified (MDS-U). In certain embodiments, the MDS is a primary MDS or a secondary MDS.

[0054] In some embodiments, the ALL is selected from B-cell acute lymphoblastic leukemia (B-ALL) and T-cell acute lymphoblastic leukemia (T-ALL). In some embodiments, the MPN is selected from polycythaemia vera, essential thrombocythemia (ET), and myelofibrosis. In some embodiments, the non-Hodgkin lymphoma is selected from B-cell lymphoma and T-cell lymphoma. In some embodiments, the lymphoma is selected from chronic lymphocytic leukemia (CLL), lymphoblastic lymphoma (LPL), diffuse large B-cell lymphoma (DLBCL), Burkitt lymphoma (BL), primary mediastinal large B-cell lymphoma (PMBL), follicular lymphoma, mantle cell lymphoma, hairy cell leukemia, plasma cell myeloma (PCM) or multiple myeloma

(MM), mature T/NK neoplasms, and histiocytic neoplasms. In certain embodiments, the cancer expresses CLEC12A.

BRIEF DESCRIPTION OF THE DRAWINGS

[0055] **FIG. 1** is a representation of a heterodimeric, multispecific antibody, *e.g.,* a trispecific binding protein (TriNKET). Each arm can represent either the NKG2D-binding domain, or the binding domain corresponding to a tumor-associated antigen. In some embodiments, the NKG2D binding domain and the tumor-associated antigen binding domains can share a common light chain.

[0056] **FIGs. 2A-2E** illustrate five exemplary formats of a multispecific binding protein, *e.g.,* a trispecific binding protein (TriNKET). As shown in **FIG. 2A**, either the NKG2D-binding domain or the tumor-associated antigen binding domain can take the scFv format (left arm). An antibody that contains a NKG2D-targeting scFv, a tumor-associated antigen targeting Fab fragment, and a heterodimerized antibody constant region is referred herein as the F3-TriNKET. An antibody that contains a tumor-associated antigen targeting scFv, a NKG2D-targeting Fab fragment, and a heterodimerized antibody constant region/domain that binds CD16 is referred herein as the F3'-TriNKET (**FIG. 2E**). As shown in **FIG. 2B**, both the NKG2D-binding domain and tumor-associated antigen binding domain can take the scFv format. **FIGs. 2C to 2D** are illustrations of an antibody with three antigen-binding sites, including two antigen-binding sites that bind the tumor-associated antigen, and the NKG2D-binding site fused to the heterodimerized antibody constant region. These antibody formats are referred herein as F4-TriNKET. **FIG. 2C** illustrates that the two tumor-associated antigen binding sites are in the Fab fragment format, and the NKG2D binding site in the scFv format. **FIG. 2D** illustrates that the tumor-associated antigen binding sites are in the scFv format, and the NKG2D binding site is in the scFv format. **FIG. 2E** represents a trispecific antibody (TriNKET) that contains a tumor-targeting scFv, a NKG2D-targeting Fab fragment, and a heterodimerized antibody constant region/domain ("CD domain") that binds CD16. The antibody format is referred herein as F3'-TriNKET. In certain exemplary multispecific binding proteins, heterodimerization mutations on the antibody constant region include K360E and K409W on one constant domain; and Q347R, D399V and F405T on the opposite constant domain (shown as a triangular lock-and-key shape in

the CD domains). The bold bar between the heavy and the light chain variable domains of the Fab fragments represents a disulfide bond.

[0057] **FIG. 3** is a representation of a TriNKET in the Triomab form, which is a trifunctional, bispecific antibody that maintains an IgG-like shape. This chimera consists of two half antibodies, each with one light and one heavy chain, that originate from two parental antibodies. Triomab form may be a heterodimeric construct containing 1/2 of rat antibody and 1/2 of mouse antibody.

[0058] **FIG. 4** is a representation of a TriNKET in the KiH Common Light Chain form, which involves the knobs-into-holes (KIHs) technology. KiH is a heterodimer containing 2 Fab fragments binding to target 1 and 2, and an Fc stabilized by heterodimerization mutations. TriNKET in the KiH format may be a heterodimeric construct with 2 Fab fragments binding to target 1 and target 2, containing two different heavy chains and a common light chain that pairs with both heavy chains.

[0059] **FIG. 5** is a representation of a TriNKET in the dual-variable domain immunoglobulin (DVD-Ig™) form, which combines the target-binding domains of two monoclonal antibodies via flexible naturally occurring linkers, and yields a tetravalent IgG-like molecule. DVD-Ig™ is a homodimeric construct where variable domain targeting antigen 2 is fused to the N-terminus of a variable domain of Fab fragment targeting antigen 1. DVD-Ig™ form contains normal Fc.

[0060] **FIG. 6** is a representation of a TriNKET in the Orthogonal Fab fragment interface (Ortho-Fab) form, which is a heterodimeric construct that contains 2 Fab fragments binding to target 1 and target 2 fused to Fc. Light chain (LC)-heavy chain (HC) pairing is ensured by orthogonal interface. Heterodimerization is ensured by mutations in the Fc.

[0061] **FIG. 7** is a representation of a TriNKET in the 2-in-1 Ig format.

[0062] **FIG. 8** is a representation of a TriNKET in the ES form, which is a heterodimeric construct containing two different Fab fragments binding to target 1 and target 2 fused to the Fc. Heterodimerization is ensured by electrostatic steering mutations in the Fc.

[0063] **FIG. 9** is a representation of a TriNKET in the Fab Arm Exchange form: antibodies that exchange Fab fragment arms by swapping a heavy chain and attached light chain (half-molecule) with a heavy-light chain pair from another molecule, resulting in bispecific antibodies. Fab Arm Exchange form (cFae) is a heterodimer containing 2 Fab fragments binding to target 1 and 2, and an Fc stabilized by heterodimerization mutations.

[0064] **FIG. 10** is a representation of a TriNKET in the SEED Body form, which is a heterodimer containing 2 Fab fragments binding to target 1 and 2, and an Fc stabilized by heterodimerization mutations.

[0065] **FIG. 11** is a representation of a TriNKET in the LuZ-Y form, in which a leucine zipper is used to induce heterodimerization of two different HCs. The LuZ-Y form is a heterodimer containing two different scFabs binding to target 1 and 2, fused to Fc. Heterodimerization is ensured through leucine zipper motifs fused to C-terminus of Fc.

[0066] **FIG. 12** is a representation of a TriNKET in the Cov-X-Body form.

[0067] **FIGs. 13A-13B** are representations of TriNKETs in the κλ-Body forms, which are heterodimeric constructs with two different Fab fragments fused to Fc stabilized by heterodimerization mutations: one Fab fragment targeting antigen 1 contains kappa LC, and the second Fab fragment targeting antigen 2 contains lambda LC. **FIG. 13A** is an exemplary representation of one form of a κλ-Body; **FIG. 13B** is an exemplary representation of another κλ-Body.

[0068] **FIG. 14** is an Oasc-Fab heterodimeric construct that includes Fab fragment binding to target 1 and scFab binding to target 2, both of which are fused to the Fc domain. Heterodimerization is ensured by mutations in the Fc domain.

[0069] **FIG. 15** is a DuetMab, which is a heterodimeric construct containing two different Fab fragments binding to antigens 1 and 2, and an Fc that is stabilized by heterodimerization mutations. Fab fragments 1 and 2 contain differential S-S bridges that ensure correct light chain and heavy chain pairing.

[0070] **FIG. 16** is a CrossmAb, which is a heterodimeric construct with two different Fab fragments binding to targets 1 and 2, and an Fc stabilized by heterodimerization mutations. CL and CH1 domains, and VH and VL domains are switched, *e.g.*, CH1 is fused in-line with VL, and CL is fused in-line with VH.

[0071] **FIG. 17** is a Fit-Ig, which is a homodimeric construct where Fab fragment binding to antigen 2 is fused to the N-terminus of HC of Fab fragment that binds to antigen 1. The construct contains wild-type Fc.

[0072] **FIG. 18** is a set of traces showing Bio-Layer Interferometry (BLI) profiles of antibodies collected from the murine hybridomas supernatants binding to hCLEC12A.

[0073] **FIG. 19** is a set of sensorgrams showing SPR profiles of antibodies collected from the murine mAb subclones binding to hCLEC12A (**FIG. 19A**) and cCLEC12A (**FIG. 19B**).

[0074] **FIG. 20** is a line graph showing binding of purified CLEC12A subclones to PL21 AML cell line.

[0075] **FIG. 21** is a set of sensorgrams showing SPR profiles of antibodies 16B8.C8 and 9F11.B7 binding to glycosylated, de-glycosylated, and de-sialylated hCLEC12A.

[0076] **FIG. 22** is a set of sensorgrams showing SPR profiles of TriNKETs derived from antibody 16B8.C8.

[0077] **FIG. 23** are line graphs showing binding of hCLEC12A -targeting TriNKETs F3'-1304, F3'-1295 and a control CLEC12A-TriNKET to hCLEC12A-expressing cell line RMA-hCLEC12A.

[0078] **FIG. 24** are line graphs showing NK cell-mediated lysis of CLEC12A-expressing cancer cell line HL60 in the presence of F3'-1295 and a control CLEC12A-TriNKET.

[0079] **FIG. 25** are line graphs showing differential scanning colorimetry (DSC) analysis of TriNKETs F3'-1295 and F3'-1602.

[0080] **FIG. 26** is a set of sensorgrams showing SPR profiles of TriNKETs F3'-1295 and F3'-1602.

[0081] **FIG. 27** are line graphs showing binding of hCLEC12A -targeting TriNKETs F3'-1295, F3'-1602, and a control CLEC12A-TriNKET to hCLEC12A-expressing cell line Ba/F3 (**FIG. 27A**), wild-type Ba/F3 (**FIG. 27B**), cancer line HL60 (**FIG. 27C**), and cancer line PL21 (**FIG. 27D**).

[0082] **FIG. 28** are line graphs showing NK cell-mediated lysis of CLEC12A-expressing cancer cell lines PL21 (**FIG. 28A**) and HL60 (**FIG. 28B**) in the presence of F3'-1295, F3'-1602, and a control CLEC12A-TriNKET.

[0083] **FIG. 29** are line graphs showing isoelectric point (pI) determined by capillary isoelectric focusing (cIEF) of F3'-1295 (**FIG. 29A**) and F3'-1602 (**FIG. 29B**).

[0084] **FIG. 30** shows flow cytometry based polyspecificity reagent (PSR) analysis of F3'-1602 TriNKET and F3'-1295 TriNKET.

[0085] **FIG. 31** is a set of sensorgrams showing SPR profiles of hF3'-1602 TriNKET and F3-TriNKET AB0010.

[0086] **FIG. 32** are line graphs showing binding of hF3'-1602 TriNKET and F3-TriNKET AB0010 to Ba/F3 expressing hCLEC12A (**FIG. 32A**), cancer line HL60 (**FIG. 32B**),and wild-type Ba/F3 (**FIG. 32C**).

[0087] **FIG. 33** are line graphs showing NK cell-mediated lysis of CLEC12A-expressing cancer cell line PL21 using KHYG-CD16V cells (**FIG. 33A**) and primary NK cells (**FIG. 33B**) in the presence of hF3'-1602 TriNKET and F3-TriNKET AB0010.

[0088] **FIG. 34** are line graphs showing binding of TriNKETs derived from 9F11.B7 and hF3'-1602 TriNKET and F3-TriNKET AB0010 to Ba/F3 expressing hCLEC12A (**FIG. 34A**) and cancer line HL60 (**FIG. 34B**).

[0089] **FIG. 35** are line graphs showing NK cell-mediated lysis of CLEC12A-expressing cancer cell line HL60 in the presence of TriNKETs derived from 9F11.B7.

[0090] **FIG. 36** are line graphs showing NK cell-mediated lysis of CLEC12A-expressing cancer cell line HL60 using KHYG-CD16V cells (**FIG. 36A**) and primary NK cells (**FIG. 36B**) in the presence of hF3'-1602 TriNKET and AB0192.

[0091] **FIG. 37** are line graphs showing NK cell-mediated lysis of CLEC12A-expressing cancer cell line PL21 (**FIG. 37A**) and THP-1 (**FIG. 37B**) in the presence of hF3'-1602 TriNKET and parental mAb.

[0092] **FIG. 38** are line graphs showing binding of hF3'-1602 TriNKET to cancer cell line HL60 (**FIG. 38A**) and PL21 (**FIG. 38B**).

[0093] **FIG. 39** are line graphs showing binding of CLEC12A-targeting TriNKETs, parental mAbs, and AB0237 NKG2D dead arm variant TriNKET to Ba/F3 expressing hCLEC12A (**FIG. 39A**), and cancer cell lines HL60 (**FIG. 39B**) and PL21 (**FIG. 39C**).

[0094] **FIG. 40** are bar graphs showing surface retention of CLEC12A-targeting TriNKETs and parental mAbs to cell lines PL21 (**FIG. 40A**) and HL60 (**FIG. 40B**).

[0095] **FIG. 41** are line graphs showing NK cell-mediated lysis of CLEC12A-expressing cancer cell line PL21 (**FIG. 41A**) and HL60 (**FIG. 41B**) in the presence of hF3'-1602 TriNKET, AB0192, and parental mAbs.

[0096] **FIG. 42** are line graphs showing NK cell-mediated lysis of CLEC12A-expressing cancer cell line PL21 (**FIG. 42A**) and HL60 (**FIG. 42B**) in the presence of hF3'-1602 TriNKET.

[0097] **FIG. 43** are line graphs showing CD8-T cell-mediated lysis of CLEC12A-expressing cancer cell line PL21 in the presence of hF3'-1602 TriNKET, parental mAb, or an NKG2D-dead variant thereof.

[0098] **FIG. 44** is a set of histograms showing binding of hF3'-1602 TriNKET (grey), parental mAb (white), and control IgG (black) to blood cells.

[0099] **FIG. 45** is a set of sensorgrams showing SPR profiles of hF3'-1602 TriNKET and trastuzumab control binding to recombinant human CD64.

[0100] **FIG. 46** is a set of sensorgrams showing SPR profiles of hF3'-1602 TriNKET and trastuzumab control binding to CD32a H131.

[0101] **FIG. 47** is a set of sensorgrams showing SPR profiles of hF3'-1602 TriNKET and trastuzumab control binding to human CD32a R131 allele (FcγRIIa R131).

[0102] **FIG. 48** is a set of sensorgrams showing SPR profiles of hF3'-1602 TriNKET and trastuzumab control binding to human CD16a high affinity allele V158 (FcγRIIIa V158).

[0103] **FIG. 49** is a set of sensorgrams showing SPR profiles of hF3'-1602 TriNKET and trastuzumab control binding to human CD16a low affinity allele F158 (FcγRIIIa F158).

[0104] **FIG. 50** is a set of sensorgrams showing SPR profiles of hF3'-1602 TriNKET and trastuzumab control binding to human CD32b (FcγRIIb).

[0105] **FIG. 51** is a set of sensorgrams showing SPR profiles of hF3'-1602 TriNKET and trastuzumab control binding to human CD16b (FcγRIIIb).

[0106] **FIG. 52** is a set of sensorgrams showing SPR profiles of hF3'-1602 TriNKET and trastuzumab control binding to cynomolgus (cyno) CD16.

[0107] **FIG. 53** is a set of sensorgrams showing SPR profiles of hF3'-1602 TriNKET and trastuzumab control binding to human FcRn as measured at pH 6.0.

[0108] **FIG. 54** is a set of sensorgrams showing SPR profiles of hF3'-1602 TriNKET and trastuzumab control binding to cyno FcRn as measured at pH 6.0.

[0109] **FIG. 55** is a set of sensorgrams showing SPR profiles of hF3'-1602 TriNKET binding to human CLEC12A.

[0110] **FIG. 56** is a set of sensorgrams showing SPR profiles of hF3'-1602 TriNKET binding to human NKG2D.

[0111] **FIG. 57** is a set of sensorgrams showing SPR profiles of hF3'-1602 TriNKET binding to recombinant cyno NKG2D (cNKG2D) extracellular domain (ECD).

[0112] **FIG. 58** are line graphs showing target binding as determined by SPR for occupancy of one TriNKET arm on binding of the other TriNKET arm.

[0113] **FIG. 59** are line graphs showing target binding as determined by SPR for synergy of NKG2D TriNKET arm and CD16a.

[0114] **FIG. 60** are line graphs showing binding of hCLEC12A -TriNKETs F3'-1295, F3'-1602, and a control CLEC12A-TriNKET to hCLEC12A-expressing cell line Ba/F3 (**FIG. 60A**), wild-type Ba/F3 (**FIG. 60B**), cancer line HL60 (**FIG. 60C**), and cancer line PL21 (**FIG. 60D**).

[0115] **FIG. 61** shows flow cytometry based polyspecificity reagent (PSR) analysis of F3'-1602 TriNKET.

[0116] **FIG. 62** are bar graphs showing relative binding (Z score) of F3'-1602 TriNKET at 1 to human CLEC12A in comparison to the entire human proteome microarray

[0117] **FIG. 63** shows models of hydrophobicity patches in hF3'-1602 TriNKET CLEC12A-binding arm.

[0118] **FIG. 64** are bar graphs based on models of CDR-length, surface hydrophobicity, and surface charge in hF3'-1602 TriNKET CLEC12A-binding arm.

[0119] **FIG. 65** shows models of hydrophobicity patches in hF3'-1602 TriNKET NKG2D-binding arm.

[0120] **FIG. 66** are bar graphs based on models of CDR-length, surface hydrophobicity, and surface charge in hF3'-1602 TriNKET NKG2D-binding arm.

[0121] **FIG. 67** is a line graph showing Hydrophobic Interactions Chromatography (HIC) analysis of hF3'-1602 TriNKET.

[0122] **FIG. 68** is a line graph showing pI as determined by cIEF for hF3'-1602 TriNKET.

[0123] **FIG. 69** is a set of flow cytometry plots demonstrating sequence liability-remediated variants of hF3'-1602 binding to hCLEC12A.

[0124] **FIG. 70** are line graphs showing NK cell-mediated lysis of CLEC12A-expressing cancer cell line PL21 in the presence of hF3'-1602 TriNKET and liability-remediated variants.

[0125] **FIG. 71** is a set of colored sensorgrams showing the binding of hCLEC12A at three-fold serial dilution (300 nM to 0.41 nM) to F3'-1602 in the HST formulation. The black overlays represent the 1:1 kinetic fit of the raw data.

[0126] **FIG. 72** is a set of graphs showing the binding of F3'-1602 in the HST formulation to hNKG2D. The top panels are colored sensorgrams representing the raw data of F3'-1602

injected over captured mFc-hNKG2D (9.77 nM to 5 μM). The black overlays represent the 1:1 kinetic fit of the raw data. The bottom panels represent steady state response measurements plotted against the corresponding analyte concentrations. The blue lines represent the steady state K_D value.

[0127] **FIG. 73** is a set of colored sensorgrams showing the binding of F3'-1602 in the HST formulation to hCD16a V158.

[0128] **FIG. 74** is a graph showing the percentage lysis of PL21 cells by NKG2D- and CD16a-expressing KHYG-1-CD16a cells in the presence of stressed and control samples of F3'-1602 in the HST formulation.

[0129] **FIG. 75** is a set of extracted ion chromatograms of CDRH3 peptide in control and stressed F3'-1602.

[0130] **FIG. 76** is a set of colored sensorgrams showing the binding of hCLEC12A to F3'-1602 in the phosphate/citrate/NaCl formulation. The black overlays represent the 1:1 kinetic fit of the raw data.

[0131] **FIG. 77** is a set of graphs showing the binding of F3'-1602 in the phosphate/citrate/NaCl formulation to hNKG2D. The top panels are colored sensorgrams representing the raw data of F3'-1602 injected over captured mFc-hNKG2D (9.77 nM to 5 μM). The black overlays represent the 1:1 kinetic fit of the raw data. The bottom panels represent steady state response measurements plotted against the corresponding analyte concentrations. The blue lines represent the steady state K_D value.

[0132] **FIG. 78** is a set of colored sensorgrams showing the binding of F3'-1602 in the phosphate/citrate/NaCl formulation to hCD16a V158.

[0133] **FIG. 79** is a graph showing the percentage lysis of PL21 cells by NKG2D- and CD16a-expressing KHYG-1-CD16a cells in the presence of stressed and control samples of F3'-1602 in the phosphate/citrate/NaCl formulation.

[0134] **FIG. 80** is a set of colored sensorgrams showing the binding of hCLEC12A at three-fold serial dilution (300 nM to 0.41 nM) to F3'-1602 after incubation in the CST formulation at 40 °C for four weeks. The black overlays represent the 1:1 kinetic fit of the raw data.

[0135] **FIG. 81** is a set of colored sensorgrams showing the binding of hCLEC12A at three-fold serial dilution (300 nM to 0.41 nM) to F3'-1602 after incubation in the CST formulation at

2-8 °C and at 25 °C for four weeks. The black overlays represent the 1:1 kinetic fit of the raw data.

[0136] **FIG. 82** is a set of graphs showing the binding of F3'-1602 in the CST formulation to hNKG2D. The top panels are colored sensorgrams representing the raw data of F3'-1602 injected over captured mFc-hNKG2D (9.77 nM to 5 μM). The black overlays represent the 1:1 kinetic fit of the raw data. The bottom panels represent steady state response measurements plotted against the corresponding analyte concentrations. The blue lines represent the steady state K_D value.

[0137] **FIG. 83** is a set of colored sensorgrams showing the binding of F3'-1602 in the CST formulation to hCD16a V158.

[0138] **FIG. 84** is a graph showing the percentage lysis of PL21 cells by NKG2D- and CD16a-expressing KHYG-1-CD16a cells in the presence of stressed and control samples of F3'-1602 in the CST formulation.

[0139] **FIG. 85** is a cIEF profile of F3'-1602 after incubation under pH 5.0 stress.

[0140] **FIG. 86** is a cIEF profile of F3'-1602 after incubation under pH 8.0 stress.

[0141] **FIG. 87** is a set of colored sensorgrams showing the binding of hCLEC12A at three-fold serial dilution (300 nM to 0.41 nM) to F3'-1602 after pH 5 stress. The black overlays represent the 1:1 kinetic fit of the raw data.

[0142] **FIG. 88** is a set of colored sensorgrams showing the binding of hCLEC12A at three-fold serial dilution (300 nM to 0.41 nM) to F3'-1602 after pH 8 stress. The black overlays represent the 1:1 kinetic fit of the raw data.

[0143] **FIG. 89** is a set of graphs showing the binding of F3'-1602 to hNKG2D after pH 5 stress. The top panels are colored sensorgrams representing the raw data of F3'-1602 injected over captured mFc-hNKG2D (9.77 nM to 5 μM). The black overlays represent the 1:1 kinetic fit of the raw data. The bottom panels represent steady state response measurements plotted against the corresponding analyte concentrations. The blue lines represent the steady state K_D value.

[0144] **FIG. 90** is a set of graphs showing the binding of F3'-1602 to hNKG2D after pH 8 stress. The top panels are colored sensorgrams representing the raw data of F3'-1602 injected over captured mFc-hNKG2D (9.77 nM to 5 μM). The black overlays represent the 1:1 kinetic fit of the raw data. The bottom panels represent steady state response measurements plotted against the corresponding analyte concentrations. The blue lines represent the steady state K_D value.

[0145] **FIG. 91** is a graph showing the percentage lysis of PL21 cells by NKG2D- and CD16a-expressing KHYG-1-CD16a cells in the presence of F3'-1602 after pH 5 stress.

[0146] **FIG. 92** is a graph showing the percentage lysis of PL21 cells by NKG2D- and CD16a-expressing KHYG-1-CD16a cells in the presence of F3'-1602 after pH 8 stress.

[0147] **FIG. 93** is a set of colored sensorgrams showing the binding of hCLEC12A to F3'-1602 after forced oxidation stress. The black overlays represent the 1:1 kinetic fit of the raw data.

[0148] **FIG. 94** is a set of graphs showing the binding of F3'-1602 to hNKG2D after forced oxidation stress. The top panels are colored sensorgrams representing the raw data of F3'-1602 injected over captured mFc-hNKG2D (9.77 nM to 5 μM). The black overlays represent the 1:1 kinetic fit of the raw data. The bottom panels represent steady state response measurements plotted against the corresponding analyte concentrations. The blue lines represent the steady state K_D value.

[0149] **FIG. 95** is a graph showing the percentage lysis of PL21 cells by NKG2D- and CD16a-expressing KHYG-1-CD16a cells in the presence of F3'-1602 after forced oxidation stress.

[0150] **FIG. 96** is a set of colored sensorgrams showing the binding of hCLEC12A to F3'-1602 after low pH hold. The black overlays represent the 1:1 kinetic fit of the raw data.

[0151] **FIG. 97** is a set of graphs showing the binding of F3'-1602 to hNKG2D after low pH hold. The top panels are colored sensorgrams representing the raw data of F3'-1602 injected over captured mFc-hNKG2D (9.77 nM to 5 μM). The black overlays represent the 1:1 kinetic fit of the raw data. The bottom panels represent steady state response measurements plotted against the corresponding analyte concentrations. The blue lines represent the steady state K_D value.

[0152] **FIG. 98** is a set of colored sensorgrams showing the binding of F3'-1602 to hCD16a V158 after low pH hold.

[0153] **FIG. 99** is a graph showing the percentage lysis of PL21 cells by NKG2D- and CD16a-expressing KHYG-1-CD16a cells in the presence of F3'-1602 after low pH hold.

[0154] **FIG. 100** is a graph showing the solubility of F3'-1602 in 10 mM sodium acetate buffer pH 5.0 in PEG-6000.

[0155] **FIG. 101** is a graph showing the percentage of F3'-1602 monomer content as a function of concentration.

[0156] **FIG. 102** are graphs showing the percentage lysis of PL-21 cells by NKG2D- and CD16a-expressing KHYG-1-CD16a cells in the presence of F3'-format TriNKET F3'-1602 (**FIG. 102A**) and F3-format TriNKET AB0010 (**FIG. 102B**) after thermal stress conditions.

[0157] **FIG. 103** is an illustration of a yeast display affinity maturation library construction. **FIG. 103A**: Substitution of pET1596 scFv CDRH3 with BamHI restriction enzyme site. **FIG. 103B**: Insertion of CDRH3 mutated library oligos at the previously introduced BamHI restriction site. **FIG. 103C**: Electroporation of BamHI linearized plasmid and library oligos into yeast followed by homologous recombination in yeast.

[0158] **FIG. 104** shows the discovery process from mouse immunization to AB0089. Upper panel represents results of CLEC12A binding by surface plasmon resonance (SPR). Lower panel shows binding to CLEC12A+ PL-21 AML cancer cells. Binding affinities and EC50 for each variant are indicated. BM, backmutation.

[0159] **FIG. 105** shows FACS analysis of CDRH3 yeast library 17. First round of selection of affinity maturating yeast display library sorted at 1 nM CLEC12A-His (**FIG. 105A**). Second round of selection sorted at 1 nM CLEC12A-His (**FIG. 105B**). Third round of selection sorted at 0.1 nM CLEC12A-His (**FIG. 105C**). Binding of library 17-R3 displayed on yeast cells to 1 nM CLEC12A (**FIG. 105D**). Binding of original clone pET1596 displayed on yeast cells at 10 nM CLEC12A (**FIG. 105E**).

[0160] **FIG. 106** shows FACS analysis of CDRH2 yeast library 30. Starting yeast display library which was generated by randomizing CDRH2 built on the background of the best clone identified from library 17 (GDYGDSLDY (SEQ ID NO:322) CDRH3) (**FIG. 106A**). Sorting was performed at 1 nM CLEC12A-His for both rounds. Flow cytometry analysis after round 1 (**FIG. 106B**). and round 2 (**FIG. 106C**) selection with CLEC12A-His, respectively. Binding of pET1596 displayed on yeast cells at 10 nM CLEC12A-His (**FIG. 106D**).

[0161] **FIG. 107** is a comparison of the improved affinity clone (**FIG. 107A**) identified from Library 30 to pET1596 (**FIG. 107B**) and AB0237 (**FIG. 107C**).

[0162] **FIG. 108** is a schematic representation of AB0089. Heterodimerization mutations and an engineered interchain disulfide bridge ensure efficient chain pairing of the IgG1 Fc. The scFv is derived from the humanized and sequence liability corrected CLEC12A mAb 16B8.C8. The scFv is stabilized by an engineered disulfide bridge between VH and VL.

[0163] **FIG. 109** is an X-ray crystal structure of EW-RVT Fc heterodimer. Superposition of the overall structure of the EW-RVT Fc heterodimer with the human wild-type (WT) IgG1 Fc homodimer (PDB ID: 3AVE) (**FIG. 109A**). Close-up view of W-VT interaction pair regions (**FIG. 109B**). Close-up view of the E-R interaction pair regions (**FIG. 109C**).

[0164] **FIG. 110** shows the crystal structure of EW-RVTS–S heterodimeric Fc with a close-up view of the asymmetric disulfide bond formed between 349C(CH3A) and 354C(CH3B) residues.

[0165] **FIG. 111** shows a ribbon diagram model of the CLEC12A binding scFv in three different orientations (upper panel) and their corresponding surface charge distribution of the same orientation (lower panel). Three orientations are shown: both façades (left panel: front view; center panel: back view) and the antigen-engaging surface (right panel: top view).

[0166] **FIG. 112** shows the analyses of CDR length and surface hydrophobicity patches of the CLEC12A-targeting arm of AB0089. The arrow points to the line where CLEC12A targeting scFv of AB0089 stands in reference to advanced clinical stage mAbs. The two inner dotted lines indicate 2 SD (>95% of reference molecules within this region). The two outer most dotted lines indicate 3 SD (>99.7% of reference molecules within this region).

[0167] **FIG. 113** shows the analyses of patches containing positive (left) and negative charges (middle), as well as the symmetry (right) of these charges around the CDR regions. Surface charge and charge symmetry analysis of CLEC12A targeting arm of AB0089. The arrow points to the line where CLEC12A targeting scFv of AB0089 stands in reference to advanced clinical stage mAbs. In each plot, there are two dashed lines—one closer and the other further to the solid line. The dashed line closer to the solid line indicates 2 SD (>95% of reference molecules within this region), whereas the dashed line further to the solid line indicates 3 SD (>99.7% of reference molecules within this region).

[0168] **FIG. 114** shows NKG2D-binding Fab with ribbon diagrams of three different orientations: both façades (left panel: front view; center panel: back view) and the antigen-engaging surface (right panel: top view).

[0169] **FIG. 115** shows the CDR length and patches of surface hydrophobicity analyses of the NKG2D-targeting arm of AB0089. The arrow points to the line where NKG2D targeting arm of AB0089 stands in reference to advanced clinical stage mAbs. The two inner dotted lines

indicate 2 SD (>95% of reference molecules within this region). The two outer most dotted lines indicate 3 SD (>99.7% of reference molecules within this region).

[0170] **FIG. 116** shows the analyses of surface charge and hydrophobicity analysis of NKG2D targeting arm of AB0089. The arrows indicate the position of the NKG2D targeting arm of AB0089 in reference to a database of 377 late-stage therapeutic antibodies. In each plot, there are two dashed lines—one closer and the other further to the solid line. The dashed line closer to the solid line indicates 2 SD (>95% of reference molecules within this region), whereas the dashed line further to the solid line indicates 3 SD (>99.7% of reference molecules within this region).

[0171] **FIG. 117** shows human acceptor frameworks used in AB0089 compared to other clinical stage therapeutic mAbs. Benchmarking of frameworks used in AB0089 against human germlines frequently used in clinical stage antibodies database containing 400+ mAbs from phase I+.

[0172] **FIG. 118** shows a cartoon representation of AB0089 indicating chain composition of the molecule (**FIG. 118A**) and the positions of chain H, S, and L of AB0089 on the Treg-adjusted EpiMatrix protein immunogenicity scale (**FIG. 118B)**.

[0173] **FIG. 119** shows a TriNKET purification process flow diagram.

[0174] **FIG. 120** shows a MabSelect Protein A capture elution chromatogram.

[0175] **FIG. 121** shows a SEC analysis of Protein A eluate, pH-adjusted and filtered for IEX loading.

[0176] **FIG. 122** shows a SDS-PAGE analysis of AB0089 Protein A load, flow through, and eluate. Based on absorbance readings, 15 µl was loaded in the "Protein A load" and "Protein A FT" lanes, 2 µg was loaded in the "Protein A Eluate lane". The major band at ~120 kDa corresponds to AB0089.

[0177] **FIG. 123** shows a Poros XS cation exchange chromatogram.

[0178] **FIG. 124** shows a SDS-PAGE analysis of AB0089 CIEX load and elution fractions. Based on absorbance readings, lanes contain ~2.0 µg of protein. The major band at ~120 kDa is AB0089.

[0179] **FIG. 125** shows reduced ("R") and non-reduced ("NR") SDS-PAGE of AB0089 Lot AB0089-002. The three chains (S, H, and L) of the molecule are labeled in the R lane. F3' in the NR lane refers to AB0089.

[0180] **FIG. 126** shows SEC analysis of purified AB0089 lot AB0089-002 and indicates 100% monomer as determined by integrated peak area.

[0181] **FIG. 127** shows intact mass spectrometry analysis of AB0089 lot AB0089-002. LC-MS analysis of the intact AB0089 showed an observed mass (126,130.0 Da) that agrees well with the theoretical mass of 126,129.1 Da.

[0182] **FIG. 128** shows CE-SDS analysis of AB0089, R (left panel) and NR (right panel) CE-SDS analysis of AB0089.

[0183] **FIG. 129** shows a charge profile of AB0089 by cIEF, indicating that AB0089 showed a major peak at a pI of 8.52 ± 0.0

[0184] **FIG. 130** shows a chromatogram of the hydrophobicity analysis of AB0089 by HIC, indicating that AB0089 is highly pure and homogenous.

[0185] **FIG. 131** shows the thermal stability of AB0089 as assessed by DSC analysis in three different formulations: PBS pH 7.4 (**FIG. 131A**), HST pH 6.0 (**FIG. 131A**), and CST, pH 7.0 (**FIG. 131A**).

[0186] **FIG. 132** shows a predicted disulfide map of AB0089.

[0187] **FIG. 133** shows the extracted ion chromatogram (XICs) for the engineered disulfide pair in the scFv (non-reduced and reduced) and the most intense charge state for that peptide pair.

[0188] **FIG. 134** shows identification of CH3-CH3 intermolecular Fc engineered disulfide.

[0189] **FIG. 135** shows binding of human CLEC12A to AB0089 tested by SPR.

[0190] **FIG. 136** shows that AB0089 and tepoditamab based molecule binding of CLEC12A conforms to a two-state model.

[0191] **FIG. 137** shows FACS assessment of AB0089 binding to isogenic cell lines expressing CLEC12A, and AML cancer cell lines (PL-21 and HL-60).

[0192] **FIG. 138** shows binding of AB0089 to a genetic variant CLEC12A (Q244) (middle panel) compared to CLEC12A (K244) WT (left panel) and cyno CLEC12A (cCLEC12A) (right panel).

[0193] **FIG. 139** shows AB0089 binding to differentially glycosylated CLEC12A: hCLEC12A untreated (left panel), hCLEC12A de-sialylated (middle panel) and hCLEC12A fully deglycosylated (right panel).

[0194] **FIG. 140** shows binding of AB0089 to human NKG2D tested by SPR. Top panel: Colored sensorgrams represent raw data. Black overlays represent the 1:1 kinetic fit. Bottom panel: Steady state affinity fit. Data from four independent Biacore channels are shown. The line represents the steady state KD value.

[0195] **FIG. 141** shows binding of AB0089 and trastuzumab to recombinant human CD16a (V158).

[0196] **FIG. 142** shows binding of AB0089 and trastuzumab to recombinant human CD64 (FcγRI).

[0197] **FIG. 143** shows binding of AB0089 and trastuzumab to cynomolgus CD64 (FcγRI).

[0198] **FIG. 144** shows binding of AB0089 and trastuzumab to human CD32a H131 (FcγRIIa H131).

[0199] **FIG. 145** shows binding of AB0089 and trastuzumab to human CD32a R131 (FcγRIIa R131).

[0200] **FIG. 146** shows binding of AB0089 and trastuzumab to recombinant human CD16a F158 (FcγRIIIa F158).

[0201] **FIG. 147** shows binding of AB0089 and trastuzumab to recombinant cynomolgus CD16 (FcγRIII).

[0202] **FIG. 148** shows binding of AB0089 and trastuzumab to recombinant human CD32b (FcγRII).

[0203] **FIG. 149** shows binding of AB0089 and trastuzumab to recombinant human CD16b (FcγRIIIb).

[0204] **FIG. 150** shows binding of AB0089 and trastuzumab to recombinant human FcRn.

[0205] **FIG. 151** shows binding of AB0089 and trastuzumab to recombinant cynomolgus FcRn.

[0206] **FIG. 152** shows that simultaneous engagement of AB0089 to CD16a and NKG2D results in avid binding.

[0207] **FIG. 153** shows AB0089 simultaneous co-engagement of CLEC12A and NKG2D binding arms.

[0208] **FIG. 154** is a summary of a comparison of the binding epitope of AB0089 in relation to AB0237, AB0192 and three CLEC12A binding reference TriNKETs by SPR. AB0089 interaction with hCLEC12A was blocked by AB0237, and two control molecules, cFAE-A49

CLL1-Merus and cFAE-A49 Tepoditamab, but not by Genentech-h6E7 based molecule, and illustrates that AB0089 binding epitope overlaps with Merus-CLL1 and tepoditamab.

[0209] **FIG. 155** shows potency of AB0089 in KHYG-1-CD16aV mediated cytotoxicity assay with HL60 and PL21 cells.

[0210] **FIG. 156** shows that AB0089 potently enhances primary NK mediated cell lysis of cancer cells, outperforming parental mAb.

[0211] **FIG. 157** shows a schematic representation of a PSR assay (**FIG. 157A**), and PSR binding AB0089 in comparison with antibodies with known PSR binding (Rituximab) and an antibody with no known non-specificity (Trastuzumab) (**FIG. 157B**).

[0212] **FIG. 158** shows the relative binding (Z score) of AB0089 at 1 μg/ml to human CLEC12A in comparison to the entire human proteome microarray. Plot depicting the relative binding Z-score (y-axis) vs. the top 24 identified binding partners of AB0089 (x-axis). hCLEC12a is plotted at position 1 with a Z-score of 150.61.

[0213] **FIG. 159** shows SEC analysis of AB0089 after 4 weeks at 40˚C in HST, pH 6.0 compared to control sample, demonstrating that AB0089 exhibited high stability.

[0214] **FIG. 160** shows CE-SDS analysis of AB0089 after 4 weeks at 40°C in HST, pH 6.0, compared to control. Non-reduced (NR) (left panel) and reduced (R) (right panel).

[0215] **FIG. 161** shows that AB0089 is stable after 4 weeks at 40˚C in HST, pH 6.0 with no effect on binding to hCLEC12A (**FIG. 161A)**, hNKG2D (**FIG. 161B)**, or hCD16aV (**FIG. 161C**).

[0216] **FIG. 162** shows AB0089 potency after 4 weeks at 40°C in HST, pH 6.0.

[0217] **FIG. 163** shows that AB0089 demonstrated high stability after 4 weeks of incubation in CST, pH 7.0, at 40 °C, compared to control sample as measured by SEC analysis.

[0218] **FIG. 164** shows that no fragmentation of AB0089 was observed by CE-SDS after 4 weeks at 40°C in CST, pH 7.0 compared to control sample. NR (left panel) and R (right panel).

[0219] **FIG. 165** shows that AB0089 is stable after 4 weeks at 40˚C in CST, pH 7.0, with no effect on binding to hCLEC12A (**FIG. 165A**), hNKG2D (**FIG. 165B**), or hCD16aV (**FIG. 165C**).

[0220] **FIG. 166** shows that long term thermal stress did not affect potency of AB0089 after 4 weeks at 40˚C in CST, pH 7.0 compared to control.

[0221] **FIG. 167** is an extracted ion chromatogram of the tryptic peptide encompassing CDRH3 of CLEC12a targeting arm of AB0089, which showed no evidence of aspartic acid isomerization in the peptide encompassing the CLEC12A binding CDRH3 was observed, based on manual inspection of peak shape.

[0222] **FIG. 168** is an SEC analysis showing that there is no difference in monomer content between oxidized AB0089 and control sample after forced oxidation.

[0223] **FIG. 169** shows that no fragmentation of AB0089 was observed by CE-SDS after forced oxidation compared to control sample. NR (left panel) and R (right panel).

[0224] **FIG. 170** shows that oxidative stress had no significant effect on the active protein content or on the affinities for hCLEC12A (**FIG. 170A**, top panel), hNKG2D (**FIG. 170B**, middle panel), and hCD16Av (**FIG. 170C**, bottom panel).

[0225] **FIG. 171** shows that AB0089 is stable in forced oxidation.

[0226] **FIG. 172** is an SEC analysis showing that AB0089 is stable under high pH stress (pH 8.0, 40°C, 2 weeks).

[0227] **FIG. 173** is an CE-SDS analysis showing that AB0089 exhibited low levels of degration AB0089 after long term high pH stress (pH 8, 40°C, 2 weeks). NR (left panel) and R (right panel).

[0228] **FIG. 174** is a cIEF showing that AB0089 exhibited an acidic shift after long term high pH exposure (pH 8, 40°C, 2 weeks).

[0229] **FIG. 175** shows that there was no meaningful difference in the amount of active protein or in the affinities for hCLEC12A (**FIG. 175A**, top panel), hNKG2D (**FIG. 175B**, middle panel), or hCD16aV (**FIG. 175C**, bottom panel) between stressed and control samples after long term high pH 8.0 stress (pH 8, 40°C, 2 weeks).

[0230] **FIG. 176** shows that the potency of AB0089 was reduced approximately 2-fold after long term high pH stress (pH 8, 40°C, 2 weeks).

[0231] **FIG. 177** is an SEC analysis showing that AB0089 is highly stable under low pH stress (pH 5.0, 40°C, 2 weeks).

[0232] **FIG. 178** is a CE-SDS analysis of AB0089 after long term low pH stress (pH 5.0 40°C, 2 weeks) showing that low levels of AB0089 degradation were detected by non-reduced (left panel) and reduced (right panel) CE-SDS.

[0233] **FIG. 179** is a cIEF analysis showing that AB0089 exposed to low pH stress shows slight acidic shift in charge profile.

[0234] **FIG. 180** shows that there was no meaningful difference in active protein content or in AB0089 affinities for hCLEC12A (**FIG. 180A**, top panel), hNKG2D (**FIG. 180B**, middle panel), or hCD16aV (**FIG. 180C**, bottom panel) after long term low pH stress (pH 5.0, 40°C, 2 weeks).

[0235] **FIG. 181** shows that the potency of AB0089 remained similar to potency of the control sample after long term low pH stress (pH 5.0 40°C, 2 weeks).

[0236] **FIG. 182** is an extracted ion chromatogram of the tryptic peptide encompassing CDRH3 of CLEC12A targeting arm of AB0089, which showed no evidence of aspartic acid isomerization in the peptide encompassing the CLEC12A binding CDRH3 after long term expure tp low pH (pH 5.0), based on manual inspection of peak shape.

[0237] **FIG. 183** is an SEC analysis showing that AB0089 is stable after six cyles of freeze/thaw.

[0238] **FIG. 184** is an CE-SDS analysis of AB0089 after six freeze/thaw cycles showing that no loss of purity was detected by reduced (right panel) or non-reduced CE-SDS (left panel).

[0239] **FIG. 185** is an SEC analysis showing that AB0089 is stable after agitation stress (300 rpm at room temperature in a deep well plate for 3 days).

[0240] **FIG. 186** is an SEC analysis showing that AB0089 was able to be concentrated to >175 mg/ml with minimal loss in percent monomer.

[0241] **FIG. 187** is a graph showing that AB0089 is amendable to concentration (up to 178 mg/ml) without loss of monomer.

[0242] **FIG. 188** is an SEC analysis of Protein A eluate pre- and post- low pH hold showing that AB0089 is highly stable during low pH hold/viral inactivation conditions used in biologics manufacturing.

[0243] **FIG. 189** shows that AB0089 charge profile remains unaltered after low pH hold.

[0244] **FIG. 190** shows that the affinities of AB0089 for hCLEC12a, hNKG2D, and CD16aV were not affected by low pH hold.

[0245] **FIG. 191** shows that the potency of AB0089 was unaltered after the low pH hold step.

[0246] **FIG. 192** is an SEC analysis showing that there was no change in profile of % monomer was observed after the low pH hold.

[0247] **FIG. 193** shows that low pH hold did not have a significant effect on the charge profile of AB0089.

[0248] **FIG. 194** shows that AB0089 strongly enhances human NK cytotoxicity of PL21 AML cells. Purified human NK cells were rested overnight and, the following day, were co-cultured with labeled PL21 target cells for DELFIA assay. Dose-titrations of CLEC12A TriNKET AB0089 or parental mAb AB0305 were prepared starting at 10 nM and added to the co-cultures. Assays were performed with a total of six healthy NK cell donors; shown is a representative result. Specific lysis was plotted against test article concentration, and data were fit to a 4-parameter non-linear regression model to generate potency values. Data points represent mean ± standard deviation.

[0249] **FIG. 195** shows that AB0192 strongly enhances human NK cytotoxicity of HL60 AML cells. Purified human NK cells were rested overnight and, the following day, were co-cultured with labeled HL60 target cells for DELFIA assay. Dose-titrations of CLEC12A TriNKET AB0089 or parental mAb AB0305 were prepared starting at 10 nM and added to the co-cultures. Assays were performed with a total of four healthy NK cell donors; shown is a representative result. Specific lysis was plotted against test article concentration, and data were fit to a 4-parameter non-linear regression model to generate potency values. Data points represent mean ± standard deviation.

[0250] **FIG. 196** shows that AB0192 strongly enhances human NK cytotoxicity of PL21 AML cells. Purified human NK cells were rested overnight and, the following day, were co-cultured with labeled PL21 target cells for DELFIA assay. Dose-titrations of CLEC12A TriNKET AB0192 or parental mAb AB0306 were prepared starting at 10 nM and added to the co-cultures. Assays were performed with a total of six healthy NK cell donors; shown is a representative result. Specific lysis was plotted against test article concentration, and data were fit to a 4-parameter non-linear regression model to generate potency values. Data points represent mean ± standard deviation.

[0251] **FIG. 197** shows that AB0192 strongly enhances human NK cytotoxicity of HL60 AML cells. Purified human NK cells were rested overnight and, the following day, were co-cultured with labeled HL60 target cells for DELFIA assay. Dose-titrations of CLEC12A

TriNKET AB0192 or parental mAb AB0306 were prepared starting at 10 nM and added to the co-cultures. Assays were performed with a total of four healthy NK cell donors; shown is a representative result. Specific lysis was plotted against test article concentration, and data were fit to a 4-parameter non-linear regression model to generate potency values. Data points represent mean ± standard deviation.

[0252] **FIG. 198** shows that AB0089 activity is not influenced by the presence of soluble MIC-A. Purified human NK cells were rested overnight and, the following day, were set up in co-culture wells with DELFIA labeled PL21 target cells. Dose-titrations of AB0089 and AB0305 were prepared, and soluble MIC-A-Fc was added to 20 ng/mL into a titration series of each test article. Dose-titrations were fit to a 4-parameter non-linear regression model. Data points represent mean ± standard deviation.

[0253] **FIG. 199** shows that AB0089 induces IFNγ production and degranulation by human NK cells against PL21 AML cells. Frozen PBMCs were thawed and co-cultured with PL21 target cells in the presence of a dose-titration of AB0089, AB0305 or F3'-palivizumab. After incubation, cells were prepared for FACS analysis of CD107a degranulation and intracellular accumulation of IFNγ. The figure shown is representative of the three PBMC donors tested. The percentage of IFNγ+CD107+ NK cells induced was plotted against concentration, and data were fit to a 4-parameter non-linear regression model to generate potency values. Data points represent mean ± standard deviation.

[0254] **FIG. 200** shows that AB0089 induces IFNγ production and degranulation by human NK cells against HL60 AML cells. Frozen PBMCs were thawed and co-cultured with HL60 target cells in the presence of a dose-titration of AB0089, AB0305 or F3'-palivizumab. After incubation, cells were prepared for FACS analysis of CD107a degranulation and intracellular accumulation of IFNγ. The figure shown is representative of the three PBMC donors tested. The percentage of IFNγ+CD107+ NK cells induced was plotted against concentration, and data were fit to a 4-parameter non-linear regression model to generate potency values. Data points represent mean ± standard deviation.

[0255] **FIG. 201** shows that CLEC12A TriNKETs induce M0-macrophage ADCP activity against PL21 AML cells. *In vitro* generated M0 macrophages were labeled with Cell Trace Violet and co-cultured with Cell Trace CFSE- labeled PL21 target cells at an 8:1 E:T ratio. After two-hours, cells were prepared for flow cytometry analysis. Double-positive Cell Trace Violet/CFSE cells were considered phagocytic events. Assays were conducted with macrophages derived from three independent donors with the figure shown being a representative result.

Percentage phagocytosis of target cells was plotted against test article concentration, and data were fit to a 4-parameter non-linear regression model to generate potency values. Data points represent mean ± standard deviation.

[0256] **FIG. 202** shows that AB0089 does not stimulate CDC against PL21 AML cells. AB0089 was incubated with BATDA-labeled PL21 cells in cell culture media containing 5% human serum for 60 minutes. Human IgG1 isotype control served as a negative control, while anti-MHC class I clone W6/32 was used as a positive control. Specific lysis of target cells was plotted against concentration, and data were fit to a 4-parameter non-linear regression model to generate potency values. Data points represent mean ± standard deviation.

[0257] **FIG. 203** shows binding of CLEC12A-TriNKETs to cell lines expressing CLEC12A. Dose-response binding of CLEC12A TriNKETs and their parental mAbs were analyzed on (**FIG. 203A**) Ba/F3 cells overexpressing human CLEC12A. The human cancer cell lines (**FIG. 203B**) HL60 and (**FIG. 203C**) PL21 with endogenous expression of CLEC12A were used to corroborate results with the transfected cell line. Figures shown are representative of results from three independent experiments, which are summarized in Table 201.

[0258] **FIG. 204** shows CLEC12A surface retention on AML cell lines exposed to CLEC12A TriNKETs. CLEC12A surface retention on (**FIG. 204A**) HL60 and (**FIG. 204B**) PL21 cells was measured after exposure to test articles at 40 nM for two hours at 37°C. Test articles were used at saturation concentrations and detected using a human IgG Fc- specific secondary antibody. Staining intensity after two hours at 37°C was normalized to staining intensity of the same test article on cells incubated for two hours on ice to derive the percentage of CLEC12A retained on cell surfaces. Data bars represent the average of duplicate wells and error bars represent standard deviation. Figures shown are representative of results from three independent experiments, which are summarized in Table 202.

[0259] **FIG. 205** shows AB0089 binding normalized to AB0237 after two hours at 37°C. AB0089 and AB0237 binding were compared on HL60 cells after a two-hour incubation on ice or at 37°C. Histograms represent the following: (1st from top to bottom) AB0237 two-hours 37°C, (2nd from top to bottom) AB0237 two-hour on ice, (3rd from top to bottom) AB0089 two-hours at 37°C, (4th from top to bottom) AB0089 two-hours on ice. Binding of all test articles was detected with an anti- human IgG Fc fluorophore-conjugated antibody.

[0260] **FIG. 206** shows AB0089 binds CLEC12A+ blasts across 10 primary AML patient samples. Primary AML bone marrow and PBMC samples were obtained from commercial vendors, see Table 3. Samples were prepared for flow cytometry analysis according to the antibody panel in Table 1. Histograms represent staining on AML blasts as follows: 4th from top to bottom = hIgG1 isotype control, 3rd from top to bottom = AB0305-CF568, 2nd from top to bottom = AB0089-CF568, 1st from top to bottom = anti-CLEC12 50C1- CF568.

[0261] **FIG. 207** shows AB0089 binds CLEC12A+ CD34+CD38- cells across 10 primary AML patient samples. Primary AML bone marrow and PBMC samples were obtained from commercial vendors, see Table 200. Samples were prepared for flow cytometry analysis according to the antibody panel in Table 198. Samples were further gated on CD34+CD38- subpopulation to enrich for leukemic stem cells. Histograms represent staining on CD34+CD38- blasts as follows: 4th from top to bottom = hIgG1 isotype control, 3rd from top to bottom = AB0305-CF568, 2nd from top to bottom = AB0089-CF568, 1st from top to bottom = anti-CLEC12 50C1- CF568.

[0262] **FIG. 208** shows the path from immunization to AB0192. Upper panel represents results of CLEC12A binding by SPR. Lower panel shows binding to CLEC12A+ PL-21 AML cancer cells.

[0263] **FIG. 209** shows a schematic representation of AB0192. Proprietary heterodimerization mutations and an engineered interchain disulfide bridge ensure efficient chain pairing of the IgG1 Fc. The scFv is derived from the humanized and sequence liability corrected CLEC12A mAb 9F11.B7. The scFv is stabilized by an engineered disulfide bridge between VH and VL.

[0264] **FIG. 210** shows the amino acid sequences of the three polypeptide chains that make up AB0192. Chain S: anti-CLEC12A scFv-CH2-CH3 (humanized sequence, CDRs are bold not underlined, back mutations bold and underlined, engineered scFv disulfide in italic and bold, and Fc mutations for heterodimerization and the engineered CH3 disulfide are underlined not bold). Chain H: anti-NKGD VH-CH1-CH2-CH3 (fully human, CDRs are bold not underlined, Fc mutations for heterodimerization and the engineered CH3 disulfide are underlined not bold). Chain L: anti-NKGD VL-CL (fully human, CDRs are bold not underlined).

[0265] **FIG. 211** shows human acceptor frameworks used in AB0192 compared to other clinical stage therapeutic mAbs. Benchmarking of frameworks used in AB0192 against human

germlines frequently used in clinical stage antibodies database containing 400+ mAbs from phase I+.

[0266] **FIG. 212** shows a ribbon diagram model of the CLEC12A binding scFv in three different orientations (upper panel) and their corresponding surface charge distribution of the same orientation (lower panel). The charge distribution of anti-CLEC12A scFv is polarized ("top view", lower panel), with negatively-charged residues populated predominately within CDRH3 and CDRL2. Three orientations are shown: both façades (Left panel: front view; center panel: back view) and the antigen-engaging surface (right panel: top view).

[0267] **FIG. 213** shows the analysis of CDR length and surface hydrophobicity patches of the CLEC12A-targeting arm of AB0192. The arrow indicates where CLEC12A targeting scFv of AB0192 stands in reference to advanced clinical stage mAbs. The inner dotted lines indicate 2 SD (>95% of reference molecules within this region). The outermost dotted lines indicate 3 SD (>99.7% of reference molecules within this region).

[0268] **FIG. 214** shows the analysis of patches containing positive and negative charges, as well as the symmetry of these charges around the CDR regions. The arrow indicates where CLEC12A targeting scFv of AB0192 stands in reference to advanced clinical stage mAbs. In each plot, there are two dashed lines—one closer and the other further to the solid line. The dashed line closer to the solid line indicates 2 SD (>95% of reference molecules within this region), whereas the dashed line further to the solid line indicates 3 SD (>99.7% of reference molecules within this region).

[0269] **FIG. 215** shows a ribbon diagrams with three different orientations of the NKG2D-binding Fab arm (upper panel) and their corresponding surface charge distribution of the same orientation (lower panel). Three orientations are shown: both façades (Left panel: front view; center panel: back view) and the antigen-engaging surface (right panel: top view).

[0270] **FIG. 216** shows the CDR length and patches of surface hydrophobicity analyses of NKG2D-targeting arm of AB0192. The arrow indicates where NKG2D targeting Fab of AB0192 stands in reference to advanced clinical stage mAbs. The inner dotted lines indicate 2 SD (>95% of reference molecules within this region). The outermost dotted lines indicate 3 SD (>99.7% of reference molecules within this region).

[0271] **FIG. 217** shows the analyses of patches containing positive and negative charges, as well as the symmetry of these charges around the CDR regions. The arrows indicate the position

of the NKG2D targeting Fab of AB0192 stands in reference to a database of 377 late-stage therapeutic antibodies. In each plot, there are two dashed lines—one closer and the other further to the solid line. The dashed line closer to the solid line indicates 2 SD (>95% of reference molecules within this region), whereas the dashed line further to the solid line indicates 3 SD (>99.7% of reference molecules within this region).

[0272] **FIG. 218A** and **FIG. 218B** shows the position of AB0192 chains on the Treg-adjusted EpiMatrix protein immunogenicity scale. **FIG. 218A** shows a cartoon representation of AB0192; **FIG. 218B** shows positions of chain H, S, and L of AB0192 on Treg-Adjusted Immunogenicity Protein Scale.

[0273] **FIG. 219** shows a schematic representation of the AB0192 2 step platform purification. Left panel: SDS-PAGE analysis of AB0192 before and after first step of purification process (Protein A capture). Middle panel: SEC analysis of AB0192 after protein A step and after cIEX step. Right panel: Reduced and non-reduced SDS-PAGE of purified AB0192.

[0274] **FIG. 220** shows the intact mass analysis of AB0192 (lot AB0192-005) using LC-MS analysis. AB0192 theoretical mass = 126,429.5 Da. AB0192 Lot AB0192-005 observed mass = 126,429.9 Da.

[0275] **FIG. 221** shows a SEC (Superdex 200) analysis of purified AB0192 (lot AB0192-005), which showed >99% monomer as determined by integrated peak area.

[0276] **FIG. 222** shows the purity of AB0192 (lot AB0192-005) by non-reduced conditions ("NR"; Left Panel) and reduced conditions ("R"; Right Panel) by CE-SDS.

[0277] **FIG. 223** shows the cIEF profile of AB0192 (lot AB0192-005).

[0278] **FIG. 224** shows the hydrophobicity analysis of AB0192 by HIC.

[0279] **FIG. 225A – FIG. 225C** shows DSC analysis of AB0192 in three different buffer systems. PBS pH 7.4 (**FIG. 225A**), HST, pH 6.0 (**FIG. 225B**) and CST, pH 7.0 (**FIG. 225C**).

[0280] **FIG. 226** shows the predicted disulfide map for AB0192.

[0281] **FIG. 227** shows the extracted ion chromatogram (XICs) for the engineered disulfide pair in the scFv (non-reduced and reduced) and the most intense charge state for that peptide pair.

[0282] **FIG. 228** shows the existence of the CH3-CH3 intermolecular Fc engineered disulfide.

[0283] **FIG. 229** shows binding of AB0192 to human CLEC12A tested by SPR.

[0284] **FIG. 230** shows binding of AB0192 to a genetic variant of human CLEC12A (Q244) compared to CLEC12A (K244) WT and cyno CLEC12A tested by SPR.

[0285] **FIG. 231** shows binding of AB0192 to differentially glycosylated CLEC12A tested by SPR.

[0286] **FIG. 232** shows binding of AB0192 to CLEC12A+ isogenic and HL60 and PL21 AML cells.

[0287] **FIG. 233** shows binding of AB0192 to human NKG2D tested by SPR.

[0288] **FIG. 234** shows binding of AB0192 to hCD16a V158 allele.

[0289] **FIG. 235** shows simultaneous binding of AB0192 to CD16a and NKG2D results in avid binding. AB0192 injected over NKG2D (middle line, as indicated on right side of graph), CD16a (bottom line, as indicated on right side of graph) or mixed, CD16a and NKG2D, (top line, as indicated on right side of graph) surfaces. Note that the surface has not been optimized for a maximum avidity effect.

[0290] **FIG. 236** shows sequential saturation of captured AB0192 with hCLEC12A and hNKG2D. Targets were sequentially injected over AB0192 captured on a Biacore chip. Upper panel represents binding of hCLEC12A (100 nM) followed by binding of hNKG2D (7 μM) to captured AB0192. Lower panel depicts the reverse order of target binding (human NKG2D binding followed by hCLEC12A). Relative binding stoichiometries (relative to binding of each target to unoccupied captured AB0192) are shown in Table 218.

[0291] **FIG. 237** shows binding of AB0192 and trastuzumab to recombinant human CD64 (FcγRI). A difference in apparent maximum binding responses between the molecules is due to their difference in molecular weight.

[0292] **FIG. 238** shows binding of AB0192 and trastuzumab to recombinant human CD64 (FcγRI). A difference in apparent maximum binding responses between the molecules is due to their difference in molecular weight

[0293] **FIG. 239** shows binding of AB0192 and trastuzumab to recombinant human CD32a (FcγRIIa) H131 allele. Top panel for each molecule represents raw binding sensorgrams while the bottom panels represent fitting to a steady state affinity model. A difference in apparent maximum binding responses between the molecules is due to a difference in molecular weight.

[0294] **FIG. 240** shows binding of AB0192 and trastuzumab to recombinant human CD32a (FcγRIIa) R131 allele. Top panel for each molecule represents raw binding sensorgrams while the bottom panels represent fitting to a steady state affinity model. A difference in apparent maximum binding responses between the molecules is due to a difference in molecular weight.

[0295] **FIG. 241** shows binding of AB0192 and trastuzumab to recombinant human CD16a (FcγRIIIa) F158 allele. Top panel for each molecule represents raw binding sensorgrams while the bottom panels represent fitting to a steady state affinity model. A difference in apparent maximum binding responses between the molecules is due to a difference in molecular weight.

[0296] **FIG. 242** shows binding of AB0192 and trastuzumab to recombinant cynomolgus CD16 (FcγRIII). Top panel for each molecule represents raw binding sensorgrams while the bottom panels represent fitting to a steady state affinity model. A difference in apparent maximum binding responses between the molecules is due to a difference in molecular weight.

[0297] **FIG. 243** shows binding of AB0192 and trastuzumab to recombinant human CD32b (FcγRIIb). Top panel for each molecule represents raw binding sensorgrams while the bottom panels represent fitting to a steady state affinity model. A difference in apparent maximum binding responses between the molecules is due to a difference in molecular weight.

[0298] **FIG. 244** shows binding of AB0192 and trastuzumab to recombinant human CD16b (FcγRIIIb). Top panel for each molecule represents raw binding sensorgrams while the bottom panels represent fitting to a steady state affinity model. A difference in apparent maximum binding responses between the molecules is due to a difference in molecular weight.

[0299] **FIG. 245** shows binding of AB0192 and trastuzumab to recombinant human FcRn. Top panel for each molecule represents raw binding sensorgrams while the bottom panels represent fitting to a steady state affinity model. A difference in apparent maximum binding responses between the molecules is due to a difference in molecular weight.

[0300] **FIG. 246** shows binding of AB0192 and trastuzumab to recombinant cynomolgus FcRn. Top panel for each molecule represents raw binding sensorgrams while the bottom panels represent fitting to a steady state affinity model. A difference in apparent maximum binding responses between the molecules is due to a difference in molecular weight.

[0301] **FIG. 247** shows Epitope binning of AB0192 against other CLEC12A binding TriNKETs.

[0302] **FIG. 248** shows potency of AB0192 in primary NK mediated cytotoxicity assay compared to corresponding mAb control.

[0303] **FIG. 249A** and **FIG. 249B** show non-specificity analysis of AB0192 in PSR assay. **FIG. 249A**: schematic representation of a PSR assay; **FIG. 249B**: PSR binding AB0089 in comparison with antibodies with known PSR binding (Rituximab) and an antibody with no known non-specificity (Trastuzumab).

[0304] **FIG. 250** shows the relative Z score of AB0089 in HuProt™ human proteome microarray assay. Plot depicting the relative binding Z-score (y-axis) vs. the top 24 identified binding partners of AB0192 (x-axis). hCLEC12a is plotted at position 1 with a Z-score of 150.06.

[0305] **FIG. 251** shows an SEC analysis of AB0192 after 4 weeks at 40˚C in HST, pH6.0, compared to control.

[0306] **FIG. 252** shows a CE-SDS analysis of AB0192 after 4 weeks at 40°C in HST, pH 6.0, compared to control. Non-reduced conditions are shown in the left panel. Reduced conditions are shown in the right panel.

[0307] **FIG. 253** shows that AB0192 is stable after 4 weeks 40˚C stress in HST, pH 6.0: no effect on CLEC12A, NKG2D or CD16a binding.

[0308] **FIG. 254** shows that there was no difference in potency between the control and stressed samples of AB0192 after 4 weeks at 40°C in HST, pH 6.0 in KHYG-1-CD16a mediated cytotoxicity assay.

[0309] **FIG. 255** shows minimal aggregation of AB0192 after 4 weeks at 40°C in CST, pH 7.0, as measured by SEC analysis.

[0310] **FIG. 256** shows minimal fragmentation of AB0192 after 4 weeks at 40°C in CST, pH 7.0 compared to control, as measured by CE-SDS analysis.

[0311] **FIG. 257** shows that AB0192 is stable after 4 weeks 40˚C stress in CST, pH 7.0: no effect on CLEC12A, NKG2D or CD16a binding.

[0312] **FIG. 258** shows that there was no difference in potency between the control and stressed samples of AB0192 after 4 weeks at 40˚C. in CST, pH 7.0, in KHYG-1-CD16a cytotoxicity assay.

[0313] **FIG. 259** shows an SEC analysis of AB0192 after forced oxidation stress compared to control, and indicated no significant decrease in monomer content.

[0314] **FIG. 260** shows a CE-SDS analysis of AB0192 after forced oxidation compared to control, and indicated that purity remained high.

[0315] **FIG. 261** shows that AB0192 is stable after oxidation stress (pH 5.0, 40°C, 14 days): no effect on CLEC12A, NKG2D or CD16a binding. Slight differences in the maximum binding signal reflect differences in capture levels.

[0316] **FIG. 262** shows that the potency of AB0192 after forced oxidation in KHYG-1-CD16a mediated cytotoxicity assay was similar to the control sample.

[0317] **FIG. 263** shows an SEC analysis of AB0192 after long term low pH exposure (pH 5.0, 40°C, 14 days), and indicated no loss of monomer.

[0318] **FIG. 264** shows a CE-SDS analysis of AB0192 after long term low pH stress (pH 5.0, 40°C, 14 days), and indicated that the differences in purity detected by non-reduced and reduced CE-SDS were less than 1%. Non-reduced conditions are shown in the left panel. Reduced conditions are shown in the right panel.

[0319] **FIG. 265** shows that AB0192 is stable after low pH stress (pH 5.0, 40°C, 14 days): no effect on CLEC12A, NKG2D or CD16a binding.

[0320] **FIG. 266** shows a charge analysis of AB0192 after long term low pH stress (pH 5.0, 40°C, 14 days) by cIEF, with control and pH 5 stressed samples showing no difference.

[0321] **FIG. 267** shows that the potency of AB0192 after long term pH 5.0 stress was unchanged relative to control in KHYG-1-CD16a cytotoxicity assay.

[0322] **FIG. 268** shows an SEC analysis of AB0192 after long term high pH stress (pH 8.0, 40°C, 14 days), which indicated that there was a 1.6 % loss of monomer.

[0323] **FIG. 269** shows a CE-SDS analysis of AB0192 after long term high pH stress (pH 8.0, 40°C, 14 days). Minor differences in purity were detected by non-reduced (left) and reduced (right) conditions.

[0324] **FIG. 270** shows that AB0192 is stable after high pH stress: no effect on CLEC12A, NKG2D or CD16a binding.

[0325] **FIG. 271** shows a charge analysis of AB0192 after long term high pH stress (pH 8.0, 40°C, 14 days) by cIEF, with an acidic shift in the pH 8 stressed sample relative to the control sample.

[0326] **FIG. 272** shows the potency of AB0192 after long term exposure to high pH 8.0 stress was not significantly affected, as assessed by KHYG-1-CD16aV cytotoxicity assay.

[0327] **FIG. 273** shows an SEC analysis of AB0192 after 6 cycles of freeze/thaw compared to control, which indicated no loss in monomer.

[0328] **FIG. 274** shows a CE-SDS analysis of AB0192 after freeze thaw stress, which indicated no loss of purity by either reduced (right panel) or non-reduced (left panel) conditions.

[0329] **FIG. 275** shows an SEC analysis of AB0192 after agitation stress compared to control, which indicated no loss of monomer.

[0330] **FIG. 276** shows a CE-SDS analysis of AB0192 after agitation stress compared to control, which indicated no increase in fragmentation detected by reduced (right panel) or non-reduced (left panel).

[0331] **FIG. 277** shows an SEC analysis of pH hold sample vs control, which indicated that no change in profile was observed after low pH hold.

[0332] **FIG. 278** shows a cIEF analysis of AB0192 after low pH hold compared to control, which indiacted that the low pH hold did not have a measurable effect on the charge profile of AB0192.

[0333] **FIG. 279** shows that AB0192 is stable after low pH hold: no effect on CLEC12A, NKG2D or CD16a binding. Slight differences in the maximum binding signal reflect differences in capture levels.

[0334] **FIG. 280** shows the potency of AB0192 after low pH hold in KHYG1-CD16a mediated cytotoxicity assay, which indicated that the potency of AB0192 was unaltered after the low pH hold step.

[0335] **FIG. 281** shows binding of AB0089 to hCLEC12A pre and post low pH hold. Slight differences in absolute maximal signals reflect difference in capture levels of AB0089.

[0336] **FIG. 282** shows AB0089 is stable after low pH hold. No difference between potencies of low pH hold and control samples was observed.

DETAILED DESCRIPTION

[0337] The present application provides multispecific binding proteins that bind the NKG2D receptor and CD16 receptor on natural killer cells, and the tumor-associated antigen. In some embodiments, the multispecific proteins further include an additional antigen-binding site that binds the tumor-associated antigen. The application also provides pharmaceutical compositions comprising such multispecific binding proteins, and therapeutic methods using such

multispecific proteins and pharmaceutical compositions, for purposes such as treating autoimmune diseases and cancer. Various aspects of the multispecific binding proteins described in the present application are set forth below in sections; however, aspects of the multispecific binding proteins described in one particular section are not to be limited to any particular section.

[0338] To facilitate an understanding of the present application, a number of terms and phrases are defined below.

[0339] The terms "a" and "an" as used herein mean "one or more" and include the plural unless the context is inappropriate.

[0340] As used herein, the term "antigen-binding site" refers to the part of the immunoglobulin molecule that participates in antigen binding. In human antibodies, the antigen binding site is formed by amino acid residues of the N-terminal variable ("V") regions of the heavy ("H") and light ("L") chains. Three highly divergent stretches within the V regions of the heavy and light chains are referred to as "hypervariable regions" which are interposed between more conserved flanking stretches known as "framework regions," or "FR." Thus the term "FR" refers to amino acid sequences which are naturally found between and adjacent to hypervariable regions in immunoglobulins. In a human antibody molecule, the three hypervariable regions of a light chain and the three hypervariable regions of a heavy chain are disposed relative to each other in three-dimensional space to form an antigen-binding surface. The antigen-binding surface is complementary to the three-dimensional surface of a bound antigen, and the three hypervariable regions of each of the heavy and light chains are referred to as "complementarity-determining regions," or "CDRs." In certain animals, such as camels and cartilaginous fish, the antigen-binding site is formed by a single antibody chain providing a "single domain antibody." Antigen-binding sites can exist in an intact antibody, in an antigen-binding fragment of an antibody that retains the antigen-binding surface, or in a recombinant polypeptide such as an scFv, using a peptide linker to connect the heavy chain variable domain to the light chain variable domain in a single polypeptide.

[0341] The term "tumor-associated antigen" as used herein means any antigen including but not limited to a protein, glycoprotein, ganglioside, carbohydrate, lipid that is associated with cancer. Such antigen can be expressed on malignant cells or in the tumor microenvironment such as on tumor-associated blood vessels, extracellular matrix, mesenchymal stroma, or immune

infiltrates. In preferred embodiments of the present disclosure, the terms "tumor-associated antigen" refers to CLEC12A.

[0342] As used herein, the terms "subject" and "patient" refer to an organism to be treated by the methods and compositions described herein. Such organisms preferably include, but are not limited to, mammals (*e.g.*, murines, simians, equines, bovines, porcines, canines, felines, and the like), and more preferably include humans.

[0343] As used herein, the term "effective amount" refers to the amount of a compound (*e.g.*, a compound of the present application) sufficient to effect beneficial or desired results. An effective amount can be administered in one or more administrations, applications or dosages and is not intended to be limited to a particular formulation or administration route. As used herein, the term "treating" includes any effect, *e.g.*, lessening, reducing, modulating, ameliorating or eliminating, that results in the improvement of the condition, disease, disorder, and the like, or ameliorating a symptom thereof.

[0344] As used herein, the term "pharmaceutical composition" refers to the combination of an active agent with a carrier, inert or active, making the composition especially suitable for diagnostic or therapeutic use *in vivo* or *ex vivo*.

[0345] As used herein, the term "pharmaceutically acceptable carrier" refers to any of the standard pharmaceutical carriers, such as a phosphate buffered saline solution, water, emulsions (*e.g.*, such as an oil/water or water/oil emulsions), and various types of wetting agents. The compositions also can include stabilizers and preservatives. For examples of carriers, stabilizers and adjuvants, s*ee e.g.*, Martin, Remington's Pharmaceutical Sciences, 15th Ed., Mack Publ. Co., Easton, PA [1975].

[0346] As used herein, the term "pharmaceutically acceptable salt" refers to any pharmaceutically acceptable salt (*e.g.*, acid or base) of a compound described in the present application which, upon administration to a subject, is capable of providing a compound described in this application or an active metabolite or residue thereof. As is known to those of skill in the art, "salts" of the compounds described in the present application may be derived from inorganic or organic acids and bases. Exemplary acids include, but are not limited to, hydrochloric, hydrobromic, sulfuric, nitric, perchloric, fumaric, maleic, phosphoric, glycolic, lactic, salicylic, succinic, toluene-p-sulfonic, tartaric, acetic, citric, methanesulfonic, ethanesulfonic, formic, benzoic, malonic, naphthalene-2-sulfonic, benzenesulfonic acid, and the

like. Other acids, such as oxalic, though not in themselves pharmaceutically acceptable, may be employed in the preparation of salts useful as intermediates in obtaining the compounds described in the application and their pharmaceutically acceptable acid addition salts.

[0347] Exemplary bases include, but are not limited to, alkali metal (*e.g.*, sodium) hydroxides, alkaline earth metal (*e.g.*, magnesium) hydroxides, ammonia, and compounds of formula NW_4^+, wherein W is C_{1-4} alkyl, and the like.

[0348] Exemplary salts include, but are not limited to: acetate, adipate, alginate, aspartate, benzoate, benzenesulfonate, bisulfate, butyrate, citrate, camphorate, camphorsulfonate, cyclopentanepropionate, digluconate, dodecylsulfate, ethanesulfonate, fumarate, flucoheptanoate, glycerophosphate, hemisulfate, heptanoate, hexanoate, hydrochloride, hydrobromide, hydroiodide, 2-hydroxyethanesulfonate, lactate, maleate, methanesulfonate, 2-naphthalenesulfonate, nicotinate, oxalate, palmoate, pectinate, persulfate, phenylpropionate, picrate, pivalate, propionate, succinate, tartrate, thiocyanate, tosylate, undecanoate, and the like. Other examples of salts include anions of the compounds described in the present application compounded with a suitable cation such as Na^+, NH_4^+, and NW_4^+ (wherein W is a C_{1-4} alkyl group), and the like.

[0349] For therapeutic use, salts of the compounds described in the present application are contemplated as being pharmaceutically acceptable. However, salts of acids and bases that are non-pharmaceutically acceptable may also find use, for example, in the preparation or purification of a pharmaceutically acceptable compound.

[0350] As used herein, CLEC12A (also known as CLL-1, DCAL-2, MICL, and CD371) refers to the protein of Uniprot Accession No. Q5QGZ9 and related isoforms and orthologs.

[0351] Throughout the description, where compositions are described as having, including, or comprising specific components, or where processes and methods are described as having, including, or comprising specific steps, it is contemplated that, additionally, there are compositions described in the present application that consist essentially of, or consist of, the recited components, and that there are processes and methods according to the present application that consist essentially of, or consist of, the recited processing steps.

[0352] As a general matter, compositions specifying a percentage are by weight unless otherwise specified. Further, if a variable is not accompanied by a definition, then the previous definition of the variable controls.

Abbreviation	Convention
A49M-I	Human anti-NKG2D antibody clone A49M-I
ADCC	Antibody dependent cellular cytotoxicity
ADCP	Antibody dependent cellular phagocytosis
AML	Acute myeloid leukemia
BM	Back mutation (murine residues introduced to human mAb sequence)
cCLEC12A	Cynomolgus monkey CLEC12A
CD16	Low affinity immunoglobulin gamma Fc region receptor III-A
CD16a	Fc gamma receptor III
CDC	Complement dependent cytotoxicity
CDR	complementarity determining region
CFSE	Carboxyfluorescein succinimidyl ester
CHO	Chinese Hamster Ovary
cIEF	capillary isoelectric focusing
CIEX	Cation Ion Exchange Chromatography
CLEC12A	C-type lectin domain family 12 member A
CLEC12A	C-type lectin domain family 12 member A, major variant with K244, also known as CLEC12A (K244) or CLEC12A WT
CLEC12AL	CLEC12A-Ligand
CMP	Common myeloid precursor
ConA	Concanavalin A
CST	20 mM sodium citrate, 250 mM sucrose, 0.01% Tween-80, pH 7.0
DI water	Distilled water
DSC	Differential Scanning Calorimetry
EC50	effective concentration that gives half-maximal response
Fab	fragment antigen-binding
FACS	Fluorescence activated cell sorting
Fc	fragment crystallizable region
FcγR	Fc-gamma receptor
GMP	Granulocyte monocyte precursor
HBS	Hepes buffered saline
hcFAE-A49.CLL1-Merus	Duobody TriNKET based on CLL1 antibody from Merus
hcFAE-A49.h6E7	Duobody TriNKET based on h6E7 antibody from Genentech
hcFAE-A49.tepoditamab	Duobody TriNKET based on CLEC12A binding arm of tepoditamab from Merus
hCLEC12A	Human CLEC12A
HCT	Hematopoietic cell transfer
HI-FBS	Heat inactivated fetal bovine serum
HMWS	high molecular weight species

Abbreviation	Convention
HPLC	high performance liquid chromatography
HST	20 mM histidine, 250 mM sucrose, 0.01% polysorbate 80
HTFR	Homogenous time resolved fluorescence
IgG1	immunoglobulin G1
ITIM	Immunoreceptor tyrosine-based inhibitory motif
k_a	association rate constant
K_D	equilibrium dissociation constant
k_d	dissociation rate constant
LC	liquid chromatography
LMWS	low molecular weight species
LSC	Leukemic stem cells
mAb	Monoclonal antibody
MEP	Megakaryocyte erythroid precursor
MFI	Median Fluorescence Intensity
MHC	Major histocompatibility complex
MIC-A	MHC class I chain-related protein A
MS	mass spectrometry
MS/MS	tandem mass spectrometry
MSU	Monosodium urate
NK cell	Natural killer cell
NKG2D	NKG2-D type II integral membrane protein
PBS	phosphate buffered saline
PBSF	Phosphate Buffered Saline (0.1% Bovine Serum Albumin (BSA))
pI	isoelectric point
PI3K	phosphatidylinositol 3' kinase
PMT	Photomultiplier tube
PS-80	polysorbate-80, Tween-80
PSR	Poly Specific Reagent
RU	resonance units, a measure of mass reported by SPR
ScFv	single-chain variable fragment
SDS-CE	sodium dodecyl sulfate capillary electrophoresis
SEC	size exclusion chromatography
SH2	Src homology 2 domain
SHP1	Src homology region 2 domain-containing phosphatase-1
SHP2	Src homology region 2 domain-containing phosphatase-2
SPR	surface plasmon resonance
TAA	Tumor associated antigen
TriNKET	Trispecific Natural Killer cell Engaging Therapy
UHPLC	ultra-high performance liquid chromatography
WT	Wild-type

I. PROTEINS

[0353] The present application provides multispecific binding proteins that bind to the NKG2D receptor and CD16 receptor on natural killer cells, and CLEC12A. The multispecific binding proteins are useful in the pharmaceutical compositions and therapeutic methods described herein. Binding of the multispecific binding proteins to the NKG2D receptor and CD16 receptor on a natural killer cell enhances the activity of the natural killer cell toward destruction of tumor cells expressing the tumor antigen. Binding of the multispecific binding proteins to tumor antigen expressing tumor cells brings these cells into proximity with the natural killer cell, which facilitates direct and indirect destruction of the tumor cells by the natural killer cell. Multispecific binding proteins that bind NKG2D, CD16, and another target are disclosed in International Application Publication Nos. WO2018148445 and WO2019157366, which are not incorporated herein by reference. Further description of some exemplary multispecific binding proteins is provided below.

[0354] The first component of the multispecific binding protein is an antigen-binding site that binds to NKG2D receptor-expressing cells, which can include but are not limited to NK cells, γδ T cells and $CD8^+$ αβ T cells. Upon NKG2D binding, the multispecific binding proteins may block natural ligands, such as ULBP6 and MICA, from binding to NKG2D and activating NK cells.

[0355] The second component of the multispecific binding proteins is an antigen-binding site that binds CLEC12A, a tumor-associated antigen. The tumor-associated antigen expressing cells may be found, for example, in solid tumor indications such as gastric cancer, esophageal cancer, lung cancer, breast cancer (*e.g.*, triple-negative breast cancer), colorectal cancer, ovarian cancer, esophageal cancer, uterine cancer, cervical cancer, head and neck cancer, glioma, and pancreatic cancer, or in certain hematological malignancies such as acute myeloid leukemia.

[0356] The third component of the multispecific binding proteins is an antibody Fc domain or a portion thereof or an antigen-binding site that binds to cells expressing CD16, an Fc receptor on the surface of leukocytes including natural killer cells, macrophages, neutrophils, eosinophils, mast cells, and follicular dendritic cells.

[0357] An additional antigen-binding site of the multispecific binding proteins may bind the same tumor-associated antigen. In certain embodiments, the first antigen-binding site that binds NKG2D is an scFv, and the second and the additional antigen-binding sites that bind the tumor-

associated antigen are each a Fab fragment. In certain embodiments, the first antigen-binding site that binds NKG2D is an scFv, and the second and the additional antigen-binding sites that bind the tumor-associated antigen are each an scFv. In certain embodiments, the first antigen-binding site that binds NKG2D is a Fab fragment, and the second and the additional antigen-binding sites that bind the tumor-associated antigen are each an scFv. In certain embodiments, the first antigen-binding site that binds NKG2D is a Fab, and the second and the additional antigen-binding sites that bind the tumor-associated antigen are each a Fab fragment.

[0358] The antigen-binding sites may each incorporate an antibody heavy chain variable domain and an antibody light chain variable domain (*e.g.*, arranged as in an antibody, or fused together to form an scFv), or one or more of the antigen-binding sites may be a single domain antibody, such as a V_HH antibody like a camelid antibody or a V_{NAR} antibody like those found in cartilaginous fish.

[0359] In some embodiments, the second antigen-binding site incorporates a light chain variable domain having an amino acid sequence identical to the amino acid sequence of the light chain variable domain present in the first antigen-binding site.

[0360] The multispecific binding proteins described herein can take various formats. For example, one format is a heterodimeric, multispecific antibody including a first immunoglobulin heavy chain, a first immunoglobulin light chain, a second immunoglobulin heavy chain and a second immunoglobulin light chain (**FIG. 1**). The first immunoglobulin heavy chain includes a first Fc (hinge-CH2-CH3) domain, a first heavy chain variable domain and optionally a first CH1 heavy chain domain. The first immunoglobulin light chain includes a first light chain variable domain and optionally a first light chain constant domain. The first immunoglobulin light chain, together with the first immunoglobulin heavy chain, forms an antigen-binding site that binds NKG2D. The second immunoglobulin heavy chain comprises a second Fc (hinge-CH2-CH3) domain, a second heavy chain variable domain and optionally a second CH1 heavy chain domain. The second immunoglobulin light chain includes a second light chain variable domain and optionally a second light chain constant domain. The second immunoglobulin light chain, together with the second immunoglobulin heavy chain, forms an antigen-binding site that binds CLEC12A. In some embodiments, the first Fc domain and second Fc domain together are able to bind to CD16 (**FIG. 1).** In some embodiments, the first immunoglobulin light chain is identical to the second immunoglobulin light chain.

[0361] Another exemplary format involves a heterodimeric, multispecific antibody including a first immunoglobulin heavy chain, a second immunoglobulin heavy chain and an immunoglobulin light chain (*e.g.*, **FIG. 2A**). In some embodiments, the first immunoglobulin heavy chain includes a first Fc (hinge-CH2-CH3) domain fused via either a linker or an antibody hinge to a single-chain variable fragment (scFv) composed of a heavy chain variable domain and light chain variable domain, which pair and bind NKG2D or bind CLEC12A. The second immunoglobulin heavy chain includes a second Fc (hinge-CH2-CH3) domain, a second heavy chain variable domain and a CH1 heavy chain domain. The immunoglobulin light chain includes a light chain variable domain and a light chain constant domain. In some embodiments, the second immunoglobulin heavy chain pairs with the immunoglobulin light chain and binds to NKG2D or binds the tumor-associated antigen, with the proviso that when the first Fc domain is fused to an scFv that binds NKG2D, the second immunoglobulin heavy chain paired with the immunoglobulin light chain binds the tumor-associated antigen, but not NKG2D, and vice versa. In some embodiments, the scFv in the first immunoglobulin heavy chain binds CLEC12A; and the heavy chain variable domain in the second immunoglobulin heavy chain and the light chain variable domain in the immunoglobulin light chain, when paired, bind NKG2D (*e.g.*, **FIG. 2E**). In some embodiments, the scFv in the first immunoglobulin heavy chain binds NKG2D; and the heavy chain variable domain in the second immunoglobulin heavy chain and the light chain variable domain in the immunoglobulin light chain, when paired, bind CLEC12A. In some embodiments, the first Fc domain and the second Fc domain together are able to bind to CD16 (*e.g.*, **FIG. 2A**).

[0362] Another exemplary format involves a heterodimeric, multispecific antibody including a first immunoglobulin heavy chain, and a second immunoglobulin heavy chain (*e.g.*, **FIG. 2B**). In some embodiments, the first immunoglobulin heavy chain includes a first Fc (hinge-CH2-CH3) domain fused via either a linker or an antibody hinge to a single-chain variable fragment (scFv) composed of a heavy chain variable domain and light chain variable domain, which pair and bind NKG2D, or bind CLEC12A. In some embodiments, the second immunoglobulin heavy chain includes a second Fc (hinge-CH2-CH3) domain fused via either a linker or an antibody hinge to a single-chain variable fragment (scFv) composed of a heavy chain variable domain and light chain variable domain which pair and bind NKG2D, or bind the tumor-associated antigen, with the proviso that when the first Fc domain is fused to an scFv that binds NKG2D, the second

Fc domain fused to an scFv binds the tumor-associated antigen, but not NKG2D, and vice versa. In some embodiments, the first Fc domain and the second Fc domain together are able to bind to CD16 (*e.g.*, **FIG. 2B**).

[0363] In some embodiments, the single-chain variable fragment (scFv) described above is linked to the antibody constant domain via a hinge sequence. In some embodiments, the hinge comprises amino acids Ala-Ser or Gly-Ser. In some embodiments, the hinge connects an scFv that binds NKG2D and the antibody heavy chain constant domain comprises amino acids Ala-Ser. In some embodiments, the hinge connects an scFv that binds the tumor-associated antigen and the antibody heavy chain constant domain comprises amino acids Gly-Ser. In some other embodiments, the hinge comprises amino acids Ala-Ser and Thr-Lys-Gly. The hinge sequence can provide flexibility of binding to the target antigen, and balance between flexibility and optimal geometry.

[0364] In some embodiments, the single-chain variable fragment (scFv) described above includes a heavy chain variable domain and a light chain variable domain. In some embodiments, the heavy chain variable domain forms a disulfide bridge with the light chain variable domain to enhance stability of the scFv. For example, a disulfide bridge can be formed between the C44 residue of the heavy chain variable domain and the C100 residue of the light chain variable domain, the amino acid positions numbered under Kabat. In some embodiments, the heavy chain variable domain is linked to the light chain variable domain via a flexible linker. Any suitable linker can be used, for example, the $(G_4S)_4$ linker ($(GlyGlyGlyGlySer)_4$ (SEQ ID NO:119)). In some embodiments of the scFv, the heavy chain variable domain is positioned at the N-terminus of the light chain variable domain. In some embodiments of the scFv, the heavy chain variable domain is positioned at the C terminus of the light chain variable domain.

[0365] The multispecific binding proteins described herein can further include one or more additional antigen-binding sites. The additional antigen-binding site(s) may be fused to the N-terminus of the constant region CH2 domain or to the C-terminus of the constant region CH3 domain, optionally via a linker sequence. In certain embodiments, the additional antigen-binding site(s) takes the form of a single-chain variable region (scFv) that is optionally disulfide-stabilized, resulting in a tetravalent or trivalent multispecific binding protein. For example, a multispecific binding protein includes a first antigen-binding site that binds NKG2D, a second antigen-binding site that binds CLEC12A, an additional antigen-binding site that binds the

tumor-associated antigen, and an antibody constant region or a portion thereof sufficient to bind CD16 or a fourth antigen-binding site that binds CD16. Any one of these antigen binding sites can either take the form of a Fab fragment or an scFv, such as an scFv described above.

[0366] In some embodiments, the additional antigen-binding site binds a different epitope of the tumor-associated antigen from the second antigen-binding site. In some embodiments, the additional antigen-binding site binds the same epitope as the second antigen-binding site. In some embodiments, the additional antigen-binding site comprises the same heavy chain and light chain CDR sequences as the second antigen-binding site. In some embodiments, the additional antigen-binding site comprises the same heavy chain and light chain variable domain sequences as the second antigen-binding site. In some embodiments, the additional antigen-binding site has the same amino acid sequence(s) as the second antigen-binding site. In some embodiments, the additional antigen-binding site comprises heavy chain and light chain variable domain sequences that are different from the heavy chain and light chain variable domain sequences of the second antigen-binding site. In some embodiments, the additional antigen-binding site has an amino acid sequence that is different from the sequence of the second antigen-binding site. In some embodiments, the second antigen-binding site and the additional antigen-binding site bind different tumor-associated antigens. In some embodiments, the second antigen-binding site and the additional antigen-binding site binds different antigens. Exemplary formats are shown in **FIG. 2C** and **FIG. 2D**. Accordingly, the multispecific binding proteins can provide bivalent engagement of the tumor-associated antigen. Bivalent engagement of the tumor-associated antigen by the multispecific proteins can stabilize the tumor-associated antigen on the tumor cell surface and enhance cytotoxicity of NK cells towards the tumor cells. Bivalent engagement of the tumor-associated antigen by the multispecific proteins can confer stronger binding of the multispecific proteins to the tumor cells, thereby facilitating stronger cytotoxic response of NK cells towards the tumor cells, especially towards tumor cells expressing a low level of the tumor-associated antigen.

[0367] The multispecific binding proteins can take additional formats. In some embodiments, the multispecific binding protein is in the Triomab form, which is a trifunctional, bispecific antibody that maintains an IgG-like shape. This chimera consists of two half antibodies, each with one light and one heavy chain, that originate from two parental antibodies.

[0368] In some embodiments, the multispecific binding protein is the KiH form, which involves the knobs-into-holes (KiHs) technology. The KiH involves engineering C_H3 domains to create either a "knob" or a "hole" in each heavy chain to promote heterodimerization. The concept behind the "Knobs-into-Holes (KiH)" Fc technology was to introduce a "knob" in one CH3 domain (CH3A) by substitution of a small residue with a bulky one (*e.g.*, $T366W_{CH3A}$ in EU numbering). To accommodate the "knob," a complementary "hole" surface was created on the other CH3 domain (CH3B) by replacing the closest neighboring residues to the knob with smaller ones (*e.g.*, $T366S/L368A/Y407V_{CH3B}$). The "hole" mutation was optimized by structured-guided phage library screening (Atwell S, Ridgway JB, Wells JA, Carter P., Stable heterodimers from remodeling the domain interface of a homodimer using a phage display library, *J. Mol. Biol.* (1997) 270(1):26–35). X-ray crystal structures of KiH Fc variants (Elliott JM, Ultsch M, Lee J, Tong R, Takeda K, Spiess C, *et al.*, Antiparallel conformation of knob and hole aglycosylated half-antibody homodimers is mediated by a CH2-CH3 hydrophobic interaction. *J. Mol. Biol.* (2014) 426(9):1947–57; Mimoto F, Kadono S, Katada H, Igawa T, Kamikawa T, Hattori K. Crystal structure of a novel asymmetrically engineered Fc variant with improved affinity for FcγRs. *Mol. Immunol.* (2014) 58(1):132–8) demonstrated that heterodimerization is thermodynamically favored by hydrophobic interactions driven by steric complementarity at the inter-CH3 domain core interface, whereas the knob–knob and the hole–hole interfaces do not favor homodimerization owing to steric hindrance and disruption of the favorable interactions, respectively.

[0369] In some embodiments, the multispecific binding protein is in the dual-variable domain immunoglobulin (DVD-Ig™) form, which combines the target binding domains of two monoclonal antibodies via flexible naturally occurring linkers, and yields a tetravalent IgG-like molecule.

[0370] In some embodiments, the multispecific binding protein is in the Orthogonal Fab interface (Ortho-Fab) form. In the ortho-Fab IgG approach (Lewis SM, Wu X, Pustilnik A, Sereno A, Huang F, Rick HL, *et al.*, Generation of bispecific IgG antibodies by structure-based design of an orthogonal Fab interface. *Nat. Biotechnol.* (2014) 32(2):191–8), structure-based regional design introduces complementary mutations at the LC and $HC_{VH\text{-}CH1}$ interface in only one Fab fragment, without any changes being made to the other Fab fragment.

[0371] In some embodiments, the multispecific binding protein is in the 2-in-1 Ig format. In some embodiments, the multispecific binding protein is in the ES form, which is a heterodimeric construct containing two different Fab fragments binding to targets 1 and target 2 fused to the Fc. Heterodimerization is ensured by electrostatic steering mutations in the Fc.

[0372] In some embodiments, the multispecific binding protein is in the κλ-Body form, which is a heterodimeric construct with two different Fab fragments fused to Fc stabilized by heterodimerization mutations: Fab fragment 1 targeting antigen 1 contains kappa LC, and Fab fragment 2 targeting antigen 2 contains lambda LC. **FIG. 13A** is an exemplary representation of one form of a κλ-Body; **FIG. 13B** is an exemplary representation of another κλ-Body.

[0373] In some embodiments, the multispecific binding protein is in Fab Arm Exchange form (antibodies that exchange Fab fragment arms by swapping a heavy chain and attached light chain (half-molecule) with a heavy-light chain pair from another molecule, which results in bispecific antibodies).

[0374] In some embodiments, the multispecific binding protein is in the SEED Body form. The strand-exchange engineered domain (SEED) platform was designed to generate asymmetric and bispecific antibody-like molecules, a capability that expands therapeutic applications of natural antibodies. This protein engineering platform is based on exchanging structurally related sequences of immunoglobulin within the conserved CH3 domains. The SEED design allows efficient generation of AG/GA heterodimers, whereas disfavoring homodimerization of AG and GA SEED CH3 domains. (Muda M. *et al.*, *Protein Eng. Des. Sel.* (2011, 24(5):447-54)).

[0375] In some embodiments, the multispecific binding protein is in the LuZ-Y form, in which a leucine zipper is used to induce heterodimerization of two different HCs. (Wranik, BJ. *et al.*, *J. Biol. Chem.* (2012), 287:43331-9).

[0376] In some embodiments, the multispecific binding protein is in the Cov-X-Body form. In bispecific CovX-Bodies, two different peptides are joined together using a branched azetidinone linker and fused to the scaffold antibody under mild conditions in a site-specific manner. Whereas the pharmacophores are responsible for functional activities, the antibody scaffold imparts long half-life and Ig-like distribution. The pharmacophores can be chemically optimized or replaced with other pharmacophores to generate optimized or unique bispecific antibodies. (Doppalapudi VR *et al.*, *PNAS* (2010), 107(52);22611-22616).

[0377] In some embodiments, the multispecific binding protein is in an Oasc-Fab heterodimeric form that includes Fab fragment binding to target 1, and scFab binding to target 2 fused to Fc. Heterodimerization is ensured by mutations in the Fc.

[0378] In some embodiments, the multispecific binding protein is in a DuetMab form, which is a heterodimeric construct containing two different Fab fragments binding to antigens 1 and 2, and Fc stabilized by heterodimerization mutations. Fab fragments 1 and 2 contain differential S-S bridges that ensure correct LC and HC pairing.

[0379] In some embodiments, the multispecific binding protein is in a CrossmAb form, which is a heterodimeric construct with two different Fab fragments binding to targets 1 and 2, fused to Fc stabilized by heterodimerization. CL and CH1 domains and VH and VL domains are switched, *e.g.*, CH1 is fused in-frame with VL, and CL is fused in-frame with VH.

[0380] In some embodiments, the multispecific binding protein is in a Fit-Ig form, which is a homodimeric construct where Fab fragment binding to antigen 2 is fused to the N terminus of HC of Fab fragment that binds to antigen 1. The construct contains wild-type Fc.

[0381] Individual components of the multispecific binding proteins are described in more detail below.

NKG2D-Binding Site

[0382] Upon binding to the NKG2D receptor and CD16 receptor on natural killer cells, and CLEC12A, the multispecific binding proteins can engage more than one kind of NK-activating receptor, and may block the binding of natural ligands to NKG2D. In certain embodiments, the proteins can agonize NK cells in humans. In some embodiments, the proteins can agonize NK cells in humans and in other species such as rodents and cynomolgus monkeys. In some embodiments, the proteins can agonize NK cells in humans and in other species such as cynomolgus monkeys.

[0383] **Table 1** lists peptide sequences of heavy chain variable domains and light chain variable domains that, in combination, can bind to NKG2D. In some embodiments, the heavy chain variable domain and the light chain variable domain are arranged in Fab format. In some embodiments, the heavy chain variable domain and the light chain variable domain are fused together to form an scFv.

[0384] The NKG2D binding sites listed in Table 1 can vary in their binding affinity to NKG2D, nevertheless, they all activate human NK cells.

[0385] Unless indicated otherwise, the CDR sequences provided in Table 1 are determined under Kabat numbering.

Table 1

Clones	Heavy chain variable region amino acid sequence	Light chain variable region amino acid sequence
ADI-27705	QVQLQQWGAGLLKPSETLSLTCAVYGG SFSGYYWSWIRQPPGKGLEWIGEIDHSG STNYNPSLKSRVTISVDTSKNQFSLKLSS VTAADTAVYYCARARGPWSFDPWGQG TLVTVSS (SEQ ID NO:1) CDR1 (SEQ ID NO:2) – GSFSGYYWS CDR2 (SEQ ID NO:3) – EIDHSGSTNYNPSLKS CDR3 (SEQ ID NO:4) – ARARGPWSFDP	DIQMTQSPSTLSASVGDRVTITCRAS QSISSWLAWYQQKPGKAPKLLIYKA SSLESGVPSRFSGSGSGTEFTLTISSL QPDDFATYYCQQYNSYPITFGGGTK VEIK (SEQ ID NO:5)
ADI-27724	QVQLQQWGAGLLKPSETLSLTCAVYGG SFSGYYWSWIRQPPGKGLEWIGEIDHSG STNYNPSLKSRVTISVDTSKNQFSLKLSS VTAADTAVYYCARARGPWSFDPWGQG TLVTVSS (SEQ ID NO:1)	EIVLTQSPGTLSLSPGERATLSCRASQ SVSSSYLAWYQQKPGQAPRLLIYGA SSRATGIPDRFSGSGSGTDFTLTISRL EPEDFAVYYCQQYGSSPITFGGGTK VEIK (SEQ ID NO:6)
ADI-27740 (A40)	QVQLQQWGAGLLKPSETLSLTCAVYGG SFSGYYWSWIRQPPGKGLEWIGEIDHSG STNYNPSLKSRVTISVDTSKNQFSLKLSS VTAADTAVYYCARARGPWSFDPWGQG TLVTVSS (SEQ ID NO:1)	DIQMTQSPSTLSASVGDRVTITCRAS QSIGSWLAWYQQKPGKAPKLLIYKA SSLESGVPSRFSGSGSGTEFTLTISSL QPDDFATYYCQQYHSFYTFGGGTK VEIK (SEQ ID NO:7)
ADI-27741	QVQLQQWGAGLLKPSETLSLTCAVYGG SFSGYYWSWIRQPPGKGLEWIGEIDHSG STNYNPSLKSRVTISVDTSKNQFSLKLSS VTAADTAVYYCARARGPWSFDPWGQG TLVTVSS (SEQ ID NO:1)	DIQMTQSPSTLSASVGDRVTITCRAS QSIGSWLAWYQQKPGKAPKLLIYKA SSLESGVPSRFSGSGSGTEFTLTISSL QPDDFATYYCQQSNSYYTFGGGTK VEIK (SEQ ID NO:8)
ADI-27743	QVQLQQWGAGLLKPSETLSLTCAVYGG SFSGYYWSWIRQPPGKGLEWIGEIDHSG	DIQMTQSPSTLSASVGDRVTITCRAS QSISSWLAWYQQKPGKAPKLLIYKA

Table 1		
Clones	**Heavy chain variable region amino acid sequence**	**Light chain variable region amino acid sequence**
	STNYNPSLKSRVTISVDTSKNQFSLKLSS VTAADTAVYYCARARGPWSFDPWGQG TLVTVSS (SEQ ID NO:1)	SSLESGVPSRFSGSGSGTEFTLTISSL QPDDFATYYCQQYNSYPTFGGGTK VEIK (SEQ ID NO:9)
ADI-28153	QVQLQQWGAGLLKPSETLSLTCAVYGG SFSGYYWSWIRQPPGKGLEWIGEIDHSG STNYNPSLKSRVTISVDTSKNQFSLKLSS VTAADTAVYYCARARGPWGFDPWGQG TLVTVSS (SEQ ID NO:10)	ELQMTQSPSSLSASVGDRVTITCRTS QSISSYLNWYQQKPGQPPKLLIYWA STRESGVPDRFSGSGSGTDFTLTISSL QPEDSATYYCQQSYDIPYTFGQGTK LEIK (SEQ ID NO:11)
ADI-28226 (C26)	QVQLQQWGAGLLKPSETLSLTCAVYGG SFSGYYWSWIRQPPGKGLEWIGEIDHSG STNYNPSLKSRVTISVDTSKNQFSLKLSS VTAADTAVYYCARARGPWSFDPWGQG TLVTVSS (SEQ ID NO:1)	DIQMTQSPSTLSASVGDRVTITCRAS QSISSWLAWYQQKPGKAPKLLIYKA SSLESGVPSRFSGSGSGTEFTLTISSL QPDDFATYYCQQYGSFPITFGGGTK VEIK (SEQ ID NO:12)
ADI-28154	QVQLQQWGAGLLKPSETLSLTCAVYGG SFSGYYWSWIRQPPGKGLEWIGEIDHSG STNYNPSLKSRVTISVDTSKNQFSLKLSS VTAADTAVYYCARARGPWSFDPWGQG TLVTVSS (SEQ ID NO:1)	DIQMTQSPSTLSASVGDRVTITCRAS QSISSWLAWYQQKPGKAPKLLIYKA SSLESGVPSRFSGSGSGTDFTLTISSL QPDDFATYYCQQSKEVPWTFGQGT KVEIK (SEQ ID NO:13)
ADI-29399	QVQLQQWGAGLLKPSETLSLTCAVYGG SFSGYYWSWIRQPPGKGLEWIGEIDHSG STNYNPSLKSRVTISVDTSKNQFSLKLSS VTAADTAVYYCARARGPWSFDPWGQG TLVTVSS (SEQ ID NO:1)	DIQMTQSPSTLSASVGDRVTITCRAS QSISSWLAWYQQKPGKAPKLLIYKA SSLESGVPSRFSGSGSGTEFTLTISSL QPDDFATYYCQQYNSFPTFGGGTKV EIK (SEQ ID NO:14)
ADI-29401	QVQLQQWGAGLLKPSETLSLTCAVYGG SFSGYYWSWIRQPPGKGLEWIGEIDHSG STNYNPSLKSRVTISVDTSKNQFSLKLSS VTAADTAVYYCARARGPWSFDPWGQG TLVTVSS (SEQ ID NO:1)	DIQMTQSPSTLSASVGDRVTITCRAS QSIGSWLAWYQQKPGKAPKLLIYKA SSLESGVPSRFSGSGSGTEFTLTISSL QPDDFATYYCQQYDIYPTFGGGTKV EIK (SEQ ID NO:15)

Table 1		
Clones	**Heavy chain variable region amino acid sequence**	**Light chain variable region amino acid sequence**
ADI-29403	QVQLQQWGAGLLKPSETLSLTCAVYGG SFSGYYWSWIRQPPGKGLEWIGEIDHSG STNYNPSLKSRVTISVDTSKNQFSLKLSS VTAADTAVYYCARARGPWSFDPWGQG TLVTVSS (SEQ ID NO:1)	DIQMTQSPSTLSASVGDRVTITCRAS QSISSWLAWYQQKPGKAPKLLIYKA SSLESGVPSRFSGSGSGTEFTLTISSL QPDDFATYYCQQYDSYPTFGGGTK VEIK (SEQ ID NO:16)
ADI-29405	QVQLQQWGAGLLKPSETLSLTCAVYGG SFSGYYWSWIRQPPGKGLEWIGEIDHSG STNYNPSLKSRVTISVDTSKNQFSLKLSS VTAADTAVYYCARARGPWSFDPWGQG TLVTVSS (SEQ ID NO:1)	DIQMTQSPSTLSASVGDRVTITCRAS QSISSWLAWYQQKPGKAPKLLIYKA SSLESGVPSRFSGSGSGTEFTLTISSL QPDDFATYYCQQYGSFPTFGGGTKV EIK (SEQ ID NO:17)
ADI-29407	QVQLQQWGAGLLKPSETLSLTCAVYGG SFSGYYWSWIRQPPGKGLEWIGEIDHSG STNYNPSLKSRVTISVDTSKNQFSLKLSS VTAADTAVYYCARARGPWSFDPWGQG TLVTVSS (SEQ ID NO:1)	DIQMTQSPSTLSASVGDRVTITCRAS QSISSWLAWYQQKPGKAPKLLIYKA SSLESGVPSRFSGSGSGTEFTLTISSL QPDDFATYYCQQYQSFPTFGGGTKV EIK (SEQ ID NO:18)
ADI-29419	QVQLQQWGAGLLKPSETLSLTCAVYGG SFSGYYWSWIRQPPGKGLEWIGEIDHSG STNYNPSLKSRVTISVDTSKNQFSLKLSS VTAADTAVYYCARARGPWSFDPWGQG TLVTVSS (SEQ ID NO:1)	DIQMTQSPSTLSASVGDRVTITCRAS QSISSWLAWYQQKPGKAPKLLIYKA SSLESGVPSRFSGSGSGTEFTLTISSL QPDDFATYYCQQYSSFSTFGGGTKV EIK (SEQ ID NO:19)
ADI-29421	QVQLQQWGAGLLKPSETLSLTCAVYGG SFSGYYWSWIRQPPGKGLEWIGEIDHSG STNYNPSLKSRVTISVDTSKNQFSLKLSS VTAADTAVYYCARARGPWSFDPWGQG TLVTVSS (SEQ ID NO:1)	DIQMTQSPSTLSASVGDRVTITCRAS QSISSWLAWYQQKPGKAPKLLIYKA SSLESGVPSRFSGSGSGTEFTLTISSL QPDDFATYYCQQYESYSTFGGGTKV EIK (SEQ ID NO:20)
ADI-29424	QVQLQQWGAGLLKPSETLSLTCAVYGG SFSGYYWSWIRQPPGKGLEWIGEIDHSG STNYNPSLKSRVTISVDTSKNQFSLKLSS	DIQMTQSPSTLSASVGDRVTITCRAS QSISSWLAWYQQKPGKAPKLLIYKA SSLESGVPSRFSGSGSGTEFTLTISSL

Table 1		
Clones	**Heavy chain variable region amino acid sequence**	**Light chain variable region amino acid sequence**
	VTAADTAVYYCARARGPWSFDPWGQG TLVTVSS (SEQ ID NO:1)	QPDDFATYYCQQYDSFITFGGGTKV EIK (SEQ ID NO:21)
ADI-29425	QVQLQQWGAGLLKPSETLSLTCAVYGG SFSGYYWSWIRQPPGKGLEWIGEIDHSG STNYNPSLKSRVTISVDTSKNQFSLKLSS VTAADTAVYYCARARGPWSFDPWGQG TLVTVSS (SEQ ID NO:1)	DIQMTQSPSTLSASVGDRVTITCRAS QSISSWLAWYQQKPGKAPKLLIYKA SSLESGVPSRFSGSGSGTEFTLTISSL QPDDFATYYCQQYQSYPTFGGGTK VEIK (SEQ ID NO:22)
ADI-29426	QVQLQQWGAGLLKPSETLSLTCAVYGG SFSGYYWSWIRQPPGKGLEWIGEIDHSG STNYNPSLKSRVTISVDTSKNQFSLKLSS VTAADTAVYYCARARGPWSFDPWGQG TLVTVSS (SEQ ID NO:1)	DIQMTQSPSTLSASVGDRVTITCRAS QSIGSWLAWYQQKPGKAPKLLIYKA SSLESGVPSRFSGSGSGTEFTLTISSL QPDDFATYYCQQYHSFPTFGGGTKV EIK (SEQ ID NO:23)
ADI-29429	QVQLQQWGAGLLKPSETLSLTCAVYGG SFSGYYWSWIRQPPGKGLEWIGEIDHSG STNYNPSLKSRVTISVDTSKNQFSLKLSS VTAADTAVYYCARARGPWSFDPWGQG TLVTVSS (SEQ ID NO:1)	DIQMTQSPSTLSASVGDRVTITCRAS QSIGSWLAWYQQKPGKAPKLLIYKA SSLESGVPSRFSGSGSGTEFTLTISSL QPDDFATYYCQQYELYSYTFGGGTK VEIK (SEQ ID NO:24)
ADI-29447 (F47)	QVQLQQWGAGLLKPSETLSLTCAVYGG SFSGYYWSWIRQPPGKGLEWIGEIDHSG STNYNPSLKSRVTISVDTSKNQFSLKLSS VTAADTAVYYCARARGPWSFDPWGQG TLVTVSS (SEQ ID NO:1)	DIQMTQSPSTLSASVGDRVTITCRAS QSISSWLAWYQQKPGKAPKLLIYKA SSLESGVPSRFSGSGSGTEFTLTISSL QPDDFATYYCQQYDTFITFGGGTKV EIK (SEQ ID NO:25)
ADI-27727	QVQLVQSGAEVKKPGSSVKVSCKASGG TFSSYAISWVRQAPGQGLEWMGGIIPIFG TANYAQKFQGRVTITADESTSTAYMELS SLRSEDTAVYYCARGDSSIRHAYYYYG MDVWGQGTTVTVSS (SEQ ID NO:26)	DIVMTQSPDSLAVSLGERATINCKSS QSVLYSSNNKNYLAWYQQKPGQPP KLLIYWASTRESGVPDRFSGSGSGTD FTLTISSLQAEDVAVYYCQQYYSTPI TFGGGTKVEIK (SEQ ID NO:32) CDR1 (SEQ ID NO:33) –

Table 1		
Clones	**Heavy chain variable region amino acid sequence**	**Light chain variable region amino acid sequence**
	CDR1– GTFSSYAIS (non-Kabat) (SEQ ID NO:27) or SYAIS (SEQ ID NO:28) CDR2 (SEQ ID NO:29) – GIIPIFGTANYAQKFQG CDR3 – ARGDSSIRHAYYYYGMDV (non-Kabat) (SEQ ID NO:30) or GDSSIRHAYYYYGMDV (SEQ ID NO:31)	KSSQSVLYSSNNKNYLA CDR2 (SEQ ID NO:34) – WASTRES CDR3 (SEQ ID NO:35) – QQYYSTPIT
ADI-29443 (F43)	QLQLQESGPGLVKPSETLSLTCTVSGGSI SSSSYYWGWIRQPPGKGLEWIGSIYYSGS TYYNPSLKSRVTISVDTSKNQFSLKLSSV TAADTAVYYCARGSDRFHPYFDYWGQG TLVTVSS (SEQ ID NO:36) CDR1– GSISSSSYYWG (non-Kabat) (SEQ ID NO:37) or SSSYYWG (SEQ ID NO:38) CDR2 (SEQ ID NO:39) – SIYYSGSTYYNPSLKS CDR3 – ARGSDRFHPYFDY (non-Kabat) (SEQ ID NO:40) or GSDRFHPYFDY (SEQ ID NO:41)	EIVLTQSPATLSLSPGERATLSCRASQ SVSRYLAWYQQKPGQAPRLLIYDAS NRATGIPARFSGSGSGTDFTLTISSLE PEDFAVYYCQQFDTWPPTFGGGTKV EIK (SEQ ID NO:42) CDR1 (SEQ ID NO:43) – RASQSVSRYLA CDR2 (SEQ ID NO:44) – DASNRAT CDR3 (SEQ ID NO:45) – QQFDTWPPT
ADI-29404 (F04)	QVQLQQWGAGLLKPSETLSLTCAVYGG SFSGYYWSWIRQPPGKGLEWIGEIDHSG STNYNPSLKSRVTISVDTSKNQFSLKLSS VTAADTAVYYCARARGPWSFDPWGQG TLVTVSS (SEQ ID NO:1)	DIQMTQSPSTLSASVGDRVTITCRAS QSISSWLAWYQQKPGKAPKLLIYKA SSLESGVPSRFSGSGSGTEFTLTISSL QPDDFATYYCEQYDSYPTFGGGTKV EIK (SEQ ID NO:46)
ADI-28200	QVQLVQSGAEVKKPGSSVKVSCKASGG TFSSYAISWVRQAPGQGLEWMGGIIPIFG TANYAQKFQGRVTITADESTSTAYMELS SLRSEDTAVYYCARRGRKASGSFYYYY GMDVWGQGTTVTVSS (SEQ ID NO:47) CDR1 (SEQ ID NO:27) – GTFSSYAIS	DIVMTQSPDSLAVSLGERATINCESS QSLLNSGNQKNYLTWYQQKPGQPP KPLIYWASTRESGVPDRFSGSGSGTD FTLTISSLQAEDVAVYYCQNDYSYP YTFGQGTKLEIK (SEQ ID NO:49) CDR1 (SEQ ID NO:50) – ESSQSLLNSGNQKNYLT

Table 1		
Clones	**Heavy chain variable region amino acid sequence**	**Light chain variable region amino acid sequence**
	CDR2 (SEQ ID NO:29) – GIIPIFGTANYAQKFQG CDR3 (SEQ ID NO:48) – ARRGRKASGSFYYYYGMDV	CDR2 (SEQ ID NO:34) – WASTRES CDR3 (SEQ ID NO:51) – QNDYSYPYT
ADI-29379 (E79)	QVQLVQSGAEVKKPGASVKVSCKASGY TFTSYYMHWVRQAPGQGLEWMGIINPS GGSTSYAQKFQGRVTMTRDTSTSTVYM ELSSLRSEDTAVYYCARGAPNYGDTTHD YYYMDVWGKGTTVTVSS (SEQ ID NO:52) CDR1 (SEQ ID NO:53) – YTFTSYYMH (non-Kabat) or SYYMH (SEQ ID NO:54) CDR2 (SEQ ID NO:55) - IINPSGGSTSYAQKFQG CDR3 – ARGAPNYGDTTHDYYYMDV (non-Kabat) (SEQ ID NO:56) or GAPNYGDTTHDYYYMDV (SEQ ID NO:57)	EIVMTQSPATLSVSPGERATLSCRAS QSVSSNLAWYQQKPGQAPRLLIYGA STRATGIPARFSGSGSGTEFTLTISSL QSEDFAVYYCQQYDDWPFTFGGGT KVEIK (SEQ ID NO:58) CDR1 (SEQ ID NO:59) - RASQSVSSNLA CDR2 (SEQ ID NO:60) - GASTRAT CDR3 (SEQ ID NO:61) - QQYDDWPFT
ADI-29463 (F63)	QVQLVQSGAEVKKPGASVKVSCKASGY TFTGYYMHWVRQAPGQGLEWMGWINP NSGGTNYAQKFQGRVTMTRDTSISTAY MELSRLRSDDTAVYYCARDTGEYYDTD DHGMDVWGQGTTVTVSS (SEQ ID NO:62) CDR1 - YTFTGYYMH (non-Kabat) (SEQ ID NO:63) or GYYMH (SEQ ID NO:64) CDR2 (SEQ ID NO:65) - WINPNSGGTNYAQKFQG CDR3 – ARDTGEYYDTDDHGMDV (non-Kabat) (SEQ ID NO:66) or DTGEYYDTDDHGMDV (SEQ ID NO:67)	EIVLTQSPGTLSLSPGERATLSCRASQ SVSSNLAWYQQKPGQAPRLLIYGAS TRATGIPARFSGSGSGTEFTLTISSLQ SEDFAVYYCQQDDYWPPTFGGGTK VEIK (SEQ ID NO:68) CDR1 (SEQ ID NO:59) - RASQSVSSNLA CDR2 (SEQ ID NO:60) - GASTRAT CDR3 (SEQ ID NO:69) - QQDDYWPPT
ADI-27744 (A44)	EVQLLESGGGLVQPGGSLRLSCAASGFT FSSYAMSWVRQAPGKGLEWVSAISGSG GSTYYADSVKGRFTISRDNSKNTLYLQM	DIQMTQSPSSVSASVGDRVTITCRAS QGIDSWLAWYQQKPGKAPKLLIYA ASSLQSGVPSRFSGSGSGTDFTLTISS

Table 1		
Clones	**Heavy chain variable region amino acid sequence**	**Light chain variable region amino acid sequence**
	NSLRAEDTAVYYCAKDGGYYDSGAGD YWGQGTLVTVSS (SEQ ID NO:70) CDR1– FTFSSYAMS (non-Kabat) (SEQ ID NO:71) or SYAMS (SEQ ID NO:115) CDR2 (SEQ ID NO:72) - AISGSGGSTYYADSVKG CDR3 - AKDGGYYDSGAGDY (non-Kabat) (SEQ ID NO:73) or DGGYYDSGAGDY (SEQ ID NO:74)	LQPEDFATYYCQQGVSYPRTFGGGT KVEIK (SEQ ID NO:75) CDR1 (SEQ ID NO:76) - RASQGIDSWLA CDR2 (SEQ ID NO:77) - AASSLQS CDR3 (SEQ ID NO:78) - QQGVSYPRT
ADI-27749 (A49)	EVQLVESGGGLVKPGGSLRLSCAASGFT FSSYSMNWVRQAPGKGLEWVSSISSSSS YIYYADSVKGRFTISRDNAKNSLYLQMN SLRAEDTAVYYCARGAPMGAAAGWFD PWGQGTLVTVSS (SEQ ID NO:79) CDR1 - FTFSSYSMN (SEQ ID NO:80) (non-Kabat) or SYSMN (SEQ ID NO:81) CDR2 (SEQ ID NO:82) - SISSSSSYIYYADSVKG CDR3– ARGAPMGAAAGWFDP (SEQ ID NO:83) (non-Kabat) or GAPMGAAAGWFDP (SEQ ID NO:84)	DIQMTQSPSSVSASVGDRVTITCRAS QGISSWLAWYQQKPGKAPKLLIYAA SSLQSGVPSRFSGSGSGTDFTLTISSL QPEDFATYYCQQGVSFPRTFGGGTK VEIK (SEQ ID NO:85) CDR1 (SEQ ID NO:86) - RASQGISSWLA CDR2 (SEQ ID NO:77) - AASSLQS CDR3 (SEQ ID NO:87) - QQGVSFPRT
	scFv (VL-VH) with Q44C in VH and G100C in VL, linker italicized: DIQMTQSPSSVSASVGDRVTITCRASQGISSWLAWYQQKPGKAPKLLIYAASSLQS GVPSRFSGSGSGTDFTLTISSLQPEDFATYYCQQGVSFPRTFGCGTKVEIK*GGGGSG GGGSGGGGSGGGGS*EVQLVESGGGLVKPGGSLRLSCAASGFTFSSYSMNWVRQA PGKCLEWVSSISSSSSYIYYADSVKGRFTISRDNAKNSLYLQMNSLRAEDTAVYYC ARGAPMGAAAGWFDPWGQGTLVTVSS (SEQ ID NO:88)	
ADI-29378 (E78)	QVQLVQSGAEVKKPGASVKVSCKASGY TFTSYYMHWVRQAPGQGLEWMGIINPS GGSTSYAQKFQGRVTMTRDTSTSTVYM ELSSLRSEDTAVYYCAREGAGFAYGMD YYYMDVWGKGTTVTVSS	EIVLTQSPATLSLSPGERATLSCRASQ SVSSYLAWYQQKPGQAPRLLIYDAS NRATGIPARFSGSGSGTDFTLTISSLE PEDFAVYYCQQSDNWPFTFGGGTK VEIK

Table 1		
Clones	**Heavy chain variable region amino acid sequence**	**Light chain variable region amino acid sequence**
	(SEQ ID NO:89) CDR1 – YTFTSYYMH (SEQ ID NO:53) (non-Kabat) or SYYMH (SEQ ID NO:54) CDR2 (SEQ ID NO:55) - IINPSGGSTSYAQKFQG CDR3 – AREGAGFAYGMDYYYMDV (SEQ ID NO:90) (non-Kabat) or EGAGFAYGMDYYYMDV (SEQ ID NO:91)	(SEQ ID NO:92) CDR1 (SEQ ID NO:93) - RASQSVSSYLA CDR2 (SEQ ID NO:44) - DASNRAT CDR3 (SEQ ID NO:94) - QQSDNWPFT
A49MI	EVQLVESGGGLVKPGGSLRLSCAASGFTFSSYSMNWVRQAPGKGLEWVSSISSSSSYIYYADSVKGRFTISRDNAKNSLYLQMNSLRAEDTAVYYCARGAP**I**GAAAGWFDPWGQGTLVTVSS (SEQ ID NO:95) CDR1: FTFSSYSMN (SEQ ID NO:80) (non-Kabat) or SYSMN (SEQ ID NO:81) CDR2: SISSSSSYIYYADSVKG (SEQ ID NO:82) CDR3: ARGAP**I**GAAAGWFDP (SEQ ID NO:96) (non-Kabat) or GAP**I**GAAAGWFDP (SEQ ID NO:97)	DIQMTQSPSSVSASVGDRVTITCRASQGISSWLAWYQQKPGKAPKLLIYAASSLQSGVPSRFSGSGSGTDFTLTISSLQPEDFATYYCQQGVSFPRTFGGGTKVEIK (SEQ ID NO:85) CDR1 (SEQ ID NO:86) - RASQGISSWLA CDR2 (SEQ ID NO:77) - AASSLQS CDR3 (SEQ ID NO:87) - QQGVSFPRT
A49MQ	EVQLVESGGGLVKPGGSLRLSCAASGFTFSSYSMNWVRQAPGKGLEWVSSISSSSSYIYYADSVKGRFTISRDNAKNSLYLQMNSLRAEDTAVYYCARGAP**Q**GAAAGWFDPWGQGTLVTVSS (SEQ ID NO:98) CDR1: FTFSSYSMN (SEQ ID NO:80) (non-Kabat) or SYSMN (SEQ ID NO:81) CDR2: SISSSSSYIYYADSVKG (SEQ ID NO:82) CDR3 - ARGAP**Q**GAAAGWFDP (SEQ ID NO:99) (non-Kabat) or GAP**Q**GAAAGWFDP (SEQ ID NO:100)	DIQMTQSPSSVSASVGDRVTITCRASQGISSWLAWYQQKPGKAPKLLIYAASSLQSGVPSRFSGSGSGTDFTLTISSLQPEDFATYYCQQGVSFPRTFGGGTKVEIK (SEQ ID NO:85) CDR1 (SEQ ID NO:86) - RASQGISSWLA CDR2 (SEQ ID NO:77) - AASSLQS CDR3 (SEQ ID NO:87) - QQGVSFPRT

Table 1		
Clones	**Heavy chain variable region amino acid sequence**	**Light chain variable region amino acid sequence**
A49ML	EVQLVESGGGLVKPGGSLRLSCAASGFT FSSYSMNWVRQAPGKGLEWVSSISSSSS YIYYADSVKGRFTISRDNAKNSLYLQMN SLRAEDTAVYYCARGAP**L**GAAAGWFDP WGQGTLVTVSS (SEQ ID NO:101) CDR1: FTFSSYSMN (SEQ ID NO:80) (non-Kabat) or SYSMN (SEQ ID NO:81) CDR2: SISSSSSYIYYADSVKG (SEQ ID NO:82) CDR3 – ARGAP**L**GAAAGWFDP (SEQ ID NO:102) (non-Kabat) or GAP**L**GAAAGWFDP (SEQ ID NO:103)	DIQMTQSPSSVSASVGDRVTITCRAS QGISSWLAWYQQKPGKAPKLLIYAA SSLQSGVPSRFSGSGSGTDFTLTISSL QPEDFATYYCQQGVSFPRTFGGGTK VEIK (SEQ ID NO:85) CDR1 (SEQ ID NO:86) - RASQGISSWLA CDR2 (SEQ ID NO:77) - AASSLQS CDR3 (SEQ ID NO:87) - QQGVSFPRT
A49MF	EVQLVESGGGLVKPGGSLRLSCAASGFT FSSYSMNWVRQAPGKGLEWVSSISSSSS YIYYADSVKGRFTISRDNAKNSLYLQMN SLRAEDTAVYYCARGAP**F**GAAAGWFDP WGQGTLVTVSS (SEQ ID NO:104) CDR1: FTFSSYSMN (SEQ ID NO:80) (non-Kabat) or SYSMN (SEQ ID NO:81) CDR2: SISSSSSYIYYADSVKG (SEQ ID NO:82) CDR3 - ARGAP**F**GAAAGWFDP (SEQ ID NO:105) (non-Kabat) or GAP**F**GAAAGWFDP (SEQ ID NO:106)	DIQMTQSPSSVSASVGDRVTITCRAS QGISSWLAWYQQKPGKAPKLLIYAA SSLQSGVPSRFSGSGSGTDFTLTISSL QPEDFATYYCQQGVSFPRTFGGGTK VEIK (SEQ ID NO:85) CDR1 (SEQ ID NO:86) - RASQGISSWLA CDR2 (SEQ ID NO:77) - AASSLQS CDR3 (SEQ ID NO:87) - QQGVSFPRT
A49MV	EVQLVESGGGLVKPGGSLRLSCAASGFT FSSYSMNWVRQAPGKGLEWVSSISSSSS YIYYADSVKGRFTISRDNAKNSLYLQMN SLRAEDTAVYYCARGAP**V**GAAAGWFDP WGQGTLVTVSS (SEQ ID NO:107) CDR1: FTFSSYSMN (SEQ ID NO:80) (non-Kabat) or SYSMN (SEQ ID NO:81)	DIQMTQSPSSVSASVGDRVTITCRAS QGISSWLAWYQQKPGKAPKLLIYAA SSLQSGVPSRFSGSGSGTDFTLTISSL QPEDFATYYCQQGVSFPRTFGGGTK VEIK (SEQ ID NO:85) CDR1 (SEQ ID NO:86) - RASQGISSWLA

Table 1		
Clones	**Heavy chain variable region amino acid sequence**	**Light chain variable region amino acid sequence**
	CDR2: SISSSSSYIYYADSVKG (SEQ ID NO:82) CDR3– ARGAP**V**GAAAGWFDP (SEQ ID NO:108) (non-Kabat) or GAP**V**GAAAGWFDP (SEQ ID NO:109)	CDR2 (SEQ ID NO:77) - AASSLQS CDR3 (SEQ ID NO:87) - QQGVSFPRT
A49-consensus	EVQLVESGGGLVKPGGSLRLSCAASGFTFSSYSMNWVRQAPGKGLEWVSSISSSSSYIYYADSVKGRFTISRDNAKNSLYLQMNSLRAEDTAVYYCARGAP**X**GAAAGWFDPWGQGTLVTVSS, wherein X is M, L, I, V, Q, or F (SEQ ID NO:110) CDR1: FTFSSYSMN (SEQ ID NO:80) (non-Kabat) or SYSMN (SEQ ID NO:81) CDR2: SISSSSSYIYYADSVKG (SEQ ID NO:82) CDR3– ARGAP**X**GAAAGWFDP (SEQ ID NO:111) (non-Kabat) or GAP**X**GAAAGWFDP (SEQ ID NO:112), wherein X is M, L, I, V, Q, or F	DIQMTQSPSSVSASVGDRVTITCRASQGISSWLAWYQQKPGKAPKLLIYAASSLQSGVPSRFSGSGSGTDFTLTISSLQPEDFATYYCQQGVSFPRTFGGGTKVEIK (SEQ ID NO:85) CDR1 (SEQ ID NO:86) - RASQGISSWLA CDR2 (SEQ ID NO:77) - AASSLQS CDR3 (SEQ ID NO:87) - QQGVSFPRT
NKG2D binder in US 9,273,136	QVQLVESGGGLVKPGGSLRLSCAASGFTFSSYGMHWVRQAPGKGLEWVAFIRYDGSNKYYADSVKGRFTISRDNSKNTLYLQMNSLRAEDTAVYYCAKDRGLGDGTYFDYWGQGTTVTVSS (SEQ ID NO:113)	QSALTQPASVSGSPGQSITISCSGSSSNIGNNAVNWYQQLPGKAPKLLIYYDDLLPSGVSDRFSGSKSGTSAFLAISGLQSEDEADYYCAAWDDSLNGPVFGGGTKLTVL (SEQ ID NO:114)
NKG2D binder in US 7,879,985	QVHLQESGPGLVKPSETLSLTCTVSDDSISSYYWSWIRQPPGKGLEWIGHISYSGSANYNPSLKSRVTISVDTSKNQFSLKLSSVTAADTAVYYCANWDDAFNIWGQGTMVTVSS (SEQ ID NO:116)	EIVLTQSPGTLSLSPGERATLSCRASQSVSSSYLAWYQQKPGQAPRLLIYGASSRATGIPDRFSGSGSGTDFTLTISRLEPEDFAVYYCQQYGSSPWTFGQGTKVEIK (SEQ ID NO:117)

[0386] In certain embodiments, the first antigen-binding site that binds NKG2D (*e.g.*, human NKG2D) comprises an antibody heavy chain variable domain (VH) that comprises an amino acid sequence at least 90% (*e.g.*, at least 91%, at least 92%, at least 93%, at least 94%, at

least 95%, at least 96%, at least 97%, at least 98%, at least 99%, or 100%) identical to the VH of an antibody disclosed in Table 1, and an antibody light chain variable domain (VL) that comprises an amino acid sequence at least 90% (*e.g.*, at least 91%, at least 92%, at least 93%, at least 94%, at least 95%, at least 96%, at least 97%, at least 98%, at least 99%, or 100%) identical to the VL of the same antibody disclosed in Table 1. In certain embodiments, the first antigen-binding site comprises the heavy chain CDR1, CDR2, and CDR3 and the light chain CDR1, CDR2, and CDR3, determined under Kabat (*see* Kabat *et al.*, (1991) Sequences of Proteins of Immunological Interest, NIH Publication No. 91-3242, Bethesda), Chothia (see, *e.g.*, Chothia C & Lesk A M, (1987), J. Mol. Biol. 196: 901-917), MacCallum (*see* MacCallum R M *et al.*, (1996) J. Mol. Biol. 262: 732-745), or any other CDR determination method known in the art, of the VH and VL sequences of an antibody discloses in Table 1. In certain embodiments, the first antigen-binding site comprises the heavy chain CDR1, CDR2, and CDR3 and the light chain CDR1, CDR2, and CDR3 of an antibody disclosed in Table 1.

[0387] In certain embodiments, the first antigen-binding site that binds to NKG2D comprises a heavy chain variable domain derived from SEQ ID NO:1, such as by having an amino acid sequence at least 90% (*e.g.*, at least 90%, at least 91%, at least 92%, at least 93%, at least 94%, at least 95%, at least 96%, at least 97%, at least 98%, at least 99%, or 100%) identical to SEQ ID NO:1, and/or incorporating amino acid sequences identical to the CDR1 (SEQ ID NO:2), CDR2 (SEQ ID NO:3), and CDR3 (SEQ ID NO:4) sequences of SEQ ID NO:1. The heavy chain variable domain related to SEQ ID NO:1 can be coupled with a variety of light chain variable domains to form an NKG2D binding site. For example, the first antigen-binding site that incorporates a heavy chain variable domain related to SEQ ID NO:1 can further incorporate a light chain variable domain selected from the sequences derived from SEQ ID NOs: 5, 6, 7, 8, 9, 12, 13, 14, 15, 16, 17, 18, 19, 20, 21, 22, 23, 24, 25, and 46. For example, the first antigen-binding site incorporates a heavy chain variable domain with amino acid sequences at least 90% (*e.g.*, at least 90%, at least 91%, at least 92%, at least 93%, at least 94%, at least 95%, at least 96%, at least 97%, at least 98%, at least 99%, or 100%) identical to SEQ ID NO:1 and a light chain variable domain with amino acid sequences at least 90% (*e.g.*, at least 90%, at least 91%, at least 92%, at least 93%, at least 94%, at least 95%, at least 96%, at least 97%, at least 98%, at least 99%, or 100%) identical to any one of the sequences selected from SEQ ID NOs: 5, 6, 7, 8, 9, 12, 13, 14, 15, 16, 17, 18, 19, 20, 21, 22, 23, 24, 25, and 46.

[0388] In certain embodiments, the first antigen-binding site that binds NKG2D comprises a VH that comprises an amino acid sequence at least 90% (*e.g.*, at least 91%, at least 92%, at least 93%, at least 94%, at least 95%, at least 96%, at least 97%, at least 98%, at least 99%, or 100%) identical to the amino acid sequence of SEQ ID NO:26, and a VL that comprises an amino acid sequence at least 90% (*e.g.*, at least 91%, at least 92%, at least 93%, at least 94%, at least 95%, at least 96%, at least 97%, at least 98%, at least 99%, or 100%) identical to SEQ ID NO:32. In certain embodiments, the VH comprises CDR1, CDR2, and CDR3 comprising the amino acid sequences of SEQ ID NOs: 27 or 28, 29, and 30 or 31, respectively (*e.g.*, SEQ ID NOs: 27, 29, and 30, respectively, or SEQ ID NOs: 28, 29, and 31, respectively). In certain embodiments, the VL comprises CDR1, CDR2, and CDR3 comprising the amino acid sequences of SEQ ID NOs: 33, 34, and 35, respectively. In certain embodiments, the first antigen-binding site comprises (a) a VH that comprises CDR1, CDR2, and CDR3 comprising the amino acid sequences of SEQ ID NOs: 27 or 28, 29, and 30 or 31, respectively (*e.g.*, SEQ ID NOs: 27, 29, and 30, respectively, or SEQ ID NOs: 28, 29, and 31, respectively); and (b) a VL that comprises CDR1, CDR2, and CDR3 comprising the amino acid sequences of SEQ ID NOs: 33, 34, and 35, respectively.

[0389] In certain embodiments, the first antigen-binding site that binds NKG2D comprises a VH that comprises an amino acid sequence at least 90% (*e.g.*, at least 91%, at least 92%, at least 93%, at least 94%, at least 95%, at least 96%, at least 97%, at least 98%, at least 99%, or 100%) identical to the amino acid sequence of SEQ ID NO:36, and a VL that comprises an amino acid sequence at least 90% (*e.g.*, at least 91%, at least 92%, at least 93%, at least 94%, at least 95%, at least 96%, at least 97%, at least 98%, at least 99%, or 100%) identical to SEQ ID NO:42. In certain embodiments, the VH comprises CDR1, CDR2, and CDR3 comprising the amino acid sequences of SEQ ID NOs: 37 or 38, 39, and 40 or 41, respectively (*e.g.*, SEQ ID NOs: 37, 39, and 40, respectively, or SEQ ID NOs: 38, 39, and 41, respectively). In certain embodiments, the VL comprises CDR1, CDR2, and CDR3 comprising the amino acid sequences of SEQ ID NOs: 43, 44, and 45, respectively. In certain embodiments, the first antigen-binding site comprises (a) a VH that comprises CDR1, CDR2, and CDR3 comprising the amino acid sequences of SEQ ID NOs: 37 or 38, 39, and 40 or 41, respectively (*e.g.*, SEQ ID NOs: 37, 39, and 40, respectively, or SEQ ID NOs: 38, 39, and 41, respectively); and (b) a VL that comprises

CDR1, CDR2, and CDR3 comprising the amino acid sequences of SEQ ID NOs: 43, 44, and 45, respectively.

[0390] In certain embodiments, the first antigen-binding site that binds NKG2D comprises a VH that comprises an amino acid sequence at least 90% (*e.g.*, at least 91%, at least 92%, at least 93%, at least 94%, at least 95%, at least 96%, at least 97%, at least 98%, at least 99%, or 100%) identical to the amino acid sequence of SEQ ID NO:47, and a VL that comprises an amino acid sequence at least 90% (*e.g.*, at least 91%, at least 92%, at least 93%, at least 94%, at least 95%, at least 96%, at least 97%, at least 98%, at least 99%, or 100%) identical to SEQ ID NO:49. In certain embodiments, the VH comprises CDR1, CDR2, and CDR3 comprising the amino acid sequences of SEQ ID NOs: 27, 29, and 48, respectively. In certain embodiments, the VL comprises CDR1, CDR2, and CDR3 comprising the amino acid sequences of SEQ ID NOs: 50, 34, and 51, respectively. In certain embodiments, the first antigen-binding site comprises (a) a VH that comprises CDR1, CDR2, and CDR3 comprising the amino acid sequences of SEQ ID NOs: 27, 29, and 48, respectively; and (b) a VL that comprises CDR1, CDR2, and CDR3 comprising the amino acid sequences of SEQ ID NOs: 50, 34, and 51, respectively.

[0391] In certain embodiments, the first antigen-binding site that binds NKG2D comprises a VH that comprises an amino acid sequence at least 90% (*e.g.*, at least 91%, at least 92%, at least 93%, at least 94%, at least 95%, at least 96%, at least 97%, at least 98%, at least 99%, or 100%) identical to the amino acid sequence of SEQ ID NO:52, and a VL that comprises an amino acid sequence at least 90% (*e.g.*, at least 91%, at least 92%, at least 93%, at least 94%, at least 95%, at least 96%, at least 97%, at least 98%, at least 99%, or 100%) identical to SEQ ID NO:58. In certain embodiments, the VH comprises CDR1, CDR2, and CDR3 comprising the amino acid sequences of SEQ ID NOs: 53 or 54, 55, and 56 or 57, respectively (*e.g.*, SEQ ID NOs: 53, 55, and 56, respectively, or SEQ ID NOs: 54, 55, and 57, respectively). In certain embodiments, the VL comprises CDR1, CDR2, and CDR3 comprising the amino acid sequences of SEQ ID NOs: 59, 60, and 61, respectively. In certain embodiments, the first antigen-binding site comprises (a) a VH that comprises CDR1, CDR2, and CDR3 comprising the amino acid sequences of SEQ ID NOs: 53 or 54, 55, and 56 or 57, respectively (*e.g.*, SEQ ID NOs: 53, 55, and 56, respectively, or SEQ ID NOs: 54, 55, and 57, respectively); and (b) a VL that comprises CDR1, CDR2, and CDR3 comprising the amino acid sequences of SEQ ID NOs: 59, 60, and 61, respectively.

[0392] In certain embodiments, the first antigen-binding site that binds NKG2D comprises a VH that comprises an amino acid sequence at least 90% (*e.g.*, at least 91%, at least 92%, at least 93%, at least 94%, at least 95%, at least 96%, at least 97%, at least 98%, at least 99%, or 100%) identical to the amino acid sequence of SEQ ID NO:62, and a VL that comprises an amino acid sequence at least 90% (*e.g.*, at least 91%, at least 92%, at least 93%, at least 94%, at least 95%, at least 96%, at least 97%, at least 98%, at least 99%, or 100%) identical to SEQ ID NO:68. In certain embodiments, the VH comprises CDR1, CDR2, and CDR3 comprising the amino acid sequences of SEQ ID NOs: 63 or 64, 65, and 66 or 67, respectively (*e.g.*, SEQ ID NOs: 63, 65, and 66, respectively, or SEQ ID NOs: 64, 65, and 67, respectively). In certain embodiments, the VL comprises CDR1, CDR2, and CDR3 comprising the amino acid sequences of SEQ ID NOs: 59, 60, and 69, respectively. In certain embodiments, the first antigen-binding site comprises (a) a VH that comprises CDR1, CDR2, and CDR3 comprising the amino acid sequences of SEQ ID NOs: 63 or 64, 65, and 66 or 67, respectively (*e.g.*, SEQ ID NOs: 63, 65, and 66, respectively, or SEQ ID NOs: 64, 65, and 67, respectively); and (b) a VL that comprises CDR1, CDR2, and CDR3 comprising the amino acid sequences of SEQ ID NOs: 59, 60, and 69, respectively.

[0393] In certain embodiments, the first antigen-binding site that binds NKG2D comprises a VH that comprises an amino acid sequence at least 90% (*e.g.*, at least 91%, at least 92%, at least 93%, at least 94%, at least 95%, at least 96%, at least 97%, at least 98%, at least 99%, or 100%) identical to the amino acid sequence of SEQ ID NO:89, and a VL that comprises an amino acid sequence at least 90% (*e.g.*, at least 91%, at least 92%, at least 93%, at least 94%, at least 95%, at least 96%, at least 97%, at least 98%, at least 99%, or 100%) identical to SEQ ID NO:92. In certain embodiments, the VH comprises CDR1, CDR2, and CDR3 comprising the amino acid sequences of SEQ ID NOs: 53 or 54, 55, and 90 or 91, respectively (*e.g.*, SEQ ID NOs: 53, 55, and 90, respectively, or SEQ ID NOs: 54, 55, and 91, respectively). In certain embodiments, the VL comprises CDR1, CDR2, and CDR3 comprising the amino acid sequences of SEQ ID NOs: 93, 44, and 94, respectively. In certain embodiments, the first antigen-binding site comprises (a) a VH that comprises CDR1, CDR2, and CDR3 comprising the amino acid sequences of SEQ ID NOs: 53 or 54, 55, and 90 or 91, respectively (*e.g.*, SEQ ID NOs: 53, 55, and 90, respectively, or SEQ ID NOs: 54, 55, and 91, respectively); and (b) a VL that comprises

CDR1, CDR2, and CDR3 comprising the amino acid sequences of SEQ ID NOs: 93, 44, and 94, respectively.

[0394] In certain embodiments, the first antigen-binding site that binds NKG2D comprises a VH that comprises an amino acid sequence at least 90% (*e.g.*, at least 91%, at least 92%, at least 93%, at least 94%, at least 95%, at least 96%, at least 97%, at least 98%, at least 99%, or 100%) identical to the amino acid sequence of SEQ ID NO:70, and a VL that comprises an amino acid sequence at least 90% (*e.g.*, at least 91%, at least 92%, at least 93%, at least 94%, at least 95%, at least 96%, at least 97%, at least 98%, at least 99%, or 100%) identical to SEQ ID NO:75. In certain embodiments, the VH comprises CDR1, CDR2, and CDR3 comprising the amino acid sequences of SEQ ID NOs: 71 or 115, 72, and 73 or 74, respectively (*e.g.*, SEQ ID NOs: 71, 72, and 73, respectively, or SEQ ID NOs: 115, 72, and 74, respectively). In certain embodiments, the VL comprises CDR1, CDR2, and CDR3 comprising the amino acid sequences of SEQ ID NOs: 76, 77, and 78, respectively. In certain embodiments, the first antigen-binding site comprises (a) a VH that comprises CDR1, CDR2, and CDR3 comprising the amino acid sequences of SEQ ID NOs: 71 or 115, 72, and 73 or 74, respectively (*e.g.*, SEQ ID NOs: 71, 72, and 73, respectively, or SEQ ID NOs: 115, 72, and 74, respectively); and (b) a VL that comprises CDR1, CDR2, and CDR3 comprising the amino acid sequences of SEQ ID NOs: 76, 77, and 78, respectively.

[0395] In certain embodiments, the first antigen-binding site that binds NKG2D comprises a VH that comprises an amino acid sequence at least 90% (*e.g.*, at least 91%, at least 92%, at least 93%, at least 94%, at least 95%, at least 96%, at least 97%, at least 98%, at least 99%, or 100%) identical to the amino acid sequence of SEQ ID NO:79, and a VL that comprises an amino acid sequence at least 90% (*e.g.*, at least 91%, at least 92%, at least 93%, at least 94%, at least 95%, at least 96%, at least 97%, at least 98%, at least 99%, or 100%) identical to SEQ ID NO:85. In certain embodiments, the VH comprises CDR1, CDR2, and CDR3 comprising the amino acid sequences of SEQ ID NOs: 80 or 81, 82, and 83 or 84, respectively (*e.g.*, SEQ ID NOs: 80, 82, and 83, respectively, or SEQ ID NOs: 81, 82, and 84, respectively). In certain embodiments, the VL comprises CDR1, CDR2, and CDR3 comprising the amino acid sequences of SEQ ID NOs: 86, 77, and 87, respectively. In certain embodiments, the first antigen-binding site comprises (a) a VH that comprises CDR1, CDR2, and CDR3 comprising the amino acid sequences of SEQ ID NOs: 80 or 81, 82, and 83 or 84 respectively (*e.g.*, SEQ ID NOs: 80, 82,

and 83, respectively, or SEQ ID NOs: 81, 82, and 84, respectively); and (b) a VL that comprises CDR1, CDR2, and CDR3 comprising the amino acid sequences of SEQ ID NOs: 86, 77, and 87, respectively.

[0396] In certain embodiments, the first antigen-binding site that binds NKG2D comprises a VH that comprises an amino acid sequence at least 90% (*e.g.*, at least 91%, at least 92%, at least 93%, at least 94%, at least 95%, at least 96%, at least 97%, at least 98%, at least 99%, or 100%) identical to the amino acid sequence of SEQ ID NO:95, and a VL that comprises an amino acid sequence at least 90% (*e.g.*, at least 91%, at least 92%, at least 93%, at least 94%, at least 95%, at least 96%, at least 97%, at least 98%, at least 99%, or 100%) identical to SEQ ID NO:85. In certain embodiments, the VH comprises CDR1, CDR2, and CDR3 comprising the amino acid sequences of SEQ ID NOs: 80 or 81, 82, and 96 or 97, respectively (*e.g.*, SEQ ID NOs: 80, 82, and 96, respectively, or SEQ ID NOs: 81, 82, and 97, respectively). In certain embodiments, the VL comprises CDR1, CDR2, and CDR3 comprising the amino acid sequences of SEQ ID NOs: 86, 77, and 87, respectively. In certain embodiments, the first antigen-binding site comprises (a) a VH that comprises CDR1, CDR2, and CDR3 comprising the amino acid sequences of SEQ ID NOs: 80 or 81, 82, and 96 or 97, respectively (*e.g.*, SEQ ID NOs: 80, 82, and 96, respectively, or SEQ ID NOs: 81, 82, and 97, respectively); and (b) a VL that comprises CDR1, CDR2, and CDR3 comprising the amino acid sequences of SEQ ID NOs: 86, 77, and 87, respectively.

[0397] In certain embodiments, the first antigen-binding site that binds NKG2D comprises a VH that comprises an amino acid sequence at least 90% (*e.g.*, at least 91%, at least 92%, at least 93%, at least 94%, at least 95%, at least 96%, at least 97%, at least 98%, at least 99%, or 100%) identical to the amino acid sequence of SEQ ID NO:98, and a VL that comprises an amino acid sequence at least 90% (*e.g.*, at least 91%, at least 92%, at least 93%, at least 94%, at least 95%, at least 96%, at least 97%, at least 98%, at least 99%, or 100%) identical to SEQ ID NO:85. In certain embodiments, the VH comprises CDR1, CDR2, and CDR3 comprising the amino acid sequences of SEQ ID NOs: 80 or 81, 82, and 99 or 100, respectively (*e.g.*, SEQ ID NOs: 80, 82, and 99, respectively, or SEQ ID NOs: 81, 82, and 100, respectively). In certain embodiments, the VL comprises CDR1, CDR2, and CDR3 comprising the amino acid sequences of SEQ ID NOs: 86, 77, and 87, respectively. In certain embodiments, the first antigen-binding site comprises (a) a VH that comprises CDR1, CDR2, and CDR3 comprising the amino acid

sequences of SEQ ID NOs: 80 or 81, 82, and 99 or 100, respectively (*e.g.*, SEQ ID NOs: 80, 82, and 99, respectively, or SEQ ID NOs: 81, 82, and 100, respectively); and (b) a VL that comprises CDR1, CDR2, and CDR3 comprising the amino acid sequences of SEQ ID NOs: 86, 77, and 87, respectively.

[0398] In certain embodiments, the first antigen-binding site that binds NKG2D comprises a VH that comprises an amino acid sequence at least 90% (*e.g.*, at least 91%, at least 92%, at least 93%, at least 94%, at least 95%, at least 96%, at least 97%, at least 98%, at least 99%, or 100%) identical to the amino acid sequence of SEQ ID NO:101, and a VL that comprises an amino acid sequence at least 90% (*e.g.*, at least 91%, at least 92%, at least 93%, at least 94%, at least 95%, at least 96%, at least 97%, at least 98%, at least 99%, or 100%) identical to SEQ ID NO:85. In certain embodiments, the VH comprises CDR1, CDR2, and CDR3 comprising the amino acid sequences of SEQ ID NOs: 80 or 81, 82, and 102 or 103, respectively (*e.g.*, SEQ ID NOs: 80, 82, and 102, respectively, or SEQ ID NOs: 81, 82, and 103, respectively). In certain embodiments, the VL comprises CDR1, CDR2, and CDR3 comprising the amino acid sequences of SEQ ID NOs: 86, 77, and 87, respectively. In certain embodiments, the first antigen-binding site comprises (a) a VH that comprises CDR1, CDR2, and CDR3 comprising the amino acid sequences of SEQ ID NOs: 80 or 81, 82, and 102 or 103, respectively (*e.g.*, SEQ ID NOs: 80, 82, and 102, respectively, or SEQ ID NOs: 81, 82, and 103, respectively); and (b) a VL that comprises CDR1, CDR2, and CDR3 comprising the amino acid sequences of SEQ ID NOs: 86, 77, and 87, respectively.

[0399] In certain embodiments, the first antigen-binding site that binds NKG2D comprises a VH that comprises an amino acid sequence at least 90% (*e.g.*, at least 91%, at least 92%, at least 93%, at least 94%, at least 95%, at least 96%, at least 97%, at least 98%, at least 99%, or 100%) identical to the amino acid sequence of SEQ ID NO:104, and a VL that comprises an amino acid sequence at least 90% (*e.g.*, at least 91%, at least 92%, at least 93%, at least 94%, at least 95%, at least 96%, at least 97%, at least 98%, at least 99%, or 100%) identical to SEQ ID NO:85. In certain embodiments, the VH comprises CDR1, CDR2, and CDR3 comprising the amino acid sequences of SEQ ID NOs: 80 or 81, 82, and 105 or 106, respectively (*e.g.*, SEQ ID NOs: 80, 82, and 105, respectively, or SEQ ID NOs: 81, 82, and 106, respectively). In certain embodiments, the VL comprises CDR1, CDR2, and CDR3 comprising the amino acid sequences of SEQ ID NOs: 86, 77, and 87, respectively. In certain embodiments, the first antigen-binding

site comprises (a) a VH that comprises CDR1, CDR2, and CDR3 comprising the amino acid sequences of SEQ ID NOs: 80 or 81, 82, and 105 or 106, respectively (*e.g.*, SEQ ID NOs: 80, 82, and 105, respectively, or SEQ ID NOs: 81, 82, and 106, respectively); and (b) a VL that comprises CDR1, CDR2, and CDR3 comprising the amino acid sequences of SEQ ID NOs: 86, 77, and 87, respectively.

[0400] In certain embodiments, the first antigen-binding site that binds NKG2D comprises a VH that comprises an amino acid sequence at least 90% (*e.g.*, at least 91%, at least 92%, at least 93%, at least 94%, at least 95%, at least 96%, at least 97%, at least 98%, at least 99%, or 100%) identical to the amino acid sequence of SEQ ID NO:107, and a VL that comprises an amino acid sequence at least 90% (*e.g.*, at least 91%, at least 92%, at least 93%, at least 94%, at least 95%, at least 96%, at least 97%, at least 98%, at least 99%, or 100%) identical to SEQ ID NO:85. In certain embodiments, the VH comprises CDR1, CDR2, and CDR3 comprising the amino acid sequences of SEQ ID NOs: 80 or 81, 82, and 108 or 109, respectively (*e.g.*, SEQ ID NOs: 80, 82, and 108, respectively, or SEQ ID NOs: 81, 82, and 109, respectively). In certain embodiments, the VL comprises CDR1, CDR2, and CDR3 comprising the amino acid sequences of SEQ ID NOs: 86, 77, and 87, respectively. In certain embodiments, the first antigen-binding site comprises (a) a VH that comprises CDR1, CDR2, and CDR3 comprising the amino acid sequences of SEQ ID NOs: 80 or 81, 82, and 108 or 109, respectively (*e.g.*, SEQ ID NOs: 80, 82, and 108, respectively, or SEQ ID NOs: 81, 82, and 109, respectively); and (b) a VL that comprises CDR1, CDR2, and CDR3 comprising the amino acid sequences of SEQ ID NOs: 86, 77, and 87, respectively.

[0401] In certain embodiments, the first antigen-binding site that binds NKG2D comprises a VH that comprises an amino acid sequence at least 90% (*e.g.*, at least 91%, at least 92%, at least 93%, at least 94%, at least 95%, at least 96%, at least 97%, at least 98%, at least 99%, or 100%) identical to the amino acid sequence of SEQ ID NO:110, and a VL that comprises an amino acid sequence at least 90% (*e.g.*, at least 91%, at least 92%, at least 93%, at least 94%, at least 95%, at least 96%, at least 97%, at least 98%, at least 99%, or 100%) identical to SEQ ID NO:85. In certain embodiments, the VH comprises CDR1, CDR2, and CDR3 comprising the amino acid sequences of SEQ ID NOs: 80 or 81, 82, and 111 or 112, respectively (*e.g.*, SEQ ID NOs: 80, 82, and 111, respectively, or SEQ ID NOs: 81, 82, and 112, respectively). In certain embodiments, the VL comprises CDR1, CDR2, and CDR3 comprising the amino acid sequences

of SEQ ID NOs: 86, 77, and 87, respectively. In certain embodiments, the first antigen-binding site comprises (a) a VH that comprises CDR1, CDR2, and CDR3 comprising the amino acid sequences of SEQ ID NOs: 80 or 81, 82, and 111 or 112, respectively (*e.g.*, SEQ ID NOs: 80, 82, and 111, respectively, or SEQ ID NOs: 81, 82, and 112, respectively); and (b) a VL that comprises CDR1, CDR2, and CDR3 comprising the amino acid sequences of SEQ ID NOs: 86, 77, and 87, respectively.

[0402] In certain embodiments, the first antigen-binding site that binds NKG2D comprises a VH that comprises an amino acid sequence at least 90% (*e.g.*, at least 91%, at least 92%, at least 93%, at least 94%, at least 95%, at least 96%, at least 97%, at least 98%, at least 99%, or 100%) identical to the amino acid sequence of SEQ ID NO:113, and a VL that comprises an amino acid sequence at least 90% (*e.g.*, at least 91%, at least 92%, at least 93%, at least 94%, at least 95%, at least 96%, at least 97%, at least 98%, at least 99%, or 100%) identical to SEQ ID NO:114.

[0403] In certain embodiments, the first antigen-binding site that binds NKG2D comprises a VH that comprises an amino acid sequence at least 90% (*e.g.*, at least 91%, at least 92%, at least 93%, at least 94%, at least 95%, at least 96%, at least 97%, at least 98%, at least 99%, or 100%) identical to the amino acid sequence of SEQ ID NO:116, and a VL that comprises an amino acid sequence at least 90% (*e.g.*, at least 91%, at least 92%, at least 93%, at least 94%, at least 95%, at least 96%, at least 97%, at least 98%, at least 99%, or 100%) identical to SEQ ID NO:117.

[0404] The multispecific binding proteins can bind to NKG2D-expressing cells, which include but are not limited to NK cells, γδ T cells and $CD8^+$ αβ T cells. Upon NKG2D binding, the multispecific binding proteins may block natural ligands, such as ULBP6 and MICA, from binding to NKG2D and activating NK cells.

[0405] The multispecific binding proteins binds to cells expressing CD16, an Fc receptor on the surface of leukocytes including natural killer cells, macrophages, neutrophils, eosinophils, mast cells, and follicular dendritic cells. A protein of the present disclosure binds to NKG2D with an affinity of K_D of 2 nM to 120 nM, *e.g.*, 2 nM to 110 nM, 2 nM to 100 nM, 2 nM to 90 nM, 2 nM to 80 nM, 2 nM to 70 nM, 2 nM to 60 nM, 2 nM to 50 nM, 2 nM to 40 nM, 2 nM to 30 nM, 2 nM to 20 nM, 2 nM to 10 nM, about 15 nM, about 14 nM, about 13 nM, about 12 nM, about 11 nM, about 10 nM, about 9 nM, about 8 nM, about 7 nM, about 6 nM, about 5 nM, about

4.5 nM, about 4 nM, about 3.5 nM, about 3 nM, about 2.5 nM, about 2 nM, about 1.5 nM, about 1 nM, between about 0.5 nM to about 1 nM, about 1 nM to about 2 nM, about 2 nM to 3 nM, about 3 nM to 4 nM, about 4 nM to about 5 nM, about 5 nM to about 6 nM, about 6 nM to about 7 nM, about 7 nM to about 8 nM, about 8 nM to about 9 nM, about 9 nM to about 10 nM, about 1 nM to about 10 nM, about 2 nM to about 10 nM, about 3 nM to about 10 nM, about 4 nM to about 10 nM, about 5 nM to about 10 nM, about 6 nM to about 10 nM, about 7 nM to about 10 nM, or about 8 nM to about 10 nM. In some embodiments, NKG2D-binding sites bind to NKG2D with a K_D of 10 to 62 nM.

CLEC12A Binding Site

[0406] The tumor associated antigen-binding site of the multispecific binding protein disclosed herein comprises a heavy chain variable domain and a light chain variable domain. **Table 2** lists some exemplary sequences of heavy chain variable domains and light chain variable domains that, in combination, can bind to these tumor associated antigens.

[0407] In one aspect, the present disclosure provides multispecific binding proteins that bind to the NKG2D receptor and CD16 receptor on natural killer cells, and CLEC12A. Table 2 lists some exemplary sequences of heavy chain variable domains and light chain variable domains that, in combination, can bind to CLEC12A. CDR sequences are identified under Kabat numbering as indicated.

Table 2: Sequences of Exemplary Antigen-Binding Sites that Bind CLEC12A.

Clone	VH	VL
16B8.C8	EVQLQESGPGLVQPSQSLSITCT VSGFSLTNYGLHWVRQSPGKG LEWLGVIWSGGKTDYNTPFKS RLSISKDISKNQVFFKMNSLQP NDTAIYFCAKYDYDDSLDYWG QGTSVTVSS [SEQ ID NO:135] CDR1: GFSLTNY [SEQ ID NO:137] CDR2: WSGGK [SEQ ID NO:138] CDR3: YDYDDSLDY [SEQ ID NO:139]	DIQMNQSPSSLSASLGDTIAITCHA SQNINFWLSWYQQKPGNIPKLLIY EASNLHTGVPSRFSGSGSGTRFTLT ISSLQPEDIATYYCQQSHSYPLTFG QGTKLEIK [SEQ ID NO:136] CDR1: HASQNINFWLS [SEQ ID NO:140] CDR2: EASNLHT [SEQ ID NO:141] CDR3: QQSHSYPLT [SEQ ID NO:142]

Clone	VH	VL
Humanized 16B8.C8 in scFv-1292 / scFv-1301 (back mutations in VH and VL underlined)	QLQLQESGPGLVKPSETLSLTCT VSGFSLTNYGLHWIRQPPGKGL EWIGVIWSGGKTDYNPSLKSRV TISKDTSKNQFSLKLSSVQAND TAVYYCAKYDYDDSLDYWGQ GTLVTVSS [SEQ ID NO:143] CDR1: GFSLTNY [SEQ ID NO:137] CDR2: WSGGK [SEQ ID NO:138] CDR3: YDYDDSLDY [SEQ ID NO:139]	DIQMTQSPSSLSASVGDRVTITCHA SQNINFWLSWYQQKPGKIPKLLIY EASNLHTGVPSRFSGSGSGTRFTLT ISSLQPEDIATYYCQQSHSYPLTFG QGTKLEIK [SEQ ID NO:144] CDR1: HASQNINFWLS [SEQ ID NO:140] CDR2: EASNLHT [SEQ ID NO:141] CDR3: QQSHSYPLT [SEQ ID NO:142]
scFv of humanized 16B8.C8 scFv-1292 / scFv-1301	scFv -1292 (VH-VL): QLQLQESGPGLVKPSETLSLTCTVSGFSLTNYGLHWIRQPPGKCLEWIG VIWSGGKTDYNPSLKSRVTISKDTSKNQFSLKLSSVQANDTAVYYCAK YDYDDSLDYWGQGTLVTVSSGGGGSGGGGSGGGGSGGGGSDIQMT QSPSSLSASVGDRVTITCHASQNINFWLSWYQQKPGKIPKLLIYEASNL HTGVPSRFSGSGSGTRFTLTISSLQPEDIATYYCQQSHSYPLTFGCGTKL EIK [SEQ ID NO:145] scFv -1301 (VL-VH): DIQMTQSPSSLSASVGDRVTITCHASQNINFWLSWYQQKPGKIPKLLIY EASNLHTGVPSRFSGSGSGTRFTLTISSLQPEDIATYYCQQSHSYPLTFG CGTKLEIKGGGGSGGGGSGGGGSGGGGSQLQLQESGPGLVKPSETLS LTCTVSGFSLTNYGLHWIRQPPGKCLEWIGVIWSGGKTDYNPSLKSRV TISKDTSKNQFSLKLSSVQANDTAVYYCAKYDYDDSLDYWGQGTLVT VSS [SEQ ID NO:146]	
Humanized 16B8.C8 in scFv-1293/ scFv-1302 (back mutations in VH and VL underlined)	QLQLQESGPGLVKPSETLSLTCT VSGFSLTNYGLHWIRQPPGKGL EWIGVIWSGGKTDYNPSLKSRV TISVDTSKNQFSLKLSSVQAND TAVYYCAKYDYDDSLDYWGQ GTLVTVSS [SEQ ID NO:147] CDR1: GFSLTNY [SEQ ID NO:137]	DIQMTQSPSSLSASVGDRVTITCHA SQNINFWLSWYQQKPGKIPKLLIY EASNLHTGVPSRFSGSGSGTRFTLT ISSLQPEDIATYYCQQSHSYPLTFG QGTKLEIK [SEQ ID NO:144] CDR1: HASQNINFWLS [SEQ ID NO:140]

Clone	VH	VL
	CDR2: WSGGK [SEQ ID NO:138] CDR3: YDYDDSLDY [SEQ ID NO:139]	CDR2: EASNLHT [SEQ ID NO:141] CDR3: QQSHSYPLT [SEQ ID NO:142]
scFv of humanized 16B8.C8 scFv-1293/ scFv-1302	scFv -1293 (VH-VL): QLQLQESGPGLVKPSETLSLTCTVSGFSLTNYGLHWIRQPPGKCLEWIG VIWSGGKTDYNPSLKSRVTISVDTSKNQFSLKLSSVQANDTAVYYCAK YDYDDSLDYWGQGTLVTVSSGGGGSGGGGSGGGGSGGGGSDIQMT QSPSSLSASVGDRVTITCHASQNINFWLSWYQQKPGKIPKLLIYEASNL HTGVPSRFSGSGSGTRFTLTISSLQPEDIATYYCQQSHSYPLTFGCGTKL EIK [SEQ ID NO:149] scFv -1302 (VL-VH): DIQMTQSPSSLSASVGDRVTITCHASQNINFWLSWYQQKPGKIPKLLIY EASNLHTGVPSRFSGSGSGTRFTLTISSLQPEDIATYYCQQSHSYPLTFG CGTKLEIKGGGGSGGGGSGGGGSGGGGSQLQLQESGPGLVKPSETLS LTCTVSGFSLTNYGLHWIRQPPGKCLEWIGVIWSGGKTDYNPSLKSRV TISVDTSKNQFSLKLSSVQANDTAVYYCAKYDYDDSLDYWGQGTLVT VSS [SEQ ID NO:150]	
Humanized 16B8.C8 in scFv-1294 / scFv-1303 (back mutations in VH and VL underlined)	QLQLQESGPGLVKPSETLSLTCT VSGFSLTNYGLHWIRQPPGKGL EWIGVIWSGGKTDYNPSLKSRV TISKDTSKNQFSLKLSSVTANDT AVYYCAKYDYDDSLDYWGQG TLVTVSS [SEQ ID NO:244] CDR1: GFSLTNY [SEQ ID NO:137] CDR2: WSGGK [SEQ ID NO:138] CDR3: YDYDDSLDY [SEQ ID NO:139]	DIQMTQSPSSLSASVGDRVTITCHA SQNINFWLSWYQQKPGKIPKLLIY EASNLHTGVPSRFSGSGSGTRFTLT ISSLQPEDIATYYCQQSHSYPLTFG QGTKLEIK [SEQ ID NO:144] CDR1: HASQNINFWLS [SEQ ID NO:140] CDR2: EASNLHT [SEQ ID NO:141] CDR3: QQSHSYPLT [SEQ ID NO:142]
scFv of humanized 16B8.C8	scFv -1294 (VH-VL): QLQLQESGPGLVKPSETLSLTCTVSGFSLTNYGLHWIRQPPGKCLEWIG VIWSGGKTDYNPSLKSRVTISKDTSKNQFSLKLSSVTANDTAVYYCAK YDYDDSLDYWGQGTLVTVSSGGGGSGGGGSGGGGSGGGGSDIQMT	

Clone	VH	VL
scFv-1294 / scFv-1303	QSPSSLSASVGDRVTITCHASQNINFWLSWYQQKPGKIPKLLIYEASNL HTGVPSRFSGSGSGTRFTLTISSLQPEDIATYYCQQSHSYPLTFGCGTKL EIK [SEQ ID NO:153] scFv -1303 (VL-VH): DIQMTQSPSSLSASVGDRVTITCHASQNINFWLSWYQQKPGKIPKLLIY EASNLHTGVPSRFSGSGSGTRFTLTISSLQPEDIATYYCQQSHSYPLTFG CGTKLEIKGGGGSGGGGSGGGGSGGGGSQLQLQESGPGLVKPSETLS LTCTVSGFSLTNYGLHWIRQPPGKCLEWIGVIWSGGKTDYNPSLKSRV TISKDTSKNQFSLKLSSVTANDTAVYYCAKYDYDDSLDYWGQGTLVT VSS [SEQ ID NO:154]	
Humanized 16B8.C8 in scFv-1295 / scFv-1304 (back mutations in VH and VL underlined)	QLQLQESGPGLVKPSETLSLTCT VSGFSLTNYGLHWIRQPPGKGL EWIGVIWSGGKTDYNPSLKSRV TISKDTSKNQFSLKLSSVQAAD TAVYYCAKYDYDDSLDYWGQ GTLVTVSS [SEQ ID NO:178] CDR1: GFSLTNY [SEQ ID NO:137] CDR2: WSGGK [SEQ ID NO:138] CDR3: YDYDDSLDY [SEQ ID NO:139]	DIQMTQSPSSLSASVGDRVTITCHA SQNINFWLSWYQQKPGKIPKLLIY EASNLHTGVPSRFSGSGSGTRFTLT ISSLQPEDIATYYCQQSHSYPLTFG QGTKLEIK [SEQ ID NO:144] CDR1: HASQNINFWLS [SEQ ID NO:140] CDR2: EASNLHT [SEQ ID NO:141] CDR3: QQSHSYPLT [SEQ ID NO:142]
scFv of humanized 16B8.C8 scFv-1295 / scFv-1304	scFv -1295 (VH-VL): QLQLQESGPGLVKPSETLSLTCTVSGFSLTNYGLHWIRQPPGKCLEWIG VIWSGGKTDYNPSLKSRVTISKDTSKNQFSLKLSSVQAADTAVYYCAK YDYDDSLDYWGQGTLVTVSSGGGGSGGGGSGGGGSGGGGSDIQMT QSPSSLSASVGDRVTITCHASQNINFWLSWYQQKPGKIPKLLIYEASNL HTGVPSRFSGSGSGTRFTLTISSLQPEDIATYYCQQSHSYPLTFGCGTKL EIK [SEQ ID NO:156] scFv -1304 (VL-VH): DIQMTQSPSSLSASVGDRVTITCHASQNINFWLSWYQQKPGKIPKLLIY EASNLHTGVPSRFSGSGSGTRFTLTISSLQPEDIATYYCQQSHSYPLTFG CGTKLEIKGGGGSGGGGSGGGGSGGGGSQLQLQESGPGLVKPSETLS LTCTVSGFSLTNYGLHWIRQPPGKCLEWIGVIWSGGKTDYNPSLKSRV	

Clone	VH	VL
	TISKDTSKNQFSLKLSSVQAADTAVYYCAKYDYDDSLDYWGQGTLVT VSS [SEQ ID NO:157]	
Humanized 16B8.C8 in scFv-1296 / scFv-1305 (back mutations in VH and VL underlined)	QLQLQESGPGLVKPSETLSLTCT VSGFSLTNYGLHWIRQPPGKGL EWIGVIWSGGKTDYNPSLKSRV TISKDTSKNQFSLKLSSVQAND TAVYYCARYDYDDSLDYWGQ GTLVTVSS [SEQ ID NO:256] CDR1: GFSLTNY [SEQ ID NO:137] CDR2: WSGGK [SEQ ID NO:138] CDR3: YDYDDSLDY [SEQ ID NO:139]	DIQMTQSPSSLSASVGDRVTITCHA SQNINFWLSWYQQKPGKIPKLLIY EASNLHTGVPSRFSGSGSGTRFTLT ISSLQPEDIATYYCQQSHSYPLTFG QGTKLEIK [SEQ ID NO:144] CDR1: HASQNINFWLS [SEQ ID NO:140] CDR2: EASNLHT [SEQ ID NO:141] CDR3: QQSHSYPLT [SEQ ID NO:142]
scFv of humanized 16B8.C8 scFv-1296 / scFv-1305	scFv -1296 (VH-VL): QLQLQESGPGLVKPSETLSLTCTVSGFSLTNYGLHWIRQPPGKCLEWIG VIWSGGKTDYNPSLKSRVTISKDTSKNQFSLKLSSVQANDTAVYYCAR YDYDDSLDYWGQGTLVTVSSGGGGSGGGGSGGGGSGGGGSDIQMT QSPSSLSASVGDRVTITCHASQNINFWLSWYQQKPGKIPKLLIYEASNL HTGVPSRFSGSGSGTRFTLTISSLQPEDIATYYCQQSHSYPLTFGCGTKL EIK [SEQ ID NO:160] scFv -1305 (VL-VH): DIQMTQSPSSLSASVGDRVTITCHASQNINFWLSWYQQKPGKIPKLLIY EASNLHTGVPSRFSGSGSGTRFTLTISSLQPEDIATYYCQQSHSYPLTFG CGTKLEIKGGGGSGGGGSGGGGSGGGGSQLQLQESGPGLVKPSETLS LTCTVSGFSLTNYGLHWIRQPPGKCLEWIGVIWSGGKTDYNPSLKSRV TISKDTSKNQFSLKLSSVQANDTAVYYCARYDYDDSLDYWGQGTLVT VSS [SEQ ID NO:161]	
Humanized 16B8.C8 in scFv-1297 / scFv-1306 (back	QLQLQESGPGLVKPSETLSLTCT VSGFSLTNYGLHWIRQPPGKGL EWIGVIWSGGKTDYNPSLKSRV TISKDTSKNQFSLKLSSVQAND	DIQMTQSPSSLSASVGDRVTITCHA SQNINFWLSWYQQKPGKAPKLLIY EASNLHTGVPSRFSGSGSGTRFTLT ISSLQPEDIATYYCQQSHSYPLTFG QGTKLEIK

Clone	VH	VL
mutations in VH and VL underlined)	TAVYYCAKYDYDDSLDYWGQ GTLVTVSS [SEQ ID NO:143] CDR1: GFSLTNY [SEQ ID NO:137] CDR2: WSGGK [SEQ ID NO:138] CDR3: YDYDDSLDY [SEQ ID NO:139]	[SEQ ID NO:163] CDR1: HASQNINFWLS [SEQ ID NO:140] CDR2: EASNLHT [SEQ ID NO:141] CDR3: QQSHSYPLT [SEQ ID NO:142]
scFv of humanized 16B8.C8 scFv-1297 / scFv-1306	scFv -1297 (VH-VL): QLQLQESGPGLVKPSETLSLTCTVSGFSLTNYGLHWIRQPPGKCLEWIG VIWSGGKTDYNPSLKSRVTISKDTSKNQFSLKLSSVQANDTAVYYCAK YDYDDSLDYWGQGTLVTVSSGGGGSGGGGSGGGGSGGGGSDIQMT QSPSSLSASVGDRVTITCHASQNINFWLSWYQQKPGKAPKLLIYEASN LHTGVPSRFSGSGSGTRFTLTISSLQPEDIATYYCQQSHSYPLTFGCGTK LEIK [SEQ ID NO:164] scFv -1306 (VL-VH): DIQMTQSPSSLSASVGDRVTITCHASQNINFWLSWYQQKPGKAPKLLI YEASNLHTGVPSRFSGSGSGTRFTLTISSLQPEDIATYYCQQSHSYPLTF GCGTKLEIKGGGGSGGGGSGGGGSGGGGSQLQLQESGPGLVKPSETL SLTCTVSGFSLTNYGLHWIRQPPGKCLEWIGVIWSGGKTDYNPSLKSR VTISKDTSKNQFSLKLSSVQANDTAVYYCAKYDYDDSLDYWGQGTLV TVSS [SEQ ID NO:165]	
Humanized 16B8.C8 in scFv-1298 / scFv-1307 (back mutations in VH and VL underlined)	QLQLQESGPGLVKPSETLSLTCT VSGFSLTNYGLHWIRQPPGKGL EWIGVIWSGGKTDYNPSLKSRV TISKDTSKNQFSLKLSSVQAND TAVYYCAKYDYDDSLDYWGQ GTLVTVSS [SEQ ID NO:143] CDR1: GFSLTNY [SEQ ID NO:137] CDR2: WSGGK [SEQ ID NO:138]	DIQMTQSPSSLSASVGDRVTITCHA SQNINFWLSWYQQKPGKIPKLLIY EASNLHTGVPSRFSGSGSGTDFTLT ISSLQPEDIATYYCQQSHSYPLTFG QGTKLEIK [SEQ ID NO:167] CDR1: HASQNINFWLS [SEQ ID NO:140] CDR2: EASNLHT [SEQ ID NO:141] CDR3: QQSHSYPLT [SEQ ID NO:142]

Clone	VH	VL
	CDR3: YDYDDSLDY [SEQ ID NO:139]	
scFv of humanized 16B8.C8 scFv-1298 / scFv-1307	scFv -1298 (VH-VL): QLQLQESGPGLVKPSETLSLTCTVSGFSLTNYGLHWIRQPPGKCLEWIG VIWSGGKTDYNPSLKSRVTISKDTSKNQFSLKLSSVQANDTAVYYCAK YDYDDSLDYWGQGTLVTVSSGGGGSGGGGSGGGGSGGGGSDIQMT QSPSSLSASVGDRVTITCHASQNINFWLSWYQQKPGKIPKLLIYEASNL HTGVPSRFSGSGSGTDFTLTISSLQPEDIATYYCQQSHSYPLTFGCGTKL EIK [SEQ ID NO:168] scFv -1307 (VL-VH): DIQMTQSPSSLSASVGDRVTITCHASQNINFWLSWYQQKPGKIPKLLIY EASNLHTGVPSRFSGSGSGTDFTLTISSLQPEDIATYYCQQSHSYPLTFG CGTKLEIKGGGGSGGGGSGGGGSGGGGSQLQLQESGPGLVKPSETLS LTCTVSGFSLTNYGLHWIRQPPGKCLEWIGVIWSGGKTDYNPSLKSRV TISKDTSKNQFSLKLSSVQANDTAVYYCAKYDYDDSLDYWGQGTLVT VSS [SEQ ID NO:169]	
Humanized 16B8.C8 in scFv-1299 / scFv-1308	QLQLQESGPGLVKPSETLSLTCT VSGFSLTNYGLHWIRQPPGKGL EWIGVIWSGGKTDYNPSLKSRV TISKDTSKNQFSLKLSSVQANDTAVYYCAKYDYDDSLDYWGQ GTLVTVSS [SEQ ID NO:143] CDR1: GFSLTNY [SEQ ID NO:137] CDR2: WSGGK [SEQ ID NO:138] CDR3: YDYDDSLDY [SEQ ID NO:139]	DIQMTQSPSSLSASVGDRVTITCHA SQNINFWLSWYQQKPGKIPKLLIY EASNLHTGVPSRFSGSGSGTRFTLT ISSLQPEDFATYYCQQSHSYPLTFG QGTKLEIK [SEQ ID NO:171] CDR1: HASQNINFWLS [SEQ ID NO:140] CDR2: EASNLHT [SEQ ID NO:141] CDR3: QQSHSYPLT [SEQ ID NO:142]
scFv of humanized 16B8.C8 scFv-1299 / scFv-1308	scFv -1299 (VH-VL): QLQLQESGPGLVKPSETLSLTCTVSGFSLTNYGLHWIRQPPGKCLEWIG VIWSGGKTDYNPSLKSRVTISKDTSKNQFSLKLSSVQANDTAVYYCAK YDYDDSLDYWGQGTLVTVSSGGGGSGGGGSGGGGSGGGGSDIQMT QSPSSLSASVGDRVTITCHASQNINFWLSWYQQKPGKIPKLLIYEASNL HTGVPSRFSGSGSGTRFTLTISSLQPEDFATYYCQQSHSYPLTFGCGTKL EIK	

Clone	VH	VL
	[SEQ ID NO:172] scFv -1308 (VL-VH): DIQMTQSPSSLSASVGDRVTITCHASQNINFWLSWYQQKPGKIPKLLIY EASNLHTGVPSRFSGSGSGTRFTLTISSLQPEDFATYYCQQSHSYPLTFG CGTKLEIKGGGGSGGGGSGGGGSGGGGSQLQLQESGPGLVKPSETLS LTCTVSGFSLTNYGLHWIRQPPGKCLEWIGVIWSGGKTDYNPSLKSRV TISKDTSKNQFSLKLSSVQANDTAVYYCAKYDYDDSLDYWGQGTLVT VSS [SEQ ID NO:173]	
Humanized 16B8.C8 in scFv-1300/ scFv-1309	QLQLQESGPGLVKPSETLSLTCT VSGFSLTNYGLHWIRQPPGKGL EWIGVIWSGGKTDYNPSLKSRV TISVDTSKNQFSLKLSSVTAADT AVYYCARYDYDDSLDYWGQG TLVTVSS [SEQ ID NO:174] CDR1: GFSLTNY [SEQ ID NO:137] CDR2: WSGGK [SEQ ID NO:138] CDR3: YDYDDSLDY [SEQ ID NO:139]	DIQMTQSPSSLSASVGDRVTITCHA SQNINFWLSWYQQKPGKAPKLLIY EASNLHTGVPSRFSGSGSGTDFTLT ISSLQPEDFATYYCQQSHSYPLTFG QGTKLEIK [SEQ ID NO:175] CDR1: HASQNINFWLS [SEQ ID NO:140] CDR2: EASNLHT [SEQ ID NO:141] CDR3: QQSHSYPLT [SEQ ID NO:142]
scFv of humanized 16B8.C8 scFv-1300/ scFv-1309	scFv -1300 (VH-VL): QLQLQESGPGLVKPSETLSLTCTVSGFSLTNYGLHWIRQPPGKCLEWIG VIWSGGKTDYNPSLKSRVTISVDTSKNQFSLKLSSVTAADTAVYYCAR YDYDDSLDYWGQGTLVTVSSGGGGSGGGGSGGGGSGGGGSDIQMT QSPSSLSASVGDRVTITCHASQNINFWLSWYQQKPGKAPKLLIYEASN LHTGVPSRFSGSGSGTDFTLTISSLQPEDFATYYCQQSHSYPLTFGCGTK LEIK [SEQ ID NO:176] scFv -1309 (VL-VH): DIQMTQSPSSLSASVGDRVTITCHASQNINFWLSWYQQKPGKAPKLLI YEASNLHTGVPSRFSGSGSGTDFTLTISSLQPEDFATYYCQQSHSYPLTF GCGTKLEIKGGGGSGGGGSGGGGSGGGGSQLQLQESGPGLVKPSETL SLTCTVSGFSLTNYGLHWIRQPPGKCLEWIGVIWSGGKTDYNPSLKSR VTISVDTSKNQFSLKLSSVTAADTAVYYCARYDYDDSLDYWGQGTLV TVSS	

Clone	VH	VL
	[SEQ ID NO:177]	
Humanized 16B8.C8 in scFv-1602/ scFv-2061	QLQLQESGPGLVKPSETLSLTCT VSGFSLTNYGLHWIRQPPGKGL EWIGVIWSGGKTDYNPSLKSRV TISKDTSKNQFSLKLSSVQAAD TAVYYCAKYDYDDSLDYWGQ GTLVTVSS [SEQ ID NO:178] CDR1: GFSLTNY [SEQ ID NO:137] CDR2: WSGGK [SEQ ID NO:138] CDR3: YDYDDSLDY [SEQ ID NO:139]	DIQMTQSPSSLSASVGDRVTITCHA SQNINFWLSWYQQKPGKAPKLLIY EASNLHTGVPSRFSGSGSGTRFTLT ISSLQPEDIATYYCQQSHSYPLTFG GGTKLEIK [SEQ ID NO:289] CDR1: HASQNINFWLS [SEQ ID NO:140] CDR2: EASNLHT [SEQ ID NO:141] CDR3: QQSHSYPLT [SEQ ID NO:142]
scFv of humanized 16B8.C8 scFv-1602/ scFv-2061	scFv -1602 (VH-VL): QLQLQESGPGLVKPSETLSLTCTVSGFSLTNYGLHWIRQPPGKCLEWIG VIWSGGKTDYNPSLKSRVTISKDTSKNQFSLKLSSVQAADTAVYYCAK YDYDDSLDYWGQGTLVTVSSGGGGSGGGGSGGGGSGGGGSDIQMT QSPSSLSASVGDRVTITCHASQNINFWLSWYQQKPGKAPKLLIYEASN LHTGVPSRFSGSGSGTRFTLTISSLQPEDIATYYCQQSHSYPLTFGCGTK LEIK [SEQ ID NO:180] scFv-2061 (VL-VH): DIQMTQSPSSLSASVGDRVTITCHASQNINFWLSWYQQKPGKAPKLLI YEASNLHTGVPSRFSGSGSGTRFTLTISSLQPEDIATYYCQQSHSYPLTF GCGTKLEIKGGGGSGGGGSGGGGSGGGGSQLQLQESGPGLVKPSETL SLTCTVSGFSLTNYGLHWIRQPPGKCLEWIGVIWSGGKTDYNPSLKSR VTISKDTSKNQFSLKLSSVQAADTAVYYCAKYDYDDSLDYWGQGTLV TVSS [SEQ ID NO:181]	
Humanized 16B8.C8 consensus	QLQLQESGPGLVKPSETLSLTCT VSGFSLTNYGLHWIRQPPGKGL EWIGVIWSGGKTDYNPSLKSRV TISX1DTSKNQFSLKLSSVX2AX3 DTAVYYCAX4YDYDDSLDYWG QGTLVTVSS where X1 is V or K, X2 is T or Q, X3 is A or N, and X4 is R or K	DIQMTQSPSSLSASVGDRVTITCHA SQNINFWLSWYQQKPGKX1PKLLI YEASNLHTGVPSRFSGSGSGTX2FT LTISSLQPEDX3ATYYCQQSHSYPLT FGX4GTKLEIK where X1 is A or I, X2 is D or R, X3 is F or I, and X4 is Q or G [SEQ ID NO:151]

Clone	VH	VL
	[SEQ ID NO:182] CDR1: GFSLTNY [SEQ ID NO:137] CDR2: WSGGK [SEQ ID NO:138] CDR3: YDYDDSLDY [SEQ ID NO:139]	CDR1: HASQNINFWLS [SEQ ID NO:140] CDR2: EASNLHT [SEQ ID NO:141] CDR3: QQSHSYPLT [SEQ ID NO:142]
Humanized 16B8.C8 in AB0305/ AB5030 (Cysteine heterodimerization mutations are underlined. Such mutations can facilitate formation of a disulfide bridge between the VH and VL of the scFv.)	QLQLQESGPGLVKPSETLSLTC TVSGFSLTNYGLHWIRQPPGKG LEWIGVIWVGGATDYNPSLKS RVTISVDTSKNQFSLKLSSVQA ADTAVYYCAKGDYGDTLDYW GQGTLVTVSS [SEQ ID NO:270] QLQLQESGPGLVKPSETLSLTCT VSGFSLTNYGLHWIRQPPGKCL EWIGVIWVGGATDYNPSLKSRV TISVDTSKNQFSLKLSSVQAAD TAVYYCAKGDYGDTLDYWGQ GTLVTVSS [SEQ ID NO:335] CDR1: GFSLTNY [SEQ ID NO:137] CDR2: WVGGA [SEQ ID NO:272] CDR3: GDYGDTLDY [SEQ ID NO:273]	DIQMTQSPSSLSASVGDRVTITCHA SQNINFWLSWYQQKPGKAPKLLIY EASNLHTGVPSRFSGSGSGTDFTLT ISSLQPEDFATYYCQQSHSYPLTFG SGTKLEIK [SEQ ID NO:271] DIQMTQSPSSLSASVGDRVTITCHA SQNINFWLSWYQQKPGKAPKLLIY EASNLHTGVPSRFSGSGSGTDFTLT ISSLQPEDFATYYCQQSHSYPLTFG CGTKLEIK [SEQ ID NO:336] CDR1: HASQNINFWLS [SEQ ID NO:140] CDR2: EASNLHT [SEQ ID NO:141] CDR3: QQSHSYPLT [SEQ ID NO:142]
scFv of humanized 16B8.C8 AB0305/ AB5030	AB0305 (VH-VL): QLQLQESGPGLVKPSETLSLTCTVSGFSLTNYGLHWIRQPPGKCLEWI GVIWVGGATDYNPSLKSRVTISVDTSKNQFSLKLSSVQAADTAVYYC AKGDYGDTLDYWGQGTLVTVSSGGGGSGGGGSGGGGSGGGGSDIQ MTQSPSSLSASVGDRVTITCHASQNINFWLSWYQQKPGKAPKLLIYEA SNLHTGVPSRFSGSGSGTDFTLTISSLQPEDFATYYCQQSHSYPLTFGCG TKLEIK [SEQ ID NO:274] AB5030 (VL-VH):	

Clone	VH	VL
	DIQMTQSPSSLSASVGDRVTITCHASQNINFWLSWYQQKPGKAPKLLI YEASNLHTGVPSRFSGSGSGTDFTLTISSLQPEDFATYYCQQSHSYPLTF GCGTKLEIKGGGGSGGGGSGGGGSGGGGSQLQLQESGPGLVKPSETL SLTCTVSGFSLTNYGLHWIRQPPGKCLEWIGVIWVGGATDYNPSLKSR VTISVDTSKNQFSLKLSSVQAADTAVYYCAKGDYGDTLDYWGQGTL VTVSS [SEQ ID NO:275]	
Humanized 16B8.C8 in AB0147/ AB7410	QLQLQESGPGLVKPSETLSLTC TVSGFSLTNYGLHWIRQPPGKG LEWIGVILSGGWTDYNPSLKSR VTISKDTSKNQFSLKLSSVQAA DTAVYYCAKGDYGDALDYWG QGTLVTVSS [SEQ ID NO:294] CDR1: GFSLTNY [SEQ ID NO:137] CDR2: LSGGW [SEQ ID NO:296] CDR3: GDYGDALDY [SEQ ID NO:279]	DIQMTQSPSSLSASVGDRVTITCHA SQNINFWLSWYQQKPGKAPKLLIY EASNLHTGVPSRFSGSGSGTRFTLT ISSLQPEDIATYYCQQSHSYPLTFGS GTKLEIK [SEQ ID NO:295] CDR1: HASQNINFWLS [SEQ ID NO:140] CDR2: EASNLHT [SEQ ID NO:141] CDR3: QQSHSYPLT [SEQ ID NO:142]
scFv of humanized 16B8.C8 AB0147/ AB7410	AB0147(VH-VL) QLQLQESGPGLVKPSETLSLTCTVSGFSLTNYGLHWIRQPPGKCLEWI GVILSGGWTDYNPSLKSRVTISKDTSKNQFSLKLSSVQAADTAVYYC AKGDYGDALDYWGQGTLVTVSSGGGGSGGGGSGGGGSGGGGSDIQ MTQSPSSLSASVGDRVTITCHASQNINFWLSWYQQKPGKAPKLLIYEA SNLHTGVPSRFSGSGSGTRFTLTISSLQPEDIATYYCQQSHSYPLTFGCG TKLEIK [SEQ ID NO:280] AB7410 (VL-VH) DIQMTQSPSSLSASVGDRVTITCHASQNINFWLSWYQQKPGKAPKLLI YEASNLHTGVPSRFSGSGSGTRFTLTISSLQPEDIATYYCQQSHSYPLTF GCGTKLEIKGGGGSGGGGSGGGGSGGGGSQLQLQESGPGLVKPSETL SLTCTVSGFSLTNYGLHWIRQPPGKCLEWIGVILSGGWTDYNPSLKSR VTISKDTSKNQFSLKLSSVQAADTAVYYCAKGDYGDALDYWGQGTL VTVSS [SEQ ID NO:200]	
9F11.B7	EVQLQESGGGLVQPGGSRKLS CAASGFTFNSFGMHWVRQAPE KGLEWVAFISSGSTSIYYANTV KGRFTISRDNPKNTLFLQMTSL RSEDTAMYYCARDGYPTGGA	DIKMTQSPSSMYASLGERVTITCK ASQDIYNYLSWFQLKPGKSPRPLIY RANILVSGVPSKFSGSGSGQDYSLT INSLEYEDLGIYYCLQFDAFPFTFG SGTKLEIK

Clone	VH	VL
	MDYWGQGTSVTVSS [SEQ ID NO:193] CDR1: GFTFNSF [SEQ ID NO:192] CDR2: SSGSTS [SEQ ID NO:196] CDR3: DGYPTGGAMDY [SEQ ID NO:187]	[SEQ ID NO:194] CDR1: KASQDIYNYLS [SEQ ID NO:198] CDR2: RANILVS [SEQ ID NO:199] CDR3: LQFDAFPFT [SEQ ID NO:201]
Humanized 9F11.B7 in AB0191 / AB0185 (back mutations in VH and VL underlined)	EVQLVESGGGVVQPGGSLRLSCAASGFTFNSFGMHWVRQAPGKGLEWVAFISSGSTSIYYANTVKGRFTISRDNSKNTLYLQMNSLRAEDTAVYYCARDGYPTGGAMDYWGQGTSVTVSS [SEQ ID NO:162] CDR1: GFTFNSF [SEQ ID NO:192] CDR2: SSGSTS [SEQ ID NO:196] CDR3: DGYPTGGAMDY [SEQ ID NO:187]	DIQMTQSPSSLSASVGDRVTITCKASQDIYNYLSWFQQKPGKAPKPLIYRANILVSGVPSRFSGSGSGQDYTFTISSLQPEDIATYYCLQFDAFPFTFGSGTKLEIK [SEQ ID NO:203] CDR1: KASQDIYNYLS [SEQ ID NO:198] CDR2: RANILVS [SEQ ID NO:199] CDR3: LQFDAFPFT [SEQ ID NO:201]
scFv of humanized 9F11.B7 AB0191 / AB0185	AB0191 (VH-VL): EVQLVESGGGVVQPGGSLRLSCAASGFTFNSFGMHWVRQAPGKCLEWVAFISSGSTSIYYANTVKGRFTISRDNSKNTLYLQMNSLRAEDTAVYYCARDGYPTGGAMDYWGQGTSVTVSSGGGGSGGGGSGGGGSGGGGSDIQMTQSPSSLSASVGDRVTITCKASQDIYNYLSWFQQKPGKAPKPLIYRANILVSGVPSRFSGSGSGQDYTFTISSLQPEDIATYYCLQFDAFPFTFGCGTKLEIK [SEQ ID NO:184] AB0185 (VL-VH): DIQMTQSPSSLSASVGDRVTITCKASQDIYNYLSWFQQKPGKAPKPLIYRANILVSGVPSRFSGSGSGQDYTFTISSLQPEDIATYYCLQFDAFPFTFGCGTKLEIKGGGGSGGGGSGGGGSGGGGSEVQLVESGGGVVQPGGSLRLSCAASGFTFNSFGMHWVRQAPGKCLEWVAFISSGSTSIYYANTVKGRFTISRDNSKNTLYLQMNSLRAEDTAVYYCARDGYPTGGAMDYWGQGTSVTVSS [SEQ ID NO:185]

Clone	VH	VL
Humanized 9F11.B7 in AB0192/ AB0186 (back mutations in VH and VL underlined)	EVQLVESGGGVVQPGGSLRLSC AASGFTFNAFGMHWVRQAPG KGLEWVAFISSGSTSIYYANTV KGRFTISRDNSKNTLYLQMNSL RAEDTAVYYCARDGYPTGGAM DYWGQGTSVTVSS [SEQ ID NO:148] CDR1: GFTFNAF [SEQ ID NO:195] CDR2: SSGSTS [SEQ ID NO:196] CDR3: DGYPTGGAMDY [SEQ ID NO:187]	DIQMTQSPSSLSASVGDRVTITCKA SQDIYNYLSWFQQKPGKAPKPLIY RANILVSGVPSRFSGSGSGQDYTFT ISSLQPEDIATYYCLQFDAFPFTFGS GTKLEIK [SEQ ID NO:203] CDR1: KASQDIYNYLS [SEQ ID NO:198] CDR2: RANILVS [SEQ ID NO:199] CDR3: LQFDAFPFT [SEQ ID NO:201]
scFv of humanized 9F11.B7 AB0192/ AB0186	AB0192 (VH-VL): EVQLVESGGGVVQPGGSLRLSCAASGFTFNAFGMHWVRQAPGKCLE WVAFISSGSTSIYYANTVKGRFTISRDNSKNTLYLQMNSLRAEDTAVY YCARDGYPTGGAMDYWGQGTSVTVSSGGGGSGGGGSGGGGSGGGG SDIQMTQSPSSLSASVGDRVTITCKASQDIYNYLSWFQQKPGKAPKPLI YRANILVSGVPSRFSGSGSGQDYTFTISSLQPEDIATYYCLQFDAFPFTF GCGTKLEIK [SEQ ID NO:204] AB0186 (VL-VH): DIQMTQSPSSLSASVGDRVTITCKASQDIYNYLSWFQQKPGKAPKPLIY RANILVSGVPSRFSGSGSGQDYTFTISSLQPEDIATYYCLQFDAFPFTFG CGTKLEIKGGGGSGGGGSGGGGSGGGGSEVQLVESGGGVVQPGGSL RLSCAASGFTFNAFGMHWVRQAPGKCLEWVAFISSGSTSIYYANTVK GRFTISRDNSKNTLYLQMNSLRAEDTAVYYCARDGYPTGGAMDYWG QGTSVTVSS [SEQ ID NO:205]	
Humanized 9F11.B7 in AB0193/ AB0187 (back mutations in VH and VL underlined)	EVQLVESGGGVVQPGGSLRLSC AASGFTFNSFGMHWVRQAPGK GLEWVAFISSGSTSIYYANTVK GRFTISRDNSKNTLYLQMNSLR AEDTAVYYCARSGYPTGGAMD YWGQGTSVTVSS [SEQ ID NO:210]	DIQMTQSPSSLSASVGDRVTITCKA SQDIYNYLSWFQQKPGKAPKPLIY RANILVSGVPSRFSGSGSGQDYTFT ISSLQPEDIATYYCLQFDAFPFTFGS GTKLEIK [SEQ ID NO:203] CDR1: KASQDIYNYLS [SEQ ID NO:198]

Clone	VH	VL
	CDR1: GFTFNSF [SEQ ID NO:192] CDR2: SSGSTS [SEQ ID NO:196] CDR3: SGYPTGGAMDY [SEQ ID NO:213]	CDR2: RANILVS [SEQ ID NO:199] CDR3: LQFDAFPFT [SEQ ID NO:201]
scFv of humanized 9F11.B7 AB0193/ AB0187	AB0193 (VH-VL): EVQLVESGGGVVQPGGSLRLSCAASGFTFNSFGMHWVRQAPGKCLE WVAFISSGSTSIYYANTVKGRFTISRDNSKNTLYLQMNSLRAEDTAVY YCARSGYPTGGAMDYWGQGTSVTVSSGGGGSGGGGSGGGGSGGGG SDIQMTQSPSSLSASVGDRVTITCKASQDIYNYLSWFQQKPGKAPKPLI YRANILVSGVPSRFSGSGSGQDYTFTISSLQPEDIATYYCLQFDAFPFTF GCGTKLEIK [SEQ ID NO:208] AB0187 (VL-VH): DIQMTQSPSSLSASVGDRVTITCKASQDIYNYLSWFQQKPGKAPKPLIY RANILVSGVPSRFSGSGSGQDYTFTISSLQPEDIATYYCLQFDAFPFTFG CGTKLEIKGGGGSGGGGSGGGGSGGGGSEVQLVESGGGVVQPGGSL RLSCAASGFTFNSFGMHWVRQAPGKCLEWVAFISSGSTSIYYANTVKG RFTISRDNSKNTLYLQMNSLRAEDTAVYYCARSGYPTGGAMDYWGQ GTSVTVSS [SEQ ID NO:209]	
Humanized 9F11.B7 in AB0194/ AB0188 (back mutations in VH and VL underlined)	EVQLVESGGGVVQPGGSLRLSC AASGFTFNSFGMHWVRQAPGK GLEWVAFISSGSTSIYYANTVK GRFTISRDNSKNTLYLQMNSLR AEDTAVYYCARDGYPTGGAMD YWGQGTSVTVSS [SEQ ID NO:162] CDR1: GFTFNSF [SEQ ID NO:192] CDR2: SSGSTS [SEQ ID NO:196] CDR3: DGYPTGGAMDY [SEQ ID NO:187]	DIKMTQSPSSLSASVGDRVTITCKA SQDIYNYLSWFQQKPGKAPKPLIY RANILVSGVPSRFSGSGSGQDYTLT ISSLQPEDIATYYCLQFDAFPFTFGS GTKLEIK [SEQ ID NO:218] CDR1: KASQDIYNYLS [SEQ ID NO:198] CDR2: RANILVS [SEQ ID NO:199] CDR3: LQFDAFPFT [SEQ ID NO:201]

Clone	VH	VL
scFv of humanized 9F11.B7 AB0194/ AB0188	AB0194 (VH-VL): EVQLVESGGGVVQPGGSLRLSCAASGFTFNSFGMHWVRQAPGKCLE WVAFISSGSTSIYYANTVKGRFTISRDNSKNTLYLQMNSLRAEDTAVY YCARDGYPTGGAMDYWGQGTSVTVSSGGGGSGGGGSGGGGSGGGG SDIKMTQSPSSLSASVGDRVTITCKASQDIYNYLSWFQQKPGKAPKPLI YRANILVSGVPSRFSGSGSGQDYTLTISSLQPEDIATYYCLQFDAFPFTF GCGTKLEIK [SEQ ID NO:215] AB0188 (VL-VH): DIKMTQSPSSLSASVGDRVTITCKASQDIYNYLSWFQQKPGKAPKPLIY RANILVSGVPSRFSGSGSGQDYTLTISSLQPEDIATYYCLQFDAFPFTFG CGTKLEIKGGGGSGGGGSGGGGSGGGGSEVQLVESGGGVVQPGGSL RLSCAASGFTFNSFGMHWVRQAPGKCLEWVAFISSGSTSIYYANTVKG RFTISRDNSKNTLYLQMNSLRAEDTAVYYCARDGYPTGGAMDYWGQ GTSVTVSS [SEQ ID NO:216]	
Humanized 9F11.B7 in AB0195/ AB0189 (back mutations in VH and VL underlined)	EVQLVESGGGVVQPGGSLRLSC AASGFTFNAFGMHWVRQAPG KGLEWVAFISSGSTSIYYANTV KGRFTISRDNSKNTLYLQMNSL RAEDTAVYYCARDGYPTGGAM DYWGQGTSVTVSS [SEQ ID NO:148] CDR1: GFTFNAF [SEQ ID NO:195] CDR2: SSGSTS [SEQ ID NO:196] CDR3: DGYPTGGAMDY [SEQ ID NO:187]	DIKMTQSPSSLSASVGDRVTITCKA SQDIYNYLSWFQQKPGKAPKPLIY RANILVSGVPSRFSGSGSGQDYTLT ISSLQPEDIATYYCLQFDAFPFTFGS GTKLEIK [SEQ ID NO:218] CDR1: KASQDIYNYLS [SEQ ID NO:198] CDR2: RANILVS [SEQ ID NO:199] CDR3: LQFDAFPFT [SEQ ID NO:201]
scFv of humanized 9F11.B7 AB0195/ AB0189	AB0195 (VH-VL): EVQLVESGGGVVQPGGSLRLSCAASGFTFNAFGMHWVRQAPGKCLE WVAFISSGSTSIYYANTVKGRFTISRDNSKNTLYLQMNSLRAEDTAVY YCARDGYPTGGAMDYWGQGTSVTVSSGGGGSGGGGSGGGGSGGGG SDIKMTQSPSSLSASVGDRVTITCKASQDIYNYLSWFQQKPGKAPKPLI YRANILVSGVPSRFSGSGSGQDYTLTISSLQPEDIATYYCLQFDAFPFTF GCGTKLEIK [SEQ ID NO:252]	

Clone	VH	VL
	AB0189 (VL-VH): DIKMTQSPSSLSASVGDRVTITCKASQDIYNYLSWFQQKPGKAPKPLIY RANILVSGVPSRFSGSGSGQDYTLTISSLQPEDIATYYCLQFDAFPFTFG CGTKLEIKGGGGSGGGGSGGGGSGGGGSEVQLVESGGGVVQPGGSL RLSCAASGFTFNAFGMHWVRQAPGKCLEWVAFISSGSTSIYYANTVK GRFTISRDNSKNTLYLQMNSLRAEDTAVYYCARDGYPTGGAMDYWG QGTSVTVSS [SEQ ID NO:253]	
Humanized 9F11.B7 in AB0196/ AB0190 (back mutations in VH and VL underlined)	EVQLVESGGGVVQPGGSLRLSC AASGFTFNSFGMHWVRQAPGK GLEWVAFISSGSTSIYYANTVK GRFTISRDNSKNTLYLQMNSLR AEDTAVYYCARSGYPTGGAMD YWGQGTSVTVSS [SEQ ID NO:210] CDR1: GFTFNSF [SEQ ID NO:192] CDR2: SSGSTS [SEQ ID NO:196] CDR3: SGYPTGGAMDY [SEQ ID NO:213]	DIKMTQSPSSLSASVGDRVTITCKA SQDIYNYLSWFQQKPGKAPKPLIY RANILVSGVPSRFSGSGSGQDYTLT ISSLQPEDIATYYCLQFDAFPFTFGS GTKLEIK [SEQ ID NO:218] CDR1: KASQDIYNYLS [SEQ ID NO:198] CDR2: RANILVS [SEQ ID NO:199] CDR3: LQFDAFPFT [SEQ ID NO:201]
scFv of humanized 9F11.B7 AB0196/ AB0190	AB0196 (VH-VL): EVQLVESGGGVVQPGGSLRLSCAASGFTFNSFGMHWVRQAPGKCLE WVAFISSGSTSIYYANTVKGRFTISRDNSKNTLYLQMNSLRAEDTAVY YCARSGYPTGGAMDYWGQGTSVTVSSGGGGSGGGGSGGGGSGGGG SDIKMTQSPSSLSASVGDRVTITCKASQDIYNYLSWFQQKPGKAPKPLI YRANILVSGVPSRFSGSGSGQDYTLTISSLQPEDIATYYCLQFDAFPFTF GCGTKLEIK [SEQ ID NO:254] AB0190 (VL-VH): DIKMTQSPSSLSASVGDRVTITCKASQDIYNYLSWFQQKPGKAPKPLIY RANILVSGVPSRFSGSGSGQDYTLTISSLQPEDIATYYCLQFDAFPFTFG CGTKLEIKGGGGSGGGGSGGGGSGGGGSEVQLVESGGGVVQPGGSL RLSCAASGFTFNSFGMHWVRQAPGKCLEWVAFISSGSTSIYYANTVKG RFTISRDNSKNTLYLQMNSLRAEDTAVYYCARSGYPTGGAMDYWGQ GTSVTVSS [SEQ ID NO:255]	

Clone	VH	VL
Humanized 9F11.B7 consensus	EVQLVESGGGVVQPGGSLRLSC AASGFTFNX$_1$FGMHWVRQAPG KGLEWVAFISSGSTSIYYANTV KGRFTISRDNSKNTLYLQMNSL RAEDTAVYYCARX$_2$GYPTGGA MDYWGQGTSVTVSS where X$_1$ is S or A and X$_2$ is D or S [SEQ ID NO:249] CDR1: GFTFNXF where X is S or A [SEQ ID NO:251] CDR2: SSGSTS [SEQ ID NO:196] CDR3: XGYPTGGAMDY where X is D or S [SEQ ID NO:246]	DIX$_1$MTQSPSSLSASVGDRVTITCK ASQDIYNYLSWFQQKPGKAPKPLI YRANILVSGVPSRFSGSGSGQDYT X$_2$TISSLQPEDIATYYCLQFDAFPFT FGSGTKLEIK where X$_1$ is Q or K and X$_2$ is F or L [SEQ ID NO:250] CDR1: KASQDIYNYLS [SEQ ID NO:198] CDR2: RANILVS [SEQ ID NO:199] CDR3: LQFDAFPFT [SEQ ID NO:201]
30A9.E9	EVQLQESGPGLVQPSQSLSITCT VSGFSLTSFGVHWVRQSPGKG LEWLGVIWSGGSTDSNAAFISR LTITKDNSKSQVFFKMNSLQAT DTAIYYCARSYFAMDYWGQGT SVSVSS [SEQ ID NO:247] CDR1: GFSLTSF [SEQ ID NO:221] CDR2: WSGGS [SEQ ID NO:166] CDR3: SYFAMDY [SEQ ID NO:223]	DIVMTQSPSSLAVTAGEKVTMRCK SSQSLLWNVNQNNYLLWYQQKQ GQPPKLLIYGASIRESWVPDRFTGS GSGTDFTLTISNVHVEDLAVYYCQ HNHGSFLPYTFGGGTKLEIK [SEQ ID NO:248] CDR1: KSSQSLLWNVNQNNYLL [SEQ ID NO:240] CDR2: GASIRES [SEQ ID NO:226] CDR3: QHNHGSFLPYT [SEQ ID NO:179]
23A5.H8	QVQLRQSGPGLVQPSQSLSITC TVSGFSLTSYGVHWVRQSPGK GLEWLGVMWSGGSTDYNAAF MSRLSISKDNSKSQVFFTMNSL QADDTAIYYCARTHFGMDYW GQGTPVTVSS [SEQ ID NO:242] CDR1: GFSLTSY [SEQ ID NO:206] CDR2: WSGGS [SEQ ID NO:166]	GIVMTQSPSSLAVTAGEKVTMRCK SSQSLLWSVNQNNYLLWYQQKQG QPPKLLIYGASIRQSWVPDRFTGSG SGTDFTLSISNVHAEDLAVYYCQH NHGSFLPYTFGGGTKLEIK [SEQ ID NO:243] CDR1: KSSQSLLWSVNQNNYLL [SEQ ID NO:245] CDR2: GASIRQS [SEQ ID NO:239]

Clone	VH	VL
	CDR3: THFGMDY [SEQ ID NO:241]	CDR3: QHNHGSFLPYT [SEQ ID NO:179]
20D6.H8	EVQLQESGPGLVQPSQSLSITCT VSGFSLTSFGIHWVRQSPGKGL EWLGVIWSGGNTDSNAAFISRL SITKDISKSQVFFKMNSLQVTD TAIYYCARSYFAMDYWGQGTS VTVSS [SEQ ID NO:238] CDR1: GFSLTSF [SEQ ID NO:221] CDR2: WSGGN [SEQ ID NO:236] CDR3: SYFAMDY [SEQ ID NO:223]	GIVMTQSPSSLAVTAGEKVTMRCK SSQSLLWNVNQNNYLVWYQQKQ GQPPKLLIYGASIRESWVPDRFTGS GSGTDFTLTISNVHAEDLAVYYCQ HNHGSFLPYTFGGGTKLEIK [SEQ ID NO:237] CDR1: KSSQSLLWNVNQNNYLV [SEQ ID NO:152] CDR2: GASIRES [SEQ ID NO:226] CDR3: QHNHGSFLPYT [SEQ ID NO:179]
15A10.G8	EVQLQESGAELVRSGASIKLSC AASAFNIKDYFIHWVRQRPDQ GLEWIGWIDPENDDTEYAPKFQ DKATMTADTSSNTAYLQLSSLT SADTAVYYCNALWSRGGYFD YWGQGTTLTVSS [SEQ ID NO:155] CDR1: AFNIKDY [SEQ ID NO:159] CDR2: DPENDD [SEQ ID NO:170] CDR3: LWSRGGYFDY [SEQ ID NO:183]	EVLLTQSPAIIAASPGEKVTITCSAR SSVSYMSWYQQKPGSSPKIWIYGI SKLASGVPARFSGSGSGTYFSFTIN NLEAEDVATYYCQQRSYYPFTFGS GTKLEIK [SEQ ID NO:158] CDR1: SARSSVSYMS [SEQ ID NO:186] CDR2: GISKLAS [SEQ ID NO:188] CDR3: QQRSYYPFT [SEQ ID NO:189]
13E1.A4	EVQLQESGPELEKPGASVRISC KASGYSFTAYNMNWVKQSNG KSLEWIGNIDPSYGDATYNQKF KGKATLTVDKSSSTAYMQLKS LTSEDSAVYYCARDNYYGSGY FDYWGQGTTLTVSS [SEQ ID NO:190] CDR1: GYSFTAY [SEQ ID NO:197]	SVLMTQTPLSLPVSLGDRASISCRS SQGIVHINGNTYLEWYLQKPGQSP KLLIYKVSNRFSGVPDRFSGSGSGT DFTLKISRVEAEDLGVYYCFQGSH VPWTFGGGTKLEIK [SEQ ID NO:191] CDR1: RSSQGIVHINGNTYLE [SEQ ID NO:211]

Clone	VH	VL
	CDR2: DPSYGD [SEQ ID NO:202] CDR3: DNYYGSGYFDY [SEQ ID NO:207]	CDR2: KVSNRFS [SEQ ID NO:212] CDR3: FQGSHVPWT [SEQ ID NO:214]
12F8.H7	EVQLQESGAELVRSGASVKLSC TVSGFNIKDYYMHWVKQRPEQ GLEWIGWIDPENGDTENVPKFQ GKATMTADTSSNTAYLQLRSL TSEDTAVYYCKSYYYDSSSRY VDVWGAGTTVTVSS [SEQ ID NO:217] CDR1: GFNIKDY [SEQ ID NO:220] CDR2: DPENGD [SEQ ID NO:222] CDR3: YYYDSSSRYVDV [SEQ ID NO:257]	GIVMTQAPLTLSVTIGQPASISCKS SQSLLDSDGKTFLNWFLQRPGQSP KRLISLVSKLDSGVPDRFTGSGSGT DFTLKLSRVEPEDLGVYYCWQGT HFPYTFGGGTKLEIK [SEQ ID NO:219] CDR1: KSSQSLLDSDGKTFLN [SEQ ID NO:224] CDR2: LVSKLDS [SEQ ID NO:225] CDR3: WQGTHFPYT [SEQ ID NO:227]
9E4.B7	EVQLQESGAELMKPGASVKISC RTTGYTFSTYWIEWVKQRPGR GPEWIGELFPGNSDTTLNEKFT GKATFTADSSSNTAYMQLSSLT SEDSAVYYCARSGYYGSSLDY WGQGTTLTVSS [SEQ ID NO:228] CDR1: GYTFSTY [SEQ ID NO:230] CDR2: FPGNSD [SEQ ID NO:231] CDR3: SGYYGSSLDY [SEQ ID NO:232]	GIVMTQSPASLSASVGETVTITCRA GENIHSYLAWYQQKQGKSPQLLV YNAKTLAEGVPSRFSGSGSGTQFS LKINSLQPEDFGSYYCQHHYGTPR TFGGGTKLEIK [SEQ ID NO:229] CDR1: RAGENIHSYLA [SEQ ID NO:233] CDR2: NAKTLAE [SEQ ID NO:234] CDR3: QHHYGTPRT [SEQ ID NO:235]

[0408] In certain embodiments, the second antigen-binding site that binds CLEC12A (*e.g.*, human CLEC12A) comprises an antibody heavy chain variable domain (VH) that comprises an amino acid sequence at least 90% (*e.g.*, at least 91%, at least 92%, at least 93%, at least 94%, at least 95%, at least 96%, at least 97%, at least 98%, at least 99%, or 100%) identical to the VH of an antibody disclosed in Table 2, and an antibody light chain variable domain (VL) that

comprises an amino acid sequence at least 90% (*e.g.*, at least 91%, at least 92%, at least 93%, at least 94%, at least 95%, at least 96%, at least 97%, at least 98%, at least 99%, or 100%) identical to the VL of the same antibody disclosed in Table 2. In certain embodiments, the second antigen-binding site comprises the heavy chain CDR1, CDR2, and CDR3 and the light chain CDR1, CDR2, and CDR3, determined under Kabat (see Kabat *et al.*, (1991) Sequences of Proteins of Immunological Interest, NIH Publication No. 91-3242, Bethesda), Chothia (see, *e.g.*, Chothia C & Lesk A M, (1987), *J Mol Biol* 196: 901-917), MacCallum (see MacCallum R M *et al.*, (1996) *J Mol Biol* 262: 732-745), or any other CDR determination method known in the art, of the VH and VL sequences of an antigen-binding site disclosed in Table 2. In certain embodiments, the second antigen-binding site comprises the heavy chain CDR1, CDR2, and CDR3 and the light chain CDR1, CDR2, and CDR3 of an antibody disclosed in Table 2.

[0409] In certain embodiments, the second antigen-binding site is derived from 16B8.C8. For example, in certain embodiments, the second antigen-binding site comprises a VH that comprises an amino acid sequence at least 90% (*e.g.*, at least 91%, at least 92%, at least 93%, at least 94%, at least 95%, at least 96%, at least 97%, at least 98%, at least 99%, or 100%) identical to the amino acid sequence of SEQ ID NO:135, and a VL that comprises an amino acid sequence at least 90% (*e.g.*, at least 91%, at least 92%, at least 93%, at least 94%, at least 95%, at least 96%, at least 97%, at least 98%, at least 99%, or 100%) identical to SEQ ID NO:136. In certain embodiments, the VH comprises CDR1, CDR2, and CDR3 comprising the amino acid sequences of SEQ ID NOs: 137, 138, and 139, respectively. In certain embodiments, the VL comprises CDR1, CDR2, and CDR3 comprising the amino acid sequences of SEQ ID NOs: 140, 141, and 142, respectively. In certain embodiments, the second antigen-binding site comprises (a) a VH that comprises CDR1, CDR2, and CDR3 comprising the amino acid sequences of SEQ ID NOs: 137, 138, and 139, respectively; and (b) a VL that comprises CDR1, CDR2, and CDR3 comprising the amino acid sequences of SEQ ID NOs: 140, 141, and 142, respectively.

[0410] In certain embodiments, the second antigen-binding site is derived from scFv-1292 or scFv-1301. For example, in certain embodiments, the second antigen-binding site comprises a VH that comprises an amino acid sequence at least 90% (*e.g.*, at least 91%, at least 92%, at least 93%, at least 94%, at least 95%, at least 96%, at least 97%, at least 98%, at least 99%, or 100%) identical to the amino acid sequence of SEQ ID NO:143, and a VL that comprises an amino acid sequence at least 90% (*e.g.*, at least 91%, at least 92%, at least 93%, at least 94%, at least 95%, at

least 96%, at least 97%, at least 98%, at least 99%, or 100%) identical to SEQ ID NO:144. In certain embodiments, the VH comprises CDR1, CDR2, and CDR3 comprising the amino acid sequences of SEQ ID NOs: 137, 138, and 139, respectively. In certain embodiments, the VL comprises CDR1, CDR2, and CDR3 comprising the amino acid sequences of SEQ ID NOs: 140, 141, and 142, respectively. In certain embodiments, the second antigen-binding site comprises (a) a VH that comprises CDR1, CDR2, and CDR3 comprising the amino acid sequences of SEQ ID NOs: 137, 138, and 139, respectively; and (b) a VL that comprises CDR1, CDR2, and CDR3 comprising the amino acid sequences of SEQ ID NOs: 140, 141, and 142, respectively. In certain embodiments, the second antigen-binding site is present as an scFv, wherein the scFv comprises an amino acid sequence at least 90% (*e.g.*, at least 91%, at least 92%, at least 93%, at least 94%, at least 95%, at least 96%, at least 97%, at least 98%, at least 99%, or 100%) identical to SEQ ID NO:145 or 146.

[0411] In certain embodiments, the second antigen-binding site is derived from scFv-1293 or scFv-1302. For example, in certain embodiments, the second antigen-binding site comprises a VH that comprises an amino acid sequence at least 90% (*e.g.*, at least 91%, at least 92%, at least 93%, at least 94%, at least 95%, at least 96%, at least 97%, at least 98%, at least 99%, or 100%) identical to the amino acid sequence of SEQ ID NO:147, and a VL that comprises an amino acid sequence at least 90% (*e.g.*, at least 91%, at least 92%, at least 93%, at least 94%, at least 95%, at least 96%, at least 97%, at least 98%, at least 99%, or 100%) identical to SEQ ID NO:144. In certain embodiments, the VH comprises CDR1, CDR2, and CDR3 comprising the amino acid sequences of SEQ ID NOs: 137, 138, and 139, respectively. In certain embodiments, the VL comprises CDR1, CDR2, and CDR3 comprising the amino acid sequences of SEQ ID NOs: 140, 141, and 142, respectively. In certain embodiments, the second antigen-binding site comprises (a) a VH that comprises CDR1, CDR2, and CDR3 comprising the amino acid sequences of SEQ ID NOs: 137, 138, and 139, respectively; and (b) a VL that comprises CDR1, CDR2, and CDR3 comprising the amino acid sequences of SEQ ID NOs: 140, 141, and 142, respectively. In certain embodiments, the second antigen-binding site is present as an scFv, wherein the scFv comprises an amino acid sequence at least 90% (*e.g.*, at least 91%, at least 92%, at least 93%, at least 94%, at least 95%, at least 96%, at least 97%, at least 98%, at least 99%, or 100%) identical to SEQ ID NO:149 or 150.

[0412] In certain embodiments, the second antigen-binding site is derived from scFv-1294 or scFv-1303. For example, in certain embodiments, the second antigen-binding site comprises a VH that comprises an amino acid sequence at least 90% (*e.g.*, at least 91%, at least 92%, at least 93%, at least 94%, at least 95%, at least 96%, at least 97%, at least 98%, at least 99%, or 100%) identical to the amino acid sequence of SEQ ID NO:244, and a VL that comprises an amino acid sequence at least 90% (*e.g.*, at least 91%, at least 92%, at least 93%, at least 94%, at least 95%, at least 96%, at least 97%, at least 98%, at least 99%, or 100%) identical to SEQ ID NO:144. In certain embodiments, the VH comprises CDR1, CDR2, and CDR3 comprising the amino acid sequences of SEQ ID NOs: 137, 138, and 139, respectively. In certain embodiments, the VL comprises CDR1, CDR2, and CDR3 comprising the amino acid sequences of SEQ ID NOs: 140, 141, and 142, respectively. In certain embodiments, the second antigen-binding site comprises (a) a VH that comprises CDR1, CDR2, and CDR3 comprising the amino acid sequences of SEQ ID NOs: 137, 138, and 139, respectively; and (b) a VL that comprises CDR1, CDR2, and CDR3 comprising the amino acid sequences of SEQ ID NOs: 140, 141, and 142, respectively. In certain embodiments, the second antigen-binding site is present as an scFv, wherein the scFv comprises an amino acid sequence at least 90% (*e.g.*, at least 91%, at least 92%, at least 93%, at least 94%, at least 95%, at least 96%, at least 97%, at least 98%, at least 99%, or 100%) identical to SEQ ID NO:153 or 154.

[0413] In certain embodiments, the second antigen-binding site is derived from scFv-1295 or scFv-1304. For example, in certain embodiments, the second antigen-binding site comprises a VH that comprises an amino acid sequence at least 90% (*e.g.*, at least 91%, at least 92%, at least 93%, at least 94%, at least 95%, at least 96%, at least 97%, at least 98%, at least 99%, or 100%) identical to the amino acid sequence of SEQ ID NO:178, and a VL that comprises an amino acid sequence at least 90% (*e.g.*, at least 91%, at least 92%, at least 93%, at least 94%, at least 95%, at least 96%, at least 97%, at least 98%, at least 99%, or 100%) identical to SEQ ID NO:144. In certain embodiments, the VH comprises CDR1, CDR2, and CDR3 comprising the amino acid sequences of SEQ ID NOs: 137, 138, and 139, respectively. In certain embodiments, the VL comprises CDR1, CDR2, and CDR3 comprising the amino acid sequences of SEQ ID NOs: 140, 141, and 142, respectively. In certain embodiments, the second antigen-binding site comprises (a) a VH that comprises CDR1, CDR2, and CDR3 comprising the amino acid sequences of SEQ ID NOs: 137, 138, and 139, respectively; and (b) a VL that comprises CDR1, CDR2, and CDR3

comprising the amino acid sequences of SEQ ID NOs: 140, 141, and 142, respectively. In certain embodiments, the second antigen-binding site is present as an scFv, wherein the scFv comprises an amino acid sequence at least 90% (*e.g.*, at least 91%, at least 92%, at least 93%, at least 94%, at least 95%, at least 96%, at least 97%, at least 98%, at least 99%, or 100%) identical to SEQ ID NO:156 or 157.

[0414] In certain embodiments, the second antigen-binding site is derived from scFv-1296 or scFv-1305. For example, in certain embodiments, the second antigen-binding site comprises a VH that comprises an amino acid sequence at least 90% (*e.g.*, at least 91%, at least 92%, at least 93%, at least 94%, at least 95%, at least 96%, at least 97%, at least 98%, at least 99%, or 100%) identical to the amino acid sequence of SEQ ID NO:256, and a VL that comprises an amino acid sequence at least 90% (*e.g.*, at least 91%, at least 92%, at least 93%, at least 94%, at least 95%, at least 96%, at least 97%, at least 98%, at least 99%, or 100%) identical to SEQ ID NO:144. In certain embodiments, the VH comprises CDR1, CDR2, and CDR3 comprising the amino acid sequences of SEQ ID NOs: 137, 138, and 139, respectively. In certain embodiments, the VL comprises CDR1, CDR2, and CDR3 comprising the amino acid sequences of SEQ ID NOs: 140, 141, and 142, respectively. In certain embodiments, the second antigen-binding site comprises (a) a VH that comprises CDR1, CDR2, and CDR3 comprising the amino acid sequences of SEQ ID NOs: 137, 138, and 139, respectively; and (b) a VL that comprises CDR1, CDR2, and CDR3 comprising the amino acid sequences of SEQ ID NOs: 140, 141, and 142, respectively. In certain embodiments, the second antigen-binding site is present as an scFv, wherein the scFv comprises an amino acid sequence at least 90% (*e.g.*, at least 91%, at least 92%, at least 93%, at least 94%, at least 95%, at least 96%, at least 97%, at least 98%, at least 99%, or 100%) identical to SEQ ID NO:160 or 161.

[0415] In certain embodiments, the second antigen-binding site is derived from scFv-1297 or scFv-1306. For example, in certain embodiments, the second antigen-binding site comprises a VH that comprises an amino acid sequence at least 90% (*e.g.*, at least 91%, at least 92%, at least 93%, at least 94%, at least 95%, at least 96%, at least 97%, at least 98%, at least 99%, or 100%) identical to the amino acid sequence of SEQ ID NO:143, and a VL that comprises an amino acid sequence at least 90% (*e.g.*, at least 91%, at least 92%, at least 93%, at least 94%, at least 95%, at least 96%, at least 97%, at least 98%, at least 99%, or 100%) identical to SEQ ID NO:163. In certain embodiments, the VH comprises CDR1, CDR2, and CDR3 comprising the amino acid

sequences of SEQ ID NOs: 137, 138, and 139, respectively. In certain embodiments, the VL comprises CDR1, CDR2, and CDR3 comprising the amino acid sequences of SEQ ID NOs: 140, 141, and 142, respectively. In certain embodiments, the second antigen-binding site comprises (a) a VH that comprises CDR1, CDR2, and CDR3 comprising the amino acid sequences of SEQ ID NOs: 137, 138, and 139, respectively; and (b) a VL that comprises CDR1, CDR2, and CDR3 comprising the amino acid sequences of SEQ ID NOs: 140, 141, and 142, respectively. In certain embodiments, the second antigen-binding site is present as an scFv, wherein the scFv comprises an amino acid sequence at least 90% (*e.g.*, at least 91%, at least 92%, at least 93%, at least 94%, at least 95%, at least 96%, at least 97%, at least 98%, at least 99%, or 100%) identical to SEQ ID NO:164 or 165.

[0416] In certain embodiments, the second antigen-binding site is derived from scFv-1298 or scFv-1307. For example, in certain embodiments, the second antigen-binding site comprises a VH that comprises an amino acid sequence at least 90% (*e.g.*, at least 91%, at least 92%, at least 93%, at least 94%, at least 95%, at least 96%, at least 97%, at least 98%, at least 99%, or 100%) identical to the amino acid sequence of SEQ ID NO:143, and a VL that comprises an amino acid sequence at least 90% (*e.g.*, at least 91%, at least 92%, at least 93%, at least 94%, at least 95%, at least 96%, at least 97%, at least 98%, at least 99%, or 100%) identical to SEQ ID NO:167. In certain embodiments, the VH comprises CDR1, CDR2, and CDR3 comprising the amino acid sequences of SEQ ID NOs: 137, 138, and 139, respectively. In certain embodiments, the VL comprises CDR1, CDR2, and CDR3 comprising the amino acid sequences of SEQ ID NOs: 140, 141, and 142, respectively. In certain embodiments, the second antigen-binding site comprises (a) a VH that comprises CDR1, CDR2, and CDR3 comprising the amino acid sequences of SEQ ID NOs: 137, 138, and 139, respectively; and (b) a VL that comprises CDR1, CDR2, and CDR3 comprising the amino acid sequences of SEQ ID NOs: 140, 141, and 142, respectively. In certain embodiments, the second antigen-binding site is present as an scFv, wherein the scFv comprises an amino acid sequence at least 90% (*e.g.*, at least 91%, at least 92%, at least 93%, at least 94%, at least 95%, at least 96%, at least 97%, at least 98%, at least 99%, or 100%) identical to SEQ ID NO:168 or 169.

[0417] In certain embodiments, the second antigen-binding site is derived from scFv-1299 or scFv-1308. For example, in certain embodiments, the second antigen-binding site comprises a VH that comprises an amino acid sequence at least 90% (*e.g.*, at least 91%, at least 92%, at least

93%, at least 94%, at least 95%, at least 96%, at least 97%, at least 98%, at least 99%, or 100%) identical to the amino acid sequence of SEQ ID NO:143, and a VL that comprises an amino acid sequence at least 90% (*e.g.*, at least 91%, at least 92%, at least 93%, at least 94%, at least 95%, at least 96%, at least 97%, at least 98%, at least 99%, or 100%) identical to SEQ ID NO:171. In certain embodiments, the VH comprises CDR1, CDR2, and CDR3 comprising the amino acid sequences of SEQ ID NOs: 137, 138, and 139, respectively. In certain embodiments, the VL comprises CDR1, CDR2, and CDR3 comprising the amino acid sequences of SEQ ID NOs: 140, 141, and 142, respectively. In certain embodiments, the second antigen-binding site comprises (a) a VH that comprises CDR1, CDR2, and CDR3 comprising the amino acid sequences of SEQ ID NOs: 137, 138, and 139, respectively; and (b) a VL that comprises CDR1, CDR2, and CDR3 comprising the amino acid sequences of SEQ ID NOs: 140, 141, and 142, respectively. In certain embodiments, the second antigen-binding site is present as an scFv, wherein the scFv comprises an amino acid sequence at least 90% (*e.g.*, at least 91%, at least 92%, at least 93%, at least 94%, at least 95%, at least 96%, at least 97%, at least 98%, at least 99%, or 100%) identical to SEQ ID NO:172 or 173.

[0418] In certain embodiments, the second antigen-binding site is derived from scFv-1300 or scFv-1309. For example, in certain embodiments, the second antigen-binding site comprises a VH that comprises an amino acid sequence at least 90% (*e.g.*, at least 91%, at least 92%, at least 93%, at least 94%, at least 95%, at least 96%, at least 97%, at least 98%, at least 99%, or 100%) identical to the amino acid sequence of SEQ ID NO:174, and a VL that comprises an amino acid sequence at least 90% (*e.g.*, at least 91%, at least 92%, at least 93%, at least 94%, at least 95%, at least 96%, at least 97%, at least 98%, at least 99%, or 100%) identical to SEQ ID NO:175. In certain embodiments, the VH comprises CDR1, CDR2, and CDR3 comprising the amino acid sequences of SEQ ID NOs: 137, 138, and 139, respectively. In certain embodiments, the VL comprises CDR1, CDR2, and CDR3 comprising the amino acid sequences of SEQ ID NOs: 140, 141, and 142, respectively. In certain embodiments, the second antigen-binding site comprises (a) a VH that comprises CDR1, CDR2, and CDR3 comprising the amino acid sequences of SEQ ID NOs: 137, 138, and 139, respectively; and (b) a VL that comprises CDR1, CDR2, and CDR3 comprising the amino acid sequences of SEQ ID NOs: 140, 141, and 142, respectively. In certain embodiments, the second antigen-binding site is present as an scFv, wherein the scFv comprises an amino acid sequence at least 90% (*e.g.*, at least 91%, at least 92%, at least 93%, at least 94%,

at least 95%, at least 96%, at least 97%, at least 98%, at least 99%, or 100%) identical to SEQ ID NO:176 or 177.

[0419] In certain embodiments, the second antigen-binding site is derived from scFv-1602 or scFv-2061. For example, in certain embodiments, the second antigen-binding site comprises a VH that comprises an amino acid sequence at least 90% (*e.g.*, at least 91%, at least 92%, at least 93%, at least 94%, at least 95%, at least 96%, at least 97%, at least 98%, at least 99%, or 100%) identical to the amino acid sequence of SEQ ID NO:178, and a VL that comprises an amino acid sequence at least 90% (*e.g.*, at least 91%, at least 92%, at least 93%, at least 94%, at least 95%, at least 96%, at least 97%, at least 98%, at least 99%, or 100%) identical to SEQ ID NO:289. In certain embodiments, the VH comprises CDR1, CDR2, and CDR3 comprising the amino acid sequences of SEQ ID NOs: 137, 138, and 139, respectively. In certain embodiments, the VL comprises CDR1, CDR2, and CDR3 comprising the amino acid sequences of SEQ ID NOs: 140, 141, and 142, respectively. In certain embodiments, the second antigen-binding site comprises (a) a VH that comprises CDR1, CDR2, and CDR3 comprising the amino acid sequences of SEQ ID NOs: 137, 138, and 139, respectively; and (b) a VL that comprises CDR1, CDR2, and CDR3 comprising the amino acid sequences of SEQ ID NOs: 140, 141, and 142, respectively. In certain embodiments, the second antigen-binding site is present as an scFv, wherein the scFv comprises an amino acid sequence at least 90% (*e.g.*, at least 91%, at least 92%, at least 93%, at least 94%, at least 95%, at least 96%, at least 97%, at least 98%, at least 99%, or 100%) identical to SEQ ID NO:180 or 181.

[0420] In certain embodiments, the second antigen-binding site is derived from humanized 16B.C8. For example, in certain embodiments, the second antigen-binding site comprises a VH that comprises an amino acid sequence at least 90% (*e.g.*, at least 91%, at least 92%, at least 93%, at least 94%, at least 95%, at least 96%, at least 97%, at least 98%, at least 99%, or 100%) identical to the amino acid sequence of SEQ ID NO:182, and a VL that comprises an amino acid sequence at least 90% (*e.g.*, at least 91%, at least 92%, at least 93%, at least 94%, at least 95%, at least 96%, at least 97%, at least 98%, at least 99%, or 100%) identical to SEQ ID NO:151. In certain embodiments, the VH comprises CDR1, CDR2, and CDR3 comprising the amino acid sequences of SEQ ID NOs: 137, 138, and 139, respectively. In certain embodiments, the VL comprises CDR1, CDR2, and CDR3 comprising the amino acid sequences of SEQ ID NOs: 140, 141, and 142, respectively. In certain embodiments, the second antigen-binding site comprises

(a) a VH that comprises CDR1, CDR2, and CDR3 comprising the amino acid sequences of SEQ ID NOs: 137, 138, and 139, respectively; and (b) a VL that comprises CDR1, CDR2, and CDR3 comprising the amino acid sequences of SEQ ID NOs: 140, 141, and 142, respectively.

[0421] In certain embodiments, the second antigen-binding site is derived from AB0305 or AB5030. For example, in certain embodiments, the second antigen-binding site comprises a VH that comprises an amino acid sequence at least 90% (*e.g.*, at least 91%, at least 92%, at least 93%, at least 94%, at least 95%, at least 96%, at least 97%, at least 98%, at least 99%, or 100%) identical to the amino acid sequence of SEQ ID NO:270, and a VL that comprises an amino acid sequence at least 90% (*e.g.*, at least 91%, at least 92%, at least 93%, at least 94%, at least 95%, at least 96%, at least 97%, at least 98%, at least 99%, or 100%) identical to SEQ ID NO:271. In certain embodiments, the second antigen-binding site comprises a VH that comprises an amino acid sequence at least 90% (*e.g.*, at least 91%, at least 92%, at least 93%, at least 94%, at least 95%, at least 96%, at least 97%, at least 98%, at least 99%, or 100%) identical to the amino acid sequence of SEQ ID NO:335, and a VL that comprises an amino acid sequence at least 90% (*e.g.*, at least 91%, at least 92%, at least 93%, at least 94%, at least 95%, at least 96%, at least 97%, at least 98%, at least 99%, or 100%) identical to SEQ ID NO:336. In certain embodiments, the second antigen-binding site comprises a VH and a VL each comprises a cysteine heterodimerization mutation. Such heterodimerization mutation can facilitate formation of a disulfide bridge between the VH and VL of the scFv. In certain embodiments, the VH comprises CDR1, CDR2, and CDR3 comprising the amino acid sequences of SEQ ID NOs: 137, 272, and 273, respectively. In certain embodiments, the VL comprises CDR1, CDR2, and CDR3 comprising the amino acid sequences of SEQ ID NOs: 140, 141, and 142, respectively. In certain embodiments, the second antigen-binding site comprises (a) a VH that comprises CDR1, CDR2, and CDR3 comprising the amino acid sequences of SEQ ID NOs: 137, 272, and 273, respectively; and (b) a VL that comprises CDR1, CDR2, and CDR3 comprising the amino acid sequences of SEQ ID NOs: 140, 141, and 142, respectively. In certain embodiments, the second antigen-binding site is present as an scFv, wherein the scFv comprises an amino acid sequence at least 90% (*e.g.*, at least 91%, at least 92%, at least 93%, at least 94%, at least 95%, at least 96%, at least 97%, at least 98%, at least 99%, or 100%) identical to SEQ ID NO:274 or 275.

[0422] In certain embodiments, the second antigen-binding site is derived from AB0147 or AB7410. For example, in certain embodiments, the second antigen-binding site comprises a VH

that comprises an amino acid sequence at least 90% (*e.g.*, at least 91%, at least 92%, at least 93%, at least 94%, at least 95%, at least 96%, at least 97%, at least 98%, at least 99%, or 100%) identical to the amino acid sequence of SEQ ID NO:294, and a VL that comprises an amino acid sequence at least 90% (*e.g.*, at least 91%, at least 92%, at least 93%, at least 94%, at least 95%, at least 96%, at least 97%, at least 98%, at least 99%, or 100%) identical to SEQ ID NO:295. In certain embodiments, the VH comprises CDR1, CDR2, and CDR3 comprising the amino acid sequences of SEQ ID NOs: 137, 296, and 279, respectively. In certain embodiments, the VL comprises CDR1, CDR2, and CDR3 comprising the amino acid sequences of SEQ ID NOs: 140, 141, and 142, respectively. In certain embodiments, the second antigen-binding site comprises (a) a VH that comprises CDR1, CDR2, and CDR3 comprising the amino acid sequences of SEQ ID NOs: 137, 296, and 279, respectively; and (b) a VL that comprises CDR1, CDR2, and CDR3 comprising the amino acid sequences of SEQ ID NOs: 140, 141, and 142, respectively. In certain embodiments, the second antigen-binding site is present as an scFv, wherein the scFv comprises an amino acid sequence at least 90% (*e.g.*, at least 91%, at least 92%, at least 93%, at least 94%, at least 95%, at least 96%, at least 97%, at least 98%, at least 99%, or 100%) identical to SEQ ID NO:280 or 200.

[0423] In certain embodiments, the second antigen-binding site is derived from 9F11.B7. For example, in certain embodiments, the second antigen-binding site comprises a VH that comprises an amino acid sequence at least 90% (*e.g.*, at least 91%, at least 92%, at least 93%, at least 94%, at least 95%, at least 96%, at least 97%, at least 98%, at least 99%, or 100%) identical to the amino acid sequence of SEQ ID NO:193, and a VL that comprises an amino acid sequence at least 90% (*e.g.*, at least 91%, at least 92%, at least 93%, at least 94%, at least 95%, at least 96%, at least 97%, at least 98%, at least 99%, or 100%) identical to SEQ ID NO:194. In certain embodiments, the VH comprises CDR1, CDR2, and CDR3 comprising the amino acid sequences of SEQ ID NOs: 192, 196, and 187, respectively. In certain embodiments, the VL comprises CDR1, CDR2, and CDR3 comprising the amino acid sequences of SEQ ID NOs: 198, 199, and 201, respectively. In certain embodiments, the second antigen-binding site comprises (a) a VH that comprises CDR1, CDR2, and CDR3 comprising the amino acid sequences of SEQ ID NOs: 192, 196, and 187, respectively; and (b) a VL that comprises CDR1, CDR2, and CDR3 comprising the amino acid sequences of SEQ ID NOs: 198, 199, and 201, respectively.

[0424] In certain embodiments, the second antigen-binding site is derived from AB0191 or AB0185. For example, in certain embodiments, the second antigen-binding site comprises a VH that comprises an amino acid sequence at least 90% (*e.g.*, at least 91%, at least 92%, at least 93%, at least 94%, at least 95%, at least 96%, at least 97%, at least 98%, at least 99%, or 100%) identical to the amino acid sequence of SEQ ID NO:162, and a VL that comprises an amino acid sequence at least 90% (*e.g.*, at least 91%, at least 92%, at least 93%, at least 94%, at least 95%, at least 96%, at least 97%, at least 98%, at least 99%, or 100%) identical to SEQ ID NO:203. In certain embodiments, the VH comprises CDR1, CDR2, and CDR3 comprising the amino acid sequences of SEQ ID NOs: 192, 196, and 187, respectively. In certain embodiments, the VL comprises CDR1, CDR2, and CDR3 comprising the amino acid sequences of SEQ ID NOs: 198, 199, and 201, respectively. In certain embodiments, the second antigen-binding site comprises (a) a VH that comprises CDR1, CDR2, and CDR3 comprising the amino acid sequences of SEQ ID NOs: 192, 196, and 187, respectively; and (b) a VL that comprises CDR1, CDR2, and CDR3 comprising the amino acid sequences of SEQ ID NOs: 198, 199, and 201, respectively. In certain embodiments, the second antigen-binding site is present as an scFv, wherein the scFv comprises an amino acid sequence at least 90% (*e.g.*, at least 91%, at least 92%, at least 93%, at least 94%, at least 95%, at least 96%, at least 97%, at least 98%, at least 99%, or 100%) identical to SEQ ID NO:184 or 185.

[0425] In certain embodiments, the second antigen-binding site is derived from AB0192 or AB0186. For example, in certain embodiments, the second antigen-binding site comprises a VH that comprises an amino acid sequence at least 90% (*e.g.*, at least 91%, at least 92%, at least 93%, at least 94%, at least 95%, at least 96%, at least 97%, at least 98%, at least 99%, or 100%) identical to the amino acid sequence of SEQ ID NO:148, and a VL that comprises an amino acid sequence at least 90% (*e.g.*, at least 91%, at least 92%, at least 93%, at least 94%, at least 95%, at least 96%, at least 97%, at least 98%, at least 99%, or 100%) identical to SEQ ID NO:203. In certain embodiments, the VH comprises CDR1, CDR2, and CDR3 comprising the amino acid sequences of SEQ ID NOs: 195, 196, and 187, respectively. In certain embodiments, the VL comprises CDR1, CDR2, and CDR3 comprising the amino acid sequences of SEQ ID NOs: 198, 199, and 201, respectively. In certain embodiments, the second antigen-binding site comprises (a) a VH that comprises CDR1, CDR2, and CDR3 comprising the amino acid sequences of SEQ ID NOs: 195, 196, and 187, respectively; and (b) a VL that comprises CDR1, CDR2, and CDR3

comprising the amino acid sequences of SEQ ID NOs: 198, 199, and 201, respectively. In certain embodiments, the second antigen-binding site is present as an scFv, wherein the scFv comprises an amino acid sequence at least 90% (*e.g.*, at least 91%, at least 92%, at least 93%, at least 94%, at least 95%, at least 96%, at least 97%, at least 98%, at least 99%, or 100%) identical to SEQ ID NO:204 or 205.

[0426] In certain embodiments, the second antigen-binding site is derived from AB0193 or AB0187. For example, in certain embodiments, the second antigen-binding site comprises a VH that comprises an amino acid sequence at least 90% (*e.g.*, at least 91%, at least 92%, at least 93%, at least 94%, at least 95%, at least 96%, at least 97%, at least 98%, at least 99%, or 100%) identical to the amino acid sequence of SEQ ID NO:210, and a VL that comprises an amino acid sequence at least 90% (*e.g.*, at least 91%, at least 92%, at least 93%, at least 94%, at least 95%, at least 96%, at least 97%, at least 98%, at least 99%, or 100%) identical to SEQ ID NO:203. In certain embodiments, the VH comprises CDR1, CDR2, and CDR3 comprising the amino acid sequences of SEQ ID NOs: 192, 196, and 213, respectively. In certain embodiments, the VL comprises CDR1, CDR2, and CDR3 comprising the amino acid sequences of SEQ ID NOs: 198, 199, and 201, respectively. In certain embodiments, the second antigen-binding site comprises (a) a VH that comprises CDR1, CDR2, and CDR3 comprising the amino acid sequences of SEQ ID NOs: 192, 196, and 213, respectively; and (b) a VL that comprises CDR1, CDR2, and CDR3 comprising the amino acid sequences of SEQ ID NOs: 198, 199, and 201, respectively. In certain embodiments, the second antigen-binding site is present as an scFv, wherein the scFv comprises an amino acid sequence at least 90% (*e.g.*, at least 91%, at least 92%, at least 93%, at least 94%, at least 95%, at least 96%, at least 97%, at least 98%, at least 99%, or 100%) identical to SEQ ID NO:208 or 209.

[0427] In certain embodiments, the second antigen-binding site is derived from AB0194 or AB0188. For example, in certain embodiments, the second antigen-binding site comprises a VH that comprises an amino acid sequence at least 90% (*e.g.*, at least 91%, at least 92%, at least 93%, at least 94%, at least 95%, at least 96%, at least 97%, at least 98%, at least 99%, or 100%) identical to the amino acid sequence of SEQ ID NO:162, and a VL that comprises an amino acid sequence at least 90% (*e.g.*, at least 91%, at least 92%, at least 93%, at least 94%, at least 95%, at least 96%, at least 97%, at least 98%, at least 99%, or 100%) identical to SEQ ID NO:218. In certain embodiments, the VH comprises CDR1, CDR2, and CDR3 comprising the amino acid

sequences of SEQ ID NOs: 192, 196, and 187, respectively. In certain embodiments, the VL comprises CDR1, CDR2, and CDR3 comprising the amino acid sequences of SEQ ID NOs: 198, 199, and 201, respectively. In certain embodiments, the second antigen-binding site comprises (a) a VH that comprises CDR1, CDR2, and CDR3 comprising the amino acid sequences of SEQ ID NOs: 192, 196, and187, respectively; and (b) a VL that comprises CDR1, CDR2, and CDR3 comprising the amino acid sequences of SEQ ID NOs: 198, 199, and 201, respectively. In certain embodiments, the second antigen-binding site is present as an scFv, wherein the scFv comprises an amino acid sequence at least 90% (*e.g.*, at least 91%, at least 92%, at least 93%, at least 94%, at least 95%, at least 96%, at least 97%, at least 98%, at least 99%, or 100%) identical to SEQ ID NO:215 or 216.

[0428] In certain embodiments, the second antigen-binding site is derived from AB0195 or AB0189. For example, in certain embodiments, the second antigen-binding site comprises a VH that comprises an amino acid sequence at least 90% (*e.g.*, at least 91%, at least 92%, at least 93%, at least 94%, at least 95%, at least 96%, at least 97%, at least 98%, at least 99%, or 100%) identical to the amino acid sequence of SEQ ID NO:148, and a VL that comprises an amino acid sequence at least 90% (*e.g.*, at least 91%, at least 92%, at least 93%, at least 94%, at least 95%, at least 96%, at least 97%, at least 98%, at least 99%, or 100%) identical to SEQ ID NO:218. In certain embodiments, the VH comprises CDR1, CDR2, and CDR3 comprising the amino acid sequences of SEQ ID NOs: 195, 196, and 187, respectively. In certain embodiments, the VL comprises CDR1, CDR2, and CDR3 comprising the amino acid sequences of SEQ ID NOs: 198, 199, and 201, respectively. In certain embodiments, the second antigen-binding site comprises (a) a VH that comprises CDR1, CDR2, and CDR3 comprising the amino acid sequences of SEQ ID NOs: 195, 196, and187, respectively; and (b) a VL that comprises CDR1, CDR2, and CDR3 comprising the amino acid sequences of SEQ ID NOs: 198, 199, and 201, respectively. In certain embodiments, the second antigen-binding site is present as an scFv, wherein the scFv comprises an amino acid sequence at least 90% (*e.g.*, at least 91%, at least 92%, at least 93%, at least 94%, at least 95%, at least 96%, at least 97%, at least 98%, at least 99%, or 100%) identical to SEQ ID NO:252 or 253.

[0429] In certain embodiments, the second antigen-binding site is derived from AB0196 or AB0190. For example, in certain embodiments, the second antigen-binding site comprises a VH that comprises an amino acid sequence at least 90% (*e.g.*, at least 91%, at least 92%, at least

93%, at least 94%, at least 95%, at least 96%, at least 97%, at least 98%, at least 99%, or 100%) identical to the amino acid sequence of SEQ ID NO:210, and a VL that comprises an amino acid sequence at least 90% (*e.g.*, at least 91%, at least 92%, at least 93%, at least 94%, at least 95%, at least 96%, at least 97%, at least 98%, at least 99%, or 100%) identical to SEQ ID NO:218. In certain embodiments, the VH comprises CDR1, CDR2, and CDR3 comprising the amino acid sequences of SEQ ID NOs: 192, 196, and 213, respectively. In certain embodiments, the VL comprises CDR1, CDR2, and CDR3 comprising the amino acid sequences of SEQ ID NOs: 198, 199, and 201, respectively. In certain embodiments, the second antigen-binding site comprises (a) a VH that comprises CDR1, CDR2, and CDR3 comprising the amino acid sequences of SEQ ID NOs: 192, 196, and 213, respectively; and (b) a VL that comprises CDR1, CDR2, and CDR3 comprising the amino acid sequences of SEQ ID NOs: 198, 199, and 201, respectively. In certain embodiments, the second antigen-binding site is present as an scFv, wherein the scFv comprises an amino acid sequence at least 90% (*e.g.*, at least 91%, at least 92%, at least 93%, at least 94%, at least 95%, at least 96%, at least 97%, at least 98%, at least 99%, or 100%) identical to SEQ ID NO:254 or 255.

[0430] In certain embodiments, the second antigen-binding site is derived from humanized 9F11.B7. For example, in certain embodiments, the second antigen-binding site comprises a VH that comprises an amino acid sequence at least 90% (*e.g.*, at least 91%, at least 92%, at least 93%, at least 94%, at least 95%, at least 96%, at least 97%, at least 98%, at least 99%, or 100%) identical to the amino acid sequence of SEQ ID NO:249, and a VL that comprises an amino acid sequence at least 90% (*e.g.*, at least 91%, at least 92%, at least 93%, at least 94%, at least 95%, at least 96%, at least 97%, at least 98%, at least 99%, or 100%) identical to SEQ ID NO:250. In certain embodiments, the VH comprises CDR1, CDR2, and CDR3 comprising the amino acid sequences of SEQ ID NOs: 251, 196, and 246, respectively. In certain embodiments, the VL comprises CDR1, CDR2, and CDR3 comprising the amino acid sequences of SEQ ID NOs: 198, 199, and 201, respectively. In certain embodiments, the second antigen-binding site comprises (a) a VH that comprises CDR1, CDR2, and CDR3 comprising the amino acid sequences of SEQ ID NOs: 251, 196, and 246, respectively; and (b) a VL that comprises CDR1, CDR2, and CDR3 comprising the amino acid sequences of SEQ ID NOs: 198, 199, and 201, respectively.

[0431] In certain embodiments, the second antigen-binding site is derived from 30A9.E9. For example, in certain embodiments, the second antigen-binding site comprises a VH that comprises

an amino acid sequence at least 90% (*e.g.*, at least 91%, at least 92%, at least 93%, at least 94%, at least 95%, at least 96%, at least 97%, at least 98%, at least 99%, or 100%) identical to the amino acid sequence of SEQ ID NO:247, and a VL that comprises an amino acid sequence at least 90% (*e.g.*, at least 91%, at least 92%, at least 93%, at least 94%, at least 95%, at least 96%, at least 97%, at least 98%, at least 99%, or 100%) identical to SEQ ID NO:248. In certain embodiments, the VH comprises CDR1, CDR2, and CDR3 comprising the amino acid sequences of SEQ ID NOs: 221, 166, and 223, respectively. In certain embodiments, the VL comprises CDR1, CDR2, and CDR3 comprising the amino acid sequences of SEQ ID NOs: 240, 226, and 179, respectively. In certain embodiments, the second antigen-binding site comprises (a) a VH that comprises CDR1, CDR2, and CDR3 comprising the amino acid sequences of SEQ ID NOs: 221, 166, and 223, respectively; and (b) a VL that comprises CDR1, CDR2, and CDR3 comprising the amino acid sequences of SEQ ID NOs: 240, 226, and 179, respectively.

[0432] In certain embodiments, the second antigen-binding site is derived from 23A5.H8. For example, in certain embodiments, the second antigen-binding site comprises a VH that comprises an amino acid sequence at least 90% (*e.g.*, at least 91%, at least 92%, at least 93%, at least 94%, at least 95%, at least 96%, at least 97%, at least 98%, at least 99%, or 100%) identical to the amino acid sequence of SEQ ID NO:242, and a VL that comprises an amino acid sequence at least 90% (*e.g.*, at least 91%, at least 92%, at least 93%, at least 94%, at least 95%, at least 96%, at least 97%, at least 98%, at least 99%, or 100%) identical to SEQ ID NO:243. In certain embodiments, the VH comprises CDR1, CDR2, and CDR3 comprising the amino acid sequences of SEQ ID NOs: 206, 166, and 241, respectively. In certain embodiments, the VL comprises CDR1, CDR2, and CDR3 comprising the amino acid sequences of SEQ ID NOs: 245, 239, and 179, respectively. In certain embodiments, the second antigen-binding site comprises (a) a VH that comprises CDR1, CDR2, and CDR3 comprising the amino acid sequences of SEQ ID NOs: 206, 166, and 241, respectively; and (b) a VL that comprises CDR1, CDR2, and CDR3 comprising the amino acid sequences of SEQ ID NOs: 245, 239, and 179, respectively.

[0433] In certain embodiments, the second antigen-binding site is derived from 20D6.H8. For example, in certain embodiments, the second antigen-binding site comprises a VH that comprises an amino acid sequence at least 90% (*e.g.*, at least 91%, at least 92%, at least 93%, at least 94%, at least 95%, at least 96%, at least 97%, at least 98%, at least 99%, or 100%) identical to the amino acid sequence of SEQ ID NO:238, and a VL that comprises an amino acid sequence

at least 90% (*e.g.*, at least 91%, at least 92%, at least 93%, at least 94%, at least 95%, at least 96%, at least 97%, at least 98%, at least 99%, or 100%) identical to SEQ ID NO:237. In certain embodiments, the VH comprises CDR1, CDR2, and CDR3 comprising the amino acid sequences of SEQ ID NOs: 221, 236, and 223, respectively. In certain embodiments, the VL comprises CDR1, CDR2, and CDR3 comprising the amino acid sequences of SEQ ID NOs: 152, 226, and 179, respectively. In certain embodiments, the second antigen-binding site comprises (a) a VH that comprises CDR1, CDR2, and CDR3 comprising the amino acid sequences of SEQ ID NOs: 221, 236, and 223, respectively; and (b) a VL that comprises CDR1, CDR2, and CDR3 comprising the amino acid sequences of SEQ ID NOs: 152, 226, and 179, respectively.

[0434] In certain embodiments, the second antigen-binding site is derived from 15A10.G8. For example, in certain embodiments, the second antigen-binding site comprises a VH that comprises an amino acid sequence at least 90% (*e.g.*, at least 91%, at least 92%, at least 93%, at least 94%, at least 95%, at least 96%, at least 97%, at least 98%, at least 99%, or 100%) identical to the amino acid sequence of SEQ ID NO:155, and a VL that comprises an amino acid sequence at least 90% (*e.g.*, at least 91%, at least 92%, at least 93%, at least 94%, at least 95%, at least 96%, at least 97%, at least 98%, at least 99%, or 100%) identical to SEQ ID NO:158. In certain embodiments, the VH comprises CDR1, CDR2, and CDR3 comprising the amino acid sequences of SEQ ID NOs: 159, 170, and 183, respectively. In certain embodiments, the VL comprises CDR1, CDR2, and CDR3 comprising the amino acid sequences of SEQ ID NOs: 186, 188, and189, and respectively. In certain embodiments, the second antigen-binding site comprises (a) a VH that comprises CDR1, CDR2, and CDR3 comprising the amino acid sequences of SEQ ID NOs: 159, 170, and 183, respectively; and (b) a VL that comprises CDR1, CDR2, and CDR3 comprising the amino acid sequences of SEQ ID NOs: 186, 188, and 189, respectively.

[0435] In certain embodiments, the second antigen-binding site is derived from 13E1.A4. For example, in certain embodiments, the second antigen-binding site comprises a VH that comprises an amino acid sequence at least 90% (*e.g.*, at least 91%, at least 92%, at least 93%, at least 94%, at least 95%, at least 96%, at least 97%, at least 98%, at least 99%, or 100%) identical to the amino acid sequence of SEQ ID NO:190, and a VL that comprises an amino acid sequence at least 90% (*e.g.*, at least 91%, at least 92%, at least 93%, at least 94%, at least 95%, at least 96%, at least 97%, at least 98%, at least 99%, or 100%) identical to SEQ ID NO:191. In certain embodiments, the VH comprises CDR1, CDR2, and CDR3 comprising the amino acid sequences

of SEQ ID NOs: 197, 202, and 207, respectively. In certain embodiments, the VL comprises CDR1, CDR2, and CDR3 comprising the amino acid sequences of SEQ ID NOs: 211, 212, and 214, and respectively. In certain embodiments, the second antigen-binding site comprises (a) a VH that comprises CDR1, CDR2, and CDR3 comprising the amino acid sequences of SEQ ID NOs: 197, 202, and 207, respectively; and (b) a VL that comprises CDR1, CDR2, and CDR3 comprising the amino acid sequences of SEQ ID NOs: 211, 212, and 214, respectively.

[0436] In certain embodiments, the second antigen-binding site is derived from 12F8.H7. For example, in certain embodiments, the second antigen-binding site comprises a VH that comprises an amino acid sequence at least 90% (*e.g.*, at least 91%, at least 92%, at least 93%, at least 94%, at least 95%, at least 96%, at least 97%, at least 98%, at least 99%, or 100%) identical to the amino acid sequence of SEQ ID NO:217, and a VL that comprises an amino acid sequence at least 90% (*e.g.*, at least 91%, at least 92%, at least 93%, at least 94%, at least 95%, at least 96%, at least 97%, at least 98%, at least 99%, or 100%) identical to SEQ ID NO:219. In certain embodiments, the VH comprises CDR1, CDR2, and CDR3 comprising the amino acid sequences of SEQ ID NOs: 220, 222, and 257, respectively. In certain embodiments, the VL comprises CDR1, CDR2, and CDR3 comprising the amino acid sequences of SEQ ID NOs: 224, 225, and 227, and respectively. In certain embodiments, the second antigen-binding site comprises (a) a VH that comprises CDR1, CDR2, and CDR3 comprising the amino acid sequences of SEQ ID NOs: 220, 222, and 257, respectively; and (b) a VL that comprises CDR1, CDR2, and CDR3 comprising the amino acid sequences of SEQ ID NOs: 224, 225, and 227, respectively.

[0437] In certain embodiments, the second antigen-binding site is derived from 9E4.B7. For example, in certain embodiments, the second antigen-binding site comprises a VH that comprises an amino acid sequence at least 90% (*e.g.*, at least 91%, at least 92%, at least 93%, at least 94%, at least 95%, at least 96%, at least 97%, at least 98%, at least 99%, or 100%) identical to the amino acid sequence of SEQ ID NO:228, and a VL that comprises an amino acid sequence at least 90% (*e.g.*, at least 91%, at least 92%, at least 93%, at least 94%, at least 95%, at least 96%, at least 97%, at least 98%, at least 99%, or 100%) identical to SEQ ID NO:229. In certain embodiments, the VH comprises CDR1, CDR2, and CDR3 comprising the amino acid sequences of SEQ ID NOs: 230, 231, and 232, respectively. In certain embodiments, the VL comprises CDR1, CDR2, and CDR3 comprising the amino acid sequences of SEQ ID NOs: 233, 234, and 235, and respectively. In certain embodiments, the second antigen-binding site comprises (a) a

VH that comprises CDR1, CDR2, and CDR3 comprising the amino acid sequences of SEQ ID NOs: 230, 231, and 232, respectively; and (b) a VL that comprises CDR1, CDR2, and CDR3 comprising the amino acid sequences of SEQ ID NOs: 233, 234, and 235, respectively.

[0438] In certain embodiments, the second antigen-binding site that binds CLEC12A is an scFv. For example, in certain embodiments, the second antigen-binding site comprises the amino acid sequence of SEQ ID NO:145, 146, 149, 150, 153, 154, 156, 157, 160, 161, 164, 165, 168, 169, 172, 173, 176, 177, 180, 181, 184, 185, 204, 205, 208, 209, 215, 216, 252, 253, 254, 255, 274, 275, 280, or 281. In specific embodiments, the second antigen-binding site comprises the amino acid sequence of SEQ ID NO:180.

[0439] Alternatively, novel antigen-binding sites that can bind to CLEC12A can be identified by screening for binding to the amino acid sequence defined by SEQ ID NO:258, a variant thereof, a mature extracellular fragment thereof or a fragment containing a domain of CLEC12A.

SEQ ID NO:258

MSEEVTYADLQFQNSSEMEKIPEIGKFGEKAPPAPSHVWRPAALFLTLLCLLLLIGLGVL ASMFHVTLKIEMKKMNKLQNISEELQRNISLQLMSNMNISNKIRNLSTTLQTIATKLCRE LYSKEQEHKCKPCPRRWIWHKDSCYFLSDDVQTWQESKMACAAQNASLLKINNKNAL EFIKSQSRSYDYWLGLSPEEDSTRGMRVDNIINSSAWVIRNAPDLNNMYCGYINRLYVQ YYHCTYKKRMICEKMANPVQLGSTYFREA (Uniprot ID No. Q5QGZ9)

[0440] It is contemplated that in an scFv, a VH and a VL can be connected by a linker, *e.g.*, $(GlyGlyGlyGlySer)_4$ *i.e.* $(G_4S)_4$ linker (SEQ ID NO:119). A skilled person in the art would appreciate that any of the other disclosed linkers (see, *e.g.*, Table 10) may be used in an scFv having a VH and VL sequences disclosed herein (*e.g.*, in Table 2).

[0441] In each of the foregoing embodiments, it is contemplated herein that the scFv, VH and/or VL sequences that bind CLEC12A may contain amino acid alterations (*e.g.*, at least 1, 2, 3, 4, 5, or 10 amino acid substitutions, deletions, or additions) in the framework regions of the VH and/or VL without affecting their ability to CLEC12A. For example, it is contemplated herein that scFv, VH and/or VL sequences that bind CLEC12A may contain cysteine heterodimerization mutations, facilitating formation of a disulfide bridge between the VH and VL of the scFv.

[0442] In certain embodiments, the second antigen-binding site disclosed herein binds human CLEC12A with a K_D (*i.e.*, dissociation constant) of 1 nM or lower, 5 nM or lower, 10 nM or lower, 15 nM or lower, or 20 nM or lower, as measured by surface plasmon resonance (SPR) (*e.g.*, using the method described in Example 12) or by bio-layer interferometry (BLI), and/or binds CLEC12A from a body fluid, tissue, and/or cell of a subject. In certain embodiments, a second antigen-binding site disclosed herein has a K_d (*i.e.*, off-rate, also called K_{off}) equal to or lower than 1×10^{-5}, 1×10^{-4}, 1×10^{-3}, 5×10^{-3}, 0.01, 0.02, or 0.05 1/s, as measured by SPR (*e.g.*, using the method described in Example 12) or by BLI.

[0443] In certain embodiments, the second antigen-binding site derived from 15A10.G8 or 20D6.A8 binds cynomolgus CLEC12A with a K_D (*i.e.*, dissociation constant) of 5 nM or lower, 10 nM or lower, 15 nM or lower, 20 nM or lower, or 30 nM or lower, as measured by surface plasmon resonance (SPR) (*e.g.*, using the method described in Example 12) or by bio-layer interferometry (BLI), and/or binds CLEC12A from a body fluid, tissue, and/or cell of a subject. In certain embodiments, a second antigen-binding site disclosed herein has a K_d (*i.e.*, off-rate, also called K_{off}) equal to or lower than 1×10^{-3}, 5×10^{-3}, 0.01, 0.02, or 0.03 1/s, as measured by SPR (*e.g.*, using the method described in Example 12) or by BLI.

[0444] Variations in the glycosylation status of CLEC12A on the surface of different cell types has been reported (Marshall *et al.*, (2006) *Eur J Immunol.* 36(8):2159-69). CLEC12A expressed on the surface of AML cells from different patients may have different glycosylation patterns as well. Moreover, branched glycans can restrict accessibility to the protein component of CLEC12A, limiting diversity of available epitopes. Certain antigen-binding sites or the present application can overcome the glycosylation variations. In certain embodiments, a second antigen-binding site disclosed herein, *e.g.*, an antigen-binding site derived from 16B8.C8, a humanized 16B8.C8, 9F11.B7, or a humanized 9F11.B7, binds CLEC12A (*e.g.*, human CLEC12A) in a glycosylation independent manner, *i.e.*, binds both a glycosylated CLEC12A and a de-glycosylated CLEC12A. In certain embodiments, the ratio of the K_D at which the second antigen-binding site binds deglycosylated CLEC12A to the K_D at which the second antigen-binding site binds glycosylated CLEC12A is within the range of 1:10 to 10:1 (e.g., within the range of 1:5 to 5:1, 1:3 to 3:1, or 1:2 to 2:1). In certain embodiments, the ratio is about 1:5, about 1:3, about 1:2, about 1:1.5, about 1:1, about 1.5:1, about 2:1, about 3:1, or about 5:1. In certain embodiments, the ratio is about 1:1. In another aspect, the instant disclosure provides a

multispecific binding protein comprising (a) a first antigen-binding site that binds NKG2D; (b) a second antigen-binding site that binds CLEC12A; and (c) an antibody Fc domain or a portion thereof sufficient to bind CD16, or a third antigen-binding site that binds CD16; wherein the second antigen-binding site binds CLEC12A in a glycosylation independent manner.

[0445] CLEC12A containing a K244Q substitution is a polymorphic variant prevalent in about 30% of the human population. In some embodiments, the second antigen-binding site of a multispecific binding protein disclosed herein binds CLEC12A-K244Q. In certain embodiments, the ratio of the K_D at which the second antigen-binding site binds CLEC12A-K244Q to the K_D at which the second antigen-binding site binds wild-type CLEC12A is within the range of 1:2 to 2:1. In certain embodiments, the ratio is about 1:2, about 1:1.5, about 1:1, about 1.5:1, or about 2:1. In certain embodiments, the ratio is about 1:1.

[0446] In some embodiments, the multispecific binding proteins described herein bind to CLEC12A with an isoelectric point (pI) of about 8 to about 9. In some embodiments, the multispecific binding proteins described herein bind to CLEC12A with a pI of about 8.5 to about 8.9. In certain embodiments, the multispecific binding proteins described herein bind to CLEC12A with a pI of about 8.7.

[0447] In some embodiments, the F3' format of a CLEC12A TriNKET described herein (*e.g.*, hF3'-1602 TriNKET), has EC50 about 2-fold lower (*e.g.*, about 1-fold lower, about 2-fold lower, about 3-fold lower, about 4 fold lower, about 5-fold lower, about 6-fold lower) than that of the corresponding F3 format TriNKET, *e.g.*, AB0010, in binding to human CLEC12A on the surface of a cell, *e.g.*, a cancer cell. In some embodiments, the F3' format of a CLEC12A TriNKET described herein (*e.g.*, hF3'-1602 TriNKET), has EC50 about 50% lower (*e.g.*, about 25% lower, about 30% lower, about 40% lower, about 50% lower, about 55% lower, about 60% lower, about 70% lower, about 75% lower) than that of the corresponding F3 format TriNKET, *e.g.*, AB0010, in binding to human CLEC12A on the surface of a cell, *e.g.*, a cancer cell.

[0448] In certain embodiments, the second antigen-binding site competes for binding to CLEC12A with a corresponding antigen-binding site described above. In one aspect, the instant disclosure provides a multispecific binding protein comprising (a) a first antigen-binding site that binds NKG2D; (b) a second antigen-binding site that binds CLEC12A; and (c) an antibody Fc domain or a portion thereof sufficient to bind CD16, or a third antigen-binding site that binds CD16; wherein the second antigen-binding site competes with an antigen-binding site that binds

CLEC12A as disclosed herein. In certain embodiments, the second antigen-binding site competes with an antigen-binding site derived from 16B8.C8 disclosed above for binding to CLEC12A. In one embodiment, the second antigen-binding site competes with 16B8.C8 for binding to CLEC12A. In certain embodiments, the second antigen-binding site competes with an antigen-binding site derived from a humanized 16B8.C8 disclosed above for binding to CLEC12A. In one embodiment, the second antigen-binding site competes with a humanized 16B8.C8 for binding to CLEC12A. In certain embodiments, the second antigen-binding site competes with an antigen-binding site derived from 9F11.B7 disclosed above for binding to CLEC12A. In one embodiment, the second antigen-binding site competes with 9F11.B7 for binding to CLEC12A. In certain embodiments, the second antigen-binding site competes with an antigen-binding site derived from a humanized 9F11.B7 disclosed above for binding to CLEC12A. In one embodiment, the second antigen-binding site competes with a humanized 9F11.B7 for binding to CLEC12A. In certain embodiments, the second antigen-binding site competes with an antigen-binding site derived from 12F8.H7, 13E1.A4, 15A10.E8, 20D6.H8, or 23A5.H8 disclosed above for binding to CLEC12A. In some embodiments, the second antigen-binding site competes with 12F8.H7, 13E1.A4, 15A10.E8, 20D6.H8, or 23A5.H8 for binding to CLEC12A.

Fc domain

[0449] Within the Fc domain, CD16 binding is mediated by the hinge region and the CH2 domain. For example, within human IgG1, the interaction with CD16 is primarily focused on amino acid residues Asp 265 – Glu 269, Asn 297 – Thr 299, Ala 327 – Ile 332, Leu 234 – Ser 239, and carbohydrate residue N-acetyl-D-glucosamine in the CH2 domain (see, Sondermann *et al.*, Nature, 406 (6793):267-273). Based on the known domains, mutations can be selected to enhance or reduce the binding affinity to CD16, such as by using phage-displayed libraries or yeast surface-displayed cDNA libraries, or can be designed based on the known three-dimensional structure of the interaction. Accordingly, in certain embodiment, the antibody Fc domain or the portion thereof comprises a hinge and a CH2 domain.

[0450] The assembly of heterodimeric antibody heavy chains can be accomplished by expressing two different antibody heavy chain sequences in the same cell, which may lead to the assembly of homodimers of each antibody heavy chain as well as assembly of heterodimers. Promoting the preferential assembly of heterodimers can be accomplished by incorporating

different mutations in the CH3 domain of each antibody heavy chain constant region as shown in US13/494870, US16/028850, US11/533709, US12/875015, US13/289934, US14/773418, US12/811207, US13/866756, US14/647480, and US14/830336. For example, mutations can be made in the CH3 domain based on human IgG1 and incorporating distinct pairs of amino acid substitutions within a first polypeptide and a second polypeptide that allow these two chains to selectively heterodimerize with each other. The positions of amino acid substitutions illustrated below are all numbered according to the EU index as in Kabat.

[0451] In one scenario, an amino acid substitution in the first polypeptide replaces the original amino acid with a larger amino acid, selected from arginine (R), phenylalanine (F), tyrosine (Y) or tryptophan (W), and at least one amino acid substitution in the second polypeptide replaces the original amino acid(s) with a smaller amino acid(s), chosen from alanine (A), serine (S), threonine (T), or valine (V), such that the larger amino acid substitution (a protuberance) fits into the surface of the smaller amino acid substitutions (a cavity). For example, one polypeptide can incorporate a T366W substitution, and the other can incorporate three substitutions including T366S, L368A, and Y407V.

[0452] An antibody heavy chain variable domain described in the application can optionally be coupled to an amino acid sequence at least 90% identical to an antibody constant region, such as an IgG constant region including hinge, CH2 and CH3 domains with or without CH1 domain. In some embodiments, the amino acid sequence of the constant region is at least 90% identical to a human antibody constant region, such as a human IgG1 constant region, an IgG2 constant region, IgG3 constant region, or IgG4 constant region. In one embodiment, the antibody Fc domain or a portion thereof sufficient to bind CD16 comprises an amino acid sequence at least 90% (*e.g.*, at least 91%, at least 92%, at least 93%, at least 94%, at least 95%, at least 96%, at least 97%, at least 98%, at least 99%, or 100%) identical to wild-type human IgG1 Fc sequence DKTHTCPPCPAPELLGGPSVFLFPPKPKDTLMISRTPEVTCVVVDVSHEDPEVKFNWYV DGVEVHNAKTKPREEQYNSTYRVVSVLTVLHQDWLNGKEYKCKVSNKALPAPIEKTIS KAKGQPREPQVYTLPPSRDELTKNQVSLTCLVKGFYPSDIAVEWESNGQPENNYKTTPP VLDSDGSFFLYSKLTVDKSRWQQGNVFSCSVMHEALHNHYTQKSLSLSPG (SEQ ID NO:118). In some other embodiments, the amino acid sequence of the constant region is at least 90% identical to an antibody constant region from another mammal, such as rabbit, dog, cat, mouse, or horse.

[0453] In some embodiments, the antibody constant domain linked to the scFv or the Fab fragment is able to bind to CD16. In some embodiments, the protein incorporates a portion of an antibody Fc domain (for example, a portion of an antibody Fc domain sufficient to bind CD16), wherein the antibody Fc domain comprises a hinge and a CH2 domain (for example, a hinge and a CH2 domain of a human IgG1 antibody), and/or amino acid sequences at least 90% identical to amino acid sequence 234-332 of a human IgG antibody.

[0454] One or more mutations can be incorporated into the constant region as compared to human IgG1 constant region, for example at Q347, Y349, L351, S354, E356, E357, K360, Q362, S364, T366, L368, K370, N390, K392, T394, D399, S400, D401, F405, Y407, K409, T411 and/or K439. Exemplary substitutions include, for example, Q347E, Q347R, Y349S, Y349K, Y349T, Y349D, Y349E, Y349C, T350V, L351K, L351D, L351Y, S354C, E356K, E357Q, E357L, E357W, K360E, K360W, Q362E, S364K, S364E, S364H, S364D, T366V, T366I, T366L, T366M, T366K, T366W, T366S, L368E, L368A, L368D, K370S, N390D, N390E, K392L, K392M, K392V, K392F, K392D, K392E, T394F, T394W, D399R, D399K, D399V, S400K, S400R, D401K, F405A, F405T, Y407A, Y407I , Y407V, K409F, K409W, K409D, K409R, T411D, T411E, K439D, and K439E.

[0455] In certain embodiments, mutations that can be incorporated into the CH1 of a human IgG1 constant region may be at amino acid V125, F126, P127, T135, T139, A140, F170, P171, and/or V173. In certain embodiments, mutations that can be incorporated into the Cκ of a human IgG1 constant region may be at amino acid E123, F116, S176, V163, S174, and/or T164.

[0456] Alternatively, amino acid substitutions could be selected from the following sets of substitutions shown in Table 3.

Table 3		
	First Polypeptide	Second Polypeptide
Set 1	S364E/F405A	Y349K/T394F
Set 2	S364H/D401K	Y349T/T411E
Set 3	S364H/T394F	Y349T/F405A
Set 4	S364E/T394F	Y349K/F405A
Set 5	S364E/T411E	Y349K/D401K
Set 6	S364D/T394F	Y349K/F405A

Set 7	S364H/F405A	Y349T/T394F
Set 8	S364K/E357Q	L368D/K370S
Set 9	L368D/K370S	S364K
Set 10	L368E/K370S	S364K
Set 11	K360E/Q362E	D401K
Set 12	L368D/K370S	S364K/E357L
Set 13	K370S	S364K/E357Q
Set 14	F405L	K409R
Set 15	K409R	F405L

[0457] Alternatively, amino acid substitutions could be selected from the following sets of substitutions shown in Table 4.

Table 4		
	First Polypeptide	Second Polypeptide
Set 1	K409W	D399V/F405T
Set 2	Y349S	E357W
Set 3	K360E	Q347R
Set 4	K360E/K409W	Q347R/D399V/F405T
Set 5	Q347E/K360E/K409W	Q347R/D399V/F405T
Set 6	Y349S/K409W	E357W/D399V/F405T

[0458] Alternatively, amino acid substitutions could be selected from the following sets of substitutions shown in Table 5.

Table 5		
	First Polypeptide	Second Polypeptide
Set 1	T366K/L351K	L351D/L368E
Set 2	T366K/L351K	L351D/Y349E
Set 3	T366K/L351K	L351D/Y349D

Set 4	T366K/L351K	L351D/Y349E/L368E
Set 5	T366K/L351K	L351D/Y349D/L368E
Set 6	E356K/D399K	K392D/K409D

[0459] Alternatively, at least one amino acid substitution in each polypeptide chain could be selected from Table 6.

Table 6	
First Polypeptide	Second Polypeptide
L351Y, D399R, D399K, S400K, S400R, Y407A, Y407I, Y407V	T366V, T366I, T366L, T366M, N390D, N390E, K392L, K392M, K392V, K392F K392D, K392E, K409F, K409W, T411D and T411E

[0460] Alternatively, at least one amino acid substitution could be selected from the following sets of substitutions in Table 7, where the position(s) indicated in the First Polypeptide column is replaced by any known negatively-charged amino acid, and the position(s) indicated in the Second Polypeptide Column is replaced by any known positively-charged amino acid.

Table 7	
First Polypeptide	Second Polypeptide
K392, K370, K409, or K439	D399, E356, or E357

[0461] Alternatively, at least one amino acid substitution could be selected from the following set in Table 8, where the position(s) indicated in the First Polypeptide column is replaced by any known positively-charged amino acid, and the position(s) indicated in the Second Polypeptide Column is replaced by any known negatively-charged amino acid.

Table 8	
First Polypeptide	Second Polypeptide
D399, E356, or E357	K409, K439, K370, or K392

[0462] Alternatively, amino acid substitutions could be selected from the following sets in Table 9.

Table 9	
First Polypeptide	Second Polypeptide
T350V, L351Y, F405A, and Y407V	T350V, T366L, K392L, and T394W

[0463] Alternatively, or in addition, the structural stability of a hetero-multimeric protein may be increased by introducing S354C on either of the first or second polypeptide chain, and Y349C on the opposing polypeptide chain, which forms an artificial disulfide bridge within the interface of the two polypeptides.

[0464] In some embodiments, the amino acid sequence of one polypeptide chain of the antibody constant region differs from the amino acid sequence of an IgG1 constant region at position T366, and wherein the amino acid sequence of the other polypeptide chain of the antibody constant region differs from the amino acid sequence of an IgG1 constant region at one or more positions selected from the group consisting of T366, L368 and Y407.

[0465] In some embodiments, the amino acid sequence of one polypeptide chain of the antibody constant region differs from the amino acid sequence of an IgG1 constant region at one or more positions selected from the group consisting of T366, L368 and Y407, and wherein the amino acid sequence of the other polypeptide chain of the antibody constant region differs from the amino acid sequence of an IgG1 constant region at position T366.

[0466] In some embodiments, the amino acid sequence of one polypeptide chain of the antibody constant region differs from the amino acid sequence of an IgG1 constant region at one or more positions selected from the group consisting of E357, K360, Q362, S364, L368, K370, T394, D401, F405, and T411 and wherein the amino acid sequence of the other polypeptide chain of the antibody constant region differs from the amino acid sequence of an IgG1 constant region at one or more positions selected from the group consisting of Y349, E357, S364, L368, K370, T394, D401, F405 and T411.

[0467] In some embodiments, the amino acid sequence of one polypeptide chain of the antibody constant region differs from the amino acid sequence of an IgG1 constant region at one or more positions selected from the group consisting of Y349, E357, S364, L368, K370, T394,

D401, F405 and T411 and wherein the amino acid sequence of the other polypeptide chain of the antibody constant region differs from the amino acid sequence of an IgG1 constant region at one or more positions selected from the group consisting of E357, K360, Q362, S364, L368, K370, T394, D401, F405, and T411.

[0468] In some embodiments, the amino acid sequence of one polypeptide chain of the antibody constant region differs from the amino acid sequence of an IgG1 constant region at one or more positions selected from the group consisting of L351, D399, S400 and Y407 and wherein the amino acid sequence of the other polypeptide chain of the antibody constant region differs from the amino acid sequence of an IgG1 constant region at one or more positions selected from the group consisting of T366, N390, K392, K409 and T411.

[0469] In some embodiments, the amino acid sequence of one polypeptide chain of the antibody constant region differs from the amino acid sequence of an IgG1 constant region at one or more positions selected from the group consisting of T366, N390, K392, K409 and T411 and wherein the amino acid sequence of the other polypeptide chain of the antibody constant region differs from the amino acid sequence of an IgG1 constant region at one or more positions selected from the group consisting of L351, D399, S400 and Y407.

[0470] In some embodiments, the amino acid sequence of one polypeptide chain of the antibody constant region differs from the amino acid sequence of an IgG1 constant region at one or more positions selected from the group consisting of Q347, Y349, K360, and K409, and wherein the amino acid sequence of the other polypeptide chain of the antibody constant region differs from the amino acid sequence of an IgG1 constant region at one or more positions selected from the group consisting of Q347, E357, D399 and F405.

[0471] In some embodiments, the amino acid sequence of one polypeptide chain of the antibody constant region differs from the amino acid sequence of an IgG1 constant region at one or more positions selected from the group consisting of Q347, E357, D399 and F405, and wherein the amino acid sequence of the other polypeptide chain of the antibody constant region differs from the amino acid sequence of an IgG1 constant region at one or more positions selected from the group consisting of Y349, K360, Q347 and K409.

[0472] In some embodiments, the amino acid sequence of one polypeptide chain of the antibody constant region differs from the amino acid sequence of an IgG1 constant region at one or more positions selected from the group consisting of K370, K392, K409 and K439, and

wherein the amino acid sequence of the other polypeptide chain of the antibody constant region differs from the amino acid sequence of an IgG1 constant region at one or more positions selected from the group consisting of D356, E357 and D399.

[0473] In some embodiments, the amino acid sequence of one polypeptide chain of the antibody constant region differs from the amino acid sequence of an IgG1 constant region at one or more positions selected from the group consisting of D356, E357 and D399, and wherein the amino acid sequence of the other polypeptide chain of the antibody constant region differs from the amino acid sequence of an IgG1 constant region at one or more positions selected from the group consisting of K370, K392, K409 and K439.

[0474] In some embodiments, the amino acid sequence of one polypeptide chain of the antibody constant region differs from the amino acid sequence of an IgG1 constant region at one or more positions selected from the group consisting of L351, E356, T366 and D399, and wherein the amino acid sequence of the other polypeptide chain of the antibody constant region differs from the amino acid sequence of an IgG1 constant region at one or more positions selected from the group consisting of Y349, L351, L368, K392 and K409.

[0475] In some embodiments, the amino acid sequence of one polypeptide chain of the antibody constant region differs from the amino acid sequence of an IgG1 constant region at one or more positions selected from the group consisting of Y349, L351, L368, K392 and K409, and wherein the amino acid sequence of the other polypeptide chain of the antibody constant region differs from the amino acid sequence of an IgG1 constant region at one or more positions selected from the group consisting of L351, E356, T366 and D399.

[0476] In some embodiments, the amino acid sequence of one polypeptide chain of the antibody constant region differs from the amino acid sequence of an IgG1 constant region by an S354C substitution and wherein the amino acid sequence of the other polypeptide chain of the antibody constant region differs from the amino acid sequence of an IgG1 constant region by a Y349C substitution.

[0477] In some embodiments, the amino acid sequence of one polypeptide chain of the antibody constant region differs from the amino acid sequence of an IgG1 constant region by a Y349C substitution and wherein the amino acid sequence of the other polypeptide chain of the antibody constant region differs from the amino acid sequence of an IgG1 constant region by an S354C substitution.

[0478] In some embodiments, the amino acid sequence of one polypeptide chain of the antibody constant region differs from the amino acid sequence of an IgG1 constant region by K360E and K409W substitutions and wherein the amino acid sequence of the other polypeptide chain of the antibody constant region differs from the amino acid sequence of an IgG1 constant region by Q347R, D399V and F405T substitutions.

[0479] In some embodiments, the amino acid sequence of one polypeptide chain of the antibody constant region differs from the amino acid sequence of an IgG1 constant region by Q347R, D399V and F405T substitutions and wherein the amino acid sequence of the other polypeptide chain of the antibody constant region differs from the amino acid sequence of an IgG1 constant region by K360E and K409W substitutions.

[0480] In some embodiments, the amino acid sequence of one polypeptide chain of the antibody constant region differs from the amino acid sequence of an IgG1 constant region by a T366W substitutions and wherein the amino acid sequence of the other polypeptide chain of the antibody constant region differs from the amino acid sequence of an IgG1 constant region by T366S, T368A, and Y407V substitutions.

[0481] In some embodiments, the amino acid sequence of one polypeptide chain of the antibody constant region differs from the amino acid sequence of an IgG1 constant region by T366S, T368A, and Y407V substitutions and wherein the amino acid sequence of the other polypeptide chain of the antibody constant region differs from the amino acid sequence of an IgG1 constant region by a T366W substitution.

[0482] In some embodiments, the amino acid sequence of one polypeptide chain of the antibody constant region differs from the amino acid sequence of an IgG1 constant region by T350V, L351Y, F405A, and Y407V substitutions and wherein the amino acid sequence of the other polypeptide chain of the antibody constant region differs from the amino acid sequence of an IgG1 constant region by T350V, T366L, K392L, and T394W substitutions.

[0483] In some embodiments, the amino acid sequence of one polypeptide chain of the antibody constant region differs from the amino acid sequence of an IgG1 constant region by T350V, T366L, K392L, and T394W substitutions and wherein the amino acid sequence of the other polypeptide chain of the antibody constant region differs from the amino acid sequence of an IgG1 constant region by T350V, L351Y, F405A, and Y407V substitutions.

Exemplary multispecific binding proteins

[0484] Listed below are examples of TriNKETs comprising an antigen-binding site that binds CLEC12A and an antigen-binding site that binds NKG2D each linked to an antibody constant region, wherein the antibody constant regions include mutations that enable heterodimerization of two Fc chains.

[0485] Exemplary CLEC12A-targeting TriNKETs are contemplated in the F3' and F3 formats. As described above, in the F3' format, the antigen-binding site that binds the tumor-associated antigen is an scFv and the antigen-binding site that binds NKG2D is a Fab. In the F3 format, the antigen-binding site that binds the tumor-associated antigen is a Fab, and the antigen-binding site that binds NKG2D is an scFv. In each TriNKET, the scFv may comprise substitution of Cys in the VH and VL regions, facilitating formation of a disulfide bridge between the VH and VL of the scFv.

[0486] The VH and VL of the scFv can be connected via a linker, *e.g.*, a peptide linker. In certain embodiments, the peptide linker is a flexible linker. Regarding the amino acid composition of the linker, peptides are selected with properties that confer flexibility, do not interfere with the structure and function of the other domains of the proteins described in the present application, and resist cleavage from proteases. For example, glycine and serine residues generally provide protease resistance. In certain embodiments, the VL is linked N-terminal or C-terminal to the VH via a $(GlyGlyGlyGlySer)_4$ ($(G_4S)_4$) linker (SEQ ID NO:119).

[0487] The length of the linker (*e.g.*, flexible linker) can be "short," *e.g.*, 0, 1, 2, 3, 4, 5, 6, 7, 8, 9, 10, 11 or 12 amino acid residues, or "long," *e.g.*, at least 13 amino acid residues. In certain embodiments, the linker is 10-50, 10-40, 10-30, 10-25, 10-20, 15-50, 15-40, 15-30, 15-25, 15-20, 20-50, 20-40, 20-30, or 20-25 amino acid residues in length.

[0488] In certain embodiments, the linker comprises or consists of a $(GS)_n$ (SEQ ID NO:120), $(GGS)_n$ (SEQ ID NO:121), $(GGGS)_n$ (SEQ ID NO:122), $(GGSG)_n$ (SEQ ID NO:123), $(GGSGG)_n$ (SEQ ID NO:124), and $(GGGGS)_n$ (SEQ ID NO:125) sequence, wherein n is 1, 2, 3, 4, 5, 6, 7, 8, 9, 10, 11, 12, 13, 14, 15, 16, 17, 18, 19, or 20. In certain embodiments, the linker comprises or consists of an amino acid sequence selected from SEQ ID NO:119 and SEQ ID NO:126-134, as listed in Table 10.

Table 10	
SEQ ID	Amino Acid Sequence
SEQ ID NO:126	GSGSGSGSGSGSGSGSGS
SEQ ID NO:127	GGSGGSGGSGGSGGSGGSGGSGGSGGSGGS
SEQ ID NO:128	GGGSGGGSGGGSGGGSGGGSGGGSGGGSGGGSGGGSGGGS
SEQ ID NO:129	GGSGGGSGGGSGGGSGGGSGGGSGGGSGGGSGGGSGGGSG
SEQ ID NO:130	GGSGGGGSGGGGSGGGGSGGGGSGGGGSGGGGSGGGGSGGG GSGGGGSGG
SEQ ID NO:131	GGGGSGGGGSGGGGSGGGGSGGGGSGGGGSGGGGSGGGGSG GGGSGGGGS
SEQ ID NO:119	GGGGSGGGGSGGGGSGGGGS
SEQ ID NO:132	GGGGSGGGGSGGGGS
SEQ ID NO:133	GGGGSGGGGSGGGGSGGGGSGGGGSGGGGSGGGGSGGGGSG GGGSGGGGSGGGGSGGGGSGGGGSGGGGSGGGGSGGGGSGG GGSGGGGSGGGGSGGGGS
SEQ ID NO:134	GGSGGGGSGGGGSGGGGSGGGGSGGGGSGGGGSGGGGSGGG GSGGGGSGGGGSGGGGSGGGGSGGGGSGGGGSGGGGSGGGGS GGGGSGGGGSGGGGSGG

[0489] In the F3'-TriNKETs, the tumor-associated antigen-binding scFv is linked to the N-terminus of an Fc via a Gly-Ser linker. The Ala-Ser or Gly-Ser linker is included at the elbow hinge region sequence to balance between flexibility and optimal geometry. In certain embodiments, an additional sequence Thr-Lys-Gly can be added N-terminal or C-terminal to the Ala-Ser or Gly-Ser sequence at the hinge.

[0490] As used herein to describe these exemplary TriNKETs, an Fc includes an antibody hinge, CH2, and CH3. In each exemplary TriNKET, the Fc domain linked to an scFv comprises the mutations of Q347R, D399V, and F405T, and the Fc domain linked to a Fab comprises matching mutations K360E and K409W for forming a heterodimer. The Fc domain linked to the scFv further includes an S354C substitution in the CH3 domain, which forms a disulfide bond with a Y349C substitution on the Fc linked to the Fab. These substitutions are bold in the sequences described in this subsection.

[0491] For example, a TriNKET of the present disclosure is F3'-1602 TriNKET, also referred to herein as "hF3'-1602 TriNKET" and "AB0237". F3'-1602 TriNKET includes (a) a CLEC12A-binding scFv sequence derived from scFv -1602 of Table 2, in the orientation of VH

positioned N-terminal to VL, linked to an Fc domain and (b) an NKG2D-binding Fab fragment derived from A49MI including a heavy chain portion comprising a heavy chain variable domain and a CH1 domain, and a light chain portion comprising a light chain variable domain and a light chain constant domain, wherein the CH1 domain is connected to the Fc domain. F3'-1602 TriNKET includes three polypeptides scFv-1602-VH-VL-Fc, A49MI-VH-CH1-Fc, and A49MI-VL-CL.

scFv-1602-VH-VL-Fc (SEQ ID NO:259) ("Chain S")

QLQLQESGPGLVKPSETLSLTCTVSGFSLTNYGLHWIRQPPGKCLEWIGVIWSGGKTDY
NPSLKSRVTISKDTSKNQFSLKLSSVQAADTAVYYCAKYDYDDSLDYWGQGTLVTVSS
GGGGSGGGGSGGGGSGGGGS
DIQMTQSPSSLSASVGDRVTITCHASQNINFWLSWYQQKPGKAPKLLIYEASNLHTGVPS
RFSGSGSGTRFTLTISSLQPEDIATYYCQQSHSYPLTFGCGTKLEIK
GS
DKTHTCPPCPAPELLGGPSVFLFPPKPKDTLMISRTPEVTCVVVDVSHEDPEVKFNWYV
DGVEVHNAKTKPREEQYNSTYRVVSVLTVLHQDWLNGKEYKCKVSNKALPAPIEKTIS
KAKGQPREPRVYTLPPCRDELTKNQVSLTCLVKGFYPSDIAVEWESNGQPENNYKTTPP
VLVSDGSFTLYSKLTVDKSRWQQGNVFSCSVMHEALHNHYTQKSLSLSPG

A49MI-VH-CH1-Fc (SEQ ID NO:260) ("Chain H")

EVQLVESGGGLVKPGGSLRLSCAASGFTFSSYSMNWVRQAPGKGLEWVSSISSSSSYIY
YADSVKGRFTISRDNAKNSLYLQMNSLRAEDTAVYYCARGAPIGAAAGWFDPWGQGT
LVTVSS
ASTKGPSVFPLAPSSKSTSGGTAALGCLVKDYFPEPVTVSWNSGALTSGVHTFPAVLQSS
GLYSLSSVVTVPSSSLGTQTYICNVNHKPSNTKVDKKVEPKSCDKTHTCPPCPAPELLGG
PSVFLFPPKPKDTLMISRTPEVTCVVVDVSHEDPEVKFNWYVDGVEVHNAKTKPREEQY
NSTYRVVSVLTVLHQDWLNGKEYKCKVSNKALPAPIEKTISKAKGQPREPQVCTLPPSR
DELTENQVSLTCLVKGFYPSDIAVEWESNGQPENNYKTTPPVLDSDGSFFLYSWLTVDK
SRWQQGNVFSCSVMHEALHNHYTQKSLSLSPG

A49MI-VL-CL (SEQ ID NO:261) ("Chain L")

DIQMTQSPSSVSASVGDRVTITCRASQGISSWLAWYQQKPGKAPKLLIYAASSLQSGVPS
RFSGSGSGTDFTLTISSLQPEDFATYYCQQGVSFPRTFGGGTKVEIKRTVAAPSVFIFPPSD
EQLKSGTASVVCLLNNFYPREAKVQWKVDNALQSGNSQESVTEQDSKDSTYSLSSTLTL
SKADYEKHKVYACEVTHQGLSSPVTKSFNRGEC

[0492] scFv-1602-VH-VL-Fc represents the full sequence of a CLEC12A binding scFv linked to an Fc domain via a hinge comprising Gly-Ser. The Fc domain linked to the scFv

includes Q347R, D399V, and F405T substitutions for heterodimerization and an S354C substitution for forming a disulfide bond with a Y349C substitution in A49MI-VH-CH1-Fc as described below. The scFv has the amino acid sequence of scFv-1602, which includes a heavy chain variable domain of scFv-1602 connected to the N-terminus of a light chain variable domain of scFv-1602 via a $(G_4S)_4$ linker. scFv-1602-VH-VL-Fc comprises substitution of Cys in the VH and VL regions at G44 and S100, facilitating formation of a disulfide bridge between the VH and VL of the scFv.

[0493] A49MI-VH-CH1-Fc represents the heavy chain portion of the Fab fragment, which comprises a heavy chain variable domain (SEQ ID NO:95) of NKG2D-binding A49MI and a CH1 domain, connected to an Fc domain. The Fc domain in A49MI-VH-CH1-Fc includes a Y349C substitution in the CH3 domain, which forms a disulfide bond with an S354C substitution on the Fc in scFv-1602-VH-VL-Fc. In A49MI-VH-CH1-Fc, the Fc domain also includes K360E and K409W substitutions for heterodimerization with the Fc in scFv-1602-VH-VL-Fc.

[0494] A49MI-VL-CL represents the light chain portion of the Fab fragment comprising a light chain variable domain of NKG2D-binding A49MI (SEQ ID NO:85) and a light chain constant domain.

[0495] The DNA sequences encoding the polypeptides scFv-1602-VH-VL-Fc, A49MI-VH-CH1-Fc, and A49MI-VL-CL are provided in Table 260.

Table 260. DNA Sequences of F3'-1602 TriNKET

Polypeptide	DNA Sequence
scFv-1602-VH-VL-Fc	ATGGACATGAGGGTACCAGCTCAGCTGCTGGGCCTGCTGCTGC TTTGGCTTCCTGGCGCTAGATGCCAATTGCAGCTGCAAGAATC CGGACCAGGGCTCGTAAAACCTTCTGAAACCCTCTCCCTCACT TGCACTGTGTCTGGATTCTCTCTCACGAACTACGGGTTGCATT GGATCCGACAGCCGCCTGGCAAGTGTCTTGAGTGGATTGGCGT TATCTGGTCAGGAGGGAAGACGGATTATAATCCAAGTCTGAA ATCCAGAGTGACAATTTCTAAGGACACGTCCAAAAATCAGTTT AGCCTCAAACTTTCCTCAGTTCAGGCTGCTGATACAGCGGTGT ACTATTGCGCAAAGTACGACTATGATGACAGTTTGGACTACTG GGGACAGGGTACACTGGTAACAGTGAGTTCTGGAGGCGGCGG TAGTGGAGGCGGGGGAAGTGGTGGCGGAGGGAGTGGAGGAG GGGGCAGTGATATTCAAATGACGCAGAGCCCCAGTTCCCTTTC AGCTAGCGTTGGCGACAGAGTAACGATAACGTGTCACGCTTCC

Polypeptide	DNA Sequence
	CAGAACATTAATTTTTGGCTTAGCTGGTATCAACAGAAACCGG GAAAAGCACCCAAGCTGCTTATCTATGAAGCGTCCAATCTCCA CACGGGTGTCCCATCAAGATTTTCTGGATCAGGCAGTGGCACA CGATTCACACTGACCATTAGTTCCTTGCAGCCCGAGGATATCG CAACTTACTACTGTCAGCAAAGTCACTCTTACCCGTTGACATT CGGATGTGGAACTAAACTGGAGATTAAGGGATCCGATAAGAC CCACACCTGTCCTCCATGTCCTGCTCCAGAACTGCTCGGCGGA CCTTCCGTGTTCCTGTTTCCTCCAAAGCCTAAGGACACCCTGAT GATCAGCAGGACCCCTGAAGTGACCTGCGTGGTGGTGGATGT GTCTCACGAGGACCCAGAAGTGAAGTTCAATTGGTACGTGGA CGGCGTGGAAGTGCACAACGCCAAGACCAAGCCTAGAGAGGA ACAGTACAACAGCACCTACAGAGTGGTGTCCGTGCTGACCGT GCTGCACCAGGATTGGCTGAACGGCAAAGAGTACAAGTGCAA GGTGTCCAACAAGGCCCTGCCTGCTCCTATCGAGAAAACCATC AGCAAGGCCAAGGGCCAGCCTCGCGAGCCTAGAGTGTATACC TTGCCTCCATGCCGGGACGAGCTGACCAAGAATCAGGTGTCCC TGACCTGCCTGGTCAAGGGCTTCTACCCTTCCGATATCGCCGT GGAATGGGAGAGCAATGGCCAGCCAGAGAACAACTACAAGA CCACACCTCCTGTGCTGGTGTCCGACGGCAGCTTTACCCTGTA CAGCAAGCTGACAGTGGACAAGAGCAGATGGCAGCAGGGCA ACGTGTTCTCCTGCAGCGTGATGCACGAGGCCCTGCACAACCA CTACACCCAGAAAAGCCTGAGCCTGTCTCCTGGCTAA [SEQ ID NO:267]
A49MI-VH-CH1-Fc	ATGGGCTGGTCCTGCATCATCCTGTTTCTGGTGGCCACAGCCA CAGGCGTGCACTCTGAGGTGCAGCTGGTTGAATCTGGCGGCG GACTTGTGAAGCCTGGCGGATCTCTGAGACTGAGCTGTGCCGC CAGCGGCTTCACCTTTAGCAGCTACAGCATGAACTGGGTCCGA CAGGCCCCTGGCAAAGGCCTTGAATGGGTGTCCAGCATCAGC AGCAGCTCCAGCTACATCTACTACGCCGACAGCGTGAAGGGC AGATTCACCATCAGCCGGGACAACGCCAAGAACAGCCTGTAC CTGCAGATGAACTCCCTGAGAGCCGAGGACACCGCCGTGTAC TATTGTGCTAGAGGCGCCCCTATTGGAGCCGCCGCTGGATGGT TCGATCCTTGGGGACAGGGAACCCTGGTCACCGTTTCTTCTGC CTCTACAAAGGGCCCCAGCGTTTTCCCACTGGCTCCTAGCAGC AAGAGCACAAGCGGAGGAACAGCTGCCCTGGGCTGTCTGGTC AAGGACTACTTTCCTGAGCCTGTGACCGTGTCCTGGAACAGCG GAGCACTGACTAGCGGCGTGCACACATTTCCAGCCGTGCTGCA AAGCAGCGGCCTGTACTCTCTGAGCAGCGTCGTGACAGTGCCT AGCAGCTCTCTGGGCACCCAGACCTACATCTGCAATGTGAACC ACAAGCCTAGCAACACCAAGGTGGACAAGAAGGTGGAACCCA AGAGCTGCGACAAGACCCACACCTGTCCTCCATGTCCTGCTCC AGAACTGCTCGGCGGACCTTCCGTGTTCCTGTTTCCTCCAAAG CCTAAGGACACCCTGATGATCAGCAGAACCCCTGAAGTGACC

Polypeptide	DNA Sequence
	TGCGTGGTGGTGGATGTGTCTCACGAGGACCCCGAAGTGAAG TTCAATTGGTACGTGGACGGCGTGGAAGTGCACAACGCCAAG ACCAAGCCTAGAGAGGAACAGTACAACAGCACCTACAGAGTG GTGTCCGTGCTGACAGTGCTGCACCAGGATTGGCTGAACGGCA AAGAGTACAAGTGCAAGGTGTCCAACAAGGCCCTGCCTGCTC CTATCGAGAAAACCATCAGCAAGGCCAAGGGCCAGCCTCGCG AACCTCAAGTCTGTACACTGCCTCCTAGCCGGGATGAGCTGAC CGAGAATCAGGTGTCCCTGACCTGTCTCGTGAAGGGCTTCTAC CCCTCCGATATCGCCGTGGAATGGGAGAGCAATGGCCAGCCA GAGAACAACTACAAGACAACCCCTCCTGTGCTGGACAGCGAC GGCTCATTCTTCCTGTACAGCTGGCTGACCGTGGACAAGTCCA GATGGCAGCAGGGCAACGTGTTCTCCTGCAGCGTGATGCACG AGGCCCTGCACAACCACTACACCCAGAAGTCCCTGTCTCTGAG CCCAGGCTAA [SEQ ID NO:268]
A49MI-VL-CL	ATGGACATGAGAGTTCCAGCTCAGCTGCTGGGCCTGCTGCTGC TTTGGCTTCCTGGCGCTAGATGCGACATCCAGATGACACAGAG CCCCAGCTCCGTGTCTGCCTCTGTGGGAGACAGAGTGACCATC ACCTGTAGAGCCAGCCAGGGCATCTCTTCTTGGCTGGCCTGGT ATCAGCAGAAGCCTGGCAAGGCCCCTAAGCTGCTGATCTATGC CGCTAGCTCTCTGCAGTCTGGCGTGCCCTCTAGATTTTCTGGCA GCGGCTCTGGCACCGACTTCACCCTGACCATATCTAGCCTGCA GCCTGAGGACTTCGCCACCTACTATTGTCAGCAGGGCGTGTCC TTTCCACGGACCTTTGGCGGCGGAACAAAGGTGGAAATCAAG CGGACAGTGGCCGCTCCTAGCGTGTTCATCTTTCCACCTAGCG ACGAGCAGCTGAAGTCCGGCACAGCCTCTGTTGTGTGCCTGCT GAACAACTTCTACCCCAGAGAAGCCAAGGTGCAGTGGAAGGT GGACAATGCCCTGCAGAGCGGCAACAGCCAAGAGAGCGTGAC AGAGCAGGACAGCAAGGACTCCACCTACAGCCTGAGCAGCAC CCTGACACTGAGCAAGGCCGACTACGAGAAGCACAAAGTGTA CGCCTGCGAAGTGACCCACCAGGGCCTTTCTAGCCCTGTGACC AAGAGCTTCAACCGGGGCGAGTGTTGA [SEQ ID NO:269]

[0496] In another example, a TriNKET of the present disclosure is hF3'-2061 TriNKET, also referred to herein as F3'2061 TriNKET. F3'-2061 TriNKET includes (a) a CLEC12A-binding scFv sequence derived from scFv-2061 of Table 2, in the orientation of VH positioned C-terminal to VL, linked to an Fc domain and (b) an NKG2D-binding Fab fragment derived from A49MI including a heavy chain portion comprising a heavy chain variable domain and a CH1 domain, and a light chain portion comprising a light chain variable domain and a light chain

constant domain, wherein the CH1 domain is connected to the Fc domain. F3'-2061 TriNKET includes three polypeptides: scFv-2061-VL-VH-Fc, A49MI-VH-CH1-Fc, and A49MI-VL-CL.

scFv-2061-VL-VH-Fc (SEQ ID NO:262)

DIQMTQSPSSLSASVGDRVTITCHASQNINFWLSWYQQKPGKAPKLLIYEASNLHTGVPS
RFSGSGSGTRFTLTISSLQPEDIATYYCQQSHSYPLTFGCGTKLEIK
GGGGSGGGGSGGGGSGGGGS
QLQLQESGPGLVKPSETLSLTCTVSGFSLTNYGLHWIRQPPGKCLEWIGVIWSGGKTDY
NPSLKSRVTISKDTSKNQFSLKLSSVQAADTAVYYCAKYDYDDSLDYWGQGTLVTVSS
GS
DKTHTCPPCPAPELLGGPSVFLFPPKPKDTLMISRTPEVTCVVVDVSHEDPEVKFNWYV
DGVEVHNAKTKPREEQYNSTYRVVSVLTVLHQDWLNGKEYKCKVSNKALPAPIEKTIS
KAKGQPREP**R**VYTLPP**C**RDELTKNQVSLTCLVKGFYPSDIAVEWESNGQPENNYKTTPP
VL**V**SDGSF**T**LYSKLTVDKSRWQQGNVFSCSVMHEALHNHYTQKSLSLSPG

[0497] scFv-2061-VL-VH-Fc represents the full sequence of a tumor-associated antigen binding scFv linked to an Fc domain via a hinge comprising Gly-Ser. The Fc domain linked to the scFv includes Q347R, D399V, and F405T substitutions for heterodimerization and an S354C substitution for forming a disulfide bond with a Y349C substitution in A49MI-VH-CH1-Fc as described below. The scFv has the amino acid sequence of scFv-2061, which includes a heavy chain variable domain of scFv-2061 connected to the C-terminus of a light chain variable domain of scFv-2061 via a $(G_4S)_4$ linker. It is contemplated that scFv-2061-VL-VH-Fc may comprise substitution of Cys in the VH and VL regions, facilitating formation of a disulfide bridge between the VH and VL of the scFv.

[0498] A49MI-VH-CH1-Fc represents the heavy chain portion of the Fab fragment, which comprises a heavy chain variable domain (SEQ ID NO:95) of NKG2D-binding A49MI and a CH1 domain, connected to an Fc domain. The Fc domain in A49MI-VH-CH1-Fc includes a Y349C substitution in the CH3 domain, which forms a disulfide bond with an S354C substitution on the Fc in scFv-2061-VL-VH-Fc. In A49MI-VH-CH1-Fc, the Fc domain also includes K360E and K409W substitutions for heterodimerization with the Fc in scFv-2061-VL-VH-Fc.

[0499] A49MI-VL-CL represents the light chain portion of the Fab fragment comprising a light chain variable domain of NKG2D-binding A49MI (SEQ ID NO:85) and a light chain constant domain.

[0500] In another example, a TriNKET of the present disclosure is AB0089 TriNKET. AB0089 TriNKET includes (a) a CLEC12A-binding scFv sequence derived from AB0305 of Table 2, in the orientation of VH positioned N-terminal to VL, linked to an Fc domain and (b) an NKG2D-binding Fab fragment derived from A49MI including a heavy chain portion comprising a heavy chain variable domain and a CH1 domain, and a light chain portion comprising a light chain variable domain and a light chain constant domain, wherein the CH1 domain is connected to the Fc domain. AB0089 TriNKET includes three polypeptides AB0305-VH-VL-Fc, A49MI-VH-CH1-Fc, and A49MI-VL-CL.

AB0305-VH-VL-Fc (SEQ ID NO:276)

QLQLQESGPGLVKPSETLSLTCTVSGFSLTNYGLHWIRQPPGKCLEWIGVIWVGGATDY
NPSLKSRVTISVDTSKNQFSLKLSSVQAADTAVYYCAKGDYGDTLDYWGQGTLVTVSS
GGGGSGGGGSGGGGSGGGGS
DIQMTQSPSSLSASVGDRVTITCHASQNINFWLSWYQQKPGKAPKLLIYEASNLHTGVPS
RFSGSGSGTDFTLTISSLQPEDFATYYCQQSHSYPLTFGCGTKLEIK
GS
DKTHTCPPCPAPELLGGPSVFLFPPKPKDTLMISRTPEVTCVVVDVSHEDPEVKFNWYV
DGVEVHNAKTKPREEQYNSTYRVVSVLTVLHQDWLNGKEYKCKVSNKALPAPIEKTIS
KAKGQPREP**R**VYTLPP**C**RDELTKNQVSLTCLVKGFYPSDIAVEWESNGQPENNYKTTPP
VL**V**SDGSF**T**LYSKLTVDKSRWQQGNVFSCSVMHEALHNHYTQKSLSLSPG

[0501] AB0305-VH-VL-Fc represents the full sequence of a tumor-associated antigen binding scFv linked to an Fc domain via a hinge comprising Gly-Ser. The Fc domain linked to the scFv includes Q347R, D399V, and F405T substitutions for heterodimerization and an S354C substitution for forming a disulfide bond with a Y349C substitution in A49MI-VH-CH1-Fc as described below. The scFv includes a heavy chain variable domain of AB0305 connected to the N-terminus of a light chain variable domain of AB0305 via a $(G_4S)_4$ linker. AB0305-VH-VL-Fc comprises substitution of Cys in the VH and VL regions at G44 and S100, facilitating formation of a disulfide bridge between the VH and VL of the scFv.

[0502] A49MI-VH-CH1-Fc represents the heavy chain portion of the Fab fragment, which comprises a heavy chain variable domain (SEQ ID NO:95) of NKG2D-binding A49MI and a CH1 domain, connected to an Fc domain. The Fc domain in A49MI-VH-CH1-Fc includes a Y349C substitution in the CH3 domain, which forms a disulfide bond with an S354C substitution on the Fc in AB0305-VH-VL-Fc. In A49MI-VH-CH1-Fc, the Fc domain also

includes K360E and K409W substitutions for heterodimerization with the Fc in AB0305-VH-VL-Fc.

[0503] A49MI-VL-CL represents the light chain portion of the Fab fragment comprising a light chain variable domain of NKG2D-binding A49MI (SEQ ID NO:85) and a light chain constant domain.

[0504] In another example, a TriNKET of the present disclosure is AB0147 TriNKET. AB0147 TriNKET includes (a) a CLEC12A-binding scFv sequence derived from AB0304 of Table 2, in the orientation of VH positioned N-terminal to VL, linked to an Fc domain and (b) an NKG2D-binding Fab fragment derived from A49MI including a heavy chain portion comprising a heavy chain variable domain and a CH1 domain, and a light chain portion comprising a light chain variable domain and a light chain constant domain, wherein the CH1 domain is connected to the Fc domain. AB0147 TriNKET includes three polypeptides AB0304-VH-VL-Fc, A49MI-VH-CH1-Fc, and A49MI-VL-CL.

AB0304-VH-VL-Fc (SEQ ID NO:277)

QLQLQESGPGLVKPSETLSLTCTVSGFSLTNYGLHWIRQPPGKCLEWIGVILSGGWTDYN
PSLKSRVTISKDTSKNQFSLKLSSVQAADTAVYYCAKGDYGDALDYWGQGTLVTVSS
GGGGSGGGGSGGGGSGGGGS
DIQMTQSPSSLSASVGDRVTITCHASQNINFWLSWYQQKPGKAPKLLIYEASNLHTGVPS
RFSGSGSGTRFTLTISSLQPEDIATYYCQQSHSYPLTFGCGTKLEIK
GS
DKTHTCPPCPAPELLGGPSVFLFPPKPKDTLMISRTPEVTCVVVDVSHEDPEVKFNWYV
DGVEVHNAKTKPREEQYNSTYRVVSVLTVLHQDWLNGKEYKCKVSNKALPAPIEKTIS
KAKGQPREP**R**VYTLPP**C**RDELTKNQVSLTCLVKGFYPSDIAVEWESNGQPENNYKTTPP
VL**V**SDGSF**T**LYSKLTVDKSRWQQGNVFSCSVMHEALHNHYTQKSLSLSPG

[0505] AB0304-VH-VL-Fc represents the full sequence of a tumor-associated antigen binding scFv linked to an Fc domain via a hinge comprising Gly-Ser. The Fc domain linked to the scFv includes Q347R, D399V, and F405T substitutions for heterodimerization and an S354C substitution for forming a disulfide bond with a Y349C substitution in A49MI-VH-CH1-Fc as described below. The scFv includes a heavy chain variable domain of AB0304 connected to the N-terminus of a light chain variable domain of AB0304 via a $(G_4S)_4$ linker. AB0304-VH-VL-Fc comprises substitution of Cys in the VH and VL regions at G44 and S100, facilitating formation of a disulfide bridge between the VH and VL of the scFv.

[0506] A49MI-VH-CH1-Fc represents the heavy chain portion of the Fab fragment, which comprises a heavy chain variable domain (SEQ ID NO:95) of NKG2D-binding A49MI and a CH1 domain, connected to an Fc domain. The Fc domain in A49MI-VH-CH1-Fc includes a Y349C substitution in the CH3 domain, which forms a disulfide bond with an S354C substitution on the Fc in AB0037-VH-VL-Fc. In A49MI-VH-CH1-Fc, the Fc domain also includes K360E and K409W substitutions for heterodimerization with the Fc in AB0304-VH-VL-Fc.

[0507] A49MI-VL-CL represents the light chain portion of the Fab fragment comprising a light chain variable domain of NKG2D-binding A49MI (SEQ ID NO:85) and a light chain constant domain.

[0508] In another example, a TriNKET of the present disclosure is AB0192 TriNKET. AB0192 TriNKET includes (a) a CLEC12A-binding scFv sequence derived from AB0192 of Table 2, in the orientation of VH positioned N-terminal to VL, linked to an Fc domain and (b) an NKG2D-binding Fab fragment derived from A49MI including a heavy chain portion comprising a heavy chain variable domain and a CH1 domain, and a light chain portion comprising a light chain variable domain and a light chain constant domain, wherein the CH1 domain is connected to the Fc domain. AB0192 TriNKET includes three polypeptides AB0192-VH-VL-Fc, A49MI-VH-CH1-Fc, and A49MI-VL-CL.

AB0192-VH-VL-Fc (SEQ ID NO:278)

EVQLVESGGGVVQPGGSLRLSCAASGFTFNAFGMHWVRQAPGKCLEWVAFISSGSTSIY
YANTVKGRFTISRDNSKNTLYLQMNSLRAEDTAVYYCARDGYPTGGAMDYWGQGTSV
TVSS
GGGGSGGGGSGGGGSGGGGS
DIQMTQSPSSLSASVGDRVTITCKASQDIYNYLSWFQQKPGKAPKPLIYRANILVSGVPS
RFSGSGSGQDYTFTISSLQPEDIATYYCLQFDAFPFTFGCGTKLEIK
GS
DKTHTCPPCPAPELLGGPSVFLFPPKPKDTLMISRTPEVTCVVVDVSHEDPEVKFNWYV
DGVEVHNAKTKPREEQYNSTYRVVSVLTVLHQDWLNGKEYKCKVSNKALPAPIEKTIS
KAKGQPREP**R**VYTLPP**C**RDELTKNQVSLTCLVKGFYPSDIAVEWESNGQPENNYKTTPP
VL**V**SDGSF**T**LYSKLTVDKSRWQQGNVFSCSVMHEALHNHYTQKSLSLSPG

[0509] AB0192-VH-VL-Fc represents the full sequence of a tumor-associated antigen binding scFv linked to an Fc domain via a hinge comprising Gly-Ser. The Fc domain linked to

the scFv includes Q347R, D399V, and F405T substitutions for heterodimerization and an S354C substitution for forming a disulfide bond with a Y349C substitution in A49MI-VH-CH1-Fc as described below. The scFv includes a heavy chain variable domain of AB0192 connected to the N-terminus of a light chain variable domain of AB0192 via a $(G_4S)_4$ linker. AB0192-VH-VL-Fc comprises substitution of Cys in the VH and VL regions at G44 and S100, facilitating formation of a disulfide bridge between the VH and VL of the scFv.

[0510] A49MI-VH-CH1-Fc represents the heavy chain portion of the Fab fragment, which comprises a heavy chain variable domain (SEQ ID NO:95) of NKG2D-binding A49MI and a CH1 domain, connected to an Fc domain. The Fc domain in A49MI-VH-CH1-Fc includes a Y349C substitution in the CH3 domain, which forms a disulfide bond with an S354C substitution on the Fc in AB0192-VH-VL-Fc. In A49MI-VH-CH1-Fc, the Fc domain also includes K360E and K409W substitutions for heterodimerization with the Fc in AB0192-VH-VL-Fc.

[0511] A49MI-VL-CL represents the light chain portion of the Fab fragment comprising a light chain variable domain of NKG2D-binding A49MI (SEQ ID NO:85) and a light chain constant domain.

[0512] In another example, a TriNKET of the present disclosure is hF3'-1295 TriNKET, also referred to herein as F3'-1295 TriNKET. F3'-1295 TriNKET includes (a) a CLEC12A-binding scFv sequence derived from scFv-1295 of Table 2, in the orientation of VH positioned N-terminal to VL, linked to an Fc domain and (b) an NKG2D-binding Fab fragment derived from A49MI including a heavy chain portion comprising a heavy chain variable domain and a CH1 domain, and a light chain portion comprising a light chain variable domain and a light chain constant domain, wherein the CH1 domain is connected to the Fc domain. F3'-1295 TriNKET includes three polypeptides scFv-1295-VH-VL-Fc, A49MI-VH-CH1-Fc, and A49MI-VL-CL.

scFv-1295-VH-VL-Fc (SEQ ID NO:281)

QLQLQESGPGLVKPSETLSLTCTVSGFSLTNYGLHWIRQPPGKCLEWIGVIWSGGKTDY
NPSLKSRVTISKDTSKNQFSLKLSSVQAADTAVYYCAKYDYDDSLDYWGQGTLVTVSS
GGGGSGGGGSGGGGSGGGGS
DIQMTQSPSSLSASVGDRVTITCHASQNINFWLSWYQQKPGKIPKLLIYEASNLHTGVPS
RFSGSGSGTRFTLTISSLQPEDIATYYCQQSHSYPLTFGCGTKLEIK
GS

DKTHTCPPCPAPELLGGPSVFLFPPKPKDTLMISRTPEVTCVVVDVSHEDPEVKFNWYV
DGVEVHNAKTKPREEQYNSTYRVVSVLTVLHQDWLNGKEYKCKVSNKALPAPIEKTIS
KAKGQPREP**R**VYTLPP**C**RDELTKNQVSLTCLVKGFYPSDIAVEWESNGQPENNYKTTPP
VL**V**SDGSF**T**LYSKLTVDKSRWQQGNVFSCSVMHEALHNHYTQKSLSLSPG

[0513] scFv-1295-VH-VL-Fc represents the full sequence of a tumor-associated antigen binding scFv linked to an Fc domain via a hinge comprising Gly-Ser. The Fc domain linked to the scFv includes Q347R, D399V, and F405T substitutions for heterodimerization and an S354C substitution for forming a disulfide bond with a Y349C substitution in A49MI-VH-CH1-Fc as described below. The scFv includes a heavy chain variable domain of scFv-1295 connected to the N-terminus of a light chain variable domain of scFv-1295 via a $(G_4S)_4$ linker. scFv-1295-VH-VL-Fc comprises substitution of Cys in the VH and VL regions at G44 and S100, facilitating formation of a disulfide bridge between the VH and VL of the scFv.

[0514] A49MI-VH-CH1-Fc represents the heavy chain portion of the Fab fragment, which comprises a heavy chain variable domain (SEQ ID NO:95) of NKG2D-binding A49MI and a CH1 domain, connected to an Fc domain. The Fc domain in A49MI-VH-CH1-Fc includes a Y349C substitution in the CH3 domain, which forms a disulfide bond with an S354C substitution on the Fc in AB0192-VH-VL-Fc. In A49MI-VH-CH1-Fc, the Fc domain also includes K360E and K409W substitutions for heterodimerization with the Fc in scFv-1295-VH-VL-Fc.

[0515] A49MI-VL-CL represents the light chain portion of the Fab fragment comprising a light chain variable domain of NKG2D-binding A49MI (SEQ ID NO:85) and a light chain constant domain.

[0516] In another example, a TriNKET of the present disclosure is F3 1602 TriNKET, also referred to herein as AB0010. F3 1602 TriNKET includes (a) an NKG2D-binding scFv sequence derived from scFv-A49MI of Table 1, in the orientation of VH positioned N-terminal to VL, linked to an Fc domain and (b) a CLEC12A-binding Fab fragment derived from scFv-1602 including a heavy chain portion comprising a heavy chain variable domain and a CH1 domain, and a light chain portion comprising a light chain variable domain and a light chain constant domain, wherein the CH1 domain is connected to the Fc domain. F3 1602 TriNKET includes three polypeptides scFv-A49MI-VH-VL-Fc, 1602-VH-CH1-Fc, and 1602-VL-CL.

scFv-A49MI-VH-VL-Fc (SEQ ID NO:286)

DIQMTQSPSSVSASVGDRVTITCRASQGISSWLAWYQQKPGKAPKLLIYAASSLQSGVPS
RFSGSGSGTDFTLTISSLQPEDFATYYCQQGVSFPRTFGGGTKVEIK
GGGGSGGGGSGGGGSGGGGS
EVQLVESGGGLVKPGGSLRLSCAASGFTFSSYSMNWVRQAPGKGLEWVSSISSSSSYIY
YADSVKGRFTISRDNAKNSLYLQMNSLRAEDTAVYYCARGAPIGAAAGWFDPWGQGT
LVTVSS
GS
DKTHTCPPCPAPELLGGPSVFLFPPKPKDTLMISRTPEVTCVVVDVSHEDPEVKFNWYV
DGVEVHNAKTKPREEQYNSTYRVVSVLTVLHQDWLNGKEYKCKVSNKALPAPIEKTIS
KAKGQPREP**R**VYTLPP**C**RDELTKNQVSLTCLVKGFYPSDIAVEWESNGQPENNYKTTPP
VL**V**SDGSF**T**LYSKLTVDKSRWQQGNVFSCSVMHEALHNHYTQKSLSLSPG

1602-VH-CH1-Fc (SEQ ID NO:287)

QLQLQESGPGLVKPSETLSLTCTVSGFSLTNYGLHWIRQPPGKGLEWIGVIWSGGKTDYN
PSLKSRVTISKDTSKNQFSLKLSSVQAADTAVYYCAKYDYDDSLDYWGQGTLVTVSS
ASTKGPSVFPLAPSSKSTSGGTAALGCLVKDYFPEPVTVSWNSGALTSGVHTFPAVLQSS
GLYSLSSVVTVPSSSLGTQTYICNVNHKPSNTKVDKKVEPKSCDKTHTCPPCPAPELLGG
PSVFLFPPKPKDTLMISRTPEVTCVVVDVSHEDPEVKFNWYVDGVEVHNAKTKPREEQY
NSTYRVVSVLTVLHQDWLNGKEYKCKVSNKALPAPIEKTISKAKGQPREPQVCTLPPSR
DELTENQVSLTCLVKGFYPSDIAVEWESNGQPENNYKTTPPVLDSDGSFFLYSWLTVDK
SRWQQGNVFSCSVMHEALHNHYTQKSLSLSPG
1602-VL-CL (SEQ ID NO:288)

DIQMTQSPSSLSASVGDRVTITCHASQNINFWLSWYQQKPGKAPKLLIYEASNLHTGVPS
RFSGSGSGTRFTLTISSLQPEDIATYYCQQSHSYPLTFGGGTKLEIKRTVAAPSVFIFPPSDE
QLKSGTASVVCLLNNFYPREAKVQWKVDNALQSGNSQESVTEQDSKDSTYSLSSTLTLS
KADYEKHKVYACEVTHQGLSSPVTKSFNRGEC

[0517] scFv-A49MI-VH-VL-Fc represents the full sequence of NKG2D binding scFv A49MI linked to an Fc domain via a hinge comprising Gly-Ser. The Fc domain linked to the scFv includes Q347R, D399V, and F405T substitutions for heterodimerization and an S354C substitution for forming a disulfide bond with a Y349C substitution in A49MI-VH-CH1-Fc as described below. The scFv includes a heavy chain variable domain of scFv-1295 connected to the N-terminus of a light chain variable domain of scFv-A49MI via a $(G_4S)_4$ linker. scFv-A49MI-VH-VL-Fc comprises substitution of Cys in the VH and VL regions at G44 and S100, facilitating formation of a disulfide bridge between the VH and VL of the scFv.

[0518] 1602-VH-CH1-Fc represents the heavy chain portion of the Fab fragment, which comprises a heavy chain variable domain of CLEC12A-binding 1602 and a CH1 domain,

connected to an Fc domain. The Fc domain in 1602-VH-CH1-Fc includes a Y349C substitution in the CH3 domain, which forms a disulfide bond with an S354C substitution on the Fc in scFv-A49MI-VH-VL-Fc. In 1602-VH-CH1-Fc, the Fc domain also includes K360E and K409W substitutions for heterodimerization with the Fc in scFv-A49MI-VH-VL-Fc.

[0519] 1602-VL-CL represents the light chain portion of the Fab fragment comprising a light chain variable domain of CLEC12A-binding 1602 and a light chain constant domain.

[0520] In certain embodiments, a TriNKET of the present disclosure is identical to one of the exemplary TriNKETs described above that includes the EW-RVT Fc mutations, except that the Fc domain linked to the NKG2D-binding Fab fragment comprises the substitutions of Q347R, D399V, and F405T, and the Fc domain linked to the tumor-associated antigen binding scFv comprises matching substitutions K360E and K409W for forming a heterodimer. In certain embodiments, a TriNKET of the present disclosure is identical to one of the exemplary TriNKETs described above that includes the KiH Fc mutations, except that the Fc domain linked to the NKG2D-binding Fab fragment comprises the "hole" substitutions of T366S, L368A, and Y407V, and the Fc domain linked to the tumor-associated antigen-binding scFv comprises the "knob" substitution of T366W for forming a heterodimer.

[0521] In certain embodiments, a TriNKET of the present disclosure is identical to one of the exemplary TriNKETs described above, except that the Fc domain linked to the NKG2D-binding Fab fragment includes an S354C substitution in the CH3 domain, and the Fc domain linked to the tumor-associated antigen-binding scFv includes a matching Y349C substitution in the CH3 domain for forming a disulfide bond.

[0522] A skilled person in the art would appreciate that during production and/or storage of proteins, N-terminal glutamate (E) or glutamine (Q) can be cyclized to form a lactam (*e.g.*, spontaneously or catalyzed by an enzyme present during production and/or storage). Accordingly, in some embodiments where the N-terminal residue of an amino acid sequence of a polypeptide is E or Q, a corresponding amino acid sequence with the E or Q replaced with pyroglutamate is also contemplated herein.

[0523] A skilled person in the art would also appreciate that during protein production and/or storage, the C-terminal lysine (K) of a protein can be removed (*e.g.*, spontaneously or catalyzed by an enzyme present during production and/or storage). Such removal of K is often observed with proteins that comprise an Fc domain at its C-terminus. Accordingly, in some embodiments

where the C-terminal residue of an amino acid sequence of a polypeptide (*e.g.*, an Fc domain sequence) is K, a corresponding amino acid sequence with the K removed is also contemplated herein.

[0524] The multispecific proteins described above can be made using recombinant DNA technology well known to a skilled person in the art. For example, a first nucleic acid sequence encoding the first immunoglobulin heavy chain can be cloned into a first expression vector; a second nucleic acid sequence encoding the second immunoglobulin heavy chain can be cloned into a second expression vector; a third nucleic acid sequence encoding the immunoglobulin light chain can be cloned into a third expression vector; and the first, second, and third expression vectors can be stably transfected together into host cells to produce the multimeric proteins.

[0525] To achieve the highest yield of the multispecific protein, different ratios of the first, second, and third expression vector can be explored to determine the optimal ratio for transfection into the host cells. After transfection, single clones can be isolated for cell bank generation using methods known in the art, such as limited dilution, ELISA, FACS, microscopy, or Clonepix.

[0526] The present application also provides a nucleic acid encoding a polypeptide that is a part of a multispecific protein provided herein. In some embodiments, a multispecific protein comprises three polypeptides. In some embodiments, a multispecific protein comprises (a) a first polypeptide comprising the amino acid sequence of SEQ ID NO:276; (b) a second polypeptide comprising the amino acid sequence of SEQ ID NO:260; and (c) a third polypeptide comprising the amino acid sequence of SEQ ID NO:261. In certain embodiments, the present application provides a nucleic acid encoding each of the three polypeptides that are part of the multispecific protein. In certain embodiments, provided herein is a nucleic acid that encodes a first polypeptide comprising the amino acid sequence of SEQ ID NO:276. In certain embodiments, provided herein is a nucleic acid that encodes a second polypeptide comprising the amino acid sequence of SEQ ID NO:260. In certain embodiments, provided herein is a nucleic acid that encodes a a third polypeptide comprising the amino acid sequence of SEQ ID NO:261.

[0527] In another aspect, the present application provides a cell comprising one or more nucleic acids encoding a polypeptide that is part of a multispecific protein provided herein. In some embodiments, a cell comprises one or more nucleic acids each encoding one or more of the

three polypeptides that are part of the multispecific protein. In certain embodiments, provided herein is a cell comprising a nucleic acid that encodes a first polypeptide comprising the amino acid sequence of SEQ ID NO:276. In certain embodiments, provided herein is a cell comprising a nucleic acid that encodes a second polypeptide comprising the amino acid sequence of SEQ ID NO:260. In certain embodiments, provided herein is a cell comprising a nucleic acid that encodes a a third polypeptide comprising the amino acid sequence of SEQ ID NO:261.

[0528] Also provided herein are methods of producing or making a multispecific protein provided herein. In some embodiments, the method comprises: (a) culturing a host cell under conditions suitable for expression of the protein, wherein the host cell comprises one or more nucleic acids each encoding one or more polypeptides that is part of the multispecific protein; and (b) isolating and purifying the protein. In some embodiments, the method comprises: (a) culturing a host cell under conditions suitable for expression of the protein, wherein the host cell comprises a first nucleic acid encoding a first polypeptide comprising the amino acid sequence of SEQ ID NO:276, a second nucleic acid encoding a second polypeptide comprising the amino acid sequence of SEQ ID NO:260, and a third nucleic acid encoding a third polypeptide comprising the amino acid sequence of SEQ ID NO:261; and (b) isolating and purifying the protein.

[0529] Clones can be cultured under conditions suitable for bio-reactor scale-up and maintained expression of the multispecific protein. The multispecific proteins can be isolated and purified using methods known in the art including centrifugation, depth filtration, cell lysis, homogenization, freeze-thawing, affinity purification, gel filtration, ion exchange chromatography, hydrophobic interaction exchange chromatography, and mixed-mode chromatography.

II. CHARACTERISTICS OF THE MULTISPECIFIC PROTEINS

[0530] The multispecific proteins described herein include an NKG2D-binding site, a tumor-associated antigen binding site that binds CLEC12A, and an antibody Fc domain or a portion thereof sufficient to bind CD16, or an antigen-binding site that binds CD16. In some embodiments, the multispecific proteins contains an additional antigen-binding site that binds to the same tumor-associated antigen (CLEC12A), as exemplified in the F4-TriNKET format (*e.g.*, FIGs. 2C and 2D).

[0531] In some embodiments, the multispecific proteins display similar thermal stability to the corresponding monoclonal antibody, *i.e.,* a monoclonal antibody containing the same tumor-associated antigen binding site as the one incorporated in the multispecific proteins.

[0532] In some embodiments, the multispecific proteins simultaneously bind to cells expressing NKG2D and/or CD16, such as NK cells, and cells expressing CLEC12A, such as certain tumor cells. Binding of the multispecific proteins to NK cells can enhance the activity of the NK cells toward destruction of the tumor-associated antigen expressing tumor cells. It has been reported that NK cells exhibit more potent cytotoxicity against target cells that are stressed (*see* Chan *et al.*, (2014) Cell Death Differ. 21(1):5-14). Without wishing to be bound by theory, it is hypothesized that when NK cells are engaged to a population of cells by a TriNKET, the NK cells may selectively kill the target cells that are stressed (*e.g.*, malignant cells and cells in a tumor microenvironment). This mechanism could contribute to increased specificity and reduced toxicity of TriNKETs, making it possible to selectively clear the stressed cells even if expression of the tumor-associated antigen is not limited to the desired target cells.

[0533] In some embodiments, the multispecific proteins induce antibody dependent cellular phagocytosis (ADCP). In some embodiments, the multispecific proteins induce antibody dependent cellular cytotoxicity (ADCC)-like activity. In some embodiments, the multispecific proteins induce ADCC activity. In some embodiments, the multispecific proteins do not induce complement dependent cytotoxicity (CDC).

[0534] In some embodiments, the multispecific proteins bind to the tumor-associated antigen with a similar affinity to the corresponding the anti-tumor-associated antigen monoclonal antibody (*i.e.,* a monoclonal antibody containing the same tumor-associated antigen binding site as the one incorporated in the multispecific proteins). In some embodiments, the multispecific proteins are more effective in killing the tumor cells expressing the tumor-associated antigen than the corresponding monoclonal antibodies.

[0535] In certain embodiments, the multispecific proteins described herein, which include a binding site for a tumor-associated antigen, activate primary human NK cells when co-culturing with cells expressing that tumor-associated antigen. NK cell activation is marked by the increase in CD107a degranulation and IFN-γ cytokine production. Furthermore, compared to a corresponding anti- tumor-associated antigen monoclonal antibody, the multispecific proteins

can show superior activation of human NK cells in the presence of cells expressing the tumor-associated antigen.

[0536] In some embodiments, the multispecific proteins described herein, which include a binding site for the tumor-associated antigen, enhance the activity of rested and IL-2-activated human NK cells when co-culturing with cells expressing the tumor-associated antigen.

[0537] In some embodiments, compared to the corresponding monoclonal antibody that binds to the tumor-associated antigen, the multispecific proteins offer an advantage in targeting tumor cells that express medium and low levels of the tumor-associated antigen.

[0538] In some embodiments, the bivalent F4 format of the TriNKETs (*i.e.,* TriNKETs include an additional antigen-binding site that binds to the tumor-associated antigen) improve the avidity with which the TriNKETs bind to the tumor-associated antigen, which in effect stabilize expression and maintenance of high levels of the tumor-associated antigen on the surface of the tumor cells. In some embodiments, the F4-TriNKETs mediate more potent killing of tumor cells than the corresponding F3-TriNKETs or F3'-TriNKETs.

III. PHARMACEUTICAL FORMULATIONS

[0539] The present disclosure also provides pharmaceutical formulations that contain a therapeutically effective amount of a multispecific binding protein disclosed herein (*e.g.*, F3'-1602). The pharmaceutical formulation comprises one or more excipients and is maintained at a certain pH. The term "excipient," as used herein, means any non-therapeutic agent added to the formulation to provide a desired physical or chemical property, for example, pH, osmolarity, viscosity, clarity, color, isotonicity, odor, sterility, stability, rate of dissolution or release, adsorption, or penetration.

Excipients and pH

[0540] The one or more excipients in the pharmaceutical formulation of the multispecific binding proteins described in the present application comprises a buffering agent. The term "buffering agent," as used herein, refers to one or more components that when added to an aqueous solution is able to protect the solution against variations in pH when adding acid or alkali, or upon dilution with a solvent. In addition to phosphate buffers, glycinate, carbonate, citrate, histidine buffers and the like can be used, in which case, sodium, potassium or ammonium ions can serve as counterion.

[0541] In certain embodiments, the buffer or buffer system comprises at least one buffer that has a buffering range that overlaps fully or in part with the range of pH 7.0-9.0. In certain embodiments, the buffer has a pKa of about 7.0 ± 0.5. In certain embodiments, the buffer has a pKa of about 7.5 ± 0.5.

[0542] In certain embodiments, the buffer comprises a citrate buffer. In certain embodiments, the citrate is present at a concentration of 5 to 100 mM, 10 to 100 mM, 15 to 100 mM, 20 to 100 mM, 5 to 50 mM, 10 to 50 mM, 15 to 100 mM, 20 to 100 mM, 5 to 25 mM, 10 to 25 mM, 15 to 25 mM, 20 to 25 mM, 5 to 20 mM, 10 to 20 mM, or 15 to 20 mM. In certain embodiments, the citrate is present at a concentration of 5 mM, 10 mM, 15 mM, 20 mM, 25 mM, or 50 mM. In certain embodiments, the citrate is present at a concentration of 20 mM.

[0543] In certain embodiments, the buffer comprises or further comprise a phosphate buffer. In certain embodiments, the phosphate is present at a concentration of 5 to 100 mM, 10 to 100 mM, 15 to 100 mM, 20 to 100 mM, 5 to 50 mM, 10 to 50 mM, 15 to 100 mM, 20 to 100 mM, 5 to 25 mM, 10 to 25 mM, 15 to 25 mM, 20 to 25 mM, 5 to 20 mM, 10 to 20 mM, or 15 to 20 mM. In certain embodiments, the phosphate is present at a concentration of 5 mM, 10 mM, 15 mM, 20 mM, 25 mM, or 50 mM. In certain embodiments, the phosphate is present at a concentration of 10 mM. It is understood that phosphate is not readily compatible with a lyophilized presentation. Accordingly, in certain embodiments, the concentration of phosphate in the pharmaceutical formulation, if any, is equal to or lower than 5 mM, 4 mM, 3 mM, 2 mM, 1 mM, 0.5 mM, 0.1 mM, 50 μM, 10 μM, 5 μM, or 1 μM. In certain embodiments, the concentration of phosphate in the pharmaceutical formulation is below the detection limit. In certain embodiments, no phosphate is added when preparing the pharmaceutical formulation.

[0544] The pharmaceutical formulation of the multispecific binding proteins described in the present application may have a pH above 7.0. For example, in certain embodiments, the pharmaceutical formulation has a pH of 7.0 to 8.0 (*i.e.*, 7.5 ± 0.5), 7.0 to 7.8 (*i.e.*, 7.4 ± 0.4), 7.0 to 7.6 (*i.e.*, 7.3 ± 0.3), 7.0 to 7.4 (*i.e.*, 7.2 ± 0.2), 7.0 to 7.2 (*i.e.*, 7.1 ± 0.1), 7.1 to 7.3 (*i.e.*, 7.2 ± 0.1), 7.2 to 7.4 (*i.e.*, 7.3 ± 0.1), 7.3 to 7.5 (*i.e.*, 7.4 ± 0.1), 7.4 to 7.6 (*i.e.*, 7.5 ± 0.1), 7.5 to 7.7 (*i.e.*, 7.6 ± 0.1), 7.6 to 7.8 (*i.e.*, 7.7 ± 0.1), 7.7 to 7.9 (*i.e.*, 7.8 ± 0.1), or 7.8 to 8.0 (*i.e.*, 7.9 ± 0.1). In certain embodiments, the pharmaceutical formulation has a pH of 7.0, 7.1, 7.2, 7.3, 7.4, 7.5, 7.6, 7.7, 7.8, 7.9, or 8.0. In certain embodiments, the pharmaceutical formulation has a pH of 7.0.

Under the rules of scientific rounding, a pH greater than or equal to 6.95 and smaller than or equal to 7.05 is rounded as 7.0.

[0545] The one or more excipients in the pharmaceutical formulation of the multispecific binding proteins described in the present application further comprises a sugar or sugar alcohol. Sugars and sugar alcohols are useful in pharmaceutical formulations as a thermal stabilizer. In certain embodiments, the pharmaceutical formulation comprises a sugar, for example, a monosaccharide (glucose, xylose, or erythritol), a disaccharide (*e.g.*, sucrose, trehalose, maltose, or galactose), or an oligosaccharide (*e.g.*, stachyose). In specific embodiments, the pharmaceutical formulation comprises sucrose. In certain embodiments, the pharmaceutical composition comprises a sugar alcohol, for example, a sugar alcohol derived from a monosaccharide (*e.g.*, mannitol, sorbitol, or xylitol), a sugar alcohol derived from a disaccharide (*e.g.*, lactitol or maltitol), or a sugar alcohol derived from an oligosaccharide. In specific embodiments, the pharmaceutical formulation comprises sorbitol.

[0546] The amount of the sugar or sugar alcohol contained within the formulation can vary depending on the specific circumstances and intended purposes for which the formulation is used. In certain embodiments, the pharmaceutical formulation comprises 50 to 300 mM, 50 to 250 mM, 100 to 300 mM, 100 to 250 mM, 150 to 300 mM, 150 to 250 mM, 200 to 300 mM, 200 to 250 mM, or 250 to 300 mM of the sugar or sugar alcohol. In certain embodiments, the pharmaceutical formulation comprises 50 mM, 75 mM, 100 mM, 125 mM, 150 mM, 200 mM, 250 mM, or 300 mM of the sugar or sugar alcohol. In specific embodiments, the pharmaceutical formulation comprises 250 mM of the sugar or sugar alcohol (*e.g.*, sucrose or sorbitol).

[0547] The one or more excipients in the pharmaceutical formulation disclosed herein further comprises a surfactant. The term "surfactant," as used herein, refers to a surface active molecule containing both a hydrophobic portion (*e.g.*, alkyl chain) and a hydrophilic portion (*e.g.*, carboxyl and carboxylate groups). Surfactants are useful in pharmaceutical formulations for reducing aggregation of a therapeutic protein. Surfactants suitable for use in the pharmaceutical formulations are generally non-ionic surfactants and include, but are not limited to, polysorbates (*e.g.* polysorbates 20 or 80); poloxamers (*e.g.* poloxamer 188); sorbitan esters and derivatives; Triton; sodium laurel sulfate; sodium octyl glycoside; lauryl-, myristyl-, linoleyl-, or stearyl-sulfobetadine; lauryl-, myristyl-, linoleyl- or stearyl-sarcosine; linoleyl-, myristyl-, or cetyl-betaine; lauramidopropyl-cocamidopropyl-, linoleamidopropyl-,

myristamidopropyl-, palmidopropyl-, or isostearamidopropylbetaine (*e.g.*, lauroamidopropyl); myristamidopropyl-, palmidopropyl-, or isostearamidopropyl-dimethylamine; sodium methyl cocoyl-, or disodium methyl oleyl-taurate; and the MONAQUAT^{TM} series (Mona Industries, Inc., Paterson, N.J.), polyethylene glycol, polypropyl glycol, and copolymers of ethylene and propylene glycol (*e.g.*, Pluronics, PF68 etc.). In certain embodiments, the surfactant is a polysorbate. In certain embodiments, the surfactant is polysorbate 80.

[0548] The amount of a non-ionic surfactant contained within the pharmaceutical formulation of the multispecific binding proteins described in the present application may vary depending on the specific properties desired of the formulation, as well as the particular circumstances and purposes for which the formulations are intended to be used. In certain embodiments, the pharmaceutical formulation comprises 0.005% to 0.5%, 0.005% to 0.2%, 0.005% to 0.1%, 0.005% to 0.05%, 0.005% to 0.02%, 0.005% to 0.01%, 0.01% to 0.5%, 0.01% to 0.2%, 0.01% to 0.1%, 0.01% to 0.05%, or 0.01% to 0.02% of the non-ionic surfactant (*e.g.*, polysorbate 80). In certain embodiments, the pharmaceutical formulation comprises 0.005%, 0.01%, 0.02%, 0.03%, 0.04%, 0.05%, 0.06%, 0.07%, 0.08%, 0.09%, 0.1%, 0.15%, 0.2%, 0.25%, 0.3%, 0.35%, 0.4%, 0.45%, or 0.5% of the non-ionic surfactant (*e.g.*, polysorbate 80).

[0549] In certain embodiments, the pharmaceutical formulation is isotonic. An "isotonic" formulation is one which has essentially the same osmotic pressure as human blood. Isotonic formulations generally have an osmotic pressure from about 250 to 350 mOsmol/kgH_2O. Isotonicity can be measured using a vapor pressure or ice-freezing type osmometer. In certain embodiments, the osmolarity of the pharmaceutical formulation is 250 to 350 mOsmol/kgH_2O. In certain embodiments, the osmolarity of the pharmaceutical formulation is 300 to 350 mOsmol/kgH_2O.

[0550] Substances such as sugar, sugar alcohol, and NaCl can be included in the pharmaceutical formulation for desired osmolarity. It is understood that NaCl is not readily compatible with a lyophilized presentation. Accordingly, in certain embodiments, the concentration of NaCl in the pharmaceutical formulation, if any, is equal to or lower than 10 mM, 9 mM, 8 mM, 7 mM, 6 mM, 5 mM, 4 mM, 3 mM, 2 mM, 1 mM, 0.5 mM, 0.1 mM, 50 μM, 10 μM, 5 μM, or 1 μM. In certain embodiments, the concentration of NaCl in the pharmaceutical formulation is below the detection limit. In certain embodiments, no NaCl salt is added when preparing the pharmaceutical formulation.

[0551] The pharmaceutical formulation of the multispecific binding proteins described in the present application may further comprise one or more other substances, such as a bulking agent or a preservative. A "bulking agent" is a compound which adds mass to a lyophilized mixture and contributes to the physical structure of the lyophilized cake (*e.g.*, facilitates the production of an essentially uniform lyophilized cake which maintains an open pore structure). Illustrative bulking agents include mannitol, glycine, polyethylene glycol and sorbitol. The lyophilized formulations of the multispecific binding proteins described in the present application may contain such bulking agents. A preservative reduces bacterial action and may, for example, facilitate the production of a multi-use (multiple-dose) formulation.

Exemplary Formulations

[0552] In certain embodiments, the pharmaceutical formulation of the multispecific binding proteins described in the present application comprises the multispecific binding protein in a buffer at pH 7.0 or higher (*e.g.*, at pH 7.0 to 8.0).

[0553] In certain embodiments, the pharmaceutical formulation comprises 10 to 200 mg/mL of the multispecific binding protein, 10 to 25 mM of citrate, 200 to 300 mM of a sugar or sugar alcohol (*e.g.*, sucrose), and 0.005% to 0.05% of a polysorbate (*e.g.*, polysorbate 80), at pH 7.0 to 8.0. In certain embodiments, the pharmaceutical formulation comprises 10 to 200 mg/mL of the multispecific binding protein, 20 mM of citrate, 250 mM of a sugar or sugar alcohol (*e.g.*, sucrose), and 0.01% of a polysorbate (*e.g.*, polysorbate 80), at pH 7.0 to 8.0. In certain embodiments, the pharmaceutical formulation comprises 10 to 200 mg/mL of the multispecific binding protein, 20 mM of citrate, 250 mM of a sugar or sugar alcohol (*e.g.*, sucrose), and 0.01% of a polysorbate (*e.g.*, polysorbate 80), at pH 7.0 to 7.5 (*e.g.*, pH 7.0).

[0554] In certain embodiments, the pharmaceutical formulation comprises 10 to 50 mg/mL of the multispecific binding protein, 10 to 25 mM of citrate, 200 to 300 mM of a sugar or sugar alcohol (*e.g.*, sucrose), and 0.005% to 0.05% of a polysorbate (*e.g.*, polysorbate 80), at pH 7.0 to 8.0. In certain embodiments, the pharmaceutical formulation comprises 10 to 50 mg/mL of the multispecific binding protein, 20 mM of citrate, 250 mM of a sugar or sugar alcohol (*e.g.*, sucrose), and 0.01% of a polysorbate (*e.g.*, polysorbate 80), at pH 7.0 to 8.0. In certain embodiments, the pharmaceutical formulation comprises 10 to 50 mg/mL of the multispecific binding protein, 20 mM of citrate, 250 mM of a sugar or sugar alcohol (*e.g.*, sucrose), and 0.01% of a polysorbate (*e.g.*, polysorbate 80), at pH 7.0 to 7.5 (*e.g.*, pH 7.0).

[0555] In certain embodiments, the pharmaceutical formulation comprises 10 to 200 mg/mL of the multispecific binding protein, 5 to 20 mM of citrate, 5 to 20 mM of phosphate, and 100 to 150 mM of NaCl, at pH 7.0 to 8.0. In certain embodiments, the pharmaceutical formulation comprises 10 to 200 mg/mL of the multispecific binding protein, 10 mM of citrate, 10 mM of phosphate, and 125 mM of NaCl, at pH 7.0 to 8.0. In certain embodiments, the pharmaceutical formulation comprises 10 to 200 mg/mL of the multispecific binding protein, 10 mM of citrate, 10 mM of phosphate, and 125 mM of NaCl, at pH 7.5 to 8.0 (*e.g.*, pH 7.8).

[0556] In certain embodiments, the pharmaceutical formulation comprises 10 to 50 mg/mL of the multispecific binding protein, 5 to 20 mM of citrate, 5 to 20 mM of phosphate, and 100 to 150 mM of NaCl, at pH 7.0 to 8.0. In certain embodiments, the pharmaceutical formulation comprises 10 to 50 mg/mL of the multispecific binding protein, 10 mM of citrate, 10 mM of phosphate, and 125 mM of NaCl, at pH 7.0 to 8.0. In certain embodiments, the pharmaceutical formulation comprises 10 to 50 mg/mL of the multispecific binding protein, 10 mM of citrate, 10 mM of phosphate, and 125 mM of NaCl, at pH 7.5 to 8.0 (*e.g.*, pH 7.8).

Stability of the Multispecific Binding Protein

[0557] The pharmaceutical formulations of the multispecific binding proteins described in the present application exhibit high levels of stability. A pharmaceutical formulation is stable when the multispecific binding protein within the formulation retains an acceptable degree of physical property, chemical structure, and/or biological function after storage under defined conditions.

[0558] Stresses during manufacture, storage, and use of the pharmaceutical formulation include but are not limited to heat stress (*e.g.*, incubation at 40 °C for 4 weeks), freeze/thaw stress (*e.g.*, after 6 freeze/thaw cycles), agitation stress (*e.g.*, stirring at 60 rpm at 4 °C for 18 hours), low pH stress (*e.g.*, incubation at pH 5.0 at 40 ºC for 2 weeks), high pH stress (*e.g.*, incubation at pH 8.0 at 40 ºC for 2 weeks), oxidative stress (*e.g.*, forced oxidation in 0.02% hydrogen peroxide at room temperature for 24 hours), or low pH hold (*e.g.*, incubation at pH 3.3 at room temperature for 1.5 hours). In certain embodiments, the multispecific binding protein is stable after exposure to one or more of these stresses.

[0559] Stability can be measured by determining the percentage of the multispecific binding protein in the formulation that remains in a native conformation after storage for a

defined amount of time at a defined temperature. The percentage of a protein in a native conformation can be determined by, for example, size exclusion chromatography (*e.g.*, size exclusion high performance liquid chromatography), where a protein in the native conformation is not aggregated (eluted in a high molecular weight fraction) or degraded (eluted in a low molecular weight fraction). In certain embodiments, less than 0.5%, 0.6%, 0.7%, 0.8%, 0.9%, or 1% of the multispecific binding protein forms a high molecular weight complex (*i.e.*, having a higher molecular weight than the native protein), as determined by size-exclusion chromatography, after one or more of the stresses disclosed herein. In certain embodiments, less than 0.5%, 0.6%, 0.7%, 0.8%, 0.9%, or 1% of the multispecific binding protein is degraded (*i.e.*, having a lower molecular weight than the native protein), as determined by size-exclusion chromatography, after one or more of the stresses disclosed herein.

[0560] Stability can also be measured by determining the percentage of multispecific binding protein present in a more acidic fraction ("acidic form") relative to the main fraction of protein ("main charge form"). Though not wishing to be bound by theory, deamidation of a protein may cause it to become more negatively charged and thus more acidic relative to the non-deamidated protein (see, e.g., Robinson, Protein Deamidation, (2002) PNAS 99(8):5283-88). The percentage of the acidic form of a protein can be determined by ion exchange chromatography (e.g., cation exchange high performance liquid chromatography) or imaged capillary isoelectric focusing (icIEF). In certain embodiments, at least 30%, 40%, 50%, 60%, 70%, 80%, or 90% of the multispecific binding protein in the pharmaceutical formulation is in the main charge form, after one or more of the stresses disclosed herein. In certain embodiments, no more than 10%, 20%, 30%, 40%, or 50% of the multispecific binding protein in the pharmaceutical formulation is in an acidic form, after one or more of the stresses disclosed herein.

[0561] Stability can also be measured by determining the purity of the multispecific binding protein by electrophoresis after denaturing the protein with sodium dodecyl sulfate (SDS). The protein sample can be denatured in the presence or absence of an agent that reduces protein disulfide bonds (*e.g.*, β-mercaptoethanol). In certain embodiments, the purity of the multispecific binding protein in the pharmaceutical formulation, as measured by capillary electrophoresis after denaturing the protein sample under reducing conditions (*e.g.*, in the presence of β-mercaptoethanol), is at least 95%, 96%, 97%, 98%, or 99%, after one or more of

the stresses disclosed herein. In certain embodiments, the purity of the multispecific binding protein in the pharmaceutical formulation, as measured by capillary electrophoresis after denaturing the protein sample under reducing conditions (*e.g.*, in the presence of β-mercaptoethanol), is at least 90%, 91%, 92%, 93%, 94%, 95%, 96%, 97%, 98%, or 99%, after one or more of the stresses disclosed herein. In certain embodiments, the purity of the multispecific binding protein in the pharmaceutical formulation, as measured by capillary electrophoresis after denaturing the protein sample under non-reducing conditions, is at least 95%, 96%, 97%, 98%, or 99%, after one or more of the stresses disclosed herein. In certain embodiments, the purity of the multispecific binding protein in the pharmaceutical formulation, as measured by capillary electrophoresis after denaturing the protein sample under non-reducing conditions, is at least 85%, 86%, 87%, 88%, 89%, 90%, 91%, 92%, 93%, 94%, 95%, 96%, 97%, 98%, or 99%, after one or more of the stresses disclosed herein.

[0562] Stability can also be measured by determining the parameters of a protein solution by dynamic light scattering. The Z-average and polydispersity index (PDI) values indicate the average diameter of particles in a solution and these measures increase when aggregates are present in the solution. The monomer %Pd value indicates the spread of different monomers detected, where lower values indicate a monodispere solution, which is preferred. The monomer size detected by DLS is useful in confirming that the main population is monomer and to characterize any higher order aggregates that may be present. In certain embodiments, the Z-average value of the pharmaceutical formulation does not increase by more than 5%, 10%, or 15%, after one or more of the stresses disclosed herein. In certain embodiments, the PDI value of the pharmaceutical formulation does not increase by more than 10%, 20%, 30%, 40%, or 50%, after one or more of the stresses disclosed herein.

[0563] In addition to the assessment of the parameters above, stability can also be measured by determining the protein's functional characters. The multispecific binding proteins disclosed herein bind CLEC12A, NKG2D, and CD16. According, in certain embodiments, the binding affinity of the multispecific binding protein to CLEC12A (*e.g.*, human CLEC12A) after one or more of the stresses disclosed herein, as measured by dissociation constant (K_D) or maximal binding response (capture level), is not lower than that in the control sample (not exposed to the stress) by more than 1%, 2%, 3%, 4%, 5%, 10%, 20%, or 30%. In certain embodiments, the binding affinity of the multispecific binding protein to NKG2D (*e.g.*, human NKG2D) after one

or more of the stresses disclosed herein, as measured by dissociation constant (K_D) or maximal binding response (capture level), is not lower than that in the control sample (not exposed to the stress) by more than 1%, 2%, 3%, 4%, 5%, 10%, 20%, or 30%. In certain embodiments, the binding affinity of the multispecific binding protein to CD16 (*e.g.*, human CD16a V158) after one or more of the stresses disclosed herein, as measured by dissociation constant (K_D) or maximal binding response (capture level), is not lower than that in the control sample (not exposed to the stress) by more than 1%, 2%, 3%, 4%, 5%, 10%, 20%, or 30%.

[0564] The multispecific binding protein disclosed herein has the ability to mediate cytotoxicity against a CLEC12A-expressing tumor cell by an NK cell. In certain embodiments, the ability of the multispecific binding protein to mediate such cytotoxicity after one or more of the stresses disclosed herein, as measured by EC50 of the multispecific binding protein in a mixed culture cytotoxicity assay, is not greater than that in the control sample (not exposed to the stress) by more than 1%, 2%, 3%, 4%, 5%, 10%, 20%, or 30%. In certain embodiments, the ability of the multispecific binding protein to mediate such cytotoxicity after one or more of the stresses disclosed herein, as measured by the maximum lysis of the target cells in a mixed culture cytotoxicity assay, is not greater than that in the control sample (not exposed to the stress) by more than 1%, 2%, 3%, 4%, 5%, 10%, 20%, or 30%.

[0565] Exemplary methods to determine stability of the multispecific binding protein in the pharmaceutical formulation are described in Examples 13 and 14 of the present disclosure. Additionally, stability of the protein can be assessed by measuring the binding affinity of the multispecific binding protein to its targets or the biological activity of the multispecific binding protein in certain *in vitro* assays, such as the NK cell activation assays and cytotoxicity assays described in WO 2018/152518.

Dosage Forms

[0566] The pharmaceutical formulation can be prepared and stored as a liquid formulation or a lyophilized form. In certain embodiments, the pharmaceutical formulation is a liquid formulation for storage at 2-8 °C (*e.g.*, 4 °C) or a frozen formulation for storage at -20 °C or lower. The sugar or sugar alcohol in the formulation is used as a lyoprotectant.

[0567] Prior to pharmaceutical use, the pharmaceutical formulation can be diluted or reconstituted in an aqueous carrier is suitable for the route of administration. Other exemplary carriers include sterile water for injection (SWFI), bacteriostatic water for injection (BWFI), a

pH buffered solution (*e.g.*, phosphate-buffered saline), sterile saline solution, Ringer's solution, or dextrose solution. For example, when the pharmaceutical formulation is prepared for intravenous administration, the pharmaceutical formulation can be diluted in a 0.9% sodium chloride (NaCl) solution. In certain embodiments, the diluted pharmaceutical formulation is isotonic and suitable for administration by intravenous infusion.

[0568] The pharmaceutical formulation comprises the multispecific binding protein at a concentration suitable for storage. In certain embodiments, the pharmaceutical formulation comprises the multispecific binding protein at a concentration of 10-200 mg/mL, 10-150 mg/mL, 10-100 mg/mL, 10-50 mg/mL, 10-40 mg/mL, 10-30 mg/mL, 10-25 mg/mL, 10-20 mg/mL, 10-15 mg/mL, 20-200 mg/mL, 20-150 mg/mL, 20-100 mg/mL, 20-50 mg/mL, 20-40 mg/mL, 20-30 mg/mL, 20-25 mg/mL, 50-200 mg/mL, 50-150 mg/mL, 50-100 mg/mL, 100-200 mg/mL, 100-150 mg/mL, or 150-200 mg/mL. In certain embodiments, the pharmaceutical formulation comprises the multispecific binding protein at a concentration of 10 mg/mL, 15 mg/mL, 20 mg/mL, 25 mg/mL, 30 mg/mL, 40 mg/mL, 50 mg/mL, 60 mg/mL, 70 mg/mL, 80 mg/mL, 90 mg/mL, 100 mg/mL, 150 mg/mL, or 200 mg/mL.

[0569] In certain embodiments, the pharmaceutical formulation is packaged in a container (*e.g.*, a vial, bag, pen, or syringe). In certain embodiments, the formulation may be a lyophilized formulation or a liquid formulation. In certain embodiments, the amount of multispecific binding protein in the container is suitable for administration as a single dose. In certain embodiments, the amount of multispecific binding protein in the container is suitable for administration in multiple doses. In certain embodiments, the pharmaceutical formulation comprises the multispecific binding protein at an amount of 0.1 to 2000 mg. In certain embodiments, the pharmaceutical formulation comprises the multispecific binding protein at an amount of 1 to 2000 mg, 10 to 2000 mg, 20 to 2000 mg, 50 to 2000 mg, 100 to 2000 mg, 200 to 2000 mg, 500 to 2000 mg, 1000 to 2000 mg, 0.1 to 1000 mg, 1 to 1000 mg, 10 to 1000 mg, 20 to 1000 mg, 50 to 1000 mg, 100 to 1000 mg, 200 to 1000 mg, 500 to 1000 mg, 0.1 to 500 mg, 1 to 500 mg, 10 to 500 mg, 20 to 500 mg, 50 to 500 mg, 100 to 500 mg, 200 to 500 mg, 0.1 to 200 mg, 1 to 200 mg, 10 to 200 mg, 20 to 200 mg, 50 to 200 mg, 100 to 200 mg, 0.1 to 100 mg, 1 to 100 mg, 10 to 100 mg, 20 to 100 mg, 50 to 100 mg, 0.1 to 50 mg, 1 to 50 mg, 10 to 50 mg, 20 to 50 mg, 0.1 to 20 mg, 1 to 20 mg, 10 to 20 mg, 0.1 to 10 mg, 1 to 10 mg, or 0.1 to 1 mg. In certain embodiments, the pharmaceutical formulation comprises the multispecific binding protein at an amount of 0.1

mg, 1 mg, 2 mg, 5 mg, 10 mg, 20 mg, 30 mg, 40 mg, 50 mg, 60 mg, 70 mg, 80 mg, 90 mg, 100 mg, 150 mg, 200 mg, 250 mg, 300 mg, 400 mg, 500 mg, 600 mg, 700 mg, 800 mg, 900 mg, 1000 mg, 1500 mg, or 2000 mg.

IV. THERAPEUTIC APPLICATIONS

[0570] The present application provides methods for treating autoimmune disease or cancer using a multispecific binding protein described herein and/or a pharmaceutical composition (*e.g.*, pharmaceutical formulation) described herein. The methods may be used to treat a variety of cancers expressing CLEC12A.

[0571] The therapeutic method can be characterized according to the cancer to be treated. The cancer to be treated can be characterized according to the presence of a particular antigen expressed on the surface of the cancer cell.

[0572] Cancers characterized by the expression of CLEC12A, include, without limitation, solid tumor indications such as gastric cancer, esophageal cancer, lung cancer, triple-negative breast cancer, colorectal cancer, and head and neck cancer.

[0573] It is contemplated that the protein, conjugate, cells, and/or pharmaceutical compositions of the present disclosure can be used to treat a variety of cancers, not limited to cancers in which the cancer cells or the cells in the cancer microenvironment express CLEC12A.

[0574] The therapeutic method can be characterized according to the cancer to be treated. For example, in certain embodiments, the cancer is acute myeloid leukemia, multiple myeloma, diffuse large B cell lymphoma, thymoma, adenoid cystic carcinoma, gastrointestinal cancer, renal cancer, breast cancer, glioblastoma, lung cancer, ovarian cancer, brain cancer, prostate cancer, pancreatic cancer, or melanoma. In some embodiments, the cancer is a hematologic malignancy or leukemia. In certain embodiments, the cancer is acute myeloid leukemia (AML), acute lymphoblastic leukemia (ALL), myelodysplasia, myelodysplastic syndromes, acute T-lymphoblastic leukemia, or acute promyelocytic leukemia, chronic myelomonocytic leukemia, or myeloid blast crisis of chronic myeloid leukemia.

[0575] In certain embodiments, the AML is a minimal residual disease (MRD). In certain embodiments, the MRD is characterized by the presence or absence of a mutation selected from CLEC12A-ITD ((Fms-like tyrosine kinase 3)-internal tandem duplications (ITD)), NPM1 (Nucleophosmin 1), DNMT3A (DNA methyltransferase gene DNMT3A), and IDH (Isocitrate

dehydrogenase 1 and 2 (IDH1 and IDH2)). In certain embodiments, the MDS is selected from MDS with multilineage dysplasia (MDS-MLD), MDS with single lineage dysplasia (MDS-SLD), MDS with ring sideroblasts (MDS-RS), MDS with excess blasts (MDS-EB), MDS with isolated del(5q), and MDS, unclassified (MDS-U). In certain embodiments, the MDS is a primary MDS or a secondary MDS.

[0576] In certain embodiments, the ALL is selected from B-cell acute lymphoblastic leukemia (B-ALL) and T-cell acute lymphoblastic leukemia (T-ALL). In certain embodiments, the MPN is selected from polycythaemia vera, essential thrombocythemia (ET), and myelofibrosis. In certain embodiments, the non-Hodgkin lymphoma is selected from B-cell lymphoma and T-cell lymphoma. In certain embodiments, the lymphoma is selected from chronic lymphocytic leukemia (CLL), lymphoblastic lymphoma (LPL), diffuse large B-cell lymphoma (DLBCL), Burkitt lymphoma (BL), primary mediastinal large B-cell lymphoma (PMBL), follicular lymphoma, mantle cell lymphoma, hairy cell leukemia, plasma cell myeloma (PCM) or multiple myeloma (MM), mature T/NK neoplasms, and histiocytic neoplasms.

[0577] In certain embodiments, the cancer is a solid tumor. In certain other embodiments, the cancer is brain cancer, bladder cancer, breast cancer, cervical cancer, colon cancer, colorectal cancer, endometrial cancer, esophageal cancer, leukemia, lung cancer, liver cancer, melanoma, ovarian cancer, pancreatic cancer, prostate cancer, rectal cancer, renal cancer, stomach cancer, testicular cancer, or uterine cancer. In yet other embodiments, the cancer is a vascularized tumor, squamous cell carcinoma, adenocarcinoma, small cell carcinoma, melanoma, glioma, neuroblastoma, sarcoma (*e.g.*, an angiosarcoma or chondrosarcoma), larynx cancer, parotid cancer, biliary tract cancer, thyroid cancer, acral lentiginous melanoma, actinic keratoses, acute lymphocytic leukemia, acute myeloid leukemia, adenoid cystic carcinoma, adenomas, adenosarcoma, adenosquamous carcinoma, anal canal cancer, anal cancer, anorectum cancer, astrocytic tumor, Bartholin gland carcinoma, basal cell carcinoma, biliary cancer, bone cancer, bone marrow cancer, bronchial cancer, bronchial gland carcinoma, carcinoid, cholangiocarcinoma, chondrosarcoma, choroid plexus papilloma/carcinoma, chronic lymphocytic leukemia, chronic myeloid leukemia, clear cell carcinoma, connective tissue cancer, cystadenoma, digestive system cancer, duodenum cancer, endocrine system cancer, endodermal sinus tumor, endometrial hyperplasia, endometrial stromal sarcoma, endometrioid adenocarcinoma, endothelial cell cancer, ependymal cancer, epithelial cell cancer, Ewing's

sarcoma, eye and orbit cancer, female genital cancer, focal nodular hyperplasia, gallbladder cancer, gastric antrum cancer, gastric fundus cancer, gastrinoma, glioblastoma, glucagonoma, heart cancer, hemangioblastomas, hemangioendothelioma, hemangiomas, hepatic adenoma, hepatic adenomatosis, hepatobiliary cancer, hepatocellular carcinoma, Hodgkin's disease, ileum cancer, insulinoma, intraepithelial neoplasia, intraepithelial squamous cell neoplasia, intrahepatic bile duct cancer, invasive squamous cell carcinoma, jejunum cancer, joint cancer, Kaposi's sarcoma, pelvic cancer, large cell carcinoma, large intestine cancer, leiomyosarcoma, lentigo maligna melanomas, lymphoma, male genital cancer, malignant melanoma, malignant mesothelial tumors, medulloblastoma, medulloepithelioma, meningeal cancer, mesothelial cancer, metastatic carcinoma, mouth cancer, mucoepidermoid carcinoma, multiple myeloma, muscle cancer, nasal tract cancer, nervous system cancer, neuroepithelial adenocarcinoma nodular melanoma, non-epithelial skin cancer, non-Hodgkin's lymphoma, oat cell carcinoma, oligodendroglial cancer, oral cavity cancer, osteosarcoma, papillary serous adenocarcinoma, penile cancer, pharynx cancer, pituitary tumors, plasmacytoma, pseudosarcoma, pulmonary blastoma, rectal cancer, renal cell carcinoma, respiratory system cancer, retinoblastoma, rhabdomyosarcoma, sarcoma, serous carcinoma, sinus cancer, skin cancer, small cell carcinoma, small intestine cancer, smooth muscle cancer, soft tissue cancer, somatostatin-secreting tumor, spine cancer, squamous cell carcinoma, striated muscle cancer, submesothelial cancer, superficial spreading melanoma, T cell leukemia, tongue cancer, undifferentiated carcinoma, ureter cancer, urethra cancer, urinary bladder cancer, urinary system cancer, uterine cervix cancer, uterine corpus cancer, uveal melanoma, vaginal cancer, verrucous carcinoma, VIPoma, vulva cancer, well differentiated carcinoma, or Wilms tumor.

[0578] In certain other embodiments, the cancer is non-Hodgkin’s lymphoma, such as a B-cell lymphoma or a T-cell lymphoma. In certain embodiments, the non-Hodgkin’s lymphoma is a B-cell lymphoma, such as a diffuse large B-cell lymphoma, primary mediastinal B-cell lymphoma, follicular lymphoma, small lymphocytic lymphoma, mantle cell lymphoma, marginal zone B-cell lymphoma, extranodal marginal zone B-cell lymphoma, nodal marginal zone B-cell lymphoma, splenic marginal zone B-cell lymphoma, Burkitt lymphoma, lymphoplasmacytic lymphoma, hairy cell leukemia, or primary central nervous system (CNS) lymphoma. In certain other embodiments, the non-Hodgkin’s lymphoma is a T-cell lymphoma, such as a precursor T-lymphoblastic lymphoma, peripheral T-cell lymphoma, cutaneous T-cell lymphoma,

angioimmunoblastic T-cell lymphoma, extranodal natural killer/T-cell lymphoma, enteropathy type T-cell lymphoma, subcutaneous panniculitis-like T-cell lymphoma, anaplastic large cell lymphoma, or peripheral T-cell lymphoma.

IV. COMBINATION THERAPY

[0579] Another aspect of the present application provides for combination therapy. A multispecific binding protein described herein can be used in combination with additional therapeutic agents to treat autoimmune disease or to treat cancer.

[0580] Exemplary therapeutic agents that may be used as part of a combination therapy in treating autoimmune inflammatory diseases are described in Li *et al.* (2017) Front. Pharmacol., 8:460, and include, for example, non-steroidal anti-inflammatory drugs (NSAIDs) (*e.g.*, COX-2 inhibitors), glucocorticoids (*e.g.*, prednisone/prednisolone, methylprednisolone, and the fluorinated glucocorticoids such as dexamethasone and betamethasone), disease-modifying antirheumatic drugs (DMARDs) (*e.g.*, methotrexate, leflunomide, gold compounds, sulfasalazine, azathioprine, cyclophosphamide, antimalarials, D-penicillamine, and cyclosporine), anti-TNF biologics (*e.g.*, infliximab, etanercept, adalimumab, golimumab, Certolizumab pegol, and their biosimilars), and other biologics targeting CTLA-4 (*e.g.*, abatacept), IL-6 receptor (*e.g.*, tocilizumab), IL-1 (*e.g.*, anakinra), Th1 immune responses (IL-12/IL-23) (*e.g.*, ustekinumab), Th17 immune responses (IL-17) (*e.g.*, secukinumab) and CD20 (*e.g.*, rituximab).

[0581] Exemplary therapeutic agents that may be used as part of a combination therapy in treating cancer include, for example, radiation, mitomycin, tretinoin, ribomustin, gemcitabine, vincristine, etoposide, cladribine, mitobronitol, methotrexate, doxorubicin, carboquone, pentostatin, nitracrine, zinostatin, cetrorelix, letrozole, raltitrexed, daunorubicin, fadrozole, fotemustine, thymalfasin, sobuzoxane, nedaplatin, cytarabine, bicalutamide, vinorelbine, vesnarinone, aminoglutethimide, amsacrine, proglumide, elliptinium acetate, ketanserin, doxifluridine, etretinate, isotretinoin, streptozocin, nimustine, vindesine, flutamide, drogenil, butocin, carmofur, razoxane, sizofilan, carboplatin, mitolactol, tegafur, ifosfamide, prednimustine, picibanil, levamisole, teniposide, improsulfan, enocitabine, lisuride, oxymetholone, tamoxifen, progesterone, mepitiostane, epitiostanol, formestane, interferon-alpha, interferon-2 alpha, interferon-beta, interferon-gamma (IFN-γ), colony stimulating factor-1,

colony stimulating factor-2, denileukin diftitox, interleukin-2, luteinizing hormone releasing factor and variations of the aforementioned agents that may exhibit differential binding to its cognate receptor, or increased or decreased serum half-life.

[0582] An additional class of agents that may be used as part of a combination therapy in treating cancer is immune checkpoint inhibitors. Exemplary immune checkpoint inhibitors include agents that inhibit one or more of (i) cytotoxic T lymphocyte-associated antigen 4 (CTLA4), (ii) programmed cell death protein 1 (PD1), (iii) PDL1, (iv) LAG3, (v) B7-H3, (vi) B7-H4, and (vii) TIM3. The CTLA4 inhibitor ipilimumab has been approved by the United States Food and Drug Administration for treating melanoma.

[0583] Yet other agents that may be used as part of a combination therapy in treating cancer are monoclonal antibody agents that target non-checkpoint targets (*e.g.*, herceptin) and non-cytotoxic agents (*e.g.*, tyrosine-kinase inhibitors).

[0584] Yet other categories of anti-cancer agents include, for example: (i) an inhibitor selected from an ALK Inhibitor, an ATR Inhibitor, an A2A Antagonist, a Base Excision Repair Inhibitor, a Bcr-Abl Tyrosine Kinase Inhibitor, a Bruton's Tyrosine Kinase Inhibitor, a CDC7 Inhibitor, a CHK1 Inhibitor, a Cyclin-Dependent Kinase Inhibitor, a DNA-PK Inhibitor, an Inhibitor of both DNA-PK and mTOR, a DNMT1 Inhibitor, a DNMT1 Inhibitor plus 2-chloro-deoxyadenosine, an HDAC Inhibitor, a Hedgehog Signaling Pathway Inhibitor, an IDO Inhibitor, a JAK Inhibitor, a mTOR Inhibitor, a MEK Inhibitor, a MELK Inhibitor, a MTH1 Inhibitor, a PARP Inhibitor, a Phosphoinositide 3-Kinase Inhibitor, an Inhibitor of both PARP1 and DHODH, a Proteasome Inhibitor, a Topoisomerase-II Inhibitor, a Tyrosine Kinase Inhibitor, a VEGFR Inhibitor, and a WEE1 Inhibitor; (ii) an agonist of OX40, CD137, CD40, GITR, CD27, HVEM, TNFRSF25, or ICOS; and (iii) a cytokine selected from IL-12, IL-15, GM-CSF, and G-CSF.

[0585] Proteins of the present application can also be used as an adjunct to surgical removal of the primary lesion.

[0586] The amount of multispecific binding protein and additional therapeutic agent and the relative timing of administration may be selected in order to achieve a desired combined therapeutic effect. For example, when administering a combination therapy to a patient in need of such administration, the therapeutic agents in the combination, or a pharmaceutical composition or compositions comprising the therapeutic agents, may be administered in any

order such as, for example, sequentially, concurrently, together, simultaneously and the like. Further, for example, a multispecific binding protein may be administered during a time when the additional therapeutic agent(s) exerts its prophylactic or therapeutic effect, or *vice versa*.

V. PHARMACEUTICAL COMPOSITIONS

[0587] The present disclosure also features pharmaceutical compositions that contain a therapeutically effective amount of a protein described herein. The composition can be formulated for use in a variety of drug delivery systems. One or more physiologically acceptable excipients or carriers can also be included in the composition for proper formulation. Suitable formulations for use in the present disclosure are found in Remington's Pharmaceutical Sciences, Mack Publishing Company, Philadelphia, Pa., 17th ed., 1985. For a brief review of methods for drug delivery, *see, e.g.*, Langer (Science 249:1527-1533, 1990).

[0588] The intravenous drug delivery formulation of the present disclosure may be contained in a bag, a pen, or a syringe. In certain embodiments, the bag may be connected to a channel comprising a tube and/or a needle. In certain embodiments, the formulation may be a lyophilized formulation or a liquid formulation. In certain embodiments, the formulation may be freeze-dried (lyophilized) and contained in about 12-60 vials. In certain embodiments, the formulation may be freeze-dried and 45 mg of the freeze-dried formulation may be contained in one vial. In certain embodiments, the about 40 mg to about 100 mg of freeze-dried formulation may be contained in one vial. In certain embodiments, freeze-dried formulation from 12, 27, or 45 vials are combined to obtain a therapeutic dose of the protein in the intravenous drug formulation. In certain embodiments, the formulation may be a liquid formulation and stored as about 250 mg/vial to about 1000 mg/vial. In certain embodiments, the formulation may be a liquid formulation and stored as about 600 mg/vial. In certain embodiments, the formulation may be a liquid formulation and stored as about 250 mg/vial.

[0589] The protein could exist in a liquid aqueous pharmaceutical formulation including a therapeutically effective amount of the protein in a buffered solution forming a formulation.

[0590] These compositions may be sterilized by conventional sterilization techniques, or may be sterile filtered. The resulting aqueous solutions may be packaged for use as-is, or lyophilized, the lyophilized preparation being combined with a sterile aqueous carrier prior to administration. The pH of the preparations typically will be between 3 and 11, more preferably

between 5 and 9 or between 6 and 8, and most preferably between 7 and 8, such as 7 to 7.5. The resulting compositions in solid form may be packaged in multiple single dose units, each containing a fixed amount of the above-mentioned agent or agents. The composition in solid form can also be packaged in a container for a flexible quantity.

[0591] In certain embodiments, the present disclosure provides a formulation with an extended shelf life including a protein of the present disclosure, in combination with mannitol, citric acid monohydrate, sodium citrate, disodium phosphate dihydrate, sodium dihydrogen phosphate dihydrate, sodium chloride, polysorbate 80, water, and sodium hydroxide.

[0592] In certain embodiments, an aqueous formulation is prepared including a protein of the present disclosure in a pH-buffered solution. The buffer may have a pH ranging from about 4 to about 8, *e.g.*, from about 4.5 to about 6.0, or from about 4.8 to about 5.5, or may have a pH of about 5.0 to about 5.2. Ranges intermediate to the above recited pH's are also intended to be part of this disclosure. For example, ranges of values using a combination of any of the above recited values as upper and/or lower limits are intended to be included. Examples of buffers that will control the pH within this range include acetate (*e.g.*, sodium acetate), succinate (such as sodium succinate), gluconate, histidine, citrate and other organic acid buffers.

[0593] In certain embodiments, the formulation includes a buffer system which contains citrate and phosphate to maintain the pH in a range of about 4 to about 8. In certain embodiments the pH range may be from about 4.5 to about 6.0, or from about pH 4.8 to about 5.5, or in a pH range of about 5.0 to about 5.2. In certain embodiments, the buffer system includes citric acid monohydrate, sodium citrate, disodium phosphate dihydrate, and/or sodium dihydrogen phosphate dihydrate. In certain embodiments, the buffer system includes about 1.3 mg/mL of citric acid (*e.g.*, 1.305 mg/mL), about 0.3 mg/mL of sodium citrate (*e.g.*, 0.305 mg/mL), about 1.5 mg/mL of disodium phosphate dihydrate (*e.g.*, 1.53 mg/mL), about 0.9 mg/mL of sodium dihydrogen phosphate dihydrate (*e.g.*, 0.86 mg/mL), and about 6.2 mg/mL of sodium chloride (*e.g.*, 6.165 mg/mL). In certain embodiments, the buffer system includes about 1 to about 1.5 mg/mL of citric acid, about 0.25 to about 0.5 mg/mL of sodium citrate, about 1.25 to about 1.75 mg/mL of disodium phosphate dihydrate, about 0.7 to about 1.1 mg/mL of sodium dihydrogen phosphate dihydrate, and about 6.0 to about 6.4 mg/mL of sodium chloride. In certain embodiments, the pH of the formulation is adjusted with sodium hydroxide.

[0594] A polyol, which acts as a tonicifier and may stabilize the antibody, may also be included in the formulation. The polyol is added to the formulation in an amount which may vary with respect to the desired isotonicity of the formulation. In certain embodiments, the aqueous formulation may be isotonic. The amount of polyol added may also be altered with respect to the molecular weight of the polyol. For example, a lower amount of a monosaccharide (*e.g.*, mannitol) may be added, compared to a disaccharide (such as trehalose). In certain embodiments, the polyol which may be used in the formulation as a tonicity agent is mannitol. In certain embodiments, the mannitol concentration may be about 5 to about 20 mg/mL. In certain embodiments, the concentration of mannitol may be about 7.5 to about 15 mg/mL. In certain embodiments, the concentration of mannitol may be about 10 to about 14 mg/mL. In certain embodiments, the concentration of mannitol may be about 12 mg/mL. In certain embodiments, the polyol sorbitol may be included in the formulation.

[0595] A detergent or surfactant may also be added to the formulation. Exemplary detergents include nonionic detergents such as polysorbates (*e.g.*, polysorbates 20, 80 etc.) or poloxamers (*e.g.*, poloxamer 188). The amount of detergent added is such that it reduces aggregation of the formulated antibody and/or minimizes the formation of particulates in the formulation and/or reduces adsorption. In certain embodiments, the formulation may include a surfactant which is a polysorbate. In certain embodiments, the formulation may contain the detergent polysorbate 80 or Tween 80. Tween 80 is a term used to describe polyoxyethylene (20) sorbitanmonooleate (*see* Fiedler, Lexikon der Hifsstoffe, Editio Cantor Verlag Aulendorf, 4th ed., 1996). In certain embodiments, the formulation may contain between about 0.1 mg/mL and about 10 mg/mL of polysorbate 80, or between about 0.5 mg/mL and about 5 mg/mL. In certain embodiments, about 0.1% polysorbate 80 may be added in the formulation.

[0596] In embodiments, the protein product of the present disclosure is formulated as a liquid formulation. The liquid formulation may be presented at a 10 mg/mL concentration in either a USP / Ph Eur type I 50R vial closed with a rubber stopper and sealed with an aluminum crimp seal closure. The stopper may be made of elastomer complying with USP and Ph Eur. In certain embodiments vials may be filled with 61.2 mL of the protein product solution in order to allow an extractable volume of 60 mL. In certain embodiments, the liquid formulation may be diluted with 0.9% saline solution.

[0597] In certain embodiments, the liquid formulation of the disclosure may be prepared as a 10 mg/mL concentration solution in combination with a sugar at stabilizing levels. In certain embodiments the liquid formulation may be prepared in an aqueous carrier. In certain embodiments, a stabilizer may be added in an amount no greater than that which may result in a viscosity undesirable or unsuitable for intravenous administration. In certain embodiments, the sugar may be disaccharides, *e.g.*, sucrose. In certain embodiments, the liquid formulation may also include one or more of a buffering agent, a surfactant, and a preservative.

[0598] In certain embodiments, the pH of the liquid formulation may be set by addition of a pharmaceutically acceptable acid and/or base. In certain embodiments, the pharmaceutically acceptable acid may be hydrochloric acid. In certain embodiments, the base may be sodium hydroxide.

[0599] In addition to aggregation, deamidation is a common product variant of peptides and proteins that may occur during fermentation, harvest/cell clarification, purification, drug substance/drug product storage and during sample analysis. Deamidation is the loss of NH_3 from a protein forming a succinimide intermediate that can undergo hydrolysis. The succinimide intermediate results in a 17 dalton mass decrease of the parent peptide. The subsequent hydrolysis results in an 18 dalton mass increase. Isolation of the succinimide intermediate is difficult due to instability under aqueous conditions. As such, deamidation is typically detectable as 1 dalton mass increase. Deamidation of an asparagine results in either aspartic or isoaspartic acid. The parameters affecting the rate of deamidation include pH, temperature, solvent dielectric constant, ionic strength, primary sequence, local polypeptide conformation and tertiary structure. The amino acid residues adjacent to Asn in the peptide chain affect deamidation rates. Gly and Ser following an Asn in protein sequences results in a higher susceptibility to deamidation.

[0600] In certain embodiments, the liquid formulation of the present disclosure may be preserved under conditions of pH and humidity to prevent deamination of the protein product.

[0601] The aqueous carrier of interest herein is one which is pharmaceutically acceptable (safe and non-toxic for administration to a human) and is useful for the preparation of a liquid formulation. Illustrative carriers include sterile water for injection (SWFI), bacteriostatic water for injection (BWFI), a pH buffered solution (*e.g.*, phosphate-buffered saline), sterile saline solution, Ringer's solution or dextrose solution.

[0602] A preservative may be optionally added to the formulations herein to reduce bacterial action. The addition of a preservative may, for example, facilitate the production of a multi-use (multiple-dose) formulation.

[0603] Intravenous (IV) formulations may be the preferred administration route in particular instances, such as when a patient is in the hospital after transplantation receiving all drugs via the IV route. In certain embodiments, the liquid formulation is diluted with 0.9% Sodium Chloride solution before administration. In certain embodiments, the diluted drug product for injection is isotonic and suitable for administration by intravenous infusion.

[0604] In certain embodiments, a salt or buffer components may be added in an amount of 10 mM - 200 mM. The salts and/or buffers are pharmaceutically acceptable and are derived from various known acids (inorganic and organic) with "base forming" metals or amines. In certain embodiments, the buffer may be phosphate buffer. In certain embodiments, the buffer may be glycinate, carbonate, citrate buffers, in which case, sodium, potassium or ammonium ions can serve as counterion.

[0605] A preservative may be optionally added to the formulations herein to reduce bacterial action. The addition of a preservative may, for example, facilitate the production of a multi-use (multiple-dose) formulation.

[0606] The aqueous carrier of interest herein is one which is pharmaceutically acceptable (safe and non-toxic for administration to a human) and is useful for the preparation of a liquid formulation. Illustrative carriers include sterile water for injection (SWFI), bacteriostatic water for injection (BWFI), a pH buffered solution (*e.g.*, phosphate-buffered saline), sterile saline solution, Ringer's solution or dextrose solution.

[0607] A protein of the present disclosure could exist in a lyophilized formulation including the proteins and a lyoprotectant. The lyoprotectant may be sugar, *e.g.*, disaccharides. In certain embodiments, the lyoprotectant may be sucrose or maltose. The lyophilized formulation may also include one or more of a buffering agent, a surfactant, a bulking agent, and/or a preservative.

[0608] The amount of sucrose or maltose useful for stabilization of the lyophilized drug product may be in a weight ratio of at least 1:2 protein to sucrose or maltose. In certain embodiments, the protein to sucrose or maltose weight ratio may be of from 1:2 to 1:5.

[0609] In certain embodiments, the pH of the formulation, prior to lyophilization, may be set by addition of a pharmaceutically acceptable acid and/or base. In certain embodiments the

pharmaceutically acceptable acid may be hydrochloric acid. In certain embodiments, the pharmaceutically acceptable base may be sodium hydroxide.

[0610] Before lyophilization, the pH of the solution containing a protein of the present disclosure may be adjusted between 6 to 8. In certain embodiments, the pH range for the lyophilized drug product may be from 7 to 8.

[0611] In certain embodiments, a salt or buffer components may be added in an amount of 10 mM - 200 mM. The salts and/or buffers are pharmaceutically acceptable and are derived from various known acids (inorganic and organic) with "base forming" metals or amines. In certain embodiments, the buffer may be phosphate buffer. In certain embodiments, the buffer may be glycinate, carbonate, citrate buffers, in which case, sodium, potassium or ammonium ions can serve as counterion.

[0612] In certain embodiments, a "bulking agent" may be added. A "bulking agent" is a compound which adds mass to a lyophilized mixture and contributes to the physical structure of the lyophilized cake (*e.g.*, facilitates the production of an essentially uniform lyophilized cake which maintains an open pore structure). Illustrative bulking agents include mannitol, glycine, polyethylene glycol and sorbitol. The lyophilized formulations of the multispecific binding proteins described in the present application may contain such bulking agents.

[0613] A preservative may be optionally added to the formulations herein to reduce bacterial action. The addition of a preservative may, for example, facilitate the production of a multi-use (multiple-dose) formulation.

[0614] In certain embodiments, the lyophilized drug product may be constituted with an aqueous carrier. The aqueous carrier of interest herein is one which is pharmaceutically acceptable (*e.g.*, safe and non-toxic for administration to a human) and is useful for the preparation of a liquid formulation, after lyophilization. Illustrative diluents include sterile water for injection (SWFI), bacteriostatic water for injection (BWFI), a pH buffered solution (*e.g.*, phosphate-buffered saline), sterile saline solution, Ringer's solution or dextrose solution.

[0615] In certain embodiments, the lyophilized drug product of the current disclosure is reconstituted with either Sterile Water for Injection, USP (SWFI) or 0.9% Sodium Chloride Injection, USP. During reconstitution, the lyophilized powder dissolves into a solution.

[0616] In certain embodiments, the lyophilized protein product of the instant disclosure is constituted to about 4.5 mL water for injection and diluted with 0.9% saline solution (sodium chloride solution).

[0617] Actual dosage levels of the active ingredients in the pharmaceutical compositions of multispecific binding proteins described in this application may be varied so as to obtain an amount of the active ingredient which is effective to achieve the desired therapeutic response for a particular patient, composition, and mode of administration, without being toxic to the patient.

[0618] The specific dose can be a uniform dose for each patient, for example, 50-5000 mg of protein. Alternatively, a patient's dose can be tailored to the approximate body weight or surface area of the patient. Other factors in determining the appropriate dosage can include the disease or condition to be treated or prevented, the severity of the disease, the route of administration, and the age, sex and medical condition of the patient. Further refinement of the calculations necessary to determine the appropriate dosage for treatment is routinely made by those skilled in the art, especially in light of the dosage information and assays disclosed herein. The dosage can also be determined through the use of known assays for determining dosages used in conjunction with appropriate dose-response data. An individual patient's dosage can be adjusted as the progress of the disease is monitored. Blood levels of the targetable construct or complex in a patient can be measured to see if the dosage needs to be adjusted to reach or maintain an effective concentration. Pharmacogenomics may be used to determine which targetable constructs and/or complexes, and dosages thereof, are most likely to be effective for a given individual (Schmitz *et al.*, *Clinica Chimica Acta* 308: 43-53, 2001; Steimer *et al.*, *Clinica Chimica Acta* 308: 33-41, 2001).

[0619] In general, dosages based on body weight are from about 0.01 μg to about 100 mg per kg of body weight, such as about 0.01 μg to about 100 mg/kg of body weight, about 0.01 μg to about 50 mg/kg of body weight, about 0.01 μg to about 10 mg/kg of body weight, about 0.01 μg to about 1 mg/kg of body weight, about 0.01 μg to about 100 μg/kg of body weight, about 0.01 μg to about 50 μg/kg of body weight, about 0.01 μg to about 10 μg/kg of body weight, about 0.01 μg to about 1 μg/kg of body weight, about 0.01 μg to about 0.1 μg/kg of body weight, about 0.1 μg to about 100 mg/kg of body weight, about 0.1 μg to about 50 mg/kg of body weight, about 0.1 μg to about 10 mg/kg of body weight, about 0.1 μg to about 1 mg/kg of body weight, about 0.1 μg to about 100 μg/kg of body weight, about 0.1 μg to about 10 μg/kg of body weight, about

0.1 μg to about 1 μg/kg of body weight, about 1 μg to about 100 mg/kg of body weight, about 1 μg to about 50 mg/kg of body weight, about 1 μg to about 10 mg/kg of body weight, about 1 μg to about 1 mg/kg of body weight, about 1 μg to about 100 μg/kg of body weight, about 1 μg to about 50 μg/kg of body weight, about 1 μg to about 10 μg/kg of body weight, about 10 μg to about 100 mg/kg of body weight, about 10 μg to about 50 mg/kg of body weight, about 10 μg to about 10 mg/kg of body weight, about 10 μg to about 1 mg/kg of body weight, about 10 μg to about 100 μg/kg of body weight, about 10 μg to about 50 μg/kg of body weight, about 50 μg to about 100 mg/kg of body weight, about 50 μg to about 50 mg/kg of body weight, about 50 μg to about 10 mg/kg of body weight, about 50 μg to about 1 mg/kg of body weight, about 50 μg to about 100 μg/kg of body weight, about 100 μg to about 100 mg/kg of body weight, about 100 μg to about 50 mg/kg of body weight, about 100 μg to about 10 mg/kg of body weight, about 100 μg to about 1 mg/kg of body weight, about 1 mg to about 100 mg/kg of body weight, about 1 mg to about 50 mg/kg of body weight, about 1 mg to about 10 mg/kg of body weight, about 10 mg to about 100 mg/kg of body weight, about 10 mg to about 50 mg/kg of body weight, about 50 mg to about 100 mg/kg of body weight.

[0620] Doses may be given once or more times daily, weekly, monthly or yearly, or even once every 2 to 20 years. Persons of ordinary skill in the art can easily estimate repetition rates for dosing based on measured residence times and concentrations of the targetable construct or complex in bodily fluids or tissues. Administration of the multispecific binding proteins described in the present application could be intravenous, intraarterial, intraperitoneal, intramuscular, subcutaneous, intrapleural, intrathecal, intracavitary, by perfusion through a catheter or by direct intralesional injection. This may be administered once or more times daily, once or more times weekly, once or more times monthly, and once or more times annually.

[0621] The description above provides multiple aspects and embodiments of the multispecific binding proteins described in the application. The patent application specifically contemplates all combinations and permutations of the aspects and embodiments. The use of any and all examples, or exemplary language herein, for example, “such as” or “including,” is intended merely to illustrate better the multispecific binding proteins described in the present application, and does not pose a limitation on the scope of the disclosure, unless so expressly stated. No language in the specification should be construed as indicating any non-claimed

element as essential to the practice of the multispecific binding proteins described in the present application.

EXAMPLES

[0622] The following examples are merely illustrative and are not intended to limit the scope or content of the multispecific binding proteins described in the present application in any way.

Example 1. Characterization of supernatants of selected hybridoma clones

[0623] CLEC12A-specific antibodies were generated by immunizing BALB/c mice with hCLEC12A-His fusion protein. Supernatants of 16 hybridomas were assessed for CLEC12A binding by Bio-layer Interferometry (BLI) binding using an OctetRed384 (ForteBio). These 16 hybridomas were further analyzed for binding to human and cynomolgus CLEC12A expressed on the cell surface of isogenic RMA cells; binding to cynomolgus CLEC12A was not observed. Estimated kinetic parameters are presented in **Table 11** and binding traces are shown in **FIG. 18**. Nine clones were selected for further study. The ability of these nine clones to bind hCLEC12A-His RMA and CLEC12A-expressing cancer cell lines U937 and PL21 was further analyzed by high resolution surface plasmon resonance (SPR). The experiment was performed at 37 °C to mimic physiological temperature using a Biacore 8K instrument.

Table 11. Kinetic parameters and affinities of CLEC12A-His binding to the antibodies produced from candidate hybridomas

Test articles	Binning profile	SPR at 37 °C			Cell Binding MFI		
		k_a (1/Ms)	k_d (1/s)	K_D (nM)	RMA-hCLEC12A	k_a (1/Ms)	k_d (1/s)
9E04	competitor	247.0	3.51×10^{-2}	9E04	competitor	247.0	3.51×10^{-2}
9F11	competitor	549.0	5.57×10^{-3}	9F11	competitor	549.0	5.57×10^{-3}
11E02	-	779.0	7.28×10^{-3}	11E02	-	779.0	7.28×10^{-3}
12F08	unique	76.7	6.23×10^{-3}	12F08	unique	76.7	6.23×10^{-3}
13E01	unique	178.0	7.50×10^{-3}	13E01	unique	178.0	7.50×10^{-3}
15A10	unique	79.5	2.23×10^{-3}	15A10	unique	79.5	2.23×10^{-3}
15D11	-	372.0	6.64×10^{-3}	15D11	-	372.0	6.64×10^{-3}

Test articles	Binning profile	SPR at 37 °C			Cell Binding MFI		
		k_a (1/Ms)	k_d (1/s)	K_D (nM)	RMA-hCLEC12A	k_a (1/Ms)	k_d (1/s)
16B08	competitor	Heterogeneous binding			819.0	16B08	competitor
20D06	unique	819.0	5.25×10^{-2}	20D06	unique	819.0	5.25×10^{-2}
23A05	unique	90.2	4.49×10^{-2}	23A05	unique	90.2	4.49×10^{-2}
30A09	-	Heterogeneous binding			74.7	30A09	-
6D07	-	Non binder			247.0	6D07	-
12B06	-	Non binder			178.0	12B06	-
20G10	-	Non binder			82.2	20G10	-
30H07	-	Non binder			76.3	30H07	-
32A03	-	Non binder			71.4	32A03	-

[0624] Binning of hybridoma fusions compared to reference mAbs was performed by BLI using OctetRed384 (ForteBio). Briefly, hybridoma supernatants were loaded onto anti-mouse IgG capture sensor tips for 15 minutes and equilibrated for 5 minutes in PBSF. Sensors were dipped into 200 nM hCLEC12A-His and allowed to associate for 180 seconds followed by dipping into 100 nM reference CLEC12A mAb. The increase in response units indicated that the hybridoma was a non-competitor to the reference mAb, whereas no increase in signal indicated that the hybridoma did compete with the reference mAb. The VH and VL sequences of these reference antibodies are provided in **Table 12**.

Table 12. Reference antibodies

Anti-CLEC12A mAbs	Source	Sequence ID	Epitope
Merus-CLL1	Merus US 2014/0120096A1	VH [SEQ ID NO:263] EVQLVQSGAEVKKPGASVKVSCKASGY TFTSYYMHWVRQAPGQGLEWMGIINPS GGSTSYAQKFQGRVTMTRDTSTSTVYM ELSSLRSEDTAVYYCARGNYGDEFDYW GQGTLVTVSS VL[SEQ ID NO:264] DIQMTQSPSSLSASVGDRVTITCRASQSIS SYLNWYQQKPGKAPKLLIYAASSLQSGV PSRFSGSGSGTDFTLTISSLQPEDFATYYC QQSYSTPPTFGQGTKVEIK	unknown

Anti-CLEC12A mAbs	Source	Sequence ID	Epitope
Genentech-h6E7	Genentech US 2016/0075787A1	VH [SEQ ID NO:265] DIQMTQSPSSLSASVGDRVTITCRASQSV STSSYNYMHWYQQKPGKPPKLLIKYASN LESGVPSRFSGSGSGTDFTLTISSLQPEDF ATYYCQHSWEIPLTFGQGTKVEIK VL [SEQ ID NO:266] EVQLVQSGAEVKKPGASVKVSCKASGY SFTDYYMHWVRQAPGQGLEWIGRINPY NGAAFYSQNFKDRVTLTVDTSTSTAYLE LSSLRSEDTAVYYCAIERGADLEGYAMD YWGQGTLVTVSS	C-type lectin-like domain, residues 142-158

[0625] Binning analysis demonstrated that antibodies produced from five of the hybridomas, namely 12F8.G3, 13E01, 15A10.G8, 20D6.A8, and 23A5.D4, did not compete with the reference antibodies for binding to hCLEC12A-His. Binding of hybridomas to isogenic human CLEC12A (hCLEC12A) and cross-reactivity with cynomolgus monkey CLEC12A (cCLEC12A) were also evaluated by measuring the binding of the antibodies to isogenic RMA cells expressing CLEC12A and the U937 AML cancer cell line.

[0626] Briefly, RMA cells were transducted with a retroviral vector encoding cCLEC12A or hCLEC12A. Binding of the α-CLEC12A mAbs from crude hybridoma harvests to the hCLEC12A or cCLEC12A isogenic cell lines, as well as CLEC12A+ U937 (ATCC catalog number CRL-1593.2) cancer cell lines, was performed as follows. 100,000 RMA, REH or SEM cells were added per well of a 96 well round bottom plate. Cells were spun down and the pellet was gently dissociated by vortexing. 100 µL of Zombie live/dead dye (PBS + 1:2000 dye) were added per well and incubated in the dark at room temperature for 20 minutes. Cells were washed with 200 µL of FACS buffer (PBS + 2% FBS). 50 µL of hybridoma supernatants were added to the washed cells and the mixtures were incubated for 30 minutes on ice in the dark. Cells were washed twice with FACS buffer and then 50 µL of anti-mouse Fc-PE secondary reagent (1:200 dilution) were added and incubated for 20 minutes on ice in the dark. After the incubation, the cells were washed and then fixed with 50 µL of 4 % paraformaldehyde for 15 minutes on ice. The fixed cells were washed with FACS buffer, resuspended in 200 µL FACS buffer, and stored at 4 °C until ready for acquisition. The samples of cells resuspended in FACS buffer were run on

BD FACSCelesta equipped with an HTS (high throughput sampler) to determine the binding affinities of the antibodies to isogenic RMA cells expressing CLEC12A and the U937 AML cancer cell line.

[0627] The binding affinities of the hybridoma supernatants to PL21 AML cancer cells (DSMZ catalog number ACC536), a human AML cell line reported to express CLEC12A, were also measured. As shown in **Table 11**, nine of the clones displayed binding affinity to cancer cells expressing hCLEC12A. Binding to cCLEC12A was not observed.

Example 2. Analysis of purified anti-CLEC12A murine antibodies

[0628] In this Example, kinetic parameters and binding affinities of the purified anti-CLEC12A murine antibodies were analyzed. Based on the analysis described in Example 1, eight hybridomas (9F11.B7, 12F8.G3, 16B8.C8, 15A10.G8, 20D6.A8, 9E4.B7, 13E1.A4, and 23A5.D4) were selected for subcloning and sequencing. Each subclone was purified from the hybridoma culture, and binding to hCLEC12A-His and cCLEC12A-His was assessed by SPR as shown in **FIG. 19**. The data from these experiments are shown in **FIG. 19A**. Antibodies 9E4.B7, 9F11.B7, 12F8.G3, and 16B8.C8 bound to hCLEC12A only (**FIG. 19A**); whereas antibodies 13E1.A4, 15A10.G8, 20D6.A8, and 23A5.D4 bound to both hCLEC12A and cCLEC12A (**FIG. 19B**). Kinetic constants and binding affinities of hCLEC12A and cCLEC12A to purified murine subcloned mAbs are provided in **Table 13**.

Table 13: Kinetic parameters and affinities of hCLEC12A binding to purified murine subclones

Test Article	Human CLEC12A-His			Cyno CLEC12A-His		
	k_a ($M^{-1}s^{-1}$)	k_d (s^{-1})	K_D (nM)	k_a ($M^{-1}s^{-1}$)	k_d (s^{-1})	K_D (nM)
9E4.B7	Low affinity heterogenous interaction			No binding		
9F11.B7	1.14×10^{6}	1.57×10^{-3}	1.4	No binding		
12F8.G3	3.97×10^{5}	1.39×10^{-3}	3.5	No binding		
16B8.C8*	4.05×10^{6}	4.44×10^{-5}	0.01	No binding		
13E1.A4	Low affinity heterogenous interaction			Low affinity heterogenous interaction		
15A10.G8	3.01×10^{5}	4.94×10^{-4}	1.6	1.96×10^{5}	6.59×10^{-4}	3.3
20D6.A8	1.31×10^{7}	9.50×10^{-2}	7.2	9.16×10^{5}	2.46×10^{-2}	26
23A5.D4	Low affinity heterogenous interaction			Low affinity heterogenous interaction		

[0629] The ability of the eight purified subcloned mAbs to bind to CLEC12A expressing cells was assessed by FACS analysis with human CLEC12A-positive PL21 cancer cell line. As shown in **FIG. 20**, 9E4.B7, 9F11.B7 and 16B8.C8 all bound to the PL21 cell line with sub-nanomolar EC50 values; however, only 9F11.B7 and 16B8.C8 satisfied both recombinant protein binding and cell binding criteria, as 9E4.B7 demonstrated low affinity heterogenous binding to recombinant hCLEC12A-His (**Table 14**). Although 15A10.G8, 13E1.A4, 20D6.A8 and 23A5.D4 showed binding to recombinant human and cyno CLEC12A in the SPR assay, these mAbs failed to recognize cancer cells, suggesting conformational differences in the binding epitope between recombinant and cell surface expressed CLEC12A. As demonstrated, both Merus-CLL1 and Genentech-h6E7 mAbs bound to PL21 with significantly inferior EC50 values as compared to the novel CLEC12A hybridoma clones.

Table 14. Cell binding confirmation of purified mouse mAbs to human PL21 cell line

Test article	EC_{50} (nM)	Max MFI
9E4.B7	0.64	186
9F11.B7	0.56	217
12F8.G3	Non binder	n/a*
16B8.C8	0.18	300
13E1.A4	Non binder	n/a
15A10.G8	Non binder	n/a
20D6.A8	Non binder	n/a
23A5.D4	Non binder	n/a
Merus-CLL1[#]	2.02	201
Genentech-h6E7[#]	5	265

[0630] To assess if mAbs bind to CLEC12A in a glycosylation independent manner, binding of clones 16B8.C8 and 9F11.B7 to glycosylated, de-sialylated and PNGase-treated hCLEC12A was assessed by SPR (**FIG. 21**). As demonstrated by the sensorgrams and in **Table 15**, both 16B8.C8 and 9F11.B7 bound to de-sialylated and deglycosylated versions of hCLEC12A without loss of affinity, suggesting that the antibody interactions with hCLEC12A are not affected by glycosylation status of the target.

Table 15. Kinetic parameters and affinities of 16B8.C8 and 9F11.B7 to differentially glycosylated hCLEC12A by SPR.

Test article	Analyte	k_a ($M^{-1}s^{-1}$)	k_d (s^{-1})	K_D (nM)
Murine 16B8. mAb	Glycosylated hCLEC12A	4.05×10^{6}	4.70×10^{-5}	0.012
Murine 16B8 mAb	De-sialylated hCLEC12A	5.25×10^{6}	3.62×10^{-5}	0.007
Murine 16B8 mAb	De-glycosylated hCLEC12A	4.26×10^{6}	4.45×10^{-5}	0.011
Murine F3'-9F11	Glycosylated hCLEC12A	1.15×10^{6}	1.11×10^{-3}	0.96
Murine F3'-9F11	De-sialylated hCLEC12A	1.58×10^{6}	9.80×10^{-4}	0.62
Murine F3'-9F11	De-glycosylated hCLEC12A	1.11×10^{6}	3.74×10^{-4}	0.34

Example 3. Putative sequence liability analysis

[0631] Potential sequence liabilities in CDRs (identified under Chothia) of the 16B8.C8 and 9F11.B7 antibodies were examined. The following potential liabilities were considered: M (potential oxidation site); NG, NS and NT sequence motif (potential deamidation site); DG, DS and DT sequence motif (potential isomerization site); DP sequence motif (potential site for chemical hydrolysis). The results are summarized in **Table 16**.

Table 16. Putative sequence liabilities in the CDRs of selected murine mAbs

Clone ID	Potential sequence liability motif	Location
16B8.C8	**DS** (Isomerization site)	CDRH3
9F11.B7	**M** (Oxidation site)	CDRH3
	DG (Isomerization site)	CDRH3
	NS (Deamidation site)	CDRH1

[0632] Variants of these antibodies were designed to remove the putative sequence liability motifs.

Example 4. Humanization of subclones

[0633] Based on the data collected regarding kinetics and affinity for recombinant hCLEC12A protein, binding to cell surface expressed hCLEC12A, and binding to AML cancer

cell lines, two mouse hybridoma subclones, namely 16B8.C8 and 9F11.B7, were selected for humanization.

[0634] The 16B8.C8 antibody was humanized. Back mutations were introduced in the framework regions to create variants having the VH and VL sequences of scFv-1292 to scFv-1309, and scFv-1602 and scFv-2061.

[0635] The 9F11.B7 antibody was humanized. Back mutations were introduced in the framework regions to create variants AB0186 to AB0196.

Example 5. CLEC12A TriNKET selection

[0636] The following criteria were applied in choosing the optimal TriNKET candidate, which led to selection of F3'-1602 TriNKET as the lead candidate:

-Potent enhancement of NK activity against AML cancer cells

-Potency greater than the corresponding monoclonal antibody

-Binding to multiple AML cell lines

-High affinity for recombinant hCLEC12A

-Low affinity for human NKG2D

-Cross-reactivity with cynomolgus monkey (cyno) targets

-Good developability profile:

-Thermostability of scFv $\geq$ 65 °C

-isoelectric point (pI) between 8-9

-Hydrophobicity Interaction Chromatography (HIC) retention time similar to well behaved therapeutic mAbs

-High specificity for human CLEC12A

-Clean polyspecific reagent (PSR) profile

-Transient expression titers similar to mAb

[0637] All 18 humanized scFv variants of clone 16B8.C8 were combined with an A49MI NKG2D Fab arm to produce humanized F3' CLEC12A TriNKETs. Binding affinities of the 18 semi-purified TriNKETs for hCLEC12A were assessed by SPR in screening. Binding signals for eight F3'-TriNKETs were less than 5 RU (approximately 15% of the expected signal ran in this assay) and, therefore, these TriNKETs were considered as nonbinders to hCLEC12A. The remaining ten F3'-TriNKETs bound to hCLEC12A with <10 nM affinity, as shown in **FIG. 22**

and **Table 17**. However, a potential N-glycosylation site was involuntarily introduced in eight out of the ten F3'-TriNKETs by introducing murine back mutation N in position H85. Only constructs F3'-1295 and F3'-1304 (containing A in position H85) did not present the N-glycosylation sequence liability; therefore, only these two constructs were carried forward for further characterization.

Table 17: Kinetics and affinities of hCLEC12A binding to semi-purified humanized F3' TriNKETs.

Test article	scFv orientations	Number of back mutations and residues reverted to human	N-glycosylation sequence liability site	k_a ($M^{-1}s^{-1}$)	k_d (s^{-1})	K_D (nM)
F3'-1292	VH-VL	7 BM	Yes	4.02×10^5	1.30×10^{-3}	3.22
F3'-1293	VH-VL	6 BM, K(H71)V*	Yes	4.58×10^5	1.75×10^{-3}	3.81
F3'-1294	VH-VL	6 BM, Q(H83)T	Yes	Binding signal < 5RU		
F3'-1295	VH-VL	6 BM, N(H85)A	No	5.20×10^5	1.53×10^{-3}	2.94
F3'-1296	VH-VL	6 BM, K(H94)R	Yes	8.74×10^5	1.17×10^{-3}	1.34
F3'-1297	VH-VL	6 BM, I(L43)A	Yes	5.04×10^5	1.41×10^{-3}	2.79
F3'-1298	VH-VL	6 BM, R(L70)D	Yes	6.44×10^5	1.85×10^{-3}	2.87
F3'-1299	VH-VL	6 BM, I(L83)F	Yes	4.26×10^5	1.21×10^{-3}	2.83
F3'-1300	VH-VL	No BM	No	Binding signal < 5RU		
F3'-1301	VL-VH	7 BM	Yes	Binding signal < 5RU		
F3'-1302	VL-VH	6 BM, K(H71)V	Yes	Binding signal < 5RU		
F3'-1303	VL-VH	6 BM, Q(H83)T	Yes	Binding signal < 5RU		
F3'-1304	VL-VH	6 BM, N(H85)A	No	4.80×10^5	1.30×10^{-3}	2.70
F3'-1305	VL-VH	6 BM, K(H94)R	Yes	Binding signal < 5RU		
F3'-1306	VL-VH	6 BM, I(L43)A	Yes	9.48×10^6	4.89×10^{-2}	5.16
F3'-1307	VL-VH	6 BM, R(L70)D	Yes	9.14×10^5	1.00×10^{-3}	1.10
F3'-1308	VL-VH	6 BM, I(L83)F	Yes	Binding signal < 5RU		
F3'-1309	VL-VH	No BM	No	Binding signal < 5RU		
m16B8.C8**	Mouse mAb		Yes	3.03×10^6	2.35×10^{-5}	0.008

*In the "residues reverted to human," the first letter is a murine residue, and the letter and number in the parentheses indicate positions of reverted residues in the heavy chain and light chain, and the last letter is the human residue, *e.g.,* in K(H71)V, murine K in position 71 of the heavy chain is replaced by human residue V.

** murine parental mAb 16B8.C8 was fully purified.

[0639] F3'-1295 and F3'-1304 TriNKETs were tested for binding isogenic to hCLEC12A +RMA cells, as shown in **FIG. 23,** and using the methods as described in Example 5 or 6. Binding of F3'-1295 to cell-surface expressed hCLEC12A was comparable to hcFAE-A49.CLL1-Merus control TriNKET, derived from the Merus antibody described above in Example 1, whereas binding of F3'-1304 to cell-surface expressed hCLEC12A was poorer compared to the hcFAE-A49.CLL1-Merus control multispecific binding protein.

[0640] Potency of F3'-1295 was assessed in the primary NK cell mediated cytotoxicity assay with HL-60 AML cells, as shown in **FIG. 24,** and using the methods as described in Example 8. F3'-1295 induced potent lysis of HL60 AML cells. Cell killing EC50 was similar, and maximum percentage of cell lysis was higher than control hcFAE-A49.CLL1-Merus TriNKET (**Table 18**).

Table 18: Potency of F3'-1295 in primary NK cells mediated cytotoxicity assay.

Test articles	EC50 (nM)	Max lysis (%)
F3'-1295	1.1	59
hcFAE-A49.CLL1-Merus	1.1	43

[0641] Thermostability of F3'-1295 was evaluated by differential scanning calorimetry (DSC). To perform DSC, briefly, TriNKETs were diluted to 0.5 mg/mL with PBS. 325 µL were added to a 96-well deep well plate along with a matching buffer blank. Thermograms were generated using a MicroCal PEAQ DSC (Malvern, PA). Temperature was ramped from 20-100 °C at 90 °C/hour. Raw thermograms were background subtracted, the baseline model was splined, and data were fitted using a non-two state model.

[0642] The melting temperature of the first transition (T_{m1}) for F3'-1295 was 60.9 °C, which is 4 °C lower than pre-defined criteria of ≥ 65 °C for the T_m of the first TriNKET transition. In the process of humanization, it is possible that the introduction of the murine residue to human framework (back mutation) may have had an impact on the thermal stability. Therefore, by reverting the back mutations to human residues thermal stability of F3'-1295 may improve. Therefore, the thermal stability of the ten F3'variants was assessed by DSC regardless of the presence or absence of the N-glycosylation sequence liability, as shown in **Table 19**. The first transition T_m (attributed to the scFv domain) of F3'-1297 and F3'-1306 TriNKETs was significantly higher (66.5 °C to 67.5 °C) than the other F3' TriNKETs. Moreover, the T_{onset} of these two molecules was significantly better compared to other F3' TriNKETs tested. The sole

difference between these two F3'-TriNKETs is the orientation of scFv; F3'-1297 (VH-VL orientation) and F3'-1306 (VL-VH orientation).

[0643] To determine if the human residue in position (L43) was responsible for an increase in thermostability, in both F3'-1306 and F3'-1297, the mouse residue I(L43) was reverted back to the original human framework residue A(L43). Moreover, the murine Ile in position L43 of F3'-1295 was replaced with human Ala, and then was produced recombinantly. The new second generation humanized TriNKET derived from F3'-1295 was named F3'-1602, or F3'-1602 TriNKET.

Table 19: DSC analysis of purified F3'-TriNKETs in PBS.

Test articles	**scFv orientation**	**Mouse residues changed to human**	**T_{onset}** (°C)	**T_{m1}** (°C)	**T_{m2}** (°C)	**T_{m3}** (°C)	**T_{m4}** (°C)	**T_{m5}** (°C)
F3'-1292	VH-VL	none	51.4	60.0	67.6	76.4	81.6	83.7
F3'-1293	VH-VL	K(H71)V #	51.2	59.8	66.9	76.5	81.6	83.7
F3'-1295	VH-VL	N(H85)A	52.5	60.9	67.1	76.6	81.6	83.4
F3'-1296	VH-VL	K(H94)R	50.5	59.7	67.1	76.3	81.6	83.7
F3'-1297	VH-VL	I(L43)A	56.4	66.5*		76.0	81.5	83.6
F3'-1298	VH-VL	R(L70)D	48.7	59.2	66.5	76.0	81.7	83.8
F3'-1299	VH-VL	I(L83)F	49.6	59.8	66.1	76.0	81.8	83.8
F3'-1304	VL-VH	N(H85)A	50.5	60.1	65.5	76.3	81.7	83.5
F3'-1306	VL-VH	I(L43)A	58.5	67.5		76.2	81.6	83.7
F3'-1307	VL-VH	R(L70)D	50.5	60.2	66.0	76.0	81.8	83.9

Chothia position (mouse residue to human residue)
* Overlaps with Tm_2

[0644] Thermostability of F3'-1295 and second generation F3'-1602 TriNKETs was evaluated by DSC in PBS (**FIG. 25**). Based on the T_m of the first transition, the scFv of F3'-1602 was thermally stabilized by 7.5 ºC compared to F3'-1295, shown in **Table 20**. This stabilization is attributed to the Ile/Ala mutations. Thus, F3'-1602 met the T_{m1} cut-off at ≥65°C.

Table 20: DSC analysis of F3'-1295 and F3'-1602 TriNKETs in PBS.

Test article	**T_{onset} (°C)**	**T_{m1} (°C)**	**T_{m2} (°C)**	**T_{m3} (°C)**	**T_{m4} (°C)**
F3'-1295	52.5	60.9	67.1	76.6	81.6
F3'-1602	58.5	66.8	76.0	81.5	83.3

[0645] To understand if the I(L43)A substitution had an effect on the TriNKET affinity for hCLEC12A, binding of hCLEC12A to F3'-1295 and F3'-1602 was determined by SPR (Biacore) at 37 °C (**FIG. 26**), and using the methods as described in Example 1. The kinetic constants and equilibrium binding affinities are listed in **Table 21**. Both TriNKETs have very similar off rates, but F3'-1602 displays about 2-fold lower K_D due to its faster on rate. Therefore, the I(L43)A substitution had an effect on the K_D.

Table 21: Kinetic parameters and affinities of F3'-1295 and F3'-1602 binding to hCLEC12A by SPR.

Test article	Target	k_a ($M^{-1}s^{-1}$)	k_d (s^{-1})	K_D (nM)
F3'1295	hCLEC12A-His	4.11×10^5	5.87×10^{-4}	1.43
	hCLEC12A-His	4.15×10^5	5.89×10^{-4}	1.42
	hCLEC12A-His	4.19×10^5	6.05×10^{-4}	1.44
	hCLEC12A-His	4.16×10^5	5.96×10^{-4}	1.43
Average ± StDev		$(4.15 \pm 0.03) \times 10^5$	$(5.94 \pm 0.09) \times 10^{-4}$	1.43 ± 0.01
F3'1602	hCLEC12A-His	8.54×10^5	4.94×10^{-4}	0.58
	hCLEC12A-His	8.33×10^5	4.94×10^{-4}	0.59
	hCLEC12A-His	8.63×10^5	4.89×10^{-4}	0.57
	hCLEC12A-His	8.26×10^5	4.99×10^{-4}	0.60
Average ± StDev		$(8.44 \pm 0.17) \times 10^5$	$(4.94 \pm 0.04) \times 10^{-4}$	0.57±0.01

[0646] F3'-1295 and F3'-1602 were tested for their ability to bind isogenic Ba/F3 cells expressing human CLEC12A, in comparison to the parental Ba/F3 cells (as shown in **FIG. 27A,** and the data listed in **Table 22**) using the methods as described in Example 5 or 6. F3'-1602 was able to bind hCLEC12A+ Ba/F3 with about 2-fold lower EC50 value but with similar maximum binding MFI compared to F3'-1295. No binding to the parental Ba/F3 cell lacking expression of CLEC12A was detected by either F3'-1295 or F3'-1602 (**FIG. 27B**), suggesting high specificity of TriNKET binding to hCLEC12A.

Table 22: EC50 and max MFI of F3'-TriNKETs binding to hCLEC12A+ Ba/F3 isogenic cell line.

	hCLEC12A+Ba/F3 cell line		Ba/F3 parental cell line	
Test article	**EC50 (nM)**	**Max MFI**	**EC50 (nM)**	**Max MFI**
F3'-1295	26.1	48040	No binding	
F3'-1602	14.4	50160	No binding	
hcFAE-A49.CLL-Merus	14.3	39740	No binding	

[0647] F3'-1295 and F3'-1602 were further tested for their ability to bind HL60 (**FIG. 27C**) and PL21 (**FIG. 27D**) AML cancer cell lines, and using the methods as described in Example 5 or 6. F3'-1602 was able to bind to both cell lines with lower EC50 values but with similar maximum binding MFI as compared to F3'-1295, as shown in **Table 23**.

[0648] Potency of F3'-1295 and F3'-1602 TriNKETs was assessed in a KHYG-1-CD16aV mediated cytotoxicity assay, the results of which are shown in **FIG. 28**. Both F3'-1602 and F3'-1295 induced potent lysis of PL21 (**FIG. 28A)** and HL60 (**FIG. 28B)** AML cancer cells, and both display similar EC50 values and % max lysis, shown in **Table 23**.

Table 23: Potency of F3'-1294 and F3'1602 in KHYG-1CD16aV mediated cytotoxicity assay.

	PL21 cancer cell line		HL60 cancer cell line	
Test articles	**EC50 (nM)**	**Max cell lysis (%)**	**EC50 (nM)**	**Max cell lysis (%)**
F3'-1295	1.23	22	1.15	48
F3'-1602	1.87	25	0.90	49
hcFAE-A49.CLL-Merus	2.97	10	1.83	27

[0649] Hydrophobic properties of F3'-1295 and F3'-1602 TriNKETs were evaluated by analytical hydrophobic interaction chromatography (HIC), the results of which are shown in **Table 24**. Trastuzumab (Roche) was used as a representative control of a therapeutic antibody. The retention times (RT) for both TriNKETs were similar to the RT of Trastuzumab, suggesting that predicted aggregation propensity of both TriNKETs is low.

Table 24: HIC retention times for F3'-1295 and F3'-1602 TriNKETs compared to Trastuzumab.

Test article	**Absolute retention time (min)**	**ΔRT relative to Trastuzumab (min)**
F3'-1295	9.7	+0.6
F3'-1602	9.4	+0.3
Trastuzumab	9.1	0.0

[0650] The experimental isoelectric point (pI) of F3'-1295 (**FIG. 29A**) and F3'-1602 (**FIG. 29B**) was assessed by capillary isoelectric focusing (cIEF), as described in Example 15. Both constructs showed nearly identical pIs. The major peak of F3'-1295 has a pI of 8.73 and that of F3'-1602 has a pI of 8.81 (**Table 25**).

Table 25: pI of F3'-1295 and F3'-1602 determined by cIEF.

Test article	pI (main peak)
F3'-1295	8.73
F3'-1602	8.81

[0651] Off-target effects of a drug need to be evaluated when developing protein therapeutics. A flow cytometry based polyspecificity reagent (PSR) assay allows for determination of antibodies that have a higher probability to bind non-specifically. F3'-1295 and F3'-1602 were tested for non-specific binding to a preparation of detergent solubilized CHO cell membrane proteins in the PSR assay, using the methods as described in Example 12. Both humanized F3'-1602 and F3'-1295 did not bind to PSR (no signal shift to the right) and showed very similar profiles as the PSR control Trastuzumab, demonstrated in **FIG. 30**, suggesting high specificity of the TriNKETs. Rituximab was used as a positive control in this assay. F3'-1602 was selected for further comparison with additional TriNKETs described.

[0652] The effect of different TriNKET formats was tested experimentally for alterations in efficacy. To obtain CLEC12A TriNKET in the F3 format, humanized 16B8.C8 was converted using the same humanization variant that was used F3'-1602, into Chains VH-CH1-Fc and VL-CL, whereas NKG2D A49M-I mAb was converted into VH-VL-Fc. The protein received the designation AB0010 or F3 –1602.

[0653] Binding affinities of human CLEC12A-His for AB0010 (F3 TriNKET format) and F3'-1602 (F3' TriNKET format) were assessed by SPR (Biacore) at 37 °C. The kinetic constants and equilibrium binding affinities are shown in **Table 26**, and the raw data and fits are shown in **FIG. 31**. Overall binding affinities of both constructs were within 2-fold difference, with AB0010 forming slightly a stronger complex with CLEC12A compared to F3'-1602, as evidenced by the K_D.

Table 26: Kinetic parameters and affinities of CLEC12A binding to F3' (F3'-1602) and F3 (AB0010) TriNKETs.

Format	Test article	Target	k_a ($M^{-1}s^{-1}$)	k_d (s^{-1})	K_D (nM)
F3'	F3'1602	hCLEC12A-His	7.91×10^5	9.52×10^{-4}	1.20
F3'	F3'1602	hCLEC12A-His	7.68×10^5	9.13×10^{-4}	1.19
F3'	**Average**		**7.79×10^5**	**9.33×10^{-4}**	**1.20**
F3	AB0010	hCLEC12A-His	7.15×10^5	5.08×10^{-4}	0.71

Format	Test article	Target	k_a ($M^{-1}s^{-1}$)	k_d (s^{-1})	K_D (nM)
F3	AB0010	hCLEC12A-His	7.04×10^5	5.41×10^{-4}	0.77
F3	**Average**		**7.10×10^5**	**5.25×10^{-4}**	**0.74**

[0654] TriNKETs of different formats, F3'-1602 (F3') and AB0010 (F3), were tested for their abilities to bind Ba/F3 cells expressing human CLEC12A (**FIG. 32A**) and AML cancer cell line (**FIG. 32B**). The EC50 value for F3'-1602 was superior over AB0010 in HL-60 cells, about 2-fold decreased (**Table 27**). Neither AB0010 nor F3'-1602 showed any binding to the parental Ba/F3 cells, demonstrating high specificity of binding to CLEC12A (**FIG. 32C**).

Table 27: Binding EC50 and max MFI of F3'-1602 and AB0010 to hCLEC12A+Ba/F3 and HL60 AML cells.

Format	Test article	hCLEC12A+Ba/F3 cell line		HL60		Ba/F3 parent cell line	
		Max MFI	EC50 (nM)	Max MFI	EC50 (nM)	Max MFI	EC50 (nM)
F3'	F3'-1602	36920	3.20	3820	1.1	No binding	
F3	AB0010	54827	6.13	6064	4.2	No binding	

[0655] The potency of AB0010 and F3'-1602 TriNKETs was assessed in KHYG-1-CD16aV mediated cytotoxicity assay, shown in **FIG. 33A**. F3'-1602 induced lysis of HL60 and PL21 AML cancer cells with a 2-fold better EC50 value than AB0010 (**Table 28**). Both F3 (AB0010) and F3' (F3'-1602) TriNKETs showed superiority over corresponding humanized parental mAb (AB0037-001).

Table 28: Potency of F3'-1602 and AB0010 in KHYG-1-CD16aV mediated cytotoxicity assay.

Format	Test articles	PL21 AML cancer cell line	
		EC50 (nM)	Max cell lysis (%)
F3	AB0010	2.99	21.75
F3'	F3'-1602	1.16	20.97
mAb	AB0037-001	N/A	N/A

[0656] The potencies of AB0010 and F3'-1602 TriNKETs were assessed in a human primary NK cell mediated cytotoxicity assay (**FIG. 33B**). F3'-1602 (F3' format) induced lysis of PL21 AML cancer cells with a 2-fold lower EC50 value than AB0010 (F3 format) (**Table 29**).

Table 29: Potency of F3'1602 and AB0010 in primary NK cell mediated cytotoxicity assay.

Format	Test article	PL21 cancer cell lines	
		EC50 (nM)	Max cell lysis (%)
F3'	F3'-1602	0.13	45.85
F3	AB0010	0.30	43.82

[0657] It was observed in both KHYG-1 mediated and primary NK cell mediated cytotoxic assays that F3'-1602 (F3'-format) demonstrated about 2-fold better EC50 than AB0010 (F3-format), whereas the overall maximum percentage of killing was not affected. In accelerated stability and forced degradation studies AB0010 was less structurally stable compared to F3'-1602 (F3'-1602) (see Example 16). Therefore, the CLEC12A TriNKET in the F3' format (F3'-1602) was chosen to move forward for further study.

[0658] For generation of 9F11.B7 TriNKETs, all 12 scFv variants of 9F11.B7 were combined with A49M-I NKG2D Fab arm to produce humanized F3' TriNKETs. Affinities of the 10 semi-purified (Protein A) TriNKETs for hCLEC12A were assessed by SPR in the screening mode shown in **Table 30**. Three (AB0190, AB0193 and AB0196) 9F11.B7 based F3'-TriNKETs showed heterogenous binding and could not be fitted to a 1:1 kinetic model with high confidence. The binding kinetics of the remaining 7 TriNKETs were similar to the chimeric parent mouse 9F11.B7 mAb, suggesting that neither humanization nor conversion of Fab to scFv affected the affinity for hCLEC12A.

Table 30: Kinetics and affinities of hCLEC12A binding to semi-purified, humanized F3' TriNKETs.

Test article	k_a ($M^{-1}s^{-1}$)	k_d (s^{-1})	K_D (nM)	Comments
AB0185	7.26×10^5	1.01×10^{-3}	1.40	
AB0186	1.12×10^6	1.17×10^{-3}	1.04	
AB0188	5.69×10^5	9.01×10^{-4}	1.58	Low heterodimer yield
AB0189	1.04×10^6	1.27×10^{-3}	1.21	
AB0190	1.55×10^7	1.77×10^{-2}	1.14	Estimated/ heterogeneous binding
AB0191	7.28×10^5	1.26×10^{-3}	1.73	
AB0192	1.09×10^6	1.38×10^{-3}	1.26	
AB0193	1.97×10^7	2.07×10^{-2}	1.04	Estimated/ heterogeneous binding
AB0195	7.66×10^5	1.29×10^{-3}	1.68	
AB0196	Heterogenous weak binding; data insufficient for estimation			
m9F11-hIgG1	9.50×10^5	1.02×10^{-3}	1.07	

[0659] Binding of 9 fully purified humanized 9F11.B7 TriNKETs to hCLEC12A+Ba/F3 and HL60 AML cancer cell lines, shown in **FIG. 34A and FIG. 34B**, was tested by FACS. AB0190, AB0193 and AB0196 showed inferior binding EC50 values for both cell lines (**Table 31**), which correlates with poor behavior in SPR described in **Table 30**. EC50 values for the remaining 6 clones were similar, showing correlation with the SPR data.

Table 31: Binding EC50 and max MFI of 9F11.B7 based F3'-TriNKETs to hCLEC12A+ Ba/F3 isogenic and HL60 AML cell lines

Test Article	hCLEC12A+Ba/F3 isogenic cell line		HL60 cancer cell line	
	EC50 (nM)	Max binding MFI	EC50 (nM)	Max binding MFI
AB0185	0.7	8025	0.4	372
AB0186	0.7	8160	0.5	412
AB0189	1.3	8760	0.7	420
AB0190	2.9	5139	N/A	n/a
AB0191	0.6	7941	0.6	420
AB0192	0.7	10158	0.6	503
AB0193	2.9	7732	19	345
AB0195	0.6	10775	0.7	551
AB0196	2.7	7427	135	650
F3'-1602	2.0	14712	1.6	924

[0660] Potencies of 9F11.B7-based TriNKETs were assessed in KHYG-1-CD16aV cell mediated cytotoxicity assay (**FIG. 35** and **Table 32**). AB0190, AB0193 and AB0196 displayed minimal activity. AB0189 and AB0192 showed the highest potency among other TriNKET candidates. AB0192 TriNKET emerged as the lead TriNKET from 9F11.B7 humanization efforts.

Table 32: Potency of humanized 9F11.B7 F3'-TriNKETs in KHYG-1CD16aV mediated cytotoxicity assay.

	HL60 AML cancer cell line	
Test article	EC50 (nM)	Max cell lysis (%)
AB0185	2.0	25
AB0186	2.7	19
AB0189	0.6	18
AB0190	n/a	n/a
AB0191	3.1	22
AB0192	1.3	22

	HL60 AML cancer cell line	
Test article	**EC50 (nM)**	**Max cell lysis (%)**
AB0193	n/a	n/a
AB0195	2.2	20
AB0196	n/a	n/a

[0661] The potency of AB0192 was assessed in a KHYG-1-CD16aV cell mediated cytotoxicity assay in comparison with the F3'-1602 (**FIG. 36A**). F3'-1602 showed improved efficacy over AB0192 both in EC50 (0.4 nM and 1.3 nM, respectively) and percentage maximum HL-60 cell lysis (41% and 22%, respectively).

[0662] The potencies of AB0192 and F3'-1602 TriNKETs were further assessed in a human primary NK cell mediated cytotoxicity assay (**FIG. 36B**). F3'-1602 and AB0192 induced lysis of HL60 AML cancer with similar EC50 and % max cell killing (**Table 33**).

[0663] AB0192 satisfies TriNKET pre-developability criteria: high affinity for hCLEC12A, efficient binding to AML cells, high potency in killing AML cells in primary NK cells mediated cytotoxicity assay, high thermostability, $T_{m1} \geq 65°$ C, low hydrophobicity, $8.0<PI<9.0$, expression level in transient transfection similar to monoclonal antibody, clean PSR (**Table 33**).

[0664] F3'-1602 demonstrated better potency , higher humanness, and fewer potential sequence liabilities compared to AB0192. Structural stability of F3'-1602 was confirmed in an extensive panel of accelerated stability and forced degradation studies, described in Example 15 . Therefore, F3'-1602 was chosen for further development.

Table 33: Summary of biochemical characterization of F3'-1602 (F3'-1602) and AB0192.

Properties	**F3'-1602**	**AB0192**
Number of back mutations	5	7
% humanness T20 score	80.09 (VH), 84.67(VK)	82.3 (VH), 81.2 (VK)
Potential seq liabilities	DS (isomerization site) in CDRH3	M (oxidation site) in CDRH3 DG (isomerization site) in CDRH3 NS (deamidation site) in CDRH1
HIC retention time relative to Humira (min)	+0.91	+0.97
pI (cIEF, major peak)	8.81	N/A
Thermal stability by DSC (Tm1 °C) in PBS	66.8	65.0
Expression Titer (ExpiCHO, mg/L)	73.3 50.2	64.4

Properties	F3'-1602	AB0192
EC50 (nM): Potency (KHYG-CD16a mediated, HL60 cell line)	0.4	1.3
EC50 (nM): Potency (Primary NK cell mediated, HL60 cell line)	0.29	0.25
Affinity to hCLEC12A by SPR (K_D in nM)	0.80	1.2
PSR specificity	Clean	Clean

[0665] F3'-1602 and its corresponding humanized mAb (h16B8.C8) were assessed for cell killing by primary NK cell mediated cytotoxicity. F3'-1602 demonstrated potent killing of PL21 (**FIG. 37A**) and THP-1 (**FIG. 37B**) AML cancer cell lines, whereas the corresponding monoclonal antibody markedly reduced potency (**Table 34**).

Table 34: Potency of F3'-1602 in comparison with parental mAb in primary NK mediated cytotoxicity assay.

Cell line	F3'-1602		Parent mAb	
	EC50 (nM)	Max lysis (%)	EC50 (nM)	Max lysis (%)
PL21	0.07	35	0.5	18
THP-1	0.7	30	NA	NA

Example 6. Assessment of TriNKET binding to cell expressed human cancer antigens

[0666] Isogenic Ba/F3 cells expressing hCLEC12A, and human cancer cell lines HL60 and PL21 expressing human CLEC12A were used to assess tumor antigen binding of CLEC12A targeted TriNKETs and mAbs.

[0667] AB0089 is an F3' TriNKET derived from the same binding domain as parental mAb AB0305. AB0192 is an F3' TriNKET derived from the same binding domain as parental mAb AB0192. AB0237 is an F3' TriNKET, also referred to herein as hF3'-1602 or F3'-1602 TriNKET, and is derived from scFv-1602. AB0300 (also referred to as F3'-1602si or AB0237si) is also an F3' TriNKET from the same sequence as AB0237 but bears mutations in the CH2 domain to eliminate Fc-gamma receptor binding. F3' TriNKETs generally showed weaker binding compared to parental mAb.

[0668] To assess whether the antigen-binding site that binds NKG2D and the effector function of the Fc contributed to the cytotoxicity of AB0237, two TriNKET variants were constructed. The first variant contains mutations in the light chain variable domain of the A49 antigen-binding site that binds NKG2D. As a result, this variant does not bind human NKG2D. The amino acid sequence of the mutant light chain variable domain is DIQMTQSPSTLSASVGDRVTITCRASNSISSWLAWYQQKPGKAPKLLIYEASSTKSGVPS RFSGSGSGTEFTLTISSLQPDDFATYYCQQYDDLPTFGGGTKVEIK (SEQ ID NO:282). The amino acid sequences of this first variant are otherwise identical to those of AB0237. The second variant contains mutations in the Fc domain. Specifically, each polypeptide chain of the Fc domain contains L234A/L235A/P329G substitutions (numbered under EU numbering system), which was reported to reduce the binding of the Fc to Fcγ receptors. The amino acid sequences of this second variant are otherwise identical to those of AB0237. F3'-palivizumab contains the same NKG2D and CD16 binder sequences as in F3'-1602 and an scFv that binds an irrelevant target not expressed in either of the two cancer cell lines tested. EC50 values are provided in **Table 35**.

Table 35: EC50 values and % max cell lysis in KHYG-1-CD16aV-mediated potency assay.

	PL-21		HL-60	
Test article	**EC50 nM**	**% Max lysis**	**EC50 nM**	**% Max lysis**
F3'-1602	0.7	33	0.27	87
F3'-1602 -Dead-2D	NA	2	2.5	33
F3'-1602 si	NA	NA	NA	12
F3'-Palivizumab	NA	NA	NA	NA

[0669] The cells were then incubated with a fluorophore conjugated anti-human IgG secondary antibody and were analyzed by flow cytometry. The mean fluorescence intensity (MFI) values were normalized to secondary antibody only controls to obtain fold over background (FOB) values.

[0670] AB0237 demonstrates high affinity binding to the two AML cell lines tested, namely, HL60 (**FIG. 38A**) and PL21 (**FIG. 38B**). The EC50 for HL60 was 2.2 nM and the EC50 for PL21 was 1.2 nM.

[0671] For two of the three binders F3' TriNKETs showed higher loading onto target cells compared to its parental mAb. Mutated variants of AB0237, AB0300 and AB0237 NKG2D dead arm, showed similar binding as their parental TriNKET AB0237 to Ba/F3-hCLEC12A (**FIG. 39A**),HL-60 (**FIG. 39B**), and PL-21 (**FIG. 39C**).

Example 7. Assessment of TriNKET surface retention to cell expressed human cancer antigens

[0672] Human cancer cell lines HL60 and PL21 expressing human CLEC12A were used to assess surface retention of CLEC12A-TriNKETs after incubation with cells. PL21 or HL60 cells in duplicate plates were incubated with TriNKETs or mAbs as indicated. The first plate was moved to 37 °C for two hours, whereas the second plate was incubated on ice for 20 minutes. After the respective incubation times, cells were washed. Surface bound TriNKET or mAb was detected using a fluorescent secondary antibody for flow cytometry.

Surface retention was calculated as follows:

% surface retention = (sample MFI 2hrs/sample MFI 20 min)) * 100%

[0673] **FIG. 40A** and **FIG. 40B** show cell surface retention of TriNKETs bound to CLEC12A+ cell lines, PL21 and HL60, respectively. Monovalent binding TriNKETs, AB0089, AB0147, AB0192 and AB0237 showed high surface retention at two hours on both PL21 and HL60 cells lines. For both PL21 and HL60, bivalent binding mAb AB0037 showed lower surface retention at two hours compared to TriNKETs.

Example 8. Human NK cell cytotoxicity assay

[0674] Lysis of target cells was measured by the DELFIA cytotoxicity assay. Briefly, human cancer cell lines expressing CLEC12A were harvested from culture, washed with HBS, and resuspended in growth media at 10^6/mL for labeling with BATDA reagent (Perkin Elmer AD0116). Manufacturer instructions were followed for labeling of the target cells. After labeling, cells were washed three times with HBS, and were resuspended at 0.5-1.0x10^5/mL in culture media. 100 µl of BATDA labeled cells were added to each well of the 96-well plate. Monoclonal antibodies or TriNKETs against CLEC12A were diluted in culture media, and 50 µl of diluted mAb or TriNKET were added to each well.

[0675] To prepare NK cells, PBMCs were isolated from human peripheral blood buffy coats using density gradient centrifugation, washed, and prepared for NK cell isolation. NK cells were

isolated using a negative selection technique with magnetic beads. Purity of isolated NK cells was typically >90% CD3-CD56+. Isolated NK cells were rested overnight and harvested from culture. The cells were then washed and resuspended at concentrations of 10^5-2.0x10^6/mL in culture media for an effector-to-target (E:T) ratio of 5:1. 50 µl of NK cells were added to each well of the plate for a total of 200 µl culture volume. The plate was incubated at 37 °C with 5% CO_2 for 2-3 hours.

[0676] After the incubation, the plate was removed from the incubator and the cells were pelleted by centrifugation at 200 xg for 5 minutes. 20 µl of culture supernatant were transferred to a clean microplate and 200 µl of room temperature europium solution (Perkin Elmer C135-100) were added to each well. The plate was protected from light and incubated on a plate shaker at 250 rpm for 15 minutes, then read using SpectraMax i3X instruments.

[0677] Spontaneous release of a substance that can form a fluorescent chelate with europium was measured in target cells incubated in the absence of NK cells. Maximum release of such a substance was measured in target cells lysed with 1% Triton-X. % Specific lysis was calculated as follows:

% Specific lysis = ((Experimental release – Spontaneous release) /
(Maximum release – Spontaneous release)) * 100%.

[0678] **FIG. 41A** and **FIG. 41B** show CLEC12A-TriNKET mediated killing of PL21 and HL60 target cells by rested human NK cells, respectively. AB0037 a CLEC12A targeted monoclonal antibody showed little enhancement of NK cell mediated lysis of PL21 and HL60 target cells. All three CLEC12A targeted TriNKETs (AB0237, AB0192 and AB0089) showed superior lysis of target cells compared to the CLEC12A targeted monoclonal antibody. EC50 values are shown in **Table 36**.

Table 36: Potency of F3'-1602 in comparison with parental mAb in primary NK mediated cytotoxicity assay.

Cell line	**F3'-1602**		**Parent mAb**	
	EC50 (nM)	Max lysis (%)	EC50 (nM)	Max lysis (%)
PL-21	0.07	35	0.5	18
THP-1	0.7	30	NA	NA

[0679] To confirm the cytoxicity findings, a second NK cell line, KHYG-1-CD16aV was engineered to stably express CD16aV and NKG2D, and the assay was conducted as described above. Cytotoxicity of PL21 is shown in **FIG. 42A**; Cytotoxicity of HL60 is shown in **FIG. 42B**. The EC50 values and maximum lysis values were derived from the cell lysis curves by the GraphPad Prism software using four parameter logistic non-linear regression curve fitting model (**Table 37**). F3'-1602 shows subnanomolar EC50 and high efficiency maximum lysis in the KHYG-1 CD16A mediated cytotoxicity assay.

Table 37: Potency of F3'-1602 in KHYG-1-CD16aV mediated cytotoxicity assay.

Test articles	Cell line	EC50	% Max lysis
F3'-1602 #1	PL21	0.3	66
F3'-1602 #2	HL60	0.2	77

Example 9. Primary human CD8+ T cell cytotoxicity assay

[0680] Lysis of target cells was measured by the DELFIA cytotoxicity assay as described in Example 8, except that CD8+ T cells were used as immune effector cells. CD8+ T cells were prepared as follows: Human PBMCs were isolated from human peripheral blood buffy coats using density gradient centrifugation with Lymphoprep and SepMate 50, according to the manufacturer's instructions. Isolated PBMCs were stimulated with 1 μg/mL ConA (an IL-2 culture supplement) in culture media at 37 °C for 18 hours. ConA was then removed and PBMCs were cultured with 25 units/mL IL-2 at 37 °C for 4 days. CD8+ T cells were purified using a negative selection technique with magnetic beads (EasySep™ Human CD8+ T Cell Isolation Kit), according to the manufacturer's instructions. CD8+ T cells were cultured in media containing 10 ng/mL IL-15 at 37 °C for 6-13 days before using in the cytolysis assay.

[0681] As shown in **FIG. 43**, AB0237 TriNKET, but not parental AB0037 mAb, significantly enhanced the ability of CD8 T cell to lyse target cells. AB0237 TriNKET increased CD8+ T cell-mediated lysis of cells in a dose-dependent manner.

[0682] To assess whether the antigen-binding site that binds NKG2D and the effector function of the Fc contributed to the cytotoxicity of AB0237 TriNKET, a TriNKET variant was constructed. The variant contains mutations in the light chain variable domain of the A49 antigen-binding site that binds NKG2D. As a result, this variant does not bind human NKG2D.

The amino acid sequence of the mutant light chain variable domain is DIQMTQSPSTLSASVGDRVTITCRASNSISSWLAWYQQKPGKAPKLLIYEASSTKSGVPS RFSGSGSGTEFTLTISSLQPDDFATYYCQQYDDLPTFGGGTKVEIK (SEQ ID NO:282). The amino acid sequences of this first variant are otherwise identical to those of AB0237 TriNKET.

[0683] The ability of the variant to induce NK cell-mediated lysis of target cells was assessed using the DELFIA cytotoxicity assay described above. As shown in **FIG. 43**, the mutations in the NKG2D-targeting domain substantially reduced cytotoxicity. This result suggested that binding to NKG2D and binding to Fcγ receptors both contributed to the cytotoxic activity of AB0237 TriNKET.

Example 10. Assessment of TriNKET or mAb binding to whole human blood

[0684] The ability of AB0237 and mAb AB0037 to bind different types of blood cells was assessed. Briefly, human whole blood was incubated with AB0237 (grey), mAb AB0037 (white), or a human IgG1 isotype control antibody (black). The blood cells were analyzed by flow cytometry and binding of AB0237, mAb AB0037, or the isotype control antibody was detected using a fluorophore conjugated anti-human IgG secondary antibody.

[0685] As shown in **FIG. 44**, staining was observed on monocytes, granulocytes, and a proportion of dendritic cells in whole blood for AB0237 and its parental mAb AB0037.

Example 11. Binding of F3'-1602 TriNKET to Fc Receptors: Label Free Surface Plasmon Resonance Characterization

[0686] The binding affinities of F3'-1602 TriNKET for recombinant human and cynomolgus Fcγ Receptors was determined and compared the binding affinities of an IgG1 isotype control, trastuzumab. Binding affinity of F3'-1602 TriNKET to human and cynomolgus monkey (cyno) FcRn at pH 6.0 and pH 7.4 was also determined.

FcγR binding

[0687] Human and cyno CD64, high and low affinity alleles of CD16a (V158 and F158, respectively), two alleles of CD32a (H131 and R131), CD16b, CD32b and cynomolgus CD16 were captured via biotin on a primed Biacore chip, prepared according to the manufacturer's instructions. Prior to FcγR binding experiment requiring a high starting concentration, F3'-1602 TriNKET and trastuzumab, samples were buffer exchanged into 1x HBS-EP+ SPR running

buffer by three consecutive dilution and concentration cycles with the use of a 0.5 mL concentrator unit, resulting in >300-fold dilution of original buffer components while maintaining a high concentration of protein. Protein concentration was measured at absorbance of A280 on a NanoDrop instrument with the use of sample appropriate theoretical molar extinction coefficients (198405 $M^{-1}cm^{-1}$ for F3'-1602 TriNKET and standard IgG setting for trastuzumab).

[0688] Each FcγR binding experiment was performed with multiple cycles utilizing 2-fold serially diluted F3'-1602 TriNKET or trastuzumab. For no-signal reference, a 0 nM blank cycle at the start of each concentration series and receptor free chip surface were used. Each experimental cycle included association, dissociation and regeneration steps. All steps were executed at a flow rate of 30 μL/min and at 25 °C. Analyte (F3'-1602 TriNKET or trastuzumab) concentrations, association and dissociation times, and regeneration parameters were FcγR-specific (**Table 38**).

Table 38: Parameters used in Biacore FcγR binding experiments

Parameter	**hCD64, cyno CD64**	**hCD16a V158**	**hCD16a F158**	**cyno CD16**	**hCD32a H131, R131**	**hCD16b**	**hCD32b**
Type of chip	CAP chip	Type S SA chip					
FcγR capture level, RU	35-50	34-37	24-27		5-15	10-15	
Concentration range, nM	400-1.56	1500-0.023	6000 – 0.023		16000-125	24000 -188	
Association time, sec	240	150			60	60	
Dissociation time, sec	600	300			60	150	
Surface regeneration	CAPture kit regeneration	5 sec pulse of 1- 2 mM NaOH				5 sec of 10 mM Gly, pH 3.0	

[0689] The shape of the raw sensorgrams representing F3'-1602 TriNKET and trastuzumab binding recombinant human CD64 enabled fitting the data with a 1:1 kinetic fit model. The black

traces representing the 1:1 kinetic fit closely follow the actual sensorgrams depicted in color in **FIG.45.**

[0690] The χ^2 error value calculated by the Biacore Insight evaluation software was ≤ 1.9% of calculated R_{max}, representing a good fit. **Table 39** summarizes kinetic rates and human CD64 affinity values for F3'-1602 TriNKET and trastuzumab.

Table 39: Kinetic parameters and affinity values of F3'-1602 TriNKET binding to human CD64.

Sample	k_a (1/Ms)	k_d (1/s)	K_D (nM)
F3'-1602 TriNKET	5.3×10^4	2.7×10^{-4}	5.2
	5.2×10^4	2.8×10^{-4}	5.3
	5.1×10^4	2.6×10^{-4}	5.2
	5.2×10^4	2.7×10^{-4}	5.3
Average ± SD	**$(5.2 \pm 0.1) \times 10^4$**	**$(2.7 \pm 0.1) \times 10^{-4}$**	**5.2 ± 0.1**
trastuzumab	9.6×10^4	2.3×10^{-4}	2.4
	9.6×10^4	2.3×10^{-4}	2.5
	9.6×10^4	2.3×10^{-4}	2.5
	9.2×10^4	2.3×10^{-4}	2.5
Average ± SD	**$(9.3 \pm 0.1) \times 10^4$**	**$(2.3 \pm 0.0) \times 10^{-4}$**	**2.5 ± 0.1**

[0691] Binding of F3'-1602 TriNKET to CD32a H131 was determined as described above and is shown in **FIG. 46**. The data were fit with a steady state affinity fit model; affinity values are summarized in **Table 40**.

Table 40: Affinity values of F3'-1602 TriNKET and trastuzumab for human CD32a H131.

Sample	Replicate K_D (μM)	Replicate K_D (μM)	Replicate K_D (μM)	Replicate K_D (μM)	K_D (μM) Average ± SD
F3'-1602 TriNKET	0.9	0.8	0.9	0.9	0.9 ± 0.0
trastuzumab	1.2	1.1	1.2	1.1	1.1 ± 0.1

[0692] Binding of F3'-1602 TriNKET to human CD32a R131 allele (FcγRIIa R131) was determined as described above and is shown in **FIG. 47**. The data were fit with a steady state affinity fit model; affinity values are summarized in **Table 41**.

Table 41: Affinity values of F3'-1602 TriNKET and trastuzumab for human CD32a R131.

Sample	Replicate K_D (nM)	Replicate K_D (nM)	Replicate K_D (nM)	Replicate K_D (nM)	K_D (nM) Average ± SD
F3'-1602 TriNKET	1.4	1.3	1.7	1.2	1.4 ± 0.2
trastuzumab	1.7	1.6	1.9	1.6	1.7 ± 0.2

[0693] Binding of F3'-1602 TriNKET to human CD16a high affinity allele V158 (FcγRIIIa V158) was determined as described above and is shown in **FIG. 48**. The data were fit with a 1:1 kinetic fit model; kinetic parameters and affinity values are summarized in **Table 42**. The affinity of F3'-1602 TriNKET for both alleles is comparable (three-fold or less difference) to trastuzumab's affinity for the same receptors.

Table 42: Kinetic parameters and affinity values of human CD16a V158 for F3'-1602 TriNKET and trastuzumab.

Sample	k_a (1/Ms)	k_d (1/s)	Kinetic Fit K_D (nM)
F3'-1602 TriNKET	9.6×10^4	2.2×10^{-2}	234.0
	9.5×10^4	2.2×10^{-2}	235.0
	9.3×10^4	2.3×10^{-2}	243.0
	9.3×10^4	2.2×10^{-2}	241.0
Average ± SD	**$(9.4 \pm 0.2) \times 10^4$**	**$(2.2 \pm 0.0) \times 10^{-2}$**	**238.3 ± 4.4**
trastuzumab	1.7×10^5	1.3×10^{-2}	76.5
	1.7×10^5	1.3×10^{-2}	76.0
	1.3×10^5	1.0×10^{-2}	80.3
	1.3×10^5	1.0×10^{-2}	77.7
Average ± SD	**$(1.5 \pm 0.2) \times 10^5$**	**$(1.1 \pm 0.1) \times 10^{-2}$**	**77.6 ± 1.9**

[0694] Binding of F3'-1602 TriNKET to human CD16a low affinity allele F158 (FcγRIIIa F158) was determined as described above and is shown in **FIG. 49**. The data were fit with a steady state affinity fit model; affinity values are summarized in **Table 43**.

Table 43: Affinity of F3'-1602 TriNKET and trastuzumab for human CD16a F158.

Sample	Replicate K_D (nM)	Replicate K_D (nM)	Replicate K_D (nM)	Replicate K_D (nM)	K_D (nM) Average ± SD
F3'-1602 TriNKET	1130.0	1120.0	1090.0	1090.0	1107.5 ± 20.6
trastuzumab	436.0	430.0	445.0	448.0	439.8 ± 8.3

[0695] Binding of F3'-1602 TriNKET to human CD32b (FcγRIIb) was determined as described above and is shown in **FIG. 50**. The data were fit with a steady state affinity fit model; affinity values are summarized in **Table 44**.

Table 44: Affinity of human CD32b for F3'-1602 TriNKET and trastuzumab.

Sample	Replicate K_D (μM)	Replicate K_D (μM)	Replicate K_D (μM)	Replicate K_D (μM)	K_D (μM) Average ± SD
F3'-1602 TriNKET	7.2	6.1	6.9	6.1	6.6 ± 0.6
trastuzumab	7.0	6.7	7.2	6.6	6.9 ± 0.3

[0696] Binding of F3'-1602 TriNKET to human CD16b (FcγRIIIb) was determined as described above and is shown in **FIG. 51**. The data were fit with a steady state affinity fit model; affinity values are summarized in **Table 45**.

Table 45: Affinity of human CD16b for F3'-1602 TriNKET and trastuzumab.

Sample	Replicate K_D (μM)	Replicate K_D (μM)	Replicate K_D (μM)	Replicate K_D (μM)	K_D (μM) Average ± SD
F3'-1602 TriNKET	7.6	7.2	8.6	6.5	7.5 ± 0.8
trastuzumab	4.2	4.0	4.8	3.8	4.2 ± 0.4

[0697] Binding of F3'-1602 TriNKET to cyno CD16 was measured as described above and is shown in **FIG. 52**. The data were fit with a steady state affinity fit model; affinity values are summarized in **Table 46**.

Table 46: Affinity values of F3'-1602 TriNKET and trastuzumab for cynomolgus CD16.

Sample	Replicate K_D (nM)	Replicate K_D (nM)	Replicate K_D (nM)	Replicate K_D (nM)	K_D (nM) Average ± SD
F3'-1602 TriNKET	315.0	315.0	294.0	302.0	306.5 ± 10.3
trastuzumab	148.0	141.0	164.0	149.0	150.5 ± 9.7

[0698] Binding of F3'-1602 TriNKET to human FcRn was measured at pH 6.0 as described above and is shown in **FIG. 53**. The data were fit with a steady state affinity fit model; affinity values are summarized in **Table 47**.

Table 47: Affinity values of F3'-1602 TriNKET and trastuzumab for human FcRn at pH 6.0.

Sample	Replicate K_D (μM)	Replicate K_D (μM)	Replicate K_D (μM)	Replicate K_D (μM)	K_D (μM) Average ± SD
F3'-1602 TriNKET	1.3	1.1	1.5	1.6	1.4 ± 0.2
trastuzumab	1.8	1.3	1.3	1.2	1.4 ± 0.2

[0699] Binding of F3'-1602 TriNKET to cyno FcRn was measured at pH 6.0 as described above and is shown in **FIG. 54**. The data were fit with a steady state affinity fit model; affinity values are summarized in **Table 48**.

Table 48: Affinity values of F3'-1602 TriNKET and trastuzumab for cyno FcRn at pH 6.0.

Sample	Replicate K_D (μM)	Replicate K_D (μM)	Replicate K_D (μM)	Replicate K_D (μM)	K_D (μM) Average ± SD
F3'-1602 TriNKET	1.1	1.1	1.4	1.5	1.3 ± 0.2
trastuzumab	1.6	1.6	1.2	1.3	1.4 ± 0.2

[0700] Binding of F3'-1602 TriNKET to human and cyno FcRn was measured at pH 7.4 as described above. No quantifiable binding was observed.

[0701] F3'-1602 TriNKET and IgG1 isotype control trastuzumab do not demonstrate physiologically meaningful differences (less than 3-fold difference) and are comparable in their binding to human and cynomolgus CD64 (FcγRI), CD16 (FcγRIII) recombinant receptors tested (**Table 49**). F3'-1602 TriNKET and trastuzumab are similar (less than 1.2-fold difference) in

their binding to human CD32 (FcγRII) receptors (**Table 49**). F3'-1602 TriNKET is similar to trastuzumab in its affinity for human and cynomolgus FcRn at pH 6.0. F3'-1602 TriNKET and trastuzumab did not demonstrate any detectable binding at the concentrations tested at pH 7.4 (**Table 50**).

Table 49: Summary of FcγRs affinities for F3'-1602 TriNKET and trastuzumab.

Sample	Human CD64 K_D, nM	Cyno CD64 K_D, nM	Human CD32a K_D, μM		Human CD16a K_D, nM		Human CD32b K_D, μM	Human CD16b K_D, μM	Cyno CD16 K_D, nM
			H131	R131	V158	F158			
F3'-1602 TriNKET	5.2 ± 0.1	2.0 ± 0.0	0.9 ± 0.0	1.4 ± 0.2	238.2 ± 4.4	1107.5 ± 20.6	6.6 ± 0.6	7.5 ± 0.8	306.5 ± 10.3
trastuzumab	2.5 ± 0.1	0.9 ± 0.0	1.1 ± 0.1	1.7 ± 0.2	77.6 ± 1.9	439.8 ± 8.3	6.9 ± 0.3	4.2 ± 0.4	150.5 ± 9.7

Table 50: Summary of F3'-1602 TriNKET and trastuzumab binding human and cynomolgus FcRn.

Sample	Human FcRn, pH 6.0 K_D, μM	Human FcRn, pH 7.4 K_D, μM	Cyno FcRn, pH 6.0 K_D, μM	Cyno FcRn, pH 7.4 K_D, μM
F3'-1602 TriNKET	**1.4 ± 0.2**	No quantifiable binding	**1.3 ± 0.2**	No quantifiable binding
trastuzumab	**1.4 ± 0.2**	No quantifiable binding	**1.4 ± 0.2**	No quantifiable binding

FcRn Binding

[0702] Recombinant human or cynomolgus monkey (cyno) FcRn was directly immobilized via amine coupling at a density of 169-216 RU. F3'-1602 TriNKET and commercial trastuzumab as an IgG1 assay control were buffer exchanged into MBS-EP+, pH 6.0 as described above before the SPR binding experiment. Each FcRn binding experiment consisted of multiple cycles utilizing varying concentrations of analytes. Two-fold dilution series (12 μM – 0.023 μM) of F3'-1602 TriNKET and trastuzumab were used. As no-signal, negative controls, a 0 nM blank cycle was placed at the start of each concentration series, and a blank amine coupling modified chip surface lacking FcRn were used. Each experimental cycle included association, dissociation, and regeneration steps. The association step consisted of 60 sec analyte injection and was followed by a 60 sec dissociation step. Surface regeneration (60 sec injection of HBS-EP+ buffer, pH 7.4) completed each kinetic cycle. All steps were executed at a flow rate of 30 μL/min and at 25 °C. MBS-EP+ buffer, pH 6.0 was used as a running buffer. The data were fitted to a

steady state affinity model with Biacore Insight evaluation software. Chi^2 (calculated by the software) related to the calculated R_{max} was used to assess goodness of the fit.

Example 12. Molecular format and design, structure, affinity, potency, specificity and cross-reactivity analysis of F3'-1602 TriNKET

Surface Plasmon Resonance (SPR)

[0703] Binding affinities of F3'-1602 TriNKET for recombinant human CLEC12A (hCLEC12A) or cyno CLEC12A (cCLEC12A) were measured by SPR using a Biacore 8K instrument at physiological temperature of 37 °C. Briefly, human Fc specific antibodies were covalently immobilized at a density of about 8000-10000 resonance units (RU) on carboxy methyl dextran matrix of a CM5 biosensor chip to create an anti-hFc IgG chip. F3'-1602 TriNKET samples were injected on the anti-hFc IgG chip at a flow rate of 10 µL/min for 60 seconds to achieve an about 250 RU capture level. hCLEC12A-His or cCLEC12A-His was serially diluted (100 nM-0.14 nM) in three-fold dilutions with running buffer and injected at a flow rate of 30 µl/min over the captured test articles. Association was monitored for 300 seconds, and dissociation was monitored for 900 seconds. Surfaces were regenerated between cycles with three pulses of 10 mM glycine-HCl (pH 1.7) injected for 20 seconds at 100 µL/min.

[0704] The kinetic constants and equilibrium binding affinities are provided in **Table 51**, and raw data and fits are shown in **FIG. 55**. The molecule binds strongly to CLEC12A and weakly to NKG2D and CD16a. The complex between F3'-1602 TriNKET and human CLEC12A is strong as evidenced from the slow rate dissociation constant $4.94 \pm 0.09 \times 10^{-4}$ s^{-1}. The equilibrium binding affinity K_D for F3'-1602 TriNKET was 0.59 ± 0.01 nM.

Table 51: Comparison of kinetic parameters of F3'-1602 TriNKET to human CLEC12A at pH 7.4 and pH 6.0.

Test article	Target	k_a ($M^{-1}s^{-1}$)	k_d (s^{-1})	K_D(nM)
F3'-1602 TriNKET #1	hCLEC12A-His	8.54×10^5	4.94×10^{-4}	0.58
F3'-1602 TriNKET #2	hCLEC12A-His	8.33×10^5	4.94×10^{-4}	0.59
F3'-1602 TriNKET #3	hCLEC12A-His	8.63×10^5	4.89×10^{-4}	0.57
F3'-1602 TriNKET #4	hCLEC12A-His	8.26×10^5	4.99×10^{-4}	0.60
Average ± Std Dev	**hCLEC12A-His**	**$(8.44 \pm 0.03) \times 10^5$**	**$(4.94 \pm 0.09) \times 10^{-4}$**	**0.59 ± 0.01**

[0705] Further, polymorphic variant CLEC12A-K244Q is prevalent in about 30% of the population. Binding of F3'-1602 TriNKET to CLEC12A-K244Q was examined by SPR and compared its affinity to wild-type CLEC12A. As shown in **Table 52**, binding kinetics of F3'-1602 TriNKET for wild-type and the K244Q variant of CLEC12A are similar.

Table 52: Kinetic parameters and affinities of F3'-1602 TriNKET for human CLEC12A-K244Q.

Test articles	Target	k_a ($M^{-1}s^{-1}$)	k_d (s^{-1})	K_D (nM)
F3'-1602 TriNKET	hCLEC12A WT	8.26×10^5	4.96×10^{-4}	0.60
F3'-1602 TriNKET	hCLEC12A-K244Q	5.65×10^5	4.36×10^{-4}	0.77

[0706] Binding affinities of F3'-1602 TriNKET for recombinant human NKG2D were measured by SPR using a Biacore 8K instrument at physiological temperature of 37 °C. Briefly, mouse (mFc) specific antibodies were covalently immobilized at a density of about 8000-10000 RU on carboxy methyl dextran matrix of a CM5 biosensor chip to create an anti-mFc IgG chip. mFc-tagged human NKG2D was captured on the anti-mFc IgG chip at a flow rate of 10 µL/min for 60 seconds to achieve an about 35 RU capture level. F3'-1602 TriNKET was buffer exchanged into running buffer and serially diluted (5000 nM – 9.78 nM) in two-fold dilutions with 1x HBS-EP+. F3'-1602 TriNKET was injected at a flow rate of 30 µl/min over the captured test articles. Association was monitored for 60 seconds, and dissociation was monitored for 60 seconds. Surfaces were regenerated between cycles with three pulses of 10 mM glycine-HCl (pH 1.7) injected for 20 seconds at 100 µL/min.

[0707] **FIG. 56** shows F3'-1602 TriNKET binding sensorgrams to human NKG2D. Two different fits were utilized to obtain the equilibrium affinity data: steady state affinity fit and kinetic fit. The kinetic constants and equilibrium affinity constants are shown in **Table 54**. The dissociation rate constant was $(1.30 \pm 0.03) \times 10^{-1}$ s^{-1}. Equilibrium affinity constants (K_D) obtained by kinetics fit and steady state affinity fit were, 721 ± 21 nM and 727 ± 22 nM respectively.

Table 54: Kinetic parameters and affinities of F3'-1602 TriNKET for human NKG2D measured by SPR.

Test articles	Target	k_a($M^{-1}s^{-1}$)	k_d (s^{-1})	Kinetic Fit K_D (nM)	Steady State Affinity fit K_D (nM)
F3'-1602 TriNKET #1	hNKG2D	1.80 x 10^5	1.26 x 10^{-1}	703	709
F3'-1602 TriNKET #2	hNKG2D	1.84 x 10^5	1.30x 10^{-1}	705	709
F3'-1602 TriNKET #3	hNKG2D	1.75 x 10^5	1.31 x 10^{-1}	745	751
F3'-1602 TriNKET #4	hNKG2D	1.80 x 10^5	1.32 x 10^{-1}	732	740
Average ± StDev	**hNKG2D**	**(1.80±0.04)x10^5**	**(1.30±0.03)x10^{-1}**	**721 ± 21**	**727 ± 22**

[0708] Cross-reactivity of F3'-1602 TriNKET with cyno NKG2D was further investigated by SPR as described in Example 5 or 6. F3'-1602 TriNKET was tested for binding to recombinant cyno NKG2D (cNKG2D) extracellular domain (ECD) by SPR (Biacore) at 37 °C (**FIG. 57**). NKG2D is a dimer in nature, therefore recombinant mFc-tagged cyno NKG2D dimer was used for this experiment. The binding affinities are shown in **Table 55**. Binding affinities were obtained from kinetic fit (K_D 839 ± 67 nM) and steady fit (K_D 828 ± 88 nM), and were similar to the binding affinity observed with hCLEC12A (K_D 721 ± 21 nM obtained with kinetic fit).

Table 55: Kinetic parameters and affinities of F3'-1602 TriNKET for cyno NKG2D measured by SPR.

Test articles	Target	k_a ($M^{-1}s^{-1}$)	k_d (s^{-1})	Kinetics fit K_D (nM)	Steady State Affinity fit K_D (nM)
F3'-1602 TriNKET #1	cNKG2D	1.77 X 10^5	1.47 X 10^{-1}	831	829
F3'-1602 TriNKET #2	cNKG2D	1.64 X 10^5	1.36 X 10^{-1}	825	828
F3'-1602 TriNKET #3	cNKG2D	1.56 X 10^5	1.45 X 10^{-1}	931	935
F3'-1602 TriNKET #4	cNKG2D	1.76 X 10^5	1.35 X 10^{-1}	769	719
Average ± StDev	**cNKG2D**	**(1.68 ± 0.1) x 10^5**	**(1.41 ± 0.06) x 10^{-1}**	**839 ± 67**	**828 ± 88**

Simultaneous engagement of CLEC12A and NKG2D

[0709] F3'-1602 TriNKET was diluted in 1x HBS-EP+ buffer containing 0.1 mg/mL BSA and was captured on an anti-human Fc surface of CM5 chip at a flow rate 5 μL/min for 60 sec to achieve capture level of 150-250 RU. The net difference between baseline signal and the signal after completion of F3'-1602 TriNKET injection representing the amount of F3'-1602 captured was recorded. hCLEC12A-His (100 nM) or mFc-hNKG2D (7 μM) was injected over captured F3'-1602 TriNKET at 30 μL/min for 90 sec to reach saturation. This injection was immediately followed by an injection of a pre-incubated mixture of hCLEC12A-His (100 nM) and mFc-hNKG2D (7 μM) at a flow rate of 30 μL/min for 90 sec with the use of the A-B-A injection command in the Biacore 8K control software (the second target was pre-mixed with the first target to assure all binding sites for the first target are occupied). The chip was regenerated by two 20 second pulses of 10 mM Glycine (pH 1.7) at 100 μL/min. The experiment was conducted at 37 °C to mimic physiological temperature. An average relative binding stoichiometry of each target bound to captured F3'-1602 TriNKET that is already saturated with the other target (injected second) was expressed as a fraction of the full capacity binding to unoccupied F3'-1602 TriNKET.

[0710] Target binding sensorgrams as shown in **FIG. 58** demonstrate that the occupancy status of the CLEC12A domain does not interfere with NKG2D binding and occupancy status of the NKG2D domain does not interfere with CLEC12A binding. Similarity in shapes of the respective sensorgram segments depicting binding of each target to free F3'-1602 TriNKET and F3'-1602 TriNKET that has been saturated with the other target suggests that the kinetic parameters are not meaningfully affected by the target occupancy status of the F3'-1602 TriNKET molecule. For instance, the shape of the CLEC12A binding segment of the sensorgrams is similar in both panels. Saturating concentration of the NKG2D was maintained throughout the entire experiment, represented in the lower panel due to the fast dissociation rate of the target. Additionally, the lack of any impact on relative stoichiometry of each target binding (when compared to binding to unoccupied F3'-1602) signifies full independence of NKG2D and CLEC12A binding sites on F3'-1602 TriNKET (**Table 56**).

Table 56: Relative binding stoichiometries of F3'-1602 TriNKET for CLEC12A and NKG2D, expressed relative to binding of each target to unoccupied captured F3'-1602 TriNKET.

	CLEC12A, relative binding stoichiometry	**NKG2D, relative binding stoichiometry**
Target Bound to F3'-1602 TriNKET unoccupied with another target (injected first)	1.00	1.00
Target Bound to F3'-1602 TriNKET saturated with another target (injected second)	1.21 ± 0.06	1.19 ± 0.04

NKG2D-CD16a synergy

[0712] Synergistic NKG2D and CD16a binding was evaluated by SPR. 233 RU of hNKG2D alone, 618 RU of CD16a F158 allele alone, and 797 RU of the mixture of hNKG2D and CD16a(F158) were amino-coupled to the surface of the CM5 Series S Biacore chip. 2.8 μM F3'-1602 TriNKET or trastuzumab were injected for 150 sec at 10 μL/min. Dissociation phase was observed for 180 seconds when regeneration was not needed and 1500 second when natural regeneration of the surface (almost complete dissociation of analyte) was needed between the cycles at the same flow rate.

[0713] As shown in **FIG. 59**, while F3'-1602 TriNKET binds with low affinity to CD16a or NKG2D alone, F3'-1602 TriNKET injected over the mixed surface manifests in avidity of simultaneous CD16a and NKG2D binding through much slower off-rate (**FIG. 59A**). Experimental control trastuzumab does not bind immobilized NKG2D and exhibits the same apparent off-rate when injected over both mixed (CD16a + NKG2D) and CD16a-only surfaces (**FIG. 59B**). The data indicate that F3'-1602 TriNKET avidly engages both CD16a and NKG2D.

Binding unrelated recombinant proteins and cell binding specificity

[0714] Specificity for CLEC12A was tested by SPR against five different unrelated proteins at concentrations as high as 500 nM and is shown in **FIG. 60**. No non-specific binding was observed to any of the unrelated recombinant targets (**FIG. 60B**, **FIG. 60C**), whereas positive control (CLEC12A) showed binding of 50 RU at 100 nM concentration (**FIG. 60A**). Specificity was also tested against proteins expressed on the surface of the Ba/F3 cell line. No non-

nonspecific binding of F3'-1602 at a concentration of 333 nM to the Ba/F3 parental cell line was observed (**FIG. 60E**), whereas Ba/F3 cell lines engineered to express CLEC12A, used as a positive control, showed a significant shift by flow cytometry (**FIG. 60D**).

Non-specific binding to polyspecific reagent (PSR)

[0715] A flow cytometry based PSR assay allows the filtering out of antibodies that have a higher probability to bind non-specifically to unrelated proteins. As part of the developability assessment, F3'-1602 was tested for non-specific binding to a preparation of detergent solubilized membrane proteins in a PSR assay (**FIG. 61**). PSR assay correlates well with cross-interaction chromatography, a surrogate for antibody solubility, as well as with baculovirus particle enzyme-linked immunosorbent assay, a surrogate for *in vivo* clearance (Xu *et. al* (2013). Addressing polyspecificity of antibodies selected from an in vitro yeast presentation system: a FACS-based, high-throughput selection and analytical tool. *Protein engineering design and selection*, 26, 663-670).

[0716] 50 µL of 100 nM TriNKET or control mAb in PBSF were incubated with pre-washed 5 µL protein A dyna beads slurry (Invitrogen, catalog # 10001D) for 30 minutes at room temperature. TriNKET or mAb bound magnetic beads were allowed to stand on a magnetic rack for 60 seconds and the supernatant was discarded. The bound beads were washed with 100 µL PBSF. Beads were incubated for 20 minutes on ice with 50 µL of biotinylated PSR reagent which was diluted 25-fold from the stock (Xu *et. al.*, (2013) *Protein engineering design and selection*, 26, 663-670). Samples were put on the magnetic rack, supernatant discarded, and washed with 100 µL of PBSF. A secondary FACS reagent, to detect binding of biotinylated PSR reagent to TriNKETs or control mAbs, was made as follows: 1:250 µL of Streptavidin-PE (Biologend, catalog # 405204) and 1:100 donkey anti-human Fc were combined in PBSF. To each sample, 100 µL of the secondary reagents were added and allowed to incubate for 20 minutes on ice. The beads were washed twice with 100 µL PBSF, and samples were analyzed on a FACS Celesta (BD). Two PSR controls, Rituximab (PSR positive) and Trastuzumab (PSR clean), were used in the assay.

High-Spec® cross reactivity assay on HuProt™ human proteome assays

[0717] To examine specificity of F3'-1602 TriNKET, a protein array technology was used. The HuProt™ human proteome microarray provides the largest database of individually purified human full length proteins on a single microscopic slide. An array consisting of 22,000 full-length human proteins are expressed in yeast *S.cerevisiae*, purified, and subsequently printed in duplicate on a mircoarray glass slide that allows thousands of interactions to be profiled in a high-throughput manner.

[0718] Specificity of F3'-1602 TriNKET was tested at 0.1 µg/mL and 1 µg/mL concentration against native Huprot human proteome array embedded on microslides at CDI laboratories (Baltimore, MD), according to their standard procedure.

[0719] **FIG. 62** shows the relative binding (Z score) of F3'-1602 TriNKET at 1 µg/mL to human CLEC12A in comparison to the entire human proteome microarray. Z score is the average binding score of two duplicates of a given protein. For comparison purpose, the top 24 proteins with residual background binding to F3'-1602 TriNKET were also provided in **FIG. 62**. **Table 57** shows the Z and S scores of F3'-1602 TriNKET to human CLEC12A and the top 6 proteins from the microarray. S score is the difference of Z score of a given protein and the one rank next to it. If the S score of the top hit is > 3 an antibody is considered to be highly specific to its target. Based on the Z and S score criteria, F3'-1602 TriNKET showed high specificity to human and lack of off-target binding in the HuProt™ human proteome assay.

Table 57: Z and S scores of F3'-1602 TriNKET in HuProt™ human proteome microarray assay.

Name	Rank	Protein-ID	Z score	S score
hCLEC12A	1		150.21	144.62
MFF	2	JHU15965.P1168B06	5.60	0.59
RPLP0	3	JHU16464.P173H05	5.01	0.12
PARS2	4	JHU06781.P071H01	4.89	0.062
HMGA1_frag	5	JHU16418.P173B08	4.83	0.27
THEMIS2_frag	6	JHU15201.P160B01	4.56	0.37
HAGHL	7	JHU08774.P092D12	4.19	0.01

Molecular modeling

[0721] Anti-CLEC12A and anti-NKG2D binding arms of F3'-1602 TriNKET were compared with 377 post Phase I biotherapeutic molecules using Therapeutic Antibody Profiler (TAP) available at the SAbPred website. TAP used ABodyBuilder to generate a model for F3'-1602 TriNKET with side chains by PEARS. The CDRH3 was built by MODELLER due to its diversity.

[0722] Five different parameters were evaluated:

Total CDR length

Patches of surface hydrophobicity (PSH) across the CDR vicinity

Patches of positive charge (PPC) across the CDR vicinity

Patches of negative charge (PNC) across the CDR vicinity

Structural Fv charge symmetry parameter (sFvCSP)

[0723] These parameters of F3'-1602 TriNKET were then compared with the profile distributions of therapeutic antibodies to predict the developability and any potential issues that might cause downstream challenges.

[0724] **FIG. 63** illustrates a ribbon diagram model of the CLEC12A binding scFv in three different orientations (upper panel) and their corresponding surface charge distribution of the same orientation (lower panel). The charge distribution of anti-CLEC12A scFv is polarized ("top view", lower panel), with negatively-charged residues populated predominately within CDRH3 and CDRL2. The uneven distribution of electrostatic patches on the paratope is likely to be target-related and reflects the complementarity of charge distribution on its cognate epitope, which may likely contribute to the high affinity interaction between CLEC12A and the scFv of F3'-1602 TriNKET.

[0725] **FIG. 64** shows the CDR length and surface hydrophobicity analyses of scFv CLEC12A targeting arm of F3'-1602 TriNKET. The length of CDRs for the CLEC12A binding arm of F3'-1602 TriNKET are typical for late stage therapeutic antibodies.

[0726] The hydrophobicity of a monoclonal antibody is an important biophysical property relevant for its developability into a therapeutic. Hydrophobic patch analysis of the CDRs of an antibody is predictive of its behavior. The CLEC12A arm of F3'-1602 TriNKET has much lower hydrophobicity comparing to other reference molecules. Based on the modeling, there is no

hydrophobic patch of significant size on the surface of CLEC12A-binding arm of F3'-1602 TriNKET.

[0727] The charge distribution of anti-CLEC12A scFv is polarized, with negatively-charged residues populated predominately within CDRH3 and CDRL2 (as shown in **FIG. 63**). Although the positively charged patches and charge symmetry are within the norm, without wishing to be bound by theory, it is hypothesized that the distinct negatively charged patches on the paratope is target-related and reflects the complementarity of charge distribution on its cognate epitope, which may contribute to its high affinity interaction with CLEC12A.

[0728] The NKG2D-binding Fab arm of F3'-1602 TriNKET is shown in ribbon diagrams with three different orientations (**FIG. 65**) and their corresponding surface charge distribution of the same orientation are provided in **FIG. 65** (lower panel). In contrast to CLEC12A binding arm, the surface charge distribution on NKG2D A49M-I arm is more evenly distributed.

[0729] **FIG. 66** shows the CDR length and patches of surface hydrophobicity analyses of NKG2D-targeting arm of F3'-1602 TriNKET. Analysis was performed using TAP and was benchmarked 377 late-stage therapeutic antibodies. It appears that the CDR length, the hydrophobic properties, the positive/negative charge distributions, and the Fc charge symmetry of the NKG2D-targeting arm of F3'-1602 TriNKET are well within the norm of existing therapeutic antibodies. The modelling suggests that F3'-1602 TriNKET will not have developability complications during the manufacturing processes.

Hydrophobic Interactions Chromatography

[0730] The hydrophobicity prediction data was confirmed by investigating F3'-1602 TriNKET behavior with analytical Hydrophobic Interactions Chromatography (HIC), a technique that relies upon proteins with significant patches of exposed hydrophobic patches being more prone to aggregation. To perform HIC, briefly, injections of TriNKETs (5 μg of protein) were prepared in a 5:4 ratio of high salt buffer (100 mM sodium phosphate, 1.8 M ammonium sulfate, pH 6.5) to sample. Samples were analyzed using an Agilent 1260 Infinity II HPLC equipped with a Sepax Proteomix HIC Butyl-NP5 5uM column held at 25 °C. The gradient was run from 0% low salt buffer (100 mM sodium phosphate, pH 6.5) to 100% low salt buffer over 6.5 minutes at a flow rate of 1.0 mL/minute. Chromatograms were monitored at 280 nm. Retention times of F3'-1602 TriNKET on the analytical HIC column is shown in **Table 58**

and HIC profile in **FIG. 67**. Commercial trastuzumab (Roche) was used as an example of a well-behaved biologic and functioned as an internal control for the assay. F3'-1602 TriNKET has a retention time of 9.8 minutes, compared to 9.6 minutes for trastuzumab. Thus, experimental hydrophobicity analysis suggests that the hydrophobic properties of F3'-1602 TriNKET are acceptable for further development.

Table 58: HIC retention time of F3'-1602 TriNKET in comparison with trastuzumab.

Test article	HIC retention time (min)
F3'-1602 TriNKET	9.8
Trastuzumab	9.6

Capillary Isoelectric Focusing (cIEF)

[0731] Experimental pI of F3'-1602 was obtained by cIEF, as described in Example 15 (**FIG. 68**). Commercial grade Trastuzumab was included in the assay as an internal control. The cIEF profile of F3'-1602 TriNKET was typical for a monoclonal antibody, with a main peak at pI 8.80 (**Table 59**). The presence of minor amounts of acidic and basic species were also observed.

Table 59: pI of scFv-1602 F3' by cIEF compared to trastuzumab.

Test article	pI (major peak)
scFv-1602 F3'	8.80
Trastuzumab	8.91

Immunogenicity assessment

[0732] Immunogenicity assessment was performed using the EpiMatrix algorithm from EpiVax was used as described in Cohen et al. (2010) A method for individualizing the prediction of immunogenicity of protein vaccines and biologic therapeutics: individualized T cell epitope measure (iTEM). *J.Biomed. Biotechnol.* 961752. The T_{reg} adjusted Epimatrix Protein Score, which ranges from -80 (no immunogenicity) to 80 (highly immunogenic), for the sequences of

the three chains of scFv-1602 F3' are VH-CH1-Fc: -33.39, VH-VL-Fc: -26.4 and VL-CL: -27.4. Thus, the predicted risk of immunogenicity for the scFv-1602 F3' appears to be low.

Example 13. F3'-1602 TriNKET analysis of putative sequence liabilities

[0733] The amino acid sequences of the three polypeptide chains of F3'-1602 TriNKET was analyzed for putative sequence liabilities as described in Example 3. Putative sequence liabilities are shown in **Table 60**.

Table 60: Putative sequence liabilities in F3'-1602 TriNKET. CDRs are under Chothia numbering.

VL-CL	VH-CH1-Fc	VH-VL-Fc
None	**DP** in CDRH3 (potential chemical instability)	**DS** in CDRH3 (potential aspartate isomerization)

[0734] To examine the liabilities, accelerated stability (4 weeks at 40°C) and forced degradation studies were performed. The DP in the CDRH3 of VH-CH1-Fc was not modified in accelerated stability studies or forced degradation studies, and therefore, no further analysis was necessary. However, it was observed that modification of the DS in the CDRH3 in the scFv led to a reduction in CLEC12A binding and decreased potency of F3'-1602 TriNKET in accelerated stability studies, as described in Example 14.

[0735] To replace the DS in CDRH3, yeast display was performed to identify alternative sequence motifs without the DS site. Three variants, namely YDYD**DA**LDY (SEQ ID NO:283) YDYD**DI**LDY (SEQ ID NO:284) and YDYD**DL**LDY (SEQ ID NO:285), were identified that showed binding to hCLEC12A albeit with weaker binding signal compared to the parent scFv (YDYD**DS**LDY) (SEQ ID NO:139), while variants YDYD**DV**LDY (SEQ ID NO:290), YDYD**DT**LDY (SEQ ID NO:291), and YDYD**ES**LDY (SEQ ID NO:292) were identified as non-binders. Based on the binding analysis only variants YDYD**DA**LDY ((SEQ ID NO:283), AB0053) and YDYD**DI**LDY ((SEQ ID NO:284), AB0085) were considered for mammalian production and further characterization. Binding of AB0053 and AB0085 to hCLEC12A-His was characterized using Surface Plasmon Resonance (SPR) at 37 °C. Both mutations introduced to remove DS sequence liability had an effect on the binding to hCLEC12A-His (**Table 61**). **FIG. 69** demonstrates FACS analysis of binding to hCLEC12A-his using yeast libraries generated to remove the sequence liability in CDRH3. The data showed complete loss of binding in the DS to

DI engineered variant (AB0085). Introduction of DA in place of DS (AB0053) did not eliminate binding completely but lead to apparent heterogeneity in binding sensorgram. Following SPR analysis, potency of the liability-remediated variants (AB0053 and AB0085) were tested in KHYG-1-CD16aV mediated cytotoxicity assay (**FIG. 70**, **Table 62**). AB0085 lost ability to kill AML cells as determined by significantly reduced percentage of maximum killing. EC50 for AB0053 construct increased ~ 3-fold compared to F3'-1602 TriNKET (AB0237) control, whereas percentage of maximum killing was not affected. This finding is in line with the 3-fold change in overall affinity for hCLEC12A established in the SPR experiment (**Table 61**).

[0736] Binding affinities of F3'-1602 TriNKET to recombinant human CLEC12A were measured by SPR at 37 ºC using a Biacore 8K instrument. Briefly, human Fc specific antibodies were covalently immobilized at a density ~8000-10000 resonance units (RU) on carboxy methyl dextran matrix of a CM5 biosensor chip via amine-coupling chemistry to create an anti-hFc IgG chip. F3'-1602 TriNKET samples were captured on the anti-hFc IgG chip at a concentration of 1.5 µg/mL at a flow rate of 10 µL/min for 60 seconds to achieve ~150-250 RU capture level. hCLEC12A-His was serially diluted (100 nM-0.046 nM) in three-fold dilutions with HBS-EP+ buffer (1X; 10 mM HEPES, 150 mM NaCl, 3 mM EDTA, 0.05% P20 pH 7.4) with 0.1 mg/mL bovine serum albumin (BSA) and injected at a flow rate of 30 µl/min over the captured test articles. Association was monitored for 300 seconds and dissociation was monitored for 600 seconds. Surfaces were regenerated between cycles with three pulses of 10 mM glycine-HCl, pH 1.7 injected for 20 seconds at 100 µL/min. HBS-EP+ (1X) with 0.1 mg/mL BSA buffer was used throughout the experiment. Data were analyzed using Biacore 8K Insight Evaluation software (GE Healthcare).

Table 61: Kinetic parameters and affinities of DS engineered clones for hCLEC12A for CLEC12A.

Test Article	k_a ($M^{-1}s^{-1}$)	k_d (s^{-1})	K_D (nM)	Notes
AB0053	$1.63 \times 10^{6*}$	$k_{d1} = 1.57 \times 10^{-2}$ and $k_{d2} = 9.49 \times 10^{-4}$	2.41	Two-state fit
AB0085	No Binding			
F3'-1602 (AB0237)	1.11×10^{6}	8.95×10^{-4}	0.80	Classical 1:1 fit

*k_{a2} value was insignificant compared to the k_{a1} value. Therefore, only k_{a1} value is shown.

Table 62: Comparison of potency of DS engineered TriNKETs in KHYG-1-CD16aV cytotoxicity assay.

Test Article	PL-21 cells	
	EC50 (nM)	**Max lysis (%)**
F3'-1602 TriNKET (AB0237)	0.12	98.96
AB0053	0.39	105.10
AB0085	N/D*	N/D

*N/D not determined

[0737] As the library approach produced AB0053 as the only hit, and that hit demonstrated kinetics of binding to hCLEC12A significantly different from F3'-1602 TriNKET and inferior potency in the cytotoxicity assay, it was concluded that the DS motif is necessary for maintaining architecture of CDRH3 and therefore cannot be effectively removed. The DS liability was instead controlled with formulation, as described in Example 14.

Example 14. Formulations of F3'-1602

[0738] In Example 13, sequence liability sites were found to be critical for the ability of F3'-1602 to bind CLEC12A and therefore cannot be removed. This example was designed to assess the formulations that may maintain the stability of F3'-1602 despite the presence of the sequence liabilities.

[0739] Briefly, three formulations were tested for F3'-1602:
(1) 20 mM histidine, 250 mM sucrose, and 0.01% polysorbate 80, at pH of 6.0, referred to herein as the "HST formulation." F3'-1602 was diafiltered into the HST buffer and the recovered sample was passed through a 0.2 μm filter. The final concentration of F3'-1602 was 19.7 mg/mL, as measured by absorbance at 280 nm (A280).
(2) 20 mM potassium phosphate, 10 mM sodium citrate, and 125 mM sodium chloride, at pH 7.8, referred to herein as the "phosphate/citrate/NaCl formulation." F3'-1602 was buffer switched into the phosphate/citrate/NaCl formulation buffer using an Amicon Ultra 0.5 mL 30K device and Zeba Desalting Columns, and the recovered sample was passed through a 0.2 μm filter. The final concentration of F3'-1602 was 20.6 mg/mL, as measured by A280.
(3) 20 mM citrate, 250 mM sucrose, and 0.01% polysorbate 80, at pH 7.0, referred to herein as the "CST formulation." F3'-1602 was diafiltered into the CST formulation buffer and the

recovered sample was passed through a 0.2 μm filter. The final concentration of F3'-1602 was 20 mg/mL, as measured by A280.

Stability of F3'-1602 in the HST formulation

[0740] An accelerated stability study was carried out in the HST buffer at 40 °C for four weeks. Size exclusion chromatography (SEC) was used to monitor the formation of high molecular weight species (HMWS) and low molecular weight species (LMWS) as a function of storage conditions. Briefly, 50 μg of test material was injected onto an Agilent 1260 Infinity II high pressure liquid chromatography (HPLC) instrument with 1260 Quat Pump, 1260 Vialsampler, 1260 VWD. The sample was separated on a Tosoh TSKgel G3000SWxl, 7.8 mm I.D. x 30 cm, 5 μm column. SEC running buffer was PBS, pH 7.0, flowing at 0.50 ml/min. Absorbance was monitored at both 214 and 280 nm, peak areas were manually integrated and the percent of HMWS, LMWS, and monomer were reported.

[0741] At the onset of the study, F3'-1602 was analyzed by SEC and was 99.6% monomer. After four weeks at 40 ºC, monomer decreased to 93.1%. LMWS were not detected in the control and increased to 5.4% after four weeks at 40 ºC. HMWS were present in the control at 0.4% and increased to 1.5% after four weeks at 40 ºC (**Table 63**). These data suggest that F3'-1602 degrades primarily through the formation of LMW species (fragmentation).

Table 63. Summary of SEC % monomer, HMW, and LMW (accelerated stability in the HST formulation)

Test article	Monomer (%)	HMW (%)	LMW (%)
Control	99.6	0.4	ND
1 week	99.0	0.7	0.3
2 weeks	98.5	1.0	0.5
3 weeks	97.8	1.5	0.8
4 weeks	93.1	1.5	5.4

ND: none detected

[0742] The binding affinities of F3'-1602 samples to recombinant human CLEC12A were measured by SPR at 37 ºC using a Biacore 8K instrument. Briefly, human Fc specific antibodies were covalently immobilized at a density ~8000-10000 resonance units (RU) on carboxy methyl dextran matrix of a CM5 biosensor chip via amine-coupling chemistry to create an anti-hFc IgG chip. F3'-1602 samples were captured on the anti-hFc IgG chip at a concentration of 1.5 μg/mL at a flow rate of 10 μL/min for 60 seconds to achieve ~150-250 RU capture level. hCLEC12A-

His was serially diluted (100 nM-0.046 nM) in three-fold dilutions with HBS-EP+ (1X) with 0.1 mg/mL bovine serum albumin (BSA) buffer and injected at a flow rate of 30 µl/min over the captured test articles. Association was monitored for 300 seconds and dissociation was monitored for 600 seconds. Surfaces were regenerated between cycles with three pulses of 10 mM glycine-HCl, pH 1.7 injected for 20 seconds at 100 µL/min. HBS-EP+ (1X) with 0.1 mg/mL BSA buffer was used throughout the experiment. Data were analyzed using Biacore 8K Insight evaluation software (GE Healthcare). The kinetic rate constants and overall affinity were obtained using 1:1 kinetic fit binding model.

[0743] After four weeks of incubation at 40 ºC in the HST formulation, binding of F3'-1602 to human CLEC12A was decreased (**FIG. 71**). The difference in association and dissociation rate constants between the control and 40 ºC stressed sample are within the experimental variability of the assay (**Table 64**); however, the maximal binding response expressed in resonance units (RU) decreased more than fivefold after the incubation at 40 °C (**FIG. 71**). The nominal capture of F3'-1602 protein was the same for both, stressed and control, samples. Under such circumstances, R_{max} is roughly proportional to the active concentration of F3'-1602 captured on the Biacore chip. This result in turn indicates that after thermal stress in the HST formulation, more than 80% of F3'-1602 molecules lost the ability to bind CLEC12A (**Table 64**).

Table 64. Summary of kinetic parameters and binding affinity of F3'-1602 for hCLEC12A (accelerated stability in the HST formulation)

Test article	Target	k_a ($M^{-1}s^{-1}$)	k_d (s^{-1})	K_D (nM)	Capture level (RU)
F3'-1602 Control	hCLEC12A	$7.91x10^5$	$8.73x10^{-4}$	1.11	83.8
F3'-1602 in the HST formulation, 40 ºC 4 wks	hCLEC12A	$1.24x10^6$	$2.14x10^{-3}$	1.69	84.2

Results are an average of n = 2 replicates

[0744] The binding affinities of F3'-1602 samples to recombinant human NKG2D were measured by SPR at 37 ºC using a Biacore 8K instrument. Briefly, mFc specific antibodies were covalently immobilized at a density of ~8000-10000 RU on carboxy methyl dextran matrix of a CM5 biosensor chips via amine coupling chemistry to create an anti-mFc IgG chip. mFc-tagged human NKG2D was captured on the anti-mFc IgG chip at a concentration of 0.2 µg/mL at a flow

rate of 10 µL/min for 60 seconds to achieve ~35 RU capture level. F3'-1602 was buffer exchanged into HBS-EP+ (1X) buffer and serially diluted (5000 nM – 9.78 nM) in two-fold dilutions with HBS-EP+. Analyte (F3'-1602) was injected at a flow rate of 30 µL/min over the captured test articles. Association was monitored for 60 seconds and dissociation was monitored for 60 seconds. Surfaces were regenerated between cycles with three pulses of 10 mM glycine-HCl, pH 1.7 injected for 20 seconds at 100 µL/min. HBS-EP+ (1X) buffer was used throughout the experiment. Data were analyzed using Biacore 8K Insight evaluation software (GE Healthcare). The binding affinity and kinetic rates were obtained with the use of both 1:1 kinetic and steady-state affinity model fits.

[0745] After four weeks of incubation at 40 ºC in the HST formulation, binding of F3'-1602 to human NKG2D was unaltered (**FIG. 72, Table 65**). The difference in association and dissociation rate constants as well as overall affinity for NKG2D between the control and 40 ºC stressed sample were within the experimental variability of the assay. Maximal binding response did not change significantly. The results indicate that F3'-1602 maintained the ability to bind NKG2D under these thermal stress conditions.

Table 65. Summary of kinetic parameters and binding affinity of F3'-1602 for hNKG2D (accelerated stability in the HST formulation)

Test article	Target	k_a ($M^{-1}s^{-1}$)	k_d (s^{-1})	1:1 Kinetic Fit K_D (nM)	Steady state K_D (nM)	Capture level (RU)
F3'-1602 Control	hNKG2D	$1.70x10^5$	$1.29x10^{-1}$	760	771	50.1
F3'-1602 in the HST formulation, 40 ºC, 4 wks	hNKG2D	$1.29x10^5$	$9.86x10^{-2}$	762	776	47.4

[0746] The binding affinities of F3'-1602 samples to biotinylated recombinant CD16a V158 (FcγRIIIa V158) receptor were measured by SPR. Briefly, FcγRIIIa V158 was captured on a SA Series S Biacore chip prior to the kinetic evaluation experiment to achieve capture ~ 10-25 RU. Trastuzumab, a well characterized IgG1 biologic drug, was used as an experimental control. The evaluation used injections of varying concentrations of ligand (F3'-1602 or trastuzumab) titrated over the captured receptor (1500 nM – 11.7 nM in 1:1 serial dilution and 0 nM). Each injection

cycle consisted of association, dissociation and regeneration steps. Association consisted of 150 seconds of ligand injection, dissociation was monitored for 300 seconds and then the surface was regenerated between cycles with 2 mM sodium hydroxide injected for 5 seconds. All steps were executed at a flow rate of 30 µL/min. 1x HBS-EP+ buffer solution was used as a running/sample dilution buffer. Data were analyzed using Biacore 8K Insight evaluation software (GE Healthcare). The data were fit with a 1:1 kinetic model.

[0747] After four weeks of incubation at 20 mg/mL, 40 ºC in the HST formulation, binding of F3'-1602 to human CD16a V158 was unaltered (**FIG. 73 and Table 66**). The difference in binding affinity between the control and 40 ºC stressed sample as well as maximal binding response (R_{max}) were within the experimental variability of the assay. The results indicate that F3'-1602 retained affinity for human CD16a under these accelerated storage conditions.

Table 66. Summary of kinetic parameters and binding affinity of F3'-1602 for hNKG2D (accelerated stability in the HST formulation)

Test article	Target	k_a ($M^{-1}s^{-1}$)	k_d (s^{-1})	K_D (nM)	Capture level (RU)
F3'-1602 Control	hCD16aV	$(1.13\pm0.04)x10^{5}$	$(2.40\pm0.09)x10^{-2}$	212±1	13.7
F3'-1602 in the HST formulation, 40 ºC, 4 wks	hCD16aV	$(8.24\pm0.78)x10^{4}$	$(1.65\pm0.06)x10^{-2}$	201±12	14.2

Results are an average of n = 3 replicates

[0748] The effect of accelerated stability on F3'-1602 function was also assessed in a cytotoxicity assay using KHYG-1-CD16a cells engineered to express CD16a in addition to NKG2D. $CLEC12A^{+}$ human cancer cell lines (PL-21) were labeled with BATDA reagent. After labeling, cells were washed and resuspended in primary cell culture media. BATDA labeled cells, F3'-1602, and rested KHYG-1-CD16V cells were added to the wells of a 96-well plate. Additional wells were prepared for maximum lysis of target cells by addition of 1% Triton-X. Spontaneous release was monitored from wells with only BATDA-labeled cells. After three hours of culture, the cells were pelleted, the culture supernatant was transferred to a clean microplate, and room temperature europium solution was added to each well. The plate was protected from light and incubated on a plate-shaker at 250 rpm for 15 minutes. Plates were read using a SpectraMax i3X instrument. The % Specific lysis was calculated as follows:

% Specific lysis = ((Experimental release – Spontaneous release) / (Maximum release – Spontaneous release)) * 100%

[0749] As shown in **FIG. 74** and **Table 67**, the ability of F3'-1602 to kill PL21 CLEC12A$^+$ cancer cells decreased by approximately 7-fold after 4 weeks at 40 ºC in the HST formulation, whereas max% lysis decreased only slightly (5%).

Table 67. EC50 and maximum lysis of CLEC12A+ PL21 cells by F3'-1602 (accelerated stability in the HST formulation)

Test article	EC50 (nM)	Max. lysis (%)
F3'-1602 Control	0.17	63
F3'-1602 in the HST formulation, 40 ºC, 4 wks	1.21	58

[0750] The significant loss of binding to hCLEC12A after 40 °C incubation and the corresponding loss in potency led to an investigation into the root cause of this behavior. UHPLC-MS/MS peptide mapping revealed that an aspartic acid in the anti-CLEC12A scFv (CDR-H3) was undergoing isomerization (**FIG. 75**).

[0751] F3'-1602 CDRH3, as defined under Chothia, contains four aspartic acids (DYDDSLDY [SEQ ID NO:293]). MS/MS was used to determine which of them was undergoing isomerization by monitoring the succinimide intermediate. Conversion to isoaspartic acid does not result in a mass difference, whereas the succinimide intermediate corresponds to a loss of water (approximately 18 Da). This mass shift can be used to identify the aspartic acid which is isomerizing. MS/MS spectra of the unmodified chymotryptic peptide and the corresponding succinimide variant showed that the aspartic acid at position H99 (Chothia) in the scFv VH (DYDDSLDY [SEQ ID NO:293]) was responsible for the isomerization.

Stability of F3'-1602 in the phosphate/citrate/NaCl formulation

[0752] Attempts to remove the liability by mutagenesis revealed that the aspartic acid at position H99 of the CLEC12A-binding scFv is an important determinant of CDR structure and cannot be easily replaced without the loss of binding to the target. Therefore, limited pre-formulation development was performed to identify a formulation with a more basic pH since isomerization rate is pH dependent. The pH dependence was confirmed by stressing F3'-1602 in citrate and phosphate buffer covering pH 5.5-7.5. After 4 weeks at 40 ºC in phosphate buffer (pH

6.5/7.0/7.5), F3'-1602 showed a pH-dependent loss of binding to CLEC12A. Interestingly, there was no trend observed in citrate buffer (pH 5.5/6.0/6.5). Additional formulations were designed based on these results, and common excipients (NaCl, sucrose, EDTA) were screened for their ability to stabilize CLEC12A binding (**Table 68**). This screening indicated that high pH and NaCl had a protective effect on CLEC12A binding.

Table 68. Phosphate/Citrate formulation buffers

Buffer #	Citrate (mM)	Phosphate (mM)	EDTA (mM)	Sucrose (mM)	NaCl (mM)	pH
1	50	0	0	0	0	7.0
2	20	50	0	0	0	7.0
3	20	50	0	0	0	7.5
4	20	50	0	0	0	8.0
5	0	50	10	0	0	7.0
6	0	50	10	0	0	7.5
7	0	50	10	0	0	8.0
8	50	0	0	250	0	7.0
9	50	0	0	0	250	7.0

[0753] Based on these results, F3'-1602 was formulated in 20 mM potassium phosphate, 10 mM sodium citrate, 125 mM sodium chloride, pH 7.8 (the phosphate/citrate/NaCl formulation).

[0754] The formation of HMWS and LMWS was assessed by SEC as described in the "Stability of F3'-1602 in the HST formulation" subsection. F3'-1602 was incubated at 40 ºC for 4 weeks. At the onset of the study, F3'-1602 was analyzed by SEC and was 97.9% monomer. After four weeks at 40 ºC, monomer decreased to 91.4%. LMWS increased from 1.8 to 5.0% after four weeks at 40 ºC. HMWS were present in the control at 0.3% and increased to 3.6% after four weeks at 40 ºC (**Table 69**). These data suggest that in the phosphate/citrate/NaCl formulation, F3'-1602 degraded through both aggregation (HMWS) and fragmentation (LMWS).

Table 69. Summary of SEC % monomer, HMW, and LMW (accelerated stability in the phosphate/citrate/NaCl formulation)

Test article	Monomer (%)	HMW (%)	LMW (%)
F3'-1602 control	97.9	0.3	1.8
F3'-1602, 4 weeks, 40 ˚C	91.4	3.6	5.0

[0755] Fragmentation and aggregation of intact F3'-1602 was assessed in the accelerated stability study by non-reduced sodium dodecyl sulfate capillary electrophoresis (SDS-CE). Briefly, F3'-1602 was diluted to 0.5 mg/mL with 1X Sample Buffer to achieve a final sample volume of 50 µL. Internal standard and iodoacetamide were added to samples, which were then incubated at 70 ºC for 10 minutes in a heat block, followed by an ice bath for 5 minutes. Samples were transferred to a 96-well plate, centrifuged, and loaded into the instrument. Individual samples were loaded into the capillary for 40 seconds at 4600 volts and separated for 35 minutes at 5750 volts on a Maurice (ProteinSimple, San Jose, CA).

[0756] The F3'-1602 main peak purity decreased from 97.0% to 91.2% by the end of the 4-week incubation. There was a corresponding increase in LMWS from 3.0% to 8.4% (**Table 70**). There was a slight increase in HMWS (none detected to 0.4%) throughout the duration of the study as determined by non-reduced SDS-CE. The difference in migration time of the main peak in the overlay was within the experimental variability of this assay.

Table 70. Summary of non-reduced SDS-CE purity (accelerated stability in the phosphate/citrate/NaCl formulation)

Test article	LMW (%)	Main (%)	HMW (%)
F3'-1602 control	3.0	97.0	ND
F3'-1602 4 weeks, 40˚C	8.4	91.2	0.4

ND, none detected

[0757] Fragmentation of the three individual polypeptide chains of F3'-1602 was assessed at each timepoint in the accelerated stability study by reduced SDS-CE. In this assay, purity was determined by the sum of the three chains. Over the course of the study, purity decreased from 97.4% to 95.2% (**Table 71**). This decrease in purity was the result of increased LMWS, which agrees with the SEC and non-reduced SDS-CE results. The difference in migration times of the main peaks in the overlay was within the experimental variability of this assay.

Table 71. Summary of reduced SDS-CE purity (accelerated stability in the phosphate/citrate/NaCl formulation)

Test article	Light chain (%)	Heavy chain (%)	scFv-Fc chain (%)	Purity (%)
F3'-1602 control	17.9	39.2	40.3	97.4

Test article	Light chain (%)	Heavy chain (%)	scFv-Fc chain (%)	Purity (%)
F3'-1602 4 weeks, 40°C	20.3	39.4	35.5	95.2

[0758] The binding affinities of F3'-1602 samples to recombinant human CLEC12A were measured by SPR as described in the "Stability of F3'-1602 in the HST formulation" subsection. After four weeks of incubation in the phosphate/citrate/NaCl formulation, human CLEC12A binding was reduced to some extent (**FIG. 76**). The difference in association and dissociation rate constants between the control and 40 ºC stressed sample were within the experimental variability of the assay (**Table 72**), whereas the maximal binding response (Rmax) adjusted for capture differences decreased approximately 10% after incubation at 40 °C. Such a loss was significantly less than more than 80% that was observed after 4 weeks of incubation in the HST formulation, indicating that the phosphate/citrate/NaCl formulation was able to stabilize F3'-1602 under accelerated (40 °C) conditions. Therefore, the isomerization of H99, as described in the "stability of F3'-1602 in the HST formulation" subsection, was substantially reduced by formulation development.

Table 72. Summary of kinetic parameters and binding affinity of F3'-1602 for hCLEC12A (accelerated stability in the phosphate/citrate/NaCl formulation)

Test article	Target	k_a ($M^{-1}s^{-1}$)	k_d (s^{-1})	K_D (nM)	Capture level (RU)
F3'-1602 control	hCLEC12A	$7.79x10^5$	$9.33x10^{-4}$	1.20	160.6
F3'-1602 in the phosphate/ Citrate/NaCl formulation, 40 ºC, 4 wks	hCLEC12A	$8.29x10^5$	$9.48x10^{-4}$	1.14	146.7

Results are an average of n = 2 replicates

[0759] The binding affinities of F3'-1602 samples to recombinant human NKG2D were measured by SPR as described in the "Stability of F3'-1602 in the HST formulation" subsection. After four weeks of incubation at 20 mg/mL, 40 ºC in the phosphate/citrate/NaCl formulation, binding of F3'-1602 to human NKG2D was unaltered (**FIG. 77 and Table 73**). The difference in equilibrium binding affinity as well as Rmax between the control and 40 ºC stressed sample were within the experimental variability of the assay. This indicates that F3'-1602 retained affinity for human NKG2D under these accelerated storage conditions.

Table 73. Summary of kinetic parameters and binding affinity of F3'-1602 for hNKG2D (accelerated stability in the phosphate/citrate/NaCl formulation)

Test article	Target	k_a ($M^{-1}s^{-1}$)	k_d (s^{-1})	1:1 Kinetic Fit K_D (nM)	Steady state K_D (nM)	Capture level (RU)
F3'-1602 Control	hNKG2D	$1.93x10^5$	$1.53x10^{-1}$	790	791	34.5
F3'-1602 in the phosphate/ citrate/NaCl formulation, 40 °C, 4 wks	hNKG2D	$1.53x10^5$	$1.33x10^{-1}$	869	872[a]	31.4

Results are an average of n = 2 replicates

[0760] The binding affinities of F3'-1602 samples to biotinylated recombinant CD16a V158 (FcγRIIIa V158) receptor were measured by SPR as described in the "Stability of F3'-1602 in the HST formulation" subsection. After four weeks of incubation at 20 mg/mL, 40 °C in the phosphate/citrate/NaCl formulation, binding of F3'-1602 to human CD16a V158 was unaltered (**FIG. 78 and Table 74**). The difference in binding affinity as well as apparent maximal binding response between the control and 40 °C stressed sample are within the experimental variability of the assay. This indicates that F3'-1602 retains affinity for human CD16a under these accelerated storage conditions.

Table 74. Summary of kinetic parameters and binding affinity of F3'-1602 for hCD16a V158 (accelerated stability in the phosphate/citrate/NaCl formulation)

Test article	Target	k_a ($M^{-1}s^{-1}$)	k_d (s^{-1})	K_D (nM)	Capture level (RU)
F3'-1602 Control[a]	hCD16aV	$(1.13\pm0.04)x10^5$	$(2.40\pm0.09)x10^{-2}$	212±1	13.7
F3'-1602 in the phosphate/citrate/ NaCl formulation, 40 °C, 4 wks	hCD16aV	$9.67x10^4$	$2.09x10^{-2}$	216	14.0

[0761] The effect of accelerated stability on F3'-1602 function was also assessed in a cytotoxicity assay using NKG2D- and CD16a-expressing KHYG-1-CD16a cells, as described in the "Stability of F3'-1602 in the HST formulation" subsection. The ability of F3'-1602 to kill PL-21 CLEC12A+ cancer cells was unaltered after 4 weeks incubation at 40 °C in the

phosphate/citrate/NaCl formulation at a concentration of 20 mg/mL (**FIG. 79 and Table 75**). This result was in stark contrast to what was observed after incubation in the HST formulation, and indicates that F3'-1602 was stabilized in 20 mM phosphate, 10 mM citrate, 125 mM NaCl, pH 7.8.

Table 75. EC50 and maximum lysis of CLEC12A+ PL-21 cells by F3'-1602 (accelerated stability in the phosphate/citrate/NaCl formulation)

Test article	EC50 (nM)	Max. lysis (%)
F3'-1602 Control	0.26	90
F3'-1602 in the phosphate/citrate/NaCl formulation, 40 ºC, 4 wks	0.29	93

Stability of F3'-1602 in the CST formulation

[0762] Based on the stability data in the phosphate/citrate/NaCl formulation, it was concluded that the loss of activity at 40 °C could be minimized in a liquid formulation. Stability of F3'-1602 was further analyzed in a lyophilization-compatible liquid formulation containing sucrose as a lyoprotectant.

[0763] An accelerated stability study at 20 mg/mL was carried out in 20 mM citrate, 250 mM sucrose, 0.01% Tween-80, pH 7.0 (the CST formulation) at refrigerated (2-8 °C) and accelerated (25 and 40 °C) conditions for four weeks. A full suite of analytics was carried out on the 40°C stressed samples while only binding to CLEC12A (SPR) and potency were monitored for the 2-8 °C and 25 °C arms.

[0764] The formation of HMWS and LMWS was assessed by SEC as described in the "Stability of F3'-1602 in the HST formulation" subsection. At the onset of the study, F3'-1602 was analyzed by SEC and was 99.6% monomer. After four weeks at 40 ºC, monomer decreased to 98.6%. LMWS were not detected in the control and increased to 0.5% after four weeks at 40 ºC. HMWS were present in the control at 0.4% and increased to 1.0% after four weeks at 40 ºC (**Table 76**). These data suggest that F3'-1602 was resistant to both aggregation and fragmentation under accelerated conditions in the CST formulation.

Table 76. Summary of SEC % monomer, HMW, and LMW (accelerated stability in the CST formulation)

Test article	Monomer (%)	HMW (%)	LMW (%)
Control	99.6	0.4	ND
1 week	99.3	0.5	0.2
2 weeks	99.0	0.7	0.3
3 weeks	98.7	0.9	0.4
4 weeks	98.6	1.0	0.5

ND, none detected

[0765] Fragmentation of intact F3'-1602 was assessed at each timepoint in the accelerated stability study by non-reduced SDS-CE, as described in the "Stability of F3'-1602 in the phosphate/citrate/NaCl formulation" subsection. The F3'-1602 main peak purity decreased from 96.1% to 91.0% by the end of the 4-week incubation. There was a corresponding increase in LMWS from 3.9% to 9.0% (**Table 77**). There was no increase in HMWS throughout the duration of the study as determined by non-reduced SDS-CE. The difference in migration time of the main peak in the overlay was within the experimental variability of this assay.

Table 77. Summary of non-reduced SDS-CE purity (accelerated stability in the CST formulation)

Test article	LMW (%)	Main (%)	HMW (%)
Control	3.9	96.1	ND
1 week	4.8	95.2	ND
2 weeks	6.6	93.4	ND
3 weeks	5.3	94.7	ND
4 weeks	9.0	91.0	ND

ND: none detected

[0766] Fragmentation of the three individual polypeptide chains of F3'-1602 was assessed at each timepoint in the accelerated stability study by reduced SDS-CE, as described in the "Stability of F3'-1602 in the phosphate/citrate/NaCl formulation" subsection. In this assay, purity was determined by the sum of the three chains. Over the course of the study, purity decreased from 98.3% to 97.7% (**Table 78**). The difference in migration times of the main peaks in the overlay was within the experimental variability of this assay.

Table 78. Summary of reduced SDS-CE purity (accelerated stability in the CST formulation)

Test article	Purity (%)
Control	98.3
1 week	98.0
2 weeks	98.0
3 weeks	97.8
4 weeks	97.7

Purity was the sum of chain L, H, and S % area

[0767] The binding affinities of F3'-1602 samples to recombinant human CLEC12A were measured by SPR as described in the "Stability of F3'-1602 in the HST formulation" subsection. After four weeks of incubation at 20 mg/mL, 40 ºC in the CST formulation, human CLEC12A binding was reduced (**FIG. 80 and Table 79**). The difference in association and dissociation rate constants between the control and 40 ºC stressed sample are within the experimental variability of the assay, however apparent binding response decreased about 15-17% after the stress at 40°C. This indicates that 15-17% of F3'-1602 lost the ability to bind CLEC12A after 4 weeks under these thermal stress conditions. While the classical SPR binding assay is a good indicator of potential loss of activity when it comes to stark differences in binding (20% or more), it is not reliable enough to address the impact of the smaller changes in activity of the sample (especially at the low replicate number); other analytical methods are used to elucidate the changes with more scientific certainty if needed.

Table 79. Summary of kinetic parameters and binding affinity of F3'-1602 for hCLEC12A (40 °C accelerated stability in the CST formulation)

Test article	Target	k_a ($M^{-1}s^{-1}$)	k_d (s^{-1})	K_D (nM)	Capture level (RU)
F3'-1602 control	hCLEC12A	$7.50x10^5$	$7.35x10^{-4}$	0.98	221.3
F3'-1602 in the CST formulation, 40 ºC, 4 wks	hCLEC12A	$7.84x10^5$	$6.74x10^{-4}$	0.86	211.5

Results are an average of n = 2 replicates

[0768] At the lower temperatures (refrigerated and 25 °C), no difference in affinity to hCLEC12A or apparent binding adjusted for differences in capture levels were observed after 4 weeks in the CST formulation (**FIG. 81, Table 80, and Table 81**).

Table 80. Summary of kinetic parameters and binding affinity of F3'-1602 for hCLEC12A (2-8 °C stability in the CST formulation)

Test article	Target	k_a ($M^{-1}s^{-1}$)	k_d (s^{-1})	K_D (nM)	Capture level (RU)
F3'-1602 control	hCLEC12A	$7.50x10^5$	$7.35x10^{-4}$	0.98	221.3
F3'-1602 in the CST formulation, 2-8 °C, 2 wk	hCLEC12A	$6.72x10^5$	$6.00x10^{-4}$	0.89	352.4
F3'-1602 in the CST formulation, 2-8 °C, 4 wk	hCLEC12A	$7.76x10^5$	$7.08x10^{-4}$	0.91	222.8

Results are an average of n = 2 replicates

Table 81. Summary of kinetic parameters and binding affinity of F3'-1602 for hCLEC12A (25 °C stability in the CST formulation)

Test article	Target	k_a ($M^{-1}s^{-1}$)	k_d (s^{-1})	K_D (nM)	Capture level (RU)
F3'-1602 control	hCLEC12A	$7.50x10^5$	$7.35x10^{-4}$	0.98	221.3
F3'-1602 in the CST formulation, 25 °C, 2 wk	hCLEC12A	$8.24x10^5$	$7.65x10^{-4}$	0.93	187.6
F3'-1602 in the CST formulation, 25 °C, 4 wk	hCLEC12A	$7.88x10^5$	$7.19x10^{-4}$	0.91	179.9

Results are an average of n = 2 replicates

[0769] The binding affinities of F3'-1602 samples to recombinant human NKG2D were measured by SPR as described in the "Stability of F3'-1602 in the HST formulation" subsection. After four weeks of incubation at 20 mg/mL, 40 °C in the CST formulation, binding of F3'-1602 to human NKG2D was unaltered (**FIG. 82 and Table 82**). The difference in equilibrium binding affinity as well as apparent Rmax between the control and 40 °C stressed sample were within the experimental variability of the assay. This indicates that F3'-1602 retained affinity for human NKG2D under these accelerated storage conditions.

Table 82. Summary of kinetic parameters and binding affinity of F3'-1602 for hNKG2D (accelerated stability in the CST formulation)

Test article	Target	k_a ($M^{-1}s^{-1}$)	k_d (s^{-1})	1:1 Kinetic Fit K_D (nM)	Steady State K_D (nM)	Capture level (RU)
F3'-1602 Control	hNKG2D	(2.11±0.06) x10^5	(1.39±0.03) x10^{-1}	661±9	664±10	34.5
F3'-1602 in the CST formulation, 40 °C, 4 wks	hNKG2D	(1.98±0.11) x10^5	(1.40±0.08) x10^{-1}	708±45	711±45	33.2

Results are an average n = 3 measurements

[0770] The binding affinities of F3'-1602 samples to biotinylated recombinant CD16a V158 (FcγRIIIa V158) receptor were measured by SPR as described in the "Stability of F3'-1602 in the HST formulation" subsection. After four weeks of incubation at 20 mg/mL, 40 °C in the CST formulation, binding of F3'-1602 to human CD16a V158 was unaltered (**FIG. 83 and Table 83**). The difference in binding affinity and apparent R_{max} between the control and 40 °C stressed sample are within the experimental variability of the assay. This indicates that F3'-1602 retains affinity for human CD16a under these accelerated storage conditions.

Table 83. Summary of kinetic parameters and affinity of F3'-1602 for hCD16a V158 (accelerated stability in the CST formulation)

Test article	Target	k_a ($M^{-1}s^{-1}$)	k_d (s^{-1})	K_D (nM)	Capture level (RU)
F3'-1602 Control	hCD16aV	(1.13±0.04)x10^5	(2.40±0.09)x10^{-2}	212±1	13.7
F3'-1602, CST, pH 7.0, 40 °C, 4 wks	hCD16aV	(1.05±0.04)x10^5	(2.25±0.09)x10^{-2}	213±3	13.6

Results are an average of n = 3 replicates

[0771] The effect of accelerated stability on F3'-1602 function was also assessed in a cytotoxicity assay using NKG2D- and CD16a-expressing KHYG-1-CD16a cells, as described in the "Stability of F3'-1602 in the HST formulation" subsection. The ability of F3'-1602 to kill PL-21 CLEC12A+ cancer cells was unaltered after 4 weeks incubation at 40 °C in the CST formulation at a concentration of 20 mg/mL (**FIG. 84 and Table 84**).

Table 84. EC50 and maximum lysis of CLEC12A+ PL-21 cells by F3'-1602 (accelerated stability in CST pH 7.0)

Test article	EC50 (nM)	Max. lysis (%)
F3'-1602 Control	0.51	78.6
F3'-1602 in the CST formulation, 40 ºC, 1 wk	0.47	77.7
F3'-1602 in the CST formulation, 40 ºC, 2 wk	0.52	74.7
F3'-1602 in the CST formulation, 40 ºC, 3 wk	0.47	74.9
F3'-1602 in the CST formulation, 40 ºC, 4 wk	0.53	74.9

Example 15. Manufacturability of F3'-1602 in the CST formulation

[0772] Various conditions throughout manufacturing of F3'-1602 could affect its stability. This example was designed to assess the stability of F3'-1602 in the CST formulation through freeze/thaw, agitation, low and high pH, forced oxidation, and low pH hold. The methods of measuring protein integrity and function, where provided in Example 14, are not repeated in this example.

Freeze/thaw

[0773] Stability during freeze/thaw cycles is important for biotherapeutics as process intermediates and bulk drug substance may be frozen to ensure stability between process steps. To create freeze/thaw stress, 8.0 mg F3'-1602 was buffer switched into 20 mM sodium citrate, 250 mM sucrose, 0.01% Tween-80, pH 7.0 using Amicon Ultra 15 ml 30K devices and brought to 400 µL with the same buffer (~20 mg/mL F3'-1602, concentration was confirmed by A280 with a Nanodrop One spectrophotometer). The concentrated sample was divided into 4 x 100 µL aliquots. The control was immediately stored at -80 ºC. The remaining three aliquots were subjected to freeze/thaw cycles at -80 °C in a Styrofoam container to slow the freezing process. At cycles 2, 4, and 6, an aliquot was removed and transferred to -80 ºC storage until analysis.

[0774] The freeze/thaw stability of F3'-1602 was assessed by measuring protein concentration by A280 at the completion of the study. F3'-1602 concentration was 20.4 mg/mL in the control and 20.2 mg/mL after 6 freeze/thaw cycles indicating that there was no loss of protein due to the freeze/thaw stress.

[0775] To assess whether F3'-1602 is stable through the freeze/thaw cycles, test article was frozen and thawed six times and analyzed by SEC after cycles 2, 4, and 6. F3'-1602 at time 0

was 99.5% monomer and the % monomer remained unchanged through all six freeze/thaw cycles (**Table 85**). This result indicates that F3'-1602 was resistant to both aggregation and fragmentation during freeze/thaw stress.

Table 85. Summary of SEC % monomer, HMW, and LMW (freeze/thaw stability)

Test article	Monomer (%)	HMW (%)	LMW (%)
Control	99.5	0.5	ND
2 F/T cycles	99.8	0.2	ND
4 F/T cycles	99.8	0.2	ND
6 F/T cycles	99.8	0.2	ND

ND: none detected

[0776] Fragmentation of intact F3'-1602 was assessed in the freeze/thaw stability study by non-reduced SDS-CE. The F3'-1602 main peak purity decreased minimally (96.1% to 95.5%) after 6 freeze/thaw cycles. There was a corresponding increase in LMWS from 3.9% to 4.5% (**Table 86**). No HMWS was detected throughout the duration of the study. These results indicate that F3'-1602 was resistant to fragmentation in 20 mM citrate, 250 mM sucrose, 0.01% Tween-80, pH 7.0. The difference in migration time of the main peak in the overlay was within the experimental variability of this assay.

Table 86. Summary of non-reduced SDS-CE purity (freeze/thaw stability)

Test article	LMW (%)	Main (%)	HMW (%)
Control	3.9	96.1	ND
2 F/T cycles	4.3	95.7	ND
4 F/T cycles	4.4	95.6	ND
6 F/T cycles	4.5	95.5	ND

ND: none detected

[0777] Fragmentation of the 3 individual polypeptide chains of F3'-1602 was assessed in the freeze/thaw stability study by reduced SDS-CE. In this assay, purity was determined by the sum of the three chains. F3'-1602 purity was unchanged after 6 freeze/thaw cycles (**Table 87**). These results indicate that F3'-1602 was resistant to fragmentation in 20 mM citrate, 250 mM sucrose, 0.01% Tween-80, pH 7.0. The difference in migration times of the main peaks in the overlay was within the experimental variability of this assay.

Table 87. Summary of reduced SDS-CE purity (freeze/thaw stability)

Test article	Purity (%)
Control	98.3
2 F/T cycles	98.0
4 F/T cycles	98.0
6 F/T cycles	98.0

Purity was the sum of chain L, H, and S percent area

Agitation

[0778] Stability during agitation is important for biotherapeutics as process intermediates and bulk drug substance may experience shear stress during processing steps. To create agitation stress, 8.0 mg F3'-1602 was buffer switched into 20 mM sodium citrate, 250 mM sucrose, 0.01% Tween-80, pH 7.0 using Amicon Ultra 15 mL 30K devices and brought to 400 µL with the same buffer (~20 mg/mL F3'-1602, concentration was confirmed by A280 with a Nanodrop One spectrophotometer). The concentrated sample was transferred into glass vial with stir bar, placed on stir plate and stirred at 60 rpm at 4 °C for 18 hours. After the agitation, the sample was stored at -80 °C until analysis.

[0779] The agitation stability of F3'-1602 was assessed. After agitation, there was visible protein precipitation. The sample was spun down, and supernatant was used in all characterization assays. Protein concentration in the supernatant was assessed by A280. F3'-1602 concentration was 20.4 mg/mL in the control and 16.8 mg/mL after agitation stress.

[0780] To determine if F3'-1602 is stable during agitation stress, test article was analyzed by SEC before and after agitation. F3'-1602 control was 99.5% monomer and the % monomer remained unchanged after agitation (**Table 88**). This indicates that F3'-1602 was resistant to both aggregation and fragmentation during agitation.

Table 88. Summary of SEC % monomer, HMW, and LMW (agitation stability)

Test article	HMW (%)	Monomer (%)	LMW (%)
Control	0.5	99.5	ND
Post-agitation	0.7	99.3	ND

ND: none detected

[0781] Fragmentation of intact F3'-1602 was assessed after agitation by non-reduced SDS-CE. The F3'-1602 main peak purity decreased minimally (96.1% to 95.5%) after agitation. There was a corresponding increase in LMWS from 3.9% to 4.5% (**Table 89**). No HMWS was detected throughout the duration of the study. These results indicate that F3'-1602 was resistant to fragmentation in 20 mM citrate, 250 mM sucrose, 0.01% Tween-80, pH 7.0. The difference in migration time of the main peak in the overlay was within the experimental variability of this assay.

Table 89. Summary of SEC % monomer, HMW, and LMW (agitation stability)

Test article	LMW (%)	Main (%)	HMW (%)
Control	3.9	96.1	ND
Post-agitation	3.8	96.2	ND

ND: none detected

[0782] Fragmentation of the three individual polypeptide chains of F3'-1602 was assessed in the agitation study by reduced SDS-CE. In this assay, purity was determined by the sum of the three chains. F3'-1602 purity was unchanged after agitation stress (**Table 90**). These results indicate that F3'-1602 was resistant to fragmentation in 20 mM citrate, 250 mM sucrose, 0.01% Tween-80, pH 7.0. The difference in migration times of the main peaks in the overlay was within the experimental variability of this assay.

Table 90. Summary of reduced SDS-CE purity (agitation stability)

Test article	Purity (%)
Control	98.3
Post-agitation	98.2

Purity was the sum of chains L, H, and S percent area

Low and high pH

[0783] To create low pH stress, 1.0 mg of F3'-1602 was buffer switched into 20 mM sodium acetate, pH 5.0 using Amicon Ultra 0.5 mL 10K devices and brought to 1.0 mL with the same buffer (~1 mg/mL F3'-1602, concentration was confirmed by A280 with a Nanodrop One spectrophotometer). The sample was split. Half was stored at -80 ºC as a control and the other

half was incubated at 40 ºC for 2 weeks. After the incubation, the sample was stored at -80 ºC until analysis.

[0784] To create high pH stress, 1.0 mg of F3'-1602 was buffer switched into 20 mM Tris, pH 8.3 using Amicon Ultra 0.5 mL 10K devices and brought to 1.0 mL with the same buffer (~1 mg/mL F3'-1602, concentration was confirmed by A280 on the Nanodrop One). The sample was split. Half was stored at -80 ºC as a control and the other half was incubated at 40 ºC for 2 weeks. After the incubation, the sample was stored at -80 ºC until analysis. The pKa of Tris will change as a result of temperature. At 40 ºC, the pH 8.3 buffer was ~pH 8.0.

[0785] To assess the chemical stability of F3'-1602, test article was held at pH 5.0 and pH 8.0 for two weeks at 40 °C. At low pH, typical chemical modifications are aspartic acid isomerization and fragmentation, while at high pH, the primary degradation pathways are deamidation and oxidation. To confirm the integrity of F3'-1602 post-incubation, control and stressed samples were analyzed by SEC (**Table 91**). The results indicate that F3'-1602 remained largely intact with low levels of fragmentation as would be expected under these harsh conditions.

Table 91. Summary of SEC % monomer, HMW, and LMW (pH 5 and 8 stress)

Test article	Monomer (%)	HMW (%)	LMW (%)
F3'-1602 pH 5 control	99.8	0.2	ND
F3'-1602 pH 5 stressed	99.4	0.2	0.3
F3'-1602 pH 8 control	99.0	1.0	ND
F3'-1602 pH 8 stressed	95.2	0.9	3.9

ND: none detected

[0786] Chemical modification of amino acid side chains can typically be observed at a global scale with capillary isoelectric focusing (cIEF). To assess the modification of F3'-1602 samples held at low pH and high pH, F3'-1602 was diluted to 1 mg/mL with MilliQ water, 15 µL of sample was added to 60 µL of master mix (water, methyl cellulose, Pharmalyte 3-10, arginine, pI markers 4.05 and 9.99), vortexed, and centrifuged briefly. 60 µL of sample was aspirated from the top of the solution and added to a 96-well plate and centrifuged before testing. During the experiment, the sample was separated for one minute at 1500 volts followed by 8 minutes at 3000 volts on a Maurice (ProteinSimple, San Jose, CA).

[0787] The cIEF profile of F3'-1602 after being held at pH 5.0 for two weeks showed an increase in basic species from 8.9 to 39.1% (**FIG. 85 and Table 92**). A similar increase in acidic

species was detected by cIEF after F3'-1602 was held at pH 8.0. A corresponding decrease in the main peak intensity (from 51.4 to 29.0%) was also observed (**FIG. 86 and Table 92**). Without wishing to be bound by theory, it is possible that deamidation throughout the F3'-1602 sequence lead to this acidic shift.

Table 92. Summary of F3'-1602 % acidic, main, and basic species (pH 5 and 8 stress)

Test article	Acidic (%)	Main (%)	Basic (%)
pH 5.0, control	39.8	51.4	8.9
pH 5.0, 2 wks, 40 °C	32.0	29.0	39.1
pH 8.0, control	39.6	52.2	8.4
pH 8.0, 2 wks, 40 °C	66.7	24.6	8.8

[0788] To determine whether the pH stress induced changes observed by cIEF was due to the modification in the complementarity determining regions (CDRs), the same pH 5 and pH 8 stressed samples were analyzed by LC-MS/MS peptide map. Briefly, 50 µg of F3'-1602 was diluted with 6 M guanidine hydrochloride in 250 mM Tris, pH 8.5, and disulfide bonds were reduced with 25 mM dithiothreitol for 30 minutes at 40 °C in a thermomixer. The reduced cysteines were then alkylated with 50 mM iodoacetamide for 60 minutes at room temperature in the dark. The reduced and alkylated protein was buffer-switched into 50 mM Tris, pH 8.0 and digested with trypsin (1:25 enzyme:substrate) for 1 hour at 37 °C. LC-MS/MS was carried out on a Thermo Vanquish UHPLC coupled to a QExactive+ mass spectrometer. Briefly, 5 µg of protein digest was separated on a Waters UPLC BEH Peptide C18 column (2.1 x 150 mm) over 150 minutes using a 2% to 40% acetonitrile gradient at 0.3 mL/min. Mass spectra were acquired from 230-2000 m/z in positive mode at 35,000 resolution for the full MS scan and 17,500 resolution for the Top10 MS/MS scans. The UPLC-MS/MS files were analyzed using the Byos PTM workflow (Protein Metrics). Peptides were identified using accurate mass and MS/MS searching the F3'-1602 sequence.

[0789] Based on the peptide map data, all but one of the CDRs in F3'-1602 were resistant to modification during low and high pH stress. Only CDRH3 of the CLEC12A-binding scFv-Fc chain showed evidence of modification (isomerization) after the pH 5 stress (**Table 93**). This modification is the same one identified in the accelerated (40 °C) stability study.

Table 93. Post-translational modifications in F3'-1602 CDRs (pH 5.0 and pH 8.0)

				Relative abundance (%)			
				pH 5		pH 8	
Target	CDR	Sequence (Chothia)	Potential liability	control	stressed	control	stressed
CLEC 12A	H1	GFSLTNY (SEQ ID NO:137)	None	NA	NA	NA	NA
	H2	WSGGK (SEQ ID NO:138)	None	NA	NA	NA	NA
	H3	YDYDDSLDY (SEQ ID NO:139)	Isomerization	ND	Observed	ND	ND
	L1	HASQNINFWLS (SEQ ID NO:140)	None	NA	NA	NA	NA
	L2	EASNLHT (SEQ ID NO:141)	None	NA	NA	NA	NA
	L3	QQSHSYPLT (SEQ ID NO:142)	None	NA	NA	NA	NA
NKG2D	H1	GFTFSSY (SEQ ID NO:297)	None	NA	NA	NA	NA
	H2	SSSSSY (SEQ ID NO:298)	None	NA	NA	NA	NA
	H3	GAPIGAAAGW FDP (SEQ ID NO:97)	Truncation	ND	ND	ND	ND
	L1	RASQGISSWLA (SEQ ID NO:86)	None	NA	NA	NA	NA
	L2	AASSLQS (SEQ ID NO:77)	None	NA	NA	NA	NA
	L3	QQGVSFPRT (SEQ ID NO:87)	None	NA	NA	NA	NA

ND: none detected; NA: not applicable

[0790] The binding affinities of F3'-1602 samples to recombinant human CLEC12A were measured by SPR as described in Example 14. After two weeks of incubation at 40 ºC in 20 mM sodium acetate, pH 5.0, binding of F3'-1602 to human CLEC12A was decreased (**FIG. 87 and Table 94**). The difference in association and dissociation rate constants between the control and low pH 40 ºC stressed sample were within the experimental variability of the assay, however, apparent maximal binding response of the stressed sample was about half of the control after pH 5 stress. This indicates that F3'-1602 had a reduced ability to bind CLEC12A under these conditions. After two weeks of incubation at 40 ºC in 20 mM Tris, pH 8.0, binding of F3'-1602 to human CLEC12A was unaltered (**FIG. 88 and Table 94**). This indicates that F3'-1602 retained affinity for CLEC12A under these accelerated pH stress conditions.

Table 94. Summary of kinetic parameters and binding affinity of F3'-1602 for hCLEC12A (pH 5.0 and pH 8.0 stress)

Test article	Target	k_a ($M^{-1}s^{-1}$)	k_d (s^{-1})	K_D (nM)	Capture level (RU)
F3'-1602 Control	hCLEC12A	$7.99x10^5$	$8.53x10^{-4}$	1.07	76.2
F3'-1602, pH 5.0, 40 °C, 2 wks	hCLEC12A	$8.65x10^5$	$8.71x10^{-4}$	1.01	87.4
F3'-1602 Control	hCLEC12A	8.01x105	8.40x10-4	1.1	86.9
F3'-1602, pH 8.0, 40 °C, 2 wks	hCLEC12A	8.35x105	8.45x10-4	1.0	82.8

Results are an average of n = 2 replicates

[0791] The binding affinities of F3'-1602 samples to recombinant human NKG2D were measured by SPR as described in Example 14. After two weeks of incubation at 40 °C in 20 mM sodium acetate, pH 5.0, binding of F3'-1602 to human NKG2D was unaltered (**FIG. 89 and Table 95**). This indicates that F3'-1602 retained affinity for NKG2D under these accelerated pH stress conditions. After two weeks of incubation at 40 °C in 20 mM tris, pH 8.0, binding of F3'-1602 to human NKG2D was unaltered (**FIG. 90 and Table 95**). This indicates that F3'-1602 retained affinity for NKG2D under these accelerated pH stress conditions.

Table 95. Summary of kinetic parameters and binding affinity of F3'-1602 for hNKG2D (pH 5.0 and pH 8.0 stress)

Test article	Target	k_a ($M^{-1}s^{-1}$)	k_d (s^{-1})	1:1 Kinetic Fit K_D (nM)	Steady state K_D (nM)	Capture level (RU)
F3'-1602 Control	hNKG2D	$1.89x10^5$	$1.28x10^{-1}$	678	684	51.9
F3'-1602, pH 5.0, 40 °C, 2 wks	hNKG2D	$1.88x10^5$	$1.27x10^{-1}$	675	677	46.2
F3'-1602 Control	hNKG2D	$1.80x10^5$	$1.25x10^{-1}$	694	695	47.2
F3'-1602, pH 8.0, 40 °C, 2 wks	hNKG2D	$1.35x10^5$	$1.22x10^{-1}$	905	919	51.0

[0792] The effect of low and high pH stress on F3'-1602 function was assessed in a cytotoxicity assay using NKG2D- and CD16a-expressing KHYG-1-CD16a cells as described in Example 14. After pH 5.0 and 8.0 stress, F3'-1602 potency against PL-21 CLEC12A+ cancer cells reflected by EC50 and maximum lysis was reduced ~2-fold after pH 5 stress (**FIG. 91 and Table 96**) and was unchanged after pH 8 stress (**FIG. 92 and Table 96**). Without wishing to be

bound by theory, it is possible that the loss of potency after pH 5 stress was due to the same isomerization of the scFv CDR-H3 aspartic acid identified in the initial accelerated stability study. The differences in the pH 5 and pH 8 results further demonstrates that F3'-1602 was more stable at elevated pH.

Table 96. EC50 and maximum lysis of CLEC12A+ PL-21 cells by F3'-1602 (pH 5.0 and pH 8.0 stress)

Test article	EC50 (nM)	Maximum Lysis (%)
F3'-1602 Control	0.18	91%
F3'-1602 pH 5.0, 2 wks, 40 °C	0.34	93%
F3'-1602Control	0.19	95%
F3'-1602 pH 8.0, 2 wks, 40 °C	0.24	90%

Forced oxidation

[0793] One of the most common stability indicating modifications of proteins is oxidation of methionine residues. To identify oxidation hot spots, 1.0 mg of F3'-1602 was diluted to 1 mg/mL with phosphate buffered saline (PBS). 3.3 µL of 3% hydrogen peroxide was added to a 0.5 mL aliquot of F3'-1602 (0.02% hydrogen peroxide). Oxidation of F3'-1602 proceeded for 24 hours at room temperature in the dark. After 24 hours, the sample was buffer switched into PBS, pH 7.4 using Amicon Ultra 0.5 mL 10K MWCO devices following the manufacturer's instructions. The un-oxidized control (0.5 mL) was stored at -80 °C.

[0794] After forced oxidation, there were no significant differences in F3'-1602 % monomer, HMWS or LMWS (**Table 97**).

Table 97. Summary of SEC % monomer, HMW, and LMW (forced oxidation)

Test article	Monomer (%)	HMW (%)	LMW (%)
F3'-1602 Control	99.9	0.1	ND
F3'-1602 0.02% H_2O_2, 24 hrs	99.9	0.1	ND

ND: none detected

[0795] After forced oxidation, the purity of F3'-1602 by non-reduced SDS-CE was decreased by less than 1% (**Table 98**). This indicates that F3'-1602 was resistant to fragmentation during forced oxidation. There were no new fragments detected after forced oxidation. The peak shape of the oxidized sample changed after the oxidative stress. Without wishing to be bound by theory, this may indicate that there was no longer a homogeneous

population and that the high levels of oxidation resulted in a conformational change not present in the control sample of F3'-1602. The difference in migration times of the main peaks in the overlay was within the experimental variability of this assay.

Table 98. Summary of non-reduced SDS-CE purity (forced oxidation)

Test article	LMW (%)	Main (%)	HMW (%)
F3'-1602, Control	3.9	96.1	ND
F3'-1602, 0.02% H_2O_2, 24 hrs	4.7	95.2	ND

ND: none detected

[0796] After forced oxidation, the purity of F3'-1602 by reduced SDS-CE was unchanged (**Table 99**). This indicates that F3'-1602 was resistant to fragmentation during forced oxidation. There were no new fragments detected after forced oxidation. The difference in migration times of the main peaks in the overlay was within the experimental variability of this assay.

Table 99. Summary of reduced SDS-CE purity (forced oxidation)

Test article	Chain L (%)	Chain H(%)	Chain S (%)	Purity (%)
F3'-1602, Control	17.7	40.1	40.5	98.3
F3'-1602, 0.02% H_2O_2, 24 hrs	17.8	40.0	40.4	98.2

[0797] In addition to determining the biophysical effects of forced oxidation by SEC, it is important to understand which amino acids are most susceptible to oxidation. There are no methionine residues in the F3'-1602 CDRs, however, several methionines are found in the framework and constant domains. Levels of oxidation were low at all sites in the control and only two sites showed significant increases in oxidation after exposure to hydrogen peroxide (**Table 100**). Low levels of oxidation have been observed in other therapeutic mAbs.

Table 100. Summary of site-specific percent oxidation in F3'-1602 (forced oxidation)

Peptide Sequence	SEQ ID NO	Chain	Position	Relative abundance (%)	
				Control	Oxidized
LSCAASGFTFSSYSMNWVR	299	H	34	0.6	0.8
NSLYLQMNSLR	300	H	83	0.2	0.3
DTLMISR	301	H/S*	257/283	2.3	71.3

Peptide Sequence	SEQ ID NO	Chain	Position	Relative abundance (%)	
				Control	Oxidized
WQQGNVFSCSVMHEALHNHYTQK	302	H/S*	433/454	1.5	47.4
DIQMTQSPSSVSASVGDR	303	L	4	0.3	0.4
YDYDDSLDYWGQGTLVTVSSGGGGSGGGGSGGGGSGGGGSDIQMTQSPSSLSASVGDRVTITCHASQNINFWLSWYQQKPGKAPK	304	S	141	ND	ND

* peptide is found in chain H and S; ND, none detected

[0798] The binding affinities of forced oxidation stressed F3'-1602 samples to recombinant human CLEC12A were measured by SPR as described in Example 14. After 24 hours of incubation at room temperature in presence of 0.02% hydrogen peroxide, kinetics and affinity of binding of F3'-1602 to human CLEC12A as well as apparent R_{max} was unaltered (**FIG. 93 and Table 101**). This indicates that F3'-1602 retained binding to CLEC12A after forced oxidation and modifications of methionines in the constant regions and framework did not affect the affinity of the F3'-1602 for hCLEC12A.

Table 101. Summary of kinetic parameters and binding affinity of F3'-1602 for hCLEC12A (forced oxidation)

Test article	Target	k_a ($M^{-1}s^{-1}$)	k_d (s^{-1})	K_D (nM)	Capture level (RU)
F3'-1602 Control	hCLEC12A	$7.99x10^5$	$8.58x10^{-4}$	1.1	78.6
F3'-1602 Forced Oxidized	hCLEC12A	$8.06x10^5$	$8.70x10^{-4}$	1.1	76.8

Results are an average of n = 2 replicates

[0799] The binding affinities of forced oxidation stressed F3'-1602 samples to recombinant human NKG2D were measured by SPR as described in Example 14. After 24 hours of incubation at room temperature in presence of 0.02% hydrogen peroxide, kinetics and affinity of binding of F3'-1602 to human NKG2D was unaltered (**FIG. 94 and Table 102**). This indicates that F3'-1602 retains binding to NKG2D after forced oxidation and modifications of methionines in the constant regions and framework do not affect the affinity of the F3'-1602 for hNKG2D.

Table 102. Summary of kinetic parameters and binding affinity of F3'-1602 for hNKG2D (forced oxidation)

Test article	Target	k_a ($M^{-1}s^{-1}$)	k_d (s^{-1})	1:1 Kinetic Fit K_D (nM)	Steady state K_D (nM)	Capture level (RU)
F3'-1602 Control	hNKG2D	(1.43±0.03) x10^5	(1.07±0.04) x10^{-1}	750±23	759±23	44.1
F3'-1602, 0.02% H_2O_2, 24 hrs	hNKG2D	(1.48±0.06) x10^5	(1.07±0.04) x10^{-1}	722±6	732±7	48.2

[0800] The effect of forced oxidation stress on F3'-1602 function was assessed in a cytotoxicity assay using NKG2D- and CD16a-expressing KHYG-1-CD16a cells as described in Example 14. As shown in **FIG. 95 and Table 103**, after oxidative stress, F3'-1602 potency (EC50 and maximum lysis) was unchanged.

Table 103. EC50 and maximum lysis of CLEC12A+ PL-21 cells by F3'-1602 (forced oxidation)

Test article	EC50 (nM)	Maximum Lysis (%)
F3'-1602 Control	0.26	60%
F3'-1602 0.02% H_2O_2, 24 hrs	0.28	63%

Low pH hold

[0801] Viral inactivation by low pH hold is an important step in biologics manufacturing. To assess the stability of F3'-1602 at low pH hold, F3'-1602 was captured on a MabSelect Sure Protein A column and eluted with 100 mM glycine, pH 3.0. Peak fractions were pooled, and the 12 mL of the protein A eluate was pH was adjusted to pH 3.3 with additional 100 mM glycine pH 3.0 buffer. The pH-adjusted eluate was held at room temperature. After 1.5 hours, the eluate was brought to neutral pH with 1.0 M Tris-HCl, pH 8.3. The pH-hold sample was further purified by cation exchange chromatography. The final product was buffer exchanged to PBS pH 7.4 for analysis.

[0802] After incubation at low pH, F3'-1602 was analyzed by SEC to determine if the hold caused aggregation. There was no increase in HMW and LMW content in F3'-1602 due to the low pH hold step (**Table 104**).

Table 104. Summary of SEC % monomer, HMW, and LMW (low pH hold)

Test article	Monomer (%)	HMW (%)	LMW (%)
F3'-1602 Control, ProA eluate	77.4	11.5	11.1
F3'-1602 low pH hold, ProA eluate	86.4	3.4	10.2

[0803] After low pH hold, the purity of F3'-1602 by non-reduced SDS-CE was unchanged (**Table 105**). This indicates that F3'-1602 was resistant to fragmentation during low pH hold. There were no new fragments detected after the low pH hold. The difference in migration times of the main peaks in the overlay was within the experimental variability of this assay.

Table 105. Summary of non-reduced SDS-CE purity (low pH hold)

Test article	LMW (%)	Main (%)	HMW (%)
F3' -1602 Control	1.3	98.7	ND
F3' -1602 low pH hold	1.1	98.9	ND

ND, none detected

[0804] After low pH hold, the purity of F3'-1602 by reduced SDS-CE was unchanged (**Table 106**). This indicates that F3'-1602 was resistant to fragmentation during low pH hold. There were no new fragments detected after the low pH hold.

Table 106. Summary of reduced SDS-CE purity (low pH hold)

Test article	Light chain (%)	Heavy chain (%)	scFv-Fc chain (%)	Purity (%)
F3'-1602 Control	18.1	39.9	40.4	98.4
F3'-1602 low pH hold	17.6	39.7	41.1	98.4

[0805] Chemical modification of amino acid side chains can typically be observed at a global scale with cIEF. The cIEF profiles of F3'-1602 control and low pH hold lot were visually very similar and the relative quantitation of acid, main, and basic species are all within 1% of each other, indicating that the low pH hold did not have a measurable effect on the charge profile of F3'-1602 (**Table 107**).

Table 107. Summary of F3'-1602 % acidic, main, and basic species (low pH hold)

Test article	pI	Acidic species (%)	Main species (%)	Basic species (%)
F3'-1602 control	8.75	42.4	48.5	9.1
F3'-1602, low pH hold	8.80	42.7	49.1	8.2

[0806] F3'-1602 samples were analyzed by intact mass to monitor modification and fragmentation as a result of the low pH hold. The observed mass for both the control and low pH hold sample matched each other and the theoretical F3'-1602 mass (G0F/G0F glycoform: 126,360.4 Da). Low pH hold did not affect the mass of F3'-1602 (**Table 108**) and fragmentation was not observed.

Table 108. F3'-1602 theoretical and observed masses (low pH hold)

Test article	Theor. Mass (Da)	Obs. Mass (Da)	Delta mass (Da)	Mass accuracy (ppm)
F3'-1602 control	126,360.4	126,360.8	+0.4	3.2
F3'-1602 low pH hold	126,360.4	126,360.7	+0.3	2.4

[0807] Low pH hold did not induce any change in kinetics or affinity of F3'-1602 binding to human CLEC12A (**FIG. 96 and Table 109**). The difference in association and dissociation rate constants as well as apparent maximal binding response (Rmax) between the control and low pH hold sample were within the experimental variability of the assay. This indicates that F3'-1602 retained affinity for CLEC12A after a low pH hold step of biotherapeutic manufacturing.

Table 109. Summary of kinetic parameters and binding affinity of F3'-1602 for hCLEC12A (low pH hold)

Test article	Target	k_a ($M^{-1}s^{-1}$)	k_d (s^{-1})	K_D (nM)	Capture level (RU)
F3'-1602 Control	hCLEC12A	$(6.78\pm0.13)\times10^{5}$	$(4.33\pm0.20)\times10^{-4}$	0.638±0.028	176±19
F3'-1602 Low pH hold	hCLEC12A	$(7.15\pm0.10)\times10^{5}$	$(4.61\pm0.03)\times10^{-4}$	0.644±0.008	157±7

Results are an average of n = 4 replicates

[0808] After low pH hold, human NKG2D binding was unaltered (**FIG. 97 and Table 110**). The differences in steady state affinity and apparent maximal binding response affinity between the control and 40 ºC stressed sample were within the experimental variability of the assay. This indicates that F3'-1602 retained affinity for human NKG2D after low pH hold.

Table 110. Summary of kinetic parameters and binding affinity of F3'-1602 for hNKG2D (low pH hold)

Test article	Target	k_a ($M^{-1}s^{-1}$)	k_d (s^{-1})	1:1 Kinetic Fit K_D (nM)	Steady state K_D (nM)	Capture level (RU)
F3'-1602 Control	hNKG2D	(2.06±0.09) x10^5	(1.46±0.08) x10^{-1}	714±62	710±63	34.0
F3'-1602, low pH hold	hNKG2D	(2.07±0.08) x10^5	(1.39±0.02) x10^{-1}	671±20	672±18	33.7

Results are an average of n = 3 measurements

[0809] After low pH hold, binding of F3'-1602 to human CD16a V158 was unaltered (**FIG. 98 and Table 111**). The difference in binding affinity and maximal binding response between the control and low pH hold sample were within the experimental variability of the assay. This indicates that F3'-1602 retained affinity for human CD16a under these accelerated storage conditions.

Table 111. Summary of kinetic parameters and affinity of F3'-1602 for hCD16a V158 (low pH hold)

Test article	Target	k_a ($M^{-1}s^{-1}$)	k_d (s^{-1})	K_D (nM)	Capture level (RU)
F3'-1602 Control	hCD16aV	(1.13±0.04) x10^5	(2.40±0.09) x10^{-2}	212±1	13.7
F3'-1602, low pH hold	hCD16aV	(1.09±0.04) x10^5	(2.29±0.04) x10^{-2}	210±3	14.1

Results are an average of n = 3 replicates

[0810] In addition to compromising biophysical stability and integrity, low pH could cause chemical degradation of amino acid side chains, in particular, aspartic acid isomerization. Chemical degradation of F3'-1602 in regions that are critical for function, if any, should manifest as reduced efficacy in a potency assay. Therefore, the potency of F3'-1602 against $CLEC12A^+$ PL-21 cancer cells were tested after low pH hold in the KHYG1-CD16V bioassay. The potency of F3'-1602 was unaltered by the low pH hold (**FIG. 99 and Table 112**).

Table 112. EC50 and maximum lysis of CLEC12A+ PL-21 cells by F3'-1602 (low pH hold)

Test article	EC50 (nM)	Maximum Lysis (%)
F3'-1602 Control	0.27	61
F3'-1602 Low pH hold	0.15	54

Colloidal stability

[0811] PEG precipitation was used to assess the colloidal stability of F3'-1602. Briefly, concentrated F3'-1602 (~20 mg/mL) was diluted to 1 mg/mL in 100 µL aliquots (10 mM sodium acetate, pH 5.0) with final concentrations of PEG 6000 ranging from 0 to 30% (w/v). The aliquots were thoroughly mixed and placed at 2-8 ºC overnight. The following day, the tubes were centrifuged to pellet any precipitation and the concentration of the supernatant was measured by A280 on a Lunatic (Unchained Labs).

[0812] The solubility of F3'-1602 in acetate buffer pH 5.0 with increasing concentration of PEG 6000 (0% - 30%) was monitored by A280. The midpoint transition (Cm) in 10 mM sodium acetate, pH 5.0 was 24.5%, indicating that F3'-1602 has high solubility in this buffer (**FIG. 100**). As comparators, trastuzumab and adalimumab were also assessed in the PEG precipitation assay in 10 mM sodium acetate, pH 5.0. The midpoint transitions of trastuzumab and adalimumab, used as assay controls, were >30% and 11.7% PEG-6000, respectively.

[0813] F3'-1602 was then concentrated using 30 kDa molecular weight cutoff devices in PBS, pH 7.4. Concentration was determined by A280 on a Nanodrop and product quality was monitored by SEC. Test material was injected onto an Agilent 1260 Infinity II high pressure liquid chromatography instrument with 1260 Quat Pump, 1260 Vialsampler, 1260 VWD. The sample was separated on a Superdex200 Increase 10/300 GL column. SEC running buffer was PBS, pH 7.4, flowing at 0.60 mL/min. Absorbance was monitored at both 214 and 280 nm, peak areas were manually integrated and the percent of HMWS, LMWS, and monomer were reported.

[0814] F3'-1602 was concentrated to approximately 25, 50, 100, and 150 mg/mL in PBS, pH 7.4 and recovery was monitored by visual inspection, concentration (A280), and SEC. F3'-1602 was able to be concentrated to >150 mg/mL in PBS, pH 7.4 with minimal loss in percent monomer and no visible precipitation (**FIG. 101 and Table 113**).

Table 113. F3'-1602 HMWS, Monomer, and LMWS content as a function of concentration

Concentration (mg/mL)	HMWS (%)	Monomer (%)	LMWS (%)
4.1	ND	98.3	1.7
26.0	0.1	97.7	2.3
58.4	0.1	97.7	2.2
89.2	0.2	97.0	2.9
158.8	0.2	96.6	3.2

Example 16. Stability and manufacturability of F3'-1602 and AB0010

[0815] F3'-1602 and AB0010 are TriNKETs in the F3' and F3 formats, respectively, that have CLEC12A-binding sites derived from the same humanized anti-CLEC12A antibody. As described in Example 5 or 6, these two TriNKETs have similar binding affinity to CLEC12A. This example was designed to compare the stability and manufacturability of F3'-1602 and AB0010.

[0816] Briefly, F3'-1602 and AB0010 were formulated in 20 mM sodium phosphate, 10 mM sodium citrate, 125 mM NaCl, and 0.01% PS-80, at pH 7.8, as described in Example 14. The formulated proteins were subject to thermal stress at 40 °C for four weeks and their stabilities were assessed by the non-reduced SDS-CE, reduced SDS-CE, SEC, and cytotoxicity assays, as described in Example 14.

[0817] Data presented in Table 114 shows that the LMW fraction of the stressed AB0010 sample increased significantly more than that of the stressed F3'-1602 sample. Data presented in Table 115 shows that the purity of the stressed AB0010 sample decreased significantly more than that of the stressed F3'-1602 sample. These results indicate that AB0010 degraded significantly more than F3'-1602 under the thermal stress condition.

Table 114. Summary of non-reduced SDS-CE purity of F3'-1602 and AB0010

Test article	LMW (%)	Main (%)	HMW (%)
F3'-1602 Control	3.0	97.0	ND
F3'-1602 40°C 4 wks	8.4	91.2	0.4
AB0010 Control	8.4	90.4	1.2
AB0010 40°C 4 wks	27.8	71.4	0.9

ND, none detected

Table 115. Summary of reduced SDS-CE purity of F3'-1602 and AB0010

Test article	Purity (%)
F3'-1602 Control	97.4
F3'-1602 40°C 4 wks	95.2
AB0010 Control	95.0
AB0010 40°C 4 wks	89.3

[0818] As shown in Table 116, the amount of HMWS in the stressed AB0010 sample increased significantly more than that of the stressed F3'-1602 sample. This result suggests that AB0010 aggregated significantly more than F3'-1602 under the thermal stress conditions.

Table 116. Summary of SEC % monomer, HMW, and LMW of F3'-1602 and AB0010

Test article	HMWS (%)	Monomer (%)	LMWS (%)
F3'-1602 Control	0.3	97.9	1.8
F3'-1602 40°C 4 wks	3.6	91.4	5.0
AB0010 Control	0.8	99.2	0.1
AB0010 40°C 4 wks	13.8	81.7	4.5

[0819] As described in Example 14, sucrose is more compatible with a lyophilized presentation than NaCl. Therefore, F3'-1602 and AB0010 were also formulated in 20 mM sodium phosphate, 10 mM sodium citrate, 250 mM sucrose, and 0.01% polysorbate 80, at pH 7.8. The TriNKET proteins in each formulation were then subject to thermal stress at 40 °C for four weeks, and their ability to mediate NK cell-mediated cytotoxicity were assessed by the cytotoxicity assay as described in Example 14. As shown in FIGs. 102A and 102B and Table 117, the ability of F3'-1602 and AB0010 to mediate killing of PL21 CLEC12A^{+} cancer cells by NKG2D- and CD16a-expressing KHYG-1-CD16a cells was not significantly affected by the thermal stress.

Table 117. EC50 and maximum lysis of CLEC12A+ PL21 cells by F3'-1602 or AB0010

Test article	EC50 (nM)	Max. lysis (%)
F3'-1602 Control	0.26	90
F3'-1602 40 °C, 4 wks in 20 mM sodium phosphate, 10 mM sodium citrate, 250 mM sucrose, and 0.01% polysorbate 80, at pH 7.8	0.34	93

F3'-1602 40 °C, 4 wks in 20 mM sodium phosphate, 10 mM sodium citrate, 125 mM NaCl, and 0.01% polysorbate 80, at pH 7.8	0.29	93
AB0010 Control	0.57	74
AB0010 40 °C, 4 wks in 20 mM sodium phosphate, 10 mM sodium citrate, 250 mM sucrose, and 0.01% polysorbate 80, at pH 7.8	0.75	74
AB0010 40 °C, 4 wks in 20 mM sodium phosphate, 10 mM sodium citrate, 125 mM NaCl, and 0.01% polysorbate 80, at pH 7.8	0.58	78

Example 17. Molecular Format, Design, Structure, and Characteristics of CLEC12A TriNKET AB0089

Objective

[0820] The objectives of this study are to describe the molecular format, design, structure, and characteristics of CLEC12A TriNKET AB0089. AB0089 is an improved version of AB0237, in which the primary sequence of the CLEC12A binding VH was optimized to remove the isomerization sequence liability while retaining affinity for CLEC12A and potency in cytotoxic lysis of CLEC12A+ AML cells. In addition, we aimed at reduction of the number of murine backmutations in the framework regions which increased humanness of the molecule. In particular, in this report we a) describe molecular format and design of AB0089; b) outline protein engineering efforts to remove sequence liability in CDRH3; c) describe protein engineering efforts to reduce number of murine backmutations; d) provide information about expression and purification of AB0089; e) describe basic biochemical and biophysical characterization of the molecule; f) determine the affinity of AB0089 for recombinant human targets (CLEC12A, NKG2D and CD16a); g) demonstrate AB0089 binding to AML cancer cell lines expressing human CLEC12A; h) demonstrate selectivity of AB0089; i) determine potency of AB0089 in killing AML cancer cells; j) assess binding epitope; k) assess binding to FcγR and FcR and compare with IgG1 mAb control; and l) describe behavior of AB0089 in developability studies including accelerated stability, forced degradation, and manufacturability.

Study Design

[0821] During the developability assessment of CLEC12A specific AB0237 TriNKET, an isomerization liability in the CDRH3 was identified, which led to a reduction in binding to CLEC12A and potency under harsh stresses.Yeast display was used to remove the sequence

liability and optimize CMC properties of the molecule. In addition, the framework of the molecule was further optimized to remove murine backmutations and replace them with the corresponding human residues, thus improving the humanness of the molecule. Properties of AB0089 were assessed by binding to recombinant hCLEC12A, binding to isogenic and cancer cells expressing CLEC12A as well as potency of the molecule against CLEC12A+ AML cancer cells. The biophysical and biochemical characteristics of AB0089 including thermal stability (DSC), hydrophobicity (HIC), and pI (cIEF) were determined. Molecular modeling was used to assess charge and hydrophobic patch distribution on the surface of AB0089 and to benchmark with clinical stage monoclonal antibodies. Specificity of binding was assessed by PSR, binding to cells not expressing the target of interest, and by HuProt™ Array. AB0089 was expressed in two different mammalian cell lines (Expi293 and ExpiCHO) and purified using Dragonfly Tx 2-step platform purification method. The binding properties of AB0089, including CLEC12A, NKG2D, CD16a (V158 and F158), an extended panel of Fcγ receptors (CD32a (H131 and R131), CD16b, CD32b, cynomolgus CD16, human and cynomolgus CD64), and FcRn (human and cynomolgus) were fully characterized. Lastly, AB0089 was assessed in a full developability panel of assays, including accelerated (40°C) stability in a platform formulation (20 mM histidine, 250 mM sucrose, 0.01% Tween-80, pH 6.0) and 20 mM citrate, 250 mM sucrose, 0.01% Tween-80, pH 7.0 buffers, forced degradation (long term pH 5, pH 8 stress, forced oxidation), and manufacturability (freeze/thaw, agitation, low pH hold).

Materials and Methods

Materials

Test Articles

Table 118: Summary of test articles.

Name	Lot	Expression host
AB0237	AB0237-002; 06Sep19AB	ExpiCHO
AB0089	AB0089-001	Expi293
AB0089	AB0089-002 (developability)	ExpiCHO
AB0089	AB0089-003 (low pH hold)	ExpiCHO
AB0089	AB0089-004 (low pH hold)	ExpiCHO

Name	Lot	Expression host
AB0192	AB0192-005	ExpiCHO

Protein reagents

Table 119: Summary of protein reagents.

Name	Manufacturer	Lot
Human CLEC12A-His	Dragonfly Tx	16Oct18GL
Human CLEC12A-K244Q-His	Dragonfly Tx	30Apr18AC
Cyno CLEC12A-His	Dragonfly Tx	30May18AC
Biotinylated CLEC12A-His	Dragonfly Tx	17Apr19GL
mFc-hNKG2D	Dragonfly Tx	01Dec17AB
mFc-cNKG2D	Dragonfly Tx	28Sep18GL
humanized mAb 16B8.C8	Dragonfly Tx	AB0037-001
hcFAE-A49.CLL1-Merus (duobody TriNKET)	Dragonfly Tx	10May18DF
hcFAE-A49.h6E7 (duobody TriNKET)	Dragonfly Tx	05Feb19DF
hcFAE-A49.tepoditamab (duobody TriNKET)	Dragonfly Tx	27Aug19XL
Trastuzumab	Roche	N3017H05
Adalimumab	AbbVie	83364XH07
Rituximab	Dragonfly Tx	19Apr19 MH

Table 120: Summary of recombinant Fc receptor proteins.

Reagent	Vendor	Catalog Number
Human CD64	ACRO Biosystems	FCA-H82E8
Cynomolgus CD64	ACRO Biosystems	FCA-C82E8
Human CD32a H131	ACRO Biosystems	CDA-H82E6
Human CD32a R131	ACRO Biosystems	CDA-H82E7
Human CD32b	ACRO Biosystems	CDB-H82E0
Human CD16a V158	Sino Biologicals	10389-H27H1-B

Reagent	Vendor	Catalog Number
Human CD16a F158	Sino Biologicals	10389-H27H-B
Human CD16b	ACRO Biosystems	CDB-H82E4
Cynomolgus CD16	ACRO Biosystems	FC6-C82E0
Human FcRn	ACRO Biosystems	FCM-H5286
Cynomolgus FcRn	ACRO Biosystems	FCM-C5284

Methods

Cell binding by flow cytometry

[0822] Binding of AB0089 to isogenic CLEC12A expressing cells and to PL-21 cancer cells was performed as described in detail in Example 19. The EC50 values were derived from the cell binding curves using GraphPad Prism software (four parameter logistic non-linear regression curve fitting model).

Yeast library construction and evaluation

[0823] A walking mutagenesis strategy was employed using a synthetic CDRH3 oligonucleotide pool to construct a yeast display affinity library (referred to as Library 17) where each residue of the AB0237 CDRH3 (YDYDDSLDY, SEQ ID NO:139) was substituted with a randomization of all 20 amino acids, as a single site or in pairs (FIG. 103).

[0824] First, a synthetic scFv double stranded DNA was designed by replacing the CDRH3 with a unique BamH1 restriction site. Then, the scFv was cloned into the yeast display plasmid (pYES-Aga2 vector) by Hifi cloning method, resulting in pYES-Aga2-scFv-BamH1 plasmid. DNA oligos with regions homologous to the vector were designed with the following randomizations introduced in the original CDRH3 (YDYDDSLDY, SEQ ID NO:139) to XDYDDSLDY (SEQ ID NO:305), YXYDDSLDY (SEQ ID NO:306), YDXDDSLDY (SEQ ID NO:307), YDYXDSLDY (SEQ ID NO:308), YDYDXSLDY (SEQ ID NO:309), YDYDDXLDY (SEQ ID NO:310), YDYDDSXDY (SEQ ID NO:311), YDYDDSLXY (SEQ ID NO:312), YDYDDSLDX (SEQ ID NO:313), XXYDDSLDY (SEQ ID NO:314), XDXDDSLDY (SEQ ID NO:315), XDYXDSLDY (SEQ ID NO:316), XDYDXSLDY (SEQ ID NO:317), XDYDDXLDY (SEQ ID NO:318), XDYDDSXDY (SEQ ID NO:319), XDYDDSLXY (SEQ ID NO:320), XDYDDSLDX (SEQ ID NO:321), where X = any amino acid) and pooled

together. pYES-Aga2-scFv-BamHI vector was then digested with BamHI and this digested plasmid was electroporated with DNA oligo pools to yield the finalized yeast display Library 17. Through the process of homologous recombination, the yeast internally ligates the library oligos with the linearized plasmid, resulting in each yeast cell containing one plasmid with one CDRH3 mutated oligo. Following selection and characterization of Library 17 outputs, a similar affinity maturation strategy was employed targeting CDRH2 for walking mutagenesis in the background of a single optimized CDRH3. The library for this second round of affinity maturation is herein referred to as Library 30.

[0825] The library was assessed by FACS sorting after growing in D-UT media. 24 hours prior to sorting, the yeast were re-seeded to a final concentration of 0.5 O.D./ml (as measured by a visible light spectrophotometer), spun down, washed twice in GR-UT media, and then left to incubate overnight in the same media. On the day of the experiment, 3 O.D. of cells were taken be tested and placed in the well of a 96-well U-bottom plate. This was repeated up to the number of antigens desired to be tested. The cells were then washed twice with PBS-F (PBS+0.25% BSA), and then various concentrations of biotinylated CLEC12A-His were incubated for 30 min. Yeast cells were then stained with FITC labeled anti-Flag and streptavidin PE and sorted using the BD FACSAria for the highest affinity binders.

[0826] The final yeast libraries were analyzed by flow cytometry. The yeast library was initially seeded in D-UT media 24 hours prior to characterization. 24 hours prior to flow cytometry, the yeast were reseeded to a final concentration of 0.5 O.D./ml, spun down, washed twice in GR-UT media, and then left to incubate overnight in the same media. On the day of the experiment, 0.2 O.D. of cells were taken per antigen to be tested and placed in each well of a 96-well U-bottom plate. The cells were washed in PBS-F (PBS+0.25% BSA), and then biotinylated CLEC12A-His was added to a final concentration of 10 nM for 30 mins. The cells were washed again and non-biotinylated CLEC12A-His (final concentration 1μM) was added for an additional 40 mins, with samples being pulled out every 20 minutes. Anti-Flag-FITC and streptavidin PE were added and incubated for 30mins in the dark, on ice, washed twice, resuspended in PBS-F, and analyzed using the FACS Celesta.

Site-directed mutagenesis

[0827] The gBlock (double stranded DNA fragment) with DS to DT mutation encoding AB0089 scFv targeting CLEC12A arm was ordered from Integrated DNA Technologies (Coralville, IA). It was cloned into pcDNA3.4 vector following the protocol as described in below.

Codon optimization

[0828] DNA codon optimization of the scFv portion of AB0089 Chain S was performed via Codon Optimization Tool from Integrated DNA Technologies (Coralville, IA), while the linker and Fc portion was codon optimized (as part of the vector backbone) using the Codon Optimization Tool from GeneArt Gene Synthesis (Thermo Fisher Scientific, Waltham, MA, USA). DNA codon optimization for the expression of AB0089 Chain H and Chain L were performed using the Codon Optimization Tool from GeneArt Gene Synthesis (Thermo Fisher Scientific, Waltham, MA, USA). The goal was to achieve high expression level in Expi293 cells (Thermo Fisher Scientific, Waltham, MA, USA).

Cloning into vectors for transient expression

[0829] AB0089 Chain H and L were synthesized and cloned into pcDNA3.4 vector using Thermo Fisher Scientific's GeneArt gene synthesis platform. The vector backbone for cloning AB0089 Chain S was prepared internally using the pcDNA3.4 vector (Thermo Fisher Scientific, Waltham, MA, USA), by creating KpnI and BamHI restriction sites for linearization and cloning using the NEBuilder HiFi Technology from New England Biolabs (Ipswich, MA). The general protocol for cloning using the NEBuilder HiFi Technology was followed. Briefly, the gBlocks (double stranded DNA fragments) expressing the gene of interest were cloned into the vector backbone, transformed using the TG-1 bacterial cells, DNA was harvested using the Zyppy Plasmid Miniprep Kit (Zymo Research, Irvine, CA) and the plasmid sequence was corroborated by Sanger sequencing (Genewiz, South Plainfield, NJ). Once sequence corroborated, maxi-preps were performed to isolate plasmid DNA using the Nucleo Bond Xtra Maxi EF Kit (Macherey-Nagel, Bethlehem, PA).

Expression

Transient expression in Expi293 cells

[0830] Transient transfection of Expi293 cells was performed according to the general protocol provided by manufacturer (Life Technologies, Thermo Fisher Scientific, Waltham, MA) with the exception that PEI reagent was used for transfection. Expi293 cells were transfected with the 3 DNA chains created for transient expression of the 3 polypeptides that make up AB0089: pETseq0854 (Chain H), pETseq0424 (Chain L) and pETseq1739 (Chain S) using the plasmid ratio 4:1:1 to achieve a high percentage of heterodimer. Briefly, DNA-PEI complexes were created by mixing DNA and PEIpro Reagent (Polyplus Transfection; Illkirch, France) separately first in OptiMEM media (Life Technologies, Thermo Fisher Scientific, Waltham, MA), followed by mixing and subsequent addition to the Expi293 cells (>95% viability; VCD of $2.5x10^6$/mL). Following transfection, the cells were cultured in a humidified shaker-incubator at 37°C and 8% CO_2. The cell supernatant was harvested 5 days later.

Transient expression in ExpiCHO cells

[0831] Transient transfections of ExpiCHO cells were performed according to the general protocol outlined by the manufacturer (Life Technologies, Thermo Fisher Scientific, Waltham, MA). ExpiCHO cells were transfected with the 3 DNA chains created for expression of the 3 polypeptides that make up AB0089: pETseq0854 (Chain H), pETseq0424 (Chain L) and pETseq1739 (Chain S) using the plasmid ratio 4:1:1 to achieve a high percentage of heterodimer. Briefly, DNA-Expifectamine complexes were created by mixing DNA and Expifectamine Reagent (Life Technologies) separately first in OptiPro media (Life Technologies), followed by mixing and subsequent addition to the ExpiCHO cells (>95% viability; VCD of 6x106/mL). Following transfection, the cells were cultured in a humidified shaker-incubator at 37°C and 8% CO_2. ExpiCHO Feed and enhancer were added 18-20 hours later to boost protein expression, as per the protocol. The cell supernatant was harvested 9-11 days later, depending on cell viability (>70%).

Harvest

[0832] For harvest of AB0089, the cell culture supernatants were transferred to 500 mL or 1 L polycarbonate centrifuge bottles and spun at 7500 rpm for 35 mins at 4°C, followed by

filtration using 0.2-micron filtration bottles. Below materials/reagents (vendor; catalog number) were used:

- Vi-CELL XR Cell Counter (Beckman Coulter)
- Vi-CELL 4mL sample cups (Beckman Coulter; 08229NT2)
- Vi-Cell Reagent Pack (Beckman Coulter; B94987)
- 1L Polycarbonate Centrifuge bottle (Beckman Coulter; 366751)
- 500 mL Polycarbonate Centrifuge bottle (Beckman Coulter; 355649)
- Nalgene® Rapid-Flow™ Filter Units and Bottle Top Filters, PES Membrane, Sterile, Thermo Scientific, 1L (VWR; 73520-986)
- Nalgene® Rapid-Flow™ Filter Units and Bottle Top Filters, PES Membrane, Sterile, Thermo Scientific, 500 mL (VWR; 73520-984)

Purification

Protein A capture chromatography

[0833] A 5.0 cm diameter SNAP column was packed to a bed height of 5.6 cm with Protein A MabSelect SuRe gel for a column volume of approximately 110 ml. Protein A method steps and buffers are shown in Table 121. Elution fractions were neutralized to approximately pH 7.0 using 1.0 M Tris, pH 8.3 (5-10% of elution volume). Below materials/reagents (vendor; catalog number) were used:

- SNAP Column (Essential Life Solutions; S-50/125-PASS-OE-FP10)
- MabSelect SuRe Protein A Gel (GE Healthcare; 175-43-802)
- 5x Protein A Binding Buffer (500 mM Sodium Phosphate, 750 mM Sodium Chloride pH 7.2) (Boston Bioproducts; C-6332)
- 1x Protein A Binding Buffer (100 mM Sodium Phosphate, 150 mM Sodium Chloride, pH 7.2) (Diluted 5x stock)
- 100 mM Glycine pH 3.0 (Boston Bioproducts; BB-95-100mM)
- 1.0 M Tris, pH 8.3 (Boston Bioproducts; LT-783)
- 10.0 N Sodium Hydroxide (VWR; BDH7247-4)
- 0.1 N Sodium Hydroxide (Diluted 10.0N stock)

Table 121: Protein A MabSelect Sure chromatography method steps.

Step	Buffer/Material	Volume (CV)	Flow Rate (mL/min)
Equilibration	1x Protein A Binding Buffer	5	10
Sample Application	Conditioned Media		10
Wash	1x Protein A Binding Buffer	20	10
Elution	100 mM Glycine, pH 3.0	7	10
Strip	0.1 N Sodium Hydroxide	4	10
Re-Equilibration	1x Protein A Binding Buffer	5	10

Cation exchange chromatography

[0834] Cation Exchange chromatography (CIEX) was performed using Poros XS resin packed to a bed height of approximately 24.5 cm in a XK-26 column body for a final column volume of 130 ml. Equilibration and wash buffer (Buffer A) was 50 mM sodium acetate pH 5.0 with 10 mM sodium chloride. Elution buffer (Buffer B) was 50 mM sodium acetate pH 5.0 with 1.0 M sodium chloride.

[0835] The eluate from the Protein A column was pH- and conductivity-adjusted by diluting at least five-fold with Buffer A. After washing the loaded column, the protein was eluted with steps of increasing sodium chloride concentration. The IEX chromatography method steps are shown in Table 122.

Table 122: Cation exchange chromatography method steps.

Step	Buffer	% B	Volume (CV)	Flow Rate (mL/min)
Equilibration	50 mM Sodium Acetate, 10 mM NaCl, pH 5.0	0	7	15.0
Sample Application	Neutralized ProA EL Buffer, Diluted ~10x with IEX EQ buffer	0	NA	15.0
Wash	50 mM Sodium Acetate, 10 mM NaCl, pH 5.0	0	5	15.0
Elution Step	Buffer A: 50 mM NaOAc, 10 mM NaCl, pH 5.0 Buffer B: 50 mM NaOAc, 1 M NaCl, pH 5.0	10	4	15.0
Elution Step		15	15	15.0
Elution Step		18	15	15.0
Elution Step		20	15	15.0
Elution Step		30	7	15.0
Elution Step		100	7	15.0

Step	Buffer	% B	Volume (CV)	Flow Rate (mL/min)
Strip/Sanitization	0.1 N NaOH	0	5	15.0

Buffer exchange by G25 chromatography and diafiltration

[0836] The IEX product was buffer exchanged to PBS pH 7.4 (ThermoFisher Scientific, P/N 10010023) by gel filtration chromatography using Sephadex™ G25 Fine resin (GE Healthcare, P/N 17-0032-01) packed in a XK-26 column to a bed height of 30 cm (160 ml column volume). Alternatively, the product was buffer exchanged and concentrated by discontinuous diafiltration using Amicon Ultra 15 centrifugal filters (Millipore, P/N: UFC903024).

SDS-PAGE

[0837] NuPAGE 4-12% Bis-Tris gels were run with MES running buffer. Wells were loaded with 2-3 µg of sample for both non-reduced and reduced preparations. Reduced samples were treated with 20 mM DTT and heated at 70°C for 10 minutes. Gel power supply settings were constant 200V for 50 minutes. Protein bands were visualized by staining with Novex SimplyBlue SafeStain according to manufacturer's instructions. Gels were scanned on an Azure Biosystems C600 imager. The below materials/reagents (vendor; catalog number) were used:

- XCell SureLock Mini-Cell (Thermo Fisher; EI0001)
- PowerEase™ 300W Power Supply (Thermo Fisher; PS0301)
- Isotemp Digital Heat Block (Fisher Scientific; 88-860-022)
- NuPAGE MES SDS Running Buffer (20X) (Thermo Fisher; NP0002)
- SimplyBlue SafeStain (Thermo Fisher; LC6065)
- NuPAGE LDS Sample Buffer (4X) (Thermo Fisher; NP0007)
- Novex Sharp Prestained Protein Standard (Thermo Fisher; LC5800)
- 2-MERCAPTOETHANOL (MP Biomedical; 194705)
- Azure c600 imager (Azure Biosystems)

Analytical size exclusion chromatography (Superdex 200)

[0838] Analytical size exclusion chromatography was performed with a Superdex 200 Increase 10/300 column installed on an Agilent 1260 HPLC system. Mobile phase was PBS pH 7.4 (ThermoFisher Scientific, P/N 10010023). Flow rate was 0.5 ml/min with run time of 45 minutes. Absorbance was measured at 214 nm and 280 nm. Peaks were integrated by the Open

Lab CDS Data Analysis Software Version 2.3 using the GC/LC Area Percent Method. Peaks below the threshold of detection were integrated by manually defining the baseline.

Intact mass

[0839] 10 µg of AB0089 was diluted to 0.25 µg/µL with 0.1% formic acid and 1 µg was injected onto a MabPac 2.1 x 100 mM column and analyzed using a Thermo Vanquish UHPLC coupled to a QExactive+ mass spectrometer with the Biopharma option. Spectra were acquired in high-mass range mode at 17,500 resolution. Data was analyzed using the Sliding Window ReSpect algorithm in the BioPharma Finder data analysis software package. The below materials/reagents (vendor; catalog number) were used: 0.1% formic acid in water (Honeywell; LC452-2.5) and MAbPac RP 2.1 x 100 mm, 4µm column (Thermo Scientific; 088647).

Endotoxin

[0840] Endotoxin readings were performed on an Endosafe® nexgen MCS cartridge reader (Charles River Laboratories) and cartridges (Charles River Laboratories P/N PTS2001F). Samples were prepared for assay by diluting in either endotoxin-free water or sterile PBS pH 7.4 (ThermoFisher Scientific, P/N 10010023). An assay was considered valid if all assay performance parameters and controls are within specification.

Hydrophobic interaction chromatography (HIC)

[0841] Injections of AB0089 (5 µg) were prepared in a 5:4 ratio of high salt buffer (100 mM sodium phosphate, 1.8 M ammonium sulfate, pH 6.5) to sample. Samples were analyzed using an Agilent 1260 Infinity II HPLC equipped with a Sepax Proteomix HIC Butyl-NP5 5uM column held at 25 ºC. The gradient runs from 0% low salt buffer (100 mM sodium phosphate, pH 6.5) to 100% low salt buffer over 6.5 minutes at a flow rate of 1.0 mL/minute. Chromatograms were monitored at 280 nm. The below materials/reagents (vendor; catalog number) were used:

- Proteomix HIC Butyl-NP5 5uM Column, 4.6x35 mm (Sepax; 431NP5-4603)
- Sodium Phosphate Monobasic (Sigma Aldrich; RES20906-A702X)
- Sodium Phosphate Dibasic (Fisher Bioreagents; BB332-500)
- Ammonium Sulfate, >99.0% (Sigma; A4418-500G)
- Sodium Hydroxide, 10.0 N (Avantor Materials; 5000-03)
- Hydrochloric Acid, 10.0 N (Ricca Chemical Company; 3770-32)

Non-reduced CE-SDS

[0842] AB0089 was diluted to 0.5 mg/mL with 1x sample buffer to achieve a final sample volume of 50 µL. Internal standard and iodoacetamide were added to samples, which were then incubated at 70 °C for 10 minutes in a heat block, followed by an ice bath for 5 minutes. Samples were transferred to a 96-well plate, centrifuged, and loaded into the instrument. Individual samples were loaded into the capillary for 40 seconds at 4600 volts and separated for 35 minutes at 5750 volts on a Maurice instrument (ProteinSimple, San Jose, CA). The below materials/reagents (vendor; catalog number) were used:

- 25x Internal Standard (ProteinSimple; 046-016)
- CE-SDS Plus Cartridge (ProteinSimple; 090-157)
- Iodoacetamide (Sigma-Aldrich; 16125-5G)
- Maurice CE-SDS PLUS Application Kit Reagents (Bottom Running Buffer, Separation Matrix, Wash Solution, Conditioning Solution 1 & 2, 1X Sample Buffer) (ProteinSimple; 046-571)
- Top Running Buffer (ProteinSimple; 046-384)

Reduced CE-SDS

[0843] AB0089 was diluted to 0.5 mg/mL with 1X sample buffer to achieve a final sample volume of 50 µL. Internal standard and beta-mercaptoethanol (Bio-Rad, #161-0710) were added to samples, which were then incubated at 70 °C for 10 minutes in a heat block, followed by an ice bath for 5 minutes. Samples were transferred to a 96-well plate, centrifuged, and loaded into the instrument. Individual samples were loaded into the capillary for 40 seconds at 4600 volts and separated for 31.2 minutes at 5750 volts on a Maurice instrument (ProteinSimple, San Jose, CA).

Capillary isoelectric focusing (cIEF)

[0844] AB0089 was diluted to 1 mg/mL with MilliQ water, 15 µL of sample was added to 60 µL of master mix (water, methyl cellulose, Pharmalyte 3-10, arginine, pI markers 4.05 and 9.99), vortexed, and centrifuged briefly. 60 µL of sample was aspirated from the top of the solution and added to a 96-well plate and centrifuged before testing. The sample was separated for one minute at 1500 volts followed by 8 minutes at 3000 volts on a Maurice instrument

(ProteinSimple, San Jose, CA). The below materials/reagents (vendor; catalog number) were used:

- 0.5% Methyl Cellulose (ProteinSimple; 102730)
- 1% Methyl Cellulose (ProteinSimple; 101876)
- 500 mM arginine (ProteinSimple; 042-691)
- Anolyte (ProteinSimple; 102727)
- Catholyte (ProteinSimple; 102728)
- cIEF Cartridge (ProteinSimple; 090-101)
- Fluorescence calibration standard (ProteinSimple; 046-025)
- Pharmalytes 3-10 (Sigma Aldrich; P1522-25ML)
- pI Marker 4.05 (ProteinSimple; 046-029)
- pI Marker 9.99 (ProteinSimple; 046-034)
- System suitability mix (ProteinSimple; 046-027)
- System suitability peptide panel (ProteinSimple; 046-026)

Differential scanning calorimetry (DSC)

[0845] AB0089 was prepared at 0.5 mg/mL in 1X PBS (Gibco, #10010-031) or alternative formulations. 325 µL was added to a 96-well deep well plate along with a matching buffer blank. Thermograms were generated using a MicroCal PEAQ DSC (Malvern, PA). Temperature was ramped from 20-100 °C at 60 °C/hour. Raw thermograms were background subtracted, the baseline model was spline, and data were fitted using a non-two state model.

SPR instrument and reagents

[0846] Biacore 8K (Instrument ID: 2222251, GE Healthcare Life Sciences) was used to run the kinetic measurements and Biacore 8K Insight Evaluation Software was used for analysis of experimental data. The below materials/reagents (vendor; catalog number) were used:

- 10 mM sodium acetate, pH 5.0 (Cytiva; BR100351)
- 10 mM Glycine, pH 1.7 (Boston BioProducts; BB-2413D)
- 10xHBS-EP+ (Cytiva; BR1006-69)
- 1xHBS-EP+ Prepared in house from 10x stock solution
- 1xMBS-EP+, pH6.0 (Prepared in house)
- BSA Fraction V (7.5%) (Gibco; 15260-037)

- NaCl (Fisher Scientific; S271-1)
- NaOH (Cytiva; BR100358)
- Amine coupling kit (Cytiva; BR-1000-50)
- Mouse antibody capture kit (Cytiva; BR100838)
- CM5 Chip (Cytiva; 29-1496-03)
- Series S Sensor Chip SA (Cytiva; BR-1005-31)
- SA Chip (Cytiva; BR100531)
- Biotin CAPture kit (Cytiva; 28-9202-34)
- Goat anti-human IgG Fc cross-absorbed secondary antibody (Invitrogen; 31125)
- Micro Bio-Spin 30 columns (Bio-Rad; 732-6223)
- Amicon Ultra 0.5 mL Centrifugal Filters 10,000 NMWL (Millipore Sigma; UFC501096)

CLEC12A affinity by SPR

[0847] Binding affinities of AB0089 to recombinant human CLEC12A (Dragonfly Tx) were measured by SPR using a Biacore 8K instrument. Briefly, human Fc specific antibodies were covalently immobilized at a density ~8000-10000 resonance units (RU) on carboxy methyl dextran matrix of a CM5 biosensor chip via amine-coupling chemistry to create an anti-hFc IgG chip. AB0089 samples were captured on the anti-hFc IgG chip at a concentration of 1.5 µg/mL at a flow rate of 10 µL/min for 60 seconds to achieve approximately 150 RU capture level. hCLEC12A-His was serially diluted (100 nM-0.14 nM) in three-fold dilutions SPR running buffer and injected at a flow rate of 30 µl/min over the captured test articles. Association was monitored for 300 seconds and dissociation was monitored for 600 seconds. Surfaces were regenerated between cycles with three pulses of 10 mM glycine-HCl, pH 1.7 injected for 20 seconds at 100 µl/min. HBS-EP+ (1X) with 0.1 mg/ml BSA was used as running buffer throughout the experiment. Experiments were performed at physiological temperature of 37°C. To obtain kinetic rate constants and overall binding affinity, double-referenced data were fit to a two-state kinetic model using Biacore 8K Insight Evaluation software (Cytiva). Justification for the use of the two-state model is provided below.The goodness of the fit between the fitted curve and the experimental data were expressed by the evaluation software as Chi^2.

NKG2D affinity by SPR

[0848] Binding affinity of AB0089 for recombinant human NKG2D (Dragonfly Tx) was measured by SPR using a Biacore 8K instrument. Briefly, mFc specific antibodies were covalently immobilized at a density of ~8000-10000 RU on carboxy methyl dextran matrix of a CM5 biosensor chip via amine coupling chemistry to create an anti-mFc IgG chip. mFc-tagged human NKG2D was captured on the anti-mFc IgG chip at a concentration of 0.2 µg/mL at a flow rate 10 µL/min for 60 seconds to achieve approximately 30 RU capture level. AB0089 was buffer exchanged into HBS-EP+ (1X) buffer and serially diluted (5000 nM – 9.77 nM) in two-fold dilutions with HBS-EP+. Analyte (AB0089) was injected at a flow rate of 30 µl/min over the captured test articles. Association was monitored for 60 seconds and dissociation was monitored for 60 seconds. Surfaces were regenerated between cycles with three pulses of 10 mM glycine-HCl, pH 1.7 injected for 20 seconds at 100 µl/min. HBS-EP+ (1X) was used as running buffer throughout the experiment. Experiments were performed at physiological temperature of 37°C. Double-referenced data were fit to a 1:1 kinetic and a Steady State interaction models using Biacore 8K Insight Evaluation software (GE Healthcare) with global fit analysis in the 1:1 kinetic fit model. Since the samples had been buffer exchanged into the running buffer prior to each experiment, offset for a steady state fit was set to constant (0). The goodness of the fit was expressed by the evaluation software as Chi^2 that was considered in the context of R_{max} value.

Synergy of simultaneous binding of CD16a and NKG2D

[0849] Synergistic NKG2D and CD16a binding was evaluated by SPR. hNKG2D alone (12.3 µg/mL), CD16a F158 allele alone (9 µg/mL) and the mixture of hNKG2D and CD16a F158 at the same concentration each were amine-coupled to the surface of the CM5 Series S Biacore chip for 1 minute. 1.8 µM AB0089 or trastuzumab were injected for 150 sec at 10 µL/min. Dissociation phase was observed for 180 sec when regeneration was not needed and 1800 sec when natural regeneration of the surface (almost complete dissociation of analyte) was needed between the cycles at the same flow rate. 1x HBS-EP+ buffer was used as running and sample dilution buffer.

Co-engagement (CLEC12A and NKG2D)

[0850] AB0089 was diluted in 1x HBS-EP+ buffer containing 0.1 mg/ml BSA and was captured on an anti-human Fc surface of CM5 chip at a flow rate 5 µL/min for 60 sec to achieve

capture level of 150-250 RU. The net difference between baseline signal and the signal after completion of AB0089 injection representing the amount of AB0089 captured was recorded. hCLEC12A-His (200 nM) or mFc-hNKG2D (7 μM) was injected over captured AB0089 at 20 μl/min for 90 sec to reach saturation. This injection was immediately followed by an injection of pre-incubated mixture of hCLEC12A-His (200 nM) and mFc-hNKG2D (7 μM) at a flow rate of 20 μl/min for 90 sec with the use of the A-B-A injection command in the Biacore 8K control software (second target was pre-mixed with the first target to assure all binding sites for the first target are occupied). The chip was regenerated by two 20 sec pulses of 10 mM Glycine (pH 1.7) at 100 μL/min. The experiment was conducted at 37°C and 1x HBS-EP+ buffer containing 0.1 mg/ml BSA was used as a running buffer. Binding of each antigen, expressed in RU, was recorded as the net difference between the baseline signal prior and after the injection of individual antigen. An average relative binding ratio of each target bound to AB0089 unoccupied with another target (injected first) was assigned a value of 1.0. An average relative binding stoichiometry of each target bound to captured AB0089 that is already saturated with the other target (injected second) was expressed as a fraction of the full capacity binding to unoccupied AB0089.

Epitope binning

[0851] Anti-CLEC12A antibody or TriNKET was directly immobilized to the active flow cell of a Series S CM5 sensor chip via amino coupling at 3 μg/mL concentration for a final density of 370-1070 RU. A classic sandwich assay run at 25°C was used for epitope binning. The first injection was a 120 second association of 200 nM CLEC12A-His followed directly by 200 nM of the sandwiching antibody/TriNKET. The sandwiching antibody/TriNKET had a 120 seconds association time and 120 seconds dissociation time. Both analyte and sandwiching molecule injections were run at 30 μL/min. A 20 second pulse of 10 mM glycine pH 1.7 injected at 100 μL/min was used to regenerate the chip surface after dissociation. The first cycle included buffer injections for both the analyte and sandwiching molecule. The second cycle included 200 nM hCLEC12A-His analyte followed by a buffer injection for sandwiching molecule. Subsequent cycles included 200 nM hCLEC12A-His analyte injection followed by 200 nM sandwiching molecule. 1x HBS-EP+ running buffer was used throughout experiment. Sensorgrams were visualized using Biacore Insight Evaluation software.

FcγR binding

[0852] Human and cynomolgus CD64, high and low affinity alleles of CD16a (V158 and F158, respectively), two alleles of CD32a (H131 and R131), CD16b, CD32b and cynomolgus CD16 were captured via biotin on a primed (according to the manufacturers instruction) Biacore chip. Table 123 summarizes respective capture levels and types of the Biacore chips used. Due to irreversibility of streptavidin - biotin interaction, the capture step for all receptors except FcγRI (CD64) was performed just once prior to the start of the binding experiment. hCD64 and cyno CD64 capture on the CAP chip surface was performed during each cycle in accordance with the manufacturer's instructions for the Biotin CAPture kit.

[0853] Prior to any FcγR binding experiment requiring a high starting concentration, AB0089 and trastuzumab, samples were buffer exchanged into 1x HBS-EP+ SPR running buffer by three consecutive dilution/concentration cycles with the use of a 0.5 mL concentrator unit resulting in >300-fold dilution of original buffer components while maintaining high concentration of protein. Protein concentration was measured at A280 on a NanoDrop instrument and with the use of sample appropriate theoretical molar extinction coefficients (196790 $M^{-1}cm^{-1}$ for AB0089 and standard IgG setting for trastuzumab).

[0854] Each FcγR binding experiment consisted of multiple cycles utilizing 2-fold serially diluted AB0089 or trastuzumab. 0 nM blank cycle placed at the start of each concentration series and receptor free chip surface were used for referencing. Each experimental cycle included association, dissociation and regeneration steps. Analyte (AB0089 or trastuzumab) concentrations, association and dissociation times, and regeneration parameters were FcγR-specific (Table 123). All steps were executed at a flow rate of 30 μL/min and at 25°C.

Table 123: Parameters used in SPR FcγR binding experiments.

Parameter	hCD64, cyno CD64	hCD16a V158	hCD16a F158	cyno CD16	hCD32a H131, R131	hCD16b	hCD32b
Type of chip	CAP chip	Type S SA chip					
FcγR capture level, RU	35-50	10-27	10-27		7-25	10-23	
Concentration range, nM	400-1.56	1500-0.023	6000 – 0.023		16000-125	24000 -188	
Association time, sec	240	150			60	60	
Dissociation time, sec	600	300			60	150	
Surface regeneration	CAPture kit regeneration	5 sec pulse of 1- 2 mM NaOH					

[0855] A series of 2-5 blank experimental cycles with the use of experiment appropriate running buffer in place of analyte was performed prior to sample analysis to stabilize the chip surface. Raw data was fitted to either a 1:1 kinetic model or a steady state affinity model using Biacore Insight evaluation software. Chi^2 (calculated by the software) related to either calculated R_{max} or apparent maximal binding response was used to assess goodness of the fit. All reported values were rounded to one decimal place after the calculation.

FcRn binding

[0856] Recombinant human or cynomolgus monkey (cyno) FcRn was captured on a surface of an SA series S chip at a concentration of 0.25 μg/mL for 1 minute. AB0089 and commercial trastuzumab (IgG1 assay control) were buffer exchanged into MBS-EP+, pH 6.0 prior to the SPR binding experiment. Each FcRn binding experiment consisted of multiple cycles utilizing varying concentrations of analytes. Two-fold dilution series (12 μM – 0.023 μM) of AB0089 and trastuzumab were used. 0 nM blank cycle placed at the start of each concentration series and a blank amine coupling modified chip surface lacking FcRn were used for referencing. Each experimental cycle included association, dissociation and regeneration steps. The association step consisted of 60 sec analyte injection and was followed by a 60 sec dissociation step. Surface regeneration (60 sec injection of HBS-EP+ buffer, pH 7.4) completed each kinetic cycle. All

steps were executed at a flow rate of 30 µL/min and at 25°C. MBS-EP+ buffer, pH 6.0 was used as a running buffer. The data were fitted to a steady state affinity model with Biacore Insight evaluation software. Chi^2 (calculated by the software) related to the calculated R_{max} was used to assess goodness of the fit. All reported values were rounded to one decimal place.

KHYG-1-CD16aV mediated cytotoxicity assay

[0857] The potency of AB0089 was tested with KHYG-1-CD16aV cells. The EC50 and maximum lysis values were derived from the cell lysis curves using GraphPad Prism software (four parameter logistic non-linear regression curve fitting model).

Primary NK cells mediated cytotoxicity assay

[0858] The potency of AB0089 was tested with primary NK cells. The EC50 and maximum lysis values were derived from the cell lysis curves using GraphPad Prism software (four parameter logistic non-linear regression curve fitting model).

Non-specific binding to polyspecific reagent (PSR)

[0859] 50 µL of 100 nM TriNKET or control mAb in PBSF were incubated with pre-washed 5 µL protein A dyna beads slurry for 30 mins at room temperature. TriNKETs or mAb bound magnetic beads were allowed to stand on a magnetic rack for 60 seconds and the supernatant was discarded. The bound beads were washed with 100 µL PBSF. Beads were incubated for 20 minutes on ice with 50 µL of biotinylated PSR reagent which was diluted 25-fold from the stock (Xu *et al.*, (2013) *Protein engineering design and selection*, 26, 663-670). Samples were put on the magnetic rack, supernatant discarded, and washed with 100 µL of PBSF. A secondary FACS reagent, to detect binding of biotinylated PSR reagent to TriNKETs or control mAbs, was made as follows: 1:250 µL of Streptavidin-PE and 1:100 donkey anti-human Fc were combined in PBSF. To each sample, 100 µL of the secondary reagents were added and allowed to incubate for 20 minutes on ice. The beads were washed twice with 100 µL PBSF. Samples were analyzed on a BDFACS Celesta. Two PSR controls, Rituximab (PSR positive) and Trastuzumab (PSR negative), were used in the assay. The below materials/reagents (vendor; catalog number) were used: PBSF (1X PBS pH 7.4 + 0.25% BSA) (Dragonfly Tx), Dyna beads (Invitrogen; 10001D), Streptavidin-PE (Biolegend; 405204), and Donkey anti-human Fc Ab (Jackson ImmunoResearch; 709-096-149).

High-Spec® cross reactivity assay using HuProt™ arrays

[0860] The specificity of AB0089 was tested at 0.1 µg/ml and 1 µg/ml concentration against native HuProt human proteome array immobilized on microslides. The assay was performed at CDI laboratories (Baltimore, MD).

Immunogenicity assessment

[0861] EpiMatrix program from EpiVax was used for all calculations as described in Cohen *et al.* (2013) *Mol Cancer Ther*, 12, 2748–59.

Molecular modeling

[0862] Molecular modelling was performed using the SAbPred website (opig.stats.ox.ac.uk/webapps/newsabdab/sabpred/). CLEC12A and NKG2D binding arms were compared with 377 post Phase I biotherapeutic molecules using Therapeutic Antibody Profiler (TAP). TAP used ABodyBuilder to generate a model for AB0089 with side chains by PEARS. The CDRH3 was built by MODELLER, since this loop is the most diverse of all CDRs.

[0863] Five different parameters were evaluated:

1. Total CDR length
2. Patches of surface hydrophobicity (PSH) across the CDR vicinity
3. Patches of positive charge (PPC) across the CDR vicinity
4. Patches of negative charge (PNC) across the CDR vicinity
5. Structural Fv charge symmetry parameter (sFvCSP) for CLEC12A binding scFv and NKG2D binding Fab

Developability

Accelerated (40°C) stability in HST, pH 6.0

[0864] AB0089 lot AB0089-002 was concentrated and diafiltered into 20 mM histidine, 250 mM sucrose, 0.01% Tween-80, pH 6.0 (HST, pH 6.0) using an Amicon Ultra15 30K device. The concentration of the recovered sample was determined by A280 and the sample was diluted to 20 mg/ml with HST buffer. A 0.2 ml aliquot was immediately frozen at -80°C as the control and two 0.15 ml aliquots were stored at 40°C in the dark. An aliquot was removed after 2 and 4 weeks and immediately frozen at -80°C until analysis. The below materials/reagents were used:

- Amicon Ultra15 Centrifugal Filters (30K MWCO) (Millipore; UFC903024)

- Hydrochloric acid, 10N (RICCA; 3770-32)
- L-Histidine (MP Biomedicals; 101954)
- Sodium hydroxide, 10N (JT Baker; 5000-03)
- Sucrose (VWR; M117-500G)
- Tween-80 (VWR; 0442-1L)

Accelerated (40°C) *stability* in CST, pH 7.0

[0865] AB0089 lot AB0089-002 was concentrated and diafiltered into 20 mM sodium citrate, 250 mM sucrose, 0.01% Tween-80, pH 7.0 using an Amicon Ultra15 30K device. The concentration of the recovered sample was determined by A280 and the sample was diluted to 20 mg/ml with CST buffer. A 0.4 ml aliquot was immediately frozen at -80°C as the control and four 0.15 ml aliquots were stored at 40°C in the dark. An aliquot was removed weekly and immediately frozen at -80°C until analysis. The below materials/reagents were used:

- Amicon Ultra15 Centrifugal Filters (30K MWCO) (Millipore; UFC903024)
- Hydrochloric acid, 10N (RICCA; 3770-32)
- Sodium Citrate Dihydrate (Fisher Chemical; S466)
- Sodium hydroxide, 10N (JT Baker; 5000-03)
- Sucrose (VWR; M117-500G)
- Tween-80 Solution (10%) (Sigma: PB192-10ML)

Forced oxidation

[0866] AB0089 lot AB0089-002 was diluted to 1 mg/ml with phosphate buffered saline (PBS). 6.7 µL of 3% hydrogen peroxide was added to a 1.0 ml aliquot of AB0089 to obtain a final concentration of 0.02% hydrogen peroxide. Oxidation of AB0089 proceeded for 24 hours at room temperature in the dark. After 24 hours, the sample was buffer switched into PBS, pH 7.4 using Amicon Ultra 0.5 ml 10K MWCO devices following the manufacturer's instructions. The un-oxidized control (0.5 ml) was stored at -80°C. The below materials/reagents were used: 30% hydrogen peroxide (VWR; BDH7690-1), Gibco PBS pH 7.4 (1x) (ThermoFisher; 10010-031), and Zeba Desalting Columns (Thermo Scientifc; 89890).

pH 5 stress

[0867] Concentrated AB0089 lot AB0089-002 was diluted to 1.0 mg/ml with 20 mM sodium acetate, pH 5.0. Concentration was corroborated by A280 with a Nanodrop One spectrophotometer. The sample was split. Half was stored at -80 ºC as a control and the other half was incubated at 40 ºC for 2 weeks. After the incubation, the sample was stored at -80 ºC until analysis. Sodium acetate buffer (1 M, pH 5.0) (Boston Bioproducts; BB-60) was used.

pH 8 stress

[0868] Concentrated AB0089 lot AB0089-002 was diluted to 1.0 mg/ml with 20 mM Tris, pH 8.3. Concentration was corroborated by A280 on the Nanodrop One spectrophotometer. The sample was split. Half was stored at -80 ºC as a control and the other half was incubated at 40 ºC for 2 weeks. After the incubation, the sample was stored at -80 ºC until analysis. The pKa of Tris is temperature dependent. Tris, pH 8.3 measured at 25ºC is expected to have a pH of ~8.0 at 40ºC. Tris buffer (1 M, pH 8.3) (Boston Bioproducts; LT-783) was used.

Freeze/thaw

[0869] Three 0.1 ml aliquots of 20 mg/ml AB0089 lot AB0089-002 in CST, pH 7.0 buffer were subjected to freeze/thaw cycles at -80 °C in a Styrofoam container to slow the freezing process. At cycles 2, 4, and 6, an aliquot was removed and transferred to -80 ºC storage until analysis.

Agitation

[0870] 0.5 ml aliquots of 10 mg/ml AB0089 lot AB0089-002 in 20 mM sodium citrate, 250 mM sucrose, pH 7.0 or 20 mM sodium citrate, 250 mM sucrose, 0.01% Tween-80, pH 7.0 were added to a deep well plate (Thermo, #278752), the place was sealed, covered with foil and shaken at room temperature at 300 rpm for 3 days. After 3 days the plate was spun down and analyzed by A280 (concentration), A340 (turbidity), and SEC (aggregation).

Low pH hold

[0871] AB0089 was captured on a MabSelect Sure Protein A column and eluted with 100 mM glycine, pH 3.0. Peak fractions were pooled, and 12 ml of the protein A eluate was pH was adjusted to pH 3.3 with 100 mM glycine pH 3.0 buffer. The pH-adjusted eluate was held at room temperature. After 1.5 hours, the eluate was brought to neutral pH with 1.0 M Tris-HCl, pH 8.3.

The pH-hold sample was further purified by cation exchange chromatography. The final product was buffer exchanged to PBS pH 7.4 for analysis and received designation AB0089 lot AB0089-003.

High concentration

[0872] AB0089 Lot AB0089-002 was concentrated using 30 kDa molecular weight cutoff devices in PBS, pH 7.4. Concentration was determined by A280 on a Nanodrop and product quality was monitored by SEC as described above.

Size exclusion chromatography (TSKgel G3000SWxl)

[0873] The following method was used for assessment of developability samples. 50 µg of test material was injected onto an Agilent 1260 Infinity II high pressure liquid chromatography (HPLC) instrument with 1260 Quat Pump, 1260 Vialsampler, 1260 VWD. The sample was separated on a Tosoh TSKgel G3000SWxl, 7.8 mm I.D. x 30 cm, 5 µm column. SEC running buffer was PBS, pH 7.0, flowing at 0.50 ml/min. Absorbance was monitored at both 214 and 280 nm, peak areas were manually integrated and the percent of high molecular weight species (HMWS), low molecular weight species (LMWS), and monomer were reported. The below materials/reagents (vendor; catalog number) were used: gel filtration standards (Bio-Rad; 1511901), SEC buffer (20 mM Sodium Phosphate Monobasic Monohydrate/Sodium Phosphate Dibasic Heptahydrate, 0.3 M Sodium Chloride, pH 7.0) (Boston BioProducts; C-5194D), and TSKgel G3000SWxl, 7.8 mm x 30 cm, 5 µm column (Tosoh; 08541).

LC-MS/MS tryptic peptide mapping

[0874] 50 µg of AB0089 was diluted with 6 M guanidine hydrochloride in 250 mM Tris, pH 8.5 and disulfide bonds were reduced with 25 mM dithiothreitol for 30 minutes at 40°C in a thermomixer. The reduced cysteines were then alkylated with 50 mM iodoacetamide for 60 minutes at room temperature in the dark. The reduced and alkylated protein was buffer-switched into 50 mM Tris, pH 8.0 and digested with trypsin (1:25 enzyme:substrate) for 1 hour at 37°C. LC-MS/MS was carried out on a Thermo Vanquish UHPLC coupled to a QExactive+ mass spectrometer. Briefly, 5 µg of protein digest was separated on a Waters UPLC BEH Peptide C18 column (2.1 x 150 mm) over 150 minutes using a 2% to 40% acetonitrile gradient at 0.3 ml/min. Mass spectra were acquired from 230-2000 m/z in positive mode at 35,000 resolution for the full

MS scan and 17,500 resolution for the Top10 MS/MS scans. The UPLC-MS/MS files were analyzed using the Byos PTM workflow (Protein Metrics). Peptides were identified using accurate mass and MS/MS searching the AB0089 sequence. Settings for peptide identification were as follows:

- Precursor Mass Tolerance 6.00 ppm
- Fragment Mass Tolerance 20.00 ppm
- Cleavage Site(s) RK, C-terminal
- Digestion Specificity Fully specific
- Missed Cleavages 2
- Modifications Carbamidomethyl / +57.021464 @ C, fixed
- DTT / +151.994915 @ C
- Oxidation / 15.994915 @ M, W
- Dethiomethyl / -48.003371 @ M
- Deamidated / +0.984016 @ N, Q
- pyro-Glu / -17.026549 @ NTerm Q
- pyro-Glu / -18.010565 @ NTerm E
- Carbamyl / +43.005814 @ NTerm, K, R
- Acetyl / +42.010565 @ Protein NTerm
- Ammonia-loss / -17.026549 @ N
- Dioxidation / +31.989829 @ W
- Kynurenine / +3.994915 @ W
- N-glycan 50 common

[0875] The following materials/reagents (vendor; catalog number) were used:

- 0.1% formic acid in acetonitrile (JT Baker; LC441-2.5)
- 0.1% formic acid in water (JT Baker; LC452-2.5)
- Formic acid (Thermo Scientific; 28905)
- Guanidine HCl (Alfa Aesar; A13543)
- Hydrochloric acid, 6 N (Avantor; 4103-01)
- No-weigh dithiothreitol (Thermo Scientific; 20291)
- No-weigh iodoacetamide (Thermo Scientific; 90034)

- Sodium hydroxide, 6 N (Avantor; 5672-02)
- Tris Base (Avantor; 4109-01)
- Trypsin (Thermo Scientific; 90057)
- UPLC BEH Peptide C18 column (2.1 x 150 mm) (Waters; 186003556)
- Zeba spin desalting columns (Thermo Scientific; 89882)

Results

Discovery

[0876] Hybridoma subclone 16B8.C8 (from which sequence optimized AB0089 and its predecessor AB0237 were derived) was discovered through immunization of BALB/c mice with recombinant human CLEC12A-His protein (FIG. 104). A detailed description of the immunization process, antibody screening, assessment of recombinant and cell surface expressed CLEC12A binding, and epitope binning are described.

[0877] During the developability assessment of AB0237, an aspartic acid isomerization liability was identified in CDRH3 of the CLEC12A binding scFv. Attempts to remove this liability by single amino acid substitution or by targeted yeast display approaches (randomization of "DS" or "S") resulted in low expression yield and significant loss of binding to CLEC12A, suggesting that this motif may be important for maintaining CDR architecture. Therefore, an affinity maturation effort focusing on optimization of CDRH3 and CDRH2 was undertaken to further improve affinity for CLEC12A, and then the DS sequence was replaced by DT on the background of the optimized CDRH3. In addition, we sought to improve the humanness of the molecule by reducing the number of murine backmutations in the framework. We hypothesized that only one backmutation in position H83 was required, while other backmutations were not obligatory for maintaining CDRs architecture. The optimized scFv framework that contained a single backmutation was named pET1596 and was used as the background for all additional engineering. Later, the (H94)K backmutation was brought back to provide additional stabilization of the molecule. These engineering efforts resulted in the discovery of the AB0089 molecule, which retained high affinity for human CLEC12A and potency towards AML cancer cell lines, while both removing the isomerization liability and improving humanness.

Sequence optimization

CDRH3 focused randomized affinity maturation library

[0878] A yeast display affinity maturation library (referred to as Library 17) was created successfully by mutating CDRH3 residues (YDYDDSLDY, SEQ ID NO:139) of pET1596 at each position one at a time or by changing two amino acid residues to all 20 amino acids as described above. To enrich for scFvs that have higher affinity towards hCLEC12A in library 17, three rounds of selections were carried out with biotinylated CLEC12A-His at 1 nM (1st and 2nd round of selection; FIG. 105 A, B) and 0.1 nM (3rd round of selection; FIG. 105C). The affinities between the parental clone pET1596 and the library clones were compared and could be accurately discriminated, allowing a quantitative selection in real time (FIG. 105 B, C, D). After 3 rounds of FACS sorting to isolate clones, one clone that contained 2 amino acid differences compared to the parental clone (**G**DY**G**DSLDY) (SEQ ID NO:322) exhibited higher binding affinity for CLEC12A than the parental clone (FIG. 105 D, E).

CDRH3 focused combinatory affinity maturation library

[0879] Outcomes from the CDRH3 focused library demonstrated an improvement in affinity, however further improvement was highly desirable. Thus, Library 30 was created by incorporating the CDRH2 combinatory library (WSGGK (SEQ ID NO:138) to XSGGK (SEQ ID NO:323), WXGGK (SEQ ID NO:324), WSXGK (SEQ ID NO:325), WSGXK (SEQ ID NO:326), WSGGX (SEQ ID NO:327), XXGGK (SEQ ID NO:328), XSXGK (SEQ ID NO:329), XSGXK (SEQ ID NO:330), XSGGX (SEQ ID NO:331), WXXGK (SEQ ID NO:332), WXGXK (SEQ ID NO:333), WXGGX (SEQ ID NO:334), where X = any amino acid) into the optimized CDRH3 backbone. The goal was to engineer and select binders with better affinity than the parental clone (pET1596) or CDRH3 optimized variant. This created a library with a randomized CDRH2 while retaining a fixed CDRH3. Two rounds of FACS sorting were performed on this affinity maturation yeast display library (Library 30) to enrich for high affinity binders (FIG. 106).

[0880] After 2 rounds of FACS sorting, one clone with changes in CDRH2 from WSGGK (SEQ ID NO:138) to WVGGA (SEQ ID NO:272) on the GDYGDSLDY (SEQ ID NO:322) CDRH3 background had the highest affinity for CLEC12A (FIG. 107). This clone showed a significant improvement in CLEC12A affinity compared to parental pET1596 and AB0237.

Remediation of DS sequence liability

[0881] Once the affinity matured clone was identified, site-directed mutagenesis was used to produce a rational variant (CDRH3: GDYGD**S**LDY (SEQ ID NO:322) to GDYGD**T**LDY (SEQ ID NO:273)), resulting in a CLEC12A targeting scFv that does not contain the isomerization liability, while maintaining high affinity binding to the target. The comparison of the CDRs of the optimized AB0089 molecule and AB0237 is shown in Table 124.

Table 124: Comparison of CLEC12A binding CDRs in AB0089 and AB0237.

TriNKETs	CDRH1	CDRH2	CDRH3
AB0237	GFSLTNY (SEQ ID NO:137)	WSGGK (SEQ ID NO:138)	YDYDDSLDY (SEQ ID NO:139)
AB0089	GFSLTNY (SEQ ID NO:137)	W**V**GG**A** (SEQ ID NO:272)	**G**DY**G**D**T**LDY (SEQ ID NO:273)

[0882] Sequence differences obtained as a result of affinity maturation are underlined. Isomerization liability correction obtained by site-directed mutagenesis (DS to DT) is shown in green.

[0883] Based on the structural modeling, we decided to re-introduce a murine residue in position H94 to provide additional support for the CDR architecture. AB0089 contains only 2 murine residues in position H83 and H94 in the VH of the CLEC12A binding scFv, while there are 5 murine backmutations in AB0237. The rest of the backmutations were reverted to human germline, thus improving the humanness of AB0089 (Table 125).

Table 125: Murine backmutations in the frameworks of AB0089 and AB0237.

Chain	AB0089	AB0237
VH		(H71)K
VH	(H83)Q	(H83)Q
VH	(H94)K	(H94)K
VL		(L70)R
VL		(L83)I

Molecular format and design

[0884] AB0089 is a heterodimeric tri-functional antibody that redirects NK and T cell activity against CLEC12A-expressing cancer cells. AB0089 contains three chains: Chain H,

Chain L and Chain S. The schematic representation of the AB0089 molecule is provided in FIG. 108. Chain H is the heavy chain of A49M-I NKG2D-targeting antibody that was selected for having low affinity while being a potent agonist of NKG2D receptors on NK and cytotoxic T cells. The M-I mutation was introduced to eliminate Met102 residue in the CDRH3 that is sensitive to oxidation and therefore may present a potential liability. Chain L is the light chain of the NKG2D-targeting antibody A49M-I. Chain S contains a scFv that binds with high affinity to CLEC12A on AML cancer cells. Both scFv and Fab domains are fused to a human IgG1 Fc. Both chains bear several mutations in the CH3 domain introduced to ensure stable heterodimerization of two Fc monomers. There are seven such mutations in the IgG1 Fc of the AB0089: three mutations in Chain H and four mutations in Chain S. Two of these mutations are involved in the formation of a stabilizing S-S bridge (Y349C and S354C) between Chains H and Chain S (EU nomenclature). The scFv (VH-VL orientation) in Chain S is stabilized by two mutations introducing a S-S bridge ((H44)C and (L100)C, Chothia nomenclature). Chain S also contains a $(G_4S)_4$ non-immunogenic linker between VH and VL of the scFv. The amino acid sequence of the CLEC12A-targeting scFv is based on the sequence of humanized 16B8.C8 antibody, obtained from hybridoma (Green Mountain Antibodies). The amino acid sequence of the NKG2D Fab is based on the fully human antibody A49M-I, obtained using human yeast display technology (Adimab).

Amino acid sequence

[0885] The amino acid sequences of the three polypeptide chains that make up AB0089 are shown below. CDRs are defined using Chothia nomenclature and are represented in Table 126. The C-terminal K, commonly processed and cleaved in IgG1, is deleted in Chain S and Chain H to prevent heterogeneity.

[0886] **Chain S:** CLEC12A targeting scFv-CH2-CH3 (humanized sequence, CDRs are italicized, back mutations are double underlined, engineered scFv disulfide in lower case letters, and Fc mutations for heterodimerization and the engineered CH3 disulfide are single underlined).

[0887] QLQLQESGPGLVKPSETLSLTCTVS***GFSLTNY***GLHWIRQPPGK**c**LEWIGVI***WV GGA***TDYNPSLKSRVTISVDTSKNQFSLKLSSV**Q**AADTAVYYCA**K**_K_***GDYGDTLDY***WGQGT LVTVSSGGGGSGGGGSGGGGSGGGGSDIQMTQSPSSLSASVGDRVTITC***HASQNINFWL S***WYQQKPGKAPKLLIY***EASNLHT***GVPSRFSGSGSGTDFTLTISSLQPEDFATYYC***QQSHS***

YPLTFG**c**GTKLEIKGSDKTHTCPPCPAPELLGGPSVFLFPPKPKDTLMISRTPEVTCVVVD VSHEDPEVKFNWYVDGVEVHNAKTKPREEQYNSTYRVVSVLTVLHQDWLNGKEYKC KVSNKALPAPIEKTISKAKGQPREP**R**VYTLPP**C**RDELTKNQVSLTCLVKGFYPSDIAVEW ESNGQPENNYKTTPPVL**V**SDGSF**T**LYSKLTVDKSRWQQGNVFSCSVMHEALHNHYTQK SLSLSPG (SEQ ID NO:276)

[0888] **Chain H:** NKG2D targeting VH-CH1-CH2-CH3 (fully human, CDRs are italicized, Fc mutations for heterodimerization and the engineered CH3 disulfide are underlined).

[0889] EVQLVESGGGLVKPGGSLRLSCAAS***GFTFSSY***SMNWVRQAPGKGLEWVSSI***S SSSSY***IYYADSVKGRFTISRDNAKNSLYLQMNSLRAEDTAVYYCAR***GAPIGAAAGWFDP*** WGQGTLVTVSSASTKGPSVFPLAPSSKSTSGGTAALGCLVKDYFPEPVTVSWNSGALTS GVHTFPAVLQSSGLYSLSSVVTVPSSSLGTQTYICNVNHKPSNTKVDKKVEPKSCDKTH TCPPCPAPELLGGPSVFLFPPKPKDTLMISRTPEVTCVVVDVSHEDPEVKFNWYVDGVE VHNAKTKPREEQYNSTYRVVSVLTVLHQDWLNGKEYKCKVSNKALPAPIEKTISKAKG QPREPQV**C**TLPPSRDELT**E**NQVSLTCLVKGFYPSDIAVEWESNGQPENNYKTTPPVLDSD GSFFLYS**W**LTVDKSRWQQGNVFSCSVMHEALHNHYTQKSLSLSPG (SEQ ID NO:260)

[0890] **Chain L:** NKG2D targeting VL-CL (fully human, CDRs are italicized).

[0891] DIQMTQSPSSVSASVGDRVTITC***RASQGISSWLA***WYQQKPGKAPKLLIY***AASS LQS***GVPSRFSGSGSGTDFTLTISSLQPEDFATYYC***QQGVSFPRT***FGGGTKVEIKRTVAAPS VFIFPPSDEQLKSGTASVVCLLNNFYPREAKVQWKVDNALQSGNSQESVTEQDSKDSTY SLSSTLTLSKADYEKHKVYACEVTHQGLSSPVTKSFNRGEC (SEQ ID NO:261)

Table 126: AB0089 CDRs sequences.

AB0089	Variable region	Framework	CDR1	CDR2	CDR3
Chain S	VH	VH4-59	GFSLTNY (SEQ ID NO:137)	WVGGA (SEQ ID NO:272)	GDYGDTLDY (SEQ ID NO:273)
Chain S	VL	VK1-12	HASQNINFWLS (SEQ ID NO:140)	EASNLHT (SEQ ID NO:141)	QQSHSYPLT (SEQ ID NO:142)
Chain H	VH	VH3-21	GFTFSSY (SEQ ID NO:297)	SSSSY (SEQ ID NO:298)	GAPIGAAAGWFDP (SEQ ID NO:97)

AB0089	Variable region	Framework	CDR1	CDR2	CDR3
Chain L	VL	VK1-2	RASQGISSWLA (SEQ ID NO:86)	AASSLQS (SEQ ID NO:77)	QQGVSFPRT (SEQ ID NO:87)

CDRs are identified by Chothia

Analysis of potential sequence liabilities in CDRs

[0892] Chain L (NKG2D binding light chain) has no predicted liabilities. Chain H (NKG2D binding heavy chain) has a DP in CDRH3. This motif is not affected by forced degradation (as in other constructs, data not shown). As such, this sequence was not altered in AB0089. Chain S (CLEC12A binding scFv-Fc chain) has no predicted liabilities.

Description of heterodimerization mutations

[0893] EU-numbering convention was used to annotate the amino acid residues in the Fc. Chain H contains the following mutations:

K360E – Heterodimerization mutation in the CH3 domain of the Fc region.

K409W – Heterodimerization mutation in the CH3 domain of the Fc region.

Y349C – Inter-subunit disulfide stabilization mutation in the CH3 domain of the Fc region.

[0894] The K360E/K409W mutations in the Fc region of Chain H are designed to render heterodimer-favoring interactions with Chain S due to hydrophobic/steric complementarity plus long-range electrostatic interactions (Choi *et al.*, (2013) *Mol Cancer Ther*, 12, 2748–59; Choi *et al.*, (2015) *Mol Immuno*l, 65, 377–83). The mutation Y349C was introduced to generate an additional inter-chain disulfide bond Y349C-(CH3-ChainH) – S354C(CH3-ChainS) pair (Choi *et al.*, (2015) *Mol Immuno*l, 65, 377–83).

Chain S contains the following mutations:

G44C – Disulfide stabilization mutation in V_H region of the scFv.

S100C – Disulfide stabilization mutation in V_L region of the scFv.

Q347R – Heterodimerization mutation in the CH3 domain of the Fc region.

D399V – Heterodimerization mutation in the CH3 domain of the Fc region.

F405T – Heterodimerization mutation in the CH3 domain of the Fc region.

S354C – Inter-subunit disulfide stabilization mutation in the CH3 domain of the Fc region.

[0895] The mutations G44C and S100C were introduced to stabilize the scFv by an engineered disulfide bond between the VH and the VL. The disulfide stabilization improves structural and thermal stability of scFv. The Q347R/D399V/F405T mutations in the Fc region of Chain S were designed to render heterodimer-favoring interactions with Chain H due to hydrophobic/steric complementarity plus long-range electrostatic interactions (Choi *et al*, (2013) *Mol Cancer Ther*, 12, 2748–59). The mutation S354C was introduced to generate an additional inter-CH3 disulfide bond with a Y349C(CH3-ChainH) – S354C(CH3-ChainS) pair (Choi *et al*, (2015) *Mol Immuno*l, 65, 377–83).

[0896] The heterodimerization of the Chain H and Chain S is based on five mutations, so called, EW-RVT, with the interaction pairs K409W(CH3A)–D399V/F405T(CH3B) (dubbed the W-VT pair) and K360E(CH3A)–Q347R(CH3B) (dubbed the E-R pair), which were designed to replace the conserved electrostatic interactions with asymmetric hydrophobic interactions and to add asymmetric long-range electrostatic interactions at the rim of the heterodimeric CH3 interface, respectively (Choi *et al*., (2013) *Mol Cancer Ther*, 12, 2748–59). Detailed analysis of the heterodimeric CH3A–CH3B inter-face revealed very few structural perturbations resulting from mutations at the interface compared to the native IgG1 Fc (FIG. 109). Backbone and side-chain conformations of the residues adjacent to the interfacial mutations in Fc-EW-RVT are almost the same as those in Fc-WT, except for the side-chain substitutions of the mutated residues (FIG. 109A). The residues of W-VT mutation pairs, i.e., K409W(CH3A)–D399V(CH3B)/F405T(CH3B), were in close proximity to form complementary contacts in mostly buried CH3A–CH3B interfaces (FIG. 109B), suggesting that W-VT pairs strengthen the hydrophobic interface between CH3A–CH3B by forming optimal hydrophobic interactions. The residues of the E-R mutation pair, K360ECH3A–Q347RCH3B, were located sufficiently close at 3.45 Å to form a salt bridge unlike the wild-type K-Q pair (4.61 Å) (FIG. 109C), contributing to the preferential formation of the heterodimer by strong electrostatic interactions. Thus, the mutated residues introduced to Fc-EW-RVT form non-covalent interactions in the CH3A–CH3B interface favoring heterodimer formation without significant structural perturbations to the overall CH3 domain structure.

[0897] By design the W-VT pair residues (K409W(CH3A)–D399V(CH3B)/F405T(CH3B)) and E-R pair residues (K360E(CH3A)–Q347R(CH3B)) are in the heterodimeric CH3 interface to form asymmetric, complementary hydrophobic interactions and electrostatic interactions at 3.45

Å, respectively, which preferentially favor the heterodimer. On the other hand, the respective homodimer formation was thermodynamically dis-favored due to the steric clash between 409WCH3A and F405CH3A residues as well as the repulsive electrostatic interactions between the 347R(CH3B) and K360(CH3B) residues. The loss of the wild-type electrostatic interaction residues of K409WT–D39WT also discourages homodimer formation. Additional stabilization of heterodimer is brought by the inter-CH3 disulfide-bonded EW-RVT(S–S) variant with Y349C(CH3A) and S354C(CH3B) mutations (FIG. 110). The X-ray structure of Fc-EW-RVT(S-S) has been described at 2.5 Å resolution (Choi *et al.*, (2015) *Mol Immuno*l, 65, 377–83) and was very similar to the known IgG1 structures.

Structural modeling

[0898] In the absence of a crystal structure, structural models of the variable segments of CLEC12A and NKG2D binding arms were generated for comparison. Model building was performed using the SAbPred website (opig.stats.ox.ac.uk/webapps/newsabdab/sabpred/).

Surface charge distribution and hydrophobic patch analysis of CLEC12A binding arm of AB0089

[0899] FIG. 111 illustrates a ribbon diagram model of the CLEC12A binding scFv in three different orientations (upper panel) and their corresponding surface charge distribution of the same orientation (lower panel). The charge distribution of the anti-CLEC12A scFv is polarized ("top view", lower panel), with negatively charged residues populated predominately within CDRH3 and CDRL2. The uneven distribution of electrostatic patches on the paratope is likely to be target-related and reflects the complementarity of charge distribution on its cognate epitope, which may contribute to the high affinity interaction between CLEC12A and the scFv of AB0089.

[0900] FIG. 112 shows the analysis of CDR length and surface hydrophobicity patches of the CLEC12A-targeting arm of AB0089. Analyses were performed using therapeutic antibody profiles (TAP): opig.stats.ox.ac.uk/webapps/newsabdab/sabpred/tap . It compares the candidate in reference to 377 late-stage therapeutic antibodies. The length of CDRs for the CLEC12A-binding arm of AB0089 are within the normal range for late stage therapeutic antibodies. Hydrophobic patch analysis of the CDRs of an antibody is predictive of its developability. The theoretical hydrophobic properties of the CLEC12A binding arm of AB0089 are well within the norm of commercialized biotherapeutics and late-stage therapeutic antibody candidates.

[0901] FIG. 113 shows the analyses of patches containing positive and negative charges, as well as the symmetry of these charges around the CDR regions. All three charts indicate that the charge distributions are within the norm compared with the population of therapeutic antibodies.

Surface charge distribution and hydrophobic patch analysis of NKG2D binding arm of AB0089

[0902] The NKG2D-binding Fab is shown in ribbon diagrams with three different orientations (FIG. 114, upper panel) and the corresponding surface charge distribution in the same orientation are provided (FIG. 114, lower panel). The surface charge on the NKG2D binding arm is more evenly distributed than charges on the CLEC12A targeting arm.

[0903] FIG. 115 shows the CDR length and patches of surface hydrophobicity analyses of the NKG2D-targeting arm of AB0089. It appears that the CDR length, hydrophobic properties, and positive/negative charge distribution are well within the norm of existing therapeutic antibodies.

[0904] FIG. 116 shows the analyses of patches containing positive and negative charges, as well as the symmetry of these charges around the CDR regions. All three charts indicate that the charge distributions are within the norm comparing with the population of therapeutic antibodies.

Framework assessment

[0905] The CLEC12A binding arm of AB0089 was discovered through mouse immunization. The frameworks chosen for CDR grafting are frequently used in clinical stage therapeutic monoclonal antibodies (FIG. 117). The NKG2D binding arm is fully human, is based on a framework frequently used in advanced stage mAbs and does not contain any unusual residues or deviations from the germline.

Immunogenicity prediction

[0906] Protein sequences of the three chains of AB0089 were examined for the presence of potentially immunogenic T cell epitopes and to rank the immunogenicity potential using the EpiMatrix algorithm (FIG. 118). AB0089 scores favorably on the Treg adjusted Immunogenicity Protein Scale. The Treg adjusted EpiMatrix Protein Score for the sequences of the three chains of AB0089 are -33.39 (chain H), -27.13 (chain S), and -23.49 (chain L) (Table 127). The predicted risk of immunogenicity for the AB0089 appears to be low.

Table 127: EpiVax immunogenicity analysis of AB0089.

Protein Sequence	Length	EpiMatrix Hits	EpiMatrix Score	Treg adjusted Epx Score
AB0089_CHAIN_H	451	207	5.99	-33.39
AB0089_CHAIN_L	214	98	11.17	-23.49
AB0089_CHAIN_S	472	202	-2.96	-27.13

Expression

[0907] Expression of AB0089 was achieved using Dragonfly Tx F3' TriNKET platform purification method. Briefly, AB0089 was expressed by transient transfection of Expi293 and ExpiCHO cells with three plasmids encoding the NKG2D targeting light chain (chain L), the NKG2D targeting IgG heavy chain (chain H), and the CLEC12A targeting scFv-Fc fusion (chain S). For both Expi293 and ExpiCHO expression, Chain S: Chain H: Chain L were transfected at the plasmid ratio 4:1:1 to maximize the percentage of desired heterodimer product. This ratio was empirically obtained based on previous humanized TriNKETs and was not specifically optimized for AB0089.

Purification

[0908] Purification of AB0089 was performed using F3' TriNKET platform purification methods developed by Dragonfly Therapeutics (FIG. 119). This purification process has been applied before to material expressed in Expi293, ExpiCHO and CHO-M cell cultures for many different TriNKETs. No optimization or extensive process development for AB0089 purification was performed. Two-step purification process was employed.

[0909] Two lots of AB0089 were produced in transiently transfected ExpiCHO and Expi293 cells. Table 128 summarizes the titer and final product purity for both lots. Purification of the AB0089 lot AB0089-002 expressed in ExpiCHO is described in detail below.

Table 128: Summary of AB0089 purification.

Lot	Expression host	Titer mg/L	Purity, % Monomer
AB0089-001	Expi293	16.8	>99
AB0089-002	ExpiCHO	68.3	>99

Protein A capture

[0910] AB0089 was expressed in ExpiCHO cell line as described above. Approximately 5.7 liters of filtered supernatant was loaded on a Protein A column. Load flow rate was 10 ml/min

(298 cm/h; 3.3 minute residence time). The capture step yield was approximately 752 mg. FIG. 120 shows the capture step chromatogram.

[0911] By SEC analysis, the Protein A eluate contains mainly desired heterodimeric AB0089 species (approximately 88.8%) eluting at 23.4 min (FIG. 121). Impurities include HMW aggregates and very little amount of LMW.

[0912] SDS-PAGE analysis of the Protein A load, flow-though and eluate demonstrate that capture of AB0089 was complete, based on absence of a AB0089 band in the flow through sample. The protein A eluate lane shows primarily TriNKET with additional bands corresponding to the HMW and LMW peaks observed by SEC (FIG. 122).

Cation exchange chromatography

[0913] The Protein A eluate was further purified by cation exchange chromatography using a Poros XS column (1.2 cm D x 20 cm H) operated at a flow rate of 7 ml/min (371 cm/h; 3.2-minute residence time). The product began to elute with the 15% B elution step, when conductivity reached approximately 20 mS/cm (FIG. 123). SDS-PAGE analysis of the elution fractions shows highly pure product in the first five fractions (FIG. 124). Peak tail fractions were excluded from the IEX product pool as SDS-PAGE indicates the presence of contaminating product-related proteins.

[0914] The IEX fractions were concentrated resulting in approximately 401 mg of purified AB0089. The pooled fractions were buffer exchanged to PBS pH 7.4 by dialysis. The AB0089 yield after buffer exchange was approximately 391 mg at a final concentration of 9.66 mg/ml (AB0089 lot AB0089-002). Yields and recoveries for AB0089 lot AB0089-002 production are summarized in Table 129.

Table 129: Yields and recoveries of AB0089 purification and buffer exchange process.

Step	**Total Protein (mg)**	**Step Recovery (%)**	**Total Recovery (%)**
MabSelect SuRe Capture	752	NA	NA
POROS XS Polish	401	53	53
Post Buffer Exchange	391	98	52

NA, not applicable

Characterization of AB0089 Lot AB0089-002 used in cyno study

[0915] AB0089 lot AB0089-002 intended for use in cyno study was extensively characterized for purity, identity, binding to the targets and potency. All tested criteria met specification.

Purity by SDS-PAGE

[0916] SDS-PAGE of the final sample showed major bands were consistent with expected molecular weight for both reduced and non-reduced AB0089 (FIG. 125).

Purity by analytical SEC (Superdex 200)

[0917] SEC analysis of purified AB0089 lot AB0089-002 showed 100% monomer as determined by integrated peak area (FIG. 126).

Identity by intact mass analysis

[0918] The identity of AB0089 (lot AB0089-002) was corroborated by mass spectrometry (FIG. 127). LC-MS analysis of the intact AB0089 showed an observed mass (126,130.0 Da) that agrees well with the theoretical mass of 126,129.1 Da. The major observed glycosylation pattern (G0F/G0F) is typical for an Fc-containing molecule expressed in CHO cells.

Endotoxin

[0919] The endotoxin level of the final AB0089 lot AB0089-002 was 0.259 EU/mg. All assay parameters met specification.

Biochemical and biophysical properties

[0920] AB0089 was characterized by SEC, CE, cIEF, HIC, and DSC to corroborate that is has the proper purity and pre-developability characteristics of a good biological therapeutic.

Purity

[0921] Purify of AB0089 was determined by CE-SDS (FIG. 128). Under non-reduced conditions the major impurities are method induced (free light chain and TriNKET – LC). Under reduced conditions the 3 expected chains (LC, HC, and scFv-Fc chain) are observed. The purity of AB0089 lot AB0089-002 determined by SEC, NR and R CE-SDS is summarized in Table 130.

Table 130: Purity of AB0089 by SEC and CE-SDS analysis.

Test article	SEC			NR CE-SDS	R CE-SDS
	HMW (%)	Monomer (%)	LMW (%)	Purity (%)	Purity (%)
AB0089	ND	100	ND	98.9	98.0

ND, none detected

Experimental pI and charge profile by cIEF

[0922] Charge profile of AB0089 was analyzed by cIEF (FIG. 129). AB0089 showed a major peak at a pI of 8.52 ± 0.0. Several lesser abundant, overlapping acidic peaks and minor basic peaks are also observed.

Hydrophobicity assessed by HIC.

[0923] The hydrophobic properties of AB0089 were assessed by HIC (FIG. 130, Table 131). The chromatogram revealed a single narrow peak, indicating that the molecule is highly pure and homogeneous. The HIC retention time was 10.2 minutes, which is within the range of well behaving marketed monoclonal antibodies (8.9-13.5 minutes, data not shown).

Table 131: Hydrophobicity assessment of AB0089 by HIC. Humira is used as an internal control of well-behaved IgG1 mAb.

Test article	HIC retention time (min)
AB0089	10.2
Humira	8.9

Thermal stability by DSC

[0924] The thermal stability of AB0089 was assessed by DSC in several buffers (PBS pH 7.4, HST pH 6.0, CST pH 7.0). AB0089 demonstrated high thermal stability in all buffers tested (FIG. 131). T_{m1} corresponding to the unfolding of scFv satisfied the ≥65°C criteria utilized in thermostability assessment (Table 132).

Table 132: Thermal stability of AB0089 by DSC.

Test Article	Buffer	T_{onset} (°C)	T_{m1} (°C)	T_{m2} (°C)	T_{m3} (°C)	T_{m4} (°C)
AB0089	PBS, pH 7.4	64.0	71.8	76.7	81.3	83.4
AB0089	HST, pH 6.0	61.2	69.0	78.7	84.3	86.3
AB0089	CST, pH 7.0	64.7	72.4	77.1	82.2	84.2

Disulfide bond assignment

[0925] AB0089 is an engineered molecule based on the backbone of a monoclonal IgG1 antibody. While a typical IgG1 contains 16 disulfide bonds, AB0089's F3' format has only 15 disulfide bonds. Half of AB0089 is an anti-NKG2D half antibody, as such it contains the expected seven disulfide bonds (one in each IgG domain and the intermolecular disulfide connecting the LC to the HC). The other half of AB0089 is an anti-CLEC12A scFv-Fc fusion. The scFv contains three disulfide bonds (one in each anti-CLEC12A VH and VL domains and an engineered, stabilizing disulfide bridging the variable domains) and the Fc contains the two expected disulfides in the IgG domains. The heterodimer is covalently associated with two native IgG1 hinge disulfides and one additional intermolecular engineered disulfide connecting the Fab-Fc to the scFv-Fc in the CH3 domain. Together this results in 15 expected disulfide bonds in AB0089. The predicted disulfide map for AB0089 is shown in FIG. 132.

[0926] The disulfide bond connectivity of AB0089 was corroborated by LC-MS/MS peptide mapping analysis of a non-reduced digest. Disulfide bonded peptides were identified by MS/MS database searching and corroborated by comparing their intensities in the native and reduced digests. In the tryptic digestion, the VL and engineered disulfide pairs are connected by a long peptide that contains 2 cysteines (three peptides connected by two disulfide bonds, S7:S36:S22) that is not observed in the LC-MSMS data. To detect the engineered scFv stabilizing disulfide, AB0089 was digested with both trypsin and chymotrypsin. FIG. 133 shows the extracted ion chromatogram (XICs) for the engineered disulfide pair in the scFv (non-reduced and reduced) and the most intense charge state for that peptide pair. The VL disulfide pair was not observed in the trypsin/chymotrypsin double digest, presumably because it is too small and hydrophilic to be retained on the column. All other disulfides were identified after digestion with only trypsin, including the engineered S-S bridge introduced to stabilize the Fc heterodimerization (FIG. 134).

[0927] A summary of the observed disulfide linked peptides in AB0089 is shown in Table 133. All observed disulfide linked peptides were had high mass accuracy (<4 ppm), were reducible, and were sequence corroborated by MS/MS fragmentation.

Table 133: Disulfide linked peptides theoretical and experimental masses.

Domain	Tryptic peptide	Theoretical mass (Da)	Experimental mass (Da)	Mass accuracy (ppm)
VL	L2:L7	4482.0784	4482.0786	0.4

Domain	Tryptic peptide	Theoretical mass (Da)	Experimental mass (Da)	Mass accuracy (ppm)
CL	L12:L19	3555.749	3555.755	1.8
CL-CH1 intermolecular	L20-21:H19	1260.4863	1260.4861	-0.3
VH	H3:H10	3371.4686	3371.4666	2.5
CH1	H13:H14-15	7916.9194	7916.9282	1.5
Hinge	H20-21:S17-18	5454.7834	5454.7905	1.5
CH2	H23:H30	2328.0977	2328.1018	1.8
CH3-CH3 intermolecular[a]	H36:S34-35	2757.383	2757.3855	1.6
CH3	H37:H41	4432.0675	4432.0687	0.3
scFv VH	S1-2:S8	5828.907	5828.9052	-0.1
scFv stabilizing[a]	S7:S36[b]	1011.4154	1011.4188	3.4
scFv VL	S10-11:S14	Not detected		
CH2	S20:S27	non-unique, see H23:H30		
CH3	S36:S41	3844.8236	3844.8284	1.2

[a]Engineered disulfide, [b]Trypsin/chymotrypsin double digest

Binding characteristics

Binding affinity for human CLEC12A

[0928] The affinity of AB0089 for human CLEC12A was determined by SPR at 37°C. AB0089 binds with high affinity to human CLEC12A (FIG. 135 and Table 134). However, the binding demonstrates heterogeneity and does not follow typical 1:1 binding kinetics. An experiment described below and in FIG. 136 established a two-state binding mechanism and justified the use of a two-state model for fitting the data. Similar two-state reaction kinetics was observed for CLEC12A binding arm of tepoditamab (Merus).

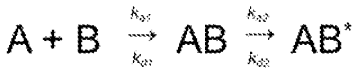
Table 134: Kinetic parameters and binding affinity of AB0089 for hCLEC12A.

Test article	k_{a1} ($M^{-1}s^{-1}$)	k_{d1} (s^{-1})	k_{a2} (s^{-1})	k_{d2} (s^{-1})	K_D (nM)
AB0089	1.09×10^{7}	4.26×10^{-2}	3.41×10^{-3}	7.28×10^{-4}	0.69
AB0089	1.06×10^{7}	4.49×10^{-2}	3.49×10^{-3}	7.48×10^{-4}	0.75
AB0089	1.02×10^{7}	4.32×10^{-2}	3.45×10^{-3}	7.41×10^{-4}	0.75
AB0089	9.99×10^{6}	4.32×10^{-2}	3.39×10^{-3}	7.49×10^{-4}	0.78

Test article	k_{a1} ($M^{-1}s^{-1}$)	k_{d1} (s^{-1})	k_{a2} (s^{-1})	k_{d2} (s^{-1})	K_D (nM)
Average ± Std Dev.	$(1.04\pm0.03)\times10^{7}$	$(4.35\pm0.12)\times10^{-2}$	$(3.43\pm0.04)\times10^{-3}$	$(7.41\pm0.10)\times10^{-4}$	0.74±0.04

[0929] A two-state binding model assumes two binding stages that are defined by two sets of kinetic constants:

1. formation of an initial CLEC12A-AB0089 complex
2. transition of the initial complex into a more stable, final complex



[0930] This mechanism implies that longer association times in an SPR experiment would lead to a higher ratio of the more stable complex on the surface and a slower apparent dissociation rate. Both AB0089 and a tepoditamab based molecule have an association time dependent apparent dissociation rate, thus corroborating the two-state interaction model (FIG. 136).

Binding to CLEC12A+ isogenic and cancer cell lines

[0931] Assessment of AB0089 binding to isogenic cell lines expressing CLEC12A and AML cancer cells was monitored by FACS (FIG. 137, Table 135). AB0089 showed high affinity for cell surface expressed CLEC12A and binds AML cell lines PL-21 and HL-60 with EC50 less than 1 nM. Specificity of AB0089 for CLEC12A was demonstrated by lack of binding to the parental Ba/F3 cells that do not express the target.

Table 135: Binding of AB0089 to isogenic and cancer cell lines expressing CLEC12A.

Cell line	EC50 (nM)
Ba/F3-hCLEC12A	4.02
Ba/F3 parental	No binding
PL21	0.45
HL-60	0.74

Binding affinity for polymorphic variant of human CLEC12A (Q244)

[0932] Polymorphic variant CLEC12A (Q244) is prevalent in 30% of population. We tested binding of AB0089 to this genetic variant by SPR and compared its affinity to the major form of CLEC12A (K244) (FIG. 138). Binding affinities of AB0089 for WT and Q244 variant of CLEC12A were similar (Table 136). Binding of AB0089 to cynomolgus monkey CLEC12A (cCLEC12A) was also tested. No binding was observed at 100 nM concentration, demonstrating that AB0089 is not cross-reactive to cynomolgus CLEC12A.

Table 136: Kinetic parameters and binding affinity of AB0089 for (K244) and (Q244) variants of human CLEC12A.

Test article	Target	k_{a1} ($M^{-1}s^{-1}$)	k_{d1} (s^{-1})	k_{a2} (s^{-1})	k_{d2} (s^{-1})	K_D (nM)
AB0089	hCLEC12A (K244) WT	(1.63±0.51) $\times 10^{7}$	(3.98±0.14) $\times 10^{-2}$	(2.95±0.06) $\times 10^{-3}$	(9.62±0.00) $\times 10^{-4}$	0.60 ± 0.26
AB0089	hCLEC12A (Q244)	(9.70±0.45) $\times 10^{6}$	(3.53±0.13) $\times 10^{-3}$	(2.67±0.06) $\times 10^{-3}$	(1.25±0.02) $\times 10^{-3}$	1.17 ± 0.00

Binding to differentially glycosylated CLEC12A

[0933] Human CLEC12A is a heavily glycosylated protein (6 potential N-glycosylation sites with an extracellular domain (ECD) compromising of 201 amino acids). Variations in the glycosylation status of CLEC12A on the surface of different cell types is documented in the literature (Marshall *et al.*, (2006) *Eur. J. Immunol.*, 36: 2159-2169). CLEC12A expressed on the surface of AML cells from different patients may have different glycosylation patterns as well. To determine if AB0089 binds to different glyco-variants of human CLEC12A, the antigen was treated with neuraminidase (to remove terminal sialic acids) or PNGaseF (to remove N-linked glycans) and affinity was compared to untreated CLEC12A by SPR (FIG. 139 and Table 137). AB0089 bound to both fully glycosylated and de-glycosylated CLEC12A and is expected to be unaffected by heterogeneity in target glycan composition.

Table 137: Kinetic parameters and binding affinity of AB0089 for differentially glycosylated CLEC12A.

Test article	Target	k_{a1} ($M^{-1}s^{-1}$)	k_{d1} (s^{-1})	k_{a2} (s^{-1})	k_{d2} (s^{-1})	K_D (nM)
AB0089	Untreated CLEC12A	(1.63±0.05) × 10^7	(3.98±0.01) × 10^{-2}	(2.95±0.06) × 10^{-3}	(9.62±0.00) × 10^{-4}	0.60 ± 0.26
AB0089	De-sialylated CLEC12A	(2.09±0.21) × 10^7	(3.29±0.18) × 10^{-2}	(3.04±0.06) × 10^{-3}	(8.63±0.24) × 10^{-4}	0.35 ± 0.47
AB0089	De-glycosylated CLEC12A	(8.96±0.86) × 10^6	(6.33±0.28) × 10^{-3}	(4.09±0.13) × 10^{-3}	(5.67±0.10) × 10^{-4}	0.09 ± 0.01

Average of 3 replicates

Binding affinity for human NKG2D

[0934] AB0089 was tested for binding to human NKG2D ECD by SPR (Biacore) at 37°C (FIG. 140). NKG2D is a dimer in nature, therefore recombinant mFc-tagged NKG2D dimer was used for this experiment. The shape of the binding sensorgrams depicted in FIG. 140 enabled two different fitting models to calculate affinity and kinetic rates data: steady state affinity fit and 1:1 kinetic fit. The kinetic constants and equilibrium affinity values are shown in Table 138. AB0089 was designed to bind to human NKG2D with low affinity, most importantly with the fast rate of dissociation. The dissociation rate constant was 1.43±0.03 x 10^{-1} s^{-1}. Affinity values (K_D) obtained by fitting the data to a 1:1 kinetic and steady state affinity models were very similar, 881 ± 10 nM and 884 ± 11 nM respectively, which suggests high confidence in the measured parameters.

Table 138: Kinetic parameters and binding affinity of AB0089 for human NKG2D.

Test article	k_a ($M^{-1}s^{-1}$)	k_d (s^{-1})	Kinetics Fit K_D (nM)	Steady State Fit K_D (nM)
AB0089	1.61 x 10^5	1.41 x 10^{-1}	872	873
AB0089	1.59 x 10^5	1.42 x 10^{-1}	892	894
AB0089	1.66 x 10^5	1.46 x 10^{-1}	880	885
Average ± Std Dev.	**(1.62±0.03) x10^5**	**(1.43±0.03) x10^{-1}**	**881 ± 10**	**884 ± 11**

Binding affinity for CD16a (FcγRIIIa)

[0935] One of the modalities of AB0089 mechanism of action is through engaging human CD16a (FcγRIIIa) that is expressed on NK cells via its Fc. Binding of AB0089 to CD16a (V158

allele) was evaluated by SPR and compared to the CD16a (V158) affinity for trastuzumab, an approved and marketed monoclonal antibody therapeutics of the same IgG1 isotype (FIG. 141, Table 139). Binding of AB0089 to CD16a is comparable to the one of trastuzumab. A 3.8-fold difference in affinity is unlikely to be of physiological consequence and is also unlikely to impact AB0089 therapeutic effect since the latter relies on synergy of simultaneous engagement of two targets on the NK cells, CD16 and NKG2D. Additionally, a slightly weaker binding to CD16a may also be of benefit for the drug's safety.

Table 139: Kinetic parameters and binding affinity of AB0089 for hCD16a (V158).

Test article	k_a ($M^{-1}s^{-1}$)	k_d (s^{-1})	K_D (nM)
AB0089	8.76×10^4	2.94×10^{-2}	336
AB0089	7.70×10^4	2.64×10^{-2}	343
AB0089	8.46×10^4	2.72×10^{-2}	321
Average ± StDev	**$(8.31 \pm 0.55) \times 10^4$**	**$(2.77 \pm 0.16) \times 10^{-2}$**	**333 ± 11**
trastuzumab	1.31×10^5	1.12×10^{-2}	86
trastuzumab	1.22×10^5	1.08×10^{-2}	89
trastuzumab	1.30×10^5	1.13×10^{-2}	87
Average ± StDev	**$(1.28 \pm 0.05) \times 10^5$**	**$(1.11 \pm 0.03) \times 10^{-2}$**	**87 ± 1**

Binding to Fcγ receptors

[0936] Since AB0089 is an IgG1 derived biologic drug candidate it is important that it maintains appropriate Fc receptor binding properties. SPR data suggest that AB0089 binds human and cynomolgus Fcγ receptors with affinities comparable to trastuzumab, a marketed IgG1 biologic that served an experimental control (Table 140). Detailed description of each individual receptor binding is presented below.

Table 140: Summary of affinities of AB0089 and trastuzumab for human and cynomolgus FcγRs.

Fcγ receptor	AB0089, K_D (nM)	trastuzumab, K_D (nM)
hFcγRI	5.1 ± 1.0	2.9 ± 0.4
cFcγRI	1.5 ± 0.3[a]	1.0 ± 0.1
hFcγRIIa H131	900.4 ± 57.1	1045.1 ± 62.2

hFcγRIIa R131	1253.3 ± 269.2	1493.2 ± 265.9
hFcγRIIIa V158	333.4 ± 11.1	87.1 ± 1.4
hFcγRIIIa F158	1271.0 ± 24.6	331.4 ± 3.3
cFcγRIII[a]	348.8 ± 2.4	128.8 ± 2.1
hFcγRIIb	6270.3 ± 1164.4	6270.3 ± 1031.7
hFcγRIIIb[a]	8851.3 ± 1454.4	3872.4 ± 486.3

[a]n=3, otherwise n=4

Binding of AB0089 to recombinant human and cynomolgus CD64 (FcγRI)

[0937] FIG. 142 and FIG. 143 depict binding of AB0089 to human and cynomolgus CD64, respectively. Table 141 demonstrates that AB0089 binds recombinant human and cynomolgus CD64 with affinities comparable (less than two-fold different) to trastuzumab.

Table 141: Binding of AB0089 and trastuzumab to human and cynomolgus CD64.

Human FcγRI	**k_a ($M^{-1}s^{-1}$)**	**k_d (s^{-1})**	**K_D (nM)**
AB0089 Lot AB0089-002	4.4×10^4	1.8×10^{-4}	6.4
AB0089 Lot AB0089-002	4.6×10^4	2.2×10^{-4}	4.7
AB0089 Lot AB0089-002	4.6×10^4	1.9×10^{-4}	4.1
AB0089 Lot AB0089-002	4.6×10^4	2.4×10^{-4}	5.2
Average ± StDev	**$(4.6 \pm 0.1) \times 10^4$**	**$(2.3 \pm 0.4) \times 10^{-4}$**	**5.1 ± 1.0**
trastuzumab	9.0×10^4	2.3×10^{-4}	2.5
trastuzumab	8.6×10^4	2.1×10^{-4}	2.5
trastuzumab	8.3×10^4	2.7×10^{-4}	3.2
trastuzumab	8.8×10^4	2.8×10^{-4}	3.2
Average ± StDev	**$(8.1 \pm 0.0) \times 10^4$**	**$(2.5 \pm 0.3) \times 10^{-4}$**	**2.9 ± 0.4**
Cynomolgus FcγRI	**k_a ($M^{-1}s^{-1}$)**	**k_d (s^{-1})**	**K_D (nM)**
AB0089 Lot AB0089-002	5.5×10^4	8.1×10^{-5}	1.5
AB0089 Lot AB0089-002	5.4×10^4	9.5×10^{-5}	1.8
AB0089 Lot AB0089-002	5.5×10^4	6.6×10^{-5}	1.2
Average ± StDev	**$(5.5 \pm 0.0) \times 10^4$**	**$(8.1 \pm 1.5) \times 10^{-5}$**	**1.5 ± 0.3**
trastuzumab	1.3×10^5	1.4×10^{-4}	1.1
trastuzumab	1.3×10^5	1.2×10^{-4}	0.9
trastuzumab	1.3×10^5	1.1×10^{-4}	0.8

trastuzumab	1.3 x 10^{5}	1.3 x 10^{-4}	1.0
Average ± StDev	**(1.3 ± 0.1) x 10^{5}**	**(1.2 ± 0.2) x 10^{-4}**	**1.0 ± 0.1**

Binding of AB0089 to recombinant human CD32a (FcγRIIa)

[0938] FIG. 144 and FIG. 145 depict binding of AB0089 and trastuzumab to CD32a (H131 and R131 alleles), respectively, tested by SPR. There is no meaningful difference between affinities of both alleles for AB0089 and trastuzumab (Table 142).

Table 142: Binding of AB0089 and trastuzumab to recombinant human CD32a (FcγRIIa).

Test article	**K_D (nM)**	
	FcgRIIa H131	**FcgRIIa R131**
AB0089 (lot AB0089-002)	953.6	1335.7
AB0089 (lot AB0089-002)	822.8	1024.1
AB0089 (lot AB0089-002)	930.1	1598.0
AB0089 (lot AB0089-002)	895.0	1055.3
Average ± StDev	**900.4 ± 57.1**	**1253.3 ± 269.2**
trastuzumab	1069.2	1488.2
trastuzumab	953.1	1381.0
trastuzumab	1090.2	1862.1
trastuzumab	1068.0	1241.4
Average ± StDev	**1045.1 ± 62.2**	**1493.2 ± 265.9**

Binding of AB0089 to human CD16a (FcγR3a) and cynomolgus CD16 (FcγR3)

[0939] Detailed description of AB0089 binding to high affinity CD16a (V158) is provided herein. Binding of AB0089 to the F158 allele of human CD16a and cynomolgus CD16 are presented in Table 143, FIG. 146 and FIG. 147. Binding of AB0089 to recombinant human CD16a (V158 and F158 alleles) and cynomolgus CD16 is comparable to a marketed IgG1 biologic drug trastuzumab. A 2.3-3.8 difference in affinity for CD16 proteins between AB0089 and trastuzumab is unlikely to be of physiological consequence and also unlikely to impact the therapeutic effect since the latter relies on the synergy of engagement of two targets on the NK cells (CD16a and NKG2D). Small difference in apparent maximum binding responses between trastuzumab and AB0089 is attributed to a difference in molecular weight. Additionally, some replicates may display slight variability in apparent maximum binding responses caused by slight

variation of receptor capture levels. Note that while the shape of the sensorgrams representing binding to human CD16a F158 allele affords fitting the interactions to both, steady-state and 1:1 kinetic, models, affinity fit (steady-state) model was used for historic reasons.

Table 143: Binding of AB0089 and trastuzumab to recombinant human CD16a F158 allele and cynomolgus CD16a.

Test article	Human FcγRIIIa F158 K_D (nM)	Cyno FcγRIII K_D (nM)
AB0089 (AB0089-002)	1250.9	351.3
AB0089 (AB0089-002)	1250.6	346.7
AB0089 (AB0089-002)	1282.2	348.3
AB0089 (AB0089-002)	1300.4	
Average ± StDev	**1271.0 ± 24.6**	**348.8 ± 2.4**
trastuzumab	332.3	127.1
trastuzumab	326.6	128.1
trastuzumab	333.8	131.1
trastuzumab	333.1	
Average ± StDev	**331.4 ± 3.3**	**128.8 ± 2.1**

Binding of AB0089 to human CD32b (FcγR2b)

[0940] FIG. 148 depicts binding to AB0089 and trastuzumab to CD32b tested by SPR. There is no meaningful difference between affinities of CD32b for AB0089 and trastuzumab (Table 144).

Table 144: Binding of AB0089 and trastuzumab to CD32b (FcγR2b).

Test article	K_D (μM)
AB0089 (lot AB0089-002)	7.1
AB0089 (lot AB0089-002)	5.3
AB0089 (lot AB0089-002)	5.3
AB0089 (lot AB0089-002)	7.4
Average ± StDev	**6.3 ± 1.2**
trastuzumab	7.1
trastuzumab	5.6

trastuzumab	5.2
trastuzumab	7.2
Average ± StDev	**6.3 ± 1.0**

Binding of AB0089 to human CD16b (FcγR3b)

[0941] FIG. 149 depicts binding of AB0089 and trastuzumab to CD16b tested by SPR. AB0089 binds human CD16b (FcγR3b) comparably to trastuzumab (Table 145). 2.3-fold difference in affinity for the receptor is unlikely to be of physiological significance.

Table 145: Binding of AB0089 and trastuzumab to recombinant human CD16b (FcγR3b).

Test Article	**K_D (μM)**
AB0089 (lot AB0089-002)	10.3
AB0089 (lot AB0089-002)	8.8
AB0089 (lot AB0089-002)	7.4
Average ± StDev	**8.9 ± 1.5**
trastuzumab	4.3
trastuzumab	3.9
trastuzumab	3.4
Average ± StDev	**3.9 ± 0.5**

Binding to FcRn

[0942] FIG. 150 and FIG. 151 depict AB0089 binding to human and cyno FcRn, respectively, tested by SPR. Affinities of AB0089 for human and cynomolgus FcRn are similar to those of trastuzumab, a marketed IgG1 biologic that served as an experimental control (Table 146).

Table 146: Summary of affinities of AB0089 and trastuzumab for human and cyno FcRn.

FcRn	**AB0089, K_D (μM)**	**trastuzumab, K_D (μM)**
hFcRn, pH 6.0	1.1 ± 0.1	1.7 ± 0.2
cFcRn, pH 6.0[a]	1.0 ± 0.1	1.5 ± 0.1

[a]n=3, otherwise n=4

Simultaneous engagement of AB0089 to CD16a and NKG2D

[0943] AB0089 is a tri-functional IgG-based biologic with two binding modalities on the NK cells: CD16a binding is achieved through the Fc and NKG2D binding is achieved through A49M-I Fab. Both interactions are important for the optimal cytotoxic activity of AB0089. To demonstrate synergy of co-engagement of human CD16a and human NKG2D binding, we performed an SPR experiment where we qualitatively compared binding of AB0089 to NKG2D, CD16a and mixed NKG2D-CD16a Biacore chip surfaces. The affinity of AB0089 for human NKG2D and human CD16a are both low, however, binding to both targets simultaneously results in an avidity effect that manifests as a slower off-rate. Thus, AB0089 can avidly engage CD16a and NKG2D (FIG. 152).

Co-engagement of CLEC12A and NKG2D

[0944] To determine if binding of one target interferes with binding of the other target to AB0089, the CLEC12A and NKG2D were sequentially injected over AB0089 captured on an anti-hFc IgG SPR chip (FIG. 153). Target binding sensorgrams demonstrate that the occupancy status of the CLEC12A domain does not interfere with NKG2D binding (FIG. 153, upper panel) and vice versa (FIG. 153, lower panel). Similarity in shapes of the respective sensorgram segments depicting binding of each target to free AB0089 and AB0089 that has been saturated with the other target suggests that the kinetic parameters are not meaningfully affected by the target occupancy status of the AB0089 molecule. For instance, the shape of the CLEC12A binding segment of the sensorgrams is similar in both panels. Note that saturating concentration of the NKG2D had to be maintained throughout the entire experiment represented in lower panel due to fast dissociation rate of this target. Additionally, the lack of any impact on relative stoichiometry of each target binding (when compared to binding to unoccupied AB0089) signifies full independence of NKG2D and CLEC12A binding sites on AB0089 (Table 147). Therefore, AB0089 may successfully achieve simultaneous co-engagement of the tumor antigen and the NKG2D targeting arm.

Table 147: Relative binding stoichiometry of AB0089 for CLEC12A and NKG2D.
Binding stoichiometries are expressed relative to binding of each target to unoccupied captured AB0089.

	CLEC12A, relative binding stoichiometry	**NKG2D,** relative binding stoichiometry
Target bound to AB0089 unoccupied with another target (injected first)	1.00	1.00
Target bound to AB0089 saturated with another target (injected second)	1.16 ± 0.02	1.16 ± 0.06

Epitope binning

[0945] We compared binding epitope of AB0089 in relation to AB0237, AB0192 and three CLEC12A binding reference TriNKETs by SPR. cFAE-A49. Tepoditamab is based on CLEC12A binding arm of a molecule from Merus (WO_2014_051433_A1), cFAE-A49. CLL1-Merus is based on the clone 4331 from Merus (WO_2014_051433_A1) and cFAE-A49. h6E7 is based on h6E7 mAb from Genentech (h6E7) (US_2016_0075787_A1). AB0089 interaction with hCLEC12A was blocked by AB0237, and two control molecules, cFAE-A49. CLL1-Merus and cFAE-A49. Tepoditamab, but not by not Genentech-h6E7 based molecule (FIG. 154) suggesting that the binding epitope of AB0089 overlaps with the epitope of tepoditamab. The results indicated that both AB0089 and AB0237 share the same epitope. This footprint is different from AB0192 which additionally cross-blocks with cFAE-A49.h6E7.

Potency

[0946] Potency of AB0089 was tested using the KHYG-1-CD16aV cytotoxicity assay with a NK cell line engineered to stably express CD16aV and NKG2D (FIG. 155 and Table 148). AB0089 demonstrated sub-nanomolar potency in driving the lysis of HL60 and PL-21 AML cells. In addition AB0089 potently enhances cytotoxic lysis of PL21 AML cells mediated by purified human primary NK cells vastly outperforming the corresponding monoclonal antibody (FIG. 156 and Table 149). Additional cytotoxicity assessment of AB0089 is described in detail in Example 18.

Table 148: Potency of AB0089 in KHYG-1-CD16aV mediated cytotoxicity assay with HL60 and PL21 cells.

Cancer cell	**EC50 (nM)**	**Max killing (%)**
HL60	0.27	111

Cancer cell	EC50 (nM)	Max killing (%)
PL21	0.16	83

Table 149: Potency of AB0089 in primary NK mediated cytotoxic killing of PL21 cells.

Test article	EC50 (nM)	Max killing (%)
AB0089	0.35	20
AB0305 - parental mAb	1.85	5

Specificity

Non-specific binding assessed by PSR

[0947] To assess the specificity of AB0089, a flow cytometry based PSR assay that measures binding to a preparation of detergent solubilized CHO cell membrane proteins was performed (FIG. 157). The PSR assay has been demonstrated to correlate with orthogonal specificity assays such as cross-interaction chromatography, and the baculovirus particle enzyme-linked immunosorbent assay. Behavior in these assays strongly associates with antibody solubility and *in vivo* clearance and therefore serves as a good developability predictive factor (Xu *et al.*, (2013) *Protein engineering design and selection*, 26, 663-670). AB0089 showed very similar profile to the low PSR control (Trastuzumab), suggesting high specificity and lack of non-specific binding to unrelated proteins (FIG. 157B). Rituximab was used as a positive control for PSR binding.

Specificity assessment of AB0089 in HuProt™ array

[0948] To directly examine the specificity of AB0089 we have explored a protein array technology. The HuProt™ human proteome microarray provides the largest database of individually purified human full-length proteins on a single microscopic slide. An array consisting of 22,000 full-length human proteins are expressed in *S.cerevisiae* yeast, purified, and are subsequently printed in duplicate on a microarray glass slide that allows thousands of interactions to be profiled in a high-throughput manner. FIG. 158 shows the relative binding (Z score) of AB0089 at 1 μg/ml to human CLEC12A in comparison to the entire human proteome microarray. For comparison purpose, the top 24 proteins with residual background binding to AB0089 were also provided. Table 150 shows the Z and S scores of AB0089 to human CLEC12A and the top 6 proteins from the microarray. S score is the difference of Z score of a

given protein and the one rank next to it. Based on the Z and S score criteria, AB0089 showed high specificity to human CLEC12A and lack of off-target binding in the HuProt™ human proteome assay.

Table 150: Summary of the top hits by HuProt™ array

Name	Rank	Protein-ID	Z score	S score
hCLEC12A	1	hCLEC12A	150.61	146.120
RPLP0	2	JHU16464.P173H05	4.49	0.051
POLR2E	3	JHU02080.P189F02	4.44	0.57
RPRD1A	4	JHU16457.P173E09	3.86	0.01
ZNF608	5	JHU13018.P136G04	3.85	0.10
ECDHDC1	6	JHU25034.P240F11	3.75	0.06
BC089418	7	JHU16002.P168E09	3.70	0.12

Developability assessment

[0949] The stability and forced degradation of AB0089 was assessed under the following conditions:

- Accelerated (40°C) stability
  - 20 mg/ml AB0089 in a formulation HST, pH 6.0 (20 mM histidine, 250 mM sucrose, 0.01% Tween-80, pH 6.0), 40°C, 4 weeks (SEC, SPR, potency, CE-SDS, peptide map).
  - 20 mg/ml AB0089 in CST, pH 7.0 (20 mM sodium citrate, 250 mM sucrose, 0.01% Tween-80, pH 7.0), 40°C, 4 weeks (SEC, SPR, potency, CE-SDS, peptide map).
- Chemical stability
  - Oxidation: 1 mg/ml AB0089 in PBS with 0.02% hydrogen peroxide, room temperature, 24 hours (SEC, CE-SDS, SPR, potency, peptide map).
  - pH 8.0: 1 mg/ml AB0089 in 20 mM Tris, 40°C, 2 weeks (cIEF, SPR, potency, peptide map).
  - pH 5.0: 1 mg/ml AB0089 in 20 mM sodium acetate, 40°C, 2 weeks (cIEF, SPR, potency, peptide map).
- Manufacturability

- Freeze/thaw: 20 mg/ml AB0089 in 20 mM sodium citrate, 250 mM sucrose, 0.01% Tween-80, pH 7.0 (SEC, SDS-CE)
- Agitation: 10 mg/ml AB0089 in 20 mM sodium citrate, 250 mM sucrose, 0.01% Tween-80, pH 7.0 (SEC, SDS-CE)
- High concentration: >150 mg/ml, PBS (SEC, A280)
- Low pH hold (mimicking conditions of viral clearance step of manufacturing process): pH 3.3, 1.5 hours, ProA eluate (SEC); fully purified AB0089 (cIEF, CE-SDS, SPR, potency)
- Low pH hold (to investigate isomerization): fully purified AB0089 was diluted with ProA elution buffer and pH adjusted to 3.5. The sample was held for 1 hour at room temperature, neutralized with Tris buffer and buffer exchanged into PBS, pH 7.4. before additional analysis (SEC, cIEF, CE-SDS, SPR, potency, peptide map).

Accelerated (40℃) stability

[0950] To assess the stability of AB0089, the molecule was staged at protein concentration of 20 mg/ml at 40 °C for 4 weeks under two different buffer conditions (1) in 20 mM histidine, 250 mM sucrose, 0.01% PS-80, pH 6.0 (HST), and (2) in 20 mM citrate, 250 mM sucrose, 0.01% PS-80, pH 7.0 (CST). Stability in both buffers was assessed by SEC, CE, SPR and potency.

Stability in HST, pH 6.0

[0951] AB0089 demonstrated high stability after 4 weeks of incubation in HST, pH 6.0, at 40 °C. No aggregation and minimal loss of monomer (1.6%) was observed by SEC (FIG. 159 and Table 151). Minimal fragmentation was detected by R CE-SDS (FIG. 160 and Table 152). Additionally, there was no meaningful difference observed in the amount of active species, binding kinetics or affinities for hCLEC12A, hNKG2D and hCD16a between control and stressed samples (FIG. 161 and Table 153). Finally, no difference in potency between the control and stressed samples was detected (FIG. 162 and Table 154).

Table 151: SEC analysis of AB0089 after 2 and 4 weeks incubation at 40°C in HST, pH 6.0.

Test Article	Monomer (%)	LMWS (%)	HMWS (%)
AB0089 control	99.5	0.5	0.0

Test Article	Monomer (%)	LMWS (%)	HMWS (%)
AB0089, HST, pH6.0, 40°C, 2 wks	99.1	0.9	ND
AB0089, HST, pH6.0, 40°C, 4 wks	98.4	1.3	0.4

Table 152: NR and R CE-SDS analysis of AB0089 after 4 weeks at 40°C in HST, pH 6.0.

Test article	NR CE Purity (%)	R CE Purity (%)
AB0089 control	98.2	94.3
AB0089, HST, pH6.0, 40°C, 4 wks	98.3	97.2

Table 153: Kinetic parameters and binding affinities of AB0089 for CLEC12A, NKG2D and CD16a after 4 weeks at 40°C in HST, pH 6.0.

Test article	Target	k_a ($M^{-1}s^{-1}$)		k_d (s^{-1})		K_D (nM)
AB0089 Control	hCLEC12A	k_{a1} ($M^{-1}s^{-1}$) (8.87±0.53) x10^6	k_{a2} (s^{-1}) (3.49±0.04) x10^{-3}	k_{d1} (s^{-1}) (4.20±0.07) x10^{-2}	k_{d2} (s^{-1}) (9.37±0.32) x10^{-4}	1.0 ± 0.0
AB0089 Stressed	hCLEC12A	k_{a1} ($M^{-1}s^{-1}$) (7.91±0.42) x10^6	k_{a2} (s^{-1}) (3.69±0.04) x10^{-3}	k_{d1} (s^{-1}) (4.24±0.17) x10^{-2}	k_{d2} (s^{-1}) (8.56±0.45) x10^{-4}	1.0 ± 0.1
AB0089 Control	hNKG2D	(1.75±0.12) x10^5		(1.35±0.08) x10^{-1}		772 ± 13
AB0089 Stressed	hNKG2D	(1.66±0.03) x10^5		(1.32±0.02) x10^{-1}		796 ± 5
AB0089 Control	CD16aV	(8.53±0.05) x10^4		(2.76±0.02) x10^{-2}		323 ± 3
AB0089 Stressed	CD16aV	(7.93±0.27) x10^4		(2.84±0.07) x10^{-2}		359 ± 6

Average of 3 replicates

Table 154: AB0089 potency after 4 weeks at 40ºC in HST, pH 6.0, in KHYG-1-CD16aV cytotoxicity assay.

Test article	EC50 (nM)	Max killing (%)
AB0089 control	0.16	83
AB0089, HST, pH 6.0, 40ºC, 4 wks	0.17	84

Stability in CST pH 7.0

[0952] AB0089 demonstrated high stability after 4 weeks of incubation in CST, pH 7.0, at 40 °C. A minimal loss monomer content (1.6%) was observed by SEC (FIG. 163 and Table 155). No fragmentation of AB0089 was observed by CE-SDS (FIG. 164 and Table 156). Additionally, there was no meaningful difference in active protein content or in binding affinities for hCLEC12A, hNKG2D and hCD16a between control and stressed samples (FIG. 165 and Table 157). Finally, long term thermal stress did not affect potency of AB0089 (FIG. 166 and Table 158).

Table 155: SEC analysis of AB0089 during weeks 1-4 at 40°C in CST, pH 7.0.

Test Article	Conc. (mg/ml)	Monomer (%)	LMWS (%)	HMWS (%)
AB0089 control	22.0	99.1	0.5	0.5
AB0089, CST, pH7.0, 40°C, 1 wk	ND	98.2	1.2	0.6
AB0089, CST, pH 7.0, 40°C, 2 wks		97.9	1.3	0.7
AB0089, CST, pH 7.0, 40°C, 3 wks		97.7	1.5	0.8
AB0089, CST, pH 7.0, 40°C, 4 wks	22.6	97.5	1.7	1.0

ND, none detected

Table 156: NR and R CE-SDS analysis of AB0089 after 4 weeks at 40°C in CST, pH 7.0.

Test article	NR CE Purity (%)	R CE Purity (%)
AB0089 control	98.6	92.7
AB0089, CST, pH 7.0, 40°C, 4 wks	96.2	96.0

Table 157: Kinetic parameters and binding affinities of AB0089 for CLEC12A, NKG2D and CD16a after 4 weeks at 40°C in CST, pH 7.0

Test article	Target	k_a ($M^{-1}s^{-1}$)		k_d (s^{-1})		K_D (nM)
AB0089 Control	hCLEC12A	k_{a1} ($M^{-1}s^{-1}$) (8.87±0.53) x10^6	k_{a2} (s^{-1}) (3.49±0.04) x10^{-3}	k_{d1} (s^{-1}) (4.20±0.07) x10^{-2}	k_{d2} (s^{-1}) (9.37±0.32) x10^{-4}	1.0 ± 0.0
AB0089 Stressed	hCLEC12A	k_{a1} ($M^{-1}s^{-1}$) (6.31±0.32) x10^6	k_{a2} (s^{-1}) (3.93±0.12) x10^{-3}	k_{d1} (s^{-1}) (3.73±0.15) x10^{-2}	k_{d2} (s^{-1}) (8.00±0.05) x10^{-4}	1.0 ± 0.0

Test article	Target	k_a ($M^{-1}s^{-1}$)	k_d (s^{-1})	K_D (nM)
AB0089 Control	hNKG 2D	(1.75±0.12) x10^{5}	(1.35±0.08) x10^{-1}	772 ± 13
AB0089 Stressed	hNKG2D	(1.60±0.04) x10^{5}	(1.26±0.06) x10^{-1}	791 ± 13
AB0089 Control	CD16aV	(8.53±0.05) x10^{4}	(2.76±0.02) x10^{-2}	323 ± 3
AB0089 Stressed	CD16aV	(8.31±0.43) x10^{4}	(2.84±0.07) x10^{-2}	342 ± 9

Average of 3 replicates

Table 158: Potency of AB0089 after 4 weeks at 40˚C in CST, pH 7.0 in KHYG1-CD16aV cytotoxicity assay.

Test article	Buffer	EC50 (nM)	Max killing (%)
AB0089 control	CST, pH 7.0	0.13	87
AB0089 stressed	CST, pH 7.0	0.16	88

Peptide map analysis of accelerated stability samples

[0953] To determine if the 40ºC stress induced modifications in the complementarity determining regions (CDRs), the control and 4-week stressed samples were analyzed by LC-MS/MS peptide mapping. Based on the peptide map data, all of the CDRs in AB0089 are resistant to modification during elevated temperature stress (Table 159). No evidence of aspartic acid isomerization in the peptide encompassing the CLEC12A binding CDRH3 was observed, based on manual inspection of peak shape (FIG. 167).

Table 159: Post-translational modifications in AB0089 CDRs after elevated temperature stress.

				Relative Abundance (%)		
Chain	**CDR**	**Sequence (Chothia)**	**Modification**	**Control**	**Stressed (CST)**	**Stressed (HST)**
S	H1	GFSLTNY (SEQ ID NO:137)	Deamidation	0.7	1.7	0.9
S	H2	WVGGA (SEQ ID NO:272)	None	NA		
S	H3	GDYGDTLDY (SEQ ID NO:273)	Isomerization	None detected		
S	L1	HASQNINFWLS (SEQ ID NO:140)	Deamidation	0.3	1.0	0.4

				Relative Abundance (%)		
Chain	**CDR**	**Sequence (Chothia)**	**Modification**	**Control**	**Stressed (CST)**	**Stressed (HST)**
S	L2	EASNLHT (SEQ ID NO:141)	Deamidation	None detected		
S	L3	QQSHSYPLT (SEQ ID NO:142)	None	NA		
H	H1	GFTFSSY (SEQ ID NO:297)	None	NA		
H	H2	SSSSSY (SEQ ID NO:298)	None	NA		
H	H3	GAPIGAAAGWFDP (SEQ ID NO:97)	Truncation	None detected		
L	L1	RASQGISSWLA (SEQ ID NO:86)	None	NA		
L	L2	AASSLQS (SEQ ID NO:77)	None	NA		
L	L3	QQGVSFPRT (SEQ ID NO:87)	None	NA		

NA: not applicable

Chemical Stability

Forced Oxidation

[0954] To assess stability of AB0089 under oxidative stress, AB0089 was incubated with 0.02% hydrogen peroxide for 24 hours at room temperature in PBS. SEC analysis showed no difference in monomer content between oxidized AB0089 and control sample (FIG. 168 and Table 160). No increase in fragmentation was detected in AB0089 by both reduced and non-reduced CE-SDS (FIG. 169 and Table 161).

Table 160: SEC analysis of AB0089 after forced oxidation compared to control.

Test article	Concentration (mg/ml)	Monomer (%)	LMWS (%)	HMWS (%)
AB0089 control	1.1	99.3	0.4	0.3
AB0089 forced oxidation	1.0	99.1	0.5	0.4

Table 161: NR and R CE-SDS analysis of AB0089 after forced oxidation.

Test article	NR CE Purity (%)	R CE Purity (%)
AB0089 control	98.9	98.0
AB0089 forced oxidization	97.4	98.1

[0955] Site-specific oxidation of methionine was monitored by tryptic peptide mapping following forced oxidation. Significant levels of oxidation were only detected at two methionines in the Fc (Table 162). Our historic data show that the same residues are modified in trastuzumab at 61.6% and 39.1% under the same conditions.

Table 162: Summary of methionine oxidation in AB0089 before and after oxidative stress.

			Relative Abundance (%)	
Sequence	**Chain**	**Position**	**Control**	**Oxidized**
LSCAASGFTFSSYS**M**NWVR (SEQ ID NO:300)	H	34	0.6	0.9
NSLYLQ**M**NSLR (SEQ ID NO:301)	H	83	0.4	0.9
DTL**M**ISR (SEQ ID NO:302)	H/S	257/278	2.1	66.7
WQQGNVFSCSV**M**HEALHNHYTQK (SEQ ID NO:303)	H/S	433/454	1.3	37.8
DIQ**M**TQSPSSVSASVGDR (SEQ ID NO:304)	L	4	0.5	1.1
GDYGDTLDYWGQGTLVTVSSGGGGSGGGGSGGGGSGGGGSDIQ**M**TQSPSSLSASVGDR (SEQ ID NO:339)	S	141	3.1	3.5

[0956] Oxidation of tryptophan residues in AB0089 CDRs was also monitored in the same experiment. None of the tryptophan residues had a significant increase in oxidation after stress (Table 163).

Table 163: Summary of tryptophan oxidation in AB0089 CDRs before and after oxidative stress.

				Relative Abundance (%)	
Sequence	**Chain**	**CDR**	**Mass shift (Da)[a]**	**Control**	**Oxidized**
WVGGA (SEQ ID NO:272)	S	H2	+16/+32/+4	ND/0.1/0.2	ND/0.2/0.3
HASQNINF**W**LS (SEQ ID NO:140)	S	L1	+16/+32/+4	ND/0.2/0.2	ND/0.3/0.3

				Relative Abundance (%)	
Sequence	**Chain**	**CDR**	**Mass shift (Da)[a]**	**Control**	**Oxidized**
GAPIGAAAGWFDP (SEQ ID NO:97)	H	H3	+16/+32/+4	0.0/0.2/0.4	0.0/0.3/0.7
RASQGISSWLA (SEQ ID NO:86)	L	L1	+16/+32/+4	0.2/0.1/0.2	0.2/0.2/0.3

[a] single oxidation (+16 Da), double oxidation (+32 Da), and kynurenine (+4 Da), ND, none detected.

[0957] Oxidative stress had no significant effect on the active protein content or on the affinities for hCLEC12A, hNKG2D, and hCD16aV (FIG. 170 and Table 164). No significant effect of oxidation on the potency of AB0089 was observed (FIG. 171 and Table 165).

Table 164: Kinetic parameters and binding affinities of AB0089 for CLEC12A, NKG2D and CD16A after forced oxidation compared to control.

Test article	**Target**	**k_a ($M^{-1}s^{-1}$)**		**k_d (s^{-1})**		**K_D (nM)**
AB0089 Control	hCLEC12A	**k_{a1} ($M^{-1}s^{-1}$)** (1.01±0.04) x10^7	**k_{a2} (s^{-1})** (3.46±0.01) x10^{-3}	**k_{d1} (s^{-1})** (4.76±0.22) x10^{-2}	**k_{d2} (s^{-1})** (8.37±0.29) x10^{-4}	0.9 ± 0.0
AB0089 Oxidized	hCLEC12A	**k_{a1} ($M^{-1}s^{-1}$)** (9.93±0.11) x10^6	**k_{a2} (s^{-1})** (3.47±0.04) x10^{-3}	**k_{d1} (s^{-1})** (4.81±0.10) x10^{-2}	**k_{d2} (s^{-1})** (8.37±0.22) x10^{-4}	0.9 ± 0.0
AB0089 Control	hNKG2D	(1.69±0.04) x10^5		(1.35±0.01) x10^{-1}		797 ± 19
AB0089 Oxidized	hNKG2D	(1.71±0.13) x10^5		(1.30±0.07) x10^{-1}		762 ± 13
AB0089 Control	hCD16aV	(8.64±0.22) x10^4		(2.78±0.05) x10^{-2}		322 ± 7
AB0089 Oxidized	hCD16aV	(8.65±0.43) x10^4		(2.77±0.05) x10^{-2}		320 ± 10

Average of 3 replicates

Table 165: AB0089 potency before and after forced oxidation in KHYG1-CD16aV cytotoxicity assay.

Test article	EC50 (nM)	Max Killing (%)
AB0089 Control	0.11	84
AB0089 Oxidized	0.16	87

pH 8 stress

[0958] Chemical stability of AB0089 was assessed by long term incubation at elevated pH (20 mM Tris, pH 8.0, 40 °C, 2 weeks). AB0089 appears to be highly stable: only 1.2 % loss of monomer was detected by SEC (FIG. 172 and Table 166).

Table 166: SEC analysis of AB0089 after long term high pH stress (pH 8.0, 40ºC, 2 wks).

Test article	Monomer (%)	LMWS (%)	HMWS (%)
AB0089 control	99.4	0.4	0.2
AB0089 pH 8 stressed	98.2	1.1	0.7

[0959] Reduced and non-reduced CE-SDS showed low levels of degradation, 1.7% and 3.9%, respectively (FIG. 173 and Table 167).

Table 167: NR and R CE-SDS analysis of AB0089 after long term high pH stress (pH 8, 40ºC, 2 wks).

Test article	NR CE Purity (%)	R CE Purity (%)
AB0089 control	98.6	98.2
AB0089 pH 8 stressed	96.9	94.3

[0960] After long term high pH stress, there was an acidic shift in the global charge profile detected by cIEF (FIG. 174 and Table 168). This acidic shift can be attributed to deamidation throughout the AB0089 sequence. A similar acidic shift was observed for trastuzumab after the same stress conditions (data not shown).

Table 168: AB0089 charge profile after long term high pH exposure (pH 8, 40°C, 2 wks).

Test article	% acidic	% main	% basic
AB0089 control	43.1	51.4	5.5
AB0089 pH 8 stressed	66.6	29.0	4.4

[0961] There was no meaningful difference in the amount of active protein or in the affinities for hCLEC12A, hNKG2D, or hCD16aV between stressed and control samples (FIG. 175 and Table 169).

Table 169: Kinetic parameters and binding affinities of AB0089 for CLEC12A, NKG2D, and CD16aV after long term high pH stress (pH 8, 40°C, 2 wks).

Test article	Target	k_a ($M^{-1}s^{-1}$)		k_d (s^{-1})		K_D (nM)
AB0089 Control	hCLEC12A	k_{a1} ($M^{-1}s^{-1}$) (1.01±0.04) x10^7	k_{a2} (s^{-1}) (3.46±0.01) x10^{-3}	k_{d1} (s^{-1}) (4.76±0.22) x10^{-2}	k_{d2} (s^{-1}) (8.37±0.29) x10^{-4}	0.9 ± 0.0
AB0089 pH 8 Stressed	hCLEC12A	k_{a1} ($M^{-1}s^{-1}$) (9.93±0.05) x10^7	k_{a2} (s^{-1}) (3.36±0.09) x10^{-3}	k_{d1} (s^{-1}) (4.90±0.24) x10^{-2}	k_{d2} (s^{-1}) (8.63±0.33) x10^{-4}	0.9 ± 0.1
AB0089 Control	hNKG2D	(1.69±0.04) x10^5		(1.35±0.01) x10^{-1}		797 ± 19
AB0089 pH 8 Stressed	hNKG2D	1.30 x10^5		1.27 x10^{-1}		983
AB0089 Control	hCD16aV	(8.64±0.22) x10^4		(2.78±0.05) x10^{-2}		322 ± 7
AB0089 pH 8 Stressed	hCD16aV	(7.94±0.28) x10^4		2.79±0.15) x10^{-2}		350 ± 11

Average of 3 replicates for all samples, except pH 8 stressed binding to hNKG2D (n = 2)

[0962] After long term high pH exposure, the potency of AB0089 was reduced approximately 2-fold (FIG. 176 and Table 170). Considering that orthogonal methods of analysis did not show any difference in binding or in the factive species content (FIG. 175), it appears that these differences may be due to potency assay variability.

Table 170: AB0089 potency after long term high pH exposure (pH 8, 40°C, 2 wks).

Test article	EC50 (nM)	Max killing (%)
AB0089 control	0.11	84
AB0089 pH 8 stressed	0.23	83

pH 5 stress

[0963] Chemical stability of AB0089 was also assessed by long term incubation at low pH (20 mM sodium acetate, pH 5.0, 40 °C, 2 weeks). DF appears to be highly stable: only 0.3% loss of monomer was detected by SEC (FIG. 177 and Table 171).

Table 171: SEC analysis of AB0089 after long term low pH stress (pH 5.0, 40°C, 2 wks).

Test article	Monomer (%)	LMWS (%)	HMWS (%)
AB0089 control	99.3	0.4	0.2
AB0089 pH 5 stressed	99.0	0.8	0.2

[0964] After long term pH 5 stress, low levels of AB0089 degradation were detected by non-reduced and reduced CE-SDS: 1.0% and 0.3% loss of monomer content, respectively (FIG. 178 and Table 172).

Table 172: NR and R CE-SDS analysis of AB0089 after long term low pH stress (pH 5.0, 40°C, 2 wks).

Test article	NR CE Purity (%)	R CE Purity (%)
AB0089 control	98.6	97.7
AB0089 pH 5 stressed	97.6	97.4

[0965] After long term pH 5 stress, there was a small acidic shift in the global charge profile detected by cIEF (FIG. 178 and Table 172), with one acidic variant in particular increasing significantly.

Table 173: Charge profile of AB0089 after long term low pH stress (pH 5.0 40°C, 2 wks).

Test article	% acidic	% main	% basic
AB0089 control	37.8	56.4	5.8
AB0089 pH 5 stressed	47.3	45.9	6.8

[0966] After long term low pH exposure, there was no meaningful difference in active protein content or in AB0089 affinities for hCLEC12A, hNKG2D, or hCD16aV (FIG. 180 and Table 174).

Table 174: Kinetic parameters and binding affinity of AB0089 for CLEC12A, NKG2D, and CD16aV after high pH stress (pH 5.0, 40°C, 2 wks).

Test article	Target	k_a ($M^{-1}s^{-1}$)		k_d (s^{-1})		K_D (nM)
AB0089 Control	hCLEC12A	k_{a1} ($M^{-1}s^{-1}$) (1.01±0.04) x10^7	k_{a2} (s^{-1}) (3.46±0.01) x10^{-3}	k_{d1} (s^{-1}) (4.76±0.22) x10^{-2}	k_{d2} (s^{-1}) (8.37±0.29) x10^{-4}	0.9 ± 0.0
AB0089 pH 5 stressed	hCLEC12A	k_{a1} ($M^{-1}s^{-1}$) (8.62±0.02) x10^6	k_{a2} (s^{-1}) (3.47±0.04) x10^{-3}	k_{d1} (s^{-1}) (4.27±0.22) x10^{-2}	k_{d2} (s^{-1}) (8.40±0.09) x10^{-4}	1.0 ± 0.0
AB0089 Control	hNKG2D	(1.69±0.04) x10^5		(1.35±0.01) x10^{-1}		797 ± 19
AB0089 pH 5 Stressed	hNKG2D	1.87 x10^5		1.31 x10^{-1}		703
AB0089 Control	CD16aV	(8.64±0.22) x10^4		(2.78±0.05) x10^{-2}		322 ± 7
AB0089 pH 5 Stressed	CD16aV	(7.54±0.36) x10^4		(2.89±0.05) x10^{-2}		383 ± 12

Average of 3 replicates for all samples, except pH 5 stressed sample binding to hNKG2D (n = 2)

[0967] Potency of AB0089 after long term pH 5 exposure remained similar to potency of the control sample (FIG. 181 and Table 175).

Table 175: AB0089 potency after long term low pH stress (pH 5.0 40°C, 2 wks) in KHYG-1-CD16aV cytotoxicity assay.

Test article	EC50 (nM)	Max killing (%)
AB0089 control	0.11	84
AB0089 pH 5 stressed	0.16	86

Peptide mapping analysis of the pH 5 and pH 8 stressed material

[0968] To determine if the pH stress induced changes observed by cIEF are due to the modification in the complementarity determining regions (CDRs), pH 5 and pH 8 stressed samples were analyzed by LC-MS/MS peptide mapping. Based on the peptide map data, all of the CDRs in AB0089 are resistant to modification during low and high pH stress (Table 176). No evidence of aspartic acid isomerization in the peptide encompassing the CDRH3 of the CLEC12A targeting arm of AB0089 was observed, based on manual inspection of peak shape (FIG. 182).

Table 176: Post-translational modifications in AB0089 CDRs after long term exposure to low and high pH (pH 5.0 and pH 8.0).

				Relative abundance (%)			
				pH 5		pH 8	
Chain	**CDR**	**Sequence (Chothia)**	**Modification**	**control**	**stressed**	**control**	**stressed**
S	H1	GFSLTNY (SEQ ID NO:137)	Deamidation	0.2	0.6	0.4	1.4
S	H2	WVGGA (SEQ ID NO:272)	None	NA			
S	H3	GDYGDTLDY (SEQ ID NO:273)	Isomerization	None detected			
S	L1	HASQNINFWLS (SEQ ID NO:140)	Deamidation	0.1	0.1	0.2	0.4
S	L2	EASNLHT (SEQ ID NO:141)	Deamidation	None detected			
S	L3	QQSHSYPLT (SEQ ID NO:142)	None	NA			
H	H1	GFTFSSY (SEQ ID NO:297)	None	NA			
H	H2	SSSSSY (SEQ ID NO:298)	None	NA			
H	H3	GAPIGAAAGWFDP (SEQ ID NO:97)	Truncation	None detected			
L	L1	RASQGISSWLA (SEQ ID NO:86)	None	NA			
L	L2	AASSLQS (SEQ ID NO:77)	None	NA			
L	L3	QQGVSFPRT (SEQ ID NO:87)	None	NA			

NA: not applicable

Manufacturability

Freeze/thaw stability

[0969] Aliquots of AB0089 (20 mg/ml in CST pH 7.0) were frozen and thawed 6 times by placing the vials in Styrofoam container (to slow the freezing rate) and placing the container at -80°C. After 6 cycles of freeze/thaw AB0089 showed no loss in monomer by SEC. Protein concentration measured by A280 remained the same (FIG. 183 and Table 177).

Table 177: SEC analysis of AB0089 after freeze/thaw stress.

Test article	Conc. (mg/ml)	Monomer (%)	LMWS (%)	HMWS (%)
AB0089 control	22.3	99.0	0.7	0.3
AB0089 after 6 F/T cycles	22.1	98.9	0.8	0.3

[0970] After 6 freeze/thaw cycles no loss of purity was detected by reduced or non-reduced CE-SDS (FIG. 184 and Table 178).

Table 178: Purity by NR and R CE-SDS analysis of AB0089 after freeze/thaw stress.

Test article	NR CE Purity (%)	R CE Purity (%)
AB0089 control	98.4	93.2
AB0089 after 6 F/T cycles	98.3	93.7

Agitation

[0971] AB0089 (at 10 mg/ml in 20 mM sodium citrate, 250 mM sucrose, pH 7.0, with or without 0.01% Tween-80) was shaken at 300 rpm at room temperature in a deep well plate for 3 days. After agitation stress, there was no loss of monomer detected by SEC (FIG. 185 and Table 179), no loss of protein concentration (A280), and no increase in turbidity (A340) was observed.

Table 179: SEC analysis of AB0089 after agitation stress.

Test article	0.01% Tween-80	Conc. (mg/ml)	Monomer (%)
AB0089 control	+	9.86	99.5
AB0089 agitation	+	9.97	99.7
AB0089 control	-	9.81	99.4
AB0089 agitation	-	9.93	99.1

High concentration

[0972] AB0089 was concentrated to approximately 10, 15, 25, 50, 100, 150 and 175 mg/ml in PBS, pH 7.4 and recovery was monitored by visual inspection, concentration (A280), and SEC. For SEC analysis, samples were injected undiluted (injection volume was normalized to the concentration). AB0089 was able to be concentrated to >175 mg/ml with minimal loss in percent monomer (FIG. 186, FIG. 187, Table 180) and no visible precipitation.

Table 180: SEC analysis of AB0089 at different concentrations.

Concentration (mg/ml)	% Monomer	% HMW
9.7	99.7	0.3
14.7	99.7	0.3
26.2	99.7	0.3
53.4	99.6	0.4
94.2	99.6	0.4
143.5	99.6	0.4
178.4	99.5	0.5

Low pH hold

[0973] Two different methods were used to assess the behavior of AB0089 during low pH hold (mock viral inactivation). The first method mimicked the manufacturing process, where the eluate from the first chromatography step (Protein A) was held at low pH before additional purification. The second method incubated fully purified AB0089 under low pH conditions. This method was used to assess potential low pH induced chemical modifications of the CDRs.

Low pH hold exposure of Protein A eluate

[0974] To determine if AB0089 is resistant to low pH hold, AB0089 Protein A eluate was adjusted to pH 3.5 and held for 2 hours at room temperature. After the hold period, the Protein A eluate was neutralized with 1.0 M Tris, pH 8.3 to achieve neutral pH. Analytical SEC was performed to determine if there were any changes in profile or aggregate content pre- and post-low pH exposure (FIG. 188). No change in the SEC profile of AB0089 was observed after low pH hold compared to "no-hold" control sample, suggesting that AB0089 is highly stable during low pH hold/viral inactivation conditions used in biologics manufacturing.

[0975] Protein was further processed through the second step of DF platform purification method and analyzed using a panel of additional assays in comparison with purified protein that

was not subjected to low pH hold. Chemical modification of amino acid side chains can typically be observed at a global scale with cIEF. The cIEF profiles of AB0089 control and low pH hold lot are visually very similar and the relative quantitation of acidic, main, and basic species are all within 5% of each other. This indicates that the low pH hold did not have a measurable effect on the charge profile of AB0089 (FIG. 189 and Table 181).

Table 181: AB0089 charge profile after low pH hold.

Test article	pI	% acidic	% main	% basic
AB0089 control	8.5	43.7	50.8	5.5
AB0089 low pH hold	8.6	39.5	54.3	6.2

[0976] The affinities of AB0089 for hCLEC12a, hNKG2D, and CD16aV were not affected by low pH hold (FIG. 190 and Table 182). No difference in active protein content was observed. The difference in binding affinity and maximal binding response between the control and low pH hold sample were within the experimental variability of the assay. This indicates that AB0089 retains affinity for all three targets after low pH hold.

Table 182: Kinetic parameters and binding affinities of AB0089 for CLEC12A, NKG2D, and CD16aV after low pH hold.

Test article	Target	k_a ($M^{-1}s^{-1}$)		k_d (s^{-1})		K_D (nM)
AB0089 Control	hCLEC12A	k_{a1} ($M^{-1}s^{-1}$) (1.04±0.03) x10^7	k_{a2} (s^{-1}) (3.43±0.04) x10^{-3}	k_{d1} (s^{-1}) (4.35±0.12) x10^{-2}	k_{d2} (s^{-1}) (7.41±0.10) x10^{-4}	0.7 ± 0.0
AB0089 low pH hold	hCLEC12A	k_{a1} ($M^{-1}s^{-1}$) (1.11±0.07) x10^7	k_{a2} (s^{-1}) (3.50±0.03) x10^{-3}	k_{d1} (s^{-1}) (4.65±0.05) x10^{-2}	k_{d2} (s^{-1}) (7.49±0.03) x10^{-4}	0.7 ± 0.0
AB0089 Control	hNKG2D	(1.62±0.03) x10^5		(1.43±0.03) x10^{-1}		881 ± 10
AB0089 low pH hold	hNKG2D	(1.59±0.07) x10^5		(1.50±0.05) x10^{-1}		941 ± 45
AB0089 Control	CD16aV	(8.31±0.55) x10^4		(2.77±0.16) x10^{-2}		333 ± 11
AB0089 low pH hold	CD16aV	(8.73±0.22) x10^4		(2.74±0.05) x10^{-2}		314 ± 8

Results are an average of 3 replicates

[0977] Potency of AB0089 subjected to low pH hold and potency of control sample were tested against CLEC12A+ HL-60 cancer cells in the KHYG1-CD16aV bioassay. The potency of AB0089 was unaltered after the low pH hold step (FIG. 191 and Table 183).

Table 183: Potency of AB0089 after low pH hold in KHYG-1-CD16aV cytotoxicity assay.

Test article	EC50 (nM)	Max killing (%)
AB0089 control	0.11	95
AB0089 low pH hold	0.11	89

Low pH hold exposure of fully purified protein

[0978] An additional low pH hold study was carried out to investigate if the DT motif in the CDRH3 (KGDYG**DT**LDY) of the CLEC12A targeting scFv would isomerize during a viral inactivation step. Low pH hold material was prepared from fully purified AB0089 material using the following steps:

1. AB0089 was diluted 1:1 with 0.1 M glycine, pH 3.0 to mimic ProA elution
2. The pH was adjusted to 3.5 ± 0.1 with 2 M acetic acid (to mimic low pH hold conditions)
3. The low pH hold was carried out for 60 min at room temperature
4. The pH was neutralized to ~7.5 with 1 M Tris, pH 8.0
5. AB0089 was buffer exchanged into PBS, pH 7.4

[0979] The final low pH hold material (AB0089 lot AB0089-004) was compared to control (AB0089 lot AB0089-002) using a panel of biological assays: SEC, cIEF, SPR binding to CLEC12A, peptide map, and potency. Analytical SEC was performed to determine if there were any changes in profile or aggregate content pre- and post- low pH exposure (FIG. 192 and Table 184). No change in profile of % monomer was observed after the low pH hold.

Table 184: SEC analysis of AB0089 after low pH hold compared to control.

Test article	Monomer (%)	LMWS (%)	HMWS (%)
AB0089 control	99.7	ND	0.3
AB0089 low pH hold	99.7	ND	0.3

ND, none detected

[0980] As was seen in the first low pH hold study, the cIEF profiles of AB0089 control and low pH hold lot are visually very similar and the relative quantitation of acidic, main, and basic species are all within 6% of each other. Hence, low pH hold did not have a significant effect on the charge profile of AB0089 (FIG. 193 and Table 185).

Table 185: Charge profile of AB0089 after low pH hold.

Test article	pI	% acidic	% main	% basic
AB0089 control	8.6	42.5	51.1	6.5
AB0089 low pH hold	8.6	38.0	56.8	5.4

[0981] The affinity of AB0089 for hCLEC12a was unaltered compared to control (FIG. 281 and Table 186). The difference in binding affinity and maximal binding response between the control and low pH hold sample are within the experimental variability of the assay. This indicates that there was no impact of low pH incubation on the binding of the CLEC12A binding arm with target antigen.

Table 186: Summary of kinetic parameters and binding affinities of AB0089 for hCLEC12A after low pH hold compared to control.

Test article	k_{a1} ($M^{-1}s^{-1}$)	k_{d1} (s^{-1})	k_{a2} (s^{-1})	k_{d2} (s^{-1})	K_D (nM)
AB0089 control	$(1.03\pm0.03)\times10^{7}$	$(2.72\pm0.11)\times10^{-2}$	$(3.59\pm0.05)\times10^{-3}$	$(8.56\pm0.32)\times10^{-4}$	0.51 ± 0.02
AB0089 low pH hold	$(1.02\pm0.06)\times10^{7}$	$(2.76\pm0.10)\times10^{-2}$	$(3.60\pm0.04)\times10^{-3}$	$(8.62\pm0.11)\times10^{-4}$	0.53 ± 0.02

Results are an average of 3 replicates

[0982] The potency of AB0089 after low pH hold against CLEC12A+ HL-60 cancer cells was assessed in the KHYG1-CD16V bioassay. No difference between potencies of low pH hold and control samples was observed (FIG. 282 and Table 187).

Table 187: Potency AB0089 after low pH hold in the KHYG1-CD16aV cytotoxicity assay.

Test article	EC50 (nM)	Maximum Lysis (%)
AB0089 control (AB0089-002)	0.04	99
AB0089 low pH hold (AB0089-004)	0.03	98

[0983] To determine if the low pH hold induced changes in the modification in the CDRs, the control and low pH hold samples were analyzed by LC-MS/MS peptide mapping. Based on the peptide map data, all of the CDRs in AB0089 are resistant to modification during low pH hold (Table 188). No evidence of aspartic acid isomerization was observed, based on manual inspection of peak shape.

Table 188: AB0089 are resistant to post-translational modifications after low pH hold.

				Relative abundance (%)	
Chain	**CDR**	**Sequence (Chothia)**	**Potential liability**	**control**	**low pH hold**
S	H1	GFSLTNY (SEQ ID NO:137)	Deamidation	0.7	1.1
S	H2	WVGGA (SEQ ID NO:272)	None	NA	
S	H3	GDYGDTLDY (SEQ ID NO:273)	Isomerization	ND	ND
S	L1	HASQNINFWLS (SEQ ID NO:140)	Deamidation	0.2	0.1
S	L2	EASNLHT (SEQ ID NO:141)	Deamidation	ND	ND
S	L3	QQSHSYPLT (SEQ ID NO:142)	None	NA	
H	H1	GFTFSSY (SEQ ID NO:297)	None	NA	
H	H2	SSSSSY (SEQ ID NO:298)	None	NA	
H	H3	GAPIGAAAGWFDP (SEQ ID NO:97)	Truncation	ND	ND
L	L1	RASQGISSWLA (SEQ ID NO:86)	None	NA	
L	L2	AASSLQS (SEQ ID NO:77)	None	NA	
L	L3	QQGVSFPRT (SEQ ID NO:87)	None	NA	

NA, not applicable

[0984] Taken together, these results demonstrate that AB0089 is an improved version of AB0192 with an optimized CMC profile. The molecular format and structure of AB0089 meets

the conceptual requirements for a new multi-specific therapeutic modality that simultaneously engages CLEC12A, NKG2D and CD16a to treat AML. AB0089 is potent and has a favorable developability profile with no sequence liabilities or significant post-translational modifications observed under any stresses. AB0089 binds to an epitope on CLEC12a similar to tepoditamab (Merus).

Example 18. AB0089 Cytotoxicity and Mechanism of Action

Objectives

[0985] Measure the activity of AB0089 in cell-based assays *in vitro* using physiologically relevant conditions to characterize AB0089's modes of action.

Study Design

[0986] The primary mechanism of action for AB0089 was tested using *in vitro* assays systems with human NK cells and CLEC12A+ cancer cells. Other effector functions aside from NK cell-mediated cytolysis were also paired with CLEC12A+ cancer cells to test additional mechanisms of action for AB0089. Macrophages were effector cells for ADCP assays and human serum was used as a source of complement to test CDC activity.

Materials and Methods

Primary cells and cell lines

[0987] Human cancer cell lines were obtained from research cell banks. Below cell lines (item number; vendor) were used: PL21 (ACC-536; DSMZ) and HL60 (CCL-240; ATCC).

[0988] Human blood was obtained from Biological Specialty Corporation (225-11-04). PBMCs were isolated by density gradient centrifugation, and NK cells were purified using negative depletion with magnetic beads (StemCell CAT#17955). The manufacturer's instructions were followed for purification of NK cells from PBMCs. Frozen NK cells were purchased from BioIVT HUMAN-HL65-U-200429 CD14+ monocytes were obtained from BioIVT (HMN370652, HMN370653, HMN370654) Frozen PBMC were purified in-house (see above) and frozen for later use.

Cell culture materials

[0989] Below items (vendor; item number) were used: RPMI-1640 (Corning; 10040CV), DMEM (Corning; 10031CV), Heat inactivated FBS (ThermoFisher; 16140-071), GlutaMax I (ThermoFisher; 35050-061), Penn/Strep (ThermoFisher; 151450-122), 2-Mercaptoethanol (MP Biomedicals; 02194705), IL-2 (PeproTech; 200-02), CFSE (ThermoFisher; C34554), Cell Trace Violet (ThermoFisher; C34557), rhM-CSF (R&D Systems; 216-MC/CF), TrypLE (ThermoFisher; 12604-013), BFA (Biolegend; 420601), Monensin (BioLegend; 420701), and Human serum (Sigma Aldrich; S1764-5X1ML).

Assay Materials

[0990] Below items (vendor; item number) were used: Hepes buffered saline (Alfa Aesar; J67502), BATDA reagent (Perkin Elmer; C136-100), TC round bottom 96- well plate (Corning; 3799), Europium solution (Perkin Elmer; C135-100), DELFIA yellow microplates 96-well (Perkin Elmer; AAAND-0001), Fixation buffer (BioLegend; 420801), Zombie NIR (BioLegend; 77184), and Anti-MHC class I clone W6/32 (Invitrogen; HLA-C1).

[0991] Below test articles (description) were used: AB0237 (CLEC12A-Targeted TriNKET with Fab NKG2D binding (A49), and scFv CLEC12A binding domain (1602)), AB0300 (AB0237 with LALAPG mutation in CH2 domain), AB0037 mAb (Humanized 1602 anti-CLEC12A mAb), AB0089 (CLEC12A-Targeted TriNKET with Fab NKG2D binding (A49) and scFv CLEC12A binding domain (1739)), AB0305 mAb (Humanized 1739 anti-CLEC12A mAb), AB0192 (CLEC12A-Targeted TriNKET with Fab NKG2D binding (A49), and scFv CLEC12A binding domain (1797)), AB0306 mAb (Humanized 1797 anti-CLEC12A mAb), and F3'-palivizumab (Non-Targeting TriNKET with Fab NKG2D binding (A49), and scFv binding domain from palivizumab).

[0992] Below instruments (serial number) were used: Attune NxT (2AFC228271119), BD Celesta (H66034400085), BD Celesta (H66034400160), Spectramax i3x (363704226) and Spectramax i3x (363703638).

Preparation of reagents

[0993] RPMI primary cell culture media was prepared starting with RPMI-1640. 10% HI-FBS, 1x GlutaMax, 1x penn/strep, and 50 μM 2-mercaptoethanol were added for complete

media. RPMI cell culture media was prepared starting with RPMI-1640. 10% HI-FBS, 1x GlutaMax, and 1x penn/strep, were added for complete media. 1x HBS was prepared by diluting 1 part of 5x HBS into 4 parts of DI water. Solution was sterile filtered before use.

DELFIA cytotoxicity assay

Labeling target cells:

[0994] Briefly, CLEC12A+ target cells were pelleted, and washed with 1x HBS. Target cells were resuspended in pre-warmed RPMI primary cell culture media at 10^6 cells/mL. BATDA reagent (bis(acetoxymethyl) 2,2':6',2''-terpyridine-6,6''-dicarboxylate) was diluted 1:400 into the cell suspension. Cells were mixed and incubated at 37°C with 5% CO_2 for 15 minutes. The labeled target cells were washed 3x with 1x HBS and resuspended at $5x10^4$ cells/mL in RPMI primary cell culture media.

Preparing the assay plate:

[0995] Rested human NK cells were removed from culture and pelleted, the cells were resuspended in RPMI primary cell culture media at $0.5x10^6$ cells/mL. 4x test articles were prepared in RPMI primary cell culture media. In a round bottom TC 96-well plate, 100 µl of labeled target cells, 50 µl of 4x TriNKET/mAb, and 50 µl of effector cells were added. Control wells for background were prepared by pelleting labeled target cells, and 100 µl of the supernatant was added to background wells, containing 100 µl of RPMI primary cell culture media. Spontaneous release wells were prepared by adding 100 µl of labeled target cells to wells containing 100 µl of RPMI primary cell culture media. Maximum release wells were prepared by adding 100 µl of labeled target cells to wells containing 80 µl of RPMI primary cell culture media and 20 µl of 10% TritonX-100 solution. The assay plate was incubated at 37°C with 5% CO_2 for 2-3 hours.

Reading the assay plate:

[0996] The assay plate was removed from the incubator and the plate was centrifuged to pellet cells. 20 µl of supernatant was removed from each well and transferred to a clean 96-well yellow DELFIA assay plate. 200 µl of room temperature Europium solution was added to each

well and the plate was placed on a plate shaker 15 minutes at 250 RPM. The plate was read using an HTRF cartridge in a SpectraMax i3x with the following PMT and optics settings:

- Integration time 0.4 ms
- Excitation time 0.05 ms
- Number of pulses 100
- Measurement delay 0.25 ms
- Read height 2.36 mm

Data analysis:

[0997] The mean of the background samples was calculated and subtracted from all samples. Specific lysis was calculated as follows:

% Specific lysis = (sample-spontaneous)/(max-spontaneous) * 100%

[0998] Data were fit to a four-parameter non-linear regression model using Prism GraphPad 7.0 or 8.0.

IFNγ and CD107a activation assays

Plate setup:

[0999] Human cancer cell lines expressing CLEC12A were harvested from culture, and cells were adjusted to $2x10^6$ cells/mL. Test articles were diluted in culture media. Rested NK cells or PBMCs were harvested from culture, cells were washed, and were resuspended at $2\text{-}4x10^6$ cells/mL in culture media. IL-2 and fluorophore conjugated anti-CD107a were added to the NK cells or PBMCs for the activation culture. Brefeldin-A (BFA) and monensin were diluted into culture media to block protein transport out of the cell for intracellular cytokine staining. Into a 96-well plate, 50 µl of tumor targets, mAbs/TriNKETs, BFA/monensin, and NK cells were added for a total culture volume of 200 µl. Plate was cultured for 4 hours before samples were prepared for FACS analysis.

Preparation of samples for FACS:

[01000] Following the 4-hour activation culture, cells were prepared for analysis by flow cytometry using fluorophore conjugated antibodies listed in Table 189. CD107a and IFNγ staining was analyzed in CD3-CD56+ populations to assess NK cell activation.

Table 189: FACS NK activation panel

Fluorophore	Target	Dilution factor
BV421	IFNy	50
BV510	CD8	100
BV605	dump	
BV785	CD3	100
PE-D594	CD56	100
PE-Cy7	CD4	100
APC	CD107a	50
A700	CD45	50
NIR	live-dead	1000
	TruStain FcX	50
	BV buffer	50
	mono block	50

[01001] Cells of interest were identified using FSC vs. SSC plot, and an appropriately shaped gate was drawn around the cells. Within the gated cells, doublet cells were removed by viewing FSC-H vs FSC-A plot. Within the single cell population, live cells were gated. Within live cells, NK cells were identified as CD56+CD3-. CD107a degranulation and intracellular (IC) IFNγ were analyzed within the NK cell population.

ADCP assays

[01002] Primary human CD14+ monocytes are obtained from BioIVT. Monocytes were isolated from peripheral blood via negative selection yielding >93% purity. Monocytes were cultured for 6 days in 50 ng/ml rhM- CSF (R&D systems), replenishing rhM-CSF every two days. After 6 days, macrophages were detached from the culture flask(s) with TrypLE Express (Gibco) and labeled with Celltrace Violet (2 μM, ThermoFisher). Target cells were labeled with CFSE (2 μM, ThermoFisher). In round-bottom 96-well plates, target cells ($1x10^4$ cells/well) are first incubated with the indicated concentrations of each test article for 30 minutes. Labeled macrophages ($8x10^4$ cells/well) are then added to the appropriate wells and plates were incubated for an additional 2 hours. Cells were stained with Zombie NIR Dye (Biolegend) for live dead discrimination and fixed. Phagocytosis is quantified by Celesta HTS (BD Biosciences), with data analysis in FlowJo 10.5.3. Data were gated on single, live cells, and % phagocytosis was calculated as follows: % phagocytosis = 100 x (count CFSE+, Celltrace Violet+ cells)/(total count CFSE+ cells). Data were graphed and analyzed using GraphPad Prism.

CDC assays

[01003] CDC was measured in a DELFIA cytotoxicity assay. PL21 cancer cell targets were labeled with BATDA labeling reagent. Labeled target cells were then incubated with the indicated concentrations of TriNKETs or mAbs for 30 min, to allow for opsonization. Human serum was added to a 5% final concentration. The plate was then incubated for 60 minutes before termination of assay. 20 µl of culture supernatant was transferred to DELFIA yellow plate. 200 µl europium solution was added per well and incubated at room temperature for 15 minutes with shaking in the dark. Fluorescence was then measured on the Spectramax plate reader.

Results and Discussion

Rested human NK cell lysis of CLEC12A+ target cells

[01004] The activities of AB0089 and AB0192 was characterized using rested primary human NK cells from healthy donors in co-culture with either human CLEC12A+ AML line PL21 or HL60. AB0089 and AB0192 were compared to their parental hIgG1 mAbs AB0305 and AB0306, respectively. **FIG. 194** shows a representative plot of PL21 leukemia target cell lysis by rested human NK cells in the presence of AB0089. AB0089 showed dose-dependent cell lysis enhancement activity that was more potent and reached a higher maximum lysis than its parental mAb AB0305. The results of similar cytotoxicity assays using NK cells derived from a total of six donors are summarized in Table 190. Across the assays, the potency AB0089 in enhancing NK cell lysis of PL21 target cells had mean EC50 value 0.25 ± 0.24 nM.

Table 190: AB0089 EC50 and % Max lysis values for rested NK cell lysis of PL21 cells
(Values represent the mean of assays with a total of six donors ± the standard deviation)

Molecule	EC50 (nM)	% Max lysis
AB0089	0.25 ± 0.24	17 ± 10
AB0305	ND	ND

ND = Not determined

[01005] **FIG. 195** shows a representative plot of HL60 leukemia target cell lysis by rested primary human NK cells in the presence of AB0089. Again, AB0089 showed more potent dose-dependent lysis and higher specific lysis overall than its parental mAb AB0305. The results of

assays using NK cells derived from four healthy donors yielded a mean EC50 of 0.09 ± 0.05 nM as summarized in Table 191.

Table 191: AB0089 EC50 and % Max lysis values for rested NK cells lysis of HL60 cells (Values represent the mean of assays with a total of four donors ± the standard deviation)

Molecule	EC50 (nM)	% Max lysis
AB0089	0.09 ± 0.05	47 ± 14
AB0305	ND	ND

ND = Not determined

[01006] **FIG. 196** shows a representative plot of PL21 leukemia target cell lysis by rested human NK cells in the presence of AB0192. AB0192 showed dose-dependent cell lysis enhancement activity that was more potent and reached a higher maximum lysis than its parental mAb AB0306. The results of similar cytotoxicity assays using NK cells derived from a total of six healthy donors are summarized in Table 192. Across the assays, the potency AB0192 in enhancing NK cell lysis of PL21 target cells had mean EC50 value 0.61 ± 0.60 nM.

Table 192: AB0192 EC50 and % Max lysis values for rested NK cell lysis of PL21 cells (Values represent the mean of assays with a total of six donors ± the standard deviation)

Molecule	EC50 (nM)	% Max lysis
AB0192	0.61 ± 0.60	18 ± 13
AB0306	ND	ND

ND = Not determined

[01007] **FIG. 197** shows a representative plot of HL60 leukemia target cell lysis by rested primary human NK cells in the presence of AB0192. Again, AB0192 showed more potent dose-dependent lysis and higher specific lysis overall than its parental mAb. The results of assays using NK cells derived from four healthy donors yielded a mean EC50 of 0.30 ± 0.27 nM as summarized in Table 193.

Table 193: AB0192 EC50 and % Max lysis values for rested NK cells lysis of HL60 cells (Values represent the mean of assays with a total of four donors ± the standard deviation)

Molecule	EC50 (nM)	% Max lysis
AB0192	0.30 ± 0.27	50 ± 14
AB0306	ND	ND

ND = Not determined

AB0089 activity in the presence of soluble MIC-A

[01008] We also tested the activity of AB0089 in the presence of soluble NKG2D ligand. For these assays, we selected to use a recombinant version of the NKG2D ligand MIC-A. MIC-A has broad expression across cancer indications and is known to shed from the cell surface resulting in accumulation in patient serum. Soluble MIC-A-Fc was added to a NK cell cytolysis assay system at 20 ng/mL, a physiologically relevant serum concentration found in cancer patients. **FIG. 198** shows the dose-response curves of AB0089 and its parental mAb AB0305 in a primary NK cell cytolysis assay against PL21 target cells in the absence and presence of soluble MIC-A. The addition of MIC-A had no effect on the potency or maximum lysis achieved by AB0089 (see Table 194 for EC50 and max lysis values).

Table 194: AB0089 EC50 and % Max lysis values for lysis of PL21 cells by NK cells with sMIC-A-Fc

Molecule	EC50 (nM)	% Max lysis
AB0089	0.32	15
AB0089 + sMIC-A-Fc	0.26	13
AB0305	ND	ND
AB0305 + sMIC-A-Fc	ND	ND

ND = Not determined

AB0089 stimulation of NK cell IFNγ production and degranulation

[01009] In addition to direct lysis of target cells, NK cells also produce cytokines upon activation. Thus, we wanted to examine alternative readouts of NK activation in addition to target cell lysis. We chose to analyze IFNγ production and CD107a degranulation from NK cells co-cultured with CLEC12A+ AML cells in the presence of AB0089. Rested NK cells within PBMCs in co-culture with PL21 and HL60 target cells showed little basal induction of CD107a degranulation or intracellular IFNγ accumulation after four hours (**FIG. 199** and **FIG. 200**,

respectively). Addition of AB0089 to the co-cultures resulted in robust induction of degranulation and IFNγ production in a dose-responsive manner. In contrast, neither parental mAb AB0305 nor non-CLEC12A-targeting TriNKET F3'-palivizumab showed a robust increase in CD107a+IFNγ+ NK cells. Assays were performed with three independent PBMC donors in co-cultures with PL21 or HL60 target cells; the results are summarized in Tables 195 and 196, respectively.

Table 195: Summary of NK cell induction of IFNγ and CD107a in co-culture with PL21 cells (Values represent the mean of assays with a total of three donors ± the standard deviation)

Molecule	EC50 (nM)	% Max
AB0089	0.08 ± 0.05	15.3 ± 4.0
AB0305	ND	ND
F3'-palivizumab	ND	ND

ND = Not determined

Table 196: Summary of NK cell induction of IFNγ and CD107a in co-culture with HL60 cells (Values represent the mean of assays with a total of three donors ± the standard deviation)

Molecule	EC50 (nM)	% Max
AB0089	0.05 ± 0.03	15.0 ± 4.6
AB0305	ND	ND
F3'-palivizumab	ND	ND

ND = Not determined

AB0089 induces ADCP activity

[01010] The Fc domain of a human IgG1 antibody can mediate three different types of effector functions.

[01011] One type of Fc-mediated effector function is ADCC, which is carried out by engagement of CD16 on NK cells; NK cell stimulation has been extensively characterized for AB0089. A second Fc-mediated effector function is ADCP, where macrophages attack and engulf cells coated with antibody. For AB0089 and alternative CLEC12A TriNKETs, we wanted to assess their ability to induce ADCP of opsonized target cells. We utilized an in vitro assay system with M0 macrophages, derived from culturing purified CD14+ monocytes with M-CSF, as effector cells. CLEC12A+ target cells were labeled with Cell Trace CFSE dye, opsonized with

test articles and co-cultured with Cell Trace Violet-labeled M0 macrophages. Phagocytosis was analyzed by flow cytometry as Cell Trace Violet+ Cell Trace CFSE+ (double-positive) events.

[01012] AB0089 and other CLEC12A TriNKETs AB0237 and AB0192 all enhanced phagocytosis of PL21 AML cells by M0 macrophages. Parental mAbs for each TriNKET also all showed an ability to induce M0 macrophage phagocytosis of opsonized target cells, but to a lower maximum level compared to their respective corresponding TriNKET (**FIG. 201**). AB0237si, which bears mutations in the CH2 domain to silence Fcγ-receptor binding, served as a negative control. As expected, AB0237si failed to mediate ADCP of opsonized target cells. Results using M0 macrophages derived from three different donors are summarized in Table 197.

Table 197: Summary of EC50 and % Max values for ADCP activity (Values represent the mean of assays with a total of three donors ± the standard deviation.)

Molecule	EC50 (nM)	% Max
AB0237si	ND	ND
AB0037	0.05 ± 0.06	11 ± 9
AB0237	0.08 ± 0.07	12 ± 8
AB0305	0.02 ± 0.01	10 ± 7
AB0089	0.03 ± 0.02	15 ± 10
AB0306	ND	ND
AB0192	0.03 ± 0.02	15 ± 7

ND = Not determined

AB0089 does not have CDC activity

[01013] A third effector function of human IgG1 isotype antibodies is initiation of the complement cascade, leading to complement dependent cytotoxicity (CDC). AB0089 is constructed using a human IgG1 Fc domain; therefore, we wanted to understand the ability of AB0089 to stimulate CDC activity. We used PL21 cells as targets and 5% human serum as a source of complement factors. Neither AB0089 nor its parental mAb AB0305 stimulated complement-mediated killing of PL21 AML cells (**FIG. 202**). In contrast, a positive control antibody against MHC class I (clone W6/32) showed dose-dependent lysis of PL21 target cells in the presence of human serum, corroborating that the serum has active complement factors. Cell

characterization analysis indicated similar expression levels of CLEC12A and MHC class I on PL21 target cells.

[01014] AB0089 demonstrated potent activity in a variety of physiologically relevant contexts. AB0089 was first tested in CLEC12A+ target cell killing assays using rested primary human NK cells. We chose to test killing of CLEC12A+ target cells derived from AML, being the indication that overexpresses CLEC12A in the clinic. For these experiments, we selected HL60 and PL21 as representative AML cell lines.

[01015] AB0089 enhanced primary NK cell cytolysis of both target cell lines and outperformed its parental hIgG1 antibody in enhancing cytolysis. We also examined the impact of soluble NKG2D ligand on the activity of AB0089 and found that physiological levels of soluble MIC-A-Fc did not alter the activity of AB0089 in cell lysis.

[01016] In addition to cell lysis, AB0089 also stimulated cytokine production from NK cells co-cultured with CLEC12A+ target cells. AB0089 enhanced intracellular accumulation of IFNγ as well as NK cell degranulation in co-cultures of human PBMCs with PL21 and HL60 AML cells. EC50 values for IFNγ and CD107a induction by AB0089 were consistent with EC50 values generated in cell lysis assays.

[01017] Finally, we investigated additional mechanisms of action for AB0089. AB0089 was demonstrated to engage macrophages to mediate ADCP of AB0089-opsonized target cells. In contrast, AB0089 does not mediate CDC of AB0089-opsonized target cells.

[01018] AB0089 was demonstrated to have potent activity against CLEC12A+ cancer cells through various effectors, including NK cells and macrophages. Moreover, the activity of AB0089 was maintained in the presence of a physiologically-relevant concentration of soluble NKG2D ligand MIC-A.

Example 19. AB0089 Binding to CLEC12A+ Cell Lines and Primary AML

Objectives

[01019] Measure the binding of AB0089 to human CLEC12A-expressing cells. Quantify CLEC12A surface retention following incubation with AB0089. Demonstrate binding of AB0089 to primary AML patient samples and compare to CLEC12A expression pattern.

Study Design

[01020] Representative cell lines with positive CLEC12A surface expression were used for characterization of AB0089 cell binding. Primary AML patient samples were obtained from Creative Bioarray and BioIVT. Binding of AB0089 and parental mAb AB0305 were compared to a commercially available CLEC12A antibody.

Materials and Methods

Primary cells and cell lines

[01021] Human cancer cell lines were obtained from research cell banks. Below cell lines (item number; vendor) were used: PL21 (ACC-536; DSMZ), HL60 (CCL-240; ATCC), Ba/F3-hCLEC12A (made in-house) and Ba/F3 (available from DSMZ ACC-300).

[01022] Human CLEC12A was introduced into Ba/F3 parental cells by retroviral transduction.

Cell culture materials

[01023] Below items (vendor; item number) were used: RPMI-1640 (Corning; 10040CV), DMEM (Corning; 10031CV), Heat inactivated FBS (ThermoFisher; 16140-071), GlutaMax I (ThermoFisher; 35050-061), Penn/Strep (ThermoFisher; 151450-122), and 2-Mercaptoethanol (MP Biomedicals; 02194705).

Assay materials

[01024] Below items (vendor; item number) were used: Hepes buffered saline (Alfa Aesar; J67502), BATDA reagent (Perkin Elmer; C136-100), TC round bottom 96- well plate (Corning; 3799), Europium solution (Perkin Elmer; C135-100), and DELFIA yellow microplates 96-well (Perkin Elmer; AAAND-0001).

[01025] Below test articles (description) were used: AB0237 (CLEC12A-Targeted TriNKET with Fab NKG2D binding (A49), and scFv CLEC12A binding domain (1602)), AB0300 (AB0237 with LALAPG mutation in CH2 domain), AB0237-Dead-2D (AB0237, NKG2D binding domain mutated to ablate binding), AB0037 mAb (Humanized 1602 anti-CLEC12A mAb), AB0089 (CLEC12A-Targeted TriNKET with Fab NKG2D binding (A49) and scFv CLEC12A binding domain (1739)), AB0305 mAb (Humanized 1739 anti-CLEC12A mAb),

AB0192 (CLEC12A-Targeted TriNKET with Fab NKG2D binding (A49), and scFv CLEC12A binding domain (1797)), AB0306 mAb (Humanized 1797 anti-CLEC12A mAb), hcFAE-A49.h6E7 (CLEC12A-Targeted TriNKET with Fab NKG2D binding (A49), and Fab CLEC12A binding domain (Genentech 6E7)) and hcFAE-A49.CLL1-Merus (CLEC12A-Targeted TriNKET with Fab NKG2D binding (A49), and Fab CLEC12A binding domain (Merus CLL-1 binder)).

[01026] Below instruments (serial number) were used: Attune NxT (2AFC228271119), BD Celesta (H66034400085), and BD Celesta (H66034400160).

Preparation of reagents

[01027] RPMI primary cell culture media was prepared starting with RPMI-1640. 10% HI-FBS, 1x GlutaMax, 1x penn/strep, and 50 μM 2-mercaptoethanol were added for complete media. RPMI cell culture media was prepared starting with RPMI-1640. 10% HI-FBS, 1x GlutaMax, and 1x penn/strep, were added for complete media. 1x HBS was prepared by diluting 1 part of 5x HBS into 4 parts of DI water. Solution was sterile filtered before use.

Binding and detection of surface bound mAb/TriNKET

[01028] 100,000 cells were seeded per well into a 96-well plate for FACS staining. Cells were washed with PBS. Cells were incubated in a 1:2000 dilution of live/dead dye in PBS for 15 minutes, then washed with FACS buffer. TriNKETs or mAbs were diluted into FACS buffer, and 50 μl containing diluted TriNKET or mAb was added to cells. Cells were incubated on ice for 20 minutes. After the incubation, cells were washed with FACS buffer. Anti-human IgG-Fc secondary antibody was diluted into FACS buffer, and 50 μl was added per well for detection of the bound TriNKETs or mAbs. Cells were incubated for 20 minutes on ice, then washed with FACS buffer. 50 μl of fixation buffer was added to each well, and cells were incubated for 10 minutes at room temperature. Cells were washed with FACS buffer and resuspended in FACS buffer for analysis with BD FACS Celesta SN# H66034400085, or BD FACS Celesta SN#H66034400160. Cells of interest were identified using FSC vs. SSC plot, and an appropriately shaped gate was drawn around the cells. Within the gated cells, doublet cells were removed by viewing FSC-H vs FSC-A plot. Within the single cell population, live cells were gated. Within the live gate, the mean fluorescence intensity (MFI) of each sample and the secondary-only control was calculated. Fold-over-background (FOB) was calculated as the ratio

of test article MFI over secondary-only background MFI. Data were fit to a four-parameter non-linear regression curve using GraphPad Prism 7.0.

Surface retention assays

[01029] 100,000 cells were seeded per well into duplicate 96-well plates for FACS staining. Cells were washed with FACS buffer. Test articles were diluted to 40 nM and were added to each of the duplicate plates. The first plate was incubated on ice for 2 hours, while the second plate was moved to 37°C for two hours. After the incubation, cells were washed with PBS and cells were incubated in a 1:2000 dilution of live/dead dye in PBS for 15 minutes, then washed with FACS buffer. Anti-human IgG-Fc secondary antibody was diluted into FACS buffer, and 50 µl was added per well for detection of the bound TriNKETs or mAbs. Cells were incubated for 20 minutes on ice, then washed with FACS buffer. 50 µl of fixation buffer was added to each well, and cells were incubated for 10 minutes at room temperature. Cells were washed with FACS buffer and resuspended in FACS buffer for analysis with BD FACS Celesta SN# H66034400085, or BD FACS Celesta SN#H66034400160. Cells of interest were identified using FSC vs. SSC plot, and an appropriately shaped gate was drawn around the cells. Within the gated cells, doublet cells were removed by viewing FSC-H vs FSC-A plot. Within the single cell population, live cells were gated. Within the live gate, the MFI of each sample was calculated. hIgG1 isotype control MFI was subtracted from all test article MFIs. Surface retention was then calculated as follows:

% surface retention = (2-hour 37°C MFI / 2-hour ice MFI) * 100

Analysis of AB0089 binding in primary AML samples

[01030] Frozen AML patient samples were thawed at 37°C and used immediately in binding assays. Test articles, hIgG1 isotype control and commercial reagent anti-CLEC12A antibody clone 50C1 were labeled using the Biotium Mix-n-Stain CF568 labeling kit; manufacturer's instructions were followed. AML samples were stained with a cocktail of antibodies as described in Tables 198 and 199. Samples were analyzed using an Attune NxT cytometer equipped with CytKick Max autosampler. Raw data was analyzed using FlowJo X software.

Table 198: AML patient sample flow cytometry panel

Fluorophore	Antigen	Dilution factor	Vendor	Cat #
BV421	CD38	100	BioLegend	368514
BV510	CD33	100	BioLegend	366610
BV605	CD15	100	BioLegend	323032
BV650	CD14	100	BioLegend	301836
BV785	CD45	50	BioLegend	368528
FITC	CD34	50	StemCell	60013FI
PE or CF568	CLEC12A		See Table 200	
PE-Cy7	CD117	100	BioLegend	313212
APC	CD13	100	BioLegend	301706
NIR	live-dead	1000	BioLegend	423105
	TruStain FcX	25	BioLegend	422302
	BV buffer	25	BD	566349
	mono block	25	BioLegend	426103

Table 199: CLEC12A antibodies and labeled test articles

Molecule	lot #
hIgG1	EXP20000921 – RMR 18Mar2020
AB0305	EXP200001542 – RMR 22May2020
AB0089	EXP200001542 – RMR 22May2020
AB0306	EXP200001542 – RMR 22May2020
AB0192	EXP200001542 – RMR 22May2020
50C1	EXP200001542 – RMR 22May2020

Table 200: Primary AML patient samples

Sample ID	Tissue	AML subtype	Vendor
19217S	PBMC	M3	Creative Bioarray
19224S	PBMC	M1	Creative Bioarray
19233S	PBMC	M1	Creative Bioarray
19246S	PBMC	M5a	Creative Bioarray
19258S	Bone marrow	M5b	Creative Bioarray
Y1724	PBMC	M4	Creative Bioarray
W5299	PBMC	M2	Creative Bioarray
W5300	PBMC	M3	Creative Bioarray
W5313	Bone marrow	M1	Creative Bioarray
W5294	PBMC	M0	Creative Bioarray

Results and Discussion

CLEC12A TriNKETs bind cell lines expressing human CLEC12A

[01031] Binding of CLEC12A TriNKETs and their parental mAbs were tested using three cell lines expressing human CLEC12A (**FIG. 203**). Mouse Ba/F3 cells were engineered to express human CLEC12A, while PL21 and HL60 are human AML cell lines with endogenous CLEC12A expression.

[01032] As comparators, two tool TriNKETs were generated using CLEC12A binding domains from Genentech (h6E7) and Merus (CLL1-Merus) known in the public domain. Duobody TriNKETs with Fab CLEC12A binding domains were paired with Fab NKG2D binder A49. Duobody TriNKET hcFAE-A49.h6E7 is derived from the Genentech binder, while hcFAE-A49.CLL1- Merus is derived from the Merus binder.

[01033] Lead TriNKET AB0089 and alternative CLEC12A TriNKETs AB0237 and AB0192 all bound CLEC12A expressing cells with nanomolar potency (Table 4). AB0089 had reduced potency but reached a higher maximum FOB compared to its parental mAb AB0305 on the three cell lines tested. AB0237 demonstrated comparable binding to its parental mAb AB0037, yielding potency values within 2-fold of each other for all three cell lines. Variants of AB0237 AB0237-Dead 2D and AB0300 bearing mutations in the NKG2D and CD16 binding domains, respectively, showed similar cell binding compared to AB0237. In contrast, AB0192 showed decreased potency and maximum FOB compared to its parental mAb AB0306.

[01034] In comparison to tool TriNKETs, AB0089 showed comparable cell loading to hcFAE- A49.CLL1-Merus and higher cell loading than hcFAE-A40.h6E7. In addition, AB0237 binding CLEC12A cell lines was more potent than hcFAE-A49.CLL1-Merus and comparable in potency to hcFAE-h6E7. All EC50 binding potencies and maximum FOB binding are summarized in Table 201.

Table 201: Summary of cell binding values

Average EC50 values in nM and mean FOB with ± standard deviation from three independent experiments.

	HL60		PL21		Ba/F3-hCLEC12A	
	EC50 nM	**FOB**	**EC50 nM**	**FOB**	**EC50 nM**	**FOB**

AB0089	1.08 ± 0.24	70 ± 28	0.34 ± 0.13	16 ± 8	2.28 ± 0.59	434 ± 258
AB0305	0.12 ± 0.01	53 ± 16	0.12 ± 0.01	15 ± 9	0.67 ± 0.20	279 ± 182
AB0192	0.61 ± 0.15	42 ± 14	0.37 ± 0.08	12 ± 5	1.33 ± 0.41	325 ± 242
AB0306	0.26 ± 0.08	47 ± 10	0.18 ± 0.05	12 ± 5	0.68 ± 0.09	303 ± 205
AB0237	1.01 ± 0.14	66 ± 18	0.52 ± 0.09	15 ± 6	1.54 ± 0.35	341 ± 249
AB0037	0.52 ± 0.12	51 ± 14	0.52 ± 0.09	13 ± 7	1.40 ± 0.24	301 ± 173
AB0237 Dead-2D	1.19 ± 0.15	59 ± 14	0.63 ± 0.14	14 ± 6	2.35 ± 0.62	357 ± 233
AB0300	1.50 ± 0.19	65 ± 20	1.58 ± 0.14	18 ± 6	2.92 ± 0.57	368 ± 249
hcFAE-A49.h6E7	1.33 ± 0.22	31 ±10	0.55 ± N/A	10 ± 5	2.87 ± 0.56	318 ± 212
hcFAE-A49.CLL1-Merus	2.79 ± 1.04	59 ± 24	1.13 ± 0.14	15 ± 10	4.45 ± 0.78	369 ± 186

CLEC12A-TriNKET surface retention

[01035] Internalization of CLEC12A following antibody ligation has been described in the literature. Leveraging on this phenomenon, antibody-drug conjugates targeting CLEC12A have been developed that depend on internalization of conjugated drugs to kill target cells. TriNKET activity, however, requires cell surface retention of CLEC12A in complex with TriNKETs to allow for NK cell engagement and effector activity against CLEC12A+ cancer cells. To better understand CLEC12A retention on cell surfaces in the presence of CLEC12A TriNKETs, we examined the binding of saturating concentrations of each TriNKET and parental mAb to CLEC12A+ cell lines after a two-hour incubation at 37°C compared to incubations on ice.

[01036] When bound to cells for 2 hours at 37°C, 90% or more of cell surface CLEC12A was retained with each of the TriNKETs. **FIG. 204** shows examples of surface retention for AB0089, AB0192, AB0237 and their parental antibodies on HL60 and PL21 AML lines. The data from three independent experiments are summarized in Table 202. AB0089 appeared to demonstrate superior surface retention compared to other CLEC12A TriNKETs and their parental mAbs.

[01037] However, AB0089 showed a lower binding signal after incubation on ice compared to AB0237 but had a similar signal after incubation at 37°C for two hours, which may have led to inflated surface retention values for AB0089 (**FIG. 205**). Nevertheless, these data suggest temperature-dependent binding of AB0089 to reach equilibrium, which could result from two-step binding mechanism suggested by kinetic binding data (Example 17).

[01038] By contrast, AB0192 and its parental mAb AB0306, which originates from a different parental murine mAb, showed similar surface retention on HL60 and PL21 cells. These data indicate that surface retention of CLEC12A may be dependent upon whether bound monovalently (as is the case for F3' TriNKETs) versus bivalently (as mAbs do) as well as the epitope of the specific binder.

Table 202: Summary of CLEC12A cell surface retention

Values indicate the average percent surface retention for a given test article after two hours at 37°C relative to the same test article after two hours on ice in three experiments ± standard deviation.

	HL60	PL21
AB0089	147 ± 13	124 ± 12
AB0305	90 ± 7	92 ± 2
AB0192	103 ± 8	101 ± 10
AB0306	114 ± 4	106 ± 9
AB0237	106 ± 4	91 ± 9
AB0037	74 ± 1	79 ± 3

AB0089 binds CLEC12A on human AML patient samples

[01039] Primary bone marrow and PBMC samples from a total of 10 AML patients were obtained (see Table 200 for sample information) to examine binding of AB0089 and its parental mAb AB0305 on primary AML cells. We compared binding patterns of fluorophore-labeled test articles AB0089 and AB0305 to a commercially available anti-CLEC12A antibody clone 50C1 (Lahoud et al, The Journal of Immunology. 2009; 182:7587- 7594). Among the 10 donors, the percentage of CLEC12A+ cells in the AML blast gate varied widely from ~ 40-95%. We analyzed AML patient samples from different FAB subtypes, which might contribute to the variation in CLEC12A expression and proportion observed.

[01040] AB0089 and AB0305 demonstrate a comparable binding pattern to anti-CLEC12A clone 50C1 across the 10 AML patient samples tested (**FIG. 206**). We further gated blasts to examine the CD34+CD38- subpopulation, which is enriched for leukemic stem cells, from each sample. Again, AB0089 and AB0305 had similar staining on CD34+CD38- blasts as clone 50C1 (**FIG. 207**). Overall, these data corroborated that AB0089 is able to bind CLEC12A on primary AML blasts as well as on the CD34+CD38- subset that is enriched for LSCs.

[01041] AB0089 and other CLEC12A TriNKETs bound to Ba/F3 cells ectopically expressing human CLEC12A as well as PL21 and HL60 AML cells expressing endogenous CLEC12A in a dose-responsive manner with similar nanomolar potencies across the lines. Despite reports in the literature of CLEC12A internalization following antibody ligation, AB0089 and both alternative CLEC12A TriNKETs AB0237 and AB0192 showed high cell surface retention of CLEC12A after two hours of incubation with HL60 and PL21 CLEC12A+ cell lines. Finally, AB0089 and its parental mAb AB0305 bound similarly to a commercial reagent anti-CLEC12A antibody clone 50C1 on bulk and CD34+CD38- blasts across primary AML patient samples from 10 donors. Together, these data support potent binding of AB0089 to cells expressing CLEC12A and indicates that AB0089 binds to primary AML blasts.

Example 20. AB0089 CLEC12A TrinKET

Objectives

[01042] The objectives of this study are to describe the molecular format, design, structure, and characteristics of CLEC12A TriNKET AB0192. In particular, in this report we a) describe the molecular format and design of AB0192, b) provide information about expression and purification of AB0192, c) describe basic biochemical and biophysical characterization of the molecule, d) determine the affinity of AB0192 for recombinant human targets (CLEC12A, NKG2D and CD16a), e) demonstrate AB0192 binding to isogenic and AML cancer cell lines expressing human CLEC12A, f) demonstrate selectivity of AB0192, g) determine potency of AB0192 in killing AML cancer cells, h) assess binding epitope, i) assess binding to FcγR and FcRn and compare with IgG1 mAb control, j) describe behavior of AB0192 in developability studies including accelerated stability, forced degradation, and manufacturability.

Study Design

[01043] Murine anti-human CLEC12A mAb (9F11.B7) was discovered by mouse immunization. 9F11.B7 was humanized, converted to a scFv and combined with A49M-I NKG2D Fab binding arm to produce an F3'-TriNKET (AB0192). AB0192 was assessed by binding to recombinant human and cyno CLEC12A, binding to isogenic and cancer cells expressing CLEC12A as well as potency of the molecule against CLEC12A+ AML cancer cells. The biophysical and biochemical characteristics of AB0192 including thermal stability (DSC),

hydrophobicity (HIC), and pI (cIEF) were determined. Specificity of binding was assessed by PSR, binding to cells not expressing the target of interest and by HuProt™ Array. AB0192 was expressed in two different mammalian cell lines (Expi293 and ExpiCHO) and purified using DragonflyTx 2-step platform purification method. Binding properties of AB0192, including CLEC12A, NKG2D, CD16a (V158 and F158), an extended panel of Fcγ receptors (CD32a (H131 and R131), CD16b, CD32b, cynomolgus CD16, human and cynomolgus CD64), and FcRn (human and cynomolgus) was fully characterized. Binding epitope was characterized in binning experiment with CLEC12A binding molecules from Merus and Genentech. Lastly, AB0192 was assessed in a full developability panel, including accelerated (40ºC) stability in the Dragonfly Tx platform formulation (20 mM histidine, 250 mM sucrose, 0.01% Tween-80, pH 6.0) and 20 mM citrate, 250 mM sucrose, 0.01% Tween-80, pH 7.0 buffer, forced degradation (long term pH 5, pH 8 stress, forced oxidation), and manufacturability (freeze/thaw, agitation, low pH hold).

Materials and Methods

[01044] Methods used to produce and characterize AB0192 are similar to the ones used in Example 17.

Test Articles

[01045] AB0192-002, (Benchling record name AB0192), humanized TriNKET expressed in Expi293 (lot AB0192-002).

[01046] AB0192-005, (Benchling record name AB0192), humanized TriNKET expressed in ExpiCHO (lot AB0192-005).

Protein reagents

Table 203: Summary of protein reagents.

Name	Manufacturer	Lot
Human CLEC12A-His	Dragonfly Tx	16Oct18GL
Human CLEC12A-K244Q-His	Dragonfly Tx	30Apr18AC
Cyno CLEC12A-His	Dragonfly Tx	30May18AC
mFc-hNKG2D	Dragonfly Tx	01Dec17AB
mFc-cNKG2D	Dragonfly Tx	28Sep18GL

Name	Manufacturer	Lot
humanized mAb 16B8.C8	Dragonfly Tx	AB0037-001
hcFAE-A49.CLL1-Merus (Duobody TriNKET)	Dragonfly Tx	10May18DF
hcFAE-A49.h6E7 (Duobody TriNKET)	Dragonfly Tx	05Feb19DF
hcFAE-A49.tepoditamab (Duobody TriNKET)	Dragonfly Tx	27Aug19XL
Trastuzumab	Roche	N3017H05
Adalimumab	AbbVie	83364XH07
Rituximab	Dragonfly Tx	19Apr19 MH

Results

Discovery of AB0192 TriNKET

[01047] Hybridoma subclone 9F11.B7 was discovered through immunization of BALB/c mouse strain with recombinant human CLEC12A-his preformed at Green Mountain Antibodies (Burlington, VT).

[01048] Murine 9F11.B7 was humanized by grafting murine CDRs to the appropriate human framework (VH3-30*02 and VK1-33) without loss of affinity for recombinant CLEC12A or cell surface expressed target (FIG. 208). 7 murine backmutations were introduced to maintain CDRs architecture. Humanized 9F11.B7 mAb was converted to a scFv and paired with NKG2D targeting A49 M-I Fab to produce F3' TriNKET (AB00192). This TriNKET was extensively characterized and designated as a candidate for CLEC12A program AB0192.

Molecular format and design

[01049] AB0192 is a heterodimeric tri-functional antibody that redirects NK and T cell activity against CLEC12A-expressing cancer cells. AB0192 contains three chains: Chain H, Chain L and Chain S. The schematic representation of the AB0192 molecule is provided in FIG. 209. Chain H is the heavy chain of A49M-I that was selected for having low affinity while being a potent agonist of NKG2D receptors on NK and cytotoxic T cells. The M-I mutation was introduced to replace the Met102 residue in the CDRH3 that is sensitive to oxidation and therefore may present a liability. Chain L is the light chain of the anti-NKG2D-targeting antibody A49M-I. Chain S contains a scFv that binds with high affinity to CLEC12A on AML cancer cells. Both scFv and Fab domains are fused to a human IgG1 Fc that has native,

unmodified sequence in the CH2 domain, where antibodies bind to Fc receptors. Both chains bear several mutations in the CH3 domain introduced to ensure stable heterodimerization of two Fc monomers. There are seven such mutations in the IgG1 Fc of the AB0192: three mutations in Chain H (K360E, K409W, Y349C) and four mutations in Chain S (Q347R, D399V, F405T and S354C). Two of these mutations are involved in the formation of a stabilizing S-S bridge (Y349C and S354C) between Chains H and Chain S (EU nomenclature). scFv (VH-VL orientation) in Chain S is stabilized by two mutations introducing a S-S bridge ((H44)C and (L100)C, Chothia nomenclature). Chain S also contains a (G4S)4 non-immunogenic linker between VH and VL of scFv. The amino acid sequence of the CLEC12A-targeting scFv is based on the sequence of humanized 9F11.B7 antibody, obtained from hybridoma (Green Mountain Antibodies, Burlington, VT). The amino acid sequence of NKG2D Fab is based on the fully human antibody A49M-I, obtained using human yeast display technology (Adimab, Lebanon, NH).

Description of heterodimerization mutants

[01050] EU-numbering convention was used to annotate the amino acid residues in the Fc.

[01051] Chain H contains the following mutations:

K360E – Heterodimerization mutation in the CH3 domain of the Fc region.

K409W – Heterodimerization mutation in the CH3 domain of the Fc region.

Y349C – Inter-subunit disulfide stabilization mutation in the CH3 domain of the Fc region.

[01052] The K360E/K409W mutations in the Fc region of Chain H are designed to render heterodimer-favoring interactions with Chain S due to hydrophobic/steric complementarity plus long-range electrostatic interactions (Choi *et al.*, (2013) *Mol Cancer Ther* 12(12):2748–59; Choi *et al.*, (2015) *Mol Immunol* 65(2):377–83). The mutation Y349C was introduced to generate an additional inter-chain disulfide bond Y349C-(CH3-ChainH) – S354C(CH3-ChainS) pair (Choi e*t al.*, (2015) *Mol Immunol* 65(2):377–83.).

[01053] Chain S contains the following mutations:

G44C – Disulfide stabilization mutation in VH region of the scFv.

Q100C – Disulfide stabilization mutation in VL region of the scFv.

Q347R – Heterodimerization mutation in the CH3 domain of the Fc region.

D399V – Heterodimerization mutation in the CH3 domain of the Fc region.

F405T – Heterodimerization mutation in the CH3 domain of the Fc region.

S354C – Inter-subunit disulfide stabilization mutation in the CH3 domain of the Fc region.

[01054] The mutations G(H44)C and Q(L100)C were introduced to stabilize the scFv by an engineered disulfide bond between the VH and the VL. The disulfide stabilization improves structural and thermal stability of scFv. The Q347R/D399V/F405T mutations in the Fc region of Chain S were designed to render heterodimer-favoring interactions with Chain H due to hydrophobic/steric complementarity plus long-range electrostatic interactions (Choi *et al*, (2013) *Mol Cancer Ther* 12(12):2748–59). The mutation S354C was introduced to generate an additional inter-CH3 disulfide bond with a Y349C(CH3-ChainH) – S354C(CH3-ChainS) pair (Choi *et al*., (2015) *Mol Immunol* 65(2):377–83).

Amino Acid sequence

[01055] The amino acid sequences of the three polypeptide chains that make up AB0192 are shown in FIG. 210. CDRs are outlined in Table 204.

Table 204: Sequences of AB0192 CDRs*.

AB0192	Variable region	Framework	CDR1	CDR2	CDR3
Chain S	VH	VH3-30	GFTFNAF (SEQ ID NO:195)	SSGSTS (SEQ ID NO:196)	DGYPTGGAMDY (SEQ ID NO:187)
Chain S	VL	VK1-33	KASQDIYNYLS (SEQ ID NO:198)	RANILVS (SEQ ID NO:199)	LQFDAFPFT (SEQ ID NO:201)
Chain H	VH	VH3-21	GFTFSSY (SEQ ID NO: 297)	SSSSY (SEQ ID NO:338)	GAPMIGAAAGWFDP (SEQ ID NO:339)
Chain L	VL	VK1-12	RASQGISSWA (SEQ ID NO:337)	AASSLQS (SEQ ID NO:77)	QQGVSFPRT (SEQ ID NO:87)

* CDRs are identified by Chothia

Analysis of potential sequence liabilities

[01056] Chain L (NKG2D binding light chain) has no predicted liabilities. Chain H (NKG2D binding heavy chain) has a DP in CDRH3. This motif is not affected by forced degradation. As such, this sequence was not altered in AB0089. Chain S contains a Met (potential oxidation site) and DG (potential isomerization site) in CDRH3. No preemptive removal of M or DG in CDRH3 was attempted. We have carefully monitored modification of these residues during accelerated stability and forced degradation studies. No modification of Met or DG was observed under any stresses tested, as shown below.

Framework assessment

[01057] The CLEC12A binding arm of AB0192 was discovered through mouse immunization. The frameworks chosen for humanization are frequently used in clinical stage therapeutic monoclonal antibodies (FIG. 211). The NKG2D binding arm is fully human, is based on a framework frequently used in advanced stage mAbs and does not contain any unusual residues or deviations from the germline.

Backmutations

[01058] Molecular modelling was used to choose murine backmutations that help maintaining CDRs architecture (Table 205). Seven backmutations: 3 in the HC and 4 in the LC were introduced.

Table 205: Summary of murine backmutations introduced in the human framework in AB0192.

Framework	Number of back mutations	Murine framework residues (Chothia)
VH	3	E(H1), R(H94), S(H108)
VL	4	F(L36), P(L46), Q(L69), Y(L71)

Structure modeling

[01059] In the absence of a crystal structure, structural models of the variable segments of CLEC12A and NKG2D binding arm were generated for comparison. Model building was performed using the SAbPred website (opig.stats.ox.ac.uk/webapps/newsabdab/sabpred/).

Surface charge distribution and hydrophobic patch analysis of CLEC12A binding arm of AB0192

[01060] FIG. 212 illustrates a ribbon diagram model of the CLEC12A binding scFv in three different orientations (upper panel) and their corresponding surface charge distribution of the same orientation (lower panel). The charge distribution of anti-CLEC12A scFv is polarized ("top view", lower panel), with negatively-charged residues populated predominately within CDRH3 and CDRL2. The uneven distribution of electrostatic patches on the paratope is likely to be target-related and reflects the complementarity of charge distribution on its cognate epitope, which may likely contribute to the high affinity interaction between CLEC12A and the scFv of AB0192.

[01061] FIG. 213 shows the analysis of CDR length and surface hydrophobicity patches of the CLEC12A-targeting arm of AB0192. Analyses were performed using therapeutic antibody profiles (TAP): opig.stats.ox.ac.uk/webapps/newsabdab/sabpred/tap. It compares the candidate in reference to 377 late-stage therapeutic antibodies. The length of CDRs for the CLEC12A-binding arm of AB0192 are within typical for late stage therapeutic antibodies. Hydrophobic patch analysis of the CDRs of an antibody is predictive of its developability. The theoretical hydrophobic properties of the TAA arm of AB0192 are well within the norm of commercialized biotherapeutics and late-stage therapeutic antibody candidates.

[01062] FIG. 214 shows the analysis of patches containing positive and negative charges, as well as the symmetry of these charges around the CDR regions. All three charts indicate that the charge distributions are within the norm compared to advanced stage therapeutic antibodies.

Surface charge distribution and hydrophobic patch analysis of NKG2D binding arm of AB0192

[01063] The NKG2D-binding Fab arm is shown in ribbon diagrams with three different orientations (FIG. 215, upper panel) and their corresponding surface charge distribution of the same orientation are provided in FIG. 215, lower panel). The surface charge distribution on NKG2D A49M-I arm is more evenly distributed than charges on CLEC12A targeting arm of the molecule.

[01064] FIG. 216 shows the CDR length and patches of surface hydrophobicity analyses of NKG2D-targeting arm of AB0192. It appears that the CDR length, the hydrophobic properties,

the positive/negative charge distributions of the NKG2D-targeting arm of AB0192 are well within the norm of existing therapeutic antibodies.

[01065] FIG. 217 shows the analyses of patches containing positive and negative charges, as well as the symmetry of these charges around the CDR regions. All three charts indicate that the charge distributions are within the norm comparing with the population of therapeutic antibodies.

Immunogeniity prediction

[01066] The protein sequences of three chains of AB0192 were examined for the presence of potentially immunogenic T cell epitopes using the EpiMatrix algorithm and to rank the immunogenicity potential (FIG. 218). AB0192 scores favorably on the Treg adjusted Immunogenicity Protein Scale. The Treg adjusted Epimatrix Protein Score for the sequences of the three chains of AB0192 are chain H: -33.39, chain S: -19.94 and chain L: -23.49 (Table 206). The predicted risk of immunogenicity for the AB0192 appears to be low.

Table 206: EpiVax immunogenicity analysis of AB0192.

Protein Sequence	Length	EpiMatrix Hits	EpiMatrix Score	Treg adjusted Score
AB0192_CHAIN_H	451	207	5.99	-33.39
AB0192_CHAIN_L	214	98	11.17	-23.49
AB0192_CHAIN_S	475	227	12.13	-19.94

Expression

[01067] Expression of AB0192 was achieved using Dragonfly Tx F3' TriNKET platform purification method. Briefly, AB0192 was expressed by transient transfection of Expi293 and ExpiCHO cells with three plasmids encoding the NKG2D targeting light chain (chain L), the NKG2D targeting IgG heavy chain (chain H), and the CLEC12A targeting scFv-Fc fusion (chain S). For both Expi293 and ExpiCHO expression, Chain S: Chain H: Chain L were transfected at the plasmid ratio 4:1:1 to maximize the percentage of desired heterodimer product. This ratio was empirically obtained based on previous humanized TriNKETs developed and was not specifically optimized for AB0192.

Purification

[01068] Purification of AB0192 was performed using 2 step F3' TriNKET platform purification method. No optimization or extensive process development for AB0192 purification was performed. The schematic representation of AB0192 purification (lot AB0192-005) expressed in ExpiCHO is shown on FIG. 219.

[01069] Two lots of AB0192 were produced in transiently transfected ExpiCHO and Expi293 cells. Table 207 summarizes the titer and final product purity for both lots.

Table 207: Summary of expression titers and final purity of two AB0192 lots.

AB0192 Lot	Expression host	Titer (mg/L)	Purity, %Monomer
AB0192-002	Expi293	16	99.5
AB0192-005	ExpiCHO	26	100.0

[01070] The identity of AB0192 was corroborated by mass spectrometry. LC-MS analysis of the intact AB0192 (lot AB0192-005) showed an observed mass (126,429.9 Da) (FIG. 220) that agrees well with the theoretical mass of 126,429.5 Da. The major observed glycosylation pattern (G0F/G0F) is typical for an Fc-containing molecule expressed in CHO cells.

Biochemical and biophysical properties

[01071] AB0192 was characterized by SEC, CE, cIEF, HIC, and DSC to corroborate that is has the proper purity and pre-developability characteristics of a good biological therapeutic.

Purity

[01072] Purity of AB0192 (lot AB0192-005) assessed by SEC, non-reduced and reduced CE-SDS is summarized Table 208.

Table 208: Purity of AB0192 by SEC and CE-SDS analysis.

Test article	SEC			NR CE-SDS	R CE-SDS
	HMW (%)	Monomer (%)	LMW (%)	Purity (%)	Purity (%)
AB0192 (lot AB0192-005)	ND	100	ND	95	98.8

Size exclusion chromatography

[01073] SEC analysis of purified AB0192 (lot AB0192-005) showed >99% monomer as determined by integrated peak area (FIG. 221).

Non-reduced and reduced CE-SDS

[01074] AB0192 has high purify by CE-SDS (FIG. 222). Under non-reduced conditions (left panel) the major impurities are method induced (free light chain and TriNKET – LC). Under reduced conditions (right panel) three expected chains (light chain (L), heavy chain (H), and scFv-Fc chain (S)) are observed.

Experimental pI and charge profile by cIEF

[01075] cIEF profile of AB0192 (lot AB0192-005) is shown on (FIG. 223). AB0192 has a major peak at a pI of 8.9 ± 0.0. Several lesser abundant, overlapping acidic peaks and minor basic peaks are also observed.

Hydrophobicity assessed by HIC

[01076] Hydrophobicity of AB0192 was assessed using hydrophobic interactions chromatography (HIC) (FIG. 224 and Table 209). The chromatogram reveals a single narrow peak, indicating that the molecule is highly pure and homogeneous. Retention time for AB0192 is comparable with retention time of Humira (a well behaved therapeutic monoclonal antibody).

Table 209: Hydrophobicity assessment of AB0192 by HIC.
Humira is used as an internal control of well-behaved IgG1 mAb.

Test article	Retention time (min)
AB0192	9.9
Humira	8.9

Thermal stability by DSC

[01077] The thermal stability of AB0192 was assessed by DSC in several buffers (PBS, pH 7.4, HST, pH 6.0, CST, pH 7.0). AB0192 demonstrated high thermal stability in all buffers tested (FIG. 225, Table 210). Tm1 corresponding to the unfolding of scFv satisfied ≥65°C criteria postulated in thermostability assessment.

Table 210: Thermal stability analysis of AB0192 in three different buffer systems by DSC.

Test Article	Buffer	T_{onset} (°C)	T_{m1} (°C)	T_{m2} (°C)	T_{m3} (°C)	T_{m4} (°C)
AB0192	PBS, pH 7.4	60.0	67.3	76.5	81.4	83.3
AB0192	HST, pH 6.0	60.8	69.0	78.8	84.0	86.1
AB0192	CST, pH 7.0	61.2	68.0	77.4	82.0	83.9

Disulfide bond assignment

[01078] AB0192 is an engineered molecule based on the backbone of a monoclonal IgG1 antibody. While a typical IgG1 contains 16 disulfide bonds, AB0192's F3' format has only 15 disulfide bonds. Half of AB0192 is an anti-NKG2D half antibody, as such it contains the expected seven disulfide bonds (one in each IgG domain and the intermolecular disulfide connecting the LC to the HC). The other half of AB0192 is an anti-CLEC12A scFv-Fc fusion. The scFv contains three disulfide bonds (one in each anti-CLEC12A VH and VL domains and an engineered, stabilizing disulfide bridging the variable domains) and the Fc contains the two expected disulfides in the IgG domains. The heterodimer is held together with two hinge disulfides and one additional intermolecular engineered disulfide connecting the Fab-Fc to the scFv-Fc in the CH3 domain. Together this results in 15 expected disulfide bonds in AB0192. The predicted disulfide map for AB0192 is shown in FIG. 226.

[01079] The disulfide bond connectivity of AB0192 was corroborated by LC-MS/MS peptide mapping analysis of a non-reduced digest. Disulfide bonded peptides were identified by MS/MS database searching and corroborated by comparing their intensities in the native and reduced digests. To observe the engineered scFv stabilizing disulfide, AB0192 was digested with both trypsin and chymotrypsin. FIG. 227 shows the extracted ion chromatogram (XICs) for the engineered disulfide pair in the scFv (non-reduced and reduced) and the most intense charge state for that peptide pair. All other disulfides were identified after digestion with only trypsin. XICs in FIG. 228 corroborates the existence of the engineered S-S bridge introduced to stabilize the Fc heterodimerization. A summary of the observed disulfide linked peptides in AB0192 is shown in Table 211. All theoretical disulfide linked peptides were observed with high mass accuracy (<5 ppm), were reducible, and were sequence corroborated by MS/MS fragmentation.

Table 211: Disulfide linked peptides theoretical and experimental masses.

Domain	Peptide	Theoretical mass (Da)	Experimental mass (Da)	Mass accuracy (ppm)
VL	L2:L7	4482.0784	4482.0791	0.5
CL	L12:L19	3555.7490	3555.7527	1.4
CL-CH1 intermolecular	L20-21:H19	1260.4863	1260.4862	0.2
VH	H3:H10	3371.4686	3371.4728	1.3
CH1	H13:H14-15	7916.9194	7916.9162	0.2
Hinge	H20-21:S20-21	5454.7834	5454.7899	1.6
CH2	H23:H30	2328.0977	2328.1015	1.5
CH3-CH3 intermolecular[a]	H36:S37-38	2757.3830	2757.3866	1.7
CH3	H37:H41	4432.0675	4432.073	1.3
scFv VL	S26:S42-44[b]	1747.8314	1747.8381	3.8
scFv VH	S2:S9	3359.4951	3359.4993	1.3
scFv stabilizing[a]	S8:S46[b]	1011.4154	1011.4198	4.4
CH2	S23:S30	non-unique, see H23:H30		
CH3	S39:S44	3844.8236	3844.8287	1.2

[a] Engineered disulfide

[b] Trypsin/chymotrypsin double digest

Binding characteristics

Binding to human CLEC12A

[01080] The affinity of AB0089 for human CLEC12A was determined by SPR at 37°C. AB0089 binds with high affinity to human CLEC12A (FIG. 229, Table 212). Per TriNKET MOA, the molecule is designed to bind strongly to TAA and weakly to NKG2D and CD16a. The complex between AB0192 and human CLEC12A is strong as evidenced from the slow rate dissociation constant $1.40 \pm 0.09 \times 10^{-3}$ s^{-1}. The equilibrium binding affinity K_D for AB0192 is 1.81 ± 0.16 nM.

Table 212: Kinetic parameters and binding affinity of AB0192 for hCLEC12A measured by SPR.

Test article	Target	k_a ($M^{-1}s^{-1}$)	k_d (s^{-1})	K_D (nM)
AB0192	hCLEC12A-His	$7.87x10^5$	$1.36x10^{-3}$	1.72
AB0192	hCLEC12A-His	$7.57x10^5$	$1.51x10^{-3}$	1.99
AB0192	hCLEC12A-His	$7.85x10^5$	$1.34x10^{-3}$	1.71
Average ± Std Dev.	**hCLEC12A-His**	**$(7.76\pm0.17)\ x10^5$**	**$(1.40\pm0.09)\ x10^{-3}$**	**1.81 ± 0.16**

Average of 3 replicates

Binding to polymorphic variant of human CLEC12A (Q244)

[01081] Polymorphic variant CLEC12A (Q244) is prevalent in 30% of population. We tested binding of AB0192 to this genetic variant by SPR and compared its affinity to CLEC12A (K244) WT (FIG. 230). Binding affinities of AB0192 for WT and (K244Q) variant of CLEC12A are within 2.5-fold (Table 213). Binding of AB0192 to cynomolgus monkey CLEC12A (cCLEC12A) was also tested. No quantifiable binding was observed at 100 nM concentration.

Table 213: Kinetic parameters and binding affinities for (K244) and (Q244) variants of human CLEC12A.

Test article	Target	k_a ($M^{-1}s^{-1}$)	k_d (s^{-1})	K_D (nM)
AB0192	hCLEC12A (K244) WT	$(6.98\pm0.09) \times 10^5$	$(1.15\pm0.01) \times 10^{-3}$	1.65 ± 0.04
AB0192	hCLEC12A (Q244)	$(8.24\pm1.33) \times 10^5$	$(3.70\pm0.38) \times 10^{-3}$	4.51 ± 0.26

Binding to differentially glycosylated CLEC12A

[01082] Human CLEC12A is a heavily glycosylated protein (6 potential N-glycosylation sites with an ECD compromising of 201 amino acids). Variations in the glycosylation status of CLEC12A on the surface of different cell types is documented in the literature (Marshall *et al.*, 2006) *Eur. J. Immunol.*, 36: 2159-2169). CLEC12A expressed on the surface of AML cells from different patients may have different glycosylation pattern as well. To determine AB0089 binds to different glyco-variants of human CLEC12A, the antigen was treated with neuraminidase (to remove terminal sialic acids) or PNGase F (to remove N-linked glycans) and affinity was compared to untreated CLEC12A by SPR. AB0192 bound to both glycosylated and de-

glycosylated variants of CLEC12A (FIG. 231 and Table 214) and is expected to be unaffected by heterogeneity in target glycan composition.

Table 214: Kinetic parameters and binding affinity of AB0192 for differentially glycosylated CLEC12A.

Test article	Target	k_a ($M^{-1}s^{-1}$)	k_d (s^{-1})	K_D (nM)
AB0192	untreated CLEC12A	(6.98±0.09) × 10^5	(1.15±0.01) × 10^{-3}	1.65 ± 0.04
AB0192	De-sialylated CLEC12A	(1.01±0.03) × 10^6	(1.04±0.00) × 10^{-3}	1.04 ± 0.03
AB0192	De-glycosylated CLEC12A	(1.31±0.02) × 10^6	(3.48±0.11) × 10^{-4}	0.27 ± 0.01

Average of 3 replicates

Binding to CLEC12A+ isogenic and cancer cell lines

[01083] Assessment of AB0192 binding to both isogenic cell lines expressing CLEC12A and AML cancer cells was monitored by FACS (FIG. 232 and Table 215). AB0192 showed high affinity for cell surface expressed CLEC12A on the isogenic Ba/F3-CLEC12A cells and binds AML cell lines PL-21 and HL-60 with EC50 of less than 1 nM. Specificity of AB0089 for CLEC12A was demonstrated by lack of binding to the parental Ba/F3 cells that do not express the target.

Table 215: Binding of AB0192 to isogenic Ba/F3-CLEC12A and cancer cell lines expressing CLEC12A.

Cell line	EC50 (nM)
Ba/F3-hCLEC12A	0.91
Ba/F3 parental	No binding
PL21	0.43
HL-60	0.6

Binding to human NKG2D

[01084] Binding of AB0192 to human NKG2D ECD by SPR at 37°C (Biacore) (FIG. 233). NKG2D is a dimer in nature, therefore recombinant mFc-tagged NKG2D dimer was used for this experiment. Affinity was determined using AB0192. FIG. 233 shows AB0192 binding sensorgrams to human NKG2D. Two different fits were utilized to obtain the equilibrium affinity data: steady state affinity fit and kinetic fit. The kinetic constants and equilibrium affinity constants are shown in Table 216. AB0192 was designed to bind to human NKG2D with low affinity, most importantly with the fast rate of dissociation. The dissociation rate constant was (1.46±0.06 x10-1 s-1). Equilibrium affinity constants (KD) obtained by kinetics fit and steady state affinity fit were very similar, 779 ± 10 nM and 781 ± 9 nM, respectively, which suggests high confidence in the measured parameters.

Table 216: Kinetic parameters and affinities of AB0192 for human NKG2D measured by SPR.

Test article	Target	k_a ($M^{-1}s^{-1}$)	k_d (s^{-1})	Kinetics Fit K_D (nM)	Steady State Fit K_D (nM)
AB0192	hNKG2D	$1.86x10^5$	$1.43x10^{-1}$	770	770
AB0192	hNKG2D	$1.96x10^5$	$1.53x10^{-1}$	778	783
AB0192	hNKG2D	$1.81x10^5$	$1.43x10^{-1}$	790	788
Average ± Std Dev.	**hNKG2D**	**$(1.88±0.08) x10^5$**	**$(1.46±0.06) x10^{-1}$**	**779 ± 10**	**781 ± 9**

Binding to human CD16a (V158 allele)

[01085] One of the modalities of AB0192 mechanism of action is through engaging human CD16a (FcγRIIIa) that is expressed on NK cells via its Fc. AB0192 binding to human CD16a was tested by SPR (FIG. 234, Table 217). CD16a high affinity V158 allele was used for this experiment. Since the literature reported Fc receptor affinity values for IgG1 vary depending on the experimental design and sourcing of the receptors, trastuzumab (Herceptin) was included as a human IgG1 control. The affinity of AB0192 for both alleles is comparable (around two-fold different) to trastuzumab's affinity for the same receptor. We do not expect this difference to have any meaningful physiological significance.

Table 217: Kinetics and affinities of AB0192 for hCD16a (V158) and trastuzumab measured by SPR.

Test article	k_a ($M^{-1}s^{-1}$)	k_d (s^{-1})	K_D (nM)
AB0192	1.03 x 10^5	1.90 x 10^{-2}	184
AB0192	1.16 x 10^5	2.01 x 10^{-2}	173
AB0192	1.16 x 10^5	2.06 x 10^{-2}	177
Average ± StDev	**(1.12±0.08) x10^5**	**(1.99±0.08) x10^{-2}**	**178 ± 6**
Trastuzumab	1.31 x 10^5	1.12 x 10^{-2}	86
Trastuzumab	1.22 x 10^5	1.08 x 10^{-2}	89
Trastuzumab	1.30 x 10^5	1.13 x 10^{-2}	87
Average ± StDev	**(1.28±0.05) x 10^5**	**(1.11±0.03) x 10^{-2}**	**87 ± 1**

Testing CD16a-NKG2D synergy

[01086] AB0192 is a tri-functional IgG-based biologic with two binding modalities on the NK cells: CD16a binding is achieved through the Fc and NKG2D binding is achieved through A49M-I Fab. Both interactions are important for the optimal cytotoxic activity of AB0192. To demonstrate synergy of co-engagement of human CD16a and human NKG2D binding, we performed an SPR experiment where we qualitatively compared binding of AB0192 to NKG2D, CD16a and mixed NKG2D-CD16a Biacore chip surfaces. The affinity of AB0192 for human NKG2D and human CD16a are both low, however, binding to both targets simultaneously results in an avidity effect that manifests as a slower off-rate (FIG. 235). Thus, AB0192 can avidly engage CD16a and NKG2D.

Co-engagement of CLEC12A and NKG2D

[01087] To determine if binding of one target interferes with binding of the other target to AB0192, CLEC12A and NKG2D were sequentially injected over AB0192 captured on an anti-hFc IgG SPR chip (FIG. 236). Target binding sensorgrams demonstrate that the occupancy status of CLEC12A does not interfere with NKG2D binding (FIG. 236 upper panel) and vice versa (FIG. 236, lower panel). Similarity in the shapes of the respective sensorgrams segments depicting binding of each target to free AB0192 and AB0192 that has been saturated with the

other target suggest that the kinetic parameters are not meaningfully affected by the target occupancy status of the AB0192 molecule. For instance, the shape of the CLEC12A binding segment of the sensorgrams is similar in both panels. Additionally, the lack of any impact on relative stoichiometry of each target binding (when compared to binding to unoccupied AB0192) signifies full independence of NKG2D and CLEC12A binding sites on AB0192 (Table 218). Therefore, AB0192 successfully achieves simultaneous co-engagement of the tumor antigen and the NKG2D targeting arm.

Table 218: Relative binding stoichiometries of AB0192 for CLEC12A and NKG2D. Binding stoichiometries are expressed relative to binding of each target to unoccupied captured AB0192.

	CLEC12A, relative binding stoichiometry	**NKG2D,** relative binding stoichiometry
Target bound to AB0192 unoccupied with another target (injected first)	1.00	1.00
Target bound to AB0192 saturated with another target (injected second)	1.03 ± 0.07	1.15 ± 0.20

Binding to Fcγ receptors

[01088] Since AB0192 is an IgG1 derived biologic drug candidate it is important that it maintains appropriate Fc receptor binding properties. SPR data suggest that AB0089 binds human and cynomolgus Fcγ receptors with affinities comparable to trastuzumab, a marketed IgG1 biologic that served an experimental control (Table 219). Detailed description of each individual receptor binding is presented below.

Table 219: Binding of AB0192 and trastuzumab binding recombinant human and cynomolgus FcγRs.

Fcγ receptor	AB0192 K_D (nM)	Trastuzumab, hIgG1 control K_D (nM)
hFcγRI	5.2 ± 1.2	2.9 ± 0.4
cFcγRI	1.9 ± 0.3	1.0 ± 0.1
hFcγRIIa H131	1011.3 ± 63.3	1045.1 ± 62.2
hFcγRIIa R131	1398.8 ± 286.1	1493.2 ± 265.9
hFcγRIIIa V158[a]	178.3 ± 5.5	87.1 ± 1.4
hFcγRIIIa F158	680.0 ± 69.6	331.4 ± 3.3
cFcγRIII[a]	203.8 ± 1.0	128.8 ± 2.1
hFcγRIIb	6062.3 ± 827.0	6270.3 ± 1031.7
hFcγRIIIb[a]	6014.8 ± 735.5	3872.4 ± 486.3

[a] n=3, otherwise n=4.

Binding to human and cynomolgus CD64 (FcγRI)

[01089] Table 220 demonstrates that AB0089 binds recombinant human and cynomolgus CD64 (FcγRI) with affinities comparable (less than two-fold different) to trastuzumab. FIG. 237 and FIG. 238 depict binding of AB0089 to human and cynomolgus CD64, respectively.

Table 220: Binding of AB0192 and trastuzumab to recombinant human and cynomolgus CD64 (FcγRI)

Test article	k_a ($M^{-1}s^{-1}$)	k_d (s^{-1})	K_D (nM)
Human CD64 (FcγRI)			
AB0192 Lot AB0192-005	4.7×10^4	2.9×10^{-4}	6.1
AB0192 Lot AB0192-005	4.7×10^4	2.6×10^{-4}	5.5
AB0192 Lot AB0192-005	4.7×10^4	2.6×10^{-4}	5.5
AB0192 Lot AB0192-005	5.2×10^4	1.8×10^{-4}	3.5
Average ± StDev	**$(4.8 \pm 0.3) 10^4$**	**$(2.5 \pm 0.5) \times 10^{-4}$**	**5.2 ± 1.2**
trastuzumab	9.0×10^4	2.3×10^{-4}	2.5

Test article	k_a ($M^{-1}s^{-1}$)	k_d (s^{-1})	K_D (nM)
trastuzumab	8.6×10^4	2.1×10^{-4}	2.5
trastuzumab	8.3×10^4	2.7×10^{-4}	3.2
trastuzumab	8.8×10^4	2.8×10^{-4}	3.2
Average ± StDev	**$(8.1 \pm 0.0) \times 10^4$**	**$(2.5 \pm 0.3) \times 10^{-4}$**	**2.9 ± 0.4**
Cynomolgus CD64 (FcγRI)			
AB0192 Lot AB0192-005	5.4×10^4	1.2×10^{-4}	2.2
AB0192 Lot AB0192-005	8.0×10^4	1.2×10^{-4}	1.5
AB0192 Lot AB0192-005	5.7×10^4	1.1×10^{-4}	1.9
AB0192 Lot AB0192-005	5.5×10^4	1.2×10^{-4}	2.1
Average ± StDev	**$(6.2 \pm 1.3) \times 10^4$**	**$(1.2 \pm 0.1) \times 10^{-4}$**	**1.9 ± 0.3**
trastuzumab	1.3×10^5	1.4×10^{-4}	1.1
trastuzumab	1.3×10^5	1.2×10^{-4}	0.9
trastuzumab	1.3×10^5	1.1×10^{-4}	0.8
trastuzumab	1.3 x 105	1.3×10^{-4}	1.0
Average ± StDev	**$(1.3 \pm 0.1) \times 10^5$**	**$(1.2 \pm 0.2) \times 10^{-4}$**	**1.0 ± 0.1**

Binding to human CD32a (FcγRIIa)

[01090] There is no meaningful difference between affinities of both alleles of human CD32a for AB0089 and trastuzumab (Table 221). FIG. 239 and FIG. 240 depict binding of AB0089 and trastuzumab to CD32a (H131 and R131 alleles), respectively, tested by SPR.

Table 221: Binding of AB0192 and trastuzumab to recombinant human CD32a (FcγRIIa) H131 and R131 alleles.

Test article	K_D (nM)	
	FcγRIIa H131	**FcγRIIa R131**
AB0192 Lot AB0192-005	1035.5	1376.1
AB0192 Lot AB0192-005	921.1	1286.2
AB0192 Lot AB0192-005	1068.0	1800.6
AB0192 Lot AB0192-005	1020.6	1132.4
Average ± StDev	**1011.3 ± 63.3**	**1398.8 ± 286.1**

Test article	K_D (nM)	
	FcγRIIa H131	**FcγRIIa R131**
trastuzumab	1069.2	1488.2
trastuzumab	953.1	1381.0
trastuzumab	1090.2	1862.1
trastuzumab	1068.0	1241.4
Average ± StDev	**1045.1 ± 62.2**	**1493.2 ± 265.9**

Binding to human CD16a F158 (FcγRIIIa F158) and cyno CD16

[01091] Detailed description of AB0192 binding CD16a V158 is provided in Section 6.9.6. Binding of AB0192 to the low affinity F158 allele of human FcγRIIIa and cynomolgus FcγRIII are presented in Table 222, FIG. 241 and FIG. 242. The AB0192 binding affinity values for recombinant human CD16a (F158 allele) and cynomolgus CD16 are comparable, less than two-fold different in affinity, to the ones of trastuzumab (Table 222).

Table 222: Binding of AB0192 and trastuzumab to recombinant human CD16a (FcγRIIIa) F158 allele and cynomolgus CD16 (FcγRIII).

Test article	Human FcγRIIIa F158 K_D (nM)	Cynomolgus FcγRIII K_D (nM)
AB0192 Lot AB0192-005	772.9	202.7
AB0192 Lot AB0192-005	633.7	204.6
AB0192 Lot AB0192-005	693.3	204.1
AB0192 Lot AB0192-005	620.0	n/a
Average ± StDev	**680.0 ± 69.6**	**203.8 ± 1.0**
trastuzumab	332.3	127.1
trastuzumab	326.6	128.1
trastuzumab	333.8	131.1
trastuzumab	333.1	n/a
Average ± StDev	**331.4 ± 3.3**	**128.8 ± 2.1**

Binding to human CD32b (FcγRIIb)

[01092] There is no meaningful difference between affinities of CD32b for AB0089 and trastuzumab (Table 223). FIG. 243 depicts binding to AB0089 and trastuzumab to CD32b tested by SPR.

Table 223: Binding of AB0192 and trastuzumab to recombinant human CD32b (FcγRIIb).

Test article	K_D (μM)
AB0192 Lot AB0192-005	6.5
AB0192 Lot AB0192-005	5.6
AB0192 Lot AB0192-005	5.2
AB0192 Lot AB0192-005	7.0
Average ± StDev	**6.1 ± 0.8**
trastuzumab	7.1
trastuzumab	5.6
trastuzumab	5.2
trastuzumab	7.2
Average ± StDev	**6.3 ± 1.0**

Binding to human CD16b (FcγRIIIb)

[01093] AB0089 binds human CD16b (FcγR3b) with affinity comparable (less than two-fold different) to the one of trastuzumab (Table 224). FIG. 244 depicts binding of AB0089 and trastuzumab to CD16b tested by SPR.

Table 224: Binding of AB0192 and trastuzumab to recombinant human CD16b (FcγRIIIb).

	K_D (μM)
AB0192 Lot AB0192-005	6.8
AB0192 Lot AB0192-005	6.0
AB0192 Lot AB0192-005	5.3
Average ± StDev	**6.0 ± 0.7**
trastuzumab	4.3
trastuzumab	3.9
trastuzumab	3.4
Average ± StDev	**3.9 ± 0.5**

Binding to human and cynomolgus FcRn

[01094] FIG. 245 and FIG. 246 depict AB0192 binding to human and cynomolgus FcRn, respectively, tested by SPR. Affinities of AB0192 for human and cynomolgus FcRn are similar to those of trastuzumab, a marketed IgG1 biologic that served as an experimental control (Table 225).

Table 225: Binding of AB0192 and trastuzumab to human and cynomolgus FcRn.

	Human FcRn K_D (μM)	**Cyno FcRn K_D (μM)**
AB0192 Lot AB0192-005	1.5	1.5
AB0192 Lot AB0192-005	1.3	1.4
AB0192 Lot AB0192-005	1.5	1.2
AB0192 Lot AB0192-005	1.5	n/a
Average ± StDev	**1.5 ± 0.1**	**1.4 ± 0.1**
trastuzumab	1.8	1.6
trastuzumab	1.5	1.6
trastuzumab	2.0	1.5
trastuzumab	1.7	n/a

	Human FcRn K_D (μM)	Cyno FcRn K_D (μM)
Average ± StDev	**1.7 ± 0.2**	**1.5 ± 0.1**

Epitope binning

[01095] We compared binding epitope of AB0192 in relation to AB0237, AB0089 and three reference controls TriNKETs by SPR (FIG. 247). cFAE-A49. Tepoditamab is based on CLEC12A binding arm of tepoditamab from Merus (WO_2014_051433_A1), cFAE-A49.CLL1-Merus is based on the clone 4331 from Merus (WO_2014_051433_A1) and cFAE-A49.h6E7 is based on h6E7 mAb from Genentech (h6E7) (US_2016_0075787_A1) AB0192 interaction with hCLEC12A was blocked by all three control molecules cFAE-A49.Tepoditamab, cFAE.A49.h6E7 and cFAE-A49.CLL1-Merus suggesting the AB0192 binding epitope is broad and overlaps with both Merus and Genentech molecules. This footprint is different from AB0237 and AB0089 which cross-block only with Merus molecules. Thus, binding epitope for AB0192 is different from AB0089 and AB0237.

Potency

[01096] The ability of AB0192 to lyse human cancer cells expressing CLEC12A was determined in the human NK cells mediated cytotoxicity assay. AB0192 demonstrated high potency in killing PL21 AML cells and vastly outperformed corresponding monoclonal antibody (FIG. 248 and Table 226).

Table 226: Potency of AB0192 in primary NK mediated cytotoxicity assay compared to corresponding mAb control.

Test article	EC50 (nM)	Max killing (%)
AB0192	1.72	24
Parental mAb (AB0306)	ND	ND

Specificity

Non-specific binding assessed by PSR assay

[01097] Non-specific binding of AB0192 was assessed by flow cytometry based PSR assay that measures binding to a preparation of detergent solubilized CHO cell membrane proteins (FIG. 249). PSR assay is known to correlate well with cross-interaction chromatography, a

surrogate for antibody solubility, as well as with baculovirus particle enzyme-linked immunosorbent assay, a surrogate for *in vivo* clearance and therefore serves as a good developability predictive factor. AB0192 showed no non-specific binding, similar to low PSR control (Trastuzumab), suggesting high specificity and lack on non-specific binding to unrelated proteins.

Specificity assessment of AB0192 in HuProt™ microarray assay

[01098] To examine specificity of AB0192 we have explored a protein array technology. The HuProt™ human proteome microarray provides the largest database of individually purified human full-length proteins on a single microscopic slide. An array consisting of 22,000 full-length human proteins are expressed in yeast *Cerevisiae*, purified, and are subsequently printed in duplicate on a microarray glass slide that allows thousands of interactions to be profiled in a high-throughput manner. FIG. 250 and shows the relative binding (Z score) of AB0192 at 1 μg/ml to human CLEC12A in comparison to the entire human proteome microarray. Z score is the average binding score of two duplicates of a given protein. For comparison purpose, the top 24 proteins with residual background binding to AB0192 were also provided in FIG. 250. Table 227 shows the Z and S scores of AB0192 to human CLEC12A and the top 6 proteins from the microarray. S score is the difference of Z score of a given protein and the one rank next to it. Based on the Z and S score criteria, AB0192 showed high specificity to human and lack of off-target binding in the HuProt™ human proteome assay.

Table 227: Summary of the top hits by HuProt™ array.

Name	Rank	Protein-ID	Z score	S score
hCLEC12A	1	hCLEC12A	150.06	144.04
MFF	2	JHU15965.P168B06	6.05	0.81
POLR2E	3	JHU02080.P189F02	5.24	0.22
HMGA1_frag	4	JHU16418.P173B08	5.02	0.12
PARS2	5	JHU06781.P071H01	4.90	0.24
THEMIS_frag	6	JHU15201.P160B01	4.66	0.23
ZNF608	7	JHU13018.P136G04	4.43	0.006

Developability assessment

[01099] The stability and forced degradation of AB0192 was assessed under the following conditions:

[01100] Accelerated (40°C) stability

- 20 mg/ml in 20 mM histidine, 250 mM sucrose, 0.01% Tween-80, pH 6.0, 40°C, 4 weeks (SEC, SPR, potency, SDS-CE)
- 20 mg/ml in 20 mM sodium citrate, 250 mM sucrose, 0.01% Tween-80, pH 7.0, 40°C, 4 weeks (SEC, SPR, potency, SDS-CE)

[01101] Chemical stability

- Oxidation: 1 mg/ml in 0.02% hydrogen peroxide, PBS, room temp., 24 hours (SEC, CE-SDS, SPR, potency, peptide map)
- pH 8.0: 1 mg/ml 20 mM Tris, 40°C, 2 weeks (cIEF, SPR, potency, peptide map)
- pH 5.0: 1 mg/ml 20 mM sodium acetate, 40°C, 2 weeks (cIEF, SPR, potency, peptide map)

[01102] Manufacturability

- Freeze/thaw: 20 mg/ml 6 cycles, 20 mM sodium citrate, 250 mM sucrose, 0.01% Tween-80, pH 7.0 (SEC, SDS-CE)
- Agitation: 20 mg/ml in 20 mM sodium citrate, 250 mM sucrose, 0.01% Tween-80, pH 7.0 (SEC, SDS-CE)
- High concentration: >150 mg/ml, PBS (SEC, A280)
- Low pH hold: pH 3.3, 1.0 hours, ProA elution buffer (SEC, cIEF, SDS-CE, intact mass, SPR, potency)

Accelerated (40°C) stability

[01103] To assess the stability of AB0192, the molecule was staged at 40 °C for 4 weeks under two different buffer conditions (1) 20 mg/ml in 20 mM histidine, 250 mM sucrose, 0.01% PS-80, pH 6.0 (HST), and (2) 20 mg/ml in 20 mM citrate, 250 mM sucrose, 0.01% PS-80, pH 7.0 (CST). Stability in both buffers was assessed by SEC, CE, SPR and potency.

Stability in HST, pH 6.0

[01104] After 4 weeks at 40 °C, AB0192 in HST, pH 6.0 showed minimal aggregation or fragmentation by SEC (FIG. 251, Table 228) or CE-SDS (FIG. 252, Table 229). Loss of monomer was 1.6% by SEC and 1% by non-reduced CE. There is no meaningful difference in the active species content or the affinities for hCLEC12A, hNKG2D and hCD16a between control and stressed samples (FIG. 253 and Table 230). Finally, there was no difference in potency between the control and stressed samples tested in KHYG-1-CD16aV cytotoxicity assay (FIG. 254 and Table 231).

Table 228: SEC analysis of AB0192 after 2 and 4 weeks at 40°C in HST, pH 6.0.

Test article	Conc. (mg/ml)	Monomer (%)	LMWS (%)	HMWS (%)
AB0192 control	20.1	98.9	1.2	0.0
AB0192 2 wks., 40˚C	20.2	98.0	2.0	0.0
AB0192, 4 wks., 40˚C	21.3	97.3	2.8	0.0

Table 229: NR and R CE-SDS analysis of AB0192 after 4 weeks at 40°C in HST pH 6.0.

Test article	NR CE purity (%)	R CE purity (%)
AB0192 control	99.1	97.5
AB0192, 4 wks., 40˚C	98.1	97.4

Table 230: Kinetic parameters and binding affinities of AB0089 for CLEC12A, NKG2D and CD16a after 4 weeks at 40˚C in HST, pH 6.0, measured by SPR.

Test article	Target	k_a ($M^{-1}s^{-1}$)	k_d (s^{-1})	K_D (nM)
AB0192 control	hCLEC12A	(7.76±0.17) x10^5	(1.40 ±0.09) x10^{-3}	1.81 ± 0.2
AB0192, 4 wks., 40˚C	hCLEC12A	(7.76±0.40) x10^5	(1.40 ±0.07) x10^{-3}	1.81 ± 0.2
AB0192 control	hNKG2D	(2.08±0.03) x10^5	(1.22±0.01) x10^{-1}	588 ± 6
AB0192, 4 wks., 40˚C	hNKG2D	(2.11±0.35) x10^5	(1.27±0.19) x10^{-1}	602 ± 9
AB0192 control	CD16aV	(1.17±0.02) x10^5	(1.99±0.05) x10^{-2}	171 ± 2
AB0192, 4 wks., 40˚C	CD16aV	(1.03±0.03) x10^5	(2.01±0.03) x10^{-2}	194 ± 4

Average of n=3 replicates

Table 231: Potency of AB0192 after 4 weeks at 40°C in HST, pH 6.0 in KHYG-1-CD16aV mediated cytotoxicity assay.

Test article	Buffer	EC50 (nM)	Max killing (%)
AB0192 control	HST	3.3	21
AB0192, 40°C 4 wks.	HST	1.6	17

Stability in CST, pH 7.0

[01105] After 4 weeks at 40 °C, AB0192 in CST, pH 7.0, showed minimal aggregation (FIG. 255 and Table 232) and fragmentation (FIG. 256 and Table 233). 1.6% and 0.8% loss of monomer was observed by SEC and non-reduced CE-SDS, respectively. There was no meaningful difference in the active species content or in the affinities for hCLEC12A, hNKG2D and hCD16a between control and stressed samples (FIG. 257 and Table 234). Finally, there was no difference in potency between the control and stressed samples in KHYG-1-CD16aV cytotoxicity assay (FIG. 258 and Table 235).

Table 232: SEC analysis of AB0192 after 1-4 weeks at 40°C in CST, pH 7.0.

Test article	Conc. (mg/ml)	Monomer (%)	LMWS (%)	HMWS (%)
AB0192 control	21.3	99.0	1.1	ND
AB0192, 1 wk., 40°C	21.4	98.1	1.5	0.4
AB0192, 2 wks., 40°C	21.4	97.9	1.6	0.5
AB0192, 3 wks., 40°C	21.7	97.8	1.7	0.5
AB0192, 4 wks., 40°C	22.2	97.4	1.8	0.8

Table 233: NR and R CE-SDS analysis of AB0192 after 4 weeks at 40°C in CST, pH 7.0.

Test article	Conc. (mg/ml)	NR CE purity (%)	R CE purity (%)
AB0192 control	21.3	98.8	97.8
AB0192, 40°C 4 wks.	22.4	98.0	97.0

Table 234: Kinetic parameters and binding affinities of AB0089 for CLEC12A, NKG2D and CD16a after 4 weeks at 40°C in CST, pH 7.0, measured by SPR.

Test article	Target	k_a ($M^{-1}s^{-1}$)	k_d (s^{-1})	K_D (nM)
AB0192 control	hCLEC12A	(7.76±0.17) x10^{5}	(1.40 ±0.09) x10^{-3}	1.81 ± 0.2
AB0192, 4 wks. 40°C	hCLEC12A	(7.49±0.22) x10^{5}	(1.47±0.12) x10^{-3}	1.96 ± 0.2

Test article	Target	k_a ($M^{-1}s^{-1}$)	k_d (s^{-1})	K_D (nM)
AB0192 control	hNKG2D	(2.08±0.03) x10^{5}	(1.22±0.01) x10^{-1}	588 ± 6
AB0192, 4 wks. 40°C	hNKG2D	(1.85±0.06) x10^{5}	(1.21±0.04) x10^{-1}	653 ± 10
AB0192 control	CD16aV	(1.17±0.02) x10^{5}	(1.99±0.05) x10^{-2}	171 ± 2
AB0192, 4 wks. 40°C	CD16aV	(1.11±0.07) x10^{5}	(1.94±0.01) x10^{-2}	174 ± 10

Average of 3 replicates

Table 235: Potency of AB0192 after 4 weeks at 40°C in CST, pH 7.0, in KHYG-1-CD16aV mediated cytotoxicity assay.

Test article	EC50 (nM)	Max killing (%)
AB0192 control	3.3	21
AB0192 40°C 4wks	1.4	19

Chemical Stability

Forced Oxidation

[01106] After 24 h of oxidative stress in 0.02% hydrogen peroxide AB0192 showed no significant decrease in monomer content (FIG. 259 and Table 236). Purity assessed by CE remained high (FIG. 260 and Table 237). Amount of active species and affinities for CLEC12A, NKG2D, and CD16aV were unaltered (FIG. 261 and Table 238), and potency was similar to the control sample (FIG. 262 and Table 239).

Table 236: SEC analysis of AB0192 after forced oxidation compared to control.

Test article	Conc. (mg/ml)	% Monomer	LMWS (%)	HMWS (%)
AB0192 control	1.1	99.4	0.7	ND
AB0192 oxidized	0.9	99.7	0.3	ND

Table 237: NR and R CE-SDS analysis of AB0192 after forced oxidation.

Test article	Conc. (mg/ml)	NR CE Purity (%)	R CE Purity (%)
AB0192 control	1.1	99.1	97.8
AB0192 oxidized	0.9	98.9	97.7

Table 238: Kinetic parameters and binding affinities of AB0089 for CLEC12A, NKG2D and CD16a after forced oxidation measured by SPR.

Test article	Target	k_a ($M^{-1}s^{-1}$)	k_d (s^{-1})	K_D (nM)
AB0192 control	hCLEC12A	(7.71±0.04) x10^5	(1.29±0.02) x10^{-3}	1.68 ± 0.0
AB0192 oxidized	hCLEC12A	(7.75±0.07) x10^5	(1.32±0.05) x10^{-3}	1.71 ± 0.1
AB0192 control	hNKG2D	(2.08±0.05) x10^5	(1.24±0.03) x10^{-1}	598 ± 9
AB0192 oxidized	hNKG2D	(1.95±0.02) x10^5	(1.19±0.03) x10^{-1}	612 ± 11
AB0192 control	CD16aV	(1.15±0.07) x10^5	(2.02±0.05) x 10^{-2}	177 ± 7
AB0192 oxidized	CD16aV	(1.19±0.04) x10^5	(1.92±0.04) x 10^{-2}	162 ± 3

Average of n=3 replicates

Table 239: Potency of AB0192 after forced oxidation stress assessed by KHYG-1-CD16aV mediated cytotoxicity assay.

Test article	EC50 (nM)	Max killing (%)
AB0192 control	1.9	18
AB0192 oxidized	2.6	18

[01107] Site-specific oxidation of methionine was monitored after forced oxidation by tryptic peptide mapping. Significant levels of oxidation were only detected at two methionines in the Fc, as expected (Table 240) as expected for an IgG1. Our historic data show that the same residues are modified in trastuzumab at 61.6% and 39.1% under the same conditions.

Table 240: Summary of methionine oxidation in AB0192 after oxidative stress.

				Relative Abundance (%)	
SEQ ID NO	**Sequence**	**Chain**	**Position**	**Control**	**Oxidized**
299	LSCAASGFTFSSYS**M**NWVR	H	34	0.5	0.8
300	NSLYLQ**M**NSLR	H	83	0.1	0.3
301	DTL**M**ISR	H/S	257/281	1.4	64.7
302	WQQGNVFSCSV**M**HEALHNHYTQK	H/S	433/457	1.2	35.9
303	DIQ**M**TQSPSSVSASVGDR	L	4	0.1	0.3
340	LSCAASGFTFNAFG**M**HWVR	S	34	0.8	0.9
341	NTLYLQ**M**NSLR	S	83	0.1	0.2
342	DGYPTGGA**M**DYWGQGTSVTVSSGGGGS GGGGSGGGGSGGGGSDIQ**M**TQSPSSLSAS VGDR[a]	S	107/110/ 144	0.2	0.9

[a] % oxidation reported as the sum of oxidation on M107, W110, and M144

[01108] Oxidation of tryptophan residues in AB0192 CDRs was also monitored in the same experiment. None of the tryptophan residues had a significant increase in oxidation after stress (Table 241).

Table 241: Summary of tryptophan oxidation in AB0192 CDRs after oxidative stress.

				Relative Abundance (%)	
Sequence	**Chain**	**CDR**	**Mass shift (Da)[a]**	**Control**	**Oxidized**
GAPIGAAAG**W**FDP (SEQ ID NO: 97)	H	H3	+16/+32/+4	ND/0.2/0.2	ND/0.1/0.0
RASQGISS**W**LA (SEQ ID NO: 86)	L	L1	+16/+32/+4	0.1/0.2/0.0	0.2/0.1/0.0

[a] single oxidation (+16 Da), double oxidation (+32 Da), and kyneurenine (+4 Da)

ND, none detected.

pH 5 stress

[01109] The chemical stability of AB0192 was assessed at low pH (20 mM sodium acetate, pH 5.0, 40 °C, 2 weeks). After 2 weeks at pH 5, no loss of monomer (FIG. 263 and Table 242) was observed by SEC. Differences in purity detected by non-reduced and reduced CE-SDS were less than 1% (FIG. 264 and Table 243). There were no meaningful differences in CLEC12A, NKG2D, or CD16aV affinity of the amount of active species observed (FIG. 265 and Table 244). A small acidic shift in the global charge profile was detected by cIEF (FIG. 266 and Table 245), however, this acidic shift did not affect AB0192 potency (FIG. 267 and Table 246).

Table 242: SEC analysis of AB0192 after long term low pH stress (pH 5.0, 40°C, 14 days).

Test article	Conc, (mg/ml)	Monomer (%)	LMWS (%)	HMWS (%)
AB0192 control	1.2	99.3	0.7	ND
AB0192, pH 5 40°C, 2 wks.	1.2	99.4	0.6	ND

Table 243: NR and R CE-SDS analysis after long term low pH stress (pH 5.0, 40°C, 14 days).

Test article	Concentration (mg/ml)	NR CE Purity (%)	R CE Purity (%)
AB0192 control	1.2	97.1	98.0
AB0192, pH 5 40°C, 2 wks.	1.2	96.3	97.8

Table 244: Kinetic parameters and binding affinities of AB0089 for CLEC12A, NKG2D and CD16a after long term low pH stress (pH 5.0, 40°C, 14 days) measured by SPR.

Test article	Target	k_a ($M^{-1}s^{-1}$)	k_d (s^{-1})	K_D (nM)
AB0192 control	hCLEC12A	(7.71±0.04) x10^5	(1.29±0.02) x10^{-3}	1.68 ± 0.0
AB0192, pH 5 40°C, 2 wks.	hCLEC12A	(7.87±0.12) x10^5	(1.30±0.03) x10^{-3}	1.65 ± 0.0

Test article	Target	k_a ($M^{-1}s^{-1}$)	k_d (s^{-1})	K_D (nM)
AB0192 control	hNKG2D	(2.08±0.03) x10^5	(1.22±0.01) x10^{-1}	588 ± 6
AB0192, pH 5 40°C, 2 wks.	hNKG2D	(2.10±0.06) x10^5	(1.20±0.01) x10^{-1}	574 ± 12
AB0192 control	CD16aV	(1.17±0.02) x10^5	(1.99±0.05) x10^{-2}	171 ± 2
AB0192, pH 5 40°C, 2 wks.	CD16aV	(1.08±0.02) x10^5	(2.08±0.04) x10^{-2}	192 ± 2

Average of 3 replicates

Table 245: Charge profile of AB0192 after long term low pH stress (pH 5.0, 40°C, 14 days).

Test article	% acidic	% main	% basic
AB0192 control	41.9	49.4	8.7
AB0192, pH 5 40°C, 2 wks.	49.8	41.4	8.8

Table 246: Potency of AB0192 after long term low pH stress (pH 5.0, 40°C, 14 days) in KHYG-1-CD16aV cytotoxicity assay.

Test article	EC50 (nM)	Max killing (%)
AB0192 control	1.9	18
AB0192, pH 5 40°C, 2 wks.	2.0	18

pH 8 stress

[01110] Chemical stability of AB0192 was also assessed by incubation at elevated pH (20 mM Tris, pH 8.0, 40 °C, 2 weeks). After 2 weeks at pH 8, there was a 1.6 % loss of monomer by SEC (FIG. 268 and Table 247). Minor differences in purity were detected by non-reduced and reduced CE-SDS (FIG. 269 and Table 248). There were no meaningful differences in CLEC12A, NKG2D, or CD16aV affinities or amount of active species observed (FIG. 270 and Table 249). A significant acidic shift in the global charge profile detected by cIEF was detected (FIG. 271

and Table 250), which can be attributed to deamidation throughout the molecule. However, this acidic shift did not have any significant effect on AB0192 potency (FIG. 272 and Table 251).

Table 247: SEC analysis of AB0192 after long term high pH stress (pH 8.0, 40C, 14 days)

Test article	Conc. (mg/ml)	Monomer (%)	LMWS (%)	HMWS (%)
AB0192 control	1.1	99.3	0.7	0.0
AB0192, pH 8 40°C, 2 wks.	1.2	97.7	1.6	0.7

Table 248: NR and R CE-SDS analysis of AB0192 after long term high pH stress (pH 8.0, 40°C, 14 days).

Test article	NR CE Purity (%)	R CE Purity
AB0192 control	97.4	98.3
AB0192, pH 8 40°C, 2 wks.	95.7	94.7

Table 249: Kinetic parameters and binding affinity of AB0089 for CLEC12A, NKG2D and CD16a after long term high pH stress (pH 8.0, 40°C, 14 days) measured by SPR.

Test article	Target	k_a ($M^{-1}s^{-1}$)	k_d (s^{-1})	K_D (nM)
AB0192 control	hCLEC12A	(7.71±0.04) x10^5	(1.29±0.02) x10^{-3}	1.68 ± 0.00
AB0192, pH 8 40°C, 2 wks.	hCLEC12A	(7.68±0.17) x10^5	(1.28±0.04) x10^{-3}	1.66 ± 0.10
AB0192 control	hNKG2D	(2.08±0.03) x10^5	(1.22±0.01) x10^{-1}	588 ± 6
AB0192, pH 8 40°C, 2 wks.	hNKG2D	(1.56±0.09) x10^5	(1.21±0.04) x10^{-1}	779 ± 45
AB0192 control	CD16aV	(1.17±0.02) x10^5	(1.99±0.05) x10^{-2}	171 ± 2

Test article	Target	k_a ($M^{-1}s^{-1}$)	k_d (s^{-1})	K_D (nM)
AB0192, pH 8 40°C, 2 wks.	CD16aV	(1.10±0.04) x10^5	(1.91±0.04) x10^{-2}	173 ± 2

Average of 3 replicates

Table 250: AB0192 charge profile after long term high pH stress (pH 8.0, 40°C, 14 days).

Test article	% acidic	% main	% basic
AB0192 control	42.7	48.6	8.7
AB0192, pH 8 40°C, 2 wks.	60.3	30.5	9.1

Table 251: Potency of AB0192 after long term high pH stress (pH 8.0, 40C, 14 days) assessed by KHYG-1-CD16aV cytotoxicity assay.

Test article	EC50 (nM)	Max killing (%)
AB0192 control	1.9	18
AB0192, pH 8 40°C, 2 wks.	3.0	18

Peptide mapping analysis of the pH 5 and pH 8 stressed material

[01111] To determine if the pH stress induced changes observed by cIEF are due to the modification in the complementarity determining regions (CDRs), the same pH 5 and pH 8 stressed samples were analyzed by LC-MS/MS peptide mapping. Based on the peptide map data, all of the CDRs in AB0192 are resistant to modification during low and high pH stress (Table 252). No evidence of aspartic acid isomerization was observed, based on manual inspection of peak shape.

Table 252: Post-translational modifications in AB0192 CDRs after low and high pH stresses.

				Relative abundance (%)			
				pH 5		pH 8	
Chain	**CDR**	**Sequence (Chothia)**	**Potential liability**	**control**	**stressed**	**control**	**stressed**
S	H1	GFTFNAF (SEQ ID NO:195)	Deamidation	NA			
S	H2	SSGSTS (SEQ ID NO:196)	None	NA			
S	H3	DGYPTGGAMDY (SEQ ID NO:187)	Isomerization	None detected			
S	L1	KASQDIYNYLS (SEQ ID NO:198)	Deamidation	NA			
S	L2	RANILVS (SEQ ID NO:199)	Deamidation	None detected			
S	L3	LQFDAFPFT (SEQ ID NO:201)	None	NA			
H	H1	GFTFSSY (SEQ ID NO:297)	None	NA			
H	H2	SSSSSY (SEQ ID NO:298)	None	NA			
H	H3	GAPIGAAAGWFDP (SEQ ID NO:97)	Truncation	None detected			
L	L1	RASQGISSWLA (SEQ ID NO:86)	None	NA			

				Relative abundance (%)			
				pH 5		pH 8	
Chain	**CDR**	**Sequence (Chothia)**	**Potential liability**	**control**	**stressed**	**control**	**stressed**
L	L2	AASSLQS (SEQ ID NO:77)	None	NA			
L	L3	QQGVSFPRT (SEQ ID NO:87)	None	NA			

NA, not applicable

Manufacturability

Freeze/thaw stability

[01112] Aliquots of AB0192 (20 mg/ml in CST pH 7.0) were frozen and thawed 6 times by placing the vials in Styrofoam container (to slow the freezing rate) and placing the container at -80°C. Once frozen, the container was placed on a lab bench and the aliquots were allowed to thaw. After 6 cycles of freeze/thaw AB0192 showed no loss in monomer by SEC and protein concentration remained the same (FIG. 273 and Table 253).

Table 253: SEC analysis of AB0192 after freeze/thaw stress.

Test article	Conc. (mg/ml)	Monomer (%)	LMWS (%)	HMWS (%)
AB0192 control	21.2	98.9	1.1	ND
AB0192 6 F/T	20.8	98.9	1.1	ND

ND, none detected

[01113] After 6 freeze/thaw cycles no loss of purity was detected by either reduced or non-reduced CE-SDS (FIG. 274 and Table 254).

Table 254: NR and R CE-SDS analysis of AB0192 after freeze/thaw stress.

Test article	NR CE Purity (%)	R CE Purity (%)
AB0192 control	99.0	97.3
AB0192 6 F/T	99.1	97.7

Agitation

[01114] Agitation study was performed in CST, pH 7.0 buffer. AB0192 was incubated for 24h at constant steering (60 rpm) in a glass vial with a micro steer bar. No loss of monomer was detected by SEC compared to the control sample (FIG. 275 and Table 255).

Table 255: SEC analysis of AB0192 after agitation stress.

Test article	Conc. (mg/ml)	Monomer (%)	LMWS (%)	HMWS (%)
AB0192 control	21.2	98.9	1.1	ND
AB0192 agitation	21.4	98.7	1.0	0.3

ND, none detected

[01115] After 24 hours of stirring, there was no increase in fragmentation detected by reduced or non-reduced CE-SDS (FIG. 276 and Table 256).

Table 256: NR and R CE-SDS analysis of AB0192 after agitation stress.

Test article	NR CE Purity (%)	R CE Purity (%)
AB0192 control	99.0	97.3
AB0192 agitation	99.2	97.1

Low pH hold

[01116] To determine if AB0192 is amendable to commonly used low pH hold protocol used for viral inactivation in biologics manufacturing, we performed low pH hold study. Incubation at low pH can potentially compromise biophysical stability and integrity of the molecule and could cause chemical degradation of amino acid side chains, in particular, aspartic acid isomerization. There is a potential sequence liability DS in CDRH3 of Chain S. Therefore, we have applied a wide range of assays to assess protein quality after low pH hold. The bulk of the AB0192 Protein A eluate was immediately adjusted to neutral pH, while a smaller sample was adjusted to pH 3.7 and held at room temperature for 1 hour to mimic a typical viral inactivation step. After the hold period, Protein A eluate was neutralized with 1.0 M Tris, pH 8.3 to achieve neutral pH. Analytical size exclusion chromatography was performed to determine if there were any changes in profile or aggregate content pre- and post- low pH exposure (FIG. 277). No change in profile

was observed after low pH hold. Both aliquots were further purified by second ion exchange chromatography and subjected to a panel of characterization assays.

[01117] Chemical modification of amino acid side chains can typically be observed at a global scale with cIEF. The cIEF profiles of AB0192 control and low pH hold lot are visually very similar and the relative quantitation of acid, main, and basic species are all within 2% of each other. Indicating that the low pH hold did not have a measurable effect on the charge profile of AB0192 (FIG. 278 and Table 257).

Table 257: Charge profile of AB0192 after low pH hold.

Test article	pI	% acidic	% main	% basic
AB0192 control	8.9	41.4	49.8	8.8
AB0192 low pH hold	8.9	43.1	48.2	8.7

[01118] After the low pH hold step, affinities for hCLEC12a, hNKG2D, and CD16aV were unaltered (FIG. 279 and Table 258). This indicates that AB0192 retains affinity for all three targets under low pH hold conditions used as viral inactivation step in biologics manufacturing

Table 258: Kinetic parameters and binding affinities of AB0192 for CLEC12A, NKG2D and CD16a after low pH hold measured by SPR.

Test article	Target	k_a ($M^{-1}s^{-1}$)	k_d (s^{-1})	K_D (nM)
AB0192 Control	hCLEC12A	6.85×10^{5}	1.25×10^{-3}	1.83
AB0192 low pH hold	hCLEC12A	$(6.90 \pm 0.17) \times 10^{5}$	$(1.15 \pm 0.01) \times 10^{-3}$	1.66 ± 0.05
AB0192 Control	hNKG2D	$(1.88 \pm 0.08) \times 10^{5}$	$(1.46 \pm 0.060) \times 10^{-1}$	779 ± 10
AB0192 low pH hold	hNKG2D	$(1.78 \pm 0.08) \times 10^{5}$	$(1.42 \pm 0.03) \times 10^{-1}$	796 ± 47
AB0192 Control	CD16aV	$(1.12 \pm 0.08) \times 10^{5}$	$(1.99 \pm 0.08) \times 10^{-2}$	178 ± 6

Test article	Target	k_a ($M^{-1}s^{-1}$)	k_d (s^{-1})	K_D (nM)
AB0192 low pH hold	CD16aV	(1.18±0.06) x10^5	(2.12±0.09) x10^{-2}	180 ± 15

[01119] Potency of low pH hold sample was further tested against CLEC12A+ PL-21 cancer cells in the KHYG1-CD16aV cytotoxicity bioassay. The potency of AB0192 was unaltered after the low pH hold step (FIG. 280 and Table 259).

Table 259: Potency of AB0192 after low pH hold in KHYG1-CD16a mediated cytotoxicity assay.

Test article	EC50 (nM)	Max killing (%)
AB0192 control	2.5	18
AB0192 low pH hold	2.0	18

[01120] Taken together, these results demonstrate that the molecular format and structure of AB0192 meets the conceptual requirements for a new multi-specific therapeutic modality that simultaneously engages CLEC12A, NKG2D and CD16a to treat AML. AB0192 is potent and has a favorable developability profile with no sequence liabilities or significant post-translational modifications observed under any stresses. AB0192 binds to an epitope different from AB0237 and AB0089 TriNKETs.

INCORPORATION BY REFERENCE

[01121] Unless stated to the contrary, the entire disclosure of each of the patent documents and scientific articles referred to herein is incorporated by reference for all purposes.

EQUIVALENTS

[01122] The application may be embodied in other specific forms without departing from the spirit or essential characteristics thereof. The foregoing embodiments are therefore to be considered in all respects illustrative rather than limiting the application described herein. Scope of the application is thus indicated by the appended claims rather than by the foregoing description, and all changes that come within the meaning and range of equivalency of the claims are intended to be embraced therein.

SEQUENCES

SEQ ID NO	Sequence
1	QVQLQQWGAGLLKPSETLSLTCAVYGGSFSGYYWSWIRQPPGKGLEWIGEIDHSGSTNYNPSLKSRVT ISVDTSKNQFSLKLSSVTAADTAVYYCARARGPWSFDPWGQGTLVTVSS
2	GSFSGYYWS
3	EIDHSGSTNYNPSLKS
4	ARARGPWSFDP
5	DIQMTQSPSTLSASVGDRVTITCRASQSISSWLAWYQQKPGKAPKLLIYKASSLESGVPSRFSGSGSG TEFTLTISSLQPDDFATYYCQQYNSYPITFGGGTKVEIK
6	EIVLTQSPGTLSLSPGERATLSCRASQSVSSSYLAWYQQKPGQAPRLLIYGASSRATGIPDRFSGSGS GTDFTLTISRLEPEDFAVYYCQQYGSSPITFGGGTKVEIK
7	DIQMTQSPSTLSASVGDRVTITCRASQSIGSWLAWYQQKPGKAPKLLIYKASSLESGVPSRFSGSGSG TEFTLTISSLQPDDFATYYCQQYHSFYTFGGGTKVEIK
8	DIQMTQSPSTLSASVGDRVTITCRASQSIGSWLAWYQQKPGKAPKLLIYKASSLESGVPSRFSGSGSG TEFTLTISSLQPDDFATYYCQQSNSYYTFGGGTKVEIK
9	DIQMTQSPSTLSASVGDRVTITCRASQSISSWLAWYQQKPGKAPKLLIYKASSLESGVPSRFSGSGSG TEFTLTISSLQPDDFATYYCQQYNSYPTFGGGTKVEIK
10	QVQLQQWGAGLLKPSETLSLTCAVYGGSFSGYYWSWIRQPPGKGLEWIGEIDHSGSTNYNPSLKSRVT ISVDTSKNQFSLKLSSVTAADTAVYYCARARGPWGFDPWGQGTLVTVSS
11	ELQMTQSPSSLSASVGDRVTITCRTSQSISSYLNWYQQKPGQPPKLLIYWASTRESGVPDRFSGSGSG TDFTLTISSLQPEDSATYYCQQSYDIPYTFGQGTKLEIK
12	DIQMTQSPSTLSASVGDRVTITCRASQSISSWLAWYQQKPGKAPKLLIYKASSLESGVPSRFSGSGSG TEFTLTISSLQPDDFATYYCQQYGSFPITFGGGTKVEIK
13	DIQMTQSPSTLSASVGDRVTITCRASQSISSWLAWYQQKPGKAPKLLIYKASSLESGVPSRFSGSGSG TDFTLTISSLQPDDFATYYCQQSKEVPWTFGQGTKVEIK
14	DIQMTQSPSTLSASVGDRVTITCRASQSISSWLAWYQQKPGKAPKLLIYKASSLESGVPSRFSGSGSG TEFTLTISSLQPDDFATYYCQQYNSFPTFGGGTKVEIK
15	DIQMTQSPSTLSASVGDRVTITCRASQSIGSWLAWYQQKPGKAPKLLIYKASSLESGVPSRFSGSGSG TEFTLTISSLQPDDFATYYCQQYDIYPTFGGGTKVEIK
16	DIQMTQSPSTLSASVGDRVTITCRASQSISSWLAWYQQKPGKAPKLLIYKASSLESGVPSRFSGSGSG TEFTLTISSLQPDDFATYYCQQYDSYPTFGGGTKVEIK
17	DIQMTQSPSTLSASVGDRVTITCRASQSISSWLAWYQQKPGKAPKLLIYKASSLESGVPSRFSGSGSG TEFTLTISSLQPDDFATYYCQQYGSFPTFGGGTKVEIK
18	DIQMTQSPSTLSASVGDRVTITCRASQSISSWLAWYQQKPGKAPKLLIYKASSLESGVPSRFSGSGSG TEFTLTISSLQPDDFATYYCQQYQSFPTFGGGTKVEIK
19	DIQMTQSPSTLSASVGDRVTITCRASQSISSWLAWYQQKPGKAPKLLIYKASSLESGVPSRFSGSGSG TEFTLTISSLQPDDFATYYCQQYSSFSTFGGGTKVEIK
20	DIQMTQSPSTLSASVGDRVTITCRASQSISSWLAWYQQKPGKAPKLLIYKASSLESGVPSRFSGSGSG TEFTLTISSLQPDDFATYYCQQYESYSTFGGGTKVEIK
21	DIQMTQSPSTLSASVGDRVTITCRASQSISSWLAWYQQKPGKAPKLLIYKASSLESGVPSRFSGSGSG TEFTLTISSLQPDDFATYYCQQYDSFITFGGGTKVEIK
22	DIQMTQSPSTLSASVGDRVTITCRASQSISSWLAWYQQKPGKAPKLLIYKASSLESGVPSRFSGSGSG TEFTLTISSLQPDDFATYYCQQYQSYPTFGGGTKVEIK
23	DIQMTQSPSTLSASVGDRVTITCRASQSIGSWLAWYQQKPGKAPKLLIYKASSLESGVPSRFSGSGSG TEFTLTISSLQPDDFATYYCQQYHSFPTFGGGTKVEIK

SEQ ID NO	Sequence
24	DIQMTQSPSTLSASVGDRVTITCRASQSIGSWLAWYQQKPGKAPKLLIYKASSLESGVPSRFSGSGSG TEFTLTISSLQPDDFATYYCQQYELYSYTFGGGTKVEIK
25	DIQMTQSPSTLSASVGDRVTITCRASQSISSWLAWYQQKPGKAPKLLIYKASSLESGVPSRFSGSGSG TEFTLTISSLQPDDFATYYCQQYDTFITFGGGTKVEIK
26	QVQLVQSGAEVKKPGSSVKVSCKASGGTFSSYAISWVRQAPGQGLEWMGGIIPIFGTANYAQKFQGRV TITADESTSTAYMELSSLRSEDTAVYYCARGDSSIRHAYYYYGMDVWGQGTTVTVSS
27	GTFSSYAIS
28	SYAIS
29	GIIPIFGTANYAQKFQG
30	ARGDSSIRHAYYYYGMDV
31	GDSSIRHAYYYYGMDV
32	DIVMTQSPDSLAVSLGERATINCKSSQSVLYSSNNKNYLAWYQQKPGQPPKLLIYWASTRESGVPDRF SGSGSGTDFTLTISSLQAEDVAVYYCQQYYSTPITFGGGTKVEIK
33	KSSQSVLYSSNNKNYLA
34	WASTRES
35	QQYYSTPIT
36	QLQLQESGPGLVKPSETLSLTCTVSGGSISSSSYYWGWIRQPPGKGLEWIGSIYYSGSTYYNPSLKSR VTISVDTSKNQFSLKLSSVTAADTAVYYCARGSDRFHPYFDYWGQGTLVTVSS
37	GSISSSSYYWG
38	SSSYYWG
39	SIYYSGSTYYNPSLKS
40	ARGSDRFHPYFDY
41	GSDRFHPYFDY
42	EIVLTQSPATLSLSPGERATLSCRASQSVSRYLAWYQQKPGQAPRLLIYDASNRATGIPARFSGSGSG TDFTLTISSLEPEDFAVYYCQQFDTWPPTFGGGTKVEIK
43	RASQSVSRYLA
44	DASNRAT
45	QQFDTWPPT
46	DIQMTQSPSTLSASVGDRVTITCRASQSISSWLAWYQQKPGKAPKLLIYKASSLESGVPSRFSGSGSG TEFTLTISSLQPDDFATYYCEQYDSYPTFGGGTKVEIK
47	QVQLVQSGAEVKKPGSSVKVSCKASGGTFSSYAISWVRQAPGQGLEWMGGIIPIFGTANYAQKFQGRV TITADESTSTAYMELSSLRSEDTAVYYCARRGRKASGSFYYYYGMDVWGQGTTVTVSS
48	ARRGRKASGSFYYYYGMDV
49	DIVMTQSPDSLAVSLGERATINCESSQSLLNSGNQKNYLTWYQQKPGQPPKPLIYWASTRESGVPDRF SGSGSGTDFTLTISSLQAEDVAVYYCQNDYSYPYTFGQGTKLEIK
50	ESSQSLLNSGNQKNYLT
51	QNDYSYPYT
52	QVQLVQSGAEVKKPGASVKVSCKASGYTFTSYYMHWVRQAPGQGLEWMGIINPSGGSTSYAQKFQGRV TMTRDTSTSTVYMELSSLRSEDTAVYYCARGAPNYGDTTHDYYYMDVWGKGTTVTVSS
53	YTFTSYYMH
54	SYYMH
55	IINPSGGSTSYAQKFQG
56	ARGAPNYGDTTHDYYYMDV
57	GAPNYGDTTHDYYYMDV
58	EIVMTQSPATLSVSPGERATLSCRASQSVSSNLAWYQQKPGQAPRLLIYGASTRATGIPARFSGSGSG TEFTLTISSLQSEDFAVYYCQQYDDWPFTFGGGTKVEIK

SEQ ID NO	Sequence
59	RASQSVSSNLA
60	GASTRAT
61	QQYDDWPFT
62	QVQLVQSGAEVKKPGASVKVSCKASGYTFTGYYMHWVRQAPGQGLEWMGWINPNSGGTNYAQKFQGRV TMTRDTSISTAYMELSRLRSDDTAVYYCARDTGEYYDTDDHGMDVWGQGTTVTVSS
63	YTFTGYYMH
64	GYYMH
65	WINPNSGGTNYAQKFQG
66	ARDTGEYYDTDDHGMDV
67	DTGEYYDTDDHGMDV
68	EIVLTQSPGTLSLSPGERATLSCRASQSVSSNLAWYQQKPGQAPRLLIYGASTRATGIPARFSGSGSG TEFTLTISSLQSEDFAVYYCQQDDYWPPTFGGGTKVEIK
69	QQDDYWPPT
70	EVQLLESGGGLVQPGGSLRLSCAASGFTFSSYAMSWVRQAPGKGLEWVSAISGSGGSTYYADSVKGRF TISRDNSKNTLYLQMNSLRAEDTAVYYCAKDGGYYDSGAGDYWGQGTLVTVSS
71	FTFSSYAMS
72	AISGSGGSTYYADSVKG
73	AKDGGYYDSGAGDY
74	DGGYYDSGAGDY
75	DIQMTQSPSSVSASVGDRVTITCRASQGIDSWLAWYQQKPGKAPKLLIYAASSLQSGVPSRFSGSGSG TDFTLTISSLQPEDFATYYCQQGVSYPRTFGGGTKVEIK
76	RASQGIDSWLA
77	AASSLQS
78	QQGVSYPRT
79	EVQLVESGGGLVKPGGSLRLSCAASGFTFSSYSMNWVRQAPGKGLEWVSSISSSSSYIYYADSVKGRF TISRDNAKNSLYLQMNSLRAEDTAVYYCARGAPMGAAAGWFDPWGQGTLVTVSS
80	FTFSSYSMN
81	SYSMN
82	SISSSSSYIYYADSVKG
83	ARGAPMGAAAGWFDP
84	GAPMGAAAGWFDP
85	DIQMTQSPSSVSASVGDRVTITCRASQGISSWLAWYQQKPGKAPKLLIYAASSLQSGVPSRFSGSGSG TDFTLTISSLQPEDFATYYCQQGVSFPRTFGGGTKVEIK
86	RASQGISSWLA
87	QQGVSFPRT
88	DIQMTQSPSSVSASVGDRVTITCRASQGISSWLAWYQQKPGKAPKLLIYAASSLQSGVPSRFSGSGSG TDFTLTISSLQPEDFATYYCQQGVSFPRTFGCGTKVEIK*GGGGSGGGGSGGGGSGGGGS*EVQLVESGG GLVKPGGSLRLSCAASGFTFSSYSMNWVRQAPGKCLEWVSSISSSSSYIYYADSVKGRFTISRDNAKN SLYLQMNSLRAEDTAVYYCARGAPMGAAAGWFDPWGQGTLVTVSS
89	QVQLVQSGAEVKKPGASVKVSCKASGYTFTSYYMHWVRQAPGQGLEWMGIINPSGGSTSYAQKFQGRV TMTRDTSTSTVYMELSSLRSEDTAVYYCAREGAGFAYGMDYYYMDVWGKGTTVTVSS
90	AREGAGFAYGMDYYYMDV
91	EGAGFAYGMDYYYMDV
92	EIVLTQSPATLSLSPGERATLSCRASQSVSSYLAWYQQKPGQAPRLLIYDASNRATGIPARFSGSGSG TDFTLTISSLEPEDFAVYYCQQSDNWPFTFGGGTKVEIK
93	RASQSVSSYLA

SEQ ID NO	Sequence
94	QQSDNWPFT
95	EVQLVESGGGLVKPGGSLRLSCAASGFTFSSYSMNWVRQAPGKGLEWVSSISSSSSYIYYADSVKGRF TISRDNAKNSLYLQMNSLRAEDTAVYYCARGAP**I**GAAAGWFDPWGQGTLVTVSS
96	ARGAP**I**GAAAGWFDP
97	GAP**I**GAAAGWFDP
98	EVQLVESGGGLVKPGGSLRLSCAASGFTFSSYSMNWVRQAPGKGLEWVSSISSSSSYIYYADSVKGRF TISRDNAKNSLYLQMNSLRAEDTAVYYCARGAP**Q**GAAAGWFDPWGQGTLVTVSS
99	ARGAP**Q**GAAAGWFDP
100	GAP**Q**GAAAGWFDP
101	EVQLVESGGGLVKPGGSLRLSCAASGFTFSSYSMNWVRQAPGKGLEWVSSISSSSSYIYYADSVKGRF TISRDNAKNSLYLQMNSLRAEDTAVYYCARGAP**L**GAAAGWFDPWGQGTLVTVSS
102	ARGAP**L**GAAAGWFDP
103	GAP**L**GAAAGWFDP
104	EVQLVESGGGLVKPGGSLRLSCAASGFTFSSYSMNWVRQAPGKGLEWVSSISSSSSYIYYADSVKGRF TISRDNAKNSLYLQMNSLRAEDTAVYYCARGAP**F**GAAAGWFDPWGQGTLVTVSS
105	ARGAP**F**GAAAGWFDP
106	GAP**F**GAAAGWFDP
107	EVQLVESGGGLVKPGGSLRLSCAASGFTFSSYSMNWVRQAPGKGLEWVSSISSSSSYIYYADSVKGRF TISRDNAKNSLYLQMNSLRAEDTAVYYCARGAP**V**GAAAGWFDPWGQGTLVTVSS
108	ARGAP**V**GAAAGWFDP
109	GAP**V**GAAAGWFDP
110	EVQLVESGGGLVKPGGSLRLSCAASGFTFSSYSMNWVRQAPGKGLEWVSSISSSSSYIYYADSVKGRF TISRDNAKNSLYLQMNSLRAEDTAVYYCARGAP**X**GAAAGWFDPWGQGTLVTVSS, wherein X is M, L, I, V, Q, or F
111	ARGAP**X**GAAAGWFDP wherein X is M, L, I, V, Q, or F
112	GAP**X**GAAAGWFDP wherein X is M, L, I, V, Q, or F
113	QVQLVESGGGLVKPGGSLRLSCAASGFTFSSYGMHWVRQAPGKGLEWVAFIRYDGSNKYYADSVKGRF TISRDNSKNTLYLQMNSLRAEDTAVYYCAKDRGLGDGTYFDYWGQGTTVTVSS
114	QSALTQPASVSGSPGQSITISCSGSSSNIGNNAVNWYQQLPGKAPKLLIYYDDLLPSGVSDRFSGSKS GTSAFLAISGLQSEDEADYYCAAWDDSLNGPVFGGGTKLTVL
115	SYAMS
116	QVHLQESGPGLVKPSETLSLTCTVSDDSISSYYWSWIRQPPGKGLEWIGHISYSGSANYNPSLKSRVT ISVDTSKNQFSLKLSSVTAADTAVYYCANWDDAFNIWGQGTMVTVSS
117	EIVLTQSPGTLSLSPGERATLSCRASQSVSSSYLAWYQQKPGQAPRLLIYGASSRATGIPDRFSGSGS GTDFTLTISRLEPEDFAVYYCQQYGSSPWTFGQGTKVEIK
118	DKTHTCPPCPAPELLGGPSVFLFPPKPKDTLMISRTPEVTCVVVDVSHEDPEVKFNWYVDGVEVHNAK TKPREEQYNSTYRVVSVLTVLHQDWLNGKEYKCKVSNKALPAPIEKTISKAKGQPREPQVYTLPPSRD ELTKNQVSLTCLVKGFYPSDIAVEWESNGQPENNYKTTPPVLDSDGSFFLYSKLTVDKSRWQQGNVFS CSVMHEALHNHYTQKSLSLSPG
119	(GlyGlyGlyGlySer)$_4$ ($(G_4S)_4$)
120	$(GS)_n$ wherein n is 1, 2, 3, 4, 5, 6, 7, 8, 9, 10, 11, 12, 13, 14, 15, 16, 17, 18, 19, or 20
121	$(GGS)_n$ wherein n is 1, 2, 3, 4, 5, 6, 7, 8, 9, 10, 11, 12, 13, 14, 15, 16, 17, 18, 19, or 20
122	$(GGGS)_n$ wherein n is 1, 2, 3, 4, 5, 6, 7, 8, 9, 10, 11, 12, 13, 14, 15, 16, 17, 18, 19, or 20

SEQ ID NO	Sequence
123	$(GGSG)_n$ wherein n is 1, 2, 3, 4, 5, 6, 7, 8, 9, 10, 11, 12, 13, 14, 15, 16, 17, 18, 19, or 20
124	$(GGSGG)_n$ wherein n is 1, 2, 3, 4, 5, 6, 7, 8, 9, 10, 11, 12, 13, 14, 15, 16, 17, 18, 19, or 20
125	$(GGGGS)_n$ wherein n is 1, 2, 3, 4, 5, 6, 7, 8, 9, 10, 11, 12, 13, 14, 15, 16, 17, 18, 19, or 20
126	GSGSGSGSGSGSGSGSGS
127	GGSGGSGGSGGSGGSGGSGGSGGSGGS
128	GGGSGGGSGGGSGGGSGGGSGGGSGGGSGGGSGGGS
129	GGSGGGSGGGSGGGSGGGSGGGSGGGSGGGSGGGSG
130	GGSGGGGSGGGGSGGGGSGGGGSGGGGSGGGGSGGGGSGGGGSGG
131	GGGGSGGGGSGGGGSGGGGSGGGGSGGGGSGGGGSGGGGSGGGGS
132	GGGGSGGGGSGGGGS
133	GGGGSGGGGSGGGGSGGGGSGGGGSGGGGSGGGGSGGGGSGGGGSGGGGSGGGGSGGGGSGGG GSGGGGSGGGGSGGGGSGGGGSGGGGSGGGGS
134	GGSGGGGSGGGGSGGGGSGGGGSGGGGSGGGGSGGGGSGGGGSGGGGSGGGGSGGGGSGGGGS GGGGSGGGGSGGGGSGGGGSGGGGSGGGGSGG
135	EVQLQESGPGLVQPSQSLSITCTVSGFSLTNYGLHWVRQSPGKGLEWLGVIWSGGKTDYNTPFKSRLS ISKDISKNQVFFKMNSLQPNDTAIYFCAKYDYDDSLDYWGQGTSVTVSS
136	DIQMNQSPSSLSASLGDTIAITCHASQNINFWLSWYQQKPGNIPKLLIYEASNLHTGVPSRFSGSGSG TRFTLTISSLQPEDIATYYCQQSHSYPLTFGQGTKLEIK
137	GFSLTNY
138	WSGGK
139	YDYDDSLDY
140	HASQNINFWLS
141	EASNLHT
142	QQSHSYPLT
143	QLQLQESGPGLVKPSETLSLTCTVSGFSLTNYGLHWIRQPPGKGLEWIGVIWSGGKTDYNPSLKSRVT ISKDTSKNQFSLKLSSVQANDTAVYYCAKYDYDDSLDYWGQGTLVTVSS
144	DIQMTQSPSSLSASVGDRVTITCHASQNINFWLSWYQQKPGKIPKLLIYEASNLHTGVPSRFSGSGSG TRFTLTISSLQPEDIATYYCQQSHSYPLTFGQGTKLEIK
145	QLQLQESGPGLVKPSETLSLTCTVSGFSLTNYGLHWIRQPPGKCLEWIGVIWSGGKTDYNPSLKSRVT ISKDTSKNQFSLKLSSVQANDTAVYYCAKYDYDDSLDYWGQGTLVTVSSGGGGSGGGGSGGGGSGGGG SDIQMTQSPSSLSASVGDRVTITCHASQNINFWLSWYQQKPGKIPKLLIYEASNLHTGVPSRFSGSGS GTRFTLTISSLQPEDIATYYCQQSHSYPLTFGCGTKLEIK
146	DIQMTQSPSSLSASVGDRVTITCHASQNINFWLSWYQQKPGKIPKLLIYEASNLHTGVPSRFSGSGSG TRFTLTISSLQPEDIATYYCQQSHSYPLTFGCGTKLEIKGGGGSGGGGSGGGGSGGGGSQLQLQESGP GLVKPSETLSLTCTVSGFSLTNYGLHWIRQPPGKCLEWIGVIWSGGKTDYNPSLKSRVTISKDTSKNQ FSLKLSSVQANDTAVYYCAKYDYDDSLDYWGQGTLVTVSS
147	QLQLQESGPGLVKPSETLSLTCTVSGFSLTNYGLHWIRQPPGKGLEWIGVIWSGGKTDYNPSLKSRVT ISVDTSKNQFSLKLSSVQANDTAVYYCAKYDYDDSLDYWGQGTLVTVSS
148	EVQLVESGGGVVQPGGSLRLSCAASGFTFNAFGMHWVRQAPGKGLEWVAFISSGSTSIYYANTVKGRF TISRDNSKNTLYLQMNSLRAEDTAVYYCARDGYPTGGAMDYWGQGTSVTVSS

SEQ ID NO	Sequence
149	QLQLQESGPGLVKPSETLSLTCTVSGFSLTNYGLHWIRQPPGKCLEWIGVIWSGGKTDYNPSLKSRVT ISVDTSKNQFSLKLSSVQANDTAVYYCAKYDYDDSLDYWGQGTLVTVSSGGGGSGGGGSGGGGSGGGG SDIQMTQSPSSLSASVGDRVTITCHASQNINFWLSWYQQKPGKIPKLLIYEASNLHTGVPSRFSGSGS GTRFTLTISSLQPEDIATYYCQQSHSYPLTFGCGTKLEIK
150	DIQMTQSPSSLSASVGDRVTITCHASQNINFWLSWYQQKPGKIPKLLIYEASNLHTGVPSRFSGSGSG TRFTLTISSLQPEDIATYYCQQSHSYPLTFGCGTKLEIKGGGGSGGGGSGGGGSGGGGSQLQLQESGP GLVKPSETLSLTCTVSGFSLTNYGLHWIRQPPGKCLEWIGVIWSGGKTDYNPSLKSRVTISVDTSKNQ FSLKLSSVQANDTAVYYCAKYDYDDSLDYWGQGTLVTVSS
151	DIQMTQSPSSLSASVGDRVTITCHASQNINFWLSWYQQKPGKX$_1$PKLLIYEASNLHTGVPSRFSGSGSG TX$_2$FTLTISSLQPEDX$_3$ATYYCQQSHSYPLTFGX$_4$GTKLEIK wherein X$_1$ is A or I, X$_2$ is D or R, X$_3$ is F or I, and X$_4$ is Q or G
152	KSSQSLLWNVNQNNYLV
153	QLQLQESGPGLVKPSETLSLTCTVSGFSLTNYGLHWIRQPPGKCLEWIGVIWSGGKTDYNPSLKSRVT ISKDTSKNQFSLKLSSVTANDTAVYYCAKYDYDDSLDYWGQGTLVTVSSGGGGSGGGGSGGGGSGGGG SDIQMTQSPSSLSASVGDRVTITCHASQNINFWLSWYQQKPGKIPKLLIYEASNLHTGVPSRFSGSGS GTRFTLTISSLQPEDIATYYCQQSHSYPLTFGCGTKLEIK
154	DIQMTQSPSSLSASVGDRVTITCHASQNINFWLSWYQQKPGKIPKLLIYEASNLHTGVPSRFSGSGSG TRFTLTISSLQPEDIATYYCQQSHSYPLTFGCGTKLEIKGGGGSGGGGSGGGGSGGGGSQLQLQESGP GLVKPSETLSLTCTVSGFSLTNYGLHWIRQPPGKCLEWIGVIWSGGKTDYNPSLKSRVTISKDTSKNQ FSLKLSSVTANDTAVYYCAKYDYDDSLDYWGQGTLVTVSS
155	EVQLQESGAELVRSGASIKLSCAASAFNIKDYFIHWVRQRPDQGLEWIGWIDPENDDTEYAPKFQDKA TMTADTSSNTAYLQLSSLTSADTAVYYCNALWSRGGYFDYWGQGTTLTVSS
156	QLQLQESGPGLVKPSETLSLTCTVSGFSLTNYGLHWIRQPPGKCLEWIGVIWSGGKTDYNPSLKSRVT ISKDTSKNQFSLKLSSVQAADTAVYYCAKYDYDDSLDYWGQGTLVTVSSGGGGSGGGGSGGGGSGGGG SDIQMTQSPSSLSASVGDRVTITCHASQNINFWLSWYQQKPGKIPKLLIYEASNLHTGVPSRFSGSGS GTRFTLTISSLQPEDIATYYCQQSHSYPLTFGCGTKLEIK
157	DIQMTQSPSSLSASVGDRVTITCHASQNINFWLSWYQQKPGKIPKLLIYEASNLHTGVPSRFSGSGSG TRFTLTISSLQPEDIATYYCQQSHSYPLTFGCGTKLEIKGGGGSGGGGSGGGGSGGGGSQLQLQESGP GLVKPSETLSLTCTVSGFSLTNYGLHWIRQPPGKCLEWIGVIWSGGKTDYNPSLKSRVTISKDTSKNQ FSLKLSSVQAADTAVYYCAKYDYDDSLDYWGQGTLVTVSS
158	EVLLTQSPAIIAASPGEKVTITCSARSSVSYMSWYQQKPGSSPKIWIYGISKLASGVPARFSGSGSGT YFSFTINNLEAEDVATYYCQQRSYYPFTFGSGTKLEIK
159	AFNIKDY
160	QLQLQESGPGLVKPSETLSLTCTVSGFSLTNYGLHWIRQPPGKCLEWIGVIWSGGKTDYNPSLKSRVT ISKDTSKNQFSLKLSSVQANDTAVYYCARYDYDDSLDYWGQGTLVTVSSGGGGSGGGGSGGGGSGGGG SDIQMTQSPSSLSASVGDRVTITCHASQNINFWLSWYQQKPGKIPKLLIYEASNLHTGVPSRFSGSGS GTRFTLTISSLQPEDIATYYCQQSHSYPLTFGCGTKLEIK
161	DIQMTQSPSSLSASVGDRVTITCHASQNINFWLSWYQQKPGKIPKLLIYEASNLHTGVPSRFSGSGSG TRFTLTISSLQPEDIATYYCQQSHSYPLTFGCGTKLEIKGGGGSGGGGSGGGGSGGGGSQLQLQESGP GLVKPSETLSLTCTVSGFSLTNYGLHWIRQPPGKCLEWIGVIWSGGKTDYNPSLKSRVTISKDTSKNQ FSLKLSSVQANDTAVYYCARYDYDDSLDYWGQGTLVTVSS
162	EVQLVESGGGVVQPGGSLRLSCAASGFTFNSFGMHWVRQAPGKGLEWVAFISSGSTSIYYANTVKGRF TISRDNSKNTLYLQMNSLRAEDTAVYYCARDGYPTGGAMDYWGQGTSVTVSS
163	DIQMTQSPSSLSASVGDRVTITCHASQNINFWLSWYQQKPGKAPKLLIYEASNLHTGVPSRFSGSGSG TRFTLTISSLQPEDIATYYCQQSHSYPLTFGQGTKLEIK
164	QLQLQESGPGLVKPSETLSLTCTVSGFSLTNYGLHWIRQPPGKCLEWIGVIWSGGKTDYNPSLKSRVT ISKDTSKNQFSLKLSSVQANDTAVYYCAKYDYDDSLDYWGQGTLVTVSSGGGGSGGGGSGGGGSGGGG

SEQ ID NO	Sequence
	SDIQMTQSPSSLSASVGDRVTITCHASQNINFWLSWYQQKPGKAPKLLIYEASNLHTGVPSRFSGSGS GTRFTLTISSLQPEDIATYYCQQSHSYPLTFGCGTKLEIK
165	DIQMTQSPSSLSASVGDRVTITCHASQNINFWLSWYQQKPGKAPKLLIYEASNLHTGVPSRFSGSGSG TRFTLTISSLQPEDIATYYCQQSHSYPLTFGCGTKLEIKGGGGSGGGGSGGGGSGGGGSQLQLQESGP GLVKPSETLSLTCTVSGFSLTNYGLHWIRQPPGKCLEWIGVIWSGGKTDYNPSLKSRVTISKDTSKNQ FSLKLSSVQANDTAVYYCAKYDYDDSLDYWGQGTLVTVSS
166	WSGGS
167	DIQMTQSPSSLSASVGDRVTITCHASQNINFWLSWYQQKPGKIPKLLIYEASNLHTGVPSRFSGSGSG TDFTLTISSLQPEDIATYYCQQSHSYPLTFGQGTKLEIK
168	QLQLQESGPGLVKPSETLSLTCTVSGFSLTNYGLHWIRQPPGKCLEWIGVIWSGGKTDYNPSLKSRVT ISKDTSKNQFSLKLSSVQANDTAVYYCAKYDYDDSLDYWGQGTLVTVSSGGGGSGGGGSGGGGSGGGG SDIQMTQSPSSLSASVGDRVTITCHASQNINFWLSWYQQKPGKIPKLLIYEASNLHTGVPSRFSGSGS GTDFTLTISSLQPEDIATYYCQQSHSYPLTFGCGTKLEIK
169	DIQMTQSPSSLSASVGDRVTITCHASQNINFWLSWYQQKPGKIPKLLIYEASNLHTGVPSRFSGSGSG TDFTLTISSLQPEDIATYYCQQSHSYPLTFGCGTKLEIKGGGGSGGGGSGGGGSGGGGSQLQLQESGP GLVKPSETLSLTCTVSGFSLTNYGLHWIRQPPGKCLEWIGVIWSGGKTDYNPSLKSRVTISKDTSKNQ FSLKLSSVQANDTAVYYCAKYDYDDSLDYWGQGTLVTVSS
170	DPENDD
171	DIQMTQSPSSLSASVGDRVTITCHASQNINFWLSWYQQKPGKIPKLLIYEASNLHTGVPSRFSGSGSG TRFTLTISSLQPEDFATYYCQQSHSYPLTFGQGTKLEIK
172	QLQLQESGPGLVKPSETLSLTCTVSGFSLTNYGLHWIRQPPGKCLEWIGVIWSGGKTDYNPSLKSRVT ISKDTSKNQFSLKLSSVQANDTAVYYCAKYDYDDSLDYWGQGTLVTVSSGGGGSGGGGSGGGGSGGGG SDIQMTQSPSSLSASVGDRVTITCHASQNINFWLSWYQQKPGKIPKLLIYEASNLHTGVPSRFSGSGS GTRFTLTISSLQPEDFATYYCQQSHSYPLTFGCGTKLEIK
173	DIQMTQSPSSLSASVGDRVTITCHASQNINFWLSWYQQKPGKIPKLLIYEASNLHTGVPSRFSGSGSG TRFTLTISSLQPEDFATYYCQQSHSYPLTFGCGTKLEIKGGGGSGGGGSGGGGSGGGGSQLQLQESGP GLVKPSETLSLTCTVSGFSLTNYGLHWIRQPPGKCLEWIGVIWSGGKTDYNPSLKSRVTISKDTSKNQ FSLKLSSVQANDTAVYYCAKYDYDDSLDYWGQGTLVTVSS
174	QLQLQESGPGLVKPSETLSLTCTVSGFSLTNYGLHWIRQPPGKGLEWIGVIWSGGKTDYNPSLKSRVT ISVDTSKNQFSLKLSSVTAADTAVYYCARYDYDDSLDYWGQGTLVTVSS
175	DIQMTQSPSSLSASVGDRVTITCHASQNINFWLSWYQQKPGKAPKLLIYEASNLHTGVPSRFSGSGSG TDFTLTISSLQPEDFATYYCQQSHSYPLTFGQGTKLEIK
176	QLQLQESGPGLVKPSETLSLTCTVSGFSLTNYGLHWIRQPPGKCLEWIGVIWSGGKTDYNPSLKSRVT ISVDTSKNQFSLKLSSVTAADTAVYYCARYDYDDSLDYWGQGTLVTVSSGGGGSGGGGSGGGGSGGGG SDIQMTQSPSSLSASVGDRVTITCHASQNINFWLSWYQQKPGKAPKLLIYEASNLHTGVPSRFSGSGS GTDFTLTISSLQPEDFATYYCQQSHSYPLTFGCGTKLEIK
177	DIQMTQSPSSLSASVGDRVTITCHASQNINFWLSWYQQKPGKAPKLLIYEASNLHTGVPSRFSGSGSG TDFTLTISSLQPEDFATYYCQQSHSYPLTFGCGTKLEIKGGGGSGGGGSGGGGSGGGGSQLQLQESGP GLVKPSETLSLTCTVSGFSLTNYGLHWIRQPPGKCLEWIGVIWSGGKTDYNPSLKSRVTISVDTSKNQ FSLKLSSVTAADTAVYYCARYDYDDSLDYWGQGTLVTVSS
178	QLQLQESGPGLVKPSETLSLTCTVSGFSLTNYGLHWIRQPPGKGLEWIGVIWSGGKTDYNPSLKSRVT ISKDTSKNQFSLKLSSVQAADTAVYYCAKYDYDDSLDYWGQGTLVTVSS
179	QHNHGSFLPYT
180	QLQLQESGPGLVKPSETLSLTCTVSGFSLTNYGLHWIRQPPGKCLEWIGVIWSGGKTDYNPSLKSRVT ISKDTSKNQFSLKLSSVQAADTAVYYCAKYDYDDSLDYWGQGTLVTVSSGGGGSGGGGSGGGGSGGGG SDIQMTQSPSSLSASVGDRVTITCHASQNINFWLSWYQQKPGKAPKLLIYEASNLHTGVPSRFSGSGS GTRFTLTISSLQPEDIATYYCQQSHSYPLTFGCGTKLEIK

SEQ ID NO	Sequence
181	DIQMTQSPSSLSASVGDRVTITCHASQNINFWLSWYQQKPGKAPKLLIYEASNLHTGVPSRFSGSGSG TRFTLTISSLQPEDIATYYCQQSHSYPLTFGCGTKLEIKGGGGSGGGGSGGGGSGGGGSQLQLQESGP GLVKPSETLSLTCTVSGFSLTNYGLHWIRQPPGKCLEWIGVIWSGGKTDYNPSLKSRVTISKDTSKNQ FSLKLSSVQAADTAVYYCAKYDYDDSLDYWGQGTLVTVSS
182	QLQLQESGPGLVKPSETLSLTCTVSGFSLTNYGLHWIRQPPGKGLEWIGVIWSGGKTDYNPSLKSRVT ISX$_1$DTSKNQFSLKLSSVX$_2$AX$_3$DTAVYYCAX$_4$YDYDDSLDYWGQGTLVTVSS; wherein X$_1$ is V or K, X$_2$ is T or Q, X$_3$ is A or N, and X$_4$ is R or K
183	LWSRGGYFDY
184	EVQLVESGGGVVQPGGSLRLSCAASGFTFNSFGMHWVRQAPGKCLEWVAFISSGSTSIYYANTVKGRF TISRDNSKNTLYLQMNSLRAEDTAVYYCARDGYPTGGAMDYWGQGTSVTVSSGGGGSGGGGSGGGGSG GGGSDIQMTQSPSSLSASVGDRVTITCKASQDIYNYLSWFQQKPGKAPKPLIYRANILVSGVPSRFSG SGSGQDYTFTISSLQPEDIATYYCLQFDAFPFTFGCGTKLEIK
185	DIQMTQSPSSLSASVGDRVTITCKASQDIYNYLSWFQQKPGKAPKPLIYRANILVSGVPSRFSGSGSG QDYTFTISSLQPEDIATYYCLQFDAFPFTFGCGTKLEIKGGGGSGGGGSGGGGSGGGGSEVQLVESGG GVVQPGGSLRLSCAASGFTFNSFGMHWVRQAPGKCLEWVAFISSGSTSIYYANTVKGRFTISRDNSKN TLYLQMNSLRAEDTAVYYCARDGYPTGGAMDYWGQGTSVTVSS
186	SARSSVSYMS
187	DGYPTGGAMDY
188	GISKLAS
189	QQRSYYPFT
190	EVQLQESGPELEKPGASVRISCKASGYSFTAYNMNWVKQSNGKSLEWIGNIDPSYGDATYNQKFKGKA TLTVDKSSSTAYMQLKSLTSEDSAVYYCARDNYYGSGYFDYWGQGTTLTVSS
191	SVLMTQTPLSLPVSLGDRASISCRSSQGIVHINGNTYLEWYLQKPGQSPKLLIYKVSNRFSGVPDRFS GSGSGTDFTLKISRVEAEDLGVYYCFQGSHVPWTFGGGTKLEIK
192	GFTFNSF
193	EVQLQESGGGLVQPGGSRKLSCAASGFTFNSFGMHWVRQAPEKGLEWVAFISSGSTSIYYANTVKGRF TISRDNPKNTLFLQMTSLRSEDTAMYYCARDGYPTGGAMDYWGQGTSVTVSS
194	DIKMTQSPSSMYASLGERVTITCKASQDIYNYLSWFQLKPGKSPRPLIYRANILVSGVPSKFSGSGSG QDYSLTINSLEYEDLGIYYCLQFDAFPFTFGSGTKLEIK
195	GFTFNAF
196	SSGSTS
197	GYSFTAY
198	KASQDIYNYLS
199	RANILVS
200	DIQMTQSPSSLSASVGDRVTITCHASQNINFWLSWYQQKPGKAPKLLIYEASNLHTGVPSRFSGSGSG TRFTLTISSLQPEDIATYYCQQSHSYPLTFGCGTKLEIKGGGGSGGGGSGGGGSGGGGSQLQLQESGP GLVKPSETLSLTCTVSGFSLTNYGLHWIRQPPGKCLEWIGVILSGGWTDYNPSLKSRVTISKDTSKNQ FSLKLSSVQAADTAVYYCAKGDYGDALDYWGQGTLVTVSS
201	LQFDAFPFT
202	DPSYGD
203	DIQMTQSPSSLSASVGDRVTITCKASQDIYNYLSWFQQKPGKAPKPLIYRANILVSGVPSRFSGSGSG QDYTFTISSLQPEDIATYYCLQFDAFPFTFGSGTKLEIK
204	EVQLVESGGGVVQPGGSLRLSCAASGFTFNAFGMHWVRQAPGKCLEWVAFISSGSTSIYYANTVKGRF TISRDNSKNTLYLQMNSLRAEDTAVYYCARDGYPTGGAMDYWGQGTSVTVSSGGGGSGGGGSGGGGSG GGGSDIQMTQSPSSLSASVGDRVTITCKASQDIYNYLSWFQQKPGKAPKPLIYRANILVSGVPSRFSG SGSGQDYTFTISSLQPEDIATYYCLQFDAFPFTFGCGTKLEIK

SEQ ID NO	Sequence
205	DIQMTQSPSSLSASVGDRVTITCKASQDIYNYLSWFQQKPGKAPKPLIYRANILVSGVPSRFSGSGSG QDYTFTISSLQPEDIATYYCLQFDAFPFTFGCGTKLEIKGGGGSGGGGSGGGGSGGGGSEVQLVESGG GVVQPGGSLRLSCAASGFTFNAFGMHWVRQAPGKCLEWVAFISSGSTSIYYANTVKGRFTISRDNSKN TLYLQMNSLRAEDTAVYYCARDGYPTGGAMDYWGQGTSVTVSS
206	GFSLTSY
207	DNYYGSGYFDY
208	EVQLVESGGGVVQPGGSLRLSCAASGFTFNSFGMHWVRQAPGKCLEWVAFISSGSTSIYYANTVKGRF TISRDNSKNTLYLQMNSLRAEDTAVYYCARSGYPTGGAMDYWGQGTSVTVSSGGGGSGGGGSGGGGSG GGGSDIQMTQSPSSLSASVGDRVTITCKASQDIYNYLSWFQQKPGKAPKPLIYRANILVSGVPSRFSG SGSGQDYTFTISSLQPEDIATYYCLQFDAFPFTFGCGTKLEIK
209	DIQMTQSPSSLSASVGDRVTITCKASQDIYNYLSWFQQKPGKAPKPLIYRANILVSGVPSRFSGSGSG QDYTFTISSLQPEDIATYYCLQFDAFPFTFGCGTKLEIKGGGGSGGGGSGGGGSGGGGSEVQLVESGG GVVQPGGSLRLSCAASGFTFNSFGMHWVRQAPGKCLEWVAFISSGSTSIYYANTVKGRFTISRDNSKN TLYLQMNSLRAEDTAVYYCARSGYPTGGAMDYWGQGTSVTVSS
210	EVQLVESGGGVVQPGGSLRLSCAASGFTFNSFGMHWVRQAPGKGLEWVAFISSGSTSIYYANTVKGRF TISRDNSKNTLYLQMNSLRAEDTAVYYCARSGYPTGGAMDYWGQGTSVTVSS
211	RSSQGIVHINGNTYLE
212	KVSNRFS
213	SGYPTGGAMDY
214	FQGSHVPWT
215	EVQLVESGGGVVQPGGSLRLSCAASGFTFNSFGMHWVRQAPGKCLEWVAFISSGSTSIYYANTVKGRF TISRDNSKNTLYLQMNSLRAEDTAVYYCARDGYPTGGAMDYWGQGTSVTVSSGGGGSGGGGSGGGGSG GGGSDIKMTQSPSSLSASVGDRVTITCKASQDIYNYLSWFQQKPGKAPKPLIYRANILVSGVPSRFSG SGSGQDYTLTISSLQPEDIATYYCLQFDAFPFTFGCGTKLEIK
216	DIKMTQSPSSLSASVGDRVTITCKASQDIYNYLSWFQQKPGKAPKPLIYRANILVSGVPSRFSGSGSG QDYTLTISSLQPEDIATYYCLQFDAFPFTFGCGTKLEIKGGGGSGGGGSGGGGSGGGGSEVQLVESGG GVVQPGGSLRLSCAASGFTFNSFGMHWVRQAPGKCLEWVAFISSGSTSIYYANTVKGRFTISRDNSKN TLYLQMNSLRAEDTAVYYCARDGYPTGGAMDYWGQGTSVTVSS
217	EVQLQESGAELVRSGASVKLSCTVSGFNIKDYYMHWVKQRPEQGLEWIGWIDPENGDTENVPKFQGKA TMTADTSSNTAYLQLRSLTSEDTAVYYCKSYYYDSSSRYVDVWGAGTTVTVSS
218	DIKMTQSPSSLSASVGDRVTITCKASQDIYNYLSWFQQKPGKAPKPLIYRANILVSGVPSRFSGSGSG QDYTLTISSLQPEDIATYYCLQFDAFPFTFGSGTKLEIK
219	GIVMTQAPLTLSVTIGQPASISCKSSQSLLDSDGKTFLNWFLQRPGQSPKRLISLVSKLDSGVPDRFT GSGSGTDFTLKLSRVEPEDLGVYYCWQGTHFPYTFGGGTKLEIK
220	GFNIKDY
221	GFSLTSF
222	DPENGD
223	SYFAMDY
224	KSSQSLLDSDGKTFLN
225	LVSKLDS
226	GASIRES
227	WQGTHFPYT
228	EVQLQESGAELMKPGASVKISCRTTGYTFSTYWIEWVKQRPGRGPEWIGELFPGNSDTTLNEKFTGKA TFTADSSSNTAYMQLSSLTSEDSAVYYCARSGYYGSSLDYWGQGTTLTVSS
229	GIVMTQSPASLSASVGETVTITCRAGENIHSYLAWYQQKQGKSPQLLVYNAKTLAEGVPSRFSGSGSG TQFSLKINSLQPEDFGSYYCQHHYGTPRTFGGGTKLEIK

SEQ ID NO	Sequence
230	GYTFSTY
231	FPGNSD
232	SGYYGSSLDY
233	RAGENIHSYLA
234	NAKTLAE
235	QHHYGTPRT
236	WSGGN
237	GIVMTQSPSSLAVTAGEKVTMRCKSSQSLLWNVNQNNYLVWYQQKQGQPPKLLIYGASIRESWVPDRF TGSGSGTDFTLTISNVHAEDLAVYYCQHNHGSFLPYTFGGGTKLEIK
238	EVQLQESGPGLVQPSQSLSITCTVSGFSLTSFGIHWVRQSPGKGLEWLGVIWSGGNTDSNAAFISRLS ITKDISKSQVFFKMNSLQVTDTAIYYCARSYFAMDYWGQGTSVTVSS
239	GASIRQS
240	KSSQSLLWNVNQNNYLL
241	THFGMDY
242	QVQLRQSGPGLVQPSQSLSITCTVSGFSLTSYGVHWVRQSPGKGLEWLGVMWSGGSTDYNAAFMSRLS ISKDNSKSQVFFTMNSLQADDTAIYYCARTHFGMDYWGQGTPVTVSS
243	GIVMTQSPSSLAVTAGEKVTMRCKSSQSLLWSVNQNNYLLWYQQKQGQPPKLLIYGASIRQSWVPDRF TGSGSGTDFTLSISNVHAEDLAVYYCQHNHGSFLPYTFGGGTKLEIK
244	QLQLQESGPGLVKPSETLSLTCTVSGFSLTNYGLHWIRQPPGKGLEWIGVIWSGGKTDYNPSLKSRVT ISKDTSKNQFSLKLSSVTANDTAVYYCAKYDYDDSLDYWGQGTLVTVSS
245	KSSQSLLWSVNQNNYLL
246	XGYPTGGAMDY wherein X is D or S
247	EVQLQESGPGLVQPSQSLSITCTVSGFSLTSFGVHWVRQSPGKGLEWLGVIWSGGSTDSNAAFISRLT ITKDNSKSQVFFKMNSLQATDTAIYYCARSYFAMDYWGQGTSVSVSS
248	DIVMTQSPSSLAVTAGEKVTMRCKSSQSLLWNVNQNNYLLWYQQKQGQPPKLLIYGASIRESWVPDRF TGSGSGTDFTLTISNVHVEDLAVYYCQHNHGSFLPYTFGGGTKLEIK
249	EVQLVESGGGVVQPGGSLRLSCAASGFTFNX$_1$FGMHWVRQAPGKGLEWVAFISSGSTSIYYANTVKGRF TISRDNSKNTLYLQMNSLRAEDTAVYYCARX$_2$GYPTGGAMDYWGQGTSVTVSS wherein X$_1$ is S or A and X$_2$ is D or S
250	DIX$_1$MTQSPSSLSASVGDRVTITCKASQDIYNYLSWFQQKPGKAPKPLIYRANILVSGVPSRFSGSGSG QDYTX$_2$TISSLQPEDIATYYCLQFDAFPFTFGSGTKLEIK wherein X$_1$ is Q or K and X$_2$ is F or L
251	GFTFNXF wherein X is S or A
252	EVQLVESGGGVVQPGGSLRLSCAASGFTFNAFGMHWVRQAPGKCLEWVAFISSGSTSIYYANTVKGRF TISRDNSKNTLYLQMNSLRAEDTAVYYCARDGYPTGGAMDYWGQGTSVTVSSGGGGSGGGGSGGGGSG GGGSDIKMTQSPSSLSASVGDRVTITCKASQDIYNYLSWFQQKPGKAPKPLIYRANILVSGVPSRFSG SGSGQDYTLTISSLQPEDIATYYCLQFDAFPFTFGCGTKLEIK
253	DIKMTQSPSSLSASVGDRVTITCKASQDIYNYLSWFQQKPGKAPKPLIYRANILVSGVPSRFSGSGSG QDYTLTISSLQPEDIATYYCLQFDAFPFTFGCGTKLEIKGGGGSGGGGSGGGGSGGGGSEVQLVESGG GVVQPGGSLRLSCAASGFTFNAFGMHWVRQAPGKCLEWVAFISSGSTSIYYANTVKGRFTISRDNSKN TLYLQMNSLRAEDTAVYYCARDGYPTGGAMDYWGQGTSVTVSS
254	EVQLVESGGGVVQPGGSLRLSCAASGFTFNSFGMHWVRQAPGKCLEWVAFISSGSTSIYYANTVKGRF TISRDNSKNTLYLQMNSLRAEDTAVYYCARSGYPTGGAMDYWGQGTSVTVSSGGGGSGGGGSGGGGSG GGGSDIKMTQSPSSLSASVGDRVTITCKASQDIYNYLSWFQQKPGKAPKPLIYRANILVSGVPSRFSG SGSGQDYTLTISSLQPEDIATYYCLQFDAFPFTFGCGTKLEIK

SEQ ID NO	Sequence
255	DIKMTQSPSSLSASVGDRVTITCKASQDIYNYLSWFQQKPGKAPKPLIYRANILVSGVPSRFSGSGSG QDYTLTISSLQPEDIATYYCLQFDAFPFTFGCGTKLEIKGGGGSGGGGSGGGGSGGGGSEVQLVESGG GVVQPGGSLRLSCAASGFTFNSFGMHWVRQAPGKCLEWVAFISSGSTSIYYANTVKGRFTISRDNSKN TLYLQMNSLRAEDTAVYYCARSGYPTGGAMDYWGQGTSVTVSS
256	QLQLQESGPGLVKPSETLSLTCTVSGFSLTNYGLHWIRQPPGKGLEWIGVIWSGGKTDYNPSLKSRVT ISKDTSKNQFSLKLSSVQANDTAVYYCARYDYDDSLDYWGQGTLVTVSS
257	YYYDSSSRYVDV
258	MSEEVTYADLQFQNSSEMEKIPEIGKFGEKAPPAPSHVWRPAALFLTLLCLLLLIGLGVLASMFHVTL KIEMKKMNKLQNISEELQRNISLQLMSNMNISNKIRNLSTTLQTIATKLCRELYSKEQEHKCKPCPRR WIWHKDSCYFLSDDVQTWQESKMACAAQNASLLKINNKNALEFIKSQSRSYDYWLGLSPEEDSTRGMR VDNIINSSAWVIRNAPDLNNMYCGYINRLYVQYYHCTYKKRMICEKMANPVQLGSTYFREA
259	QLQLQESGPGLVKPSETLSLTCTVSGFSLTNYGLHWIRQPPGKCLEWIGVIWSGGKTDYNPSLKSRVT ISKDTSKNQFSLKLSSVQAADTAVYYCAKYDYDDSLDYWGQGTLVTVSSGGGGSGGGGSGGGGSGGGG SDIQMTQSPSSLSASVGDRVTITCHASQNINFWLSWYQQKPGKAPKLLIYEASNLHTGVPSRFSGSGS GTRFTLTISSLQPEDIATYYCQQSHSYPLTFGCGTKLEIKGSDKTHTCPPCPAPELLGGPSVFLFPPPK PKDTLMISRTPEVTCVVVDVSHEDPEVKFNWYVDGVEVHNAKTKPREEQYNSTYRVVSVLTVLHQDWL NGKEYKCKVSNKALPAPIEKTISKAKGQPREPRVYTLPPCRDELTKNQVSLTCLVKGFYPSDIAVEWE SNGQPENNYKTTPPVLVSDGSFTLYSKLTVDKSRWQQGNVFSCSVMHEALHNHYTQKSLSLSPG
260	EVQLVESGGGLVKPGGSLRLSCAASGFTFSSYSMNWVRQAPGKGLEWVSSISSSSSYIYYADSVKGRF TISRDNAKNSLYLQMNSLRAEDTAVYYCARGAPIGAAAGWFDPWGQGTLVTVSSASTKGPSVFPLAPS SKSTSGGTAALGCLVKDYFPEPVTVSWNSGALTSGVHTFPAVLQSSGLYSLSSVVTVPSSSLGTQTYI CNVNHKPSNTKVDKKVEPKSCDKTHTCPPCPAPELLGGPSVFLFPPKPKDTLMISRTPEVTCVVVDVS HEDPEVKFNWYVDGVEVHNAKTKPREEQYNSTYRVVSVLTVLHQDWLNGKEYKCKVSNKALPAPIEKT ISKAKGQPREPQVCTLPPSRDELTENQVSLTCLVKGFYPSDIAVEWESNGQPENNYKTTPPVLDSDGS FFLYSWLTVDKSRWQQGNVFSCSVMHEALHNHYTQKSLSLSPG
261	DIQMTQSPSSVSASVGDRVTITCRASQGISSWLAWYQQKPGKAPKLLIYAASSLQSGVPSRFSGSGSG TDFTLTISSLQPEDFATYYCQQGVSFPRTFGGGTKVEIKRTVAAPSVFIFPPSDEQLKSGTASVVCLL NNFYPREAKVQWKVDNALQSGNSQESVTEQDSKDSTYSLSSTLTLSKADYEKHKVYACEVTHQGLSSP VTKSFNRGEC
262	DIQMTQSPSSLSASVGDRVTITCHASQNINFWLSWYQQKPGKAPKLLIYEASNLHTGVPSRFSGSGSG TRFTLTISSLQPEDIATYYCQQSHSYPLTFGCGTKLEIKGGGGSGGGGSGGGGSGGGGSQLQLQESGP GLVKPSETLSLTCTVSGFSLTNYGLHWIRQPPGKCLEWIGVIWSGGKTDYNPSLKSRVTISKDTSKNQ FSLKLSSVQAADTAVYYCAKYDYDDSLDYWGQGTLVTVSSGSDKTHTCPPCPAPELLGGPSVFLFPPK PKDTLMISRTPEVTCVVVDVSHEDPEVKFNWYVDGVEVHNAKTKPREEQYNSTYRVVSVLTVLHQDWL NGKEYKCKVSNKALPAPIEKTISKAKGQPREP**R**VYTLPP**C**RDELTKNQVSLTCLVKGFYPSDIAVEWE SNGQPENNYKTTPPVL**V**SDGSF**T**LYSKLTVDKSRWQQGNVFSCSVMHEALHNHYTQKSLSLSPG
263	EVQLVQSGAEVKKPGASVKVSCKASGYTFTSYYMHWVRQAPGQGLEWMGIINPSGGSTSYAQKFQGRV TMTRDTSTSTVYMELSSLRSEDTAVYYCARGNYGDEFDYWGQGTLVTVSS
264	DIQMTQSPSSLSASVGDRVTITCRASQSISSYLNWYQQKPGKAPKLLIYAASSLQSGVPSRFSGSGSG TDFTLTISSLQPEDFATYYCQQSYSTPPTFGQGTKVEIK
265	DIQMTQSPSSLSASVGDRVTITCRASQSVSTSSYNYMHWYQQKPGKPPKLLIKYASNLESGVPSRFSG SGSGTDFTLTISSLQPEDFATYYCQHSWEIPLTFGQGTKVEIK
266	EVQLVQSGAEVKKPGASVKVSCKASGYSFTDYYMHWVRQAPGQGLEWIGRINPYNGAAFYSQNFKDRV TLTVDTSTSTAYLELSSLRSEDTAVYYCAIERGADLEGYAMDYWGQGTLVTVSS
267	ATGGACATGAGGGTACCAGCTCAGCTGCTGGGCCTGCTGCTGCTTTGGCTTCCTGGCGCTAGATGCCA ATTGCAGCTGCAAGAATCCGGACCAGGGCTCGTAAAACCTTCTGAAACCCTCTCCCTCACTTGCACTG TGTCTGGATTCTCTCTCACGAACTACGGGTTGCATTGGATCCGACAGCCGCCTGGCAAGTGTCTTGAG

SEQ ID NO	Sequence
	TGGATTGGCGTTATCTGGTCAGGAGGGAAGACGGATTATAATCCAAGTCTGAAATCCAGAGTGACAAT TTCTAAGGACACGTCCAAAAATCAGTTTAGCCTCAAACTTTCCTCAGTTCAGGCTGCTGATACAGCGG TGTACTATTGCGCAAAGTACGACTATGATGACAGTTTGGACTACTGGGGACAGGGTACACTGGTAACA GTGAGTTCTGGAGGCGGCGGTAGTGGAGGCGGGGGAAGTGGTGGCGGAGGGAGTGGAGGAGGGGGCAG TGATATTCAAATGACGCAGAGCCCCAGTTCCCTTTCAGCTAGCGTTGGCGACAGAGTAACGATAACGT GTCACGCTTCCCAGAACATTAATTTTTGGCTTAGCTGGTATCAACAGAAACCGGGAAAAGCACCCAAG CTGCTTATCTATGAAGCGTCCAATCTCCACACGGGTGTCCCATCAAGATTTTCTGGATCAGGCAGTGG CACACGATTCACACTGACCATTAGTTCCTTGCAGCCCGAGGATATCGCAACTTACTACTGTCAGCAAA GTCACTCTTACCCGTTGACATTCGGATGTGGAACTAAACTGGAGATTAAGGGATCCGATAAGACCCAC ACCTGTCCTCCATGTCCTGCTCCAGAACTGCTCGGCGGACCTTCCGTGTTCCTGTTTCCTCCAAAGCC TAAGGACACCCTGATGATCAGCAGGACCCCTGAAGTGACCTGCGTGGTGGTGGATGTGTCTCACGAGG ACCCAGAAGTGAAGTTCAATTGGTACGTGGACGGCGTGGAAGTGCACAACGCCAAGACCAAGCCTAGA GAGGAACAGTACAACAGCACCTACAGAGTGGTGTCCGTGCTGACCGTGCTGCACCAGGATTGGCTGAA CGGCAAAGAGTACAAGTGCAAGGTGTCCAACAAGGCCCTGCCTGCTCCTATCGAGAAAACCATCAGCA AGGCCAAGGGCCAGCCTCGCGAGCCTAGAGTGTATACCTTGCCTCCATGCCGGGACGAGCTGACCAAG AATCAGGTGTCCCTGACCTGCCTGGTCAAGGGCTTCTACCCTTCCGATATCGCCGTGGAATGGGAGAG CAATGGCCAGCCAGAGAACAACTACAAGACCACACCTCCTGTGCTGGTGTCCGACGGCAGCTTTACCC TGTACAGCAAGCTGACAGTGGACAAGAGCAGATGGCAGCAGGGCAACGTGTTCTCCTGCAGCGTGATG CACGAGGCCCTGCACAACCACTACACCCAGAAAAGCCTGAGCCTGTCTCCTGGCTAA
268	ATGGGCTGGTCCTGCATCATCCTGTTTCTGGTGGCCACAGCCACAGGCGTGCACTCTGAGGTGCAGCT GGTTGAATCTGGCGGCGGACTTGTGAAGCCTGGCGGATCTCTGAGACTGAGCTGTGCCGCCAGCGGCT TCACCTTTAGCAGCTACAGCATGAACTGGGTCCGACAGGCCCCTGGCAAAGGCCTTGAATGGGTGTCC AGCATCAGCAGCAGCTCCAGCTACATCTACTACGCCGACAGCGTGAAGGGCAGATTCACCATCAGCCG GGACAACGCCAAGAACAGCCTGTACCTGCAGATGAACTCCCTGAGAGCCGAGGACACCGCCGTGTACT ATTGTGCTAGAGGCGCCCCTATTGGAGCCGCCGCTGGATGGTTCGATCCTTGGGGACAGGGAACCCTG GTCACCGTTTCTTCTGCCTCTACAAAGGGCCCCAGCGTTTTCCCACTGGCTCCTAGCAGCAAGAGCAC AAGCGGAGGAACAGCTGCCCTGGGCTGTCTGGTCAAGGACTACTTTCCTGAGCCTGTGACCGTGTCCT GGAACAGCGGAGCACTGACTAGCGGCGTGCACACATTTCCAGCCGTGCTGCAAAGCAGCGGCCTGTAC TCTCTGAGCAGCGTCGTGACAGTGCCTAGCAGCTCTCTGGGCACCCAGACCTACATCTGCAATGTGAA CCACAAGCCTAGCAACACCAAGGTGGACAAGAAGGTGGAACCCAAGAGCTGCGACAAGACCCACACCT GTCCTCCATGTCCTGCTCCAGAACTGCTCGGCGGACCTTCCGTGTTCCTGTTTCCTCCAAAGCCTAAG GACACCCTGATGATCAGCAGAACCCCTGAAGTGACCTGCGTGGTGGTGGATGTGTCTCACGAGGACCC CGAAGTGAAGTTCAATTGGTACGTGGACGGCGTGGAAGTGCACAACGCCAAGACCAAGCCTAGAGAGG AACAGTACAACAGCACCTACAGAGTGGTGTCCGTGCTGACAGTGCTGCACCAGGATTGGCTGAACGGC AAAGAGTACAAGTGCAAGGTGTCCAACAAGGCCCTGCCTGCTCCTATCGAGAAAACCATCAGCAAGGC CAAGGGCCAGCCTCGCGAACCTCAAGTCTGTACACTGCCTCCTAGCCGGGATGAGCTGACCGAGAATC AGGTGTCCCTGACCTGTCTCGTGAAGGGCTTCTACCCCTCCGATATCGCCGTGGAATGGGAGAGCAAT GGCCAGCCAGAGAACAACTACAAGACAACCCCTCCTGTGCTGGACAGCGACGGCTCATTCTTCCTGTA CAGCTGGCTGACCGTGGACAAGTCCAGATGGCAGCAGGGCAACGTGTTCTCCTGCAGCGTGATGCACG AGGCCCTGCACAACCACTACACCCAGAAGTCCCTGTCTCTGAGCCCAGGCTAA
269	ATGGACATGAGAGTTCCAGCTCAGCTGCTGGGCCTGCTGCTGCTTTGGCTTCCTGGCGCTAGATGCGA CATCCAGATGACACAGAGCCCCAGCTCCGTGTCTGCCTCTGTGGGAGACAGAGTGACCATCACCTGTA GAGCCAGCCAGGGCATCTCTTCTTGGCTGGCCTGGTATCAGCAGAAGCCTGGCAAGGCCCCTAAGCTG CTGATCTATGCCGCTAGCTCTCTGCAGTCTGGCGTGCCCTCTAGATTTTCTGGCAGCGGCTCTGGCAC CGACTTCACCCTGACCATATCTAGCCTGCAGCCTGAGGACTTCGCCACCTACTATTGTCAGCAGGGCG TGTCCTTTCCACGGACCTTTGGCGGCGGAACAAAGGTGGAAATCAAGCGGACAGTGGCCGCTCCTAGC GTGTTCATCTTTCCACCTAGCGACGAGCAGCTGAAGTCCGGCACAGCCTCTGTTGTGTGCCTGCTGAA

SEQ ID NO	Sequence
	CAACTTCTACCCCAGAGAAGCCAAGGTGCAGTGGAAGGTGGACAATGCCCTGCAGAGCGGCAACAGCC AAGAGAGCGTGACAGAGCAGGACAGCAAGGACTCCACCTACAGCCTGAGCAGCACCCTGACACTGAGC AAGGCCGACTACGAGAAGCACAAAGTGTACGCCTGCGAAGTGACCCACCAGGGCCTTTCTAGCCCTGT GACCAAGAGCTTCAACCGGGGCGAGTGTTGA
270	QLQLQESGPGLVKPSETLSLTCTVSGFSLTNYGLHWIRQPPGKGLEWIGVIWVGGATDYNPSLKSRVT ISVDTSKNQFSLKLSSVQAADTAVYYCAKGDYGDTLDYWGQGTLVTVSS
271	DIQMTQSPSSLSASVGDRVTITCHASQNINFWLSWYQQKPGKAPKLLIYEASNLHTGVPSRFSGSGSG TDFTLTISSLQPEDFATYYCQQSHSYPLTFGSGTKLEIK
272	WVGGA
273	GDYGDTLDY
274	QLQLQESGPGLVKPSETLSLTCTVSGFSLTNYGLHWIRQPPGKCLEWIGVIWVGGATDYNPSLKSRVT ISVDTSKNQFSLKLSSVQAADTAVYYCAKGDYGDTLDYWGQGTLVTVSSGGGGSGGGGSGGGGSGGGG SDIQMTQSPSSLSASVGDRVTITCHASQNINFWLSWYQQKPGKAPKLLIYEASNLHTGVPSRFSGSGS GTDFTLTISSLQPEDFATYYCQQSHSYPLTFGCGTKLEIK
275	DIQMTQSPSSLSASVGDRVTITCHASQNINFWLSWYQQKPGKAPKLLIYEASNLHTGVPSRFSGSGSG TDFTLTISSLQPEDFATYYCQQSHSYPLTFGCGTKLEIKGGGGSGGGGSGGGGSGGGGSQLQLQESGP GLVKPSETLSLTCTVSGFSLTNYGLHWIRQPPGKCLEWIGVIWVGGATDYNPSLKSRVTISVDTSKNQ FSLKLSSVQAADTAVYYCAKGDYGDTLDYWGQGTLVTVSS
276	QLQLQESGPGLVKPSETLSLTCTVSGFSLTNYGLHWIRQPPGKCLEWIGVIWVGGATDYNPSLKSRVT ISVDTSKNQFSLKLSSVQAADTAVYYCAKGDYGDTLDYWGQGTLVTVSSGGGGSGGGGSGGGGSGGGG SDIQMTQSPSSLSASVGDRVTITCHASQNINFWLSWYQQKPGKAPKLLIYEASNLHTGVPSRFSGSGS GTDFTLTISSLQPEDFATYYCQQSHSYPLTFGCGTKLEIKGSDKTHTCPPCPAPELLGGPSVFLFPPK PKDTLMISRTPEVTCVVVDVSHEDPEVKFNWYVDGVEVHNAKTKPREEQYNSTYRVVSVLTVLHQDWL NGKEYKCKVSNKALPAPIEKTISKAKGQPREP**R**VYTLPP**C**RDELTKNQVSLTCLVKGFYPSDIAVEWE SNGQPENNYKTTPPVL**V**SDGSF**T**LYSKLTVDKSRWQQGNVFSCSVMHEALHNHYTQKSLSLSPG
277	QLQLQESGPGLVKPSETLSLTCTVSGFSLTNYGLHWIRQPPGKCLEWIGVILSGGWTDYNPSLKSRVT ISKDTSKNQFSLKLSSVQAADTAVYYCAKGDYGDALDYWGQGTLVTVSSGGGGSGGGGSGGGGSGGGG SDIQMTQSPSSLSASVGDRVTITCHASQNINFWLSWYQQKPGKAPKLLIYEASNLHTGVPSRFSGSGS GTRFTLTISSLQPEDIATYYCQQSHSYPLTFGCGTKLEIKGSDKTHTCPPCPAPELLGGPSVFLFPPK PKDTLMISRTPEVTCVVVDVSHEDPEVKFNWYVDGVEVHNAKTKPREEQYNSTYRVVSVLTVLHQDWL NGKEYKCKVSNKALPAPIEKTISKAKGQPREP**R**VYTLPP**C**RDELTKNQVSLTCLVKGFYPSDIAVEWE SNGQPENNYKTTPPVL**V**SDGSF**T**LYSKLTVDKSRWQQGNVFSCSVMHEALHNHYTQKSLSLSPG
278	EVQLVESGGGVVQPGGSLRLSCAASGFTFNAFGMHWVRQAPGKCLEWVAFISSGSTSIYYANTVKGRF TISRDNSKNTLYLQMNSLRAEDTAVYYCARDGYPTGGAMDYWGQGTSVTVSSGGGGSGGGGSGGGGSG GGGSDIQMTQSPSSLSASVGDRVTITCKASQDIYNYLSWFQQKPGKAPKPLIYRANILVSGVPSRFSG SGSGQDYTFTISSLQPEDIATYYCLQFDAFPFTFGCGTKLEIKGSDKTHTCPPCPAPELLGGPSVFLF PPKPKDTLMISRTPEVTCVVVDVSHEDPEVKFNWYVDGVEVHNAKTKPREEQYNSTYRVVSVLTVLHQ DWLNGKEYKCKVSNKALPAPIEKTISKAKGQPREP**R**VYTLPP**C**RDELTKNQVSLTCLVKGFYPSDIAV EWESNGQPENNYKTTPPVL**V**SDGSF**T**LYSKLTVDKSRWQQGNVFSCSVMHEALHNHYTQKSLSLSPG
279	GDYGDALDY
280	QLQLQESGPGLVKPSETLSLTCTVSGFSLTNYGLHWIRQPPGKCLEWIGVILSGGWTDYNPSLKSRVT ISKDTSKNQFSLKLSSVQAADTAVYYCAKGDYGDALDYWGQGTLVTVSSGGGGSGGGGSGGGGSGGGG SDIQMTQSPSSLSASVGDRVTITCHASQNINFWLSWYQQKPGKAPKLLIYEASNLHTGVPSRFSGSGS GTRFTLTISSLQPEDIATYYCQQSHSYPLTFGCGTKLEIK
281	QLQLQESGPGLVKPSETLSLTCTVSGFSLTNYGLHWIRQPPGKCLEWIGVIWSGGKTDYNPSLKSRVT ISKDTSKNQFSLKLSSVQAADTAVYYCAKYDYDDSLDYWGQGTLVTVSSGGGGSGGGGSGGGGSGGGG SDIQMTQSPSSLSASVGDRVTITCHASQNINFWLSWYQQKPGKIPKLLIYEASNLHTGVPSRFSGSGS

SEQ ID NO	Sequence
	GTRFTLTISSLQPEDIATYYCQQSHSYPLTFGCGTKLEIKGSDKTHTCPPCPAPELLGGPSVFLFPPK PKDTLMISRTPEVTCVVVDVSHEDPEVKFNWYVDGVEVHNAKTKPREEQYNSTYRVVSVLTVLHQDWL NGKEYKCKVSNKALPAPIEKTISKAKGQPREP**R**VYTLPP**C**RDELTKNQVSLTCLVKGFYPSDIAVEWE SNGQPENNYKTTPPVL**V**SDGSF**T**LYSKLTVDKSRWQQGNVFSCSVMHEALHNHYTQKSLSLSPG
282	DIQMTQSPSTLSASVGDRVTITCRASNSISSWLAWYQQKPGKAPKLLIYEASSTKSGVPSRFSGSGSG TEFTLTISSLQPDDFATYYCQQYDDLPTFGGGTKVEIK
283	YDYDDALDY
284	YDYDDILDY
285	YDYDDLLDY
286	DIQMTQSPSSVSASVGDRVTITCRASQGISSWLAWYQQKPGKAPKLLIYAASSLQSGVPSRFSGSGSG TDFTLTISSLQPEDFATYYCQQGVSFPRTFGGGTKVEIKGGGGSGGGGSGGGGSGGGGSEVQLVESGG GLVKPGGSLRLSCAASGFTFSSYSMNWVRQAPGKGLEWVSSISSSSSYIYYADSVKGRFTISRDNAKN SLYLQMNSLRAEDTAVYYCARGAPIGAAAGWFDPWGQGTLVTVSSGSDKTHTCPPCPAPELLGGPSVF LFPPKPKDTLMISRTPEVTCVVVDVSHEDPEVKFNWYVDGVEVHNAKTKPREEQYNSTYRVVSVLTVL HQDWLNGKEYKCKVSNKALPAPIEKTISKAKGQPREP**R**VYTLPP**C**RDELTKNQVSLTCLVKGFYPSDI AVEWESNGQPENNYKTTPPVL**V**SDGSF**T**LYSKLTVDKSRWQQGNVFSCSVMHEALHNHYTQKSLSLSP G
287	QLQLQESGPGLVKPSETLSLTCTVSGFSLTNYGLHWIRQPPGKGLEWIGVIWSGGKTDYNPSLKSRVT ISKDTSKNQFSLKLSSVQAADTAVYYCAKYDYDDSLDYWGQGTLVTVSSASTKGPSVFPLAPSSKSTS GGTAALGCLVKDYFPEPVTVSWNSGALTSGVHTFPAVLQSSGLYSLSSVVTVPSSSLGTQTYICNVNH KPSNTKVDKKVEPKSCDKTHTCPPCPAPELLGGPSVFLFPPKPKDTLMISRTPEVTCVVVDVSHEDPE VKFNWYVDGVEVHNAKTKPREEQYNSTYRVVSVLTVLHQDWLNGKEYKCKVSNKALPAPIEKTISKAK GQPREPQVCTLPPSRDELTENQVSLTCLVKGFYPSDIAVEWESNGQPENNYKTTPPVLDSDGSFFLYS WLTVDKSRWQQGNVFSCSVMHEALHNHYTQKSLSLSPG
288	DIQMTQSPSSLSASVGDRVTITCHASQNINFWLSWYQQKPGKAPKLLIYEASNLHTGVPSRFSGSGSG TRFTLTISSLQPEDIATYYCQQSHSYPLTFGGGTKLEIKRTVAAPSVFIFPPSDEQLKSGTASVVCLL NNFYPREAKVQWKVDNALQSGNSQESVTEQDSKDSTYSLSSTLTLSKADYEKHKVYACEVTHQGLSSP VTKSFNRGEC
289	DIQMTQSPSSLSASVGDRVTITCHASQNINFWLSWYQQKPGKAPKLLIYEASNLHTGVPSRFSGSGSG TRFTLTISSLQPEDIATYYCQQSHSYPLTFGGGTKLEIK
290	YDYDDVLDY
291	YDYDDTLDY
292	YDYDESLDY
293	DYDDSLDY
294	QLQLQESGPGLVKPSETLSLTCTVSGFSLTNYGLHWIRQPPGKGLEWIGVILSGGWTDYNPSLKSRVT ISKDTSKNQFSLKLSSVQAADTAVYYCAKGDYGDALDYWGQGTLVTVSS
295	DIQMTQSPSSLSASVGDRVTITCHASQNINFWLSWYQQKPGKAPKLLIYEASNLHTGVPSRFSGSGSG TRFTLTISSLQPEDIATYYCQQSHSYPLTFGSGTKLEIK
296	LSGGW
297	GFTFSSY
298	SSSSSY
299	LSCAASGFTFSSYS**M**NWVR
300	NSLYLQ**M**NSLR
301	DTL**M**ISR
302	WQQGNVFSCSV**M**HEALHNHYTQK
303	DIQ**M**TQSPSSVSASVGDR

SEQ ID NO	Sequence
304	YDYDDSLDYWGQGTLVTVSSGGGGSGGGGSGGGGSGGGGSDIQMTQSPSSLSASVGDRVTITCHASQN INFWLSWYQQKPGKAPK
305	XDYDDSLDY, wherein X = any amino acid
306	YXYDDSLDY, wherein X = any amino acid
307	YDXDDSLDY, wherein X = any amino acid
308	YDYXDSLDY, wherein X = any amino acid
309	YDYDXSLDY, wherein X = any amino acid
310	YDYDDXLDY, wherein X = any amino acid
311	YDYDDSXDY, wherein X = any amino acid
312	YDYDDSLXY, wherein X = any amino acid
313	YDYDDSLDX, wherein X = any amino acid
314	XXYDDSLDY, wherein X = any amino acid
315	XDXDDSLDY, wherein X = any amino acid
316	XDYXDSLDY, wherein X = any amino acid
317	XDYDXSLDY, wherein X = any amino acid
318	XDYDDXLDY, wherein X = any amino acid
319	XDYDDSXDY, wherein X = any amino acid
320	XDYDDSLXY, wherein X = any amino acid
321	XDYDDSLDX, wherein X = any amino acid
322	GDYGDSLDY
323	XSGGK, wherein X = any amino acid
324	WXGGK, wherein X = any amino acid
325	WSXGK, wherein X = any amino acid
326	WSGXK, wherein X = any amino acid
327	WSGGX, wherein X = any amino acid
328	XXGGK, wherein X = any amino acid
329	XSXGK, wherein X = any amino acid
330	XSGXK, wherein X = any amino acid
331	XSGGX, wherein X = any amino acid
332	WXXGK, wherein X = any amino acid
333	WXGXK, wherein X = any amino acid
334	WXGGX, wherein X = any amino acid
335	QLQLQESGPGLVKPSETLSLTCTVSGFSLTNYGLHWIRQPPGKCLEWIGVIWVGGATDYNPSLKSRVT ISVDTSKNQFSLKLSSVQAADTAVYYCAKGDYGDTLDYWGQGTLVTVSS
336	DIQMTQSPSSLSASVGDRVTITCHASQNINFWLSWYQQKPGKAPKLLIYEASNLHTGVPSRFSGSGSG TDFTLTISSLQPEDFATYYCQQSHSYPLTFGCGTKLEIK
337	RASQGISSWA
338	SSSSY
339	GAPMIGAAAGWFDP
340	LSCAASGFTFNAFGMHWVR
341	NTLYLQMNSLR
342	DGYPTGGAMDYWGQGTSVTVSSGGGGSGGGGSGGGGSGGGGSDIQMTQSPSSLSASVGDR

WHAT IS CLAIMED IS:

1. A protein comprising:

(a) a first antigen-binding site that binds NKG2D;

(b) a second antigen-binding site that binds CLEC12A; and

(c) an antibody Fc domain or a portion thereof sufficient to bind CD16, or a third antigen-binding site that binds CD16;

wherein the second antigen-binding site that binds CLEC12A comprises:

(i) a heavy chain variable domain (VH) comprising complementarity-determining region 1 (CDR1), complementarity-determining region 2 (CDR2), and complementarity-determining region 3 (CDR3) comprising the amino acid sequences of SEQ ID NOs: 137, 272, and 273, respectively; and a light chain variable domain (VL) comprising CDR1, CDR2, and CDR3 comprising the amino acid sequences of SEQ ID NOs: 140, 141, and 142, respectively;

(ii) a VH comprising CDR1, CDR2, and CDR3 comprising the amino acid sequences of SEQ ID NOs: 137, 138, and 139, respectively; and a VL comprising CDR1, CDR2, and CDR3 comprising the amino acid sequences of SEQ ID NOs: 140, 141, and 142, respectively;

(iii) a VH comprising CDR1, CDR2, and CDR3 comprising the amino acid sequences of SEQ ID NOs: 251, 196, and 246, respectively; and a VL comprising CDR1, CDR2, and CDR3 comprising the amino acid sequences of SEQ ID NOs: 198, 199, and 201, respectively;

(iv) a VH comprising CDR1, CDR2, and CDR3 comprising the amino acid sequences of SEQ ID NOs: 221, 166, and 223, respectively; and a VL comprising CDR1, CDR2, and CDR3 comprising the amino acid sequences of SEQ ID NOs: 240, 226, and 179, respectively;

(v) a VH comprising CDR1, CDR2, and CDR3 comprising the amino acid sequences of SEQ ID NOs: 206, 166, and 241, respectively; and a VL comprising CDR1, CDR2, and CDR3 comprising the amino acid sequences of SEQ ID NOs: 245, 239, and 179, respectively;

(vi) a VH comprising CDR1, CDR2, and CDR3 comprising the amino acid sequences of SEQ ID NOs: 221, 236, and 223, respectively; and a VL comprising CDR1, CDR2, and CDR3 comprising the amino acid sequences of SEQ ID NOs: 152, 226, and 179, respectively;

(vii) a VH comprising CDR1, CDR2, and CDR3 comprising the amino acid sequences of SEQ ID NOs: 159, 170, and 183, respectively; and a VL comprising CDR1, CDR2, and CDR3 comprising the amino acid sequences of SEQ ID NOs: 186, 188, and 189, respectively;

(viii) a VH comprising CDR1, CDR2, and CDR3 comprising the amino acid sequences

of SEQ ID NOs: 197, 202, and 207, respectively; and a VL comprising CDR1, CDR2, and CDR3 comprising the amino acid sequences of SEQ ID NOs: 211, 212, and 214, respectively;

(ix) a VH comprising CDR1, CDR2, and CDR3 comprising the amino acid sequences of SEQ ID NOs: 220, 222, and 257, respectively; and a VL comprising CDR1, CDR2, and CDR3 comprising the amino acid sequences of SEQ ID NOs: 224, 225, and 227, respectively; or

(x) a VH comprising CDR1, CDR2, and CDR3 comprising the amino acid sequences of SEQ ID NOs: 230, 231, and 232, respectively; and a VL comprising CDR1, CDR2, and CDR3 comprising the amino acid sequences of SEQ ID NOs: 233, 234, and 235, respectively.

2. The protein of claim 1, wherein the second antigen-binding site that binds CLEC12A comprises

(i) a VH comprising CDR1, CDR2, and CDR3 comprising the amino acid sequences of SEQ ID NOs: 137, 272, and 273, respectively; and a VL comprising CDR1, CDR2, and CDR3 comprising the amino acid sequences of SEQ ID NOs: 140, 141, and 142, respectively; or

(ii) a VH comprising CDR1, CDR2, and CDR3 comprising the amino acid sequences of SEQ ID NOs: 137, 138, and 139, respectively; and a VL comprising CDR1, CDR2, and CDR3 comprising the amino acid sequences of SEQ ID NOs: 140, 141, and 142, respectively.

3. The protein of claim 1 or 2, wherein

(i) the VH comprises an amino acid sequence at least 90% identical to SEQ ID NO:335, and the VL comprises an amino acid sequence at least 90% identical to SEQ ID NO:336;

(ii) the VH comprises an amino acid sequence at least 90% identical to SEQ ID NO:270, and the VL comprises an amino acid sequence at least 90% identical to SEQ ID NO:271; or

(iii) the VH comprises an amino acid sequence at least 90% identical to SEQ ID NO:178, and the VL comprises an amino acid sequence at least 90% identical to SEQ ID NO:289.

4. The protein of any one of claims 1-3, wherein

(i) the VH comprises the amino acid sequence of SEQ ID NO:335, and the VL comprises the amino acid sequence of SEQ ID NO:336;

(ii) the VH comprises the amino acid sequence of SEQ ID NO:270, and the VL comprises the amino acid sequence of SEQ ID NO:271; or

(iii) the VH comprises the amino acid sequence of SEQ ID NO:178, and the VL comprises the amino acid sequence of SEQ ID NO:289.

5. The protein of claim 1 or 2, wherein the VH and the VL comprise the amino acid sequences of SEQ ID NOs: 143 and 144; 147 and 144; 244 and 144; 178 and 144; 256 and 144; 143 and 163; 143 and 167; 143 and 171; or 174 and 175, respectively.

6. The protein of any one of claims 1-5, wherein the second antigen-binding site is present as a single-chain fragment variable (scFv), and wherein the scFv comprises an amino acid sequence selected from SEQ ID NOs: 274, 145, 146, 149, 150, 153, 154, 156, 157, 160, 161, 164, 165, 168, 169, 172, 173, 176, 177, 180, and 181.

7. The protein of claim 6, wherein the scFv comprises the amino acid sequence of SEQ ID NO:274 or SEQ ID NO:180.

8. The protein of claim 1, wherein the second antigen-binding site that binds CLEC12A comprises a VH comprising CDR1, CDR2, and CDR3 comprising the amino acid sequences of SEQ ID NOs: 251, 196, and 246, respectively; and a VL comprising CDR1, CDR2, and CDR3 comprising the amino acid sequences of SEQ ID NOs: 198, 199, and 201, respectively.

9. The protein of claim 1, wherein the second antigen-binding site that binds CLEC12A comprises:

(i) a VH comprising CDR1, CDR2, and CDR3 comprising the amino acid sequences of SEQ ID NOs: 195, 196, 187, respectively; and a VL comprising CDR1, CDR2, and CDR3 comprising the amino acid sequences of SEQ ID NOs: 198, 199, 201, respectively;

(ii) a VH comprising CDR1, CDR2, and CDR3 comprising the amino acid sequences of SEQ ID NOs: 192, 196, and 187, respectively; and a VL comprising CDR1, CDR2, and CDR3 comprising the amino acid sequences of SEQ ID NOs: 198, 199, and 201, respectively; or

(iii) a VH comprising CDR1, CDR2, and CDR3 comprising the amino acid sequences of SEQ ID NOs: 192, 196, and 213, respectively; and a VL comprising CDR1, CDR2, and CDR3 comprising the amino acid sequences of SEQ ID NOs: 198, 199, and 201, respectively.

10. The protein of any one of claims 1 and 8-9, wherein the VH comprises an amino acid sequence at least 90% identical to SEQ ID NO:148, and the VL comprises an amino acid sequence at least 90% identical to SEQ ID NO:203.

11. The protein of any one of claims 1 and 8-10, wherein the VH comprises the amino acid sequence of SEQ ID NO:148, and the VL comprises the amino acid sequence of SEQ ID NO:203.

12. The protein of claim 11, wherein the VH and the VL comprise the amino acid sequences of SEQ ID NOs: 162 and 203; 210 and 203; 162 and 218; 148 and 218; or 210 and 218, respectively.

13. The protein of any one of claims 8-12, wherein second the antigen-binding site is present as an scFv, and wherein the scFv comprises an amino acid sequence selected from SEQ ID NOs: 184, 185, 204, 205, 208, 209, 215, 216, 252, 253, 254, and 255.

14. The protein of claim 13, wherein the scFv comprises the amino acid sequence of SEQ ID NO:204.

15. The protein of any one of the preceding claims, wherein the second antigen-binding site binds CLEC12A in a glycosylation independent manner.

16. A protein comprising:

(a) a first antigen-binding site that binds NKG2D;

(b) a second antigen-binding site that binds CLEC12A; and

(c) an antibody Fc domain or a portion thereof sufficient to bind CD16, or a third antigen-binding site that binds CD16;

wherein the second antigen-binding site binds CLEC12A in a glycosylation independent manner.

17. The protein of any one of claims 1-16, wherein the second antigen-binding site binds human CLEC12A with a dissociation constant (K_D) smaller than or equal to 20 nM as measured by surface plasmon resonance (SPR).

18. The protein of any one of claims 1-7 and 16-17, wherein the second antigen-binding site binds human CLEC12A with a K_D smaller than or equal to 1 nM as measured by SPR.

19. The protein of any one of claims 1-7 and 15-18, wherein the second antigen-binding site binds human CLEC12A comprising a K244Q substitution.

20. The protein of any one of claims 1-19, wherein the protein comprises an antibody Fc domain or a portion thereof sufficient to bind CD16.

21. The protein of any one of claims 1-20, wherein the first antigen-binding site that binds NKG2D is a Fab fragment, and the second antigen-binding site that binds CLEC12A is an scFv.

22. The protein of any one of claims 1-5, 8-12, and 15-20, wherein the first antigen-binding site that binds NKG2D is an scFv, and the second antigen-binding site that binds CLEC12A is a Fab fragment.

23. The protein of any one of claims 1-20, further comprising an additional antigen-binding site that binds CLEC12A.

24. The protein of claim 23, wherein the first antigen-binding site that binds NKG2D is an scFv, and the second and the additional antigen-binding sites that bind CLEC12A are each a Fab fragment.

25. The protein of claim 23, wherein the first antigen-binding site that binds NKG2D is an scFv, and the second and the additional antigen-binding sites that bind CLEC12A are each an scFv.

26. The protein of any one of claims 23-25, wherein the amino acid sequences of the second and the additional antigen-binding sites are identical.

27. A protein comprising:

(a) a first antigen-binding site that binds NKG2D;

(b) a second antigen-binding site that binds CLEC12A; and

(c) an antibody Fc domain or a portion thereof sufficient to bind CD16, or a third antigen-binding site that binds CD16;

wherein the first antigen-binding site that binds NKG2D is a Fab fragment, and the second antigen-binding site that binds CLEC12A is an scFv.

28. The protein of any one of claims 22, 24-26, wherein the scFv that binds NKG2D is linked to an antibody constant domain or a portion thereof sufficient to bind CD16, via a hinge comprising Ala-Ser or Gly-Ser.

29. The protein of any one of claims 21 and 25-28, wherein each scFv that binds CLEC12A is linked to an antibody constant domain or a portion thereof sufficient to bind CD16, via a hinge comprising Ala-Ser or Gly-Ser.

30. The protein of claim 28 or 29, wherein the hinge further comprises an amino acid sequence Thr-Lys-Gly.

31. The protein of any one of claims 22, 24-26, 28, and 30, wherein within the scFv that binds NKG2D, the heavy chain variable domain of the scFv forms a disulfide bridge with the light chain variable domain of the scFv.

32. The protein of any one of claims 21, 25-27, and 30-31, wherein within each scFv that binds CLEC12A, the heavy chain variable domain of the scFv forms a disulfide bridge with the light chain variable domain of the scFv.

33. The protein of claim 31 or 32, wherein the disulfide bridge is formed between C44 of the heavy chain variable domain and C100 of the light chain variable domain, numbered under the Kabat numbering scheme.

34. The protein of any one of claims 22, 24-26, 28, 30-31, and 33, wherein within the scFv that binds NKG2D, the heavy chain variable domain is linked to the light chain variable domain via a flexible linker.

35. The protein of any one of claims 21, 25-27, 29-30, and 32-34, wherein within each scFv that binds CLEC12A, the heavy chain variable domain is linked to the light chain variable domain via a flexible linker.

36. The protein of claim 34 or 35, wherein the flexible linker comprises $(G_4S)_4$.

37. The protein of any one of claims 22, 24-26, 28, 30-31, 33-34, and 36, wherein within the scFv that binds NKG2D, the heavy chain variable domain is positioned at the C-terminus of the light chain variable domain.

38. The protein of any one of claims 21, 25-27, 29-30, 32-33, and 35-37, wherein within each scFv that binds CLEC12A, the heavy chain variable domain is positioned at the C-terminus of the light chain variable domain.

39. The protein of any one of claims 22, 24-26, 28, 30-31, 33-34, and 36, wherein within the scFv that binds NKG2D, the heavy chain variable domain is positioned at the N-terminus of the light chain variable domain.

40. The protein of any one of claims 21, 25-27, 29-30, 32-33, 35-36, and 39, wherein within each scFv that binds CLEC12A, the heavy chain variable domain is positioned at the N-terminus of the light chain variable domain.

41. The protein of any one of claims 21, 27, 29-30, 32-33, 35-36, 38 and 40, wherein the Fab fragment that binds NKG2D is not positioned between an antigen-binding site and the Fc or the portion thereof.

42. The protein of any one of claims 22, 24, 26, 28, 30-31, 33-34, 36-37, and 39, wherein no Fab fragment that binds CLEC12A is positioned between an antigen-binding site and the Fc or the portion thereof.

43. The protein according to any one of claims 1-42, wherein the first antigen-binding site that binds NKG2D comprises a VH comprising CDR1, CDR2, and CDR3 comprising the amino acid sequences of SEQ ID NOs: 81, 82, and 112, respectively; and a VL comprising CDR1, CDR2, and CDR3 comprising the amino acid sequences of SEQ ID NOs: 86, 77, and 87, respectively.

44. The protein of any one of claims 1-42, wherein the first antigen-binding site that binds NKG2D comprises:

(i) a VH comprising CDR1, CDR2, and CDR3 comprising the amino acid sequences of SEQ ID NOs: 81, 82, and 97, respectively; and a VL comprising CDR1, CDR2, and CDR3

comprising the amino acid sequences of SEQ ID NOs: 86, 77, and 87, respectively; or

(ii) a VH comprising CDR1, CDR2, and CDR3 comprising the amino acid sequences of SEQ ID NOs: 81, 82, and 84, respectively; and a VL comprising CDR1, CDR2, and CDR3 comprising the amino acid sequences of SEQ ID NOs: 86, 77, and 87, respectively.

45. The protein of claim 43 or 44, wherein the VH of the first antigen-binding site comprises an amino acid sequence at least 90% identical to SEQ ID NO:95, and the VL of the first antigen-binding site comprises an amino acid sequence at least 90% identical to SEQ ID NO:85.

46. The protein of any one of claims 43-45, wherein the VH of the first antigen-binding site comprises the amino acid sequence of SEQ ID NO:95, and the VL of the first antigen-binding site comprises the amino acid sequence of SEQ ID NO:85.

47. The protein of any one of claims 1-46, wherein the antibody Fc domain is a human IgG1 antibody Fc domain.

48. The protein of claim 47, wherein the antibody Fc domain or the portion thereof comprises an amino acid sequence at least 90% identical to SEQ ID NO:118.

49. The protein of claim 47 or 48, wherein at least one polypeptide chain of the antibody Fc domain comprises one or more mutations, relative to SEQ ID NO:118, at one or more positions selected from Q347, Y349, L351, S354, E356, E357, K360, Q362, S364, T366, L368, K370, N390, K392, T394, D399, S400, D401, F405, Y407, K409, T411, and K439, numbered according to the EU numbering system.

50. The protein of any one of claims 47-49, wherein at least one polypeptide chain of the antibody Fc domain comprises one or more mutations, relative to SEQ ID NO:118, selected from Q347E, Q347R, Y349S, Y349K, Y349T, Y349D, Y349E, Y349C, L351K, L351D, L351Y, S354C, E356K, E357Q, E357L, E357W, K360E, K360W, Q362E, S364K, S364E, S364H, S364D, T366V, T366I, T366L, T366M, T366K, T366W, T366S, L368E, L368A, L368D, K370S, N390D, N390E, K392L, K392M, K392V, K392F, K392D, K392E, T394F, D399R, D399K, D399V, S400K, S400R, D401K, F405A, F405T, Y407A, Y407I, Y407V, K409F, K409W, K409D, T411D, T411E, K439D, and K439E, numbered according to the EU numbering system.

51. The protein of any one of claims 47-50, wherein one polypeptide chain of the antibody heavy chain constant region comprises one or more mutations, relative to SEQ ID NO:118, at one or more positions selected from Q347, Y349, L351, S354, E356, E357, K360, Q362, S364, T366, L368, K370, K392, T394, D399, S400, D401, F405, Y407, K409, T411 and K439; and the other polypeptide chain of the antibody heavy chain constant region comprises one or more mutations, relative to SEQ ID NO:118, at one or more positions selected from Q347, Y349, L351, S354, E356, E357, S364, T366, L368, K370, N390, K392, T394, D399, D401, F405, Y407, K409, T411, and K439, numbered according to the EU numbering system.

52. The protein of claim 51, wherein one polypeptide chain of the antibody heavy chain constant region comprises K360E and K409W substitutions relative to SEQ ID NO:118; and the other polypeptide chain of the antibody heavy chain constant region comprises Q347R, D399V and F405T substitutions relative to SEQ ID NO:118, numbered according to the EU numbering system.

53. The protein of claim 51 or 52, wherein one polypeptide chain of the antibody heavy chain constant region comprises a Y349C substitution relative to SEQ ID NO:118; and the other polypeptide chain of the antibody heavy chain constant region comprises an S354C substitution relative to SEQ ID NO:118, numbered according to the EU numbering system.

54. A protein comprising:

(a) a first polypeptide comprising the amino acid sequence of SEQ ID NO:259 or SEQ ID NO:276;

(b) a second polypeptide comprising the amino acid sequence of SEQ ID NO:260; and

(c) a third polypeptide comprising the amino acid sequence of SEQ ID NO:261.

55. A pharmaceutical composition comprising the protein of any one of claims 1-54 and a pharmaceutically acceptable carrier.

56. A pharmaceutical formulation comprising the protein of any one of claims 1-54 and a buffer at pH 7.0 or higher.

57. The pharmaceutical formulation of claim 56, wherein the pH of the formulation is between 7.0 and 8.0.

58. The pharmaceutical formulation of claim 56 or 57, wherein the buffer comprises citrate.

59. The pharmaceutical formulation of claim 58, wherein the concentration of citrate is 10 to 20 mM.

60. The pharmaceutical formulation of any one of claims 56-59, wherein the buffer further comprises phosphate.

61. The pharmaceutical formulation of any one of claims 56-59, further comprising a sugar or sugar alcohol.

62. The pharmaceutical formulation of claim 61, wherein the sugar or sugar alcohol is a disaccharide.

63. The pharmaceutical formulation of claim 62, wherein the disaccharide is sucrose.

64. The pharmaceutical formulation of any one of claims 61-63, wherein the concentration of the sugar or sugar alcohol in the pharmaceutical formulation is 200 to 300 mM.

65. The pharmaceutical formulation of claim 64, wherein the concentration of the sugar or sugar alcohol in the pharmaceutical formulation is about 250 mM.

66. The pharmaceutical formulation of any one of claims 56-65, further comprising a nonionic surfactant.

67. The pharmaceutical formulation of claim 66, wherein the nonionic surfactant comprises a polysorbate.

68. The pharmaceutical formulation of claim 67, wherein the polysorbate is polysorbate 80.

69. The pharmaceutical formulation of claim 68, wherein the concentration of polysorbate 80 in the pharmaceutical formulation is 0.005% to 0.05%.

70. The pharmaceutical formulation of claim 69, wherein the concentration of polysorbate 80 in the pharmaceutical formulation is about 0.01%.

71. The pharmaceutical formulation of any one of claims 56-70, wherein the concentration of NaCl, if any, is about 1 mM or lower in the pharmaceutical formulation.

72. The pharmaceutical formulation of any one of claims 56-71, wherein the concentration of the protein is 10 to 200 mg/mL.

73. The pharmaceutical formulation of claim 72, wherein the concentration of the protein is about 20 mg/mL.

74. The pharmaceutical formulation of any one of claims 56-59 and 61-73, comprising about 20 mM citrate, about 250 mM sucrose, and about 0.01% polysorbate 80, at pH 7.0.

75. The pharmaceutical formulation of any one of claims 56-60 and 72-73, comprising about 20 mg/mL of the protein, about 20 mM potassium phosphate, about 10 mM sodium citrate, and about 125 mM sodium chloride, at pH 7.8.

76. A cell comprising one or more nucleic acids encoding a protein of any one of claims 1-54.

77. A method of enhancing tumor cell death, the method comprising exposing the tumor cell and a natural killer cell to an effective amount of the protein of any one of claims 1-54, the pharmaceutical composition of claim 55, or the pharmaceutical formulation of any one of claims 56-75.

78. A method of treating cancer, the method comprising administering to a subject in need thereof an effective amount of the protein of any one of claims 1-54, the pharmaceutical composition of claim 55, or the pharmaceutical formulation of any one of claims 56-75.

79. The method of claim 78, wherein the cancer is a hematologic malignancy.

80. The method of claim 79, wherein the hematologic malignancy is selected from the group consisting of acute myeloid leukemia (AML), myelodysplastic syndrome (MDS), acute lymphoblastic leukemia (ALL), myeloproliferative neoplasms (MPNs), lymphoma, non-Hodgkin lymphomas, and classical Hodgkin lymphoma.

81. The method of claim 80, wherein the AML is selected from undifferentiated acute myeloblastic leukemia, acute myeloblastic leukemia with minimal maturation, acute myeloblastic leukemia with maturation, acute promyelocytic leukemia (APL), acute myelomonocytic leukemia, acute myelomonocytic leukemia with eosinophilia, acute monocytic leukemia, acute erythroid leukemia, acute megakaryoblastic leukemia (AMKL), acute basophilic leukemia, acute panmyelosis with fibrosis, and blastic plasmacytoid dendritic cell neoplasm (BPDCN).

82. The method of claim 80 or 81, wherein the AML is characterized by expression of CLL-1 on the AML leukemia stem cells (LSCs).

83. The method of claim 82, wherein the LSCs further express a membrane marker selected from CD34, CD38, CD123, TIM3, CD25, CD32, and CD96.

84. The method of any one of claims 80-83, wherein the AML is a minimal residual disease (MRD).

85. The method of claim 84, wherein the MRD is characterized by the presence or absence of a mutation selected from *FLT3-ITD* ((Fms-like tyrosine kinase 3)-internal tandem duplications (ITD)), *NPM1* (Nucleophosmin 1), *DNMT3A* (DNA methyltransferase gene *DNMT3A)*, and *IDH* (Isocitrate dehydrogenase 1 and 2 (IDH1 and IDH2)).

86. The method of claim 80, wherein the MDS is selected from MDS with multilineage dysplasia (MDS-MLD), MDS with single lineage dysplasia (MDS-SLD), MDS with ring sideroblasts (MDS-RS), MDS with excess blasts (MDS-EB), MDS with isolated del(5q), and MDS, unclassified (MDS-U).

87. The method of claim 80, wherein the MDS is a primary MDS or a secondary MDS.

88. The method of claim 80, wherein the ALL is selected from B-cell acute lymphoblastic leukemia (B-ALL) and T-cell acute lymphoblastic leukemia (T-ALL).

89. The method of claim 80, wherein the MPN is selected from polycythaemia vera, essential thrombocythemia (ET), and myelofibrosis.

90. The method of claim 80, wherein the non-Hodgkin lymphoma is selected from B-cell lymphoma and T-cell lymphoma.

91. The method of claim 80, wherein the lymphoma is selected from chronic lymphocytic leukemia (CLL), lymphoblastic lymphoma (LPL), diffuse large B-cell lymphoma (DLBCL), Burkitt lymphoma (BL), primary mediastinal large B-cell lymphoma (PMBL), follicular lymphoma, mantle cell lymphoma, hairy cell leukemia, plasma cell myeloma (PCM) or multiple myeloma (MM), mature T/NK neoplasms, and histiocytic neoplasms.

92. The method of any one of claims 78-91, wherein the cancer expresses CLEC12A.